THE STRUCTURAL AND METAMORPHIC DEVELOPMENT

OF THE BERGEN ARC/BERGSDALEN FORELAND

GNEISSES OF OSTERØY, S.W. NORWAY

by

Frederick William Metcalfe HOPPER

VOLUME I

Thesis submitted for the Degree of

Doctor of Philosophy

Bedford College (University of London)   February 1980

ProQuest Number: 10098381

All rights reserved

INFORMATION TO ALL USERS
The quality of this reproduction is dependent upon the quality of the copy submitted.

In the unlikely event that the author did not send a complete manuscript
and there are missing pages, these will be noted. Also, if material had to be removed,
a note will indicate the deletion.

ProQuest 10098381

Published by ProQuest LLC(2016). Copyright of the Dissertation is held by the Author.

MAPPING   FRIENDS

posterioribus

Dedicated to the memory of
   Mark Howard Johnson

North Osterøy comprises autochthonous and para-autochthonous basement
which has been reworked during the orogenic development of the adjacent
Bergsdalen and Bergen Arc nappes.

The divisions of the basement, the Southern and Northern Gneiss Units,
are composed of acid gneisses, paragneisses, migmatites, orthoamphibolites
and granites.   Three sedimentary complexes are identified, the first
(circa 1500 Ma.) resembles the Fjordane complex.   The second is correlated
with sediments in the Bergsdalen Nappes (older than 1000 Ma.), and with
the Samnanger complex in the Bergen Arcs.   The third sedimentary sequence
is the Ashgillian, Holdhus sequence of the Bergen Arcs.

The rocks of the Southern Gneiss Unit are derived from, and emplaced
over, the Northern Gneisses during four deformations, each of which is
separated by a sedimentary interval.   The deformation involves 'mylonitic'
processes acting at high temperatures and high strain rates.

The first deformation forms part of the Svecofennian orogenic cycle.
The second and third form part of the Sveconorwegian cycle and produce
folds with north-easterly trending axial traces.   The third is responsible
for the emplacement of the primary Bergsdalen Nappes and contrary to current
opinion these Nappes are thought to root in the south east.

The final deformation is part of the Caledonian orogenic cycle and
involves the development of the Bergen Arcs and their emplacement over the
Bergsdalen Nappes.   In the early stages of this cycle, structures formed
on an east-north-east Bergsdalen trend, but later, non-cyclindrical folds
with north-westerly trending axial traces developed, giving rise to the
Bergen Arc trend.   Of the two deformations which produce the Bergen Arc
and Bergsdalen Nappes, the Sveconorwegian event is the more important.

The interpretation of the geology of N. Osterøy and consideration of
its relationships to adjacent regions allows a new plate tectonic inter-
pretation of Western Norway.

ACKNOWLEDGEMENTS

CONTENTS

VOLUME 1

<u>VOLUME 2</u>

Plates 1 to 105

Map 1

Figure 158

Microfiche

1. INTRODUCTION

This thesis is based on a study of the rocks of North Osterøy, near Bergen, West Norway. The general position of the area relative to the main Caledonian Orogen is shown in figure 1.

The work forms part of a project arranged between the University of Bergen and Bedford College (London University), the aims of which are to re-examine the geology of the Bergen Arcs (Kolderup & Kolderup, 1940) and the immediate surrounding region (fig.2). The responsibility of the Bedford College contingent was to examine the geology of the basement gneisses to the east and west of the Arc structure, while the Institute in Bergen concentrated on remapping the lithologies comprising the Arcs. The area mapped (fig.9) was chosen on several counts, both logistic and academic. Less was known about the basement to the east of the Arcs than the Øygarden basement to the west, and it was felt that this should be studied first, with the object of examining the Arc basement contact.

The British contribution is financed by N.E.R.C. and directed by Professor B.C. King.

1.1. TOPOGRAPHY AND GEOLOGY

Osterøy is the only place on the eastern margin of the Arcs where the contact between the basement gneisses and the rocks of the Arcs is well exposed; elsewhere the junction is covered by sea. The rocks of the Arcs comprise the south-west portion of the island to the south and west of the central Storvatnet lake. These rocks form a fertile soil and the area is populous and well served by roads. The gneisses occupy the whole of the north-eastern portion of the island to the north and east of Storvatnet. These rocks form the highest ground of the island as

Fig 1.

THE SCANDINAVIAN CALEDONIDES

N

18 E
N 70

NORWAY / SWEDEN

TRONDHEIM

The Northwestern Gneisses

BERGEN

The Telemark Gneisses
OSLO

▨ Caledonian Allochthon

☐ Basement Gneisses

56 N
18 E

Fig 2.

Nord Hordland

N

Manger

Lindås

TYSSE

Holsnøy

Osterøy

Askøy

BERGEN

Sotra

OS

THE BERGEN ARCS

- Øygarden Gneiss Complex
- Minor Bergen Arc
- Ulriken Gneiss Complex
- Anorthosite Complex
- Major Bergen Arc
- Reworked N.E. Gneiss Complex
- North-Eastern Gneiss Complex
- Bergsdalen Nappes
- Fana Granite
- Thrust Contact

0   10
Km

Fig. 9.

NORTH
OSTERØY

PLACE NAMES
AND
MAPPING COVER

Bjorsvik

Molvik

Tyssebotnen

Fotlandsvag

Gammersvik

Stamn
-es

+HOGAFJELL

Dale

N

(STORVATNET)

Mapping scale
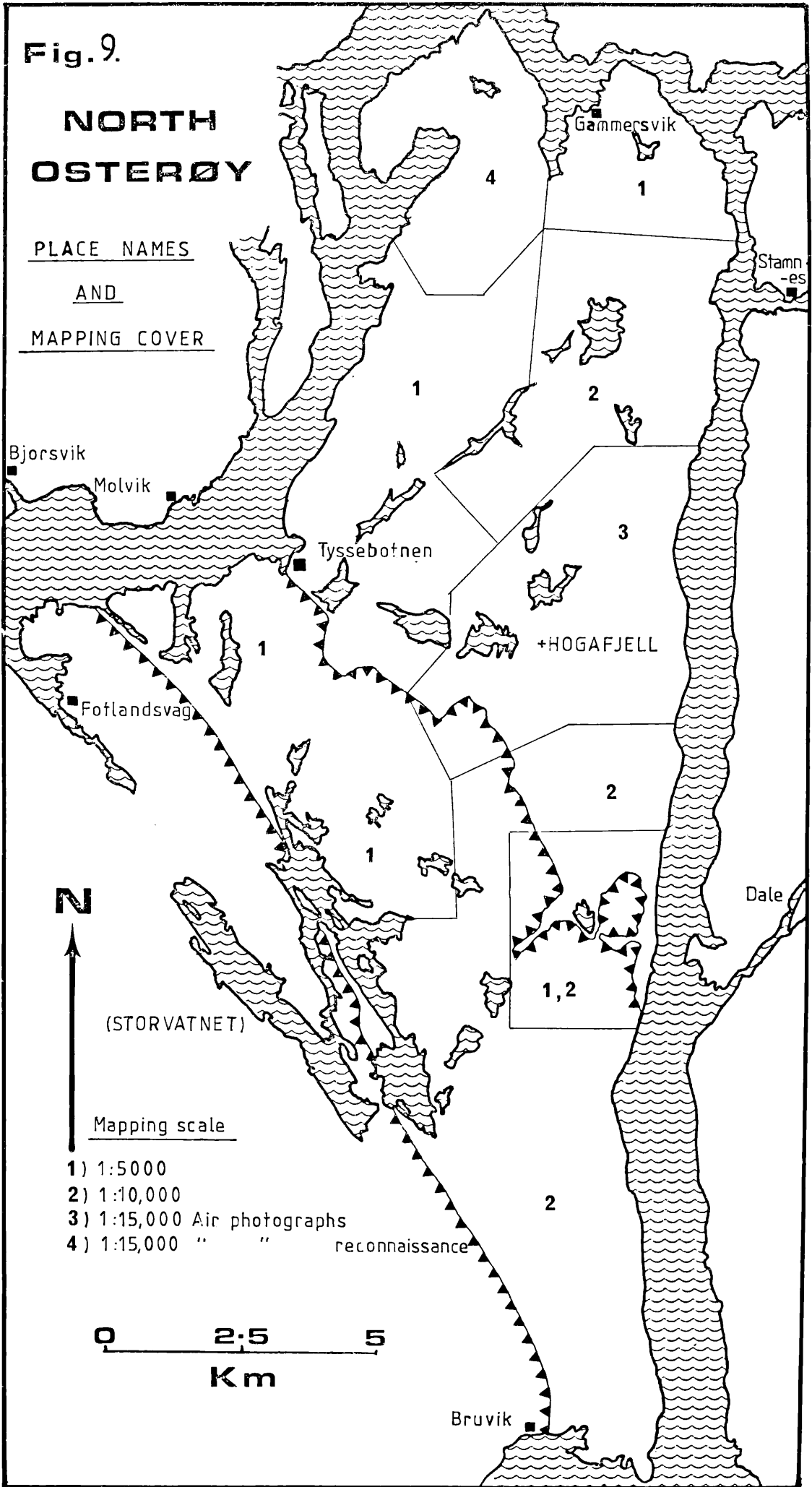
1) 1:5000
2) 1:10,000
3) 1:15,000 Air photographs
4) 1:15,000 " " reconnaissance

0   2·5   5
Km

Bruvik

they resist weathering and are for the most part exposed as barren rock. The villages are sited in the coastal valleys where glacial drift provides arable land. The tree line on this ground is at about 150 metres.

The highest point in the area mapped (the outcrop of these north-eastern gneisses) is Hogafjell, a mountain in the centre of the outcrop which rises to 869 metres. The hills are dissected by steep-sided valleys which follow sets of north-east and north-west trending joints (map 1). Numerous lakes develop at the points where these joints inter-sect. The tops of the hills are reasonably level but routes up to this plateau are scarce (map 1). Access from the fjord coast is impossible, the fjord sides are precipitous except at the mouths of rivers, which are sites of villages.

Climate

The mapping season in this area is from June to October; at other times the outcrops may be snow covered and/or the working day is too short. Rainfall is generally high throughout the year.

Mapping

The segment of basement chosen for mapping forms a triangle of gneisses between the rocks of the Bergsdalen and Bergen Arc nappes, ideally positioned to study the relationship between the two, as regards basement structure and constitution. The area north-east of the southernmost thrust on figure 9, was mapped at various scales, depending on the availability of maps. The basic mapping is at 1:5000, with the remainder of the area covered at 1:10,000, except where no maps were available, when mapping was done direct onto air photographs at a scale of 1:15,000. These photographs were later used in the construction of map 1, using the techniques of radial line plotting to transfer the more important topographic features and the geology.

Form of the Thesis

The thesis is divided into five main sections. The first places
Oster∅y in its regional setting, reviewing what is known of the geology
of the surrounding areas. The next two sections are descriptive,
dealing with rock composition, field and thin section appearance,
structure and the elucidation of structural and metamorphic history;
Any immediate conclusions that may be reached are presented as discussions
within these sections. In the process of mapping and in attempting to
understand the mineral textures observed, it became clear that a straight-
forward description of the observed features would not provide a complete
understanding of these rocks. The apparent heterogeneity of the
observed strains and the palaeometamorphic textures could only be adequately
explained in the light of recent advances in the understanding of the
nature and generation of mylonites. The fourth section is a description
of the rocks in this light and is in part theoretical. The final
section deals with the conclusions that may be drawn directly from the
area of study, incorporating the theory discussed in the fourth section.
Regional issues raised by these observations are discussed at the end
of this section.

Techniques, computer programmes and data are included as a set
of appendices.

1.2   Regional Setting

Oster∅y is an inland island, surrounded by fjords, situated 30 Km
to the north-east of the city of Bergen. It straddles the central
eastern "front" of the Bergen Arc structure. The south-western portion
of the island cuts deep into the centre of the Arcs and comprises most
of the usual lithologies encountered within the structure. The north-
east portion (the area mapped) extends into a large tract of gneissose

rocks believed to form part of the "North Western Gneisses" (Kvale,
1960), an area of basement gneisses, outcropping in the core of a major
geanticlinal structure on a north-easterly trend between Trondheim and
Bergen (fig.1), (see also Southern Norway Tectonic Map, 1975).
Immediately to the south east of Osterøy are the "Bergsdalen Nappes"
(Kvale, 1946), which continue on a north-east trend passing beneath
the "Upper Jotun Nappe" (Goldschmidt, 1916), to the north and out to sea
to the south (fig.3).

This part of south-western Norway can be divided into six main
regions (fig.4):

1) The Øygarden Basement Gneisses Complex

2) The Bergen Arc Nappe Complex

3) The North-Western Basement Gneiss Complex

(4) The Bergsdalen Nappe Complex)
(   )
(5) The Jotun Nappe Complex   )

6) The Telemark Basement Gneiss Complex

The Nappe complexes are preserved in major synformal troughs (Southern
Norway Tectonic Map, 1975). It is generally thought that the nappes
root to the north-west (Hossack, 1978) in a position presently occupied
by the North Sea, and that they once covered all of the North-Western
Basement. They have subsequently been eroded, being now only preserved
as infolds in basement depressions (Ramberg, 1977).

Figure 5 is a gravity map of the region (after Ramberg, 1977), which
shows two large areas of basement gneisses, the North-Western Gneiss
Complex and the Telemark Complex form areas of strong negative anomaly.
This indicates the crust in these regions is thick and not very dense,
comprising mainly acid material. Beneath the outcrop of the Bergen/
Jotun Nappes, however, this negative anomaly is not so marked. Indeed

Fig. 3   **8**

Principal Tectono-stratigraphic Units of the Southern Norwegian Caledonides.

LEGEND:

- Devonian
- Caledonian intrusive complexes
- Lower Palaeozoic metamorphic rocks
- Valdres Nappe (Late Precambrian – Mid Ordovician)
- Quartz-Sandstone Nappe (Late Precambrian – Mid Ordovician)
- Fanafjell Nappe, uncertain age (Bergen)
- Upper Jotun Nappe
- Hardanger – Ryfylke Nappe Complex
- Upper / Lower Bergsdalen Nappes
- Anorthosite Complex (Bergen)
- Ulriken Nappe (Bergen)
- Dalsfjord Nappe (Sunnfjord)
- In east autochtonous Lower Palaeozoic sediments In west Lower Palaeozoic sediments variably involved in thrusting and of uncertain tectonostratigraphic position
- Precambrian basement

Localities where major Middle Ordovician unconformity is preserved

S - Skudeneshavn, M - Moldvika, Os, St - Stubseid
L A - Lærdal and Aurland

After Sturt and Thon, 1978.

Fig 4

TECTONICS OF THE REGION ROUND OSTERØY.
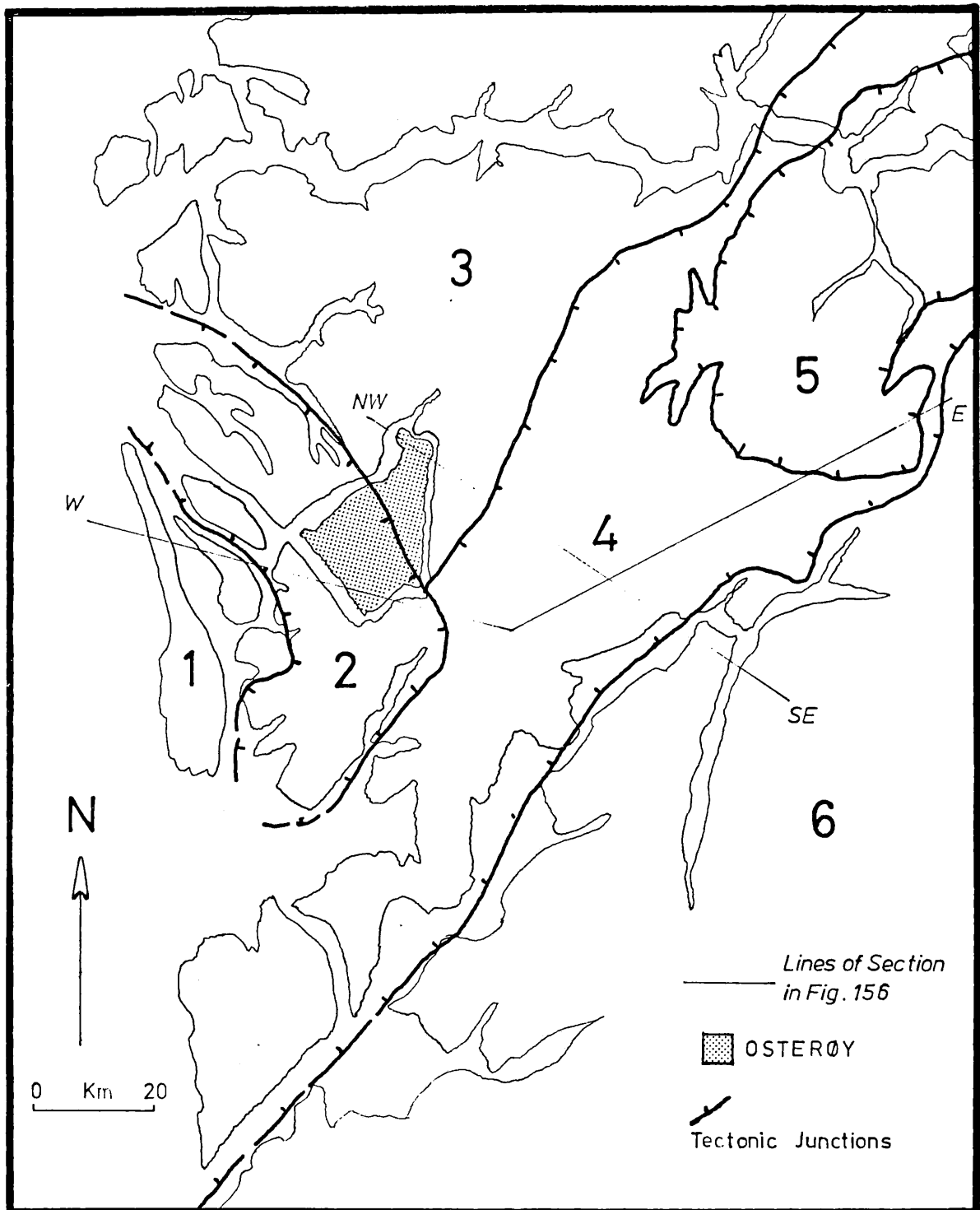
1. Øygarden Basement Gneiss Complex

2. Bergen Arc Nappe Complex

3. North Western Basement Gneiss Complex

4. Bergsdalen Nappe Complex

5. Jotun Nappe Complex

6. Telemark Basement Gneiss Complex

Fig 5.   10

BOUGUER   ANOMALY   MAP   OF

SOUTHERN   NORWAY

After RAMBERG, 1971.

[MGAL'S]
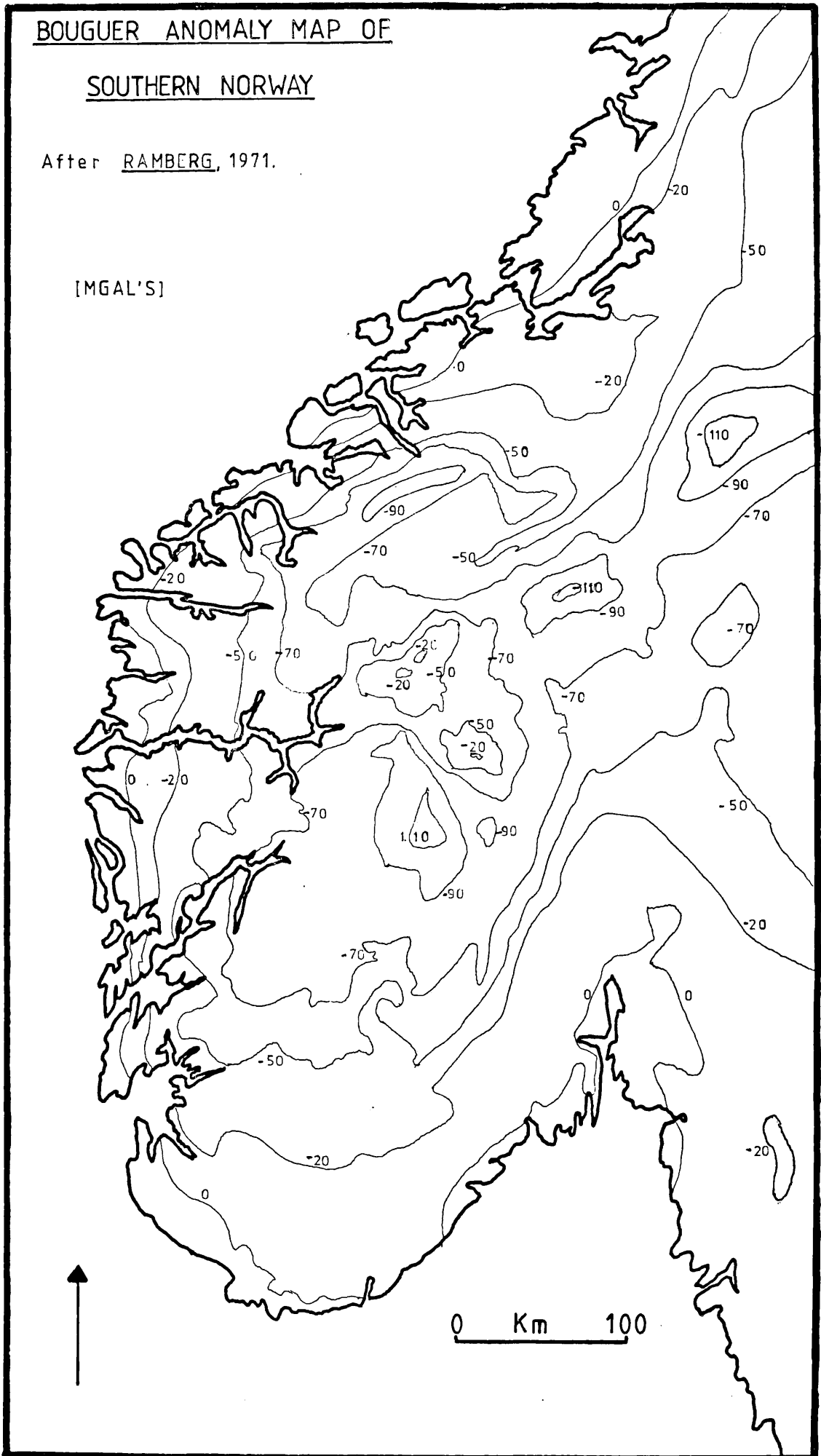
the area is anomalous in the manner in which the anomaly departs from

the general trend.   There are two possible explanations for this anomaly

(Ramberg, 1977; Smithson, Ramberg & Grönlie, 1974), either the crust

is thinner in this region, or there is more basic rock included in the

crust.

Seismic traverses over the region (Sellvoll & Warrick, 1971;

Kanestrøm & Haugland, 1971; Kanestrom, 1977) prove the crust in the region

to be 32-38 Km thick, with the thickest part lying under the outcrop of

the Bergsdalen/Jotun Nappes.   This indicates that the Bouguer anomaly

must be caused by the presence of denser rocks somewhere within the

crustal section.

The question is then one of the depth and thickness of this body of

dense rock; whether the anomaly is attributable to the rocks seen in

outcrop, or is caused by something at depth.

There is an accompanying magnetic anomaly associated with the

Bergsdalen/Jotun outcrop, which follows the gravity anomaly.   The

preferred explanation for this feature is the presence of a large mass

of gabbroic rock, about 3 Km thick (Aalstad et al., 1977).   This is at

variance with the preferred interpretation of the gravity data (Smithson

et al., 1974), which requires a thickness of at least 8 Km for the

gabbroic rock and the problem remains to be resolved.

Whatever its cause, the anomaly forms a marked linear feature in

the crust on the Bergsdalen/Jotun axis, passing to the south-east of

Osterøy.   Off the west coast of Bergen there is another strong positive

anomaly, a steep gradient on a north-south axis passes right through the

Arcs.   The cause of this is unclear, but the presence of the Viking

Graben off the coast to the west, in the North Sea (Nilsen, 1976), might

possibly offer an explanation for this.   This would mean that the gradient

through the Arcs is probably a relatively recent Mesozoic (Nilsen, 1976) modification of the older north-east - south-west trend described above.

Osterøy is thus situated just to the north-west of a major linear anomaly in the crust; it is therefore ideally placed to study how the basement has responded to the emplacement of the Bergen Arcs and Bergsdalen Nappes. If the geophysical feature has any surface expression it is likely that the rocks on Osterøy might shed some light as to its nature.

The Bergen Arcs and the Øygarden Basement

The first account of the geology around Bergen was given by Naumann (1824), who described the arcuate form of the outcrops. He was followed by Meilhau (1850), Hiortdahl and Irgens (1862), Kjerulf (1879), Reusch (1882), Kolderup (1897), Kolderup and Monckton (1912), Kolderup (1931), but it was Kolderup and Kolderup (1940) who appropriately referred to "The Bergen Arc System". This describes the two parallel belts of schists, approximately semicircular in shape and with a centre immediately to the west. The neighbouring formations are also arranged in a similar manner and so, together with the arcs s.s., form a large system of arcs of which there are five major units of differing lithology and of varying metamorphic grade. These units are separated by tectonic junctions (fig.2), which are major planes of transport for the allochthonous units, although within each unit there is much smaller scale imbrication. The five major units are, from the centre outwards:

1) Øygarden Gneiss Complex

2) Minor Bergen Arc

3) Ulriken Gneiss Complex

4) Anorthosite Complex

5) Major Bergen Arc.

The Øygarden Gneiss Complex

This is exposed as the "kernel" of the arcs and is on Sotra; it is represented by a series of granitic, granodioritic and tonalitic gneisses with amphibolites. They are considered to be of Svecofennian age (Sturt, Skarpenes, Ohanian & Pringle, 1975), but to have undergone several phases of reworking under amphibolite facies conditions with at least two stages of anatectic mobilisation, which evidently occurred in both the Grenvillian and Caledonian orogenies (Sturt et al., 1975). There is also some evidence for activity during the Grampian event.

Although no thrusts are seen in this unit and it apparently forms a local basement underlying the Bergen nappes to the east, it may itself be an allochthonous unit.

The Minor Bergen Arc

This overlies the Øygarden gneisses and crops out beneath the city of Bergen. The unit comprises metasediments and metavolcanics in which a number of impersistent horizons of gneiss occur. These usually have strong mylonitic fabrics. The contact with the underlying Øygarden unit is also a zone of intense deformation in which a great variety of mylonitic rocks are developed (Thon, Pers.Comm.,1977). To the east the Minor Arc is bounded by a major thrust underlying the Ulriken Gneiss Unit. These features suggest that the Minor Arc is a flattened zone of imbrication between the basement and a succession of thrust nappes, of which the Ulriken Gneiss Unit is the first. The Minor Arc has generally been regarded as of Lower Paleozoic age (Sturt & Thon,1978), though there is no proof of this; all that can be said is that it is pre-Ashgillian.

The Ulriken Gneiss Complex

This consists of a complex of thrust slices of gneisses with inter-
layered zones of metasedimentary rocks.   The gneisses are essentially
migmatitic with a comparatively late anatectic event at 1488 Ma. (Sturt
et al., 1975).   The gneisses are traversed by numerous zones of
mylonite and are separated from the underlying rocks of the Minor Arc by
a thick band of mylonite (Sturt et al.,1975), and at least three thrust
slices have been identified in this allochthonous basement nappe.

The Anorthosite Complex

Outcropping to the east of the Ulriken Gneiss Complex, and separated
from it by a distinct thrust contact, the Anorthosite unit comprises
a complex of imbricated and thrust plutonic igneous rocks, para- and
ortho-gneisses.   The oldest members (1775 Ma.,Sturt et al.,1975)
are anorthositic in composition.   These rocks have a protracted history
of deformation and metamorphic recrystallisation in the granulite facies
(Griffin,1972), before the intrusion of a younger suite of mangeritic
rocks (1064 Ma. Sturt et al.,1975; Sturt & Thon,1978).   The mangerites
have also been subject to granulitic facies metamorphism.   The rocks
of the Anorthosite Complex show the effects of reworking under both
amphibolite and greenschist facies conditions, which are largely
attributable to the Caledonian orogeny (Sturt & Thon,1978).

The Major Bergen Arc

The Major Arc is subdivided into two sequences separated by a major
unconformity (Sturt & Thon,1976).   The older of these sequences, the
Samnanger Complex (Faerseth, Thon, Larsen, Sivertsen & Elvestad, 1977),
comprises heterogeneous schists, quartz conglomerates, amphibolites
and greenstones, together with metaperidotites, gabbros and quartz diorites.
The rocks are characterised by highly complicated structures and several

zones of extensively mylonitised and recrystallised Precambrian gneisses within the schists. The age of these rocks is unknown, though in the literature (Faerseth et al.,1977) the sequence is assumed to be of Lower Palaeozoic age.

The Holdhus Group is unconformable on the Samnanger Complex (Faerseth et al.,1977). The Moberg conglomerate represents the oldest formation of the group, passing up into marble which is followed by the Gräsdalen Formation, including a fossiliferous Ashgillian marble.

Figure 6, after Sturt and Thon (1978), is a table of the Bergen Nappe sequence.

The Structure of the Bergen Arcs

Kolderup and Kolderup (1940) regarded the rocks of the Arc system as representing a Lower Palaeozoic metamorphic suite, containing a con- tinuous stratigraphic sequence from Precambrian gneisses through late Precambrian metasediments (the Minor Arc and Ulriken Gneiss), late Precambrian metavolcanics (the Anorthosite Complex), into fossiliferous lower Palaeozoic rocks (the Major Bergen Arc). The only basement in the area is that exposed on Øygarden. Hernes (1967) supported this view, but Kvale (1960), following Reusch (1882), interpreted the area in terms of nappe tectonics. He believed that the anorthositic and associated gneissic rocks represented an allochthonous thrust unit which overlay and separated the Major and Minor Arcs with their sequence of Lower Palaeozoic metamorphic rocks. Recent field and geochronological studies support Kvale's proposition, although the pattern of thrust tectonics is more complex than he envisaged.

Kvale regarded the Major Arc as being overlain by the anorthositic rocks, and suggested that the presence of an outlier of these rocks in the easternmost part of the Major Arc (fig.2) represented a thrust mass

Fig 6.

Bergen Nappe Sequence, Southern Norway.

	TECTONOSTRATIGRAPHIC UNITS	MAIN LITHOLOGIES	FOSSIL EVIDENCE	IGNEOUS ROCKS	CHARACTER OF DEFORMATION AND GRADE OF METAMORPHISM	RADIOMETRIC AGES
A L L O C H T H O N O U S U N I T S	FANAFJELL NAPPE	Ortho- and paragneisses. Granites, micaschists, quartzites, greenschists, minor marbles. Age uncertain.	None	Granites, Porphyries, Metadolerites.	Polyphasal deformation probably both Precambrian and Caledonian. Amphibolite facies metamorphism (probably Precambrian), Caledonian greenschist facies metamorphism.	453 ± 50 m.y. (variably sheared granites).
		THRUST CONTACT CATACLASIS AND VARIABLE BLASTOMYLONITES DEVELOPMENT. THRUST PLANE FOLDED AND CUTS ALREADY FOLDED THRUST PLANE IN SUBSTRATE.				
	ANORTHOSITE COMPLEX	Anorthosites, gabbros, mangerites. Ortho- and paragneisses with quartzites. Possibility that these rocks represent several tectono-stratigraphic units, but this awaits confirmation.	None	Anorthosites, Gabbros, minor ultramafics. Mangerites, Metadolerites, Trondhjemites.	Precambrian polyphasal deformation. Caledonian polyphasal deformation. Precambrian polyphasal granulite facies metamorphism - local eclogite development. Amphibolite facies metamorphism of Precambrian/Caledonian age. Caledonian greenschist facies overprint metamorphism.	1064 ± 24 m.y. (Mangerites) 1775 m.y. (Approx. isochron for granulite facies paragneisses, partially downgraded to amphibolite facies).
		THRUST CONTACT - EXTENSIVE BLASTOMYLONITE DEVELOPMENT. COMPLEX REFOLDING OF THRUST PLANE				
	ULRIKEN GNEISS NAPPE	Quartzites, conglomerates, micaschists Assumed Lr. Palaeozoic age.	None	None recorded.	Polyphasal Caledonian deformation Caledonian middle greenschist facies metamorphism.	None available.
		IN PART THRUST CONTACT - IN PART PRIMARY STRATIGRAPHIC UNCONFORMITY				
		Migmatitic para- and orthogneisses. Intrusive granitic complexes.	None	Granites, Pegmatites, Metadolerites.	Polyphasal Precambrian deformation. Polyphasal Caledonian reworking. Precambrian high amphibolite facies polyphasal metamorphism with extensive anatexis. Caledonian greenschist facies overprint metamorphism.	1440 ± 100 m.y. (age of late anatexis).
		The Ulrikens Nappe is multiple unit containing at least three thrust sheets, which in themselves exhibit a variety of basement/cover relations involving the above units.				
		THRUST CONTACT - EXTENSIVE BLASTOMYLONITE DEVELOPMENT. COMPLEX REFOLDING OF THRUST PLANE				
	MAJOR AND MINOR BERGEN SCHIST ARCS	(HOLDHUS GROUP) Conglomerates, phyllites, micaschists, limestones, metagreywacks	Llandoverian graptolite/brachiopod fauna. Ashgill coral shelly fauna	Lamprophyres, Trondhjemites.	Polyphasal Caledonian (late) deformation Caledonian metamorphism of middle to upper Greenschist facies.	None available
		HIGHLY DEFORMED PRIMARY STRATIGRAPHIC UNCONFORMITY				
		(SAMNANGER COMPLEX) Mica schists, quartz schists, conglomerates, marbles, greenschists, amphibolites.	None	Quartz diorites, Minor granodiorites. Gabbros, Serpentinites, Peridotites. Extensive basic lavas, in part pillowed.	Polyphasal early Caledonian deformation. Polyphasal late Caledonian reworking. Early Caledonian upper greenschist-lower amphibolite facies metamorphism. Late Caledonian greenschist facies overprint metamorphism - often pervasive.	None available
		The relations between the two complexes are often obscured by the pervasive late Caledonian polyphase deformation and metamorphism. Within these sequences occur slices of variably Caledonized basement gneisses.				
		THRUST CONTACT - EXTENSIVE BLASTOMYLONITE AND PHYLLONITE DEVELOPMENT. COMPLEX REFOLDING OF THRUST PLANE				
? A U T O C H T H O N ?	ØYGARDENS GNEISS COMPLEX	Para- and Orthogneisses with amphibolites	None	Granites, Gabbros, Metadolerites, Amphibolites, Diorites, Quartz Syenites, Pegmatites	Polyphasal Precambrian deformation. Polyphasal Caledonian reworking. Precambrian high amphibolite facies, metamorphism with relicts of older granulite facies metamorphism. Caledonian greenschist facies overprint metamorphism, may range up into amphibolite facies.	473 ± 31 m.y. ⎤ Younger 890 ± 150 m.y. ⎬ igneous 800 ± 14 m.y. ⎦ intrusions 1024 ± 85 m.y. ⎤ Presumed 1042 ± 92 m.y. ⎬ Grenville ⎦ reworking 1750 ± 60 m.y. Older gneisses
		It is not possible to say whether this is true basement or if thrust planes occur beneath sea-level.				

After Sturt & Thon, 1978.

subsequently folded into a tight synformal structure. The discovery of

the mid-Ordovician unconformity (Sturt & Thon,1976), shows that the

development of the Major Arc was a two stage process, comprising an early

deformation before the deposition of the Holdhus Group, which is

responsible for major stratigraphic inversions within the Samnanger Complex

(Faerseth et al.,1977). Further deformation causing both new folding

and secondary imbrication, affects both sequences of rocks (Ryan &

Skevington,1976; Sturt & Thon,1976; Sinha Roy,1977c; Faerseth et al.,1977

and Sturt & Thon,1978).

The youngest major feature and the highest unit within the Arcs is

the Fana Nappe (Sharman & Sturt,1977). This comprises mainly granitic

gneisses and minor amounts of metasediments transgressively emplaced

across the already folded thrust plane between the Anorthosite Complex

and the Major Bergen Arc. This late thrust is itself strongly folded

(Sturt & Thon,1978).

The Bergen Arc System can be regarded as a complexly refolded nappe

pile sitting in a synformal basement depression. Each unit is a separate

thrust sheet and the simplest explanation would be to correlate the rocks

of the Minor Bergen Arc with those of the Samnanger Complex of the Major

Arc, joining them up beneath the Anorthosite Complex. The structural

succession would then be as shown in figure 6.

The North Western Gneiss Complex

The North-Western Gneiss Complex (area 3 on fig.4), contains a great

variety of rock types, bounded in the west, along the coast, by several

synformal structures in which Devonian and what are regarded as Cambro-

Silurian rocks are preserved. These later sediments appear to be tectonically

emplaced along low lying thrusts (Bryhni, 1977; Skjerlie, 1968). In

the east, the region is bounded by a thick sequence of Eocambrian rocks

of arkosic character, while to the south is the junction between the basement gneisses and the overthrust rocks of the Bergsdalen and Jotun Nappes (Banham, 1968; Bryhni,1977).

The gneisses include obvious metasedimentary rocks, mica schists and quartz schists, together with sporadic layers of amphibolite, eclogites and anorthosites.

Until 1938, Norwegian geologists believed this area formed a Precambrian substratum to the Eocambrian and Cambro-Silurian rocks which surround it. Barth (1938) and Holtedahl (1938), however, postulated that some of the rocks in the gneisses might well be Eocambrian or Cambro-Silurian in age. Kolderup (1960) suggested that the whole of the gneissose area was produced by the granitisation and metasomatic alteration of what were originally Eocambrian and Cambro-Silurian rocks, having lithologies similar to those which surround the gneiss area. He regarded the junction between the observed Eocambrian and Cambro-Silurian rocks and the gneisses as the limit of the effects of the granitisation. He presumed the eclogites to be produced in the deep-seated heart of this area of granitisation from portions of the rocks which were originally amphibolitic in composition. This view was also supported by Hernes (1970).

More recently Bryhni(1966), subdivided the gneisses into two complexes, one of which, the Jostedal Complex, a sequence of relatively homogeneous two-feldspar gneisses, migmatites and augen gneisses, he believed to be reworked (or Caledonised) Pre-Eocambrian basement. This was considered to be overlain (in the west) by a more heterogeneous series of gneisses containing schists, quartzites, marbles, eclogites, amphibolites, peridotites and anorthosites - the Fjordane Complex. He believed this complex to be derived from rocks of Cambro-Silurian age and older elements corresponding to the Jotun thrust masses.

The two complexes (fig.7), have been widely recognised throughout the area (Brueckner et al.,1968; Strand,1969; Bryhni & Grimstad,1970; Bryhni et al.,1971; Carswell,1973). Brueckner (1977) called the two units in his area the Fetvatn Gneiss and the Vikvatn Sequence respectively, further subdividing the latter into three separate units (Bryhni,1977 and Lappin & Smith,1978).

Current argument concerns the relative ages of the two sequences and the mode of formation of the eclogites and anorthosites. Carswell (1973) believed that the Jostedal Complex was younger than the overlying Fjordane Complex and that the latter was either intruded by, or thrust over the former. The Jostedal Complex gives ages of 1000 Ma. (Bryhni, 1973, 1977) while the ages on the Fjordane Complex are nearer 1800 Ma. (Bryhni, 1973,1977). Both complexes show a retrogression, identified on the basis of individual mineral ages, between 500-350 Ma., showing they have been subject to a Caledonian reworking. However, the most recent dating seems to indicate that the Jostedal . Complex too is older than previously thought, as it has given ages of 1700 Ma. (Krogh,1977). The younger dates of 1000 Ma. come from a suite of granites, e.g. the Hestbrepiggan granite (Banham & Elliot,1965; Banham,1968 and Priem et al., 1973), which intrude this older part of the Jostedal basement. The gneisses then seem to be the produce of some ancient (pre-1000 Ma.) orogeny(s), involving a basement with a sedimentary cover sequence. It is now clear that the rocks of the Fjordane Complex are not Eocambrian or Cambro-Silurian as was once thought but represent an older Precambrian metasedimentary sequence (Brueckner,1979).

The eclogites found in this complex are an early feature in the crust, being involved in the earliest recognised deformations (Brueckner,1977). There are, however, two schools of thought as to their origin. Griffin and Bryhni (1977) and Krogh (1977), believe the eclogites in the gneisses

Fig 7.

THE UNITS OF THE N.W. GNEISS AREA

FJORDANE   COMPLEX

(Fetvatn   Gneisses)

Migmatized   Metasedimentary   Complex

+ Amphibolites + Anorthosites + Eclogites

[pre 1500 Ma]

————— Unconformity ? —————————

Granites
[1000 Ma]

JOSTEDAL   COMPLEX

(Vikvatn   Sequence)

Homogeneous   Two   Feldspar   Gneisses

[1800 - 1700 Ma]
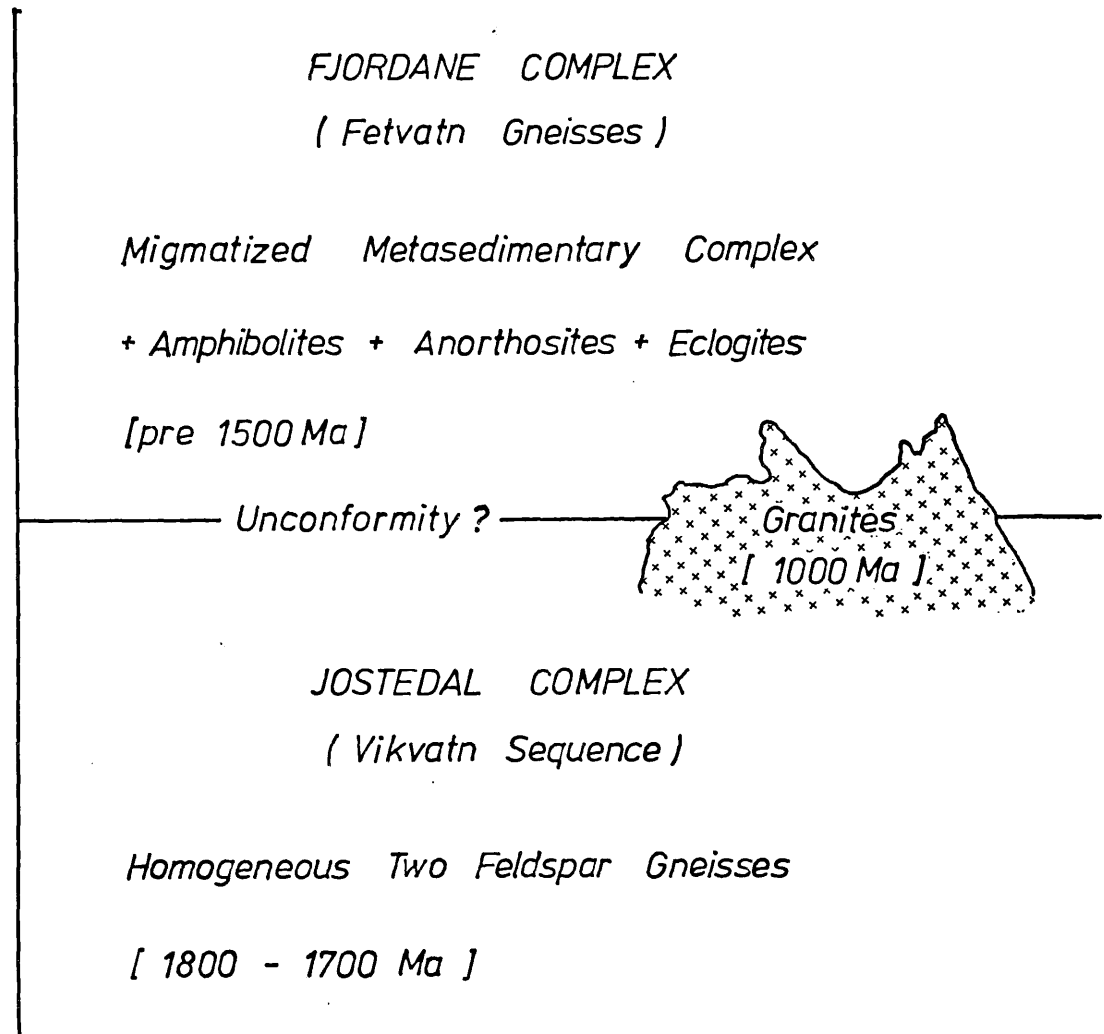
were formed in situ during the regional metamorphism of a variety of
basic rocks.   A Precambrian continent-continent collision is involved
where the environment was typified by high pressure and a very low
ppH2O.   The other school follows Eskola (1921), and is led by Lappin
and Smith (1978), who examined the mineral phases using microprobe
techniques.   They conclude that the eclogite and anorthosite rocks
crystallised at temperatures of around 1200-1370°C and pressures of around
30-40 Kb, implying therefore a mantle origin.   They propose that these
bodies of rock, occurring as aligned strings of boudins in the gneisses,
which themselves do not show such high grades of metamorphism, are mantle
wedges brought into the crust during an orogenic episode.

The Bergsdalen and Jotun Nappe Complex

This complex (areas 4 & 5 of fig.4), comprises several nappe units
of varying lithology and metamorphic grade.   The complex is preserved
in a synformal structure which runs from the coast inland on a north-
easterly trend following the Hardanger Fjord.   The dips along the north-
western margin of the structure are steeper than those along the south-
eastern border, where rivers have cut long re-entrants into the nappe
pile, forming windows through the structure.

In the eastern portion of the complex, three major nappe units are
recognised (Sturt & Thon,1978), see figure 8.   The highest unit of these,
occupying the central part of the synform, is the Upper Jotun Nappe
(Goldschmidt,1916;   Strand,1972).   This consists of a variety of rock
types (anorthosites, mangerites, jotunites and pyroxene granulites)
(Griffin,1971 & 1977;   Battey & McRitchie,1975).   Because of similarities
in lithologies with rocks of the Bergen Arcs these are therefore referred
to as the Bergen/Jotun kindred rocks.   The rocks of the Upper Jotun Nappe
preserve evidence of an early granulite facies metamorphism predating

Fig. 8.

Nappe Sequence Eastern Jotunheimen, Southern Norway.

TECTONOSTRATIGRAPHIC UNIT		MAIN LITHOLOGIES	FOSSIL EVIDENCE	IGNEOUS ROCKS	CHARACTER OF DEFORMATION & METAMORPHIC GRADE	RADIOMETRIC AGES
A L L O C H T H O N O U S U N I T S	**ØLJUVATN UNIT** (Formation)	Sandstone polymict conglomerate	None		Polyphasal deformation greenschist facies /metamorphism (probably Caledonian)	None
	PROBABLY PRIMARY UNCONFORMITY					
	UPPER JOTUN NAPPE	Anorthosites. Peridotites. Various pyroxene-granulites and gneisses in the core. In peripheral areas gabbros and granitic rocks.	None	Anorthosites, peridotites, gabbros, syenites, granites	Precambrian granulite facies, corona forming in anorthosites. Amphibolite facies (probably precamb.) Strongly developed cataclastic rocks during Caledonian thrusting, with greenschist facies metamorphic assemblages produced.	K/Ar mineral ages in the range 428 - 1280 m.y.
	THRUST CONTACT: WITH MAJOR DEVELOPMENT OF BLASTOMYLONITES					
	VALDRES OG MELLSENN GROUPS (UPPER JOTUN NAPPE)	Shales, sandstones, tillites (correlated with the thick Moelv tillite) Coarse conglomerates.	4 a	None	Polyphasal deformation with strong pebble elongation (Bygdin) cleavage formation. Recumbent folds in the Mellene area. Caledonian low greenschist facies met.	None
	THRUST CONTACT. IN PART SLIGHTLY DISTURBED PRIMARY UNCONFORMITY					
	ESPEDAL ROSSJOKOLLAN POSSIBLY GRONNESEN-KNIPA (LOWER JOTUN NAPPE)	Varied gneisses and other rocks resembling those of the Upper Jotun Nappe.	None	Granite, metagabbro, anorthosite	Amphibolite facies of probable Pre-cambrian age. Relict Precambrian granulite facies suggest by the presence of jotunperthites Caledonian cataclastic with accompanying greenschist facies metamorphism.	None
	THRUST CONTACT					
	QUARTZ-SANDSTONE NAPPE	Phyllites [Limestones locally, schist, shales and sandstones passing up into "Quartz sandstone" fine grained sandstone, coarse arkoses and quartzites (eocambrian)	3 a-h 2c 2a 1r	None	Slaty cleavage and folding. Caledonian low greenschist metamorphism	None
	THRUST PLANE					
A U T O C H T H O N	**CAMBRIAN**	Thickness < 100m. Alumschist. Dark sandy shale Thin basal conglomerate locally	Middle Cambrium (1c) in Arudal (Strand 1954).	None	Very low grade Caledonian metamorphism. Locally tectonic thickening and imbrication.	None
	PRIMARY STRATIGRAPHIC UNCONFORMITY					
	PRECAMBRIAN BASEMENT	Telemark supracrustals, metarhyolite, metabasalt and quartzites. Various gneisses (both para- and orthogneisses).	None	Granites, gabbros, dolerites	Polyphasal deformation. Mainly Precambrian amphibolite facies, also Precambrian greenschist-facies in Telemark supracrustals. Precambrian granulite facies in Arendal area.	Mainly Sveconorwegian dates 900-1200 m.y. but some older (Svecofennian) 1616 ± 38 m.y. 1700 ± 100 m.y.

Note: Numbers 1c etc. refer to standard stratigraphic subdivision of the Lower Palaeozoic sequence in the Oslo area as summarized by Henningsmoen, 1960 (p. 130 - 131,PI. 7). Geology of Norway, Norges Geol. Unders. 208, ed. Oluf Holtedahl.

After Sturt & Thon, 1978.

emplacement.   Whole rock ages of around 1280 Ma. from the granulites

date this metamorphism, whilst rocks recording retrogression due to

nappe emplacement yield mineral ages of around 428 Ma. (Sturt & Thon,1978).

Situated tectonically below the Jotun Nappe, the Valdres Nappe

consists, in its lower portions, of Precambrian crystalline basement

similar to that of the overlying Jotun Nappe (Hossack,1972 & 1976;

Heim et al.,1977).   These crystalline portions are succeeded in places

by a thick sequence of Eocambrian sparagmites which in turn pass up

through a Cambrian sequence.   The highest stratigraphical level preserved

is middle Ordovician.

The lowest of the three nappes is the Quartz Sandstone Nappe (Heim

et al.,1977;   Sturt & Thon,1978), which contains sediments ranging in

age from late Precambrian to middle Ordovician.

The rocks of these nappes show strong internal deformation (Bjorlykke,

1978;   Hossack,1978).   The nappes were apparently folded before emplace-

ment (Sturt & Thon,1978), which seems to have been a Caledonian event

occurring under greenschist facies conditions.   The thrust planes are

always marked by extensive zones of cataclastic rocks and it is thought

by many workers (Hossack,1978), that these units are far travelled, the

Upper Jotun Nappe having originated some considerable distance to the

west of the present Norwegian coast.   Such a provenance means that the

nappe sequence must have travelled from beyond the west coast of Norway

over the gneisses of the North-West Gneiss Complex.   Other workers

(Banham, Gibbs & Hopper,1979) hold the view that the nappes originated

beneath their present outcrops, and have moved to both the north and

south.   This model is consistent with the regional gravity anomaly

in the area (Smithson et al.,1974).

The western and southern portions of the complex are surprisingly

different from the patterns described above (fig.3). The thick Valdres

and Quartz Sandstone Nappes are not represented here and the rocks of

the Bergsdalen Nappes (Kvale,1946 & 1948), underlie the Jotun Nappe.

Kvale (1960), subdivided these into two units, the Upper and Lower

Bergsdalen nappes, separated by a thick unit of phyllites which are

assumed to be of Lower Palaeozoic age.

The nappes are also separated from the basement along the north-west

margin by similar phyllites (fig.3), though these are probably phyllonites.

The Bergsdalen Nappes themselves comprise an assemblage of Precambrian

gneisses and supracrustals (quartzites, conglomerates, meta-volcanics and

their mylonitic equivalents). They are intruded by a series of granitic

plutons of Precambrian age (1274 Ma. Pringle et al.,1975; Brueckner,1972;

Grey,1978 pers.comm.). As with the northern part of the complex much of

the early deformation predates the nappe transport, and took place at a

higher metamorphic grade than that coeval with the nappe transport

(middle greenschist in the phyllites and zones of cataclasis along

thrust planes, Sturt & Thon,1978).

There is much similarity between the rocks of the Bergsdalen Nappes

and those found in the Samnanger Complex of the Major Bergen Arc.

Similar rocks are also to be found all along the north-west margin of the

outcrop of the Bergsdalen/Jotun Complex (Banham et al.,1979). This

imparts an asymmetry to the rock types outcropping on either margin of

the complex; the north-west edge is very different in rock types and

has undergone much higher strain than the south-eastern margin.

In the south-west, the Bergsdalen Nappes are overlain by the Bergen

Nappe Sequence, with a contact complicated by later folding (Sturt & Thon,

1978). This suggests that the Bergen Arc structure continued to develop

after the Bergsdalen and Jotun Complex had formed.

The Telemark Basement Gneiss Complex

This area (region 6, fig.4), which underlies the whole of southern

Norway to the south of the Bergsdalen/Jotun complex, comprises granites,

gneisses, migmatites, metasediments, quartzites, metavolcanics, amphi-

bolites and anorthosites. These rocks form a vast complex wherein the

metasedimentary sequences occupy an arc, following the coast, round a

central region in which the granites, gneisses and migmatites are to be

found. The whole complex is Precambrian, yielding ages ranging from

1730-860 Ma. (O'Nions & Heier,1972; Versteeve,1975). In most respects

this basement area is very similar to that north of the Bergsdalen/Jotun

complex, in that it comprises a Precambrian metasedimentary and meta-

volcanic sequence of varied lithology overlying a more uniform gneissose

basement into which much granitic material has been intruded, the two

having been deformed together (Torske,1977). While eclogites are not

found in this southern basement, in the south the metamorphic grade does

reach granulite facies and in all other respects the lithologies present

in the southern basement are identical to those in the north-western

gneisses, even including anorthosites (Carswell,1973). The area is

interpreted as representing an ancient cordilleran-type, orogenic segment

that developed over a protracted period in Precambrian times (Torske,1977).

To the north-east in the Hardangervidda-Ryfylke area the basement

is overlain by a younger, Cambro-Ordovician autochthonous cover sequence.

This is then overthrust by a sequence of nappes which are subdivided into

five distinct tectono-stratigraphic units, two of which are attributable

to the Caledonian depositional cycle. The other three nappes are composed

of tectonised basement. These nappes continue down the west coast into

the Stavanger area. In the east, the Telemark basement is involved in

the upper Palaeozoic rifting of the Oslo Graben.

2. STRUCTURE OF THE AREA

The gneisses of north Osterøy (fig.10), are divided into the Northern
Gneiss Unit and the Southern Gneiss Unit, along a line passing through
Tysse, for the following reasons: the foliation in the Northern Gneiss
Unit strikes to the north-east paralleling the Bergsdalen front and the
structures seen within it are the oldest in the area. In contrast,
within the Southern Gneiss Unit, which structurally overlies the Northern
Gneiss Unit, the foliation strikes to the south - south-east paralleling
the outcrop of the Major Bergen Arc and the structures seen within it
are younger than those seen in the Northern Gneiss Unit.

The structural history of the two areas is described separately;
in each case starting with the oldest feature seen. The relationships
between the two units are discussed, together with the nature of the
junction between them.

References are made to the strain ellipsoid in discussion of the
deformations affecting the Osterøy gneisses. The properties of the
ellipsoid are inferred from structures present in the rocks, shape fabrics;
fold styles; general orientations or reorientations of visible structures;
schistosities, veins and igneous intrusions, etc. At no time has it been
possible directly to determine the shape of the ellipsoid by measurement
and only in one instance (D3 of the Southern Gneiss Unit), has it been
possible to define more precisely the nature of the ellipsoid.

2.1 STRUCTURAL HISTORY OF THE NORTHERN GNEISS UNIT

The deformation sequence in the Northern Gneiss Unit is summarised
in figure 36.

Fig. 10.

NORTH OSTERØY

MAJOR ROCK UNITS
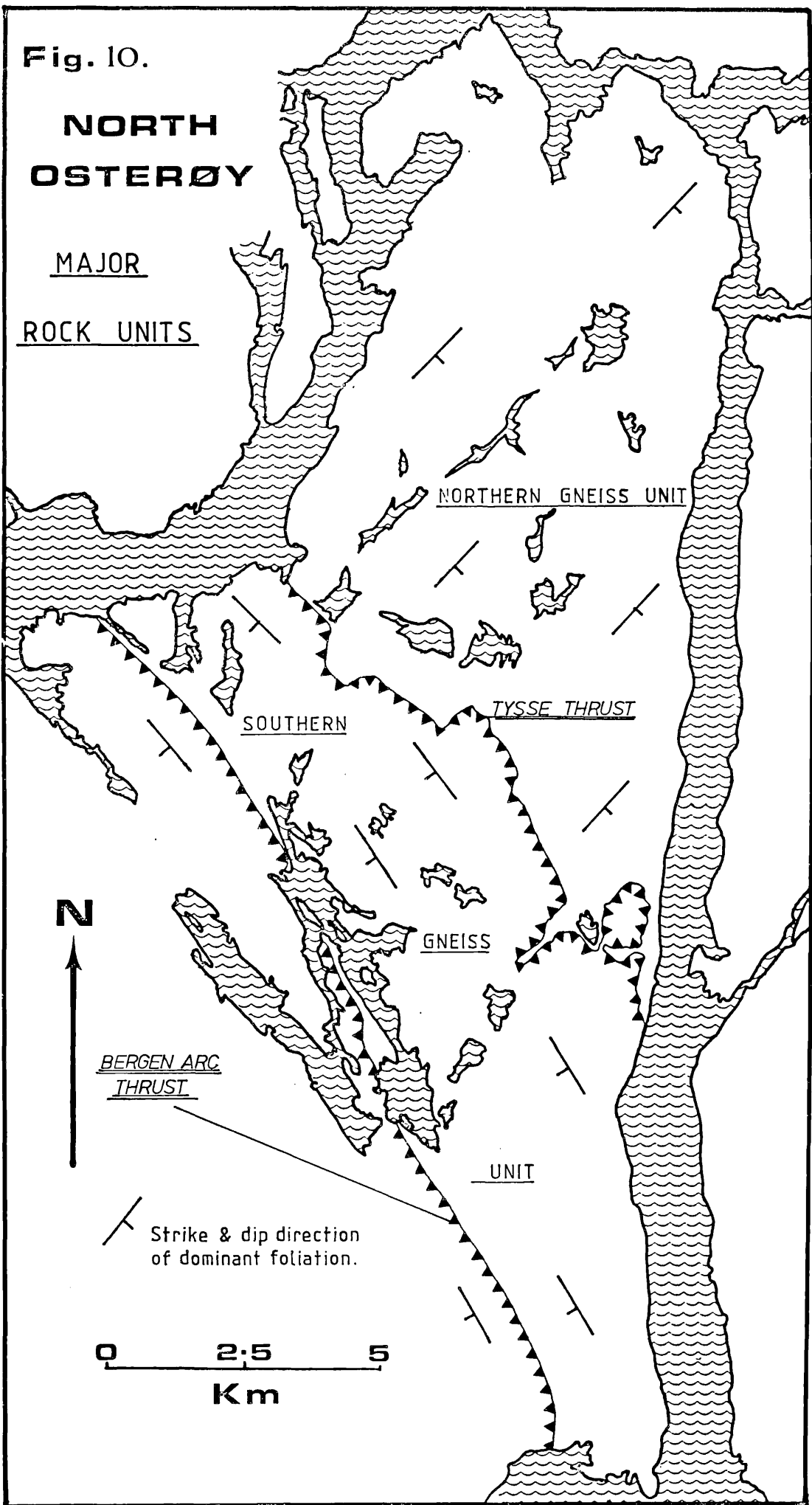
NORTHERN GNEISS UNIT

TYSSE THRUST

SOUTHERN

GNEISS

UNIT

BERGEN ARC THRUST

N

Strike & dip direction of dominant foliation.

0   2·5   5

Km

2.1.1   Early Deformations and Production of the Early Foliation "S Early"

The oldest feature seen is a gneissose banding accompanied by a layer of parallel schistocity. Over most of the area this banding is destroyed by subsequent deformations, but it is preserved at (11.37,34.85) and in exposures along the north and west coasts of Osterøy. The gneissose banding and accompanying fabric may represent primary igneous layering, migmatisation of an older complex, or earlier layering modified by an earlier tectonism.

The third of these possibilities seems the most likely because, while all the old rocks preserve the schistocity, only some of them are banded. The schistocity is best developed (as a penetrative amphibole alignment) in the more mafic components, while the banding (a compositional layering) is found in the more acid rocks. The banding is marked by leucocratic and melanocratic layers about 1-8 cm. thick (pl.1).

These features indicate that the banding and foliation are, in part at least, the product of an earlier deformation or deformations rather than a primary feature. For this reason the foliation is called "S Early" rather than "S0".

2.1.2   D1, The First Deformation Phase

Evidence for D1 is only sporadically preserved (fig.11), and is best seen at (11.37,34.85). This is the first fold-forming deformation, the folds cropping out as tight intrafolial isoclines (pl.2).

It is possible to trace the developmental history of D1 using structures developed in syntectonically intruded igneous bodies, and their relationship to periodic pegmatite emplacement.

Fig. 11

NORTH
OSTERØY

D1

PRINCIPAL D1

EXPOSURES

N

0   2·5   5
Km
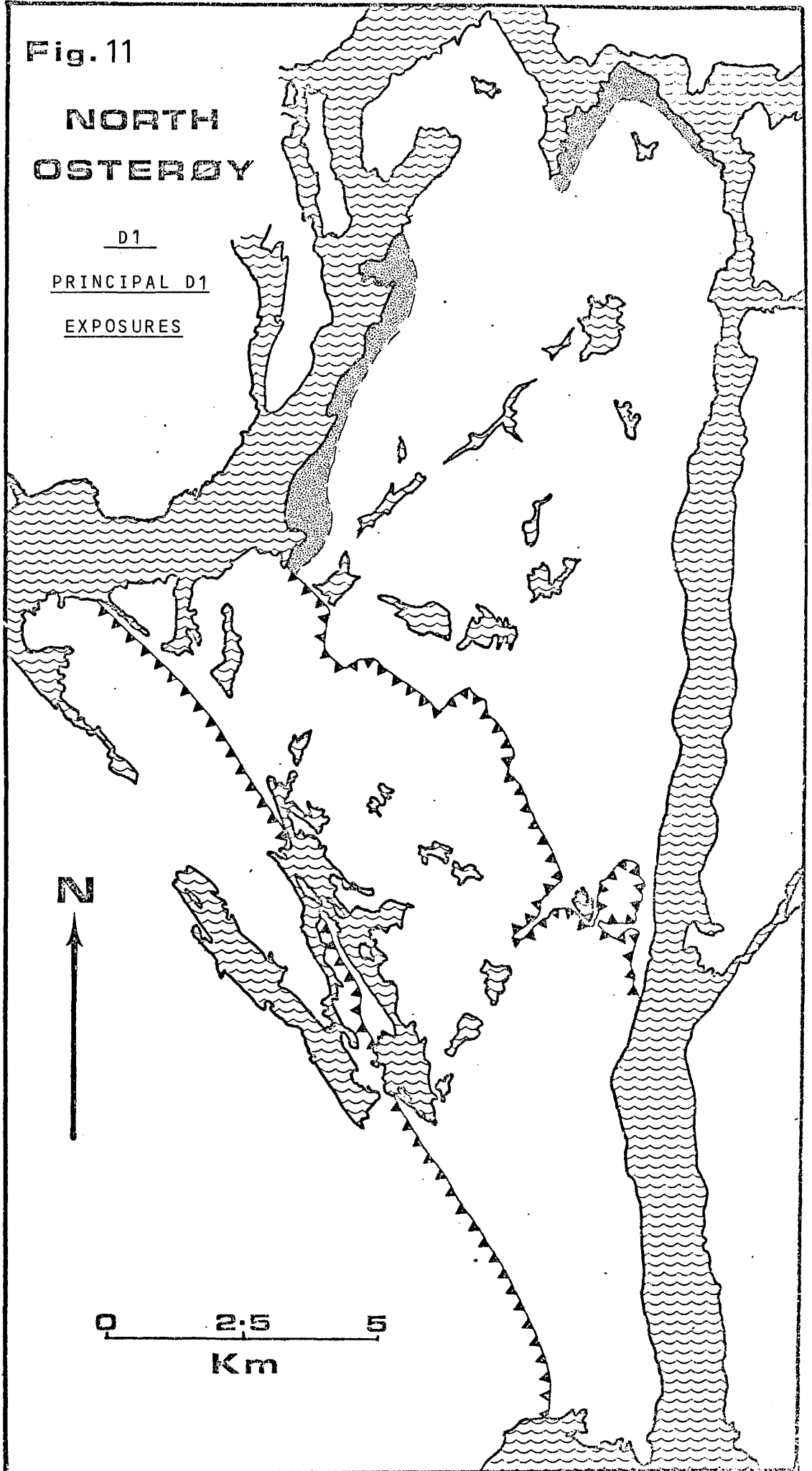
TABLE OF D1 EVENTS

D1a

1) Folding of "S Early" to form F1.

2) Intrusion of basic igneous bodies.

3) Initiation of vein development.

D1b

4) Flattening of F1 into intrafolial isoclines.

5) Flattening of the igneous bodies.

6) The development of a new foliation-S1.

7) The development of an intersection lineation (mullions in places)-L1.

8) Termination of vein emplacement started in D1a, associated with the limb regions of F1 folds.

This chronology is primarily established on evidence using the basic to ultrabasic intrusions at (11.37,34.58 and 14.65,44.63). The "S Early" foliation is isoclinally folded (pl.2), but this folding does not involve the basic bodies themselves which must therefore be intruded along the fold limbs and postdate this folding. After intrusion the basic bodies were veined by pegmatites that also started to develop in association with the limb regions of the folds (pl.3). The first stage of the D1 deformation is thus separated from the second by two intrusive events.

The second stage of the D1 deformation essentially involved flattening the pegmatitic veins in the basic bodies and those branching at an angle to the axial planes of the F1 folds became folded (fig.12), and a penetrative fabric, S1, developed axial planar to the F1 folds. The fabric is defined by the decusate texture of amphibole crystals. In fold noses its intersection with "S Early" produces a lineation (L1). Occasionally an associated, slight, coaxial mullion structure developed on the outer arc of some of the more leucocratic "S Early" bands (fig.13).

Fig 12.

ILLUSTRATION OF A POST F1 GABBRO AFFECTED BY S1 FLATTENING.
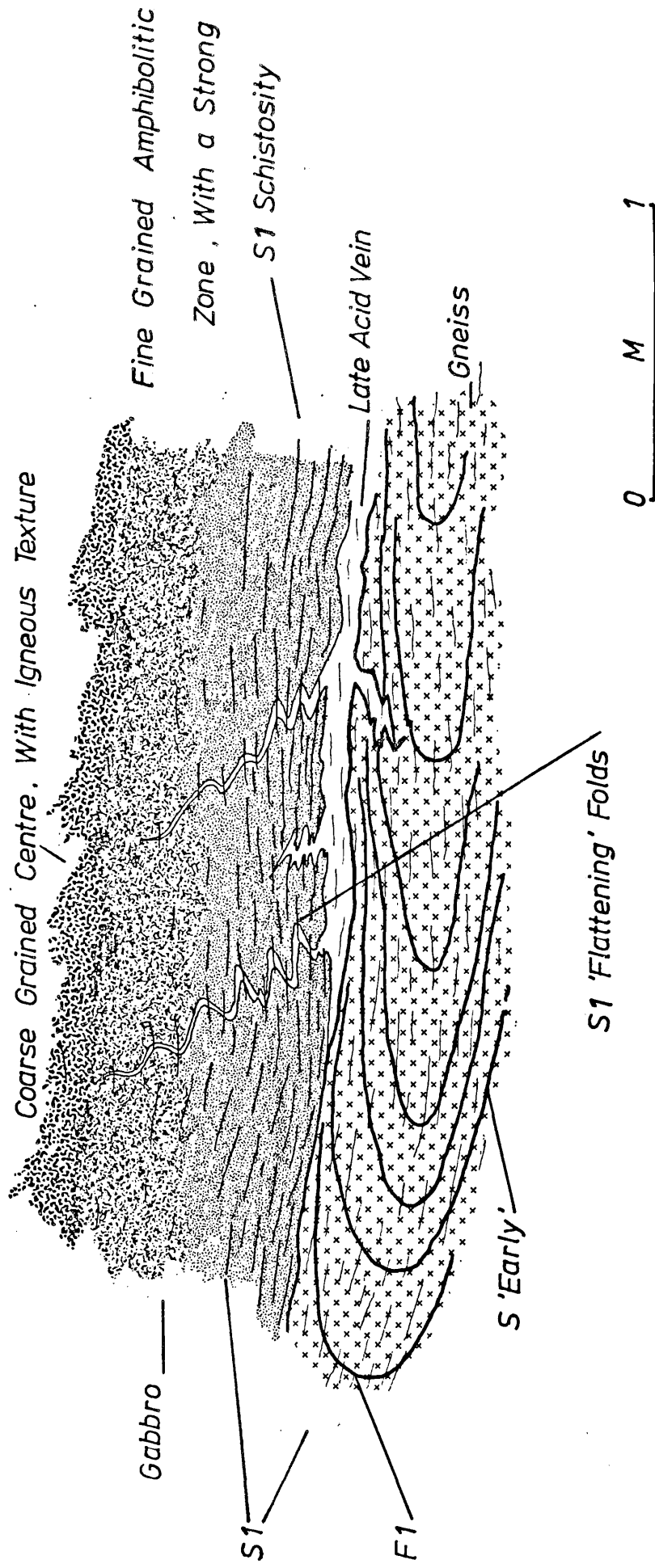
Fine Grained Amphibolitic Zone, With a Strong S1 Schistosity

Late Acid Vein

Gneiss

Coarse Grained Centre, With Igneous Texture

Gabbro

S1

F1

S 'Early'

S1 'Flattening' Folds

0   M   1

Fig 13.

SIMLIFIED GEOMETRY OF STRUCTURES PRODUCED IN D1

Plunge of F1 & L1

Limbs of F1 Folds

N

STRUCTURES ASSOCIATED WITH THE F1 FOLDS

0   M   0.5

L1 (Mullion)

Flaggy S1

L1 (Intersection)

Penetrative S1

Amphibolite Intrusion

F1

Folded D1a Pegmatite

S 'Early'
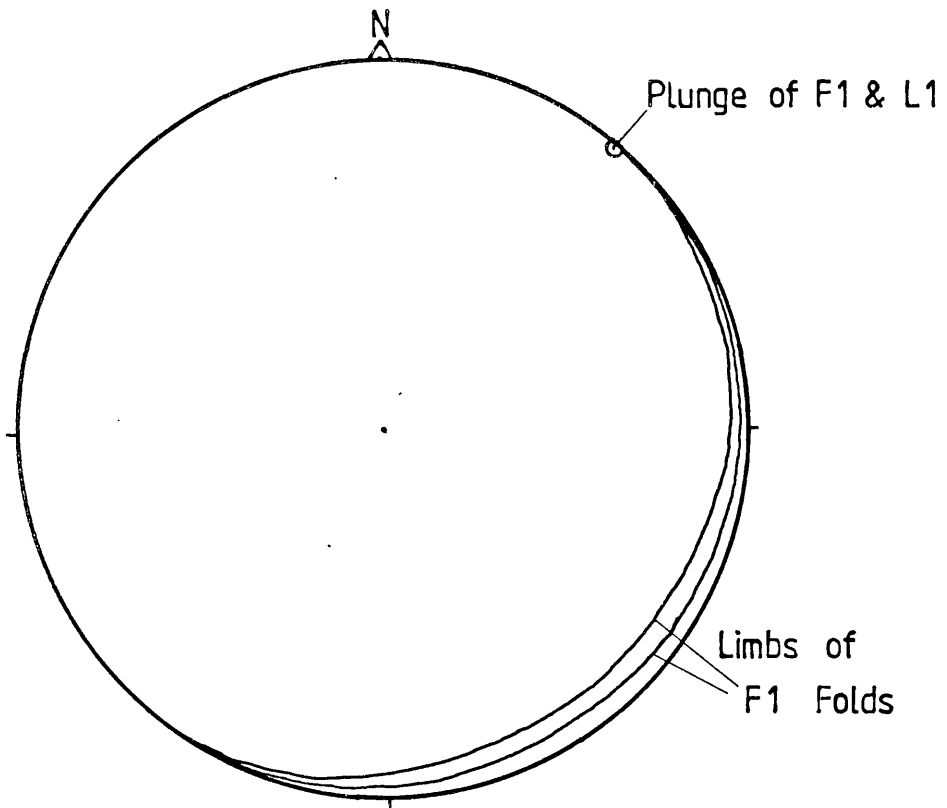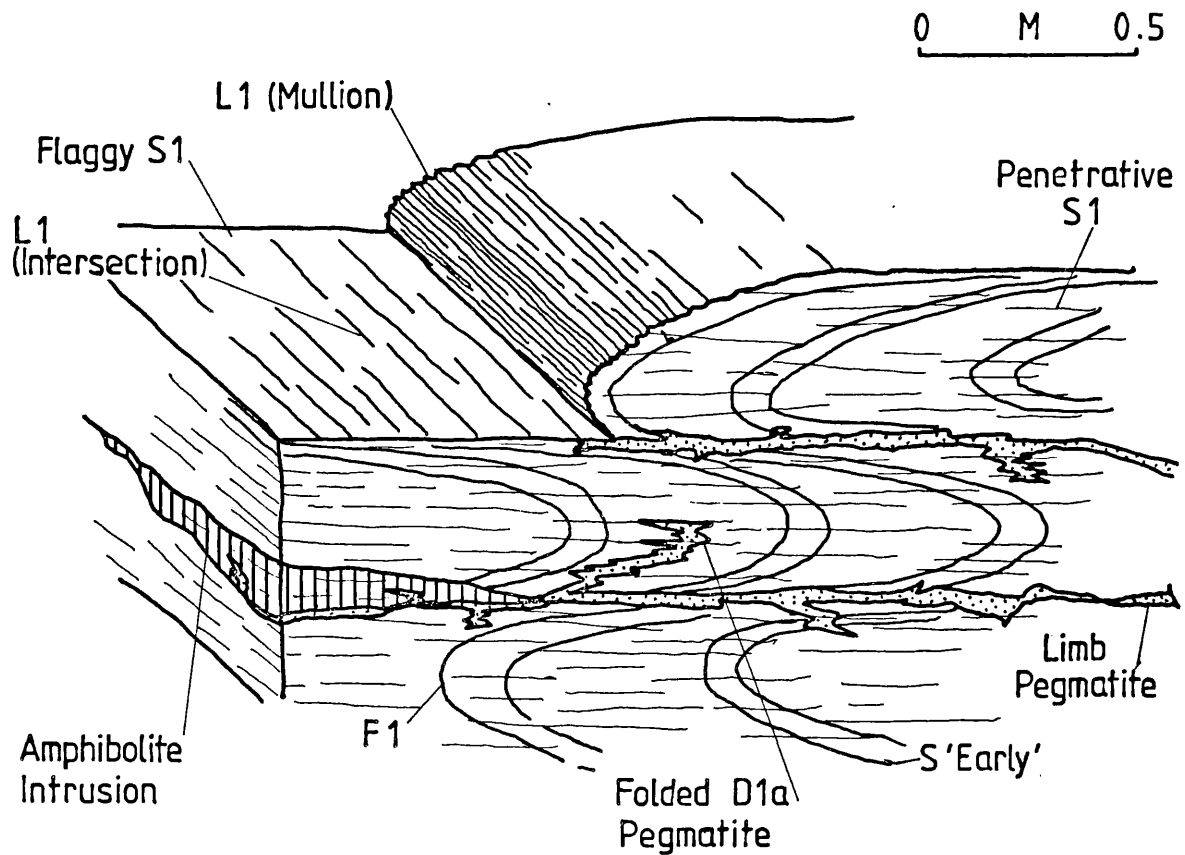
Limb Pegmatite

During the folding of the pegmatite veins the basic bodies themselves were flattened and boudinaged in the plane of the S1 schistosity. The amount of this flattening is difficult to determine because of post D1 events. The D1 flattening increases in intensity towards the margins of the larger bodies (up to 4 meters thick), and the original coarse-grained igneous texture is replaced in the flattened margins with a finer-grained tectonic fabric (fig.12).

During D1b the limbs of the F1 folds were attenuated and sheared out, leaving isolated fold noses. It is in the sheared limb areas that the new foliation is most strongly developed, along with foliation parallel pegmatitic veins (pl.4). In outcrop, therefore, the rock is divided into layers of relatively unmodified fold noses, separated by thinner layers, developed from the limbs, rich in pegmatites and showing none of the older structures. It is impossible to tell whether these pegmatites are, in Sederholm's (1967) terms, arterites or venites; they possess characteristics of both. Selvedges of mafic constituents (mainly amphibole now retrogressed to biotite) are developed at the pegmatite margins. The pegmatite vein emplacement continued throughout the flattening in the last formed shears (pl.4).

The trend of the F1 folds axes is difficult to determine because of the lack of suitable exposures and modification by later (post D1) deformations. The observed fold axes lie north-east - south-west and plunge in both directions depending on the geometry of the later folding. After removal of the later modification it is thought they were probably originally subhorizontal.

Discussion

Figure 13 shows the main structures developed in D1 and their orientation. Exposures preserving evidence for this deformation are rare (fig.11), being mainly confined to the northern and western coasts of the island. Inland, apart from the problem of weathering, which obscures detail in the exposures, the evidence for the deformation becomes masked by structures developed during post-D1 deformation. The spatial occurrence of the unmodified exposures is not haphazard and is controlled by position on later structures.

In view of the relationships described above the D1 deformation probably spanned a considerable time period, but grouping into one episode is justified on the grounds that the foliation developed in D1b is axial planar to the folds which began to form in D1a. The possibility that the D1a structures rotated into alignment with the D1b structures is recognised.

The model proposed is folding, followed by intrusion of basic lenses and pegmatites. Considering the progressive nature of the S1 development subsequent to the F1 folding, it is likely that the igneous intrusions would be in the XY plane of the developing F1 strain ellipsoid; the plane of the S1 schistosity. It also seems that because the axial planes of the F1 folds and the folds in the pegmatitic veins formed in D2b are parallel, the development of the D1 strain ellipse during D1 was, after F1, achieved with very little accompanying rotation. "a", "b" and "c" for the F1 folds can, therefore be considered to be coincident with X, Y and Z for the D1 strain ellipsoid.

2.1.3   The Period between D1 and D2

After the last stage of the D1 flattening (see above), and before the onset of the next phase of deformation, D2 (see below), two

important events, vein emplacement and the deposition of a sedimentary complex occurred.

The veining is best seen where sections at right angles to the dominant foliation are exposed. On the northern coastline, a set of veins is seen to cross-cut those developed in D1. They do not preserve the S1 fabric, but are folded by D2 structures and develop the D2 fabric (pls. 5 & 6).

Other very coarse-grained, granitic veins (frequently very rich in quartz) are found, which are difficult to place in the structural chronology since they do not preserve fabrics well; even where fabrics occur they can be attributed to either D2 or subsequent deformations. A further complication arises because migmatitic veins with a similar composition were also formed during early D2.

The sedimentary complex

In the period between D1 and D2, a sedimentary complex was either deposited or structurally emplaced in the area (map 1). The complex, described in detail in section 3.2.2, was essentially psammitic in composition with minor amounts of quartzite and mica schist. It is extensively migmatised, and all but the most quartzitic members have been altered. The migmatites are, however, distinguished from the gneisses because they do not show the intrafolial D1 isoclines and by the presence of quartzite. The basement gneisses appear to have been migmatised with the sediments, as at (11.27, 34.85) ghost D1 structures are seen in the migmatised gneiss.

Discussion

Two problems are raised: firstly, the relationship of the pegmatites to the deposition or emplacement of the sediments. No exposures in which the pegmatites intrude the migmatites were found, suggesting that the sediments postdate the pegmatites; secondly, the relative age of the sediments. If they had been deposited directly on their present basement, a basal unconformity would be expected. As no such unconformity has been identified it follows that either the unconformity is obliterated by the migmatisation and subsequent deformations, or the sediment/basement contact is entirely tectonic; the sedimentary complex may have been transported into the area during the early stages of D2.

Thin section study of the quartzite units shows several phases of fabric development. This conclusion is supported by field observations, the rocks are seen to be extensively folded. Minor thrusting accompanying the folding could account for the outcrop pattern seen at (21.00, 39.00, map 1); alternatively, the pattern could represent a refolded major D2 or D3 schuppen zone, in which case the sediments form an allochthonous nappe emplaced before the folding. In the absence of definite evidence, however, it is felt that the sediments are largely autochthonous and that the pattern is produced by original sedimentary variation; lenses of pure quartzite in a less pure sequence.

A remaining problem is the timespan indicated by the veining episode(s) and deposition of the sediments. At the close of D1 the rocks were undergoing amphibolite facies metamorphism (section 3.5.2), and since the sediments are a surface phenomenon, a considerable period of uplift and erosion is indicated. This was punctuated in the early stages by phases of vein emplacement which represent the only feature attributable to this period. The gap between D1 and D2 events is therefore probably considerable and could span the period between one orogenic cycle and the next.

2.1.4   D2, The Production of F2, S2, S3 and L2

D2 is the second deformation event to produce folds.   It can be

subdivided into two phases (table below).   The effects of the second

episode are inhomogeneously developed across the area, increasing in

intensity from west to east.

In the western half of Osterøy, F2 folds are the dominant structures

and unlike the intrafolial F1 folds, deform the dominant foliation.

They are the obvious folds seen in outcrop.

TABLE OF D2 EVENTS

D2a

1)   Migmatisation

2)   Production of a metasedimentary and migmatitic
         layering, S2

3)   Minor pre-fold thrusting ?

4)   Folding

5)   Production of S3a

6)   Production of L2

7)   Pegmatitic vein emplacement

D2b

8)   Intrusion of basic igneous bodies

9)   Pegmatitic vein emplacement

10)   Flattening and enhancement of the S3a fabric to form
          S3b.   (This event was heterogeneously developed
          across the area, being strongest on the eastern
          side of the island.)

The migmatite phase affecting the sedimentary complex has been referred

to in the previous section.   Metamorphic segregation and the development

of kyanite, almandine and hornblende in the metasediments suggests re-

working at about $600^{\circ}C$ and 20 Km burial (Miyashiro,1973).   During this

metamorphism a gneissose banding develops sub-parallel to the original

colour banding seen in the more quartz-rich sedimentary units; these

resisting migmatisation to a greater degree than the less pure components.

The colour banding appears to represent sedimentary layering, the

gneissose banding therefore probably developed tangential to the Earth's

surface rather than normal to it, and is therefore the product of hydro-

static burial during metamorphism rather than lateral compression. This

foliation is called S2 and is everywhere parallel to S1.

Except for a few arteritic (Sederholm,1967) pegmatites derived from

the migmatites, some of which are garnetiferous, the migmatite event in

the metasediments is only poorly seen in the older gneisses, which already

possessed a mineralogy stable at the almandine amphibolite facies of

metamorphism. Within the sediments there are numerous pegmatitic veins

produced during migmatisation; these are coarse-grained and very rich

in potash feldspar. Examples of these are seen at (21.50,39.00), where

dioritic granites intrude the migmatites. These diorites bear the

migmatitic fabric S2, and are now augen gneisses. They are arteritic in

origin, not a product of the migmatisation.

At locality (22.00,38.00 - map 1), schlieren of quartzite are present

in the migmatites. As has been discussed, these could point to the

presence of a hidden thrust. The picture is also confused because their

contacts are sharp and apparently tectonic. However, the schlieren are

not thought to be a schuppen zone but sedimentary/metamorphic in origin

and the tectonic contacts are thought to be produced during F2, as the

result of the first movements of folding.

F2 Folding

The F2 folds fold the S2 migmatite foliation and S1 (pls.7 & 8),

which as a composite structure form the dominant foliation of the Nord

Hordland gneiss region. The F2 folds are asymmetrical and overturned,

verging north-west and trending north-east - south-west.   The long limbs

of the folds dip south-east forming the east slopes of the local mountains,

while the short, steeply dipping north-west limbs give the topography a

sawtooth appearance.   The major folds have a wave-length of about 6 Km.

Parasitic folds are very common in the nose regions of the main folds

(e.g. the western coastline, 11.50,36.00), and range from 1 to 30 meters

in wavelength.

The plunge of the F2 folds is variable for the following reasons:

a)   They are affected by later deformations, which modify the F2 geometry.

b)   In the nose regions of the major folds the parasitic folds become

non-cylindrical, the pitch of the axis, measured in the axial plane, the

general dip of which is $110/50^\circ$, varies by as much as 50°.

c)   There is a variation in style of fold related to the rock type

involved in the folding.

Figure 14 shows the variation in plunge for the F1 folds;   the spread

in the data is a function of the non-cylindricity, while the south-west

plunges are produced by later folding.   Removing later deformation, the

general plunge of the F2 folds is to the north-east, at $045/27^\circ$.   On a

large scale these folds are cylindrical.   On the small scale however,

especially where the rocks involved have high ductility contrasts (such

as between quartzite and migmatite;   and amphibolite and migmatite) and

in the nose regions of the major folds (where the strain is constrictional)

the parasitic folds become non-cylindrical.

On Osterøy two large scale F2 fold closures are seen, one synformal

and one antiformal (fig.15).   The geometry of the synform is altered by

later thrusting, as is seen from the outcrop pattern of the quartzites

(fig.26).   The thrusting is also responsible for repetition of the

antiform closure (fig.15).

Fig 14.

Plunge of F2 Folds

PLOT OF SWIRL FOLD PLUNGE (N)

THIS PLOT HAS UNDERGONE -0- ROTATIONS

USING CORDINATE CARD   0

SAMPLING   2ACROSS/- 1DOWN   POLES PER   1PERCENT AREA   52 DATA   EQ AR

THE CONTOURS REPRESENT THE FOLLOWING PERCENTAGES

00.9<=1-2%>02.9<=3-4%>04.9<=5-6%>06.9<=7-8%>08.9<=9-10%>10.9<=11-12%>12.9
12.9<=13-14%>14.9<=15-16%>16.9<=17-18%>18.9<=19-20%>20.9<=21-22%>22.9
22.9<=23-24%>24.9<=25-26%>26.9<=27-28%>28.9<=29-30%>30.9<=31-32%>32.9
32.9<=33-34%>34.9<=35-36%>36.9<=37-38%>38.9<=39-40%>40.9<=41-42%>42.9
42.9<=43-44%>44.9<=45-46%>46.9<=47-48%>48.9<=49-50%>50.9<=51%+
NOTE A VALUE OF>0.5-0.9<=.LT.1%AND.GT.0%

Fig.15

NORTH OSTERØY

D2
F2 FOLD TRACES
AND QUARTZITE
OUTCROPS

F2

D2/
D3 THRUSTS

QUARTZITE

F2

N

0   2·5   5
Km

A new foliation, S3a, developed with the folding.   It is first

apparent in the quartzites where a muscovite and potash feldspar schistosity,

best seen in thin section, develops parallel to the axial plane of the

F2 folds, (the biotite of S2 tends to recrystallise) (fig.16).   In

the gneisses the S3a schistocity is marked by small flattened pods of

amphibole, now mainly replaced by biotite, which crosscut the earlier

S1 and S2 foliations in the nose regions of the F2 folds (pl.11).

An intersection lineation, L2, forms between the dominant S1-S2

foliations and S3a (pl.9).   The plunge of the lineation is parallel to

the F2 folds and may show a mullion-like character in the nose regions,

especially in the quartzites.   Figure 17 is a plot of all the lineations

found in the Northern Gneiss Unit;   the majority of the readings plotted

are L2, and it is clear that the orientation is similar to that for the

F2 plunges (fig.14).   The spread of the readings is not a reflection

of the non-cylindricity, because the readings were mostly made on the

limbs rather than hinges of the F2 folds.   The spread is attributed to

the effects of later folding (F3, see below), refolding this D2 lineation

so that it now plots on two small circles round the hinge of the later

(F3) folds (fig.25).

Pegmatite Relationships

The relationship between the F2 folds and the various pegmatitic

veins allows a detailed subdivision of the D2 event.   Four groups of

veins can be differentiated:

a)   The D1 limb region pegmatitic veins, now seen to be folded

round the F2 noses along with refolded F1 folds (pls.10 & 11).

b)   The pre-migmatite pegmatites, which are very difficult to

identify (see p.34), (pl.5).

Fig 16.

DEVELOPMENT OF S3a SCHISTOSITY

SKETCH OF HAND SPECIMEN (FH B39)

S3a

L2 Intersection Lineation

× $^{1}/_{2}$

S3a (Feint)

F2 Folds

Quartz Matrix

Biotite Foliation S2

SKETCH OF THIN SECTION

0   0.25mm.

F2
Microfold

Quartz Matrix

K-Feldspar S3a

Late Quartz Lath
Cleavage S5
(D4)

Folded Biotite
Foliation S2

Muscovite Books
Aligned With
S3a

Fig 17.
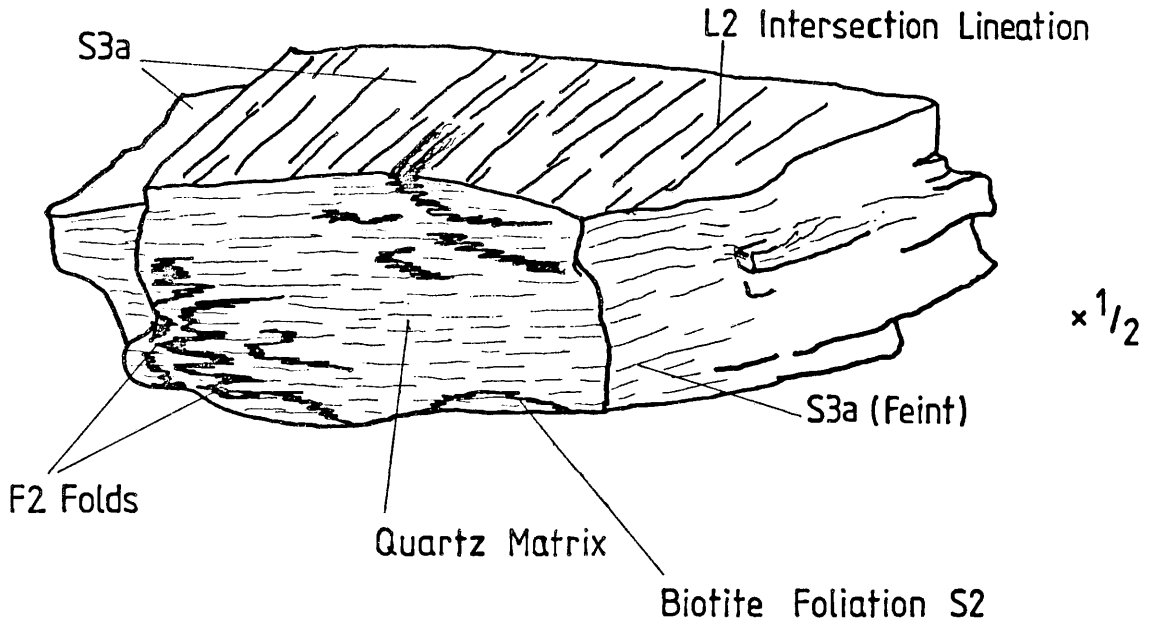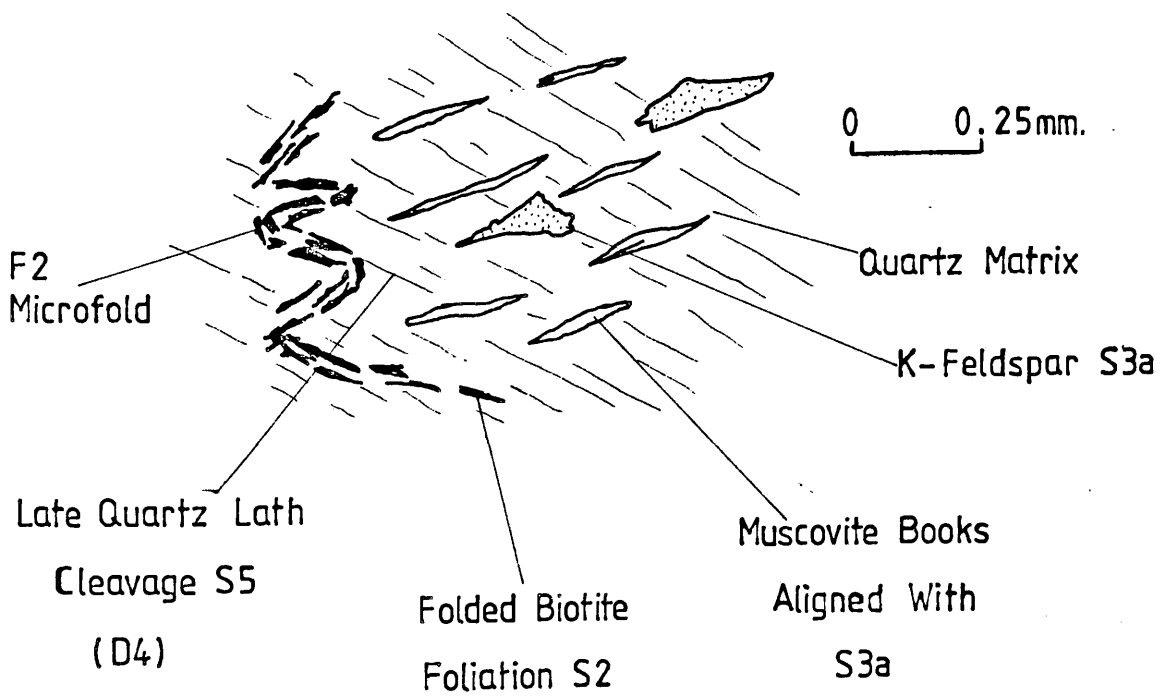
Plot of all N.Gneiss Lineations

PLOT OF NG. LINEATION (N)

THIS PLOT HAS UNDERGONE -0- ROTATIONS

USING CORDINATE CARD   0

SAMPLING   2ACROSS/- 1DOWN   POLES PER   1PERCENT AREA   155 DATA   EQ AR

THE CONTOURS REPRESENT THE FOLLOWING PERCENTAGES

00.9<=1-2%>02.9<=3-4%>04.9<=5-6%>06.9<=7-8%>08.9<=9-10%>10.9<=11-12%>12.9
12.9<=13-14%>14.9<=15-16%>16.9<=17-18%>18.9<=19-20%>20.9<=21-22%>22.9
22.9<=23-24%>24.9<=25-26%>26.9<=27-28%>28.9<=29-30%>30.9<=31-32%>32.9
32.9<=33-34%>34.9<=35-36%>36.9<=37-38%>38.9<=39-40%>40.9<=41-42%>42.9
42.9<=43-44%>44.9<=45-46%>46.9<=47-48%>48.9<=49-50%>50.9<=51%+
NOTE A VALUE OF>0.5-0.9<=.LT.1%AND.GT.0%

c)   The migmatite pegmatites and granites (pl.12)

d)   A suite of pegmatitic veins developed during the F2 folding, which lie along the axial planes of the folds (pls.10 & 11).

All these pegmatitic veins show the S3a schistosity, making detailed subdivision of the older veins difficult.   Accompanying the axial planar pegmatites, in the long limbs of the F2 folds, a suite of gabbroic igneous bodies was intruded (see 22.00,34.00).   After intrusion further pegmatitic veins were emplaced.   These coarse-grained, quartz and potash feldspar rich pegmatites cut the gabbros, F2 folds and S3a schistosity at moderately high angles, but are deformed in the D2b events (fig.21).

The D2b Flattening

The final phase of the D2 deformation is a flattening event.   Unlike the D1b flattening, which is homogeneous across the island, it increases from west to east of Osterøy (cf. pls.7,8 & 10 from the west coast, centre and east of the island).   As the F2 folding becomes tighter, the S3a schistosity is more strongly developed.   Further east the new schistosity becomes more intense, replacing S1 and S2, it forms the dominant foliation.   It imparts a flaggy nature to the outcrops on the east of Osterøy, as the F2 folds become intrafolial to S3b (intensified S3a).   On Osterøy the flattening increases with altitude and eastwards (fig.18).

It is apparent from this that the deformation increases in intensity along a vector normal to the F2 axial planes, towards the east.   The build-up to this flattening is gradual, the first effect seen is folding of the late pegmatites discussed above (pl.13).   Higher up the structural section as seen in the mountains, the flattening affects the igneous bodies and their cross-cutting pegmatites, which are boudineé within

Fig 18.

DEVELOPMENT OF D2 STRUTURES ACROSS N. OSTERØY

N

F2

S3a + S3b

S3a

0 ___ 1 Km
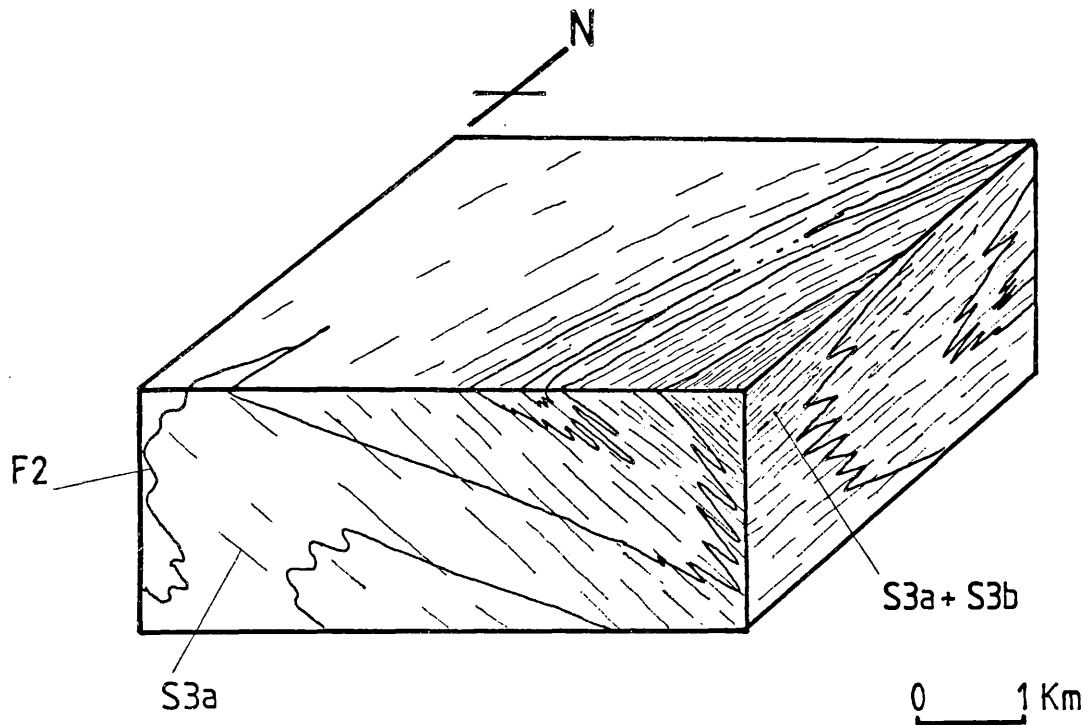
Fig 19.

DEVELOPMENT of the FLAGGY S3b SCHISTOSITY

Area of Rock Little Affected by
S3b and Still Showing Older
Features

0 M 10

S3b

Grass

F3
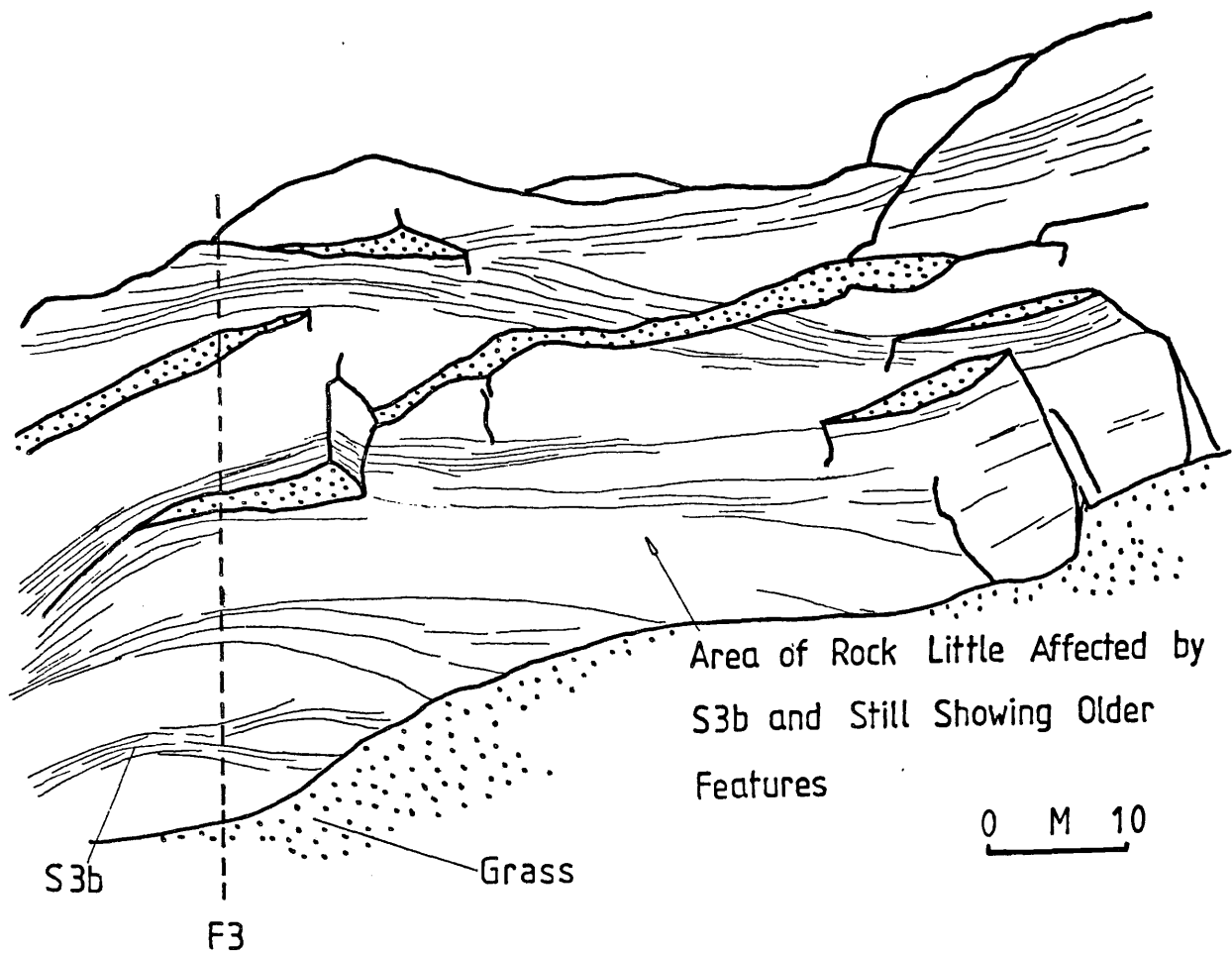
the gabbros (pl.14). Higher still, and further east the S3b foliation becomes dominant (pl.10), the foliation appearing first in the middle limbs of the F2 folds (fig.19). On the east slopes of Hogafjell (fig.9), the D1 structures start to be overprinted.

Discussion

The problems which arise when considering the D2 deformation are similar to those for D1. The grounds for grouping two phases of deformation, D2a and D2b, are that the S3b foliation is parallel to that of S3a and the development of S3b is associated with the tightening of the F2 folds, which formed in D2a.

The heterogeneity of the S3b development across the area must be of fundamental significance, it increases in intensity towards the Bergsdalen front. This observation can be interpreted in two ways:

1) The D2 deformation was associated with emplacement of the Bergsdalen Nappes and is therefore the first indication of their emplacement (see fig.20a).

2) That the site now occupied by the Bergsdalen Nappes formed a fundamental feature in the local basement, which preceded emplacement of the Bergsdalen Nappes (see fig.20b). Deformation on this feature would be responsible for the alignment of the D1 structures and the F2 folds. The intensity of the D2b flattening may be a function of absolute distance from this feature.

The sense of translation on the shears in the middle limbs of the F2 folds and their vergence is to the north-west. This, and the fact that the D1 folds axes parallel those of D2 and the presence of a further phase of folding (F3 below), indicate Figure 20b (OR) probably best explains the observations.

Fig 20a

MODEL 1 EXPLAINING THE SIGNIFICANCE OF F2 & S3b

Emplacement of the BERGSDALEN at the end of D2

F2

NW

SE

S3b
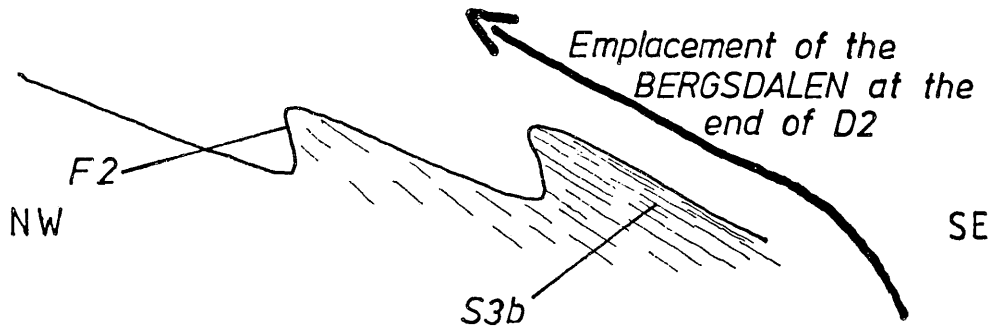
Fig 20b

MODEL 2 EXPLAINING THE SIGNIFICANCE OF F2 & S3b

First in D2

Major Crustal Feature Here in D2, an Orogen?

F2

NW

SE

S3b

Then Later, D3? D4?

EITHER

BERGSDALEN Emplaced From The NW

F2

NW

SE

S3b

Crustal D2 Feature

OR

BERGSDALEN Emplaced From The SE

F2

NW

S3b

SE
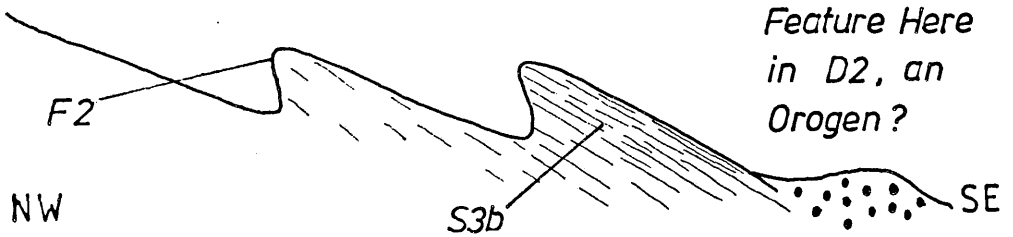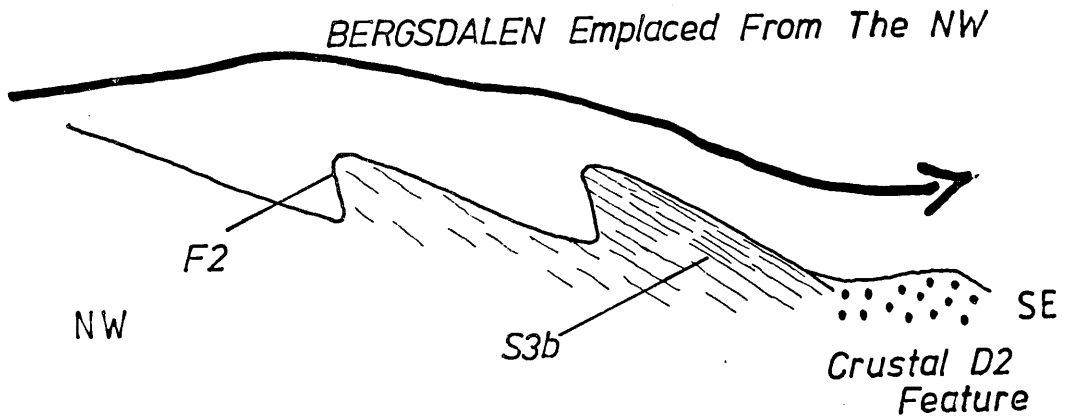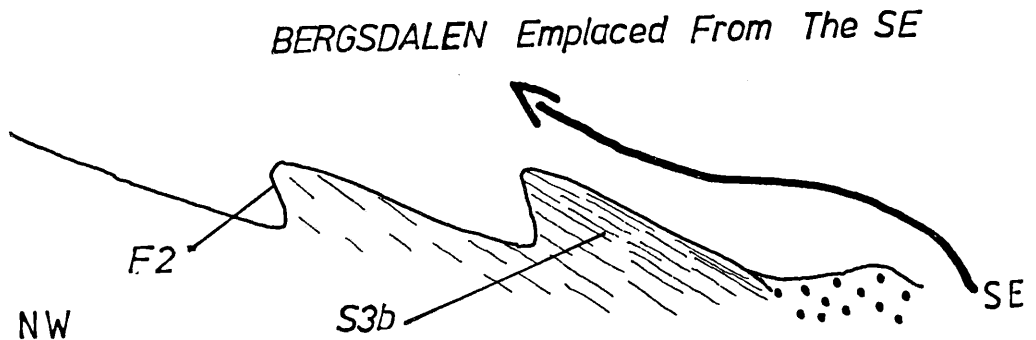
Like the D1 deformation, D2 obviously spans a considerable period. The strain ellipsoid for the event is complex; development of D2 structures is tabulated below:

a)   Initial extension parallel to the layering (D1) accompanying migmatisation, during which pegmatites were intruded.

b)   Folding of the S1/S2 layering to produce F2.

c)   Formation of a new schistosity in the X/Y plane of the F2 strain ellipsoid.

d)   Injection of gabbro and pegmatite emplacement parallel to the X/Y plane of F2 strain ellipsoid.

e)   Pegmatite emplacement in the Y/Z plane of the F2 strain ellipsoid (see fig. 21).

f)   Further modification of the F2 strain ellipsoid during D2b.

This sequence of development is very similar to that seen in D1 and is summarised in figure 22.   (Again a, b and c for the folds are assumed to be coincident with X, Y and Z for the D2 ellipsoid).

2.1.5   D3, The Production of F3, L3 and S4

D3 is the third deformation seen in the area, it is subdivided into several episodes.

TABLE OF D3 EVENTS

1)   Thrusting

2)   Production of the F3 folds

3)   Development of S4

4)   Development of the L3 lineation

5)   Pegmatite emplacement

Fig 21

D2 PEGMATITES AND THEIR RELATIONSHIP
TO THE F2 FOLDS

(D3 Pegmatite)

(D3 Fold)

D1 Pegmatite

F 2

Pegmatites in b c
Plane of the F2
Folds, Folded in D2,
-During the D2b
Flattening

S3b
in a b Plane
of the F2
Folds

0   M   1

Fig 22.   51

SIMPLIFIED GEOMETRY OF STRUCTURES PRODUCED IN D2

Steep Limb
F2

L2 and Plunge of
F2

Shallow Limb
F2

F2
Axial Plane + S3
(Composite)
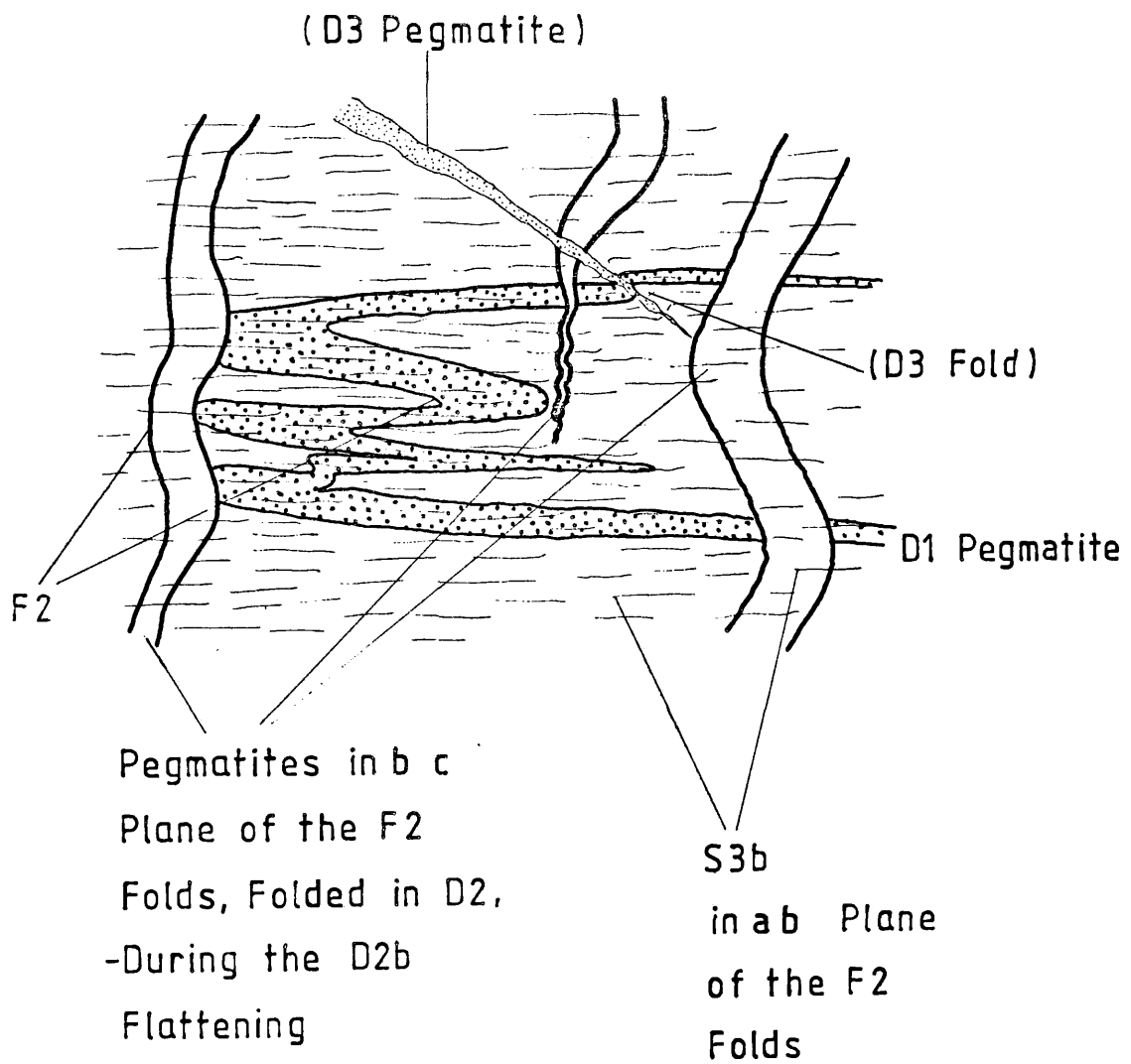
X,Y,Z = Strain
Axes for F2
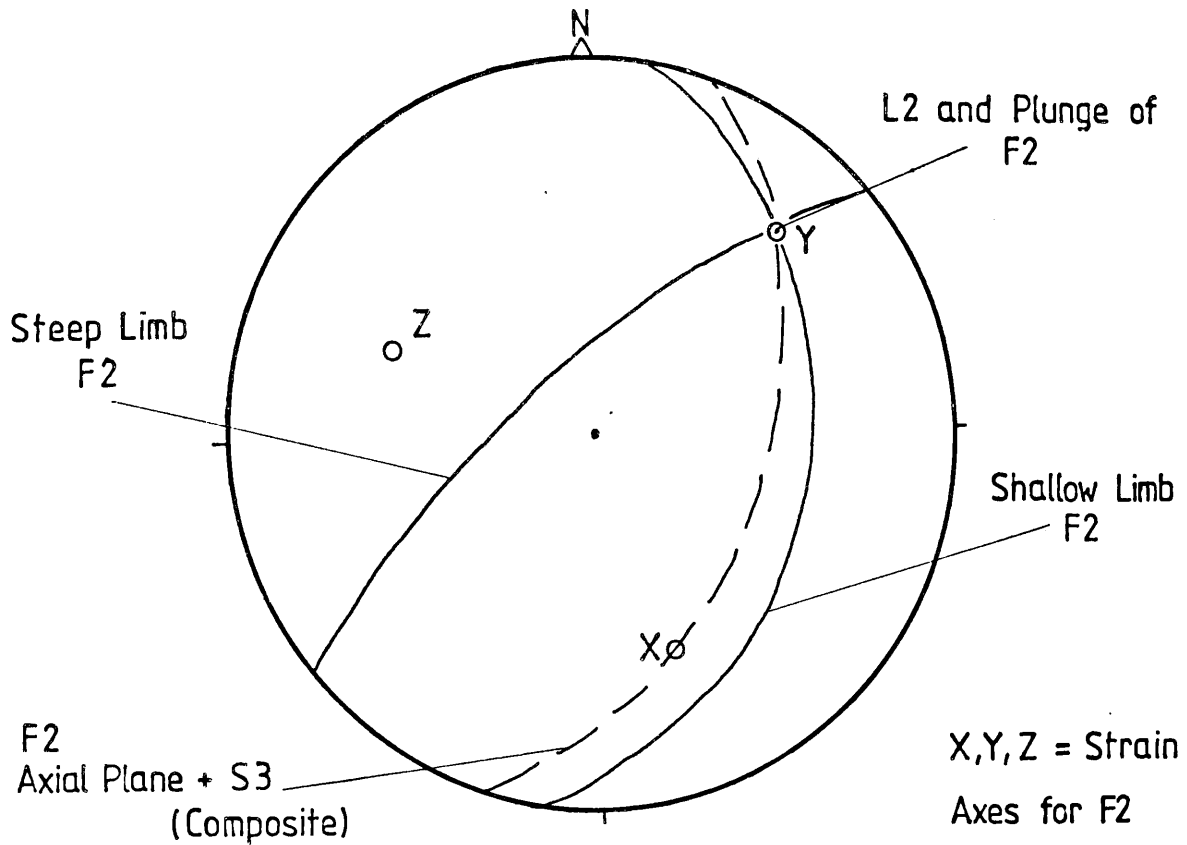
SYNOPTIC DIAGRAM OF STRUCTURES ASSOCIATED WITH THE
F2 FOLDS

S1 & S2
Composite
Foliation

Internal
F1 Structures

F 2

Axial Plane

L2

S3a + S3b

Non-cylindrical F2
Parasitic Folds
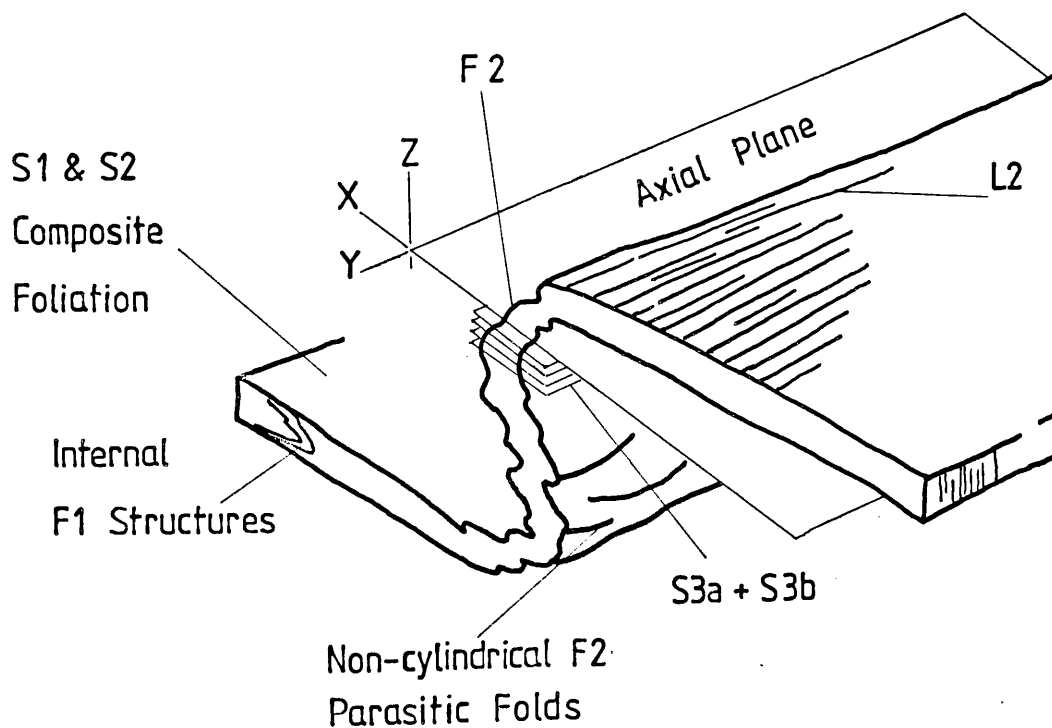
While the deformation produces some of the most obvious folds in the Northern Gneiss Unit, F3 folds only become dominant structures further east on the mainland. Like the D2b flattening, the structures produced in D3 are heterogeneously developed across the island; they are absent in the west, first seen in the centre and are moderately developed in the east.

Figure 23 shows the dominant trend of the D3 structures on north Osterøy, where they are confined to the areas where the earlier D2 deformation and S3 foliation are best developed. The F3 folds fold the D2 foliations and the D2 amphibolites (pls. 14 & 15).

The first features associated with D3, the thrusts seen on figure 23, could in fact more properly belong at the end of D2. Dipping steeply to the south-east these thrusts cross-cut the F2 folds (figs. 15, 23 & 26), displacing their axial planes. The effects of the thrusting on an F2 synformal closure are seen in the quartzite outcrop at (17.00,33.00 & 19.20,25.50); the fold nose is cut out leaving a "pipe" of quartzite running through the mountain (fig. 26). Although the thrusts are sub-axial planar to the F3 folds they are in fact slightly folded by F3; it is this which places them at the beginning of D3 or at the end of D2. The sense of translation on the thrusts, inferred from the displacement of the F2 axial planes, is from the south-east to the north-west. Typical displacements measured on the map are of the order of 100s of meters.

The F3 folds are asymmetrical and open, verging slightly to the north-west. The degree of asymmetry and amount of overturning increases east-wards. The folds are developed on a large scale, between 20 meters and 500 meters in wavelength. The open geometry and large scale of the folds makes it almost impossible to measure plunge and axial plane orientations

Fig. 23

NORTH OSTERØY

D3

THRUSTS AND

F3 FOLD TRACES

Late D2 or Early
D3 THRUSTS

TYSSE THRUST

F3 Axial
Traces

N

BERGEN ARC
THRUST

0   2·5   5

Km
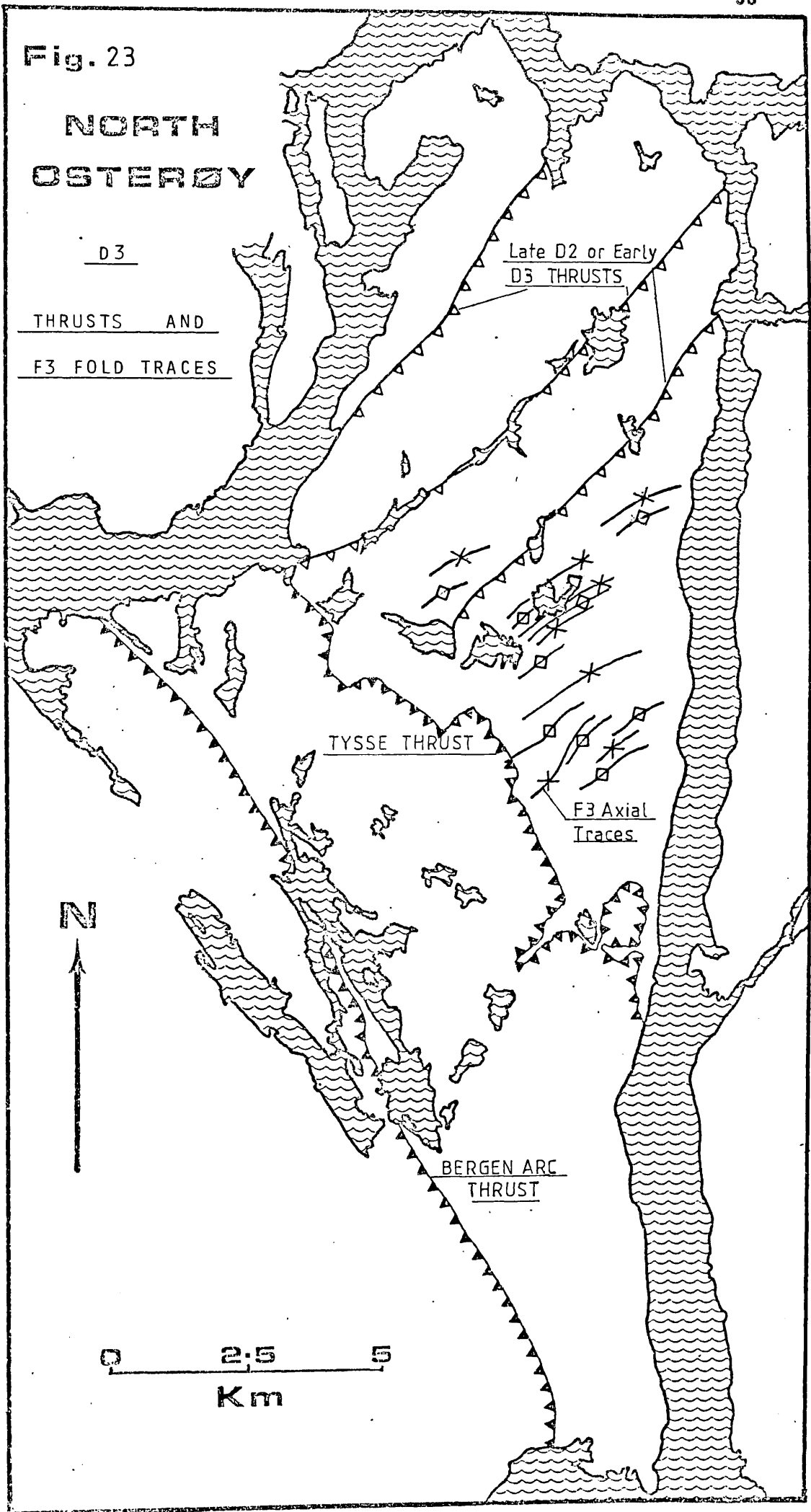
directly, these are therefore determined from readings made on the S3

schistosity, where this is strongly affected by the F3 folding.

Figure 24 indicates that the folds plunge to 080/11° and the axial planes

dip at 170/85°.   In the east of the island some of the folds are much

tighter and develop shears on their middle limbs.   In places the folds

are non-cylindrical, as is seen from the outcrop pattern at (21.50,28.50),

but this seems to be atypical.   Elsewhere the folds have a more cylindrical

geometry (pls.16 & 17).   The F3 folds are responsible for the outcrop

pattern in the amphibolites at (20.00,32.00), (fig.112).

In the east the middle limbs of the sheared folds begin to develop

a new axial plane schistosity, S4 shown by hornblende.   This is very

weak on Osterøy but strengthens eastwards, where, with the F3 axial

plane, it rotates to give progressively shallower dips to the east, as

the F3 folds become more overturned.

A strong mullion rodding, L3 tends to develop with the F3 folds even

where they are open and S4 is weak (pl.16), this becomes more pronounced

as the folds tighten.   The mullion development enhances the older

lineations (L1 and L2), over most of the area, and in the east of the

island it is L3 itself which forms the strongest feature of the topography.

It is very difficult to distinguish between L2 and L3 in outcrop and

figure 17 is therefore an amalgamation of both taken from the area as a

whole.   However, the two fold phases (F2 and F3) are not strictly

parallel;   F3 plunges to 080° while F2 plunges to 045°, thus enabling

separation of the L3 component on figure 17;   the cluster seen at 075°

is attributable to D3, while the general skewed spread of the points is

caused by the D2 lineations.   They are folded round the F3 axis on a

small circle (fig.25), (also allowing for variation caused by the non-

cylindrical nature of some of the F2 and F3 folds).   The refolding also

explains some of the spread in F2 plunges in figure 14.

Fig 24.

POLES TO S3 DEFINING THE F3 FOLDS

PLOT OF SN+3 FOLIATION FOLDED BY THE F3 FOLDS.

THIS PLOT HAS UNDERGONE -O- ROTATIONS

USING CORDINATE CARD   1

SAMPLING   2ACROSS/- 1DOWN   POLES PER   1PERCENT AREA   325 DATA   EQ AR

THE CONTOURS REPRESENT THE FOLLOWING PERCENTAGES

00.9<=1-2%>02.9<=3-4%>04.9<=5-6%>06.9<=7-8%>08.9<=9-10%>10.9<=11-12%>12.9
12.9<=13-14%>14.9<=15-16%>16.9<=17-18%>18.9<=19-20%>20.9<=21-22%>22.9
22.9<=23-24%>24.9<=25-26%>26.9<=27-28%>28.9<=29-30%>30.9<=31-32%>32.9
32.9<=33-34%>34.9<=35-36%>36.9<=37-38%>38.9<=39-40%>40.9<=41-42%>42.9
42.9<=43-44%>44.9<=45-46%>46.9<=47-48%>48.9<=49-50%>50.9<=51%+
NOTE A VALUE OF>0.5-0.9<=.LT.1%AND.GT.0%

Fig 25.

THE RELATIONSHIP BETWEEN L2 AND L3

L3 Mullion Rodding

F3

30°

S3 Foliation
Plane

L2 Refolded Round F3

Intrafolial F2
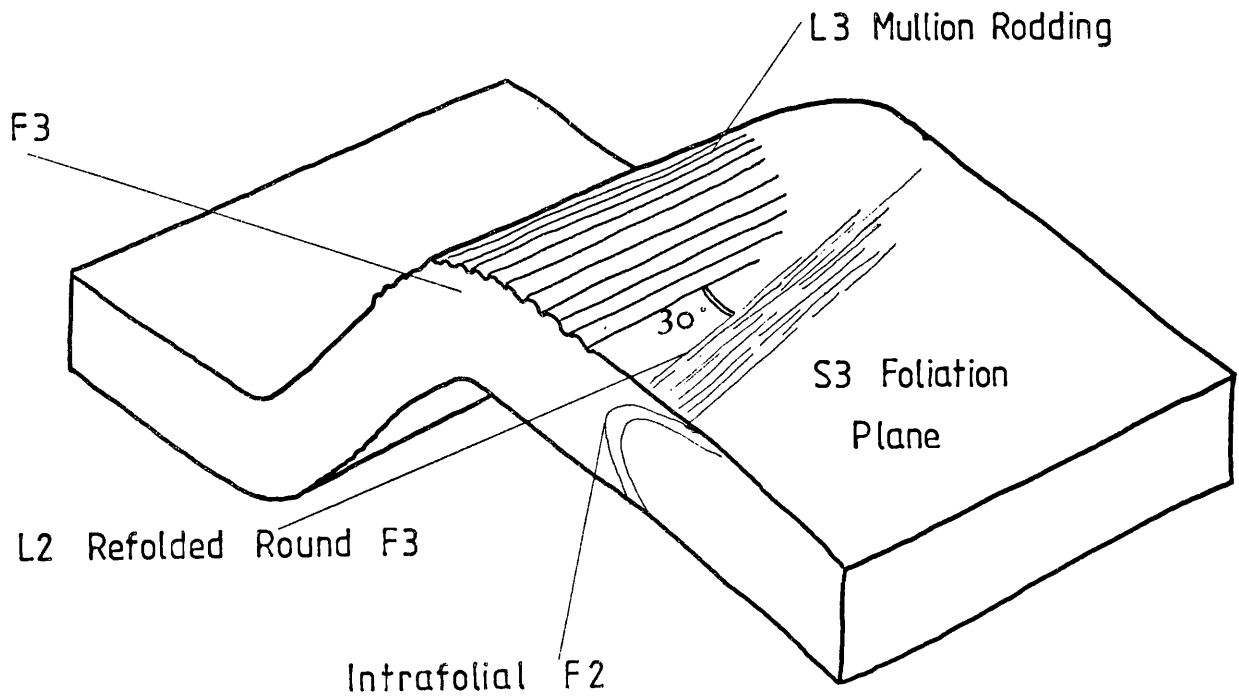
INTERPRETATION OF Fig. 17.

Small Circle
Spread of the
L2 Lineation

N

L3 and
Plunge of
F3

Fig 26.
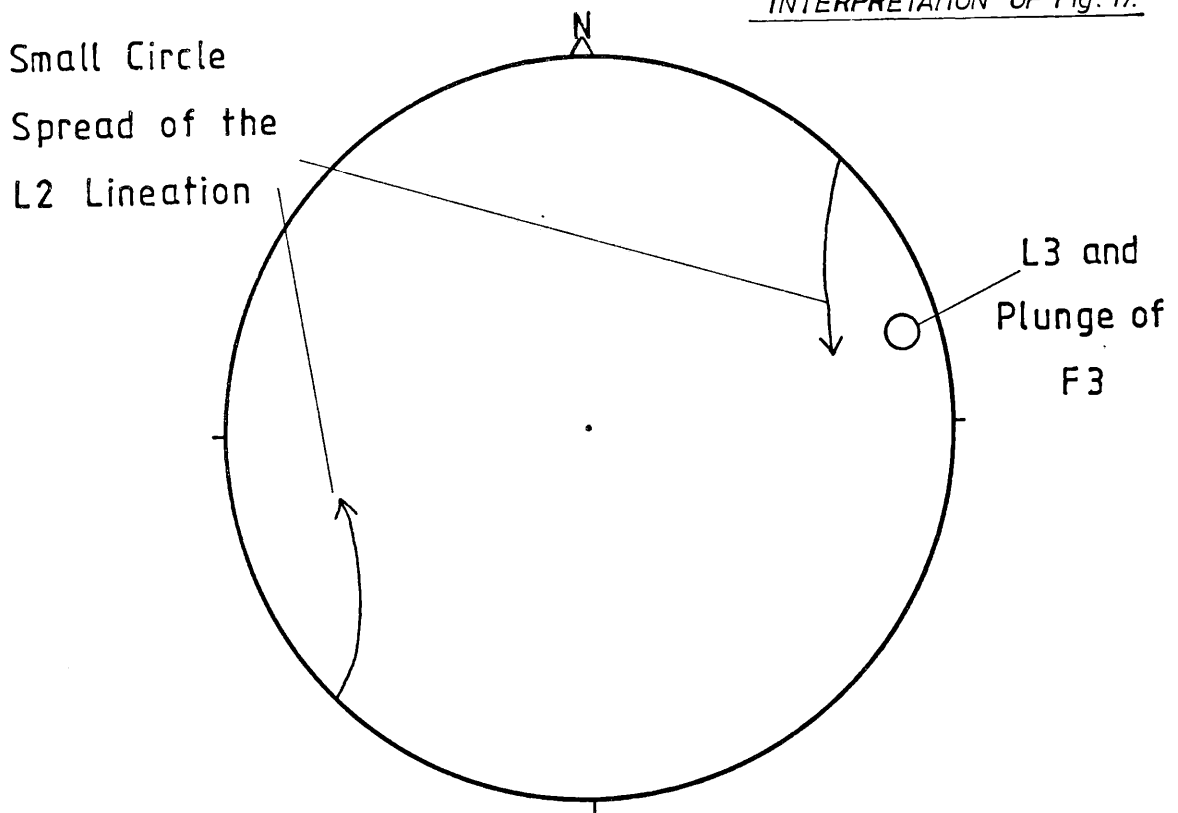
SCHEMATIC DIAGRAM TO SHOW HOW THE LATE D2 OR
EARLY D3 THRUSTS CROSS-CUT THE D2 STRUCTURES

F2 Synform

Late D2
or Early D3
Thrust

F2 Synform
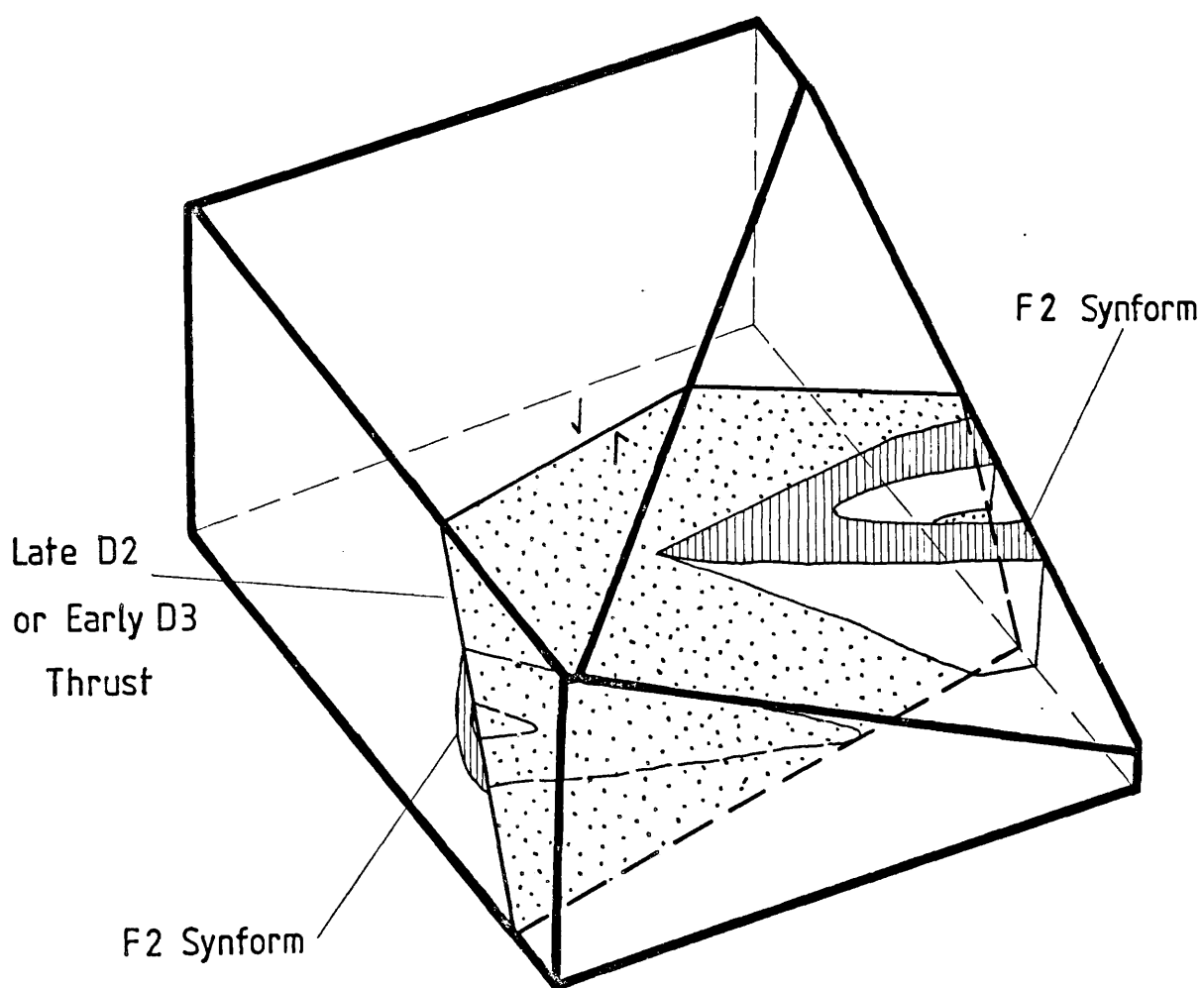
Following the F3 folding there is evidence in a few localities for a further phase of pegmatite emplacement in the Northern gneisses (fig. 21). The pegmatites are granitic in composition and intruded along the axial planes of the F3 folds at a high angle to the foliation, e.g. (11.37,34.85).

The last structural feature attributable to D3 is further thrusting. The thrusts are only seen on the small (outcrop size) scale and are the result of further development of the F3 folds, shearing out their middle limbs. The effects of this shearing increase south-eastwards where the folds are at their best developed and tightest. The translation (from the direction of overturning and displacement) is again from the south-east to the north-west.

Discussion

The most significant feature of this deformation is the orientation of the structures and their sense of translation. The repetitive history of folding along a north-east axis, observed through D1 to D3; the consistent north-westerly direction of thrusting and overturning of the fold axial surfaces, points to transport from the south-east, and is consistent with model 2 (fig. 20) proposed for D2.

The proposed development of the D3 structures was:

a) Thrusting ? shortening of the layering to produce F3.

b) A new schistosity and foliation developing in the east where the F3 folds are tightest, the schistosity forming in the X/Y plane of the F3 strain ellipsoid.

c) A new lineation L3 developing parallel to the Y axis and enhancing that previously developed in D2 (L2) because of the nature of the interference pattern between F2 and F3, (a Ramsay (1967) type 3 pattern) as proposed by Watterson (pers. comm. 1977), (fig. 27).

Fig 27.

PRODUCTION OF A PENETRATIVE L TECTONITE FABRIC BY
SUPERIMPOSED STRAINS. [After WATTERSON 1977]

Da

F1 Axial Plane

F2 Axial Plane

F1

F2

Db
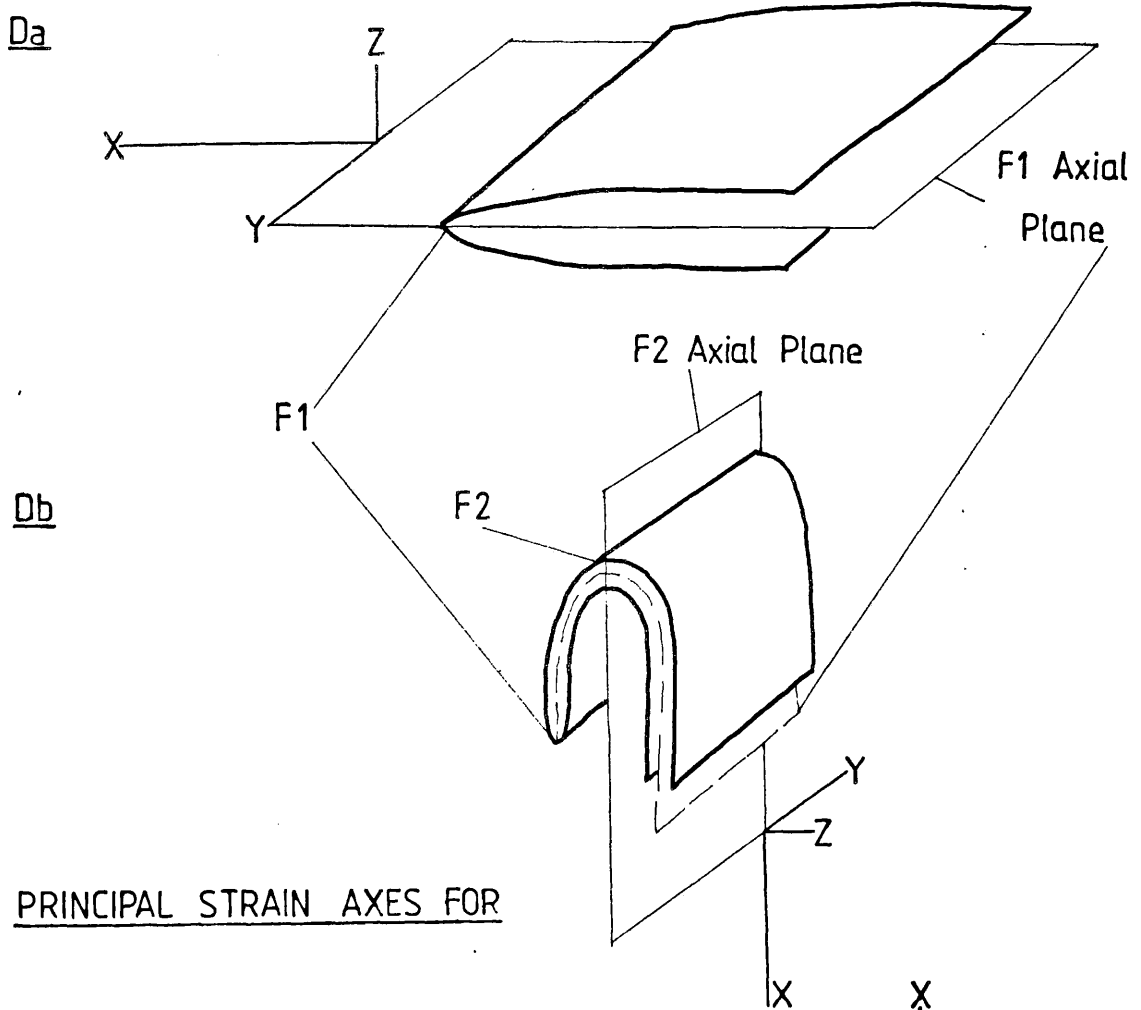
PRINCIPAL STRAIN AXES FOR

Da   and   Db
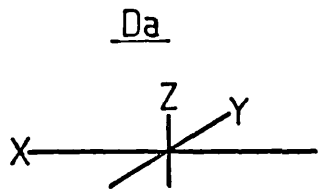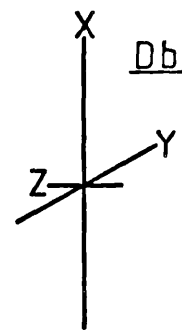
WHICH, WHEN SUPERIMPOSED PRODUCE FINITE
STRAIN AXES :-
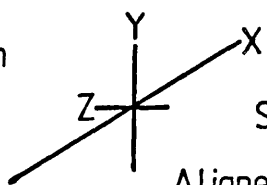
Finite Situation   Rodding
Structure
Aligned Parallel
to the Y Axis of the Folds
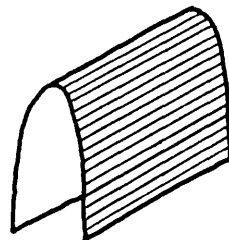
d)   Pegmatite emplacement along the X/Y plane of the F3 strain

ellipsoid (fig.21).

e)   Minor ductile thrusting in the form of shearing along the X/Y

planes of the F3 strain ellipsoid (the axial planes of the folds -

the middle limbs were sheared out).

This sequence of development is summarised in figure 28.

2.1.6   D4, The Production of F4 and S5

The D4 deformation was the last affecting the Northern Gneiss

Unit.   It is distinguishable from the preceding deformations primarily

because D4 structures are orientated at right angles to the D1-D3 trends.

TABLE OF D4 EVENTS:

1)   Development of F4 folds

2)   Local development of S5 schistosity and foliation

3)   Development of quartz veins.

In general the trend of the D4 structures in the Northern gneisses

is around 135° (fig.29), but the folds are highly non-cylindrical and

the pitch of the axis measured in the axial plane varies by as much as

90° over distances of 10 meters.   The folds are asymmetric and over-

turned, verging to the south-west.

Except where the foliation has a shallow dip, the F4 folds fold

rocks in which the dominant foliation was aligned close to the X/Z plane

of the D4 strain ellipsoid.   Well developed F4 folds are therefore very

rare in the Northern Gneiss Unit.   D4 folds are better developed in the

Southern Gneiss Unit, and it is clear that F4 folds in the Northern gneisses

are not only restricted to areas where the foliation was almost flat,

but also to bands across the Northern gneisses.   These bands are seen

Fig 28.

SIMPLIFIED GEOMETRY OF THE STRUCTURES PRODUCED IN D3

Steep Limb

oZ

N

L3 and Plunge
of F3

F3 Axial Plane,
S4 and Late
D3 Thrusts

Early D3 or
Late D2 Thrusts

Shallow Limb

X,Y,Z = F3 Strain Axes

STRUCTURES ASSOCIATED WITH THE F3 FOLDS

Early D3 or Late D2
Thrust Plane

F3 Axial Planes

L3

Tight
Non-cylindrical
F3

X

Y   Z

Inrafolial F2

Open F3

Incipient Thrusting in Middle
Limb Late in D3

S4 Late Axial Planar
D3 Pegmatite
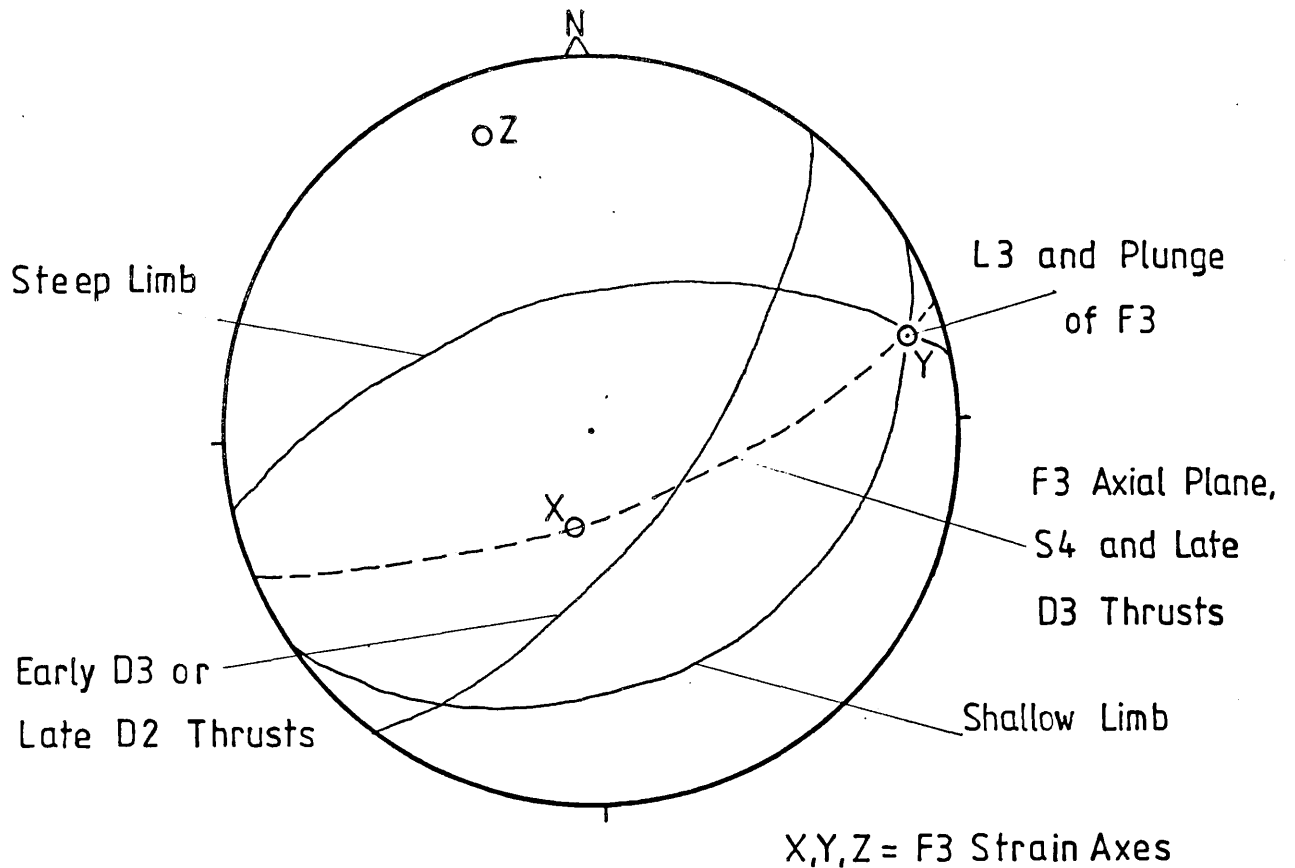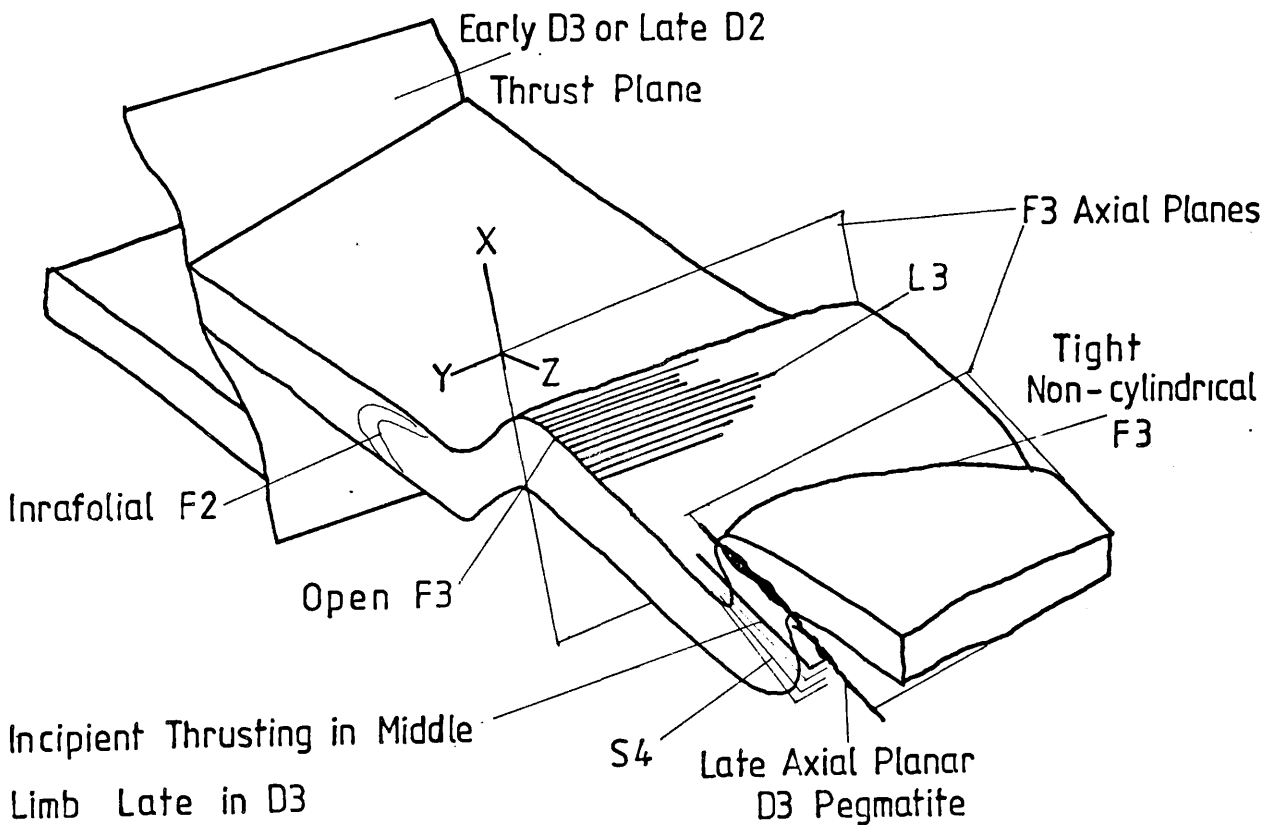
Fig. 29.

NORTH OSTERØY

D4

STRUCTURAL

TRENDS

N

—— Near Vertical Shear
Zones and Trend of F4 Fold Axes

0   2·5   5
Km
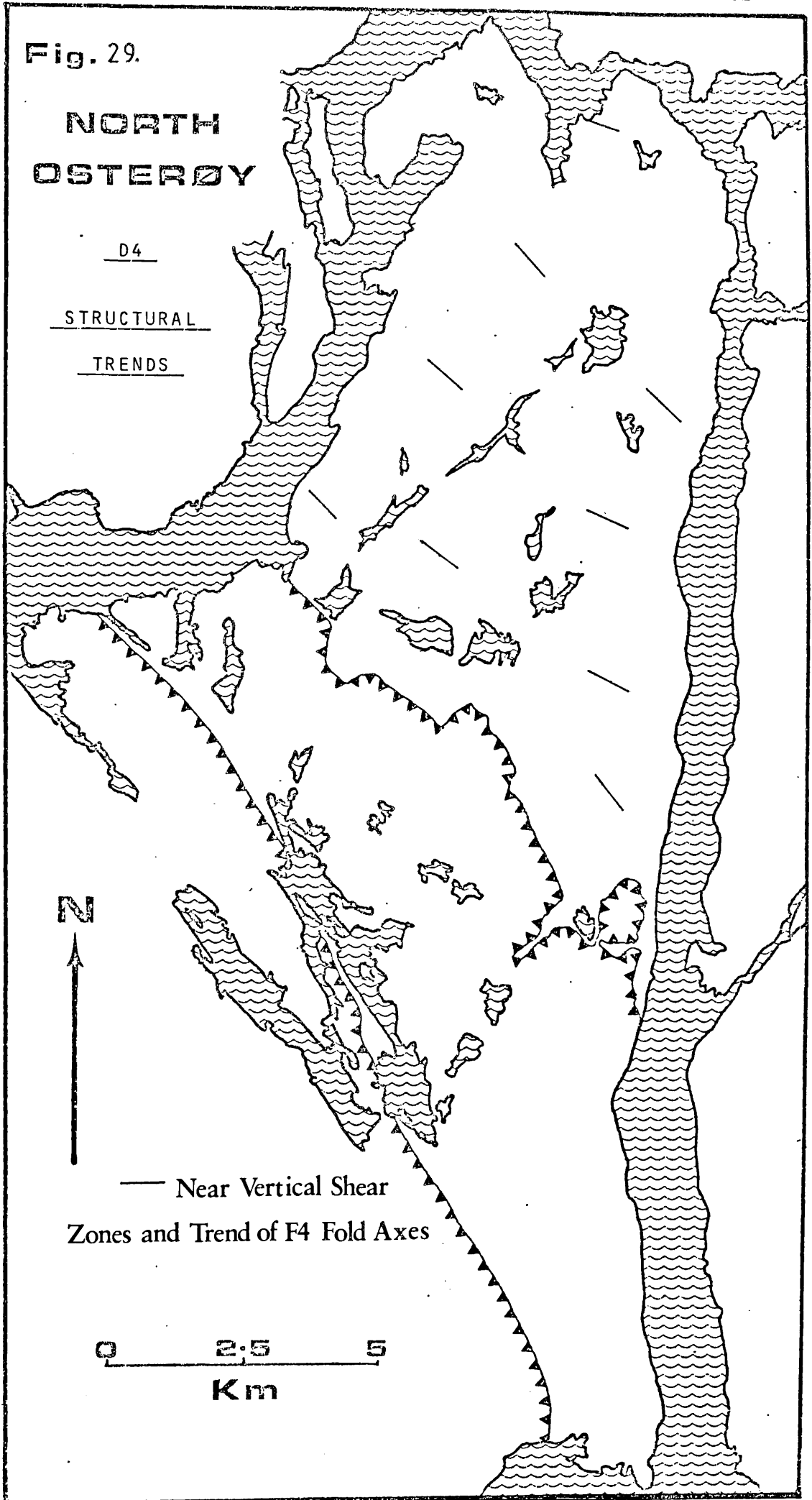
in figure 30, which is a computer generated surface representing a foliation surface across north Osterøy, constructed to enhance east-west trending structures and suppress the effects of structures in other orientations. (a) shows the resultant surface as a block diagram, (b) as a contour map. The bands represent the periodicity (wavelength) the folding would tend to assume on the larger scale. D4 structures are therefore best developed along these bands. The folds are impersistent and die out over short distances, though great numbers of parasitic folds generally occur together (e.g. 11.90,35.50). (A further account of these folds will be given in section 2.2.4 on the Southern Gneiss Unit).

Shear zones on the same general trend are also to be found throughout the Northern Gneiss Unit (pl.18). These zones are generally between 0.05 and 0.5 meters wide and 10 meters long, though much larger examples (5-20 meters wide) were found in the north of the island (pl.19). The pre-D4 foliation is deflected sharply on entering these bands. In the shear zones the texture and mineralogy is altered to produce a new schistosity and foliation: S5. Figure 31 shows examples of these shear zones from which it is clear that they are associated with the F4 folds (pl.20). The shear zones form either on the middle limbs of partially developed F4 folds or replace them. The displacement across the shears indicates a translation from the north-east to the south-west, consistent with the sense of translation on the F4 folds.

Within the quartzites (fig.15), there are thin bands of mica schist. The schistosity developed during D2 and D3, and is parallel to S3. In D4 a strong crenulation cleavage develops in these, although few F4 folds are seen. Microscopically the geometry of this crenulation cleavage is identical to that of the D4 shear zones (fig.32). These can therefore be regarded as analogous to the crenulation cleavage, which is orientated 035/17° in the mica schist.

Fig 30.

64

PERIODICITY OF THE MAJOR F4 FOLDS ACROSS THE N. GNEISSES

a
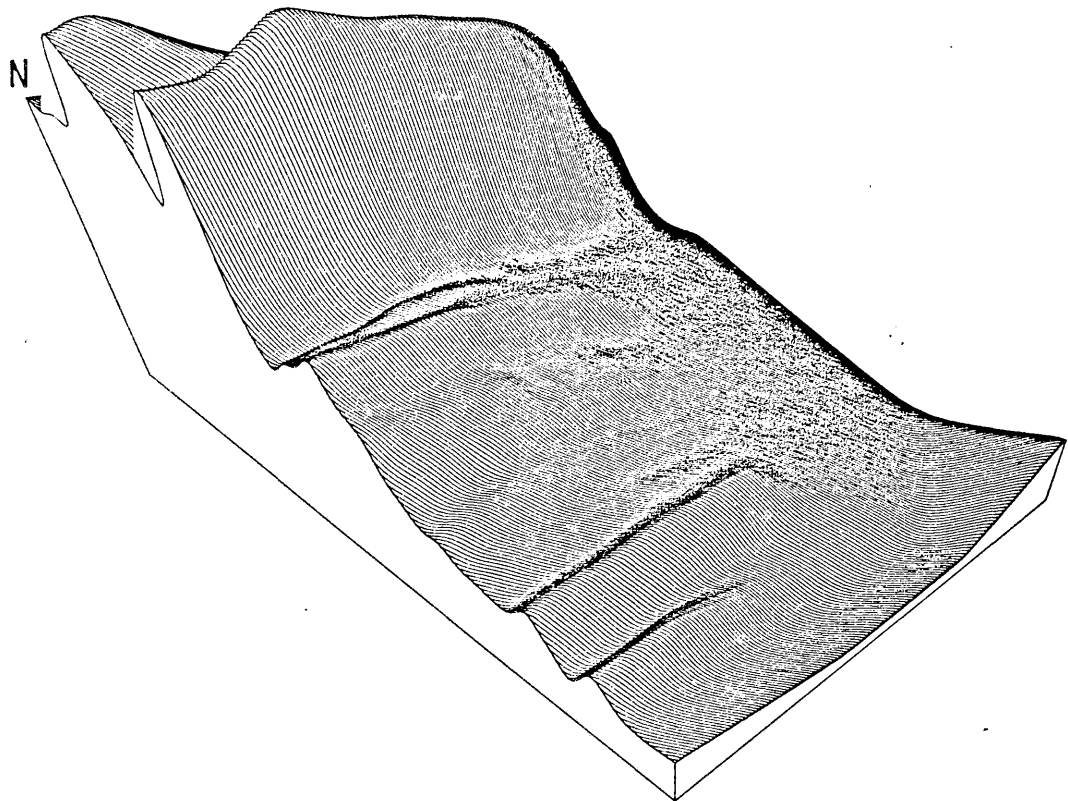
PLOT OF THE FOLIATION IN THE NORTHERN GNEISSES US INO - WDEP.TH.
AZIMUTH = .45   ALTITUDE = .55
*WIDTH = 6.00   *HEIGHT = 5.00
SMOOTHINGS = -1.00

* BEFORE FORESHORTENING 06/03/79

b

Fig 31.
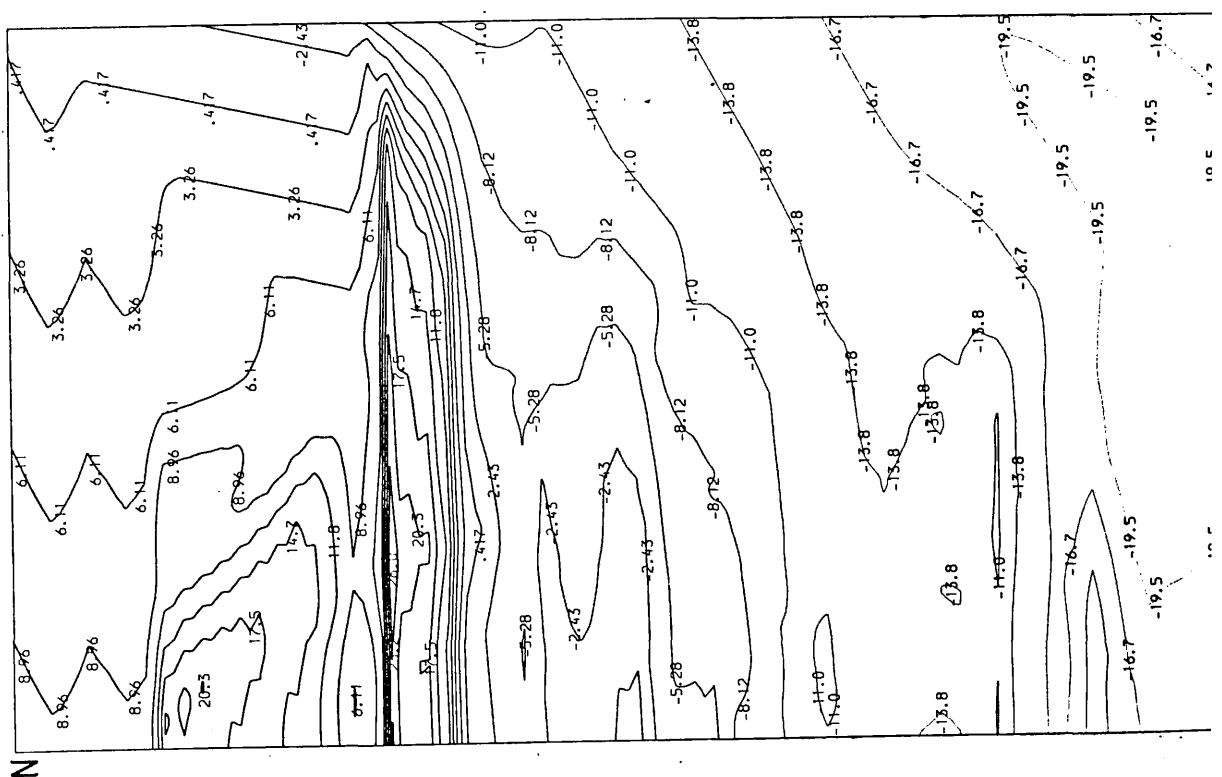
EXAMPLES OF D4 SHEAR ZONES AND S5

F4 Middle Limb Shear
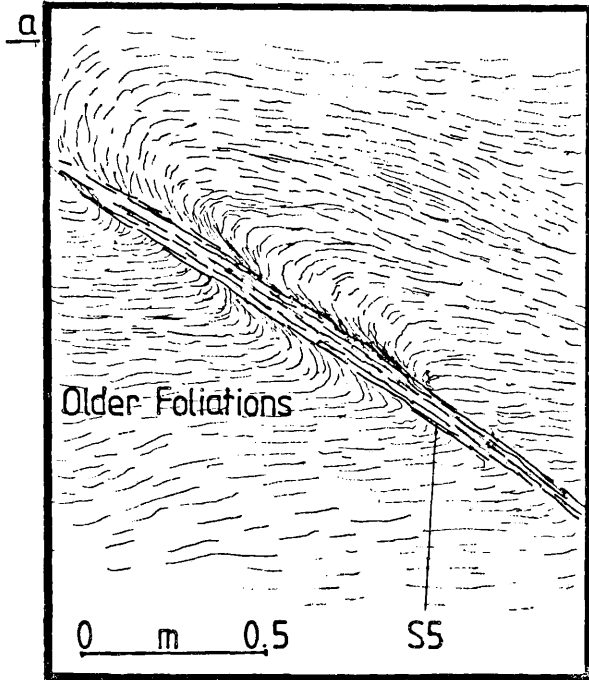
Three Dimensional View
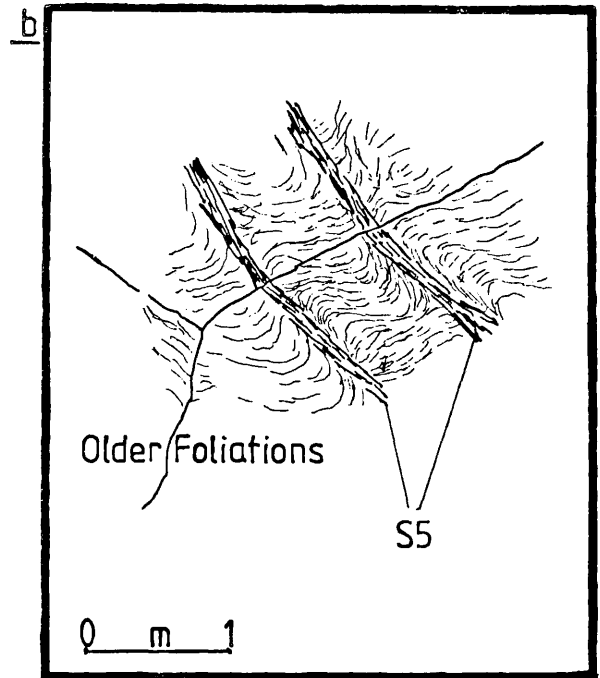
Profile View of an F4 Fold
Showing Shear & Quartz Vein
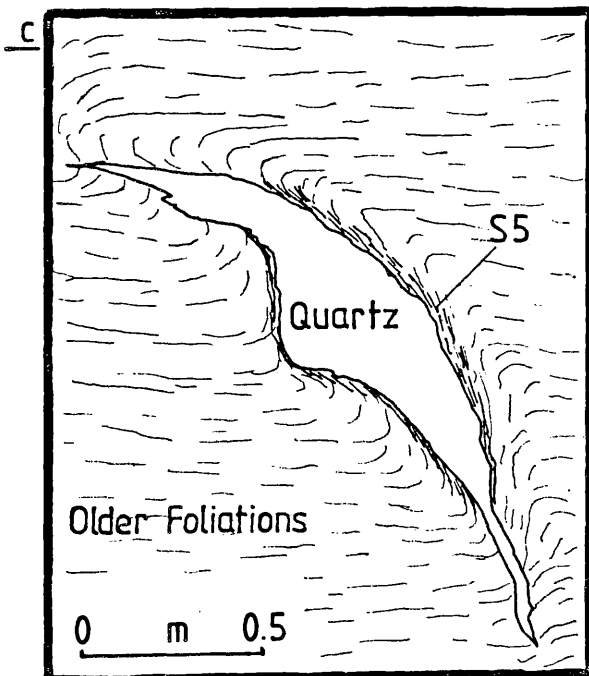
Oblique View of D4 Quartz Vein

Fig 32.
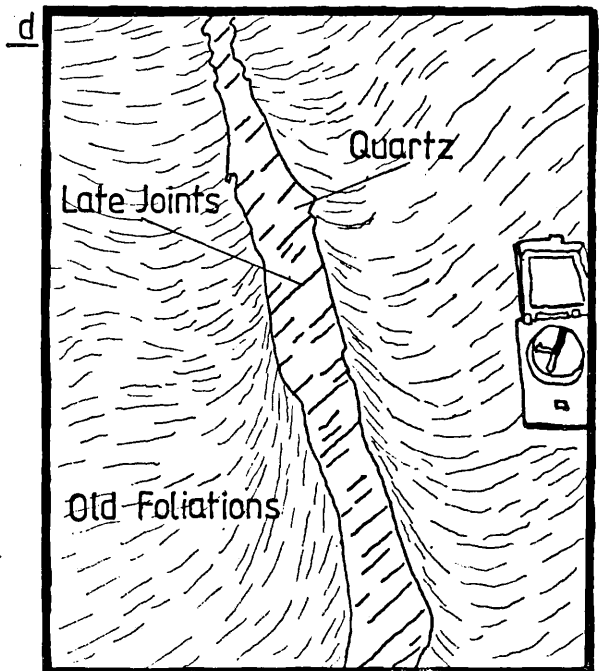
HAND SPECIMEN [FH B77] OF MICA SCHIST SHOWING THE
F4, S5 CRENULATIONS
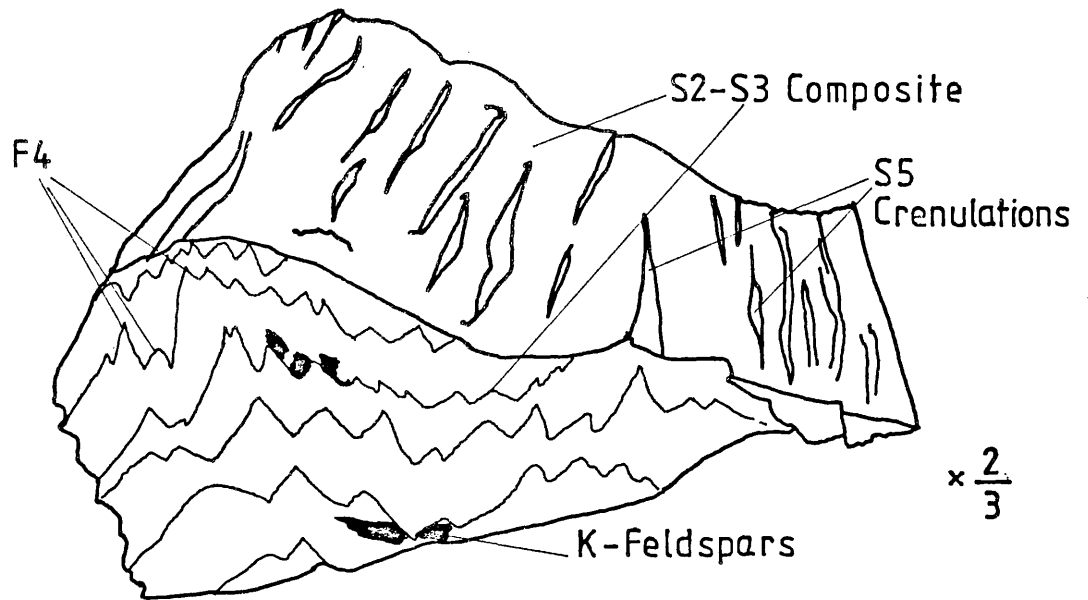
SKETCH OF THIN SECTION [FH B54] SHOWING AN OBLIQUE VIEW
OF AN F2 FOLD REFOLDED ROUND AN F4 FOLD AND FORMING
THE S5 CRENULATION CLEAVAGE

0   m m   2
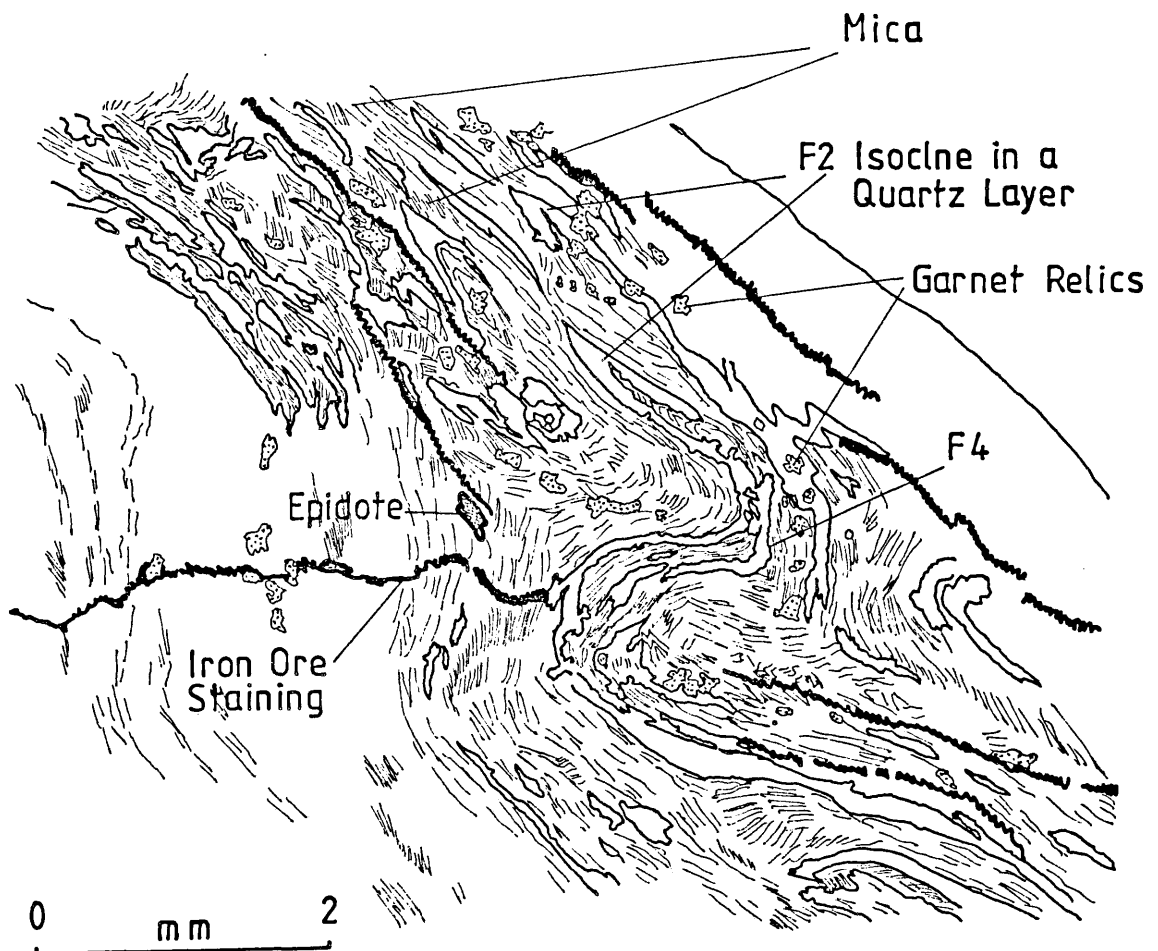
Along the axial planes of the F4 folds and within the shear zones
it is common to find large lensoid quartz veins, ranging from 0.01 meters
wide, 0.3 meters long, to 1 meter wide, 30 meters long (pl.21 and fig.
31c & d). These veins are very common and form a characteristic
feature of the Northern gneisses. Like the shear zones they are related
to the F4 folding. Figure 33 shows that the majority of the veins are
vertical and strike at 145°, the spread is the result of the non-
cylindricity of the F4 folding (see below). The plots near the centre
of the net are of veins with a morphology similar to that seen in figure 31c.

Discussion

Several relationships were observed between the F4 folds, shears
and quartz veins:

1) Folding without associated shears or quartz veins

2) Folds with shears in their middle limbs

3) Shearing with little preceding or accompanying folding
(abrupt shears) (fig.31b)

4) Folds with sheared middle limbs, cut by quartz veins

5) Shears cut by quartz veins

6) Quartz veining with little or no preceding deformation.

These observations can be explained by assuming a model for D4
where the deformation occurred in a serial manner (fig.34). The folds
were the first structure to develop, after this shearing became the
dominant deformation mechanism. Shears formed in the middle limbs of
the F4 folds, while elsewhere (where the S3 and S4 foliation is more
orientated in the X/Z plane of the D4 strain ellipsoid), they affected
undeformed rock. Next the quartz veining modified the earlier F4 folds
and shears, but also occurred in new localities in the rock.

Fig 33.

POLES TO D4 QUARTZ VEINS

PLOT OF QUARTS VEIN ORIENTATIONS

THIS PLOT HAS UNDERGONE -0- ROTATIONS

USING CORDINATE CARD   0

SAMPLING   2ACROSS/- 1DOWN   POLES PER   1PERCENT AREA   97 DATA   EQ AR

N

W-   -E

S

THE CONTOURS REPRESENT THE FOLLOWING PERCENTAGES

00.9<=1-2%>02.9<=3-4%>04.9<=5-6%>06.9<=7-8%>08.9<=9-10%>10.9<=11-12%>12.9
12.9<=13-14%>14.9<=15-16%>16.9<=17-18%>18.9<=19-20%>20.9<=21-22%>22.9·
22.9<=23-24%>24.9<=25-26%>26.9<=27-28%>28.9<=29-30%>30.9<=31-32%>32.9
32.9<=33-34%>34.9<=35-36%>36.9<=37-38%>38.9<=39-40%>40.9<=41-42%>42.9
42.9<=43-44%>44.9<=45-46%>46.9<=47-48%>48.9<=49-50%>50.9<=51%+
NOTE A VALUE OF>0.5-0.9<=.LT.1%AND.GT.0%

Fig 34.

OBSERVED RELATIONSHIPS BETWEEN THE F4 FOLDS, S5 AND
THE D4 QUARTZ VEINS

a) Folds [F4]   b) D4 Shears [S5]   c) D4 Quartz Veins

1.

2.

Older Foliations

Quartz Veins

S5 Developed in the D4 Shears

3.

No Accompanying S5
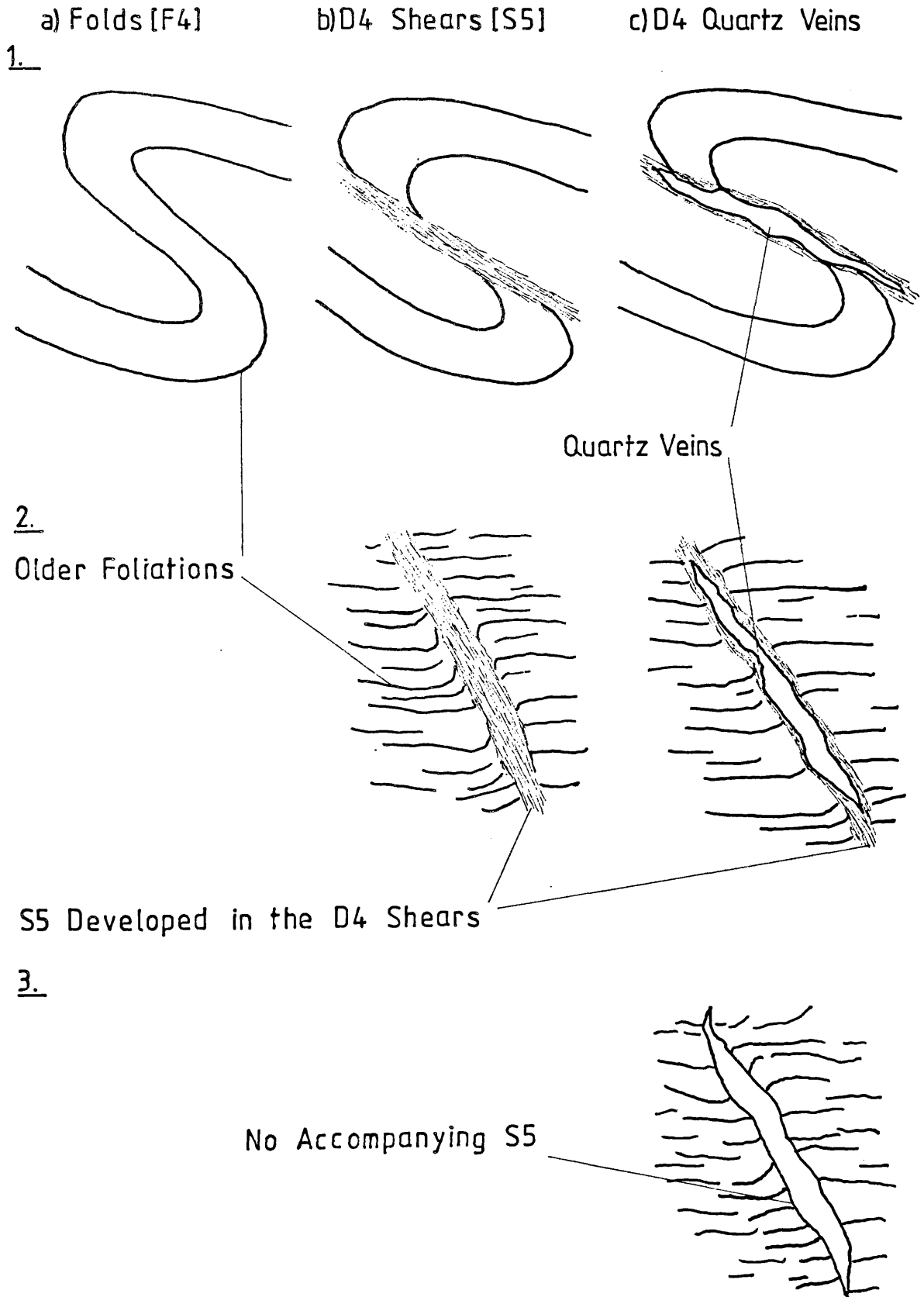
The D4 deformation also affects the Southern Gneiss Unit rocks

(see below). Here the folds are better developed and shears and quartz

veins are uncommon. The reason for this is that the pre-D4 foliation

in the Northern gneisses strikes at right angles to the F4 axial planes

and the pitch of the intersection of the foliation on the axial plane

generally exceeds 45°. The higher this angle the more difficult the

foliation is to fold, and the more restricted the style of structure

that can develop (Ramsay,1967; Cosgrove,1976): (By analogy it is like

trying to fold the spine of a telephone directory, edge on, over the edge

of a table). The deformation started as a flexural slip buckling of

suitably orientated layers, producing class 1a-c folds (Ramsay,1967).

Once these layers had folded, because the unsuitably orientated layers

could not fold, shearing took over and the shear zones were formed.

The quartz veins formed at a late stage in the process during the decay

of the stress field, the pore fluid pressures having been "pumped up"

by the early high stresses. The rock hydraulically fractures along the

planes of weakness established during the earlier part of D4; these

were the only planes with the right orientation in the waning D4

stress field.

The development of the structures seen in D4 are (fig.35):

1) Compression of the layering to produce F4.

2) Further shortening, producing shear zones, a crenulation
   cleavage and the S5 schistosity, parallel to the X Y plane
   of the F4 strain ellipsoid.

3) Hydraulic fracture and the generation of quartz veins in
   the X Y plane of the F4 strain ellipsoid along zones of
   incipient F4 and S5 deformation.

Fig 35.   71

SIMPLIFIED GEOMETRY OF STRUCTURES PRODUCED IN D4

Variation in F4
Axial Plane
Attitude

Zone of
Possible F4
Plunges

Crenulation Cleavage S5

Average Shallow
Limb

D4 Shears and
Quartz Veins

F4
Plunge

Average Shallow
Limb

STRUCTURES ASSOCIATED WITH THE F4 FOLDS

Non-cylindrical F4

S5 in a D4 Shear Zone

Axial Plane
of F4
and S5
Crenulation
Cleavage

(shallow)
Composite Older
Foliations   [F2 or F3]
(steep)

D4 Quartz Vein
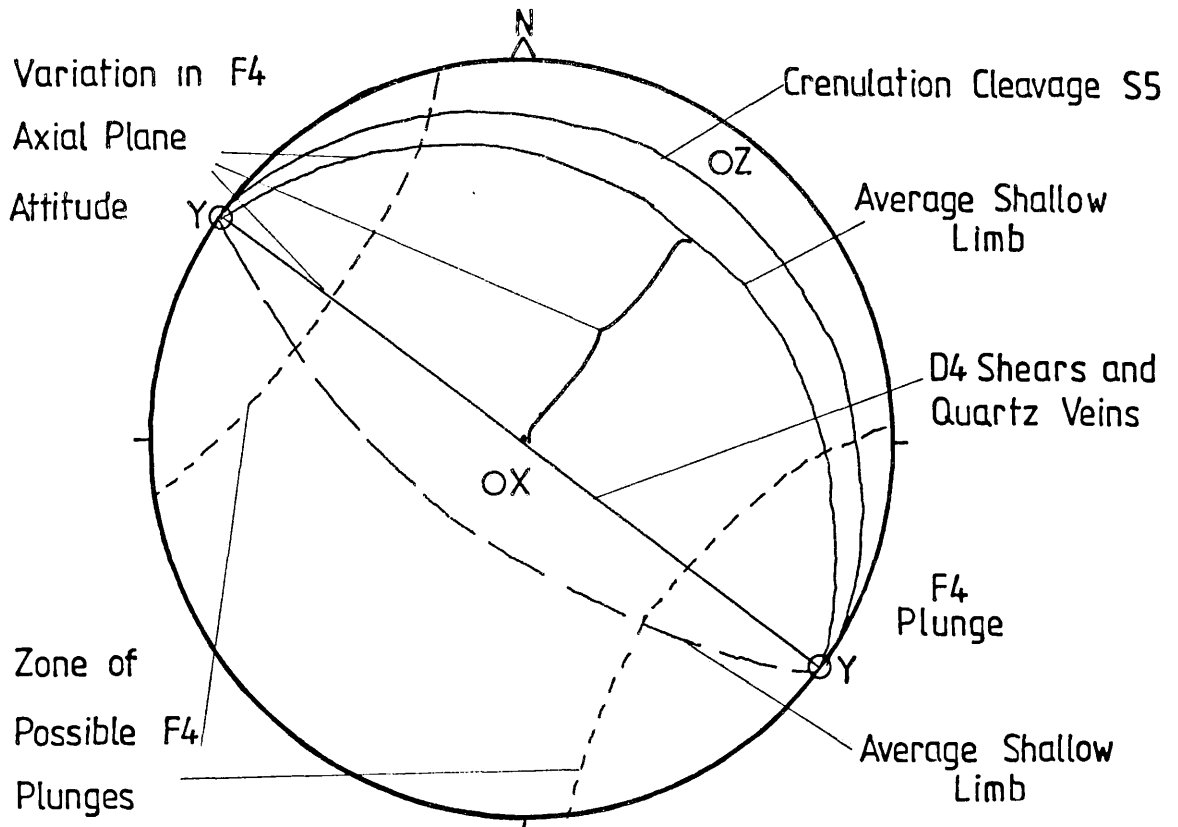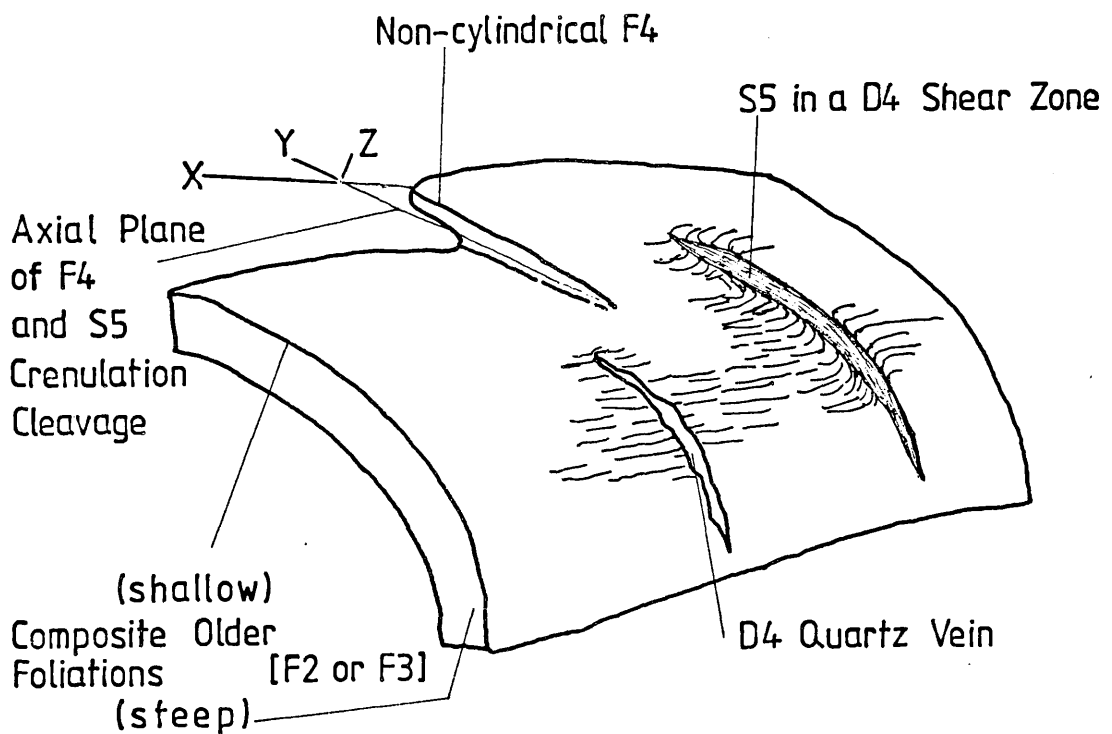
2.1.7   Discussion on the Deformation of the Northern Gneiss Unit

Figure 36 summarises the deformation history of this unit, in which several distinct trends can be seen.   Firstly, deformation was cyclic. The basic cycle seems to be:

A)   Undeformed foliation.

B)   Pegmatite emplacement at a high angle to the foliation.

C)   Folding (open folds which tend to have a parallel geometry).

D)   Pegmatite emplacement and igneous injection parallel to the
         axial planes.

E)   Pegmatite emplacement at a high angle to the axial planes.

F)   Flattening of all the above, (folding of (E) pegmatites),

         ((C) folds become isoclinal with a similar geometry).

This sequence of igneous and tectonic activity characterises one "deformation" cycle.   Occasionally, while all the structural characteristics of a cycle may be present, an igneous phase may be absent, presumably because of an independent non-tectonic control.   It is important to note that when present the igneous bodies are usually intruded in or close to the plane containing the maximum and intermediate stress axes, as defined by the geometry of local macroscopic or mesoscopic structural features.

Many authors (Price,1970,1975;   Price & Hancock,1972;   Blay et al., 1977;   Dubey & Cobbold,1977), believe that folding is a sequential dia-chronous phenomenon.   Folds may develop one at a time in a fold train, so that of any two adjacent folds one is older than the other, even though they belong to the same deformational event.   Using this theory it is possible to explain the repetition of the deformational sequence (A-F above) observed in the Osterøy basement.

Fig 36.

DEFORMATION IN THE NORTHERN GNEISSES

D "Early"	D 1	D 2	D 3	D 4	STAGE IN FIG 37.
	F 1	Thrusts F 2 S 3a L 2	Thrusts F 3 S 4 L 3	F 4 S 5	C
	Igneous activity and Pegmatites	Igneous activity and Pegmatites	Pegmatites	Quartz Veins	D E
	Flattening	Flattening	Flattening		F
S "Early"	S 1 L 1	S3b	Thrust		A
	Pegmatites	Pegmatites			B

S 2 MIGMATISATION SEDIMENTS

The model proposed makes some assumptions; that the stress strain compatibility equation $\boxed{\Delta^2 i = 0}$ (Jaeger,1956; Ramsay,1967), holds during the deformation under the crustal conditions pertinent to the north Osterøy gneisses; that the stress ellipsoid is the reciprocal of the strain ellipsoid (Ramsay,1967); that on the broad scale the maximum principal stress axis will be normal to the Earth's surface for the majority of geological time (Price,1966; Dietrich & Carter,1969). Evidently during periods of crustal shortening, it will be orientated sub-parallel to the Earth's surface.

The model relates the deformation seen in the Northern gneisses, (D1-D4), to the deformation sequence (A-F) (fig.36), by considering how the regional stress ellipsoid may develop compared to the local stress ellipsoid during an orogeny. Figure 37 summarises the model and shows that while it is possible to erect a chronology of events for the deformation and intrusion relating to one fold, this chronology is not absolute because the deformation and intrusion are diachronous; (while the axial plane pegmatites are emplaced at one locality, folds are just forming in another). The model also describes a single tectonic event, providing justification (from theory as well as observation) for the grouping of deformational features into D1-D4.

Clearly the Northern gneisses have undergone at least three of these complete tectonic cycles up to D4, at which point the record of deformation ceases. Of the three earlier cycles D2 occurred at the deepest crustal level and D4 at the shallowest (see section 3.5 below).

Another characteristic of the deformation in the Northern gneisses is the flattening that precedes the folding; this is explained in the model proposed, but in the case of D2 and D3 there is a further complication, the flattening is heterogeneous. Plate 22 shows leucocratic layers in the

Fig 37.   75

FOUR STAGE STRESS MODEL TO EXPLAIN THE RELATIONSHIP
BETWEEN BASEMENT STRUCTURAL FEATURES

A   Usual Situation

Earth's Surface

B

Buckling Situation

New Cleavage

C

Local Stress Field

D   Regional Stress Field
                                                     During Deformation

Flattening situation
E

F

====== = Igneous Intrusions   The STRESS Ellipse
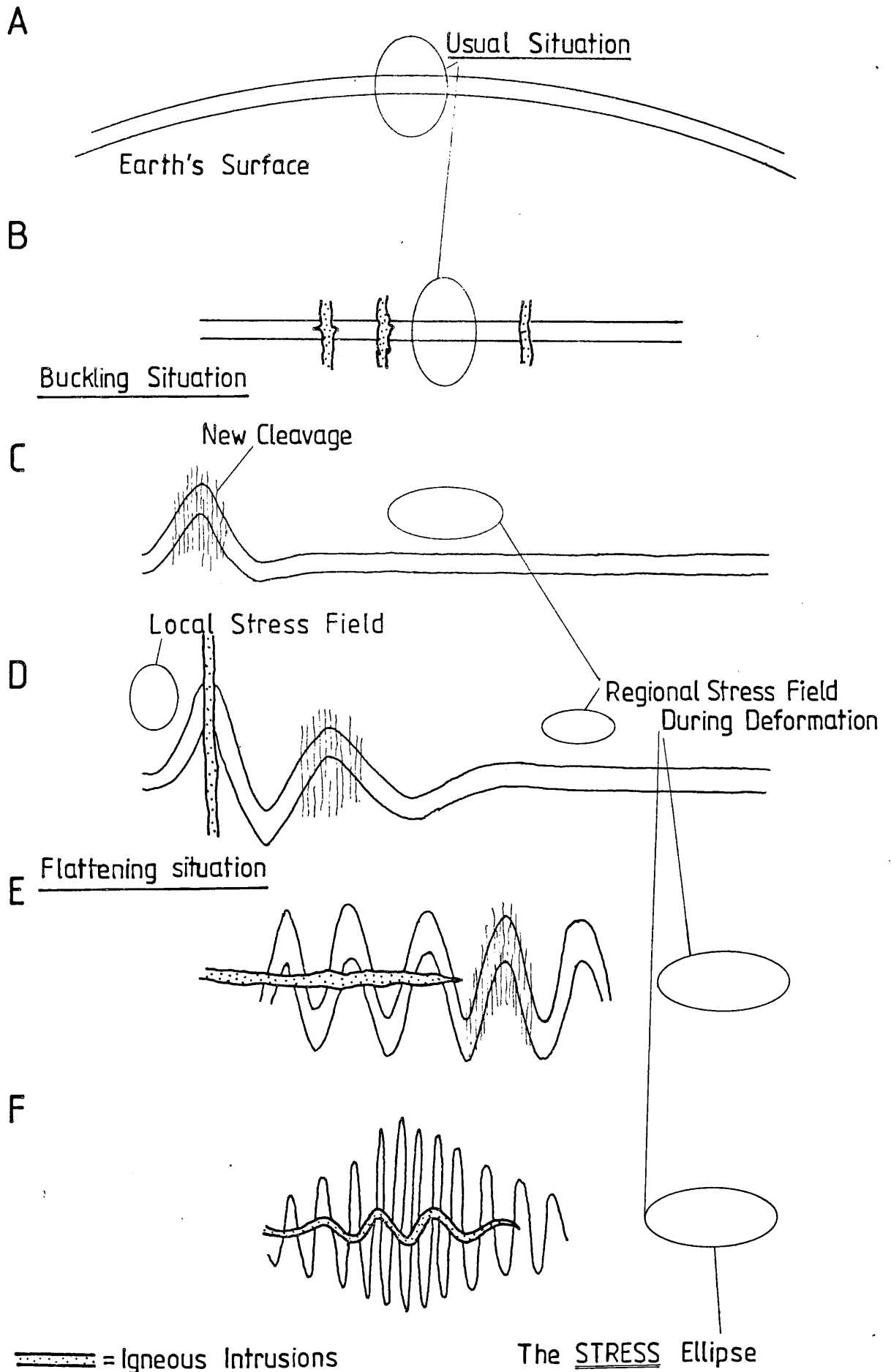
gneisses from Osterøy; some of the layers are tightly folded, yet the layers immediately above and below are less intensely deformed. This observation accords with theoretical and scale model concepts for folding (Ramberg,1959,1963; Biot,1961, 1964; Donath,1962; Chapple,1968; Cobbold et al.,1971; Cosgrove,1976), which predict that the strain round a folded layer dies out within approximately one fold wavelength from the layer in flexural slip buckling deformation. This concentration of strain round the "site of tectonic activity" is also postulated on the larger scale for continental plate boundaries (Bott & Dean,1973). This would mean that intense deformation in the orogen is not likely to extend very far into the basement and it is therefore to be expected that the intensity of deformation will decrease sharply with distance from a "site of crustal activity". We might then expect to find that the deformation in a "basement" to such a "site" would increase sharply towards the paleo-surface (contact with the overlying folded rocks) and towards the "site of activity" horizontally (fig.38). Such a model could be used to explain the observed sequence in tectonic style and intensity away from the Bergsdalen front (figs.18, 20 & 23).

A plot of the entire foliations measured on the Northern gneisses shows that the dominant structure is that of D2 (fig.39, cf.fig.24). The large (yet statistically insignificant) scatter is caused by the D4 cross folds. Figure 40 is a computer generated block diagram of the foliation surface, generated from the same data as that used in figure 39. It shows the major D2 antiformal structure with the effects of D4 suppressed, while figure 30 shows the effect of D4 with D2 structures suppressed.

Fig 38.

PERSISTENCE OF DEFORMATION AWAY FROM DEFORMATION

CENTRES

(Start Condition)

Cover

Basement

(Ramberg 1959 Model)

λ

Basement
Deformation
Dies Out Within
One Fold Wavelenth
From The Folded
Cover

λ

(Bott & Dean 1973 model)

"Site of Crustal"
Activity

Undeformed
"Foreland"

Fig 39.

78
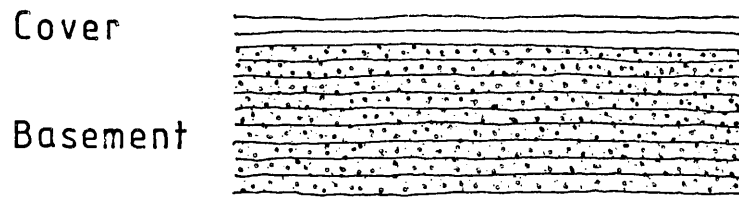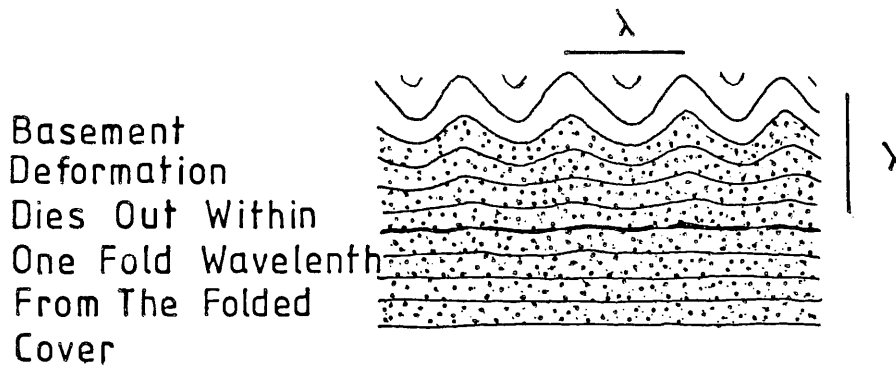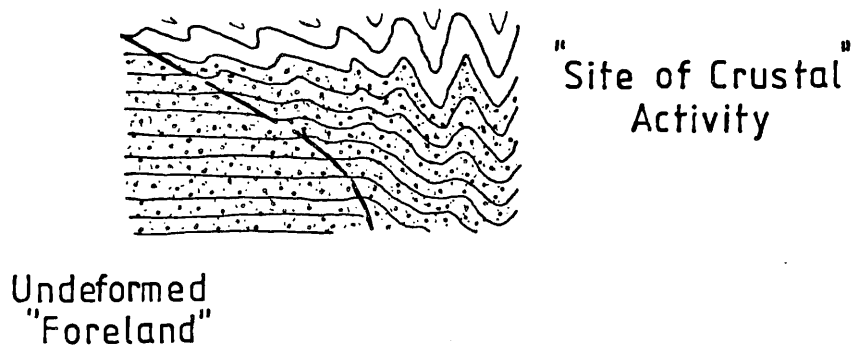
PLOT OF ALL THE FOLIATIONS MEASURED IN THE NORTHERN GNEISSES

PLOT OF NG.FOLIATION (N)

. THIS PLOT HAS UNDERGONE -0- ROTATIONS

USING CORDINATE CARD   0

SAMPLING   2ACROSS/- 1DOWN   POLES PER   1PERCENT AREA   1404 DATA   EQ AR

THE CONTOURS REPRESENT THE FOLLOWING PERCENTAGES

00.9<=1-2%>02.9<=3-4%>04.9<=5-6%>06.9<=7-8%>08.9<=9-10%>10.9<=11-12%>12.9
12.9<=13-14%>14.9<=15-16%>16.9<=17-18%>18.9<=19-20%>20.9<=21-22%>22.9
22.9<=23-24%>24.9<=25-26%>26.9<=27-28%>28.9<=29-30%>30.9<=31-32%>32.9
32.9<=33-34%>34.9<=35-36%>36.9<=37-38%>38.9<=39-40%>40.9<=41-42%>42.9
42.9<=43-44%>44.9<=45-46%>46.9<=47-48%>48.9<=49-50%>50.9<=51%+
NOTE A VALUE OF>0.5-0.9<=.LT.1%AND.GT.0%

SPATIAL REPRESENTATION OF THE DATA

STEREOGRAPHICALLY PROJECTED IN

FIG 39.

Fig 40.

PLOT OF THE FOLIATION IN THE NORTHERN GNEISSES US ING - DIEPTH.
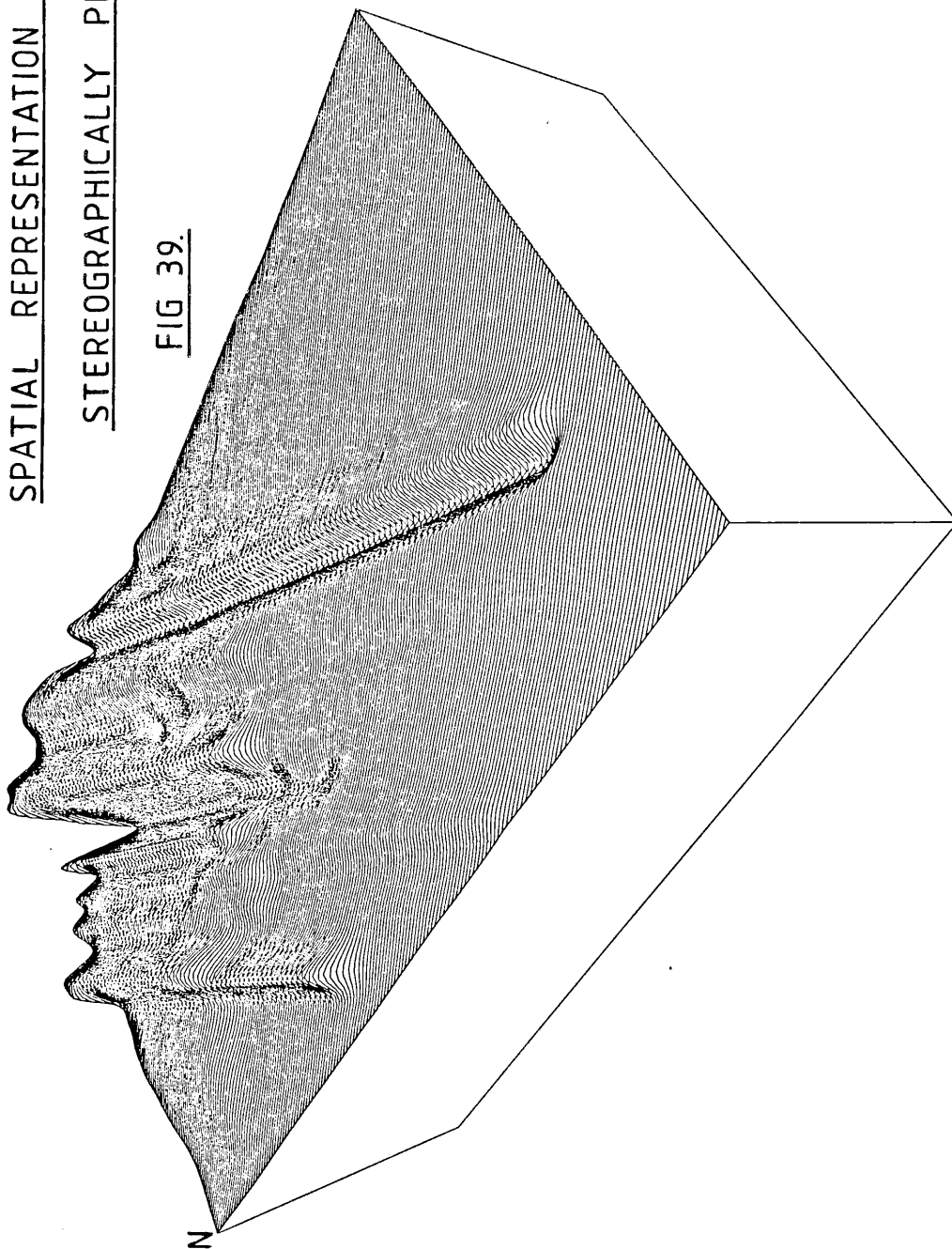
AZIMUTH = 45   ALTITUDE = 55
*WIDTH = 6.00   *HEIGHT = 5.00
SMOOTHINGS = 8.00

* BEFORE FORESHORTENING   05/12/78

2.2   STRUCTURAL HISTORY OF THE SOUTHERN GNEISS UNIT

The principal difference between the rocks comprising the Southern

and Northern units is not one of petrology, but deformation.   The

early deformation in the Southern Gneiss Unit, unlike the Northern

gneisses, proceeds to the point where the rocks develop mylonitic

characteristics.

The chronology of deformation presented in this chapter is specific

to the Southern gneisses, and cannot be directly equated with that

presented for the Northern gneisses.   Correlation between the two units

will be made in the next chapter, as part of the discussion of the nature

of the contact between the two units.

The deformation sequence in the Southern Gneiss Unit is summarised

in figure 95.

2.2.1   The Early Deformation and the Production of the Early
Foliation, S "Early".

Like the rocks of the Northern Unit the earliest deformation feature

seen in the Southern gneisses is a gneissose banding and accompanying

layer parallel schistosity. For similar reasons to those given for the

S "Early" of the Northern gneisses, this banding and schistosity are inter-

preted as being of tectonic rather than igneous or sedimentary origin.

The schistosity is seen as a penetrative amphibole (now much retrogressed

to biotite) alignment.   This is much better developed than its correlative

seen in the Northern gneisses, such that the foliation overprints all

evidence for older deformations.

S "Early" is very difficult to recognise in the field, because of

the strong development of later fabrics which overprint it.   It is most

clearly established in the nose regions of F1 folds, which are best seen

at grid reference 17.50,17.00 (pl.23, 24 & 25). The gneissose foliation is cut by early pegmatites (pl. 24 & 25), but the exact relationship between the pegmatites and the foliation is obscure; they appear as sheets sub-parallel to the schistosity, yet contain the early schistosity themselves. This is interpreted as meaning that the pegmatites were intruded into well foliated rocks, which were subsequently further flattened, such that all the features in the rock rotated into the plane of flattening. This flattening caused the development of a new fabric in the pegmatites and enhanced that fabric already present in the host rock, thereby obscuring all evidence for prior deformations.

There is also some evidence for pegmatites in the Southern gneisses that postdate D "Early" yet predate D1. These crosscut the S "Early" foliation at a shallow angle (pl.24) and do not contain the S "Early" schistosity.

Discussion

The flattening and textures seen in the Southern gneisses differ from those seen in the Northern gneisses. The gneissose banding is much finer; the leucocratic segregations are only millimeters thick rather than centimeters (cf. pls. 1 & 25). The schistosity, too, is more obvious, being present and well developed in all the rock types, rather than just the melanocratic layers. The rock seems to be generally in a much higher state of strain than for the "Early" deformation in the Northern gneisses. The presence of detectable "Early" pegmatites in the Southern gneisses also distinguishes them from the Northern rocks. It is therefore clear that correlation between S"Early" (Northern) and S "Early" (Southern) is not possible. Thus it is likely that a direct correlation of the ensuing Southern Gneiss Unit deformations with those affecting the Northern Gneiss Unit would be incorrect, despite the fact

that the rock types involved in the D "Early" deformation (discussed in section 3 below), are similar to those found in the Northern gneisses. They include metasediments, gabbros and amphibolites, set in a matrix of granitic and granodioritic gneiss.

2.2.2   D1, The Production of the First Mylonitic Textures, F1, S1 and L1

This deformation produced the first folds seen in the Southern gneisses and is the predominant deformation;   the general trend of the fold axes is shown in figure 41.   The deformation occurred at a metamorphic grade of almandine amphibolite facies (see petrological section), and imparted a strong mylonitic fabric to the rocks.   This texture generally overprints all evidence for D "Early".   A table of D1 deformational events is given below:

TABLE OF FEATURES PRODUCED IN D1

1) F1 folds

2) Rotated garnet fabrics

3) A strong "L" tectonite rodding, L1

4) An S1 schistosity and foliation

5) Mylonitization

6) Axial planar pegmatites

7) Further pegmatites emplaced at a high angle to S1

8) Gabbroic sheets intruded parallel to foliation.

In D1 the S "Early" foliation was folded by the F1 folds, and F1 folds are seen throughout the Southern Gneiss Unit.   They are also seen, equally developed, in the majority of the rocks to the south-west in the Bergen Arcs themselves.

Fig. 41.

NORTH OSTERØY

D1

GENERAL TREND OF STRUCTURES.

N
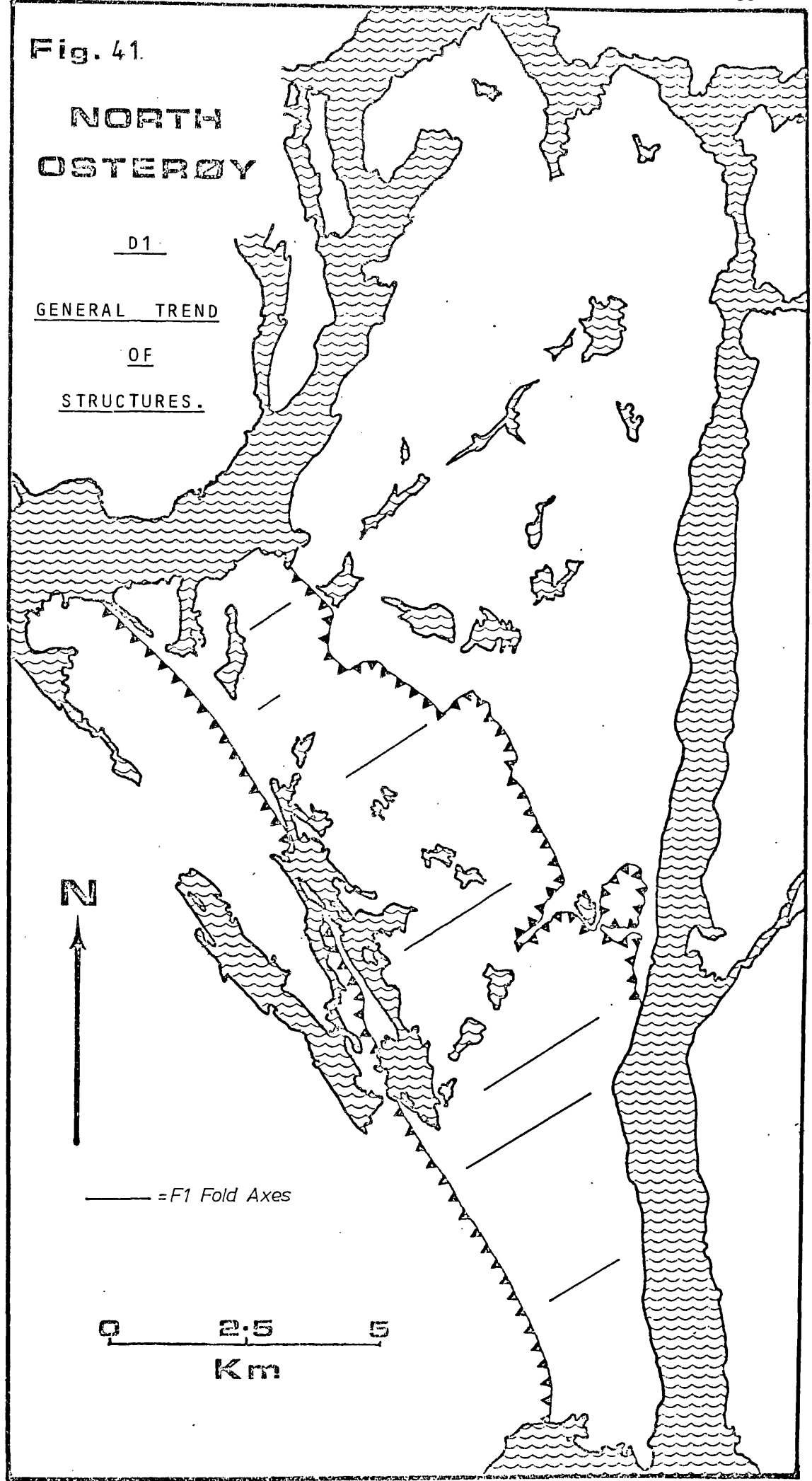
——— = F1 Fold Axes

0   2·5   5
Km

The folds are usually isoclinal and tend to be intrafolial (pl.26), however, where the D1 strain is lower, more open examples of these folds are seen (pls.23, 24 & 25).

In less flattened examples, the F1 folds are asymmetric and recumbent, frequently with sheared middle limbs (fig.42). The sense of overturning of these folds is ambiguous, as it is obscured by later deformations (fig.43), the fact that F1 folds are isoclinal and the limited nature of the exposures. After removal of the majority of the effects of the later deformation, by rotations on a stereonet, it is possible to determine that the F1 folds originally trended north-east - south-west, and had flat-lying axial planes, which must also have had a north-east - south-west strike. The original direction of plunge cannot however be determined, but it is likely that the plunge was very gentle.

During the metamorphism accompanying the folding, garnets grew in some rock types, which show rotation fabrics (fig.44, pl.56).

A strong mullion rodding is associated with the development of the F1 folds (pls.27 & 29). It is much more strongly developed than similar structures seen in the Northern gneisses, and is accompanied by a strong prolate ellipsoidal shape fabric (pl.28), with the longest axis parallel to the "b" direction of the F1 folds (pl.29, fig.45). This rodding, L1, is penetrative and developed on all scales. As with the F1 folds, the lineation is also developed in the majority of the pre-Holdhus (Faerseth et al.,1977) rocks of the Arcs and is traceable into them from the Southern Gneiss Unit. (Elongate rodded boulders are frequently used as fence posts in the area). The exact nature of L1 is complex; in part it is a true mullion structure (pl.29); in part flattened fold closures (fig.43), leucocratic segregations (pl.28), have their longest axis lying in the L1 direction and it is also defined by the penetrative

Fig 42.

GENERAL SHAPE OF F1 FOLDS

Sheared Out Middle Limb
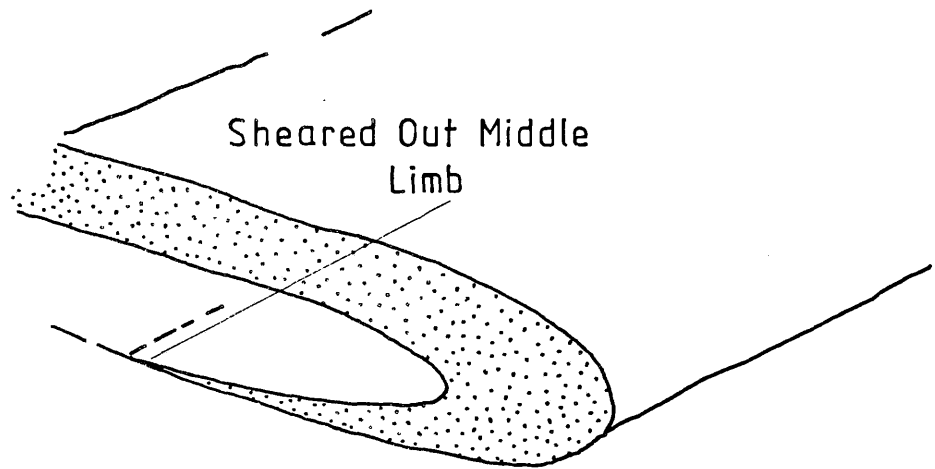
Fig 43.

GENERAL APPEARANCE AND MAIN FEATURES OF F1 FOLDS

L1   F3   F1   S1 & S2   S2 (&S1)

Detached F1 Fragments Dispersed Into S2 By The Flattening Accompanying D2

Fig 44.

86
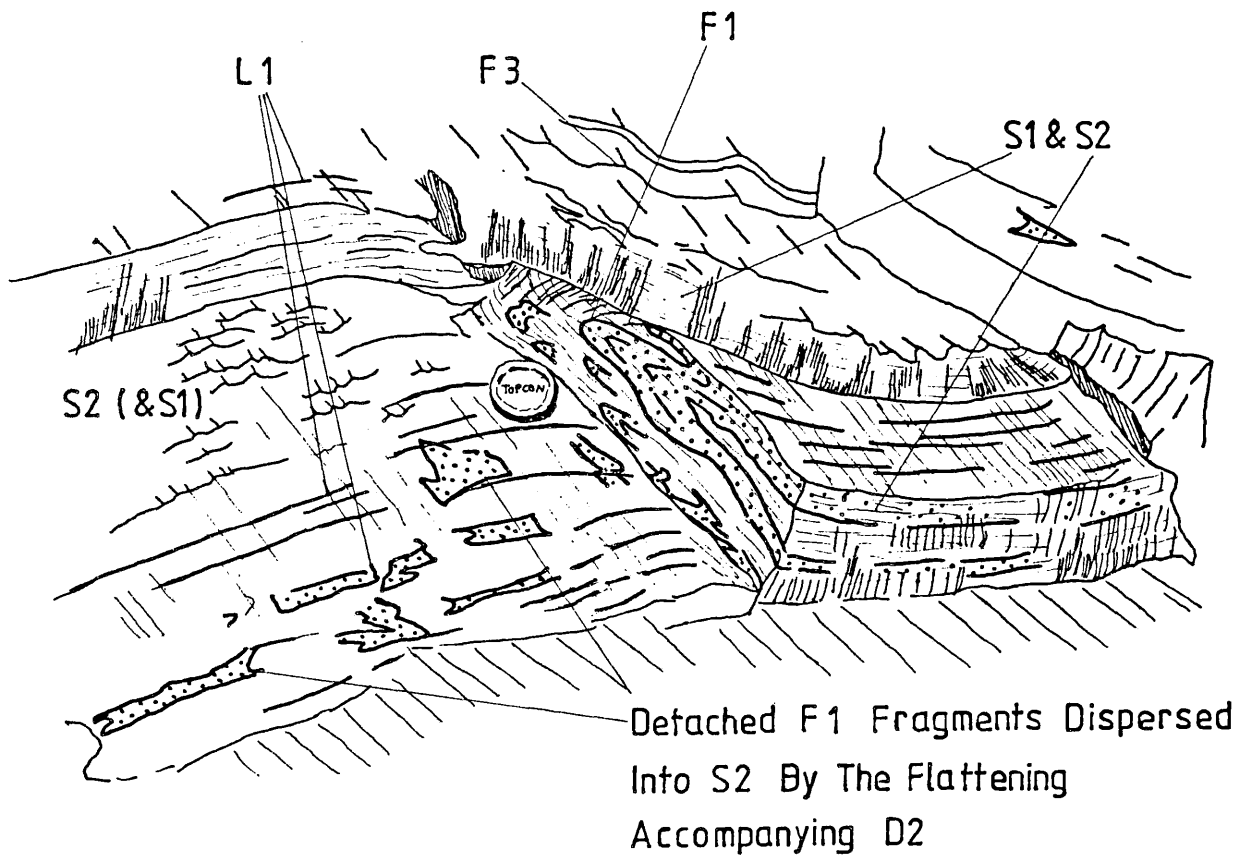
ROTATION FABRICS ASSOCIATED WITH THE F1 FOLDS

SNOWBALL GARNET ·   [Rock FH 17]
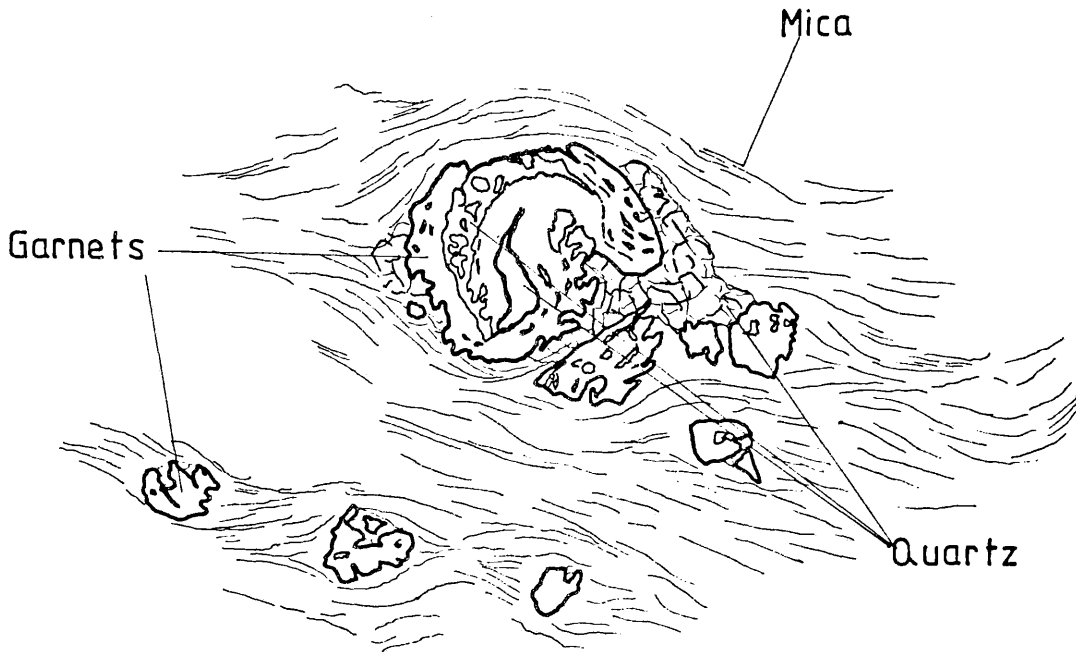
GARNET WITH ROTATIONAL INCLUSION TRAILS OF QUARTZ
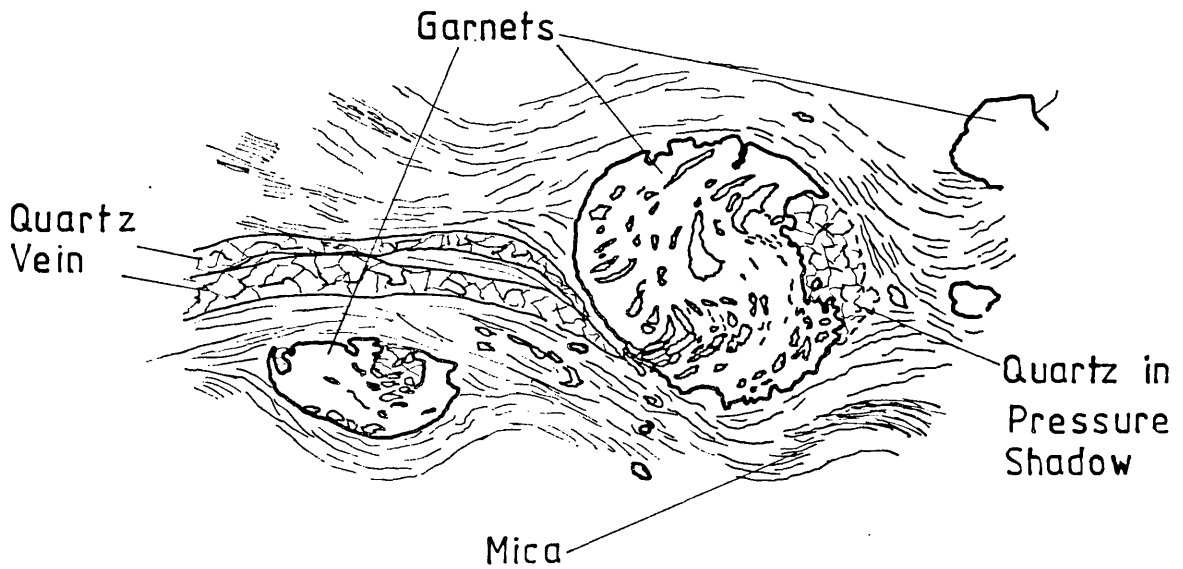
Note-Garnets now corroded and enveloped by a
new younger schistosity

0   mm   1

Fig 45.

PLOT OF THE GEOMETRY OF THE F1 FOLD AT [12.50,18.70],

SHOWING L1 LYING IN TECTONIC Y FOR THE FOLD
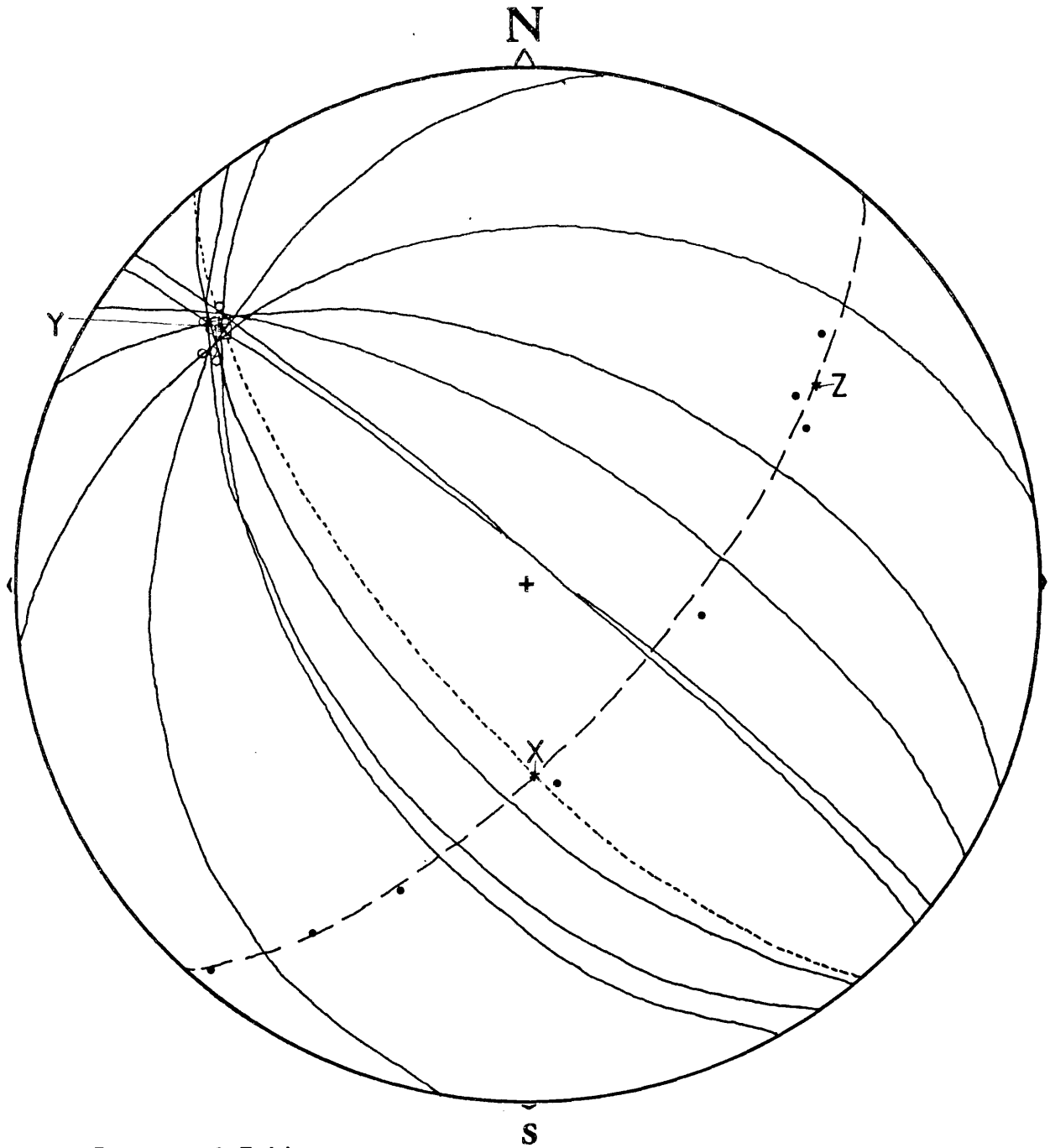
□ Plunge of Fold

○ L1

• Poles to S`Early`

.... Axial Plane

_ _ _ Fold Profile Plane

_____ S `Early`

*, X, Y, Z = Tectonic Axes for

The Fold

alignment of inequant mineral grains (pl.27). All these structures serve
to define a prolate finite strain ellipsoid and such strain geometry has
developed throughout the body of the rock, irrespective of the relative
position on the meso- and macroscopic deformation structures. A model
for the development of this strain geometry is proposed in figure 27.
The fact that this requires two phases of deformation is further indication
that S "Early" is the product of deformation rather than a primary
sedimentary or igneous layering.

A new schistosity, S1, developed axial planar to F1 folds (fig.45)
and this, although penetrative, cuts but does not overprint S "Early"
in the F1 nose regions (pl.24); in the limb regions S "Early" and S1
are coplanar. The extent of S1 development is variable; in certain rock
types (pl.26), the S "Early" foliation is overprinted to a greater extent.
The variation is governed primarily by rock type; in the thicker least
ductile units (acidic layers more than 10cm thick) the S1 schistosity is
generally less well developed. This variation in the D1 strain, allows
examination of the textural development accompanying D1. During D1
folding there was a marked grain size reduction through the Southern
gneisses, which coincided with a thermal peak in metamorphic grade;
hornblende and almandine garnet developed during (and for some time after)
the deformation (fig.44). This imposition of high strains on what were
already highly strained rocks, together with the metamorphism, caused
the development of a new "tectonic" rock type which is characteristically
fine to medium grained, has a marked colour banding (1mm to 30mm thick,
pls.24, 25 & 26), lying parallel to the S1 schistosity (fig.46), and
a flinty appearance. The textures developed and the general appearance
of the rocks, closely resembles those of the "Augen Schists" from Eribol,
Scotland (Lapworth,1885); the rocks are mylonitic.

The mylonitisation affects all the Southern Gneiss Unit, except some rare exposures of F1 fold noses, where pre-existant textures and foliations are seen.   The process accompanied the formation of the F1 isoclines and the L1 rodding and was not confined to localised zones. (The textures and structures developed as a result of this mylonitisation, and an explanation as to the processes involved are given in section 4.)

The F1 folds were intruded by two suites of pegmatites.   The earliest of these (emplaced during or soon after the F1 folding), are parallel to the axial planes of the F1 folds (pl.25).   They are granitic in composition and uncommon.

Subsequently the Southern gneisses were veined   by a suite of much thicker (up to 1m thick) granitic pegmatites that cross-cut the new S1 foliation at a high angle (pl.23).   Some portions of the Southern gneisses are very rich in these pegmatites (10.80,26.60), and can be mapped on this basis;   in other parts, however, there are no pegmatites.

The final phase of igneous activity in D1 postdated the majority of the deformation, and comprises a suite of gabbroic sills emplaced parallel to the S1 foliation, the largest of which is seen at (05.20,32.70). This particular body has a continuous outcrop for several kilometers along strike.   There are also numerous smaller bodies associated with this main intrusion, which cut across F1 folds.

These bodies are confined to the south-west margin of the Southern gneiss outcrop.   They do not contain L1 , and are not cut by the late D1 pegmatites;   this distinguishes them from the older D "Early" amphibolites and gabbros, which are cut by these pegmatites.

Discussion

The D1 deformation is seen to affect all the pre-pegmatite rocks

comprising the Southern Gneiss Unit. These include, in the south-west

region, quartz and mica schists, which were of sedimentary origin, and

a suite of granodioritic granites (which developed into augen gneisses

during D1, and therefore contain L1). They are also cut by post-

intrusional but pre-deformational quartz veins which became isoclinally

folded in D1. An age of 794.08 ± 18.82 Ma. (see appendix 1) has been

obtained on these granites. The granites contain xenoliths of the

sediments, e.g. at grid ref. (06.26,32.30), and must therefore postdate them.

The F1 folds are the earliest structures seen in the sediments and granites.

S "Early" is not present in the granites; their foliation is entirely

attributable to D1 and subsequent deformations. The identification of

the structural sequence in the sediments is however difficult because

the exposures are very limited and there is no immediate evidence as to

whether the foliation defining F1 in them is of sedimentary or tectonic

origin.

If it is tectonic, this implies that the sediments were complexly

folded with the underlying gneisses prior to the granite intrusion.

This would necessitate the introduction of a new fold phase for which

there is no other evidence; there is petrological evidence that these

sediments cannot be correlated with those seen in the Northern Gneiss

Unit (see section 3.3.1) and the sediments may be traced in outcrop into

the sediments of the Major Bergen Arc to the south-east of Osterøy.

The foliation is therefore regarded as bedding.

However, this interpretation raises problems; xenoliths of the

sediments are found in the granite, yet the outcrops of the two are

everywhere separated by at least 200 meters of gneisses. This problem

is resolved by assuming that the relationship between the sediments and

the granites has been modified by secondary imbrication of the succession

during the formation of the Bergen Arc Thrust (fig.10, section 2.3.2)
either in late D1 or D2.

On this evidence, therefore, it is possible to propose a sequence
of events preceding D1 and postdating D "Early". This was a period of
deposition of a sedimentary cover complex, followed at the start of D1
by a phase of granite intrusion. The granites were sill-like intrusions,
sub-parallel to the developing S1 schistosity.

The presence of the mica and quartz schists within the gneiss terrain
raises the problem of whether they are autochthonous or allochthonous.
If allochthonous, they must have been emplaced prior to D1. There is
however no evidence for such an additional phase of deformation. The
main translation event emplacing the Bergen Arc and Bergsdalen Nappes is
interpreted as occurring at the end of D1, with perhaps a reactivation
in D2 as discussed above. Therefore, as has been suggested, the sediments
in the gneiss terrain are correlated with those in the nappe units; they
are para-autochthonous or autochthonous. This means that as with the
time gap between D1 and D2 in the Northern gneisses, the D "Early"
deformation was followed by a period of erosion and deposition. The time
gap between D "Early" and D1 is then probably of major importance.

The most significant feature of the D1 deformation is the myloni-
tisation, which imparts a "false simplicity" to the Unit. The mylonitic
fabric is used as a "marker" in the analysis of later deformations.

The D1 strain history started with the production of F1 folds. The
L1 lineation developed parallel to the Y axis of the strain ellipsoid
as defined by F1 and the new S1 schistosity developed in the X/Y plane.
Compression continued normal to the X/Y plane and the F1 folds tightened
up, becoming isoclinal. In this process the mylonites developed.

At some stage during the compression, a suite of pegmatites and gabbros was emplaced into the gneisses, parallel to the S1 schistosity, while older pegmatites belonging to D "Early", were boudinaged in the plane of the new schistosity. Finally a new suite of pegmatites was emplaced across S1. These remain undeformed in D1 and therefore mark the close of this deformation.

The most important structural element developed in D1 is the L1 fabric, this is very marked and persists through later deformations. (It is correlated with L3 of the Northern gneisses, see correlation section 2.3.1 below).

The sequence of deformation - folding followed by flattening with igneous activity - is similar to that seen in the Northern gneisses, but the intensity of the D1 flattening is far greater than in the Northern Unit.

The features developed in D1 are summarised in figure 46.

2.2.3   D2, The Production of the Second Mylonitic Tectures, F2 and S2

The structures produced during D2 are as follows:

1)   F2 folds

2)   S2 schistosity

3)   Mylonitic fabrics

4)   Some pegmatite emplacement.

It is noteworthy that the S1 foliation is not folded by F2;   only the late cross cutting D1 pegmatites are affected (pl.23, fig.47).   On the basis of these immediate observations, it could be argued that D2 does not exist.   However, the possibility that the folding seen in the pegmatites is attributable to the D1 flattening event rather than F2,

Fig 46.

93

SIMPLIFIED GEOMETRY OF THE STRUCTURES PRODUCED IN D1

F1 Plunge

L1 Plot

General Axial
Direction of F1
and L1

S1

π Girdle of
S Early

Cluster of
Poles to S Early

STRUCTURES ASSOCIATED WITH THE F1 FOLDS

L1 Mullions

L Tectonite Rodding L1

L1 Inter-
-section
Lineation

Axial Plane

Axial
Plane
Pegmatite

S Early

S1 Cleavage

Deformed Porphyroclasts
in the Mylonite

S1 Mylonite

Boudin

0   M   0.5

Fig 47.
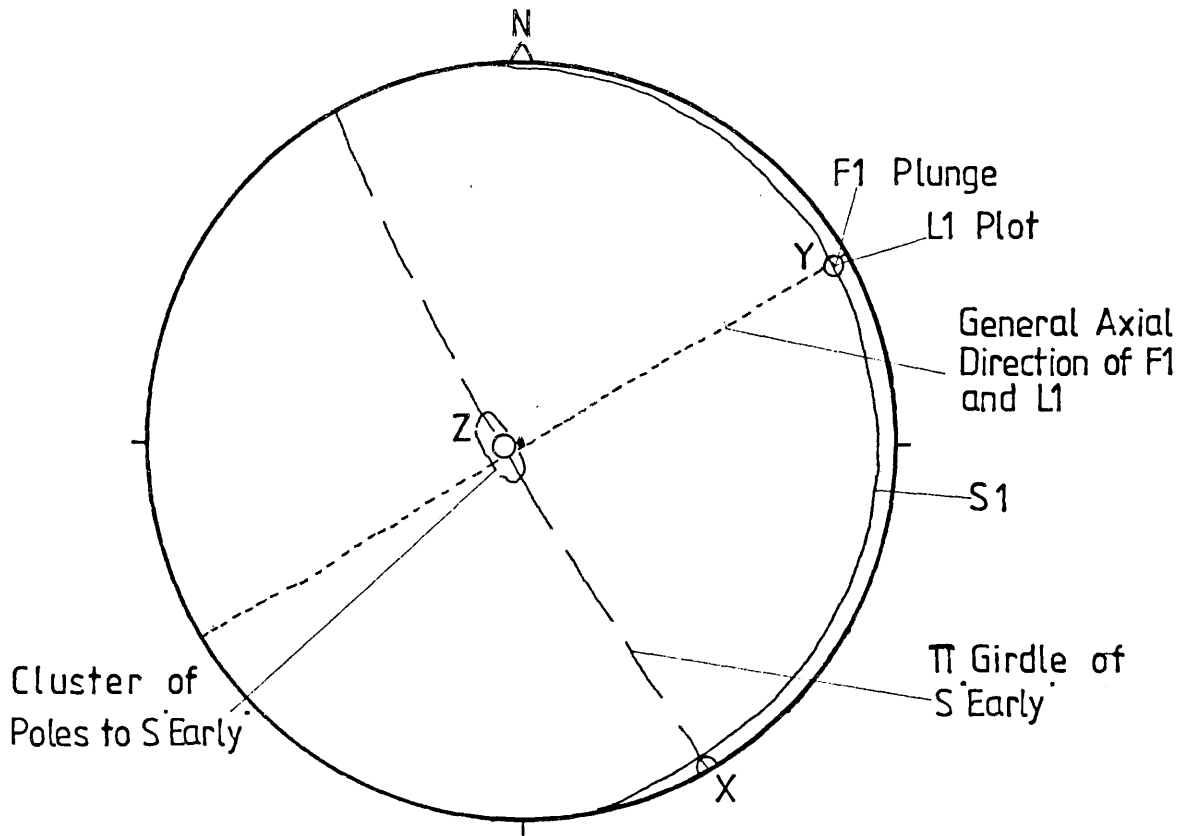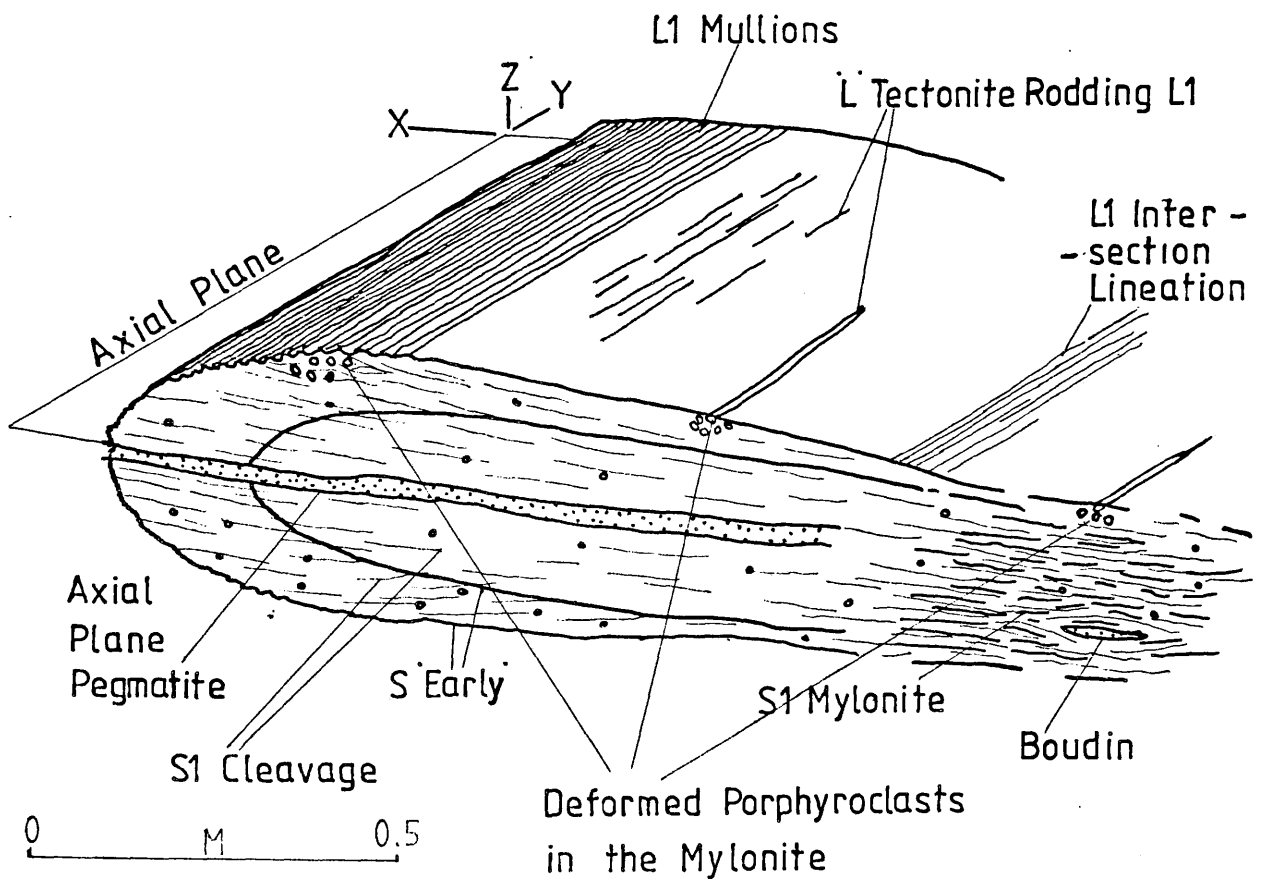
F2 AFFECTING THE LATE D1 PEGMATITES

S Early

Late D1 Pegmatite

F1

F2

S2

D1
Shear in a Middle
Limb of an F1 Fold

S1/S2 Composite

0   M   1
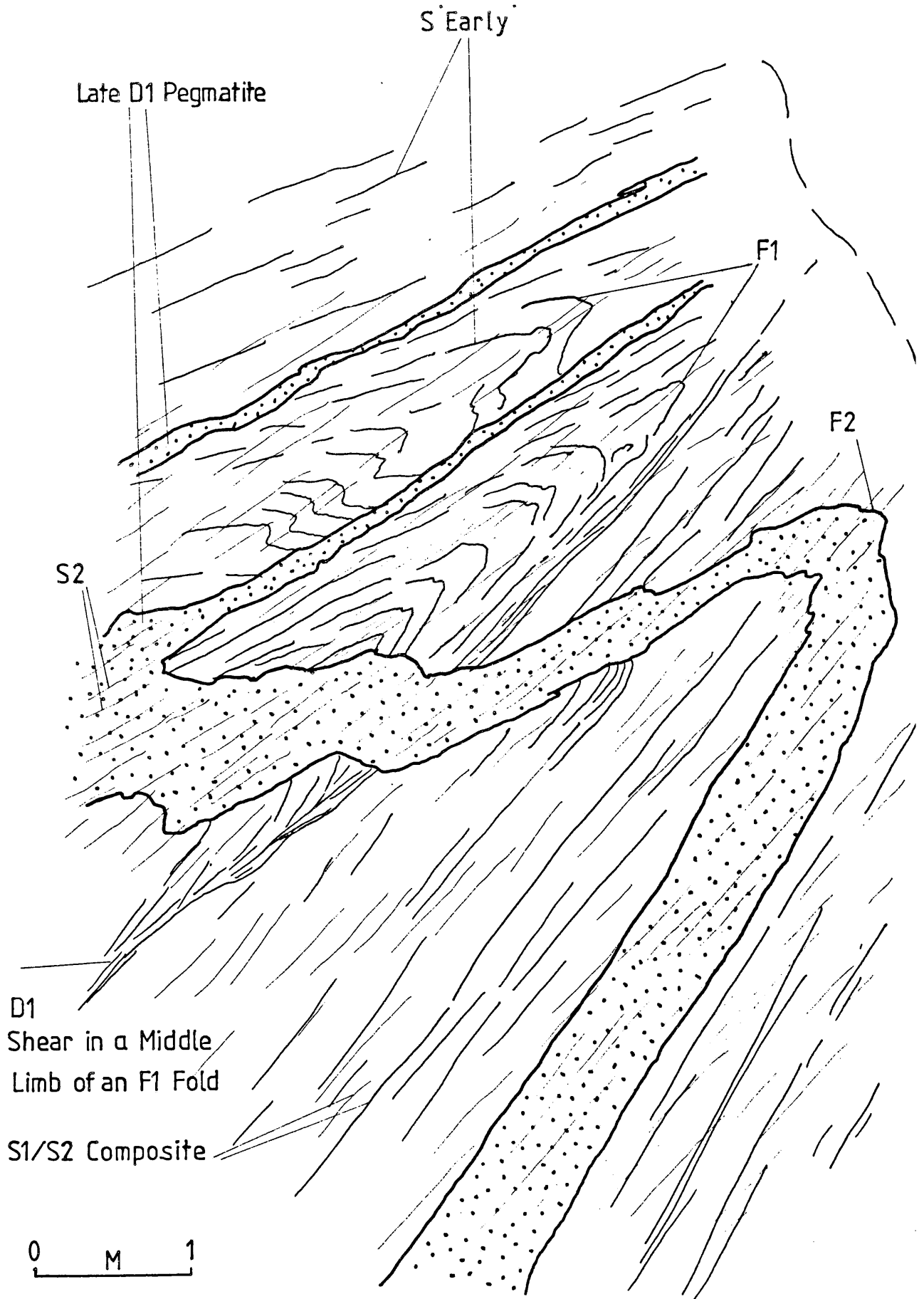
and that the D1 pegmatites were intruded earlier than indicated above,
is disproved since a new schistosity, S2, accompanies this folding and
crosscuts S1 at a shallow angle.   This is fundamentally different from
the relationships between the schistosities produced in the "double
flattenings" (stage F (fig. 37)) in the Northern gneisses; these are
parallel.   While this difference could be explained by non-coaxial strain
late in D1, F2 folds are observed within the Arcs (Faerseth et al.,1977).
D2 and F2 in the basement must therefore be considered as a separate
deformation.

The D2 deformation is heterogeneous on two counts (fig. 45); its
over-all intensity increases from north-east to south-west across the
Southern Gneiss Unit outcrop, and locally it is frequently confined to
narrow bands of intense shearing (pl. 23).   These shear zones are usually
localised on certain portions of the earlier D1 structures; they
frequently (but not always, they can cut "fresh" rock) form on the middle
limbs of the F1 folds and where the D1 mylonite development is strongest.
The intensity of the D2 fabric also tends to increase towards contacts
between different units in the gneisses.   The contact between the augen
granite and the gneisses at (18.80,09.50), providesa good example of
this and plates 42 to 45 show the textural changes moving from the centre
of the granite to the contact.   In general, the D1 and D2 deformations
seem to follow each other, where D1-S1 is strongest, then D2-S2 is strongest.
For example, the areas in which the unflattened F1 folds are seen are also
less affected by D2.   In the old amphibolites, which are cut by the
younger pegmatites that were folded in D1, the effect of D2 was to disrupt
the folding, producing a chaotic structure in which the fragments of the
folds are rotated in all directions (pl. 30).

The spatial relationship between S1 and S2 is not immediately apparent,
on superficial examination the rocks do not appear to have two schistosities.

Fig.48.

NORTH OSTERØY

D2

STRENTH OF

DEVELOPMENT

N
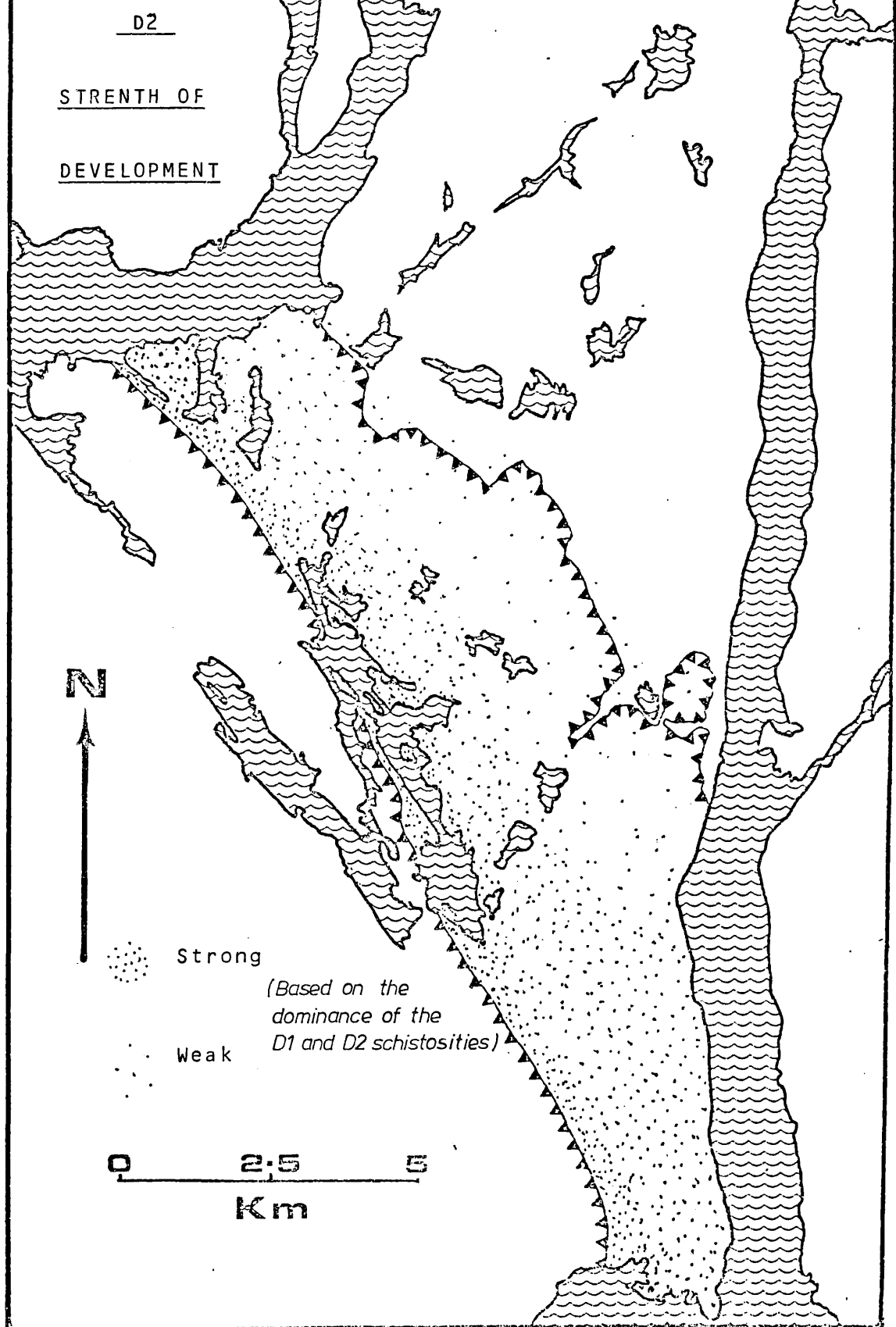
Strong

(Based on the dominance of the D1 and D2 schistosities)

Weak

0   2·5   5
Km

This is because S2 is both variably developed and, where present, lies at only 2-5° oblique to S1. The schistosity is seen in isolation only in the post-D1-flattening pegmatites, and once its presence is suspected, structures attributable to it become apparent. These include:

A) A spindle-like shape to quartz grains in the gneisses

B) The boudinage and shearing of the L1 fabric-bearing rocks to form porphyroclastic remnants in a new S2 mylonitic banding (e.g. at 07.90,29.80)

C) Boudinée of leucocratic layers.

The D1 fabric is dominantly an (L) tectonic fabric. Where this is intersected by S2 which, from the shape of porphyroclasts in areas of strong S2, appears to relate to an oblate ellipsoid, the L1 fabric is chopped up as shown in figure 49, producing spindle shaped relics. The individual rods are also separated laterally and wrapped round by S2 (fig.49), so instead of remaining as true prolate ellipsoids, they become flattened in the plane of S2. Thus the bulk of the gneisses have a good foliation on which the rock will split into flat sheets, yet on any one foliation surface there is exposed a strong linear fabric confined to that surface (pl.27). The immediate effect of D2 was to emphasise the D1 fabric, but as S2 gets stronger L1 is progressively destroyed. This effect is best seen in an along strike traverse through the middle of the Southern gneiss within one lithological unit. There is an increase in the intensity of D2 and consequent progressive destruction of L1 across strike to the south-west, and along strike to the north-west (fig.48).

During D2 there was extensive boudinage within the Southern gneisses. This not only affected the late D1 pegmatites (fig.50), but also involved leucocratic members of the gneissose banding when one of these was sandwiched between melocratic portions (fig.51). The late stage D1 boudins were also enhanced in this process.

Fig 49.

DEFORMATION OF L1 IN S2

L1 Exposed on S2

Plane of S2

Detailed
Nature of L1
After Modification
By D2

Quartz Spindle

Shape of Cross-section of
an L1 'Rod', in the S2
Schistosity
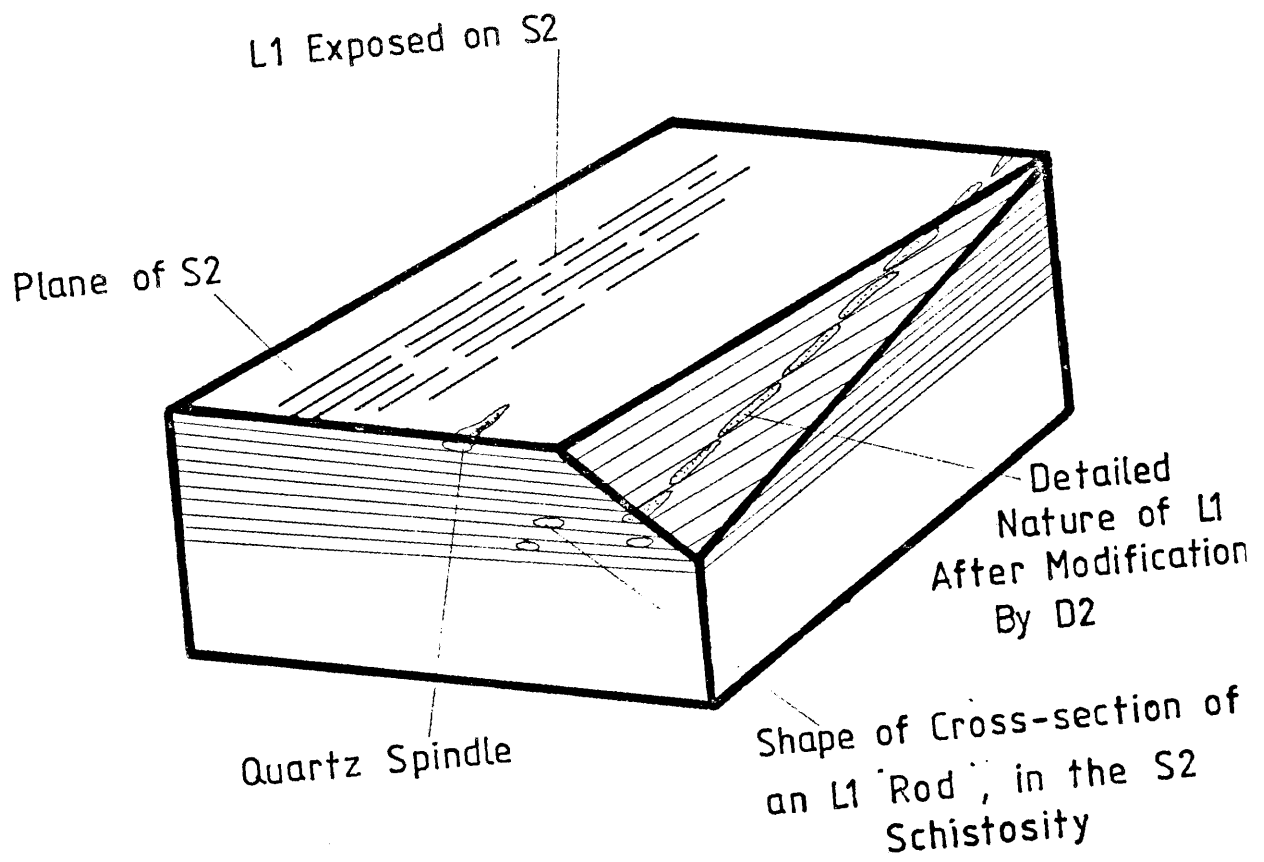
DETAIL OF A QUARTZ SPINDLE

Macroscopic
Direction of L1

'Spindle' of Mono or
Polycrystalline Quartz, the
Remnant of a D1 Rodded Structure

S2

Fig 50.
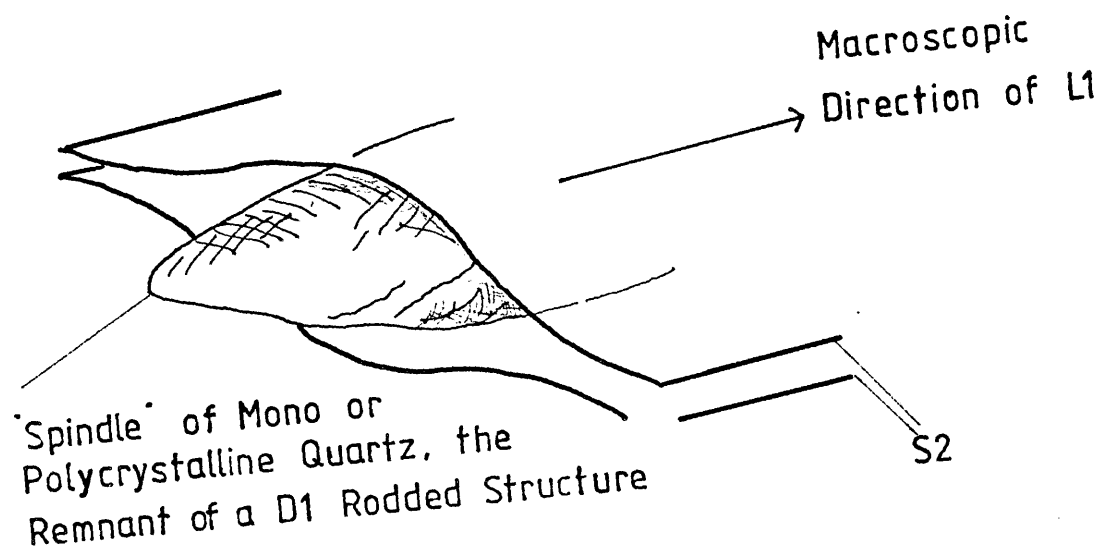
TWO EXAMPLES OF D2 BOUDINAGE

Post D2 Vein

K-Feldspar
porphyroblast

Pegmatite

Boudin

Melanocratic
Gneiss

5 Cm.

Fig 51.

Acid Gneiss

Melanocratic Gneiss

5 Cm.
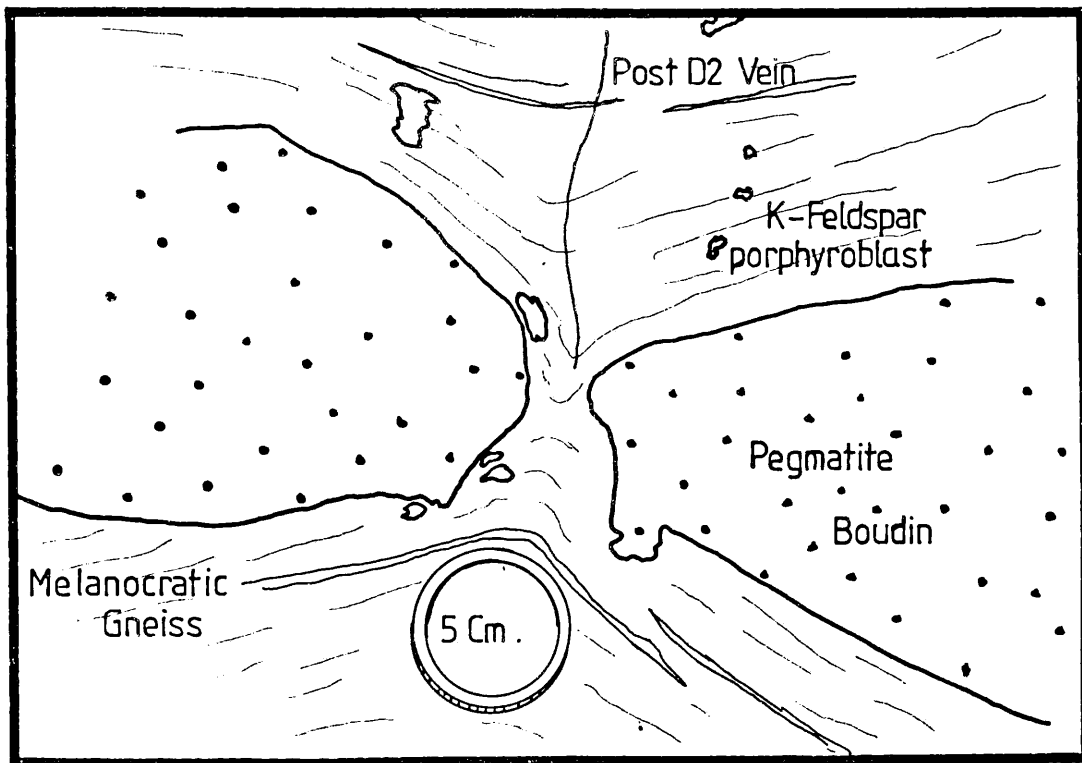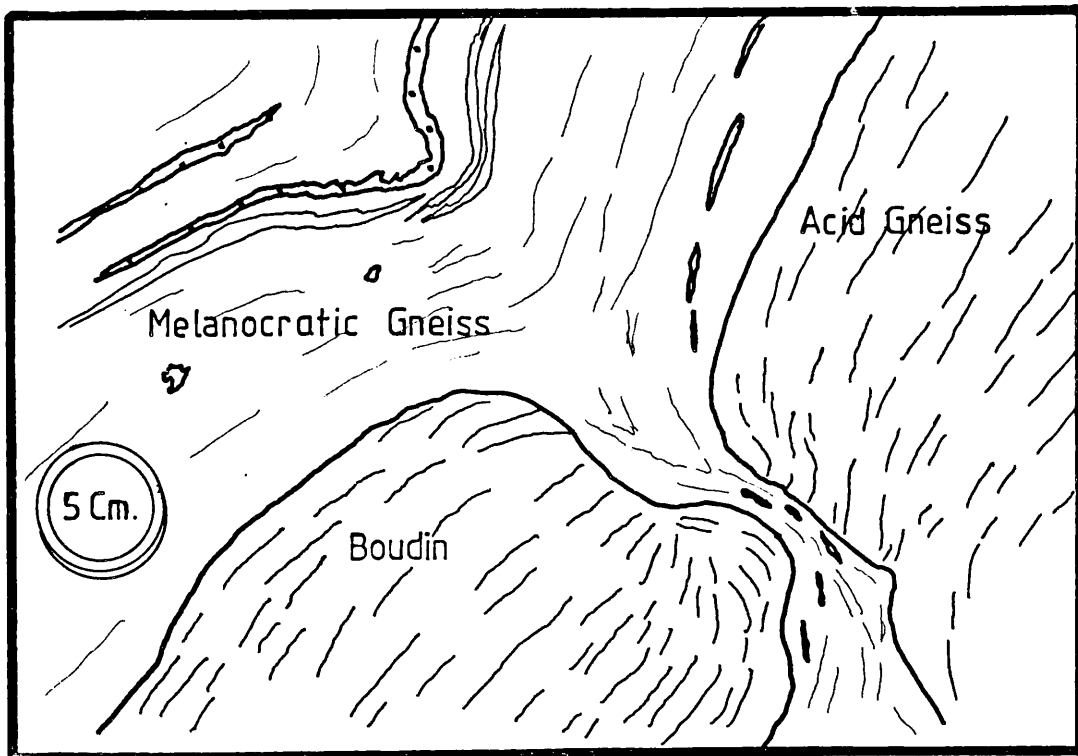
Boudin

The amount of strain involved in the D2 boudinage, gauged from the spacing between "pips", increases moving up section towards the south-west. The D2 boudinage is also seen to extend some way into the Northern gneisses.

The visible foliation in the Southern gneisses is therefore a complex structure formed by the interplay of two separate foliations of slightly different character.   As far as can be ascertained in view of the subsequent reorientation of S2 in D3 (2.2.4 below), throughout the Southern gneisses, S2 cross cuts S1 more steeply (fig. 52a).

Accompanying the formation of S2, in the regions of strong D2 development, there was grain size reduction and the growth of a new minerals of upper greenschist facies (see 3.2, petrological section);   the textures formed are mylonitic.   The principal difference between the D1 and D2 mylonites is that the D2 generation is less penetrative and confined to zones which isolate patches where the D1 fabrics remain dominant.   The D2 mylonites are best developed in a thick zone paralleling the junction with the Major Bergen Arc;   here virtually all textures are attributable to it.

The D2 structures are cut by two sets of pegmatites, both very rare.   The first of these, thin discordant sheets of fine grained grey trondhjemite, must have been emplaced during the folding because they contain a weak S2 and are only seen where they cut the folded D1 pegmatites. They are axial planar to the F2 folds (pl. 23).   The second set are coarse grained quartz, potash feldspar-rich pegmatites, only two examples of which were found.   These trend across strike and are lenticular, being about 0.5m thick and 30m long.   Their margins are diffuse;   they seem to merge with the country gneisses and are interpreted as being of local metasomatic origin (veinites).

Fig 52.

101

RELATIONSHIP BETWEEN S1 AND S2

a)

S1

a

S2

N
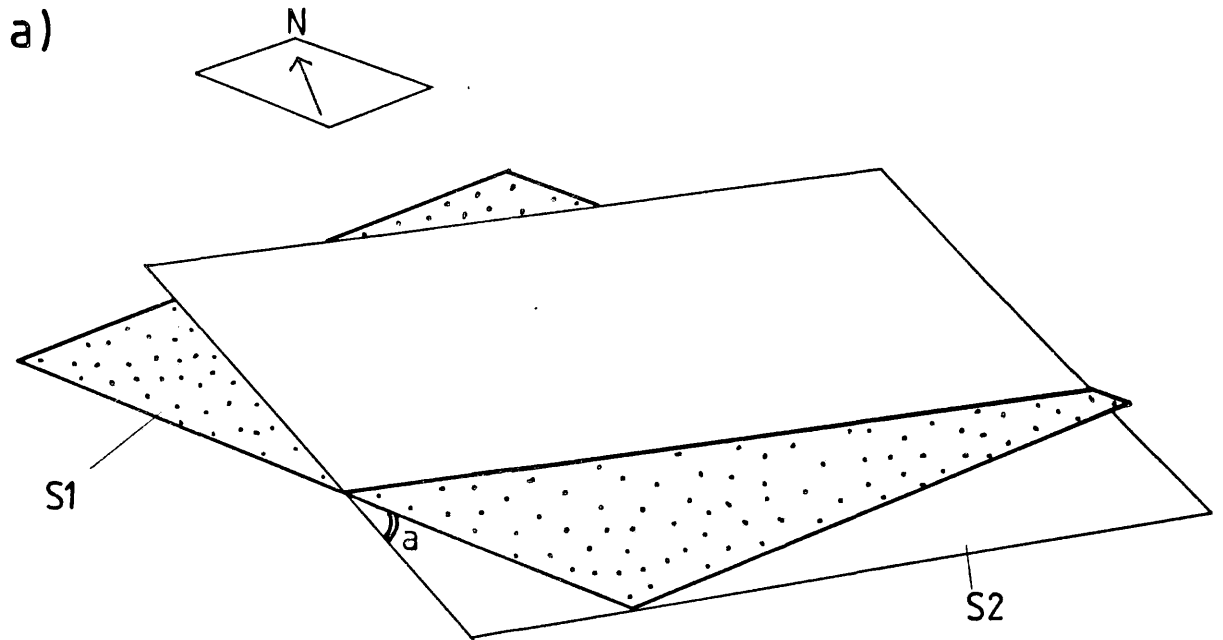
DIAGRAM SHOWING HOW THE D2 STRUCTURES IN THE BASEMENT ARE THOUGHT TO RELATE TO THOSE IN THE ARCS

b)

D2 Thrusts

F2 Folds

(Allochthon)

(Autochthon)

Sheared F2 Folds

Flattened, Reworked Basement
(Para-autochthon)

ARCS
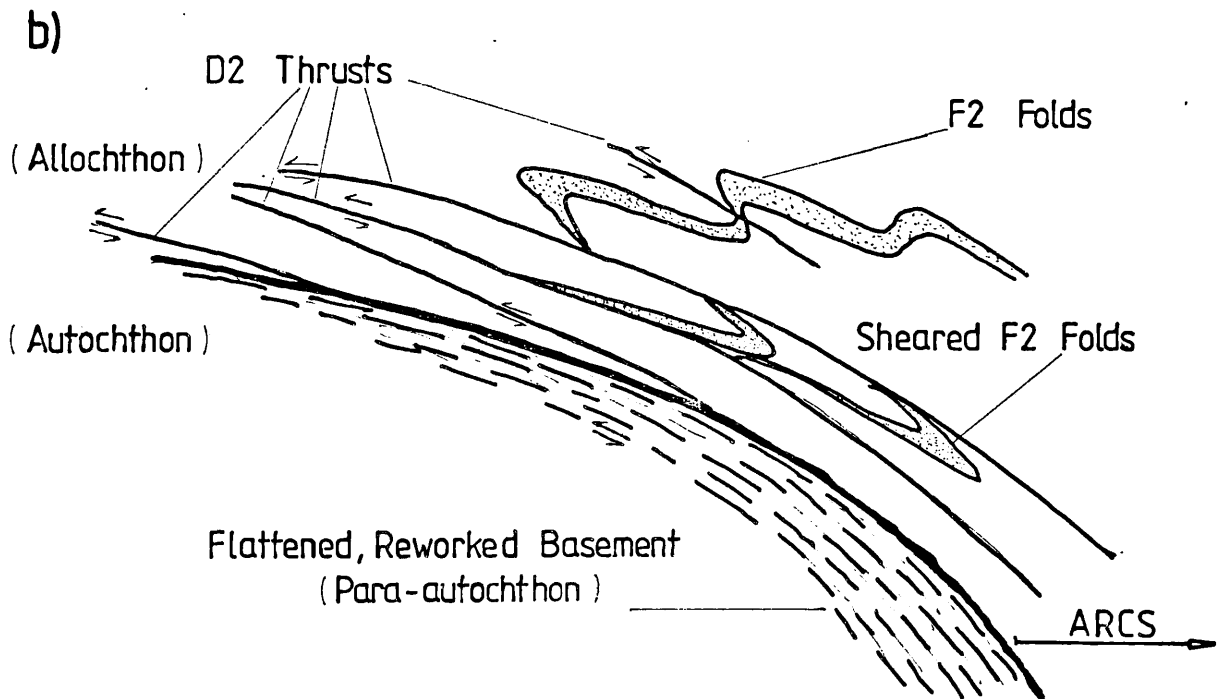
Discussion

It is apparent that in D2 the Southern gneisses were, though not folded, highly strained. A new penetrative fabric was acquired and secondary mylonitic textures pervasively developed. The D2 deformation is therefore as important as D1.

D2 displays a similar heterogeneity to that seen in D2 and D3 of the Northern gneisses (see 2.1.4 above), which increases in intensity approaching the Bergsdalen Nappes, only here there is an increase towards the Bergen Arcs as well (fig.48).

It can be proved (see 2.3.2 below), that the D2 flattening episode in the Southern gneisses must have been synchronous with a fold-producing deformation identified by Faerseth et al. (1977), within the Arcs. D2 is therefore interpreted as a basement response to deformation which at a higher level in the tectonic pile gave rise to folding. Because of the similarity in nature of the deformational effects produced in the Southern gneisses and the semi-parallelism of S1 and S2, the D2 deformations must have been very similar to those in D1. A model envisaged is given in figure 52b.

Determination of the D2 direction of tectonic transport is critical but presents a problem, because no major F2 folds are exposed in the Osterøy basement. There are four possibilities; like D1 the structures could have been aligned on a north-east (Bergsdalen) axis with transport from either the north-west or south east; or the structures could have had a north-west (Bergen Arc) axial trend, with transport from the north-east or south-west.

It is important in regional terms to decide at which stage in the deformation history of the area structures with a Bergen Arc trend first appear. The thinning and cutting out of lithologies moving along strike

in the Southern gneisses away from the Bergsdalen front (map 1), a D2

phenomenon, seems to indicate a component of transport along a north-west

vector, though as in the Arcs (Faerseth et al.,1977) this is inconclusive

because of the effects of later folding.   However, the distribution of

S2 (fig.48), which strengthens towards the Bergsdalen Nappes, suggests

D2 should be included with the Bergsdalen affiliated deformations.

The D2 strain ellipsoid is probably very similar to that formed in

D1 with some rotation, the X Y plane of the D2 ellipsoid is slightly

oblique to that of D1.   S2 is therefore a schistosity which formed in

the bc plane of a major fold phase.   The folds seen to affect the late

D1 pegmatites are the expression of these folds in the basement, and

formed during the development of D2;   S2 is axial planar to these folds.

There are several important deductions that may be made based on

observations of the D2 boudinage.   Firstly, it is the leucocratic portions

that form the boudins, and the melanocratic portions that form the "ductile"

matrix.-   This is the reverse of the situation usually seen in gneiss

terrains, where the basic portions form the boudins (as with D1 in the

gabbros of the Northern gneisses).   In the Northern gneisses the

ductility contrasts controlling boudinage were the result of elevated

temperatures (the leucocratic portion was of high ductility because it

was near its melting point).   While in the Southern gneisses the controls

were mechanical, there is a grain size difference between the two units

(the finer grained melanocratic rock was the weaker (fig.144)) and slip

on the cleavage planes of the mafic minerals (biotite and amphibole)

would have taken place.   The D2 deformation occurred at relatively lower

temperatures than D1 (Northern Unit). This is borne out by the fact that

during D2 the rocks were at a much lower grade of metamorphism than

previously seen on Osterøy (see section 3.5).

The observation that this deformation crosses into the Northern gneisses indicates conclusively that the two units were adjacent at the time of the D2 deformation.

The dominant foliation mapped in the Southern Gneiss Unit is then a complex foliation, composed in some parts mainly of S2 while in others it is dominantly an S1 surface. Separation of the two is generally impossible in outcrop because of their near parallelism. This problem also affects the lithological units mapped; in map 1 these units are not strictly lithological divisions defined on a mineralogical basis, they are a reflection of both mineralogical and textural variation. This latter variation was produced during D1 and D2 (mainly D2 because of its heterogeneous nature). The mapped units are then strictly litho-tectonic units, except for the igneous members, and all contacts are tectonic.

The structures associated with D2 are summarised in figure 53.

2.2.4   D4, The Production of F3, S3, L2 and L3

The F3 folds are the most obvious folds seen in the Southern gneisses, and within the Bergen Arcs generally. Their development will be considered in detail. It is D3 that is correlated with D4 of the Northern gneisses, for reasons which will become apparent during this description and which are discussed in the correlation section (2.3.1 below).

The structures produced in D3 are as follows:

1) F3 folds, folding the S1/S2 composite foliation

2) S3 schistosity

3) L2, mineral growth lineation

4) Folding of L1

5) An L3, S1/S2, S3 intersection lineation

6) D3 quartz veins, and hydraulic fracturing.

Fig 53   105

SIMPLIFIED GEOMETRY OF THE STRUCTURES PRODUCED IN D2
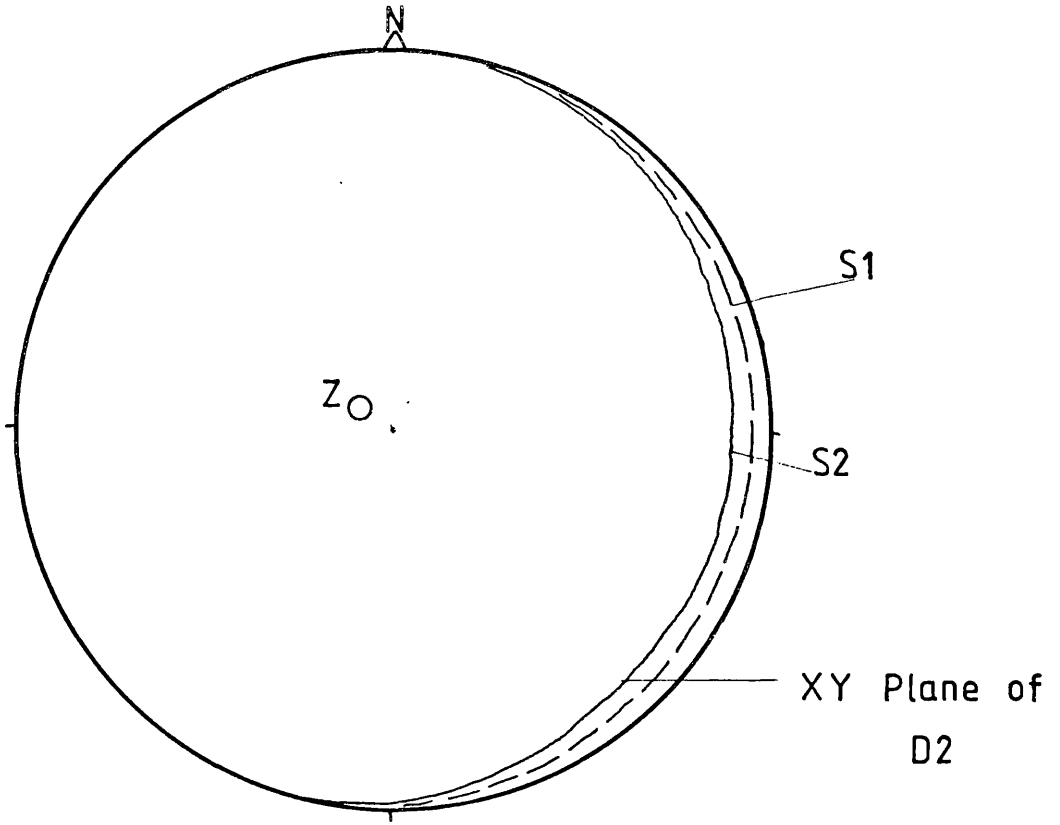
STRUCTURES ASSOCIATED WITH THE F2 FOLDS
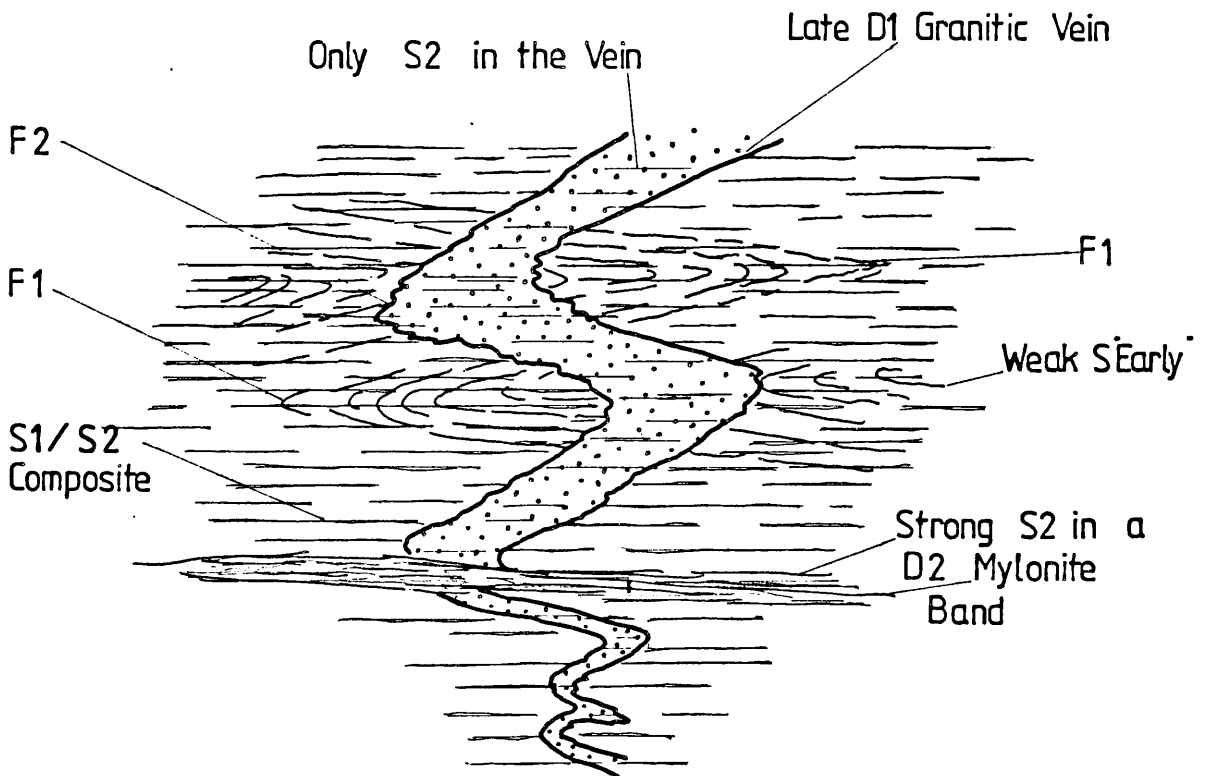
The F3 folds fold the S1/S2 composite foliation and refold F1 and F2 folds (pl.31 and figs.43 & 54). The folds are asymmetrical, non-planar, non-cylindrical, recumbent folds overturned to the south-west (towards the Bergen Arcs). The wavelength of these folds is, on the largest scale, about 10 Km. The fold style is summarised in figure 55. The whole attitude of the Southern Gneiss Unit and a large portion of the adjacent Arc units is governed by one such fold, the short steep limb occupying the region of the large lake in the centre of Osterøy (fig.56). On the smallest scale in thin section, these folds are seen to affect the S1/S2 biotite schistosity (fig.57). Between these extremes the F3 folds are pervasively developed throughout the Southern Gneiss Unit and have been traced across south Osterøy over as far as Bergen, where they have been identified in the Ulriken Gneiss Complex (Thon, pers.comm. and Faerseth et al.,1977). They are also equally well developed in the south of the Arcs at Os and in the north on Lindas. In short they form the most obvious folds in the whole Bergen area. Plates 32 and 33 and figure 58 show examples of these folds.

Figure 59 shows the variation in plunge of F3 folds. This variation is the product of a primary non-cylindricity and is clearly not the result of cross folding. The pitch of the fold axis, measured in the axial plane, may vary by up to 90° over short (0.3m) lengths of hinge, giving rise to concentric outcrop patterns, similar to a Type 1 inteference pattern (Ramsay,1967), (pl.34, fig.60). Furthermore the axial planes of the F3 folds are primarily non-planar (fig.61), and these are subsequently folded by D4 (see below). Thus while the over-all geometry of the F3 folds defines a recumbent structure (fig.55), in individual outcrops the folds may be upright. Figure 62 shows how this affects the plunge direction and therefore the variation present in figure 59.

Fig 54.

F1 FOLDS REFOLDED BY F3

F3

D3 Slide

F1 Fold
Closures

5cm. in
Diameter
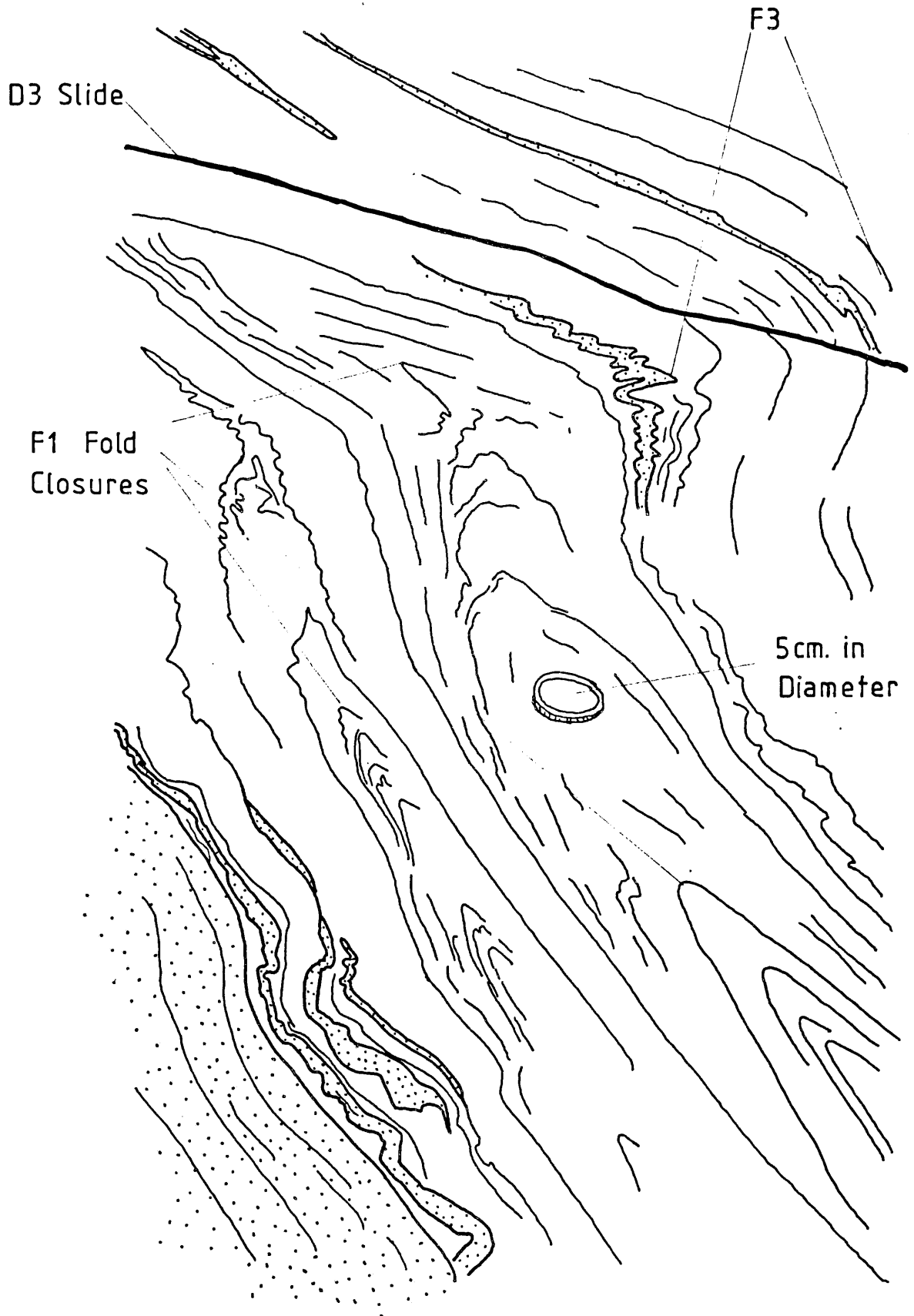
Fig 55.

DIAGRAM SHOWING THE GENERAL STYLE OF THE F3 FOLDS

Curvature of the
F3 Axis

F3 Parasites

F3

Eye Structure

S1 / S2 Composite

0   100 Metres
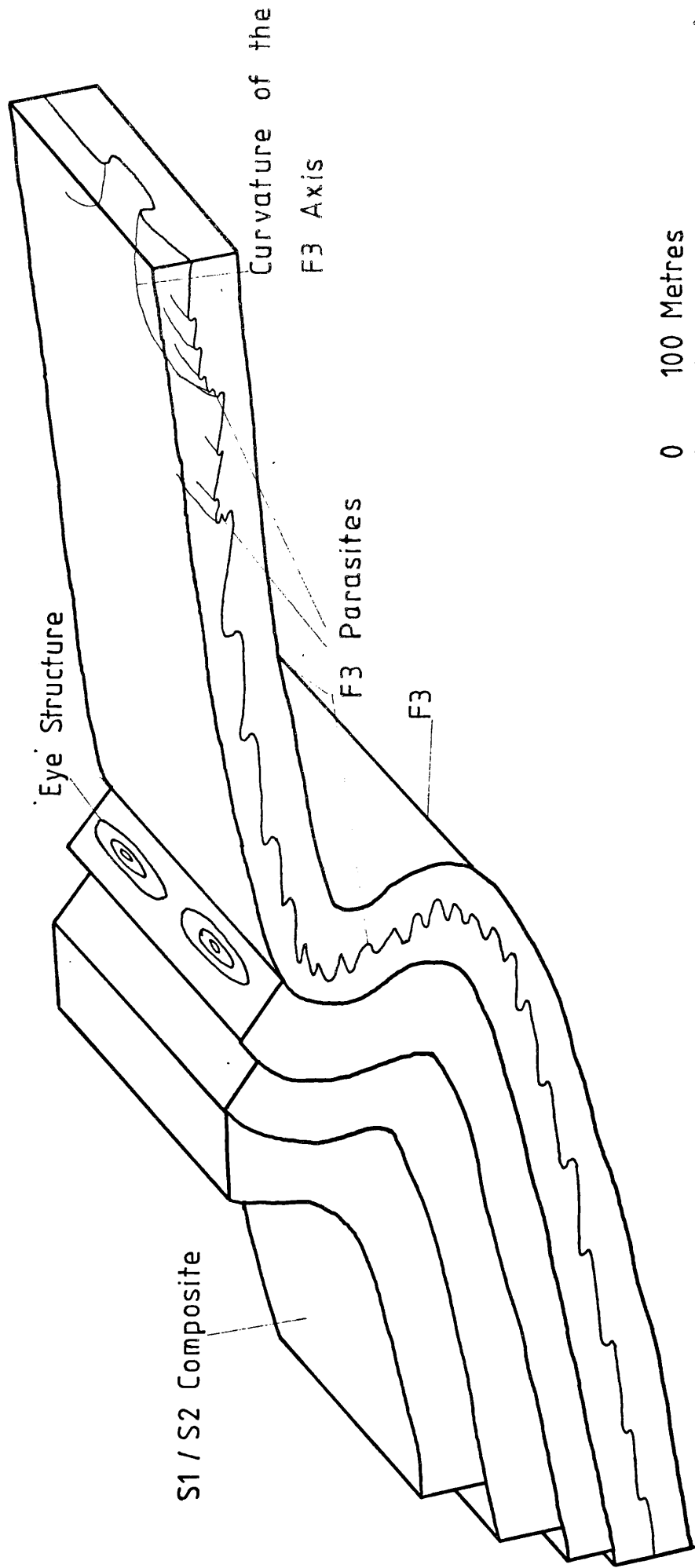
Fig.56

NORTH OSTERØY

D3

S2 Defining the Major F3 Fold

[shallow]

[steep]

N

70

45

90

27

65

20

37

90

73

0   2.5   5
Km

Fig 57.
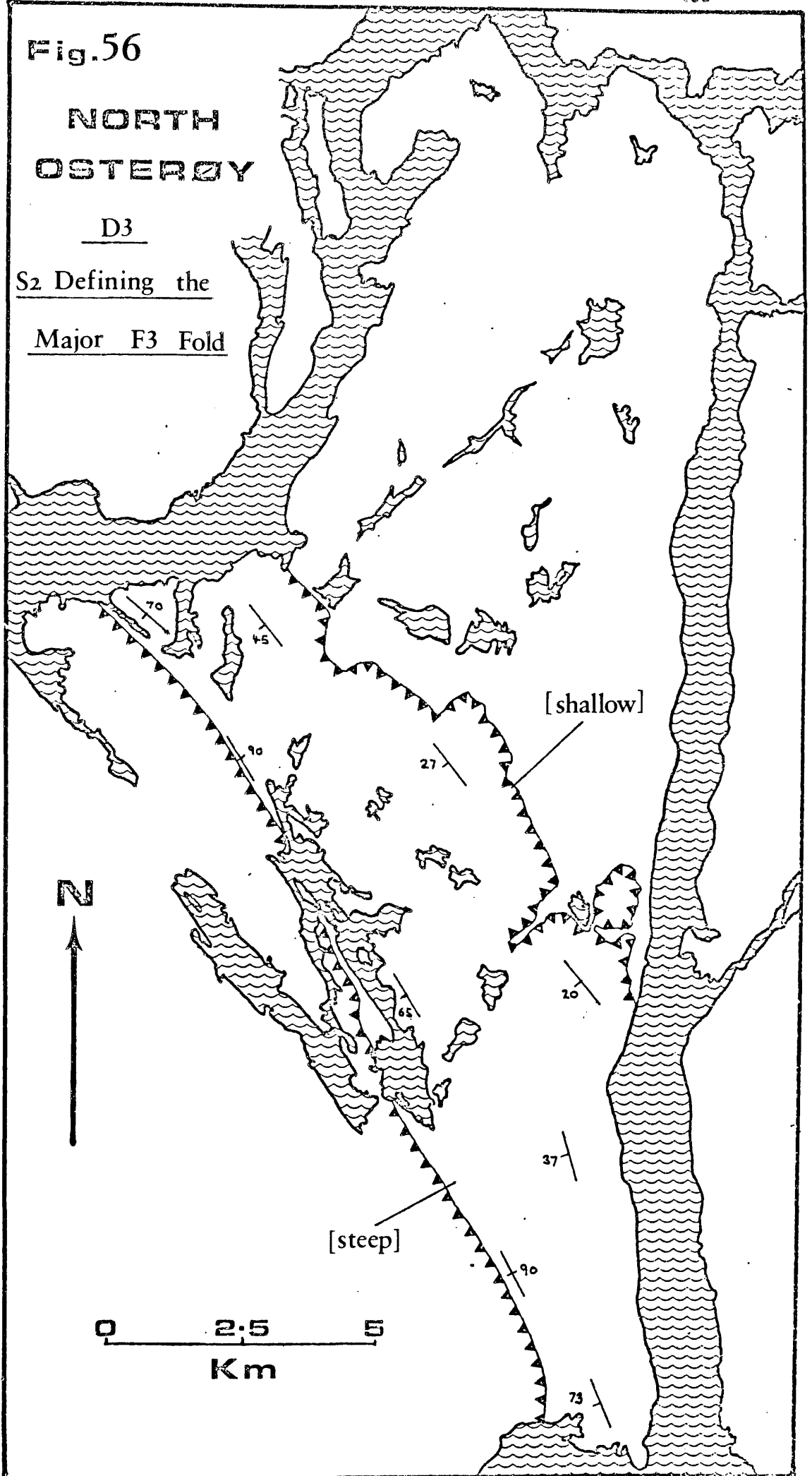
SMALL SCALE F3 CRENULATIONS AFFECTING AN OLDER (S2)
BIOTITE SCHISTOSITY

Quartz

Mica

Old Schistosity

Developing S3

0   mm   1
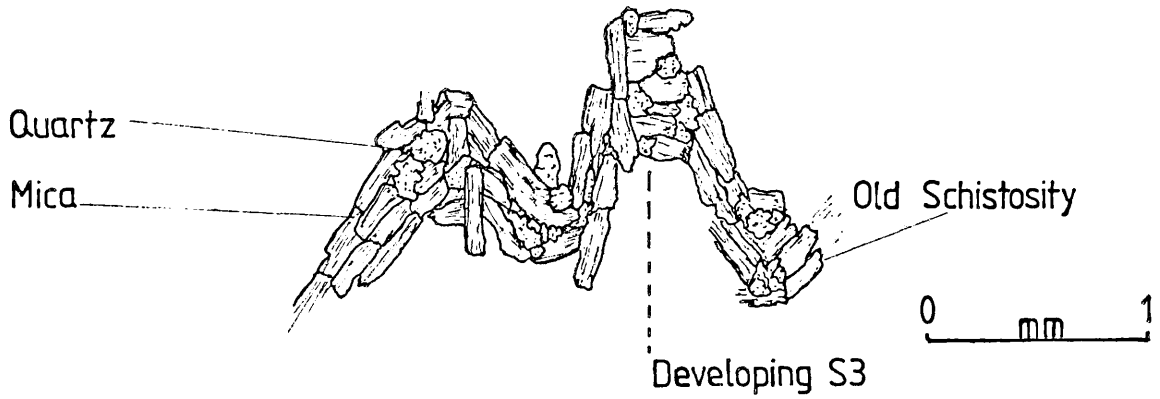
Fig 58.

SMALL F3 FOLD WITH SHEARED MIDDLE LIMB

Old S1 & S2 Foliations

The Middle
is Thinned
and Then
Translation
Occurs on it

F2 Closure

New S3 Schistosity
Develops in the
Shear, but is not
Present Outside it
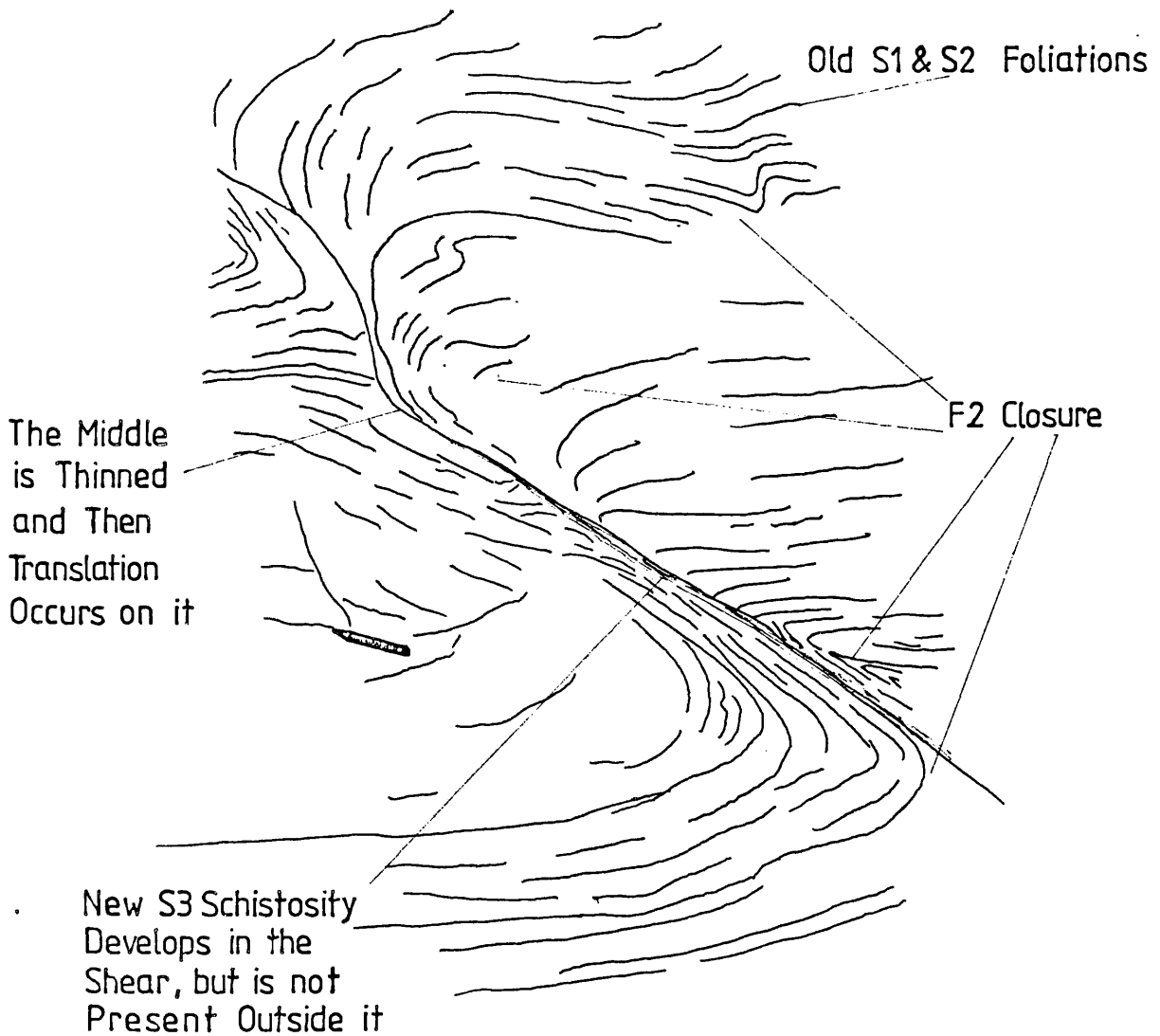
Fig 59.

PLOT OF PLUNGE OF THE F3 FOLDS

PLOT OF BERGEN ARC FOLD PLUNGE

THIS PLOT HAS UNDERGONE -0- ROTATIONS

USING CORDINATE CARD   0

SAMPLING   2ACROSS/- 1DOWN   POLES PER   1PERCENT AREA   211 DATA   EQ AR

THE CONTOURS REPRESENT THE FOLLOWING PERCENTAGES

00.9<=1-2%>02.9<=3-4%>04.9<=5-6%>06.9<=7-8%>08.9<=9-10%>10.9<=11-12%>12.9
12.9<=13-14%>14.9<=15-16%>16.9<=17-18%>18.9<=19-20%>20.9<=21-22%>22.9
22.9<=23-24%>24.9<=25-26%>26.9<=27-28%>28.9<=29-30%>30.9<=31-32%>32.9
32.9<=33-34%>34.9<=35-36%>36.9<=37-38%>38.9<=39-40%>40.9<=41-42%>42.9
42.9<=43-44%>44.9<=45-46%>46.9<=47-48%>48.9<=49-50%>50.9<=51%+
NOTE A VALUE OF>0.5-0.9<=.LT.1%AND.GT.0%

Fig 60.

OBSERVED NON-CYLYNDRICITY OF F3 FOLDS

0 M 1
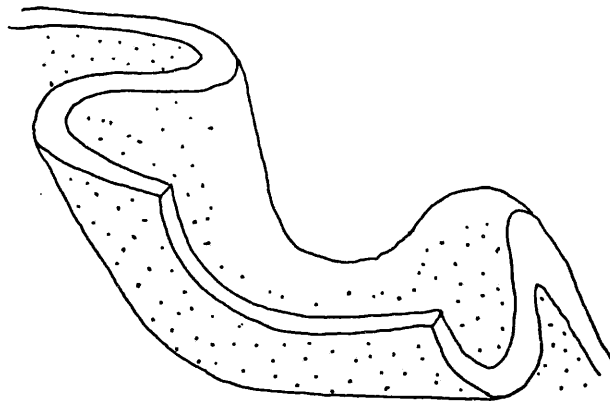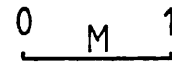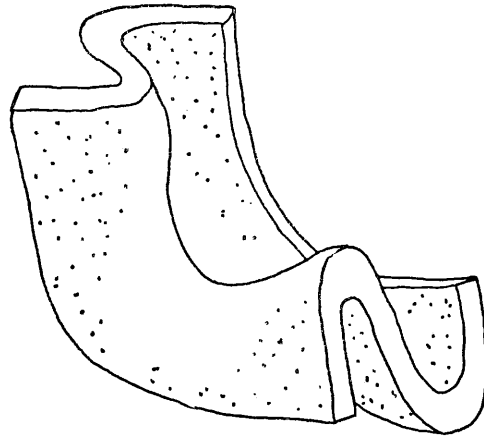
SIDE VIEW OF AN F3 FOLD HINGE

240°

Fig 61.

113
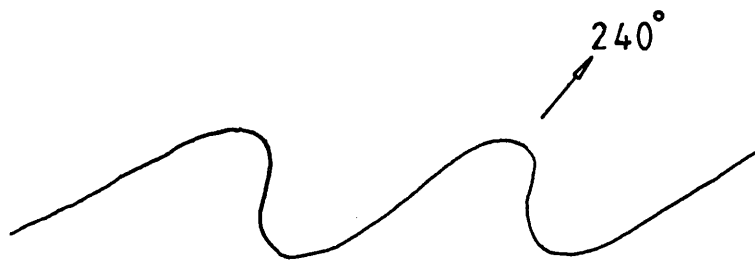
STYLE OF F3 FOLDS

Non Plane Non-Cylindrical Folds
With Cylindrical, Curviplanar
Axial Surfaces
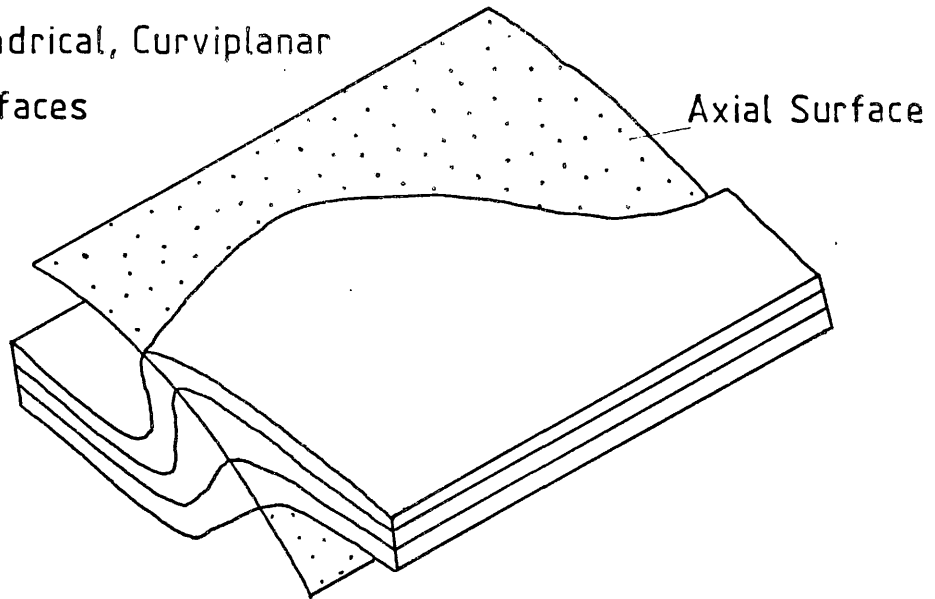
Axial Surface

Non Plane Non-Cylindrical Folds
With Non-Cylindrical
Axial Surfaces
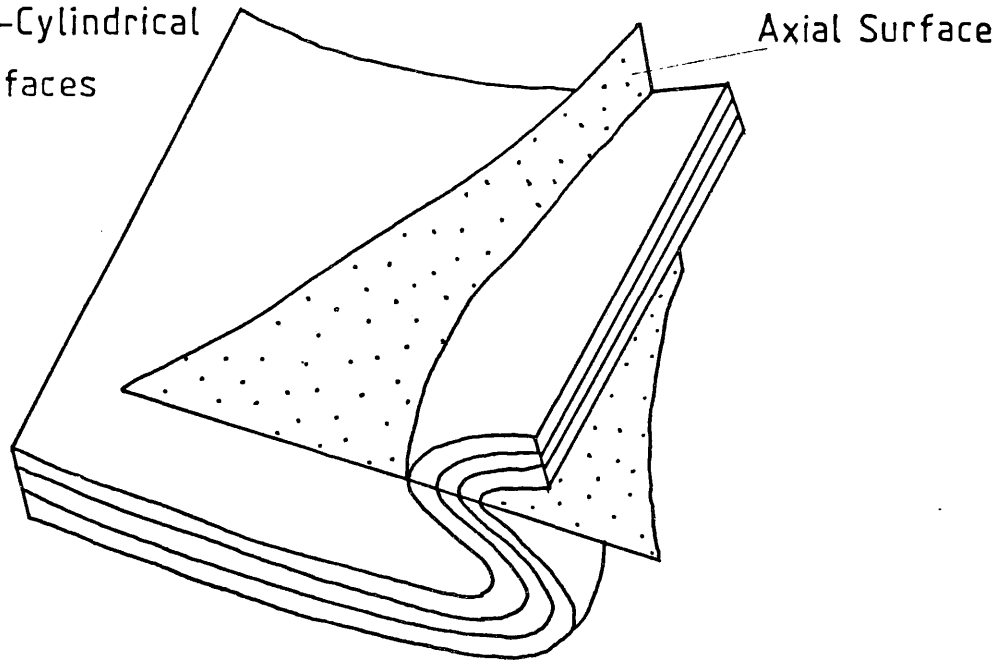
Axial Surface

Persistence of the Folds in Profile,
Along the Axial Surface.

Axial Surface

Fig 62.

114

EXPLANATION FOR THE VARIATION IN F3 PLUNGE SEEN IN
Fig 59

Plunges on a
Non-Cylindrical
Fold With
The
Axial
Plane
Horizontal
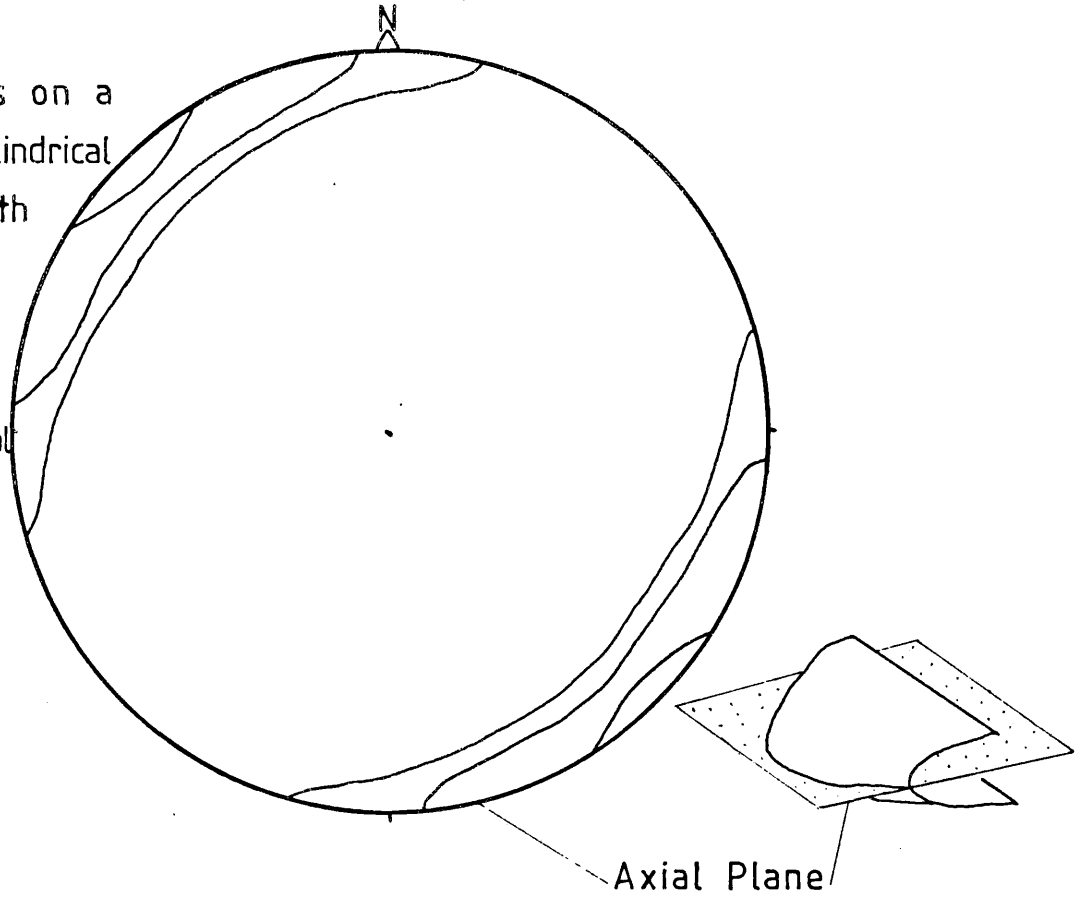
Axial Plane

Plunges on a
Non-Cylindrical
Fold With
The
Axial
Plane
Vertical

Axial Plane
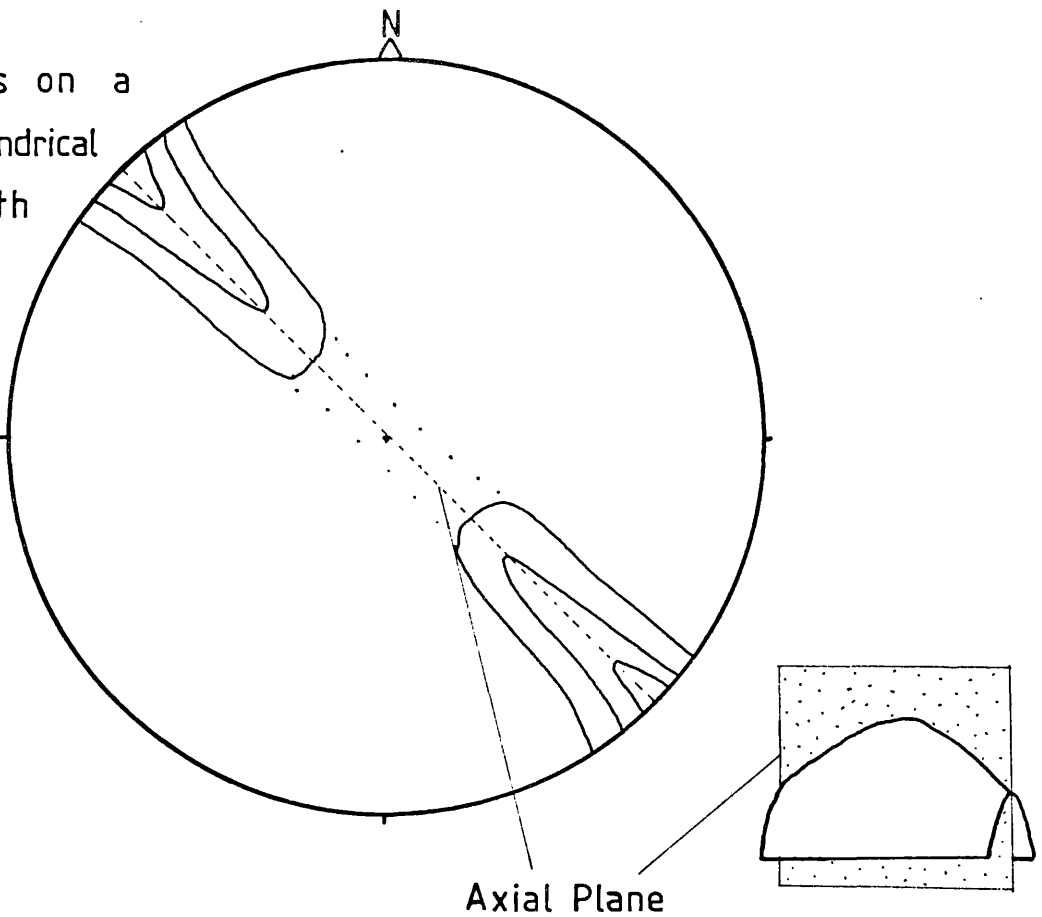
The mean plunge of F3 is 135/10° (defined by the longest portion of the more cylindrical members) and there is a slight (10°) rotation of this across Osterøy accompanying the "swing" of the Arcs. As the folds become more non-cylindrical the axial curvature becomes asymmetric, with the "culminations" pointing to 240 or 060° (fig.60). This situation is similar to that found on Sørøy (Ramsay & Sturt,1973), but in contrast the "synformal" culminations are no tighter than the "antiformal".

The non-cylindricity of F3 folds varies over the Southern gneiss outcrop and is controlled by two factors:

1)   The position of the fold in question relative to the fold on which it is parasitic.

2)   The "competence contrast" between the folded layers involved and their absolute and relative thicknesses.

The first of these controls is well known and described by Ramsay and Sturt (1973). They measured the angle between the axial plane and the mean attitude of the layering and plotted this against the axial deviation (fig.63). It is impossible to produce such a plot for F3, because, as described above, the axial plane does not provide a constant reference. Also the Osterøy gneisses do not provide adequate exposures of complete surfaces, in a limited area needed for such a diagram to be reliably constructed. It is possible, however, knowing the morphology and position of the largest scale F3 fold which affects the whole Southern gneiss outcrop, to comment objectively on the observed axial deviation in outcrop-sized minor folds in various situations on the larger structure. On the gently dipping long limb, these minor folds are markedly non-cylindrical; an example is seen in the road section at (09.50,34.60), this is typical of the style of F3 along strike. The nose of the main fold crops out in the lake at (11.50,24.00); on its north shores the

Fig 63.

NON-CYLINDRICITY AND THE ANGLE BETWEEN THE AXIAL
PLANE AND THE MEAN ATTITUDE OF THE LAYERING
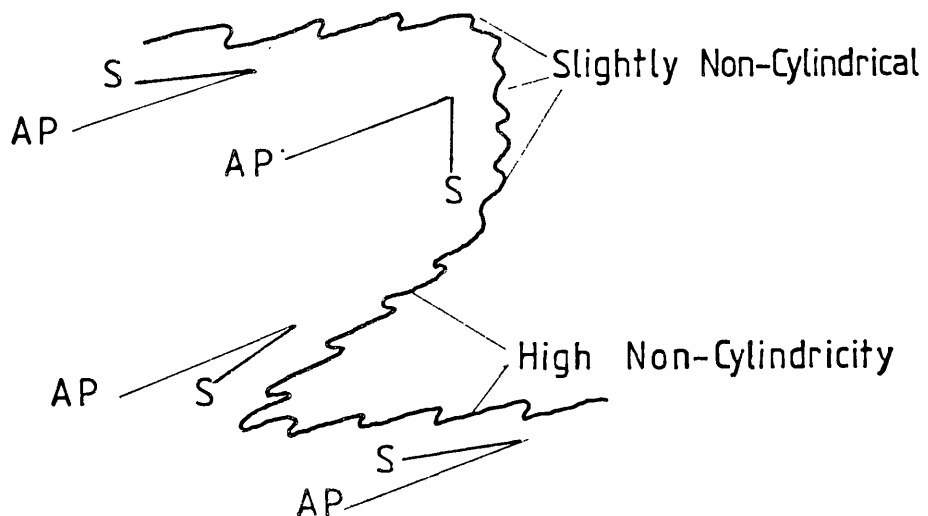
AP = Axial Plane
S = Mean Layering
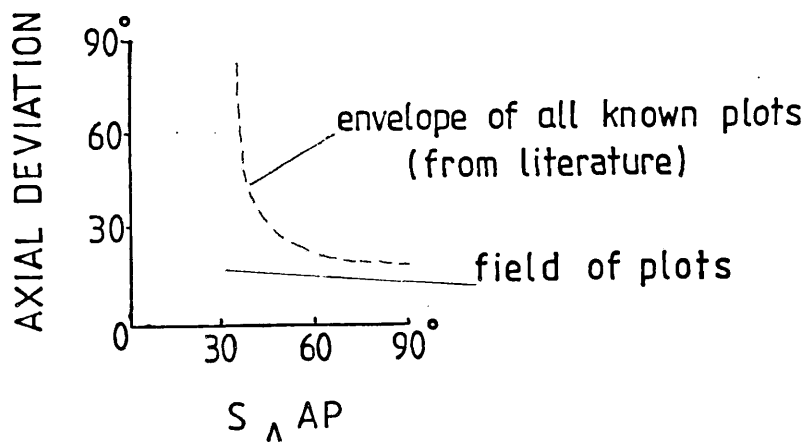
foliation is steeply dipping and the minor folds show less axial deviation, the deviation also occurs over much longer lengths of axis. The F3 folds conform then to the pattern of non-cylindricity described by Ramsay and Sturt, despite being generally more complex in development than the Sørøy examples.

A second factor is that under the prevailing metamorphic conditions (lower greenschist facies), it was the melanocratic portions of the multi-layers that were the most ductile (p.103, figs.50 & 51). Where a sequence comprising a leucocratic layer set in a melanocratic matrix was involved in F3 folding, the folds developed show extreme axial deviation regardless of position on the mother fold (pl.32). The effect becomes less marked as the relative thickness of the leucocratic layer increases and as the absolute thickness of the leucocratic layer increases while the relative thickness of the multilayer components remains constant.

Discussion on F3

The above observations provide an insight as to how non-cylindricity develops. Biot (1961 & 1964), Ramberg (1959) and Ramsay (1967), show that the wavelength of folds is dependent on the thickness of the buckling layer and the viscosity contrast between the folding layer and the matrix (virtually constant for the Southern gneisses in D3). Further, Cosgrove (1976), shows that in a multilayer in which individual layers are of varying thickness, the thinner layers fold in advance of the rest. It is therefore reasonable to assume that the extreme non-cylindricity seen in thin layers is controlled by the time of fold formation. This observation is borne out by the fact that changes in the relative and absolute thicknesses of the layers is accompanied by changes in geometry.

The obvious explanation as to why early formed folds are the most non-cylindrical is that they have been more flattened as the deformation progressed. A high degree of flattening would also be true for the folds in the major-fold limbs (fig. 63).

It follows from the non-cylindricity of folds observed in the field that it should be possible to observe a change in fold style as one moves from place to place along the axis. Unfortunately, it was not possible to do this on a single fold in the field or the laboratory, but many profile view photographs were taken of the F3 folds, then analysed by dipisogons and t'_{α} plots (Ramsay, 1967). Some of these analyses are presented (figs. 64, 65, 66 & 67). From these it is seen that the basic style of the F3 folds is class 1C, with class 1A and 1B elements appearing in some layers. This probably means that when first formed the folds were class 1A or 1B and the 1C geometry developed subsequently as they flattened. Where the middle limb of the fold begins to shear, the geometry changes from class 1C to class 2 in the shearing limb. Where the non-cylindricity begins to develop, seen as a progressive thickening of the layers in the nose region, the modification of the 1C geometry is to class 3.

This describes the over-all trend, but as is seen from figures 66 and 67, the fold geometry tends to become complex because the folding layers are not perfect and shear on the middle limbs occurs simultaneously. The situation seen in the F3 folds is summarised in figure 68, and it is important to note that any one fold dies out as one moves in any direction in the plane of the axial surface, away from the point of maximum axial deviation (fig. 61). In the third dimension, the situation is as shown in figure 69; in a profile through D where the folds are "dying out" a class 1A geometry is inevitable. It is therefore clear that the production

Fig 64.

PROFILE SECTION THROUGH AN F3 FOLD, WITH ISOGONS

Dip Isogons

[Fold Class Determined
From Isogons and
t'α Plots]

Melanocratic

Class 1C

Leucocratic

Class 1C-1B

Class 1C

Melanocratic

Fig 65.
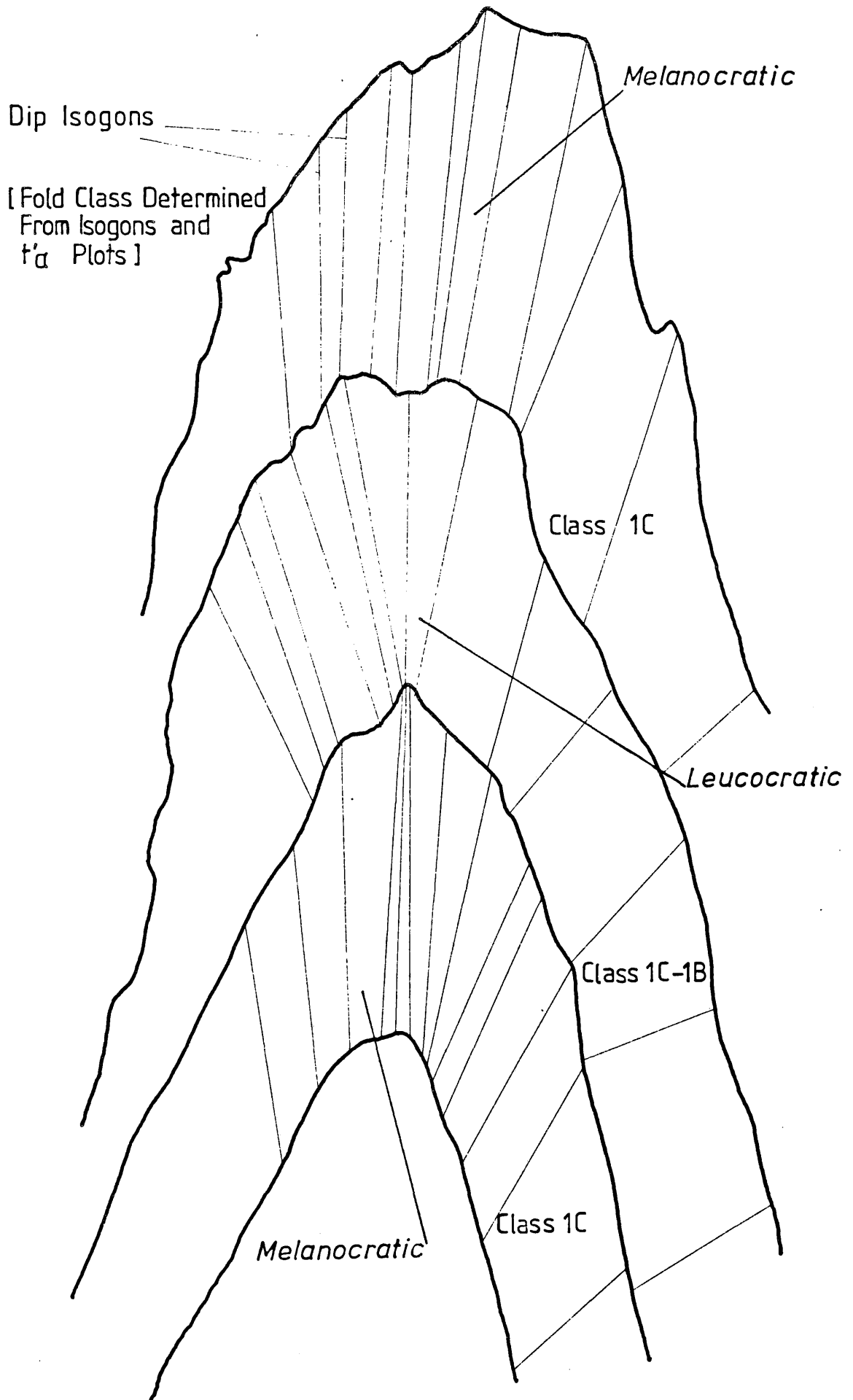
PROFILE SECTION OF AN F3 FOLD WITH DIP ISOGONS

Dip Isogons

Leucocratic

Melanocratic

Class 1C

Unclassifiable

Class 3

Class 2 Limbs

Unclassifiable

Class 1C

Leucocratic
Melanocratic

[Fold Class Determined From Isogons and t'_α Plots]

Fig 66.
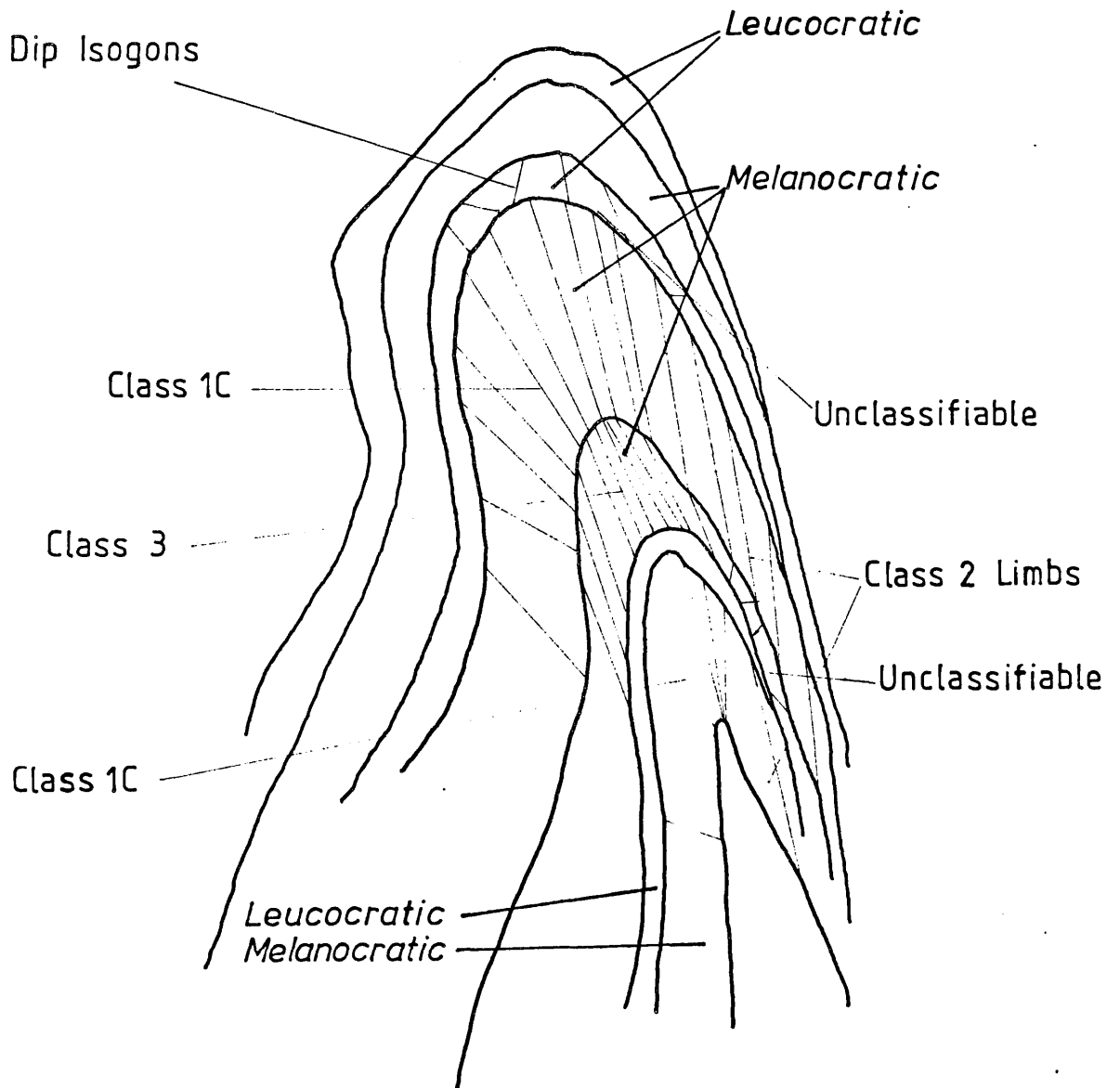
PROFILE OF AN F3 FOLD SHOWING
MODIFICATIONS CAUSED BY EXTREME
CONTRAST IN COMPETENCE BETWEEN
THE LAYERS

3

Amphibolite

Acid Gneiss

3
or 1B

Unclassifiable

1A

1C

2

Fig 67.

Isogons

Leucocratic

Layer with a 1B Geometry

1C Layer

1A Layer

Class 3 Portions

Melanocratic

[Classes Determined from the Isogons and t'_α Plots]

0   M   1

Fig 68.

GEOMETRY OF A LAYER IN SUCCESSIVE PROFILE SECTIONS
ACROSS A NON-CYLINDRICAL [F3] FOLD
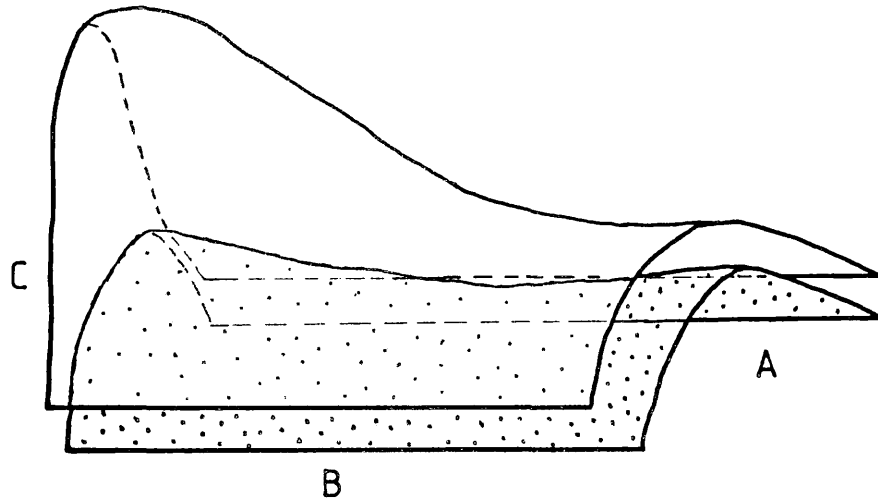
SECTION		CLASS
A		1A / 1B
B		1C
C		3

Fig 69.   124
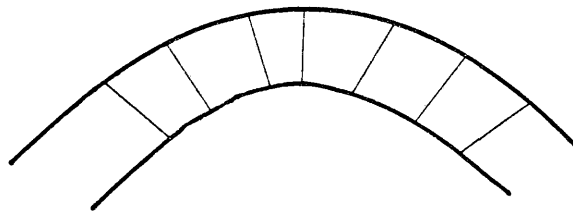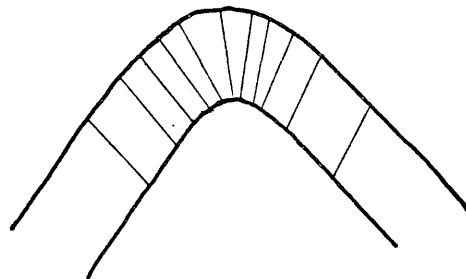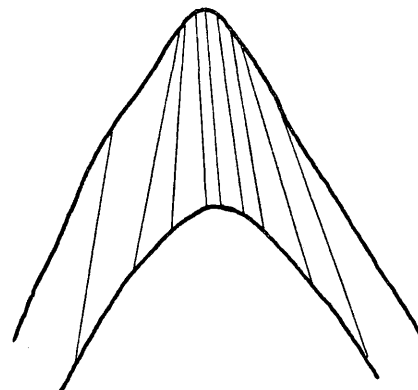
DIAGRAM EXPLAINING WHY 1A GEOMETRIES ARE FOUND IN

THE F3 FOLDS

D

Class 1A

Dip Isogons
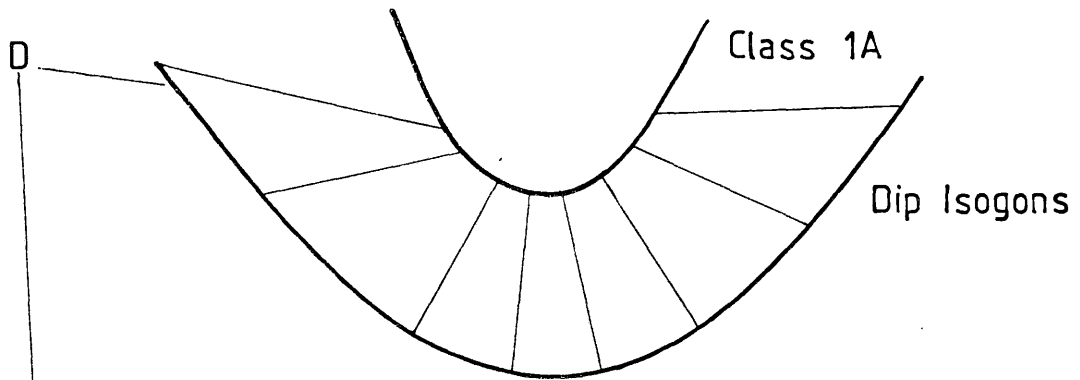
REPRESENTATIVE F3 FOLD

D
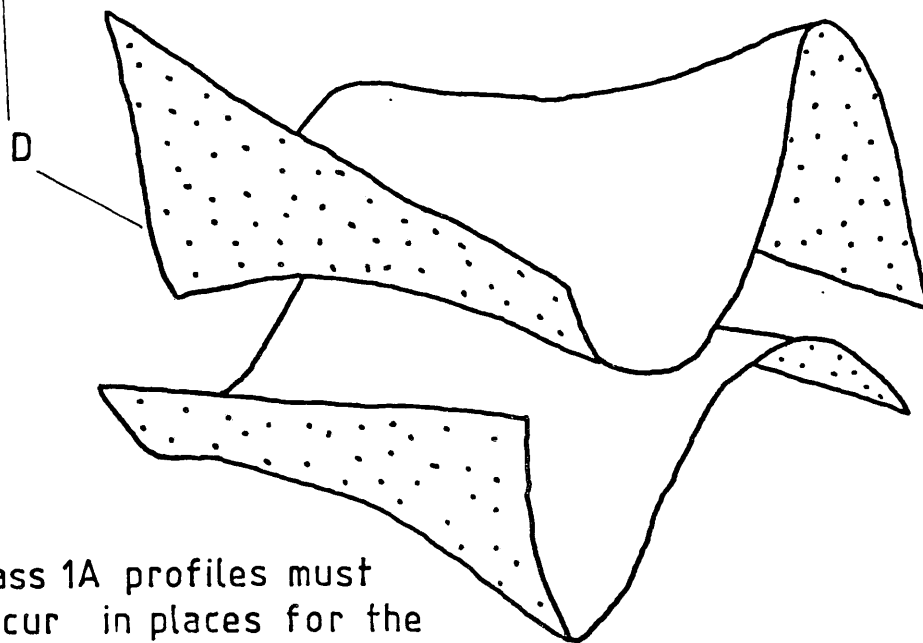
[Class 1A profiles must
occur in places for the
non-cylindrical folds to fit
together across the layering]

of non-cylindrical folds induces the production of class 1A and class

3 geometries. A single layer traced out in three dimensions is folded

in all classes (except class 2) in different parts, (the class 2

geometries being interpreted as the product of a different deformation

process which acts after the folds initiate). The fold pattern produced

interlocks, such that the total shortening across any one layer is the

same in any section cut normal to the average profile, provided a number

of whole wavelengths are involved. The layer when unfolded would be

rectangular (fig.70, pl.35).

This style of development requires the movement of material, not only

in a direction parallel to the axial plane, from the limbs to the crest,

but also in the plane of the axial plane, parallel to the crest (from

areas (a) to areas (b) fig.70). We can therefore consider the fold

geometry in a section parallel to the axial plane cut through the hinge.

Figure 71 summarises the possible geometries. The thickening in the

hinge region where the geometry parallel to the axial plane is class 1A/3,

is accommodated more by movement of material from the limbs than along

the crest. It thus accompanies the development of a class 3 profile

geometry (fig.72). This relationship is only developed if the deformation

process is one of heterogeneous simple shear.

A lineation, L2 develops with the F3 folds. This has two components;

on the layering surfaces it is defined by inequidimensional mica flakes

or mica flakes included at differing attitudes to S1/S2 and therefore

presenting elongate sections on the foliation planes. Within and on

the more leucocratic layers, the lineation is further seen as elongate,

spindleform grains of quartz or feldspar lying at an angle to the S1/S2

foliation surface. This may develop into a ridge and groove structure

closely resembling slickenside lineation where the plane of the foliation

Fig 70.

DIAGRAM OF A NON-CYLINDRICALLY FOLDED LAYER

One 'Set' of

Folds

(b)

(a)

Two 'Sets' of Folds

Showing the Inevitable

Geometry of the

Interlocking

1

2
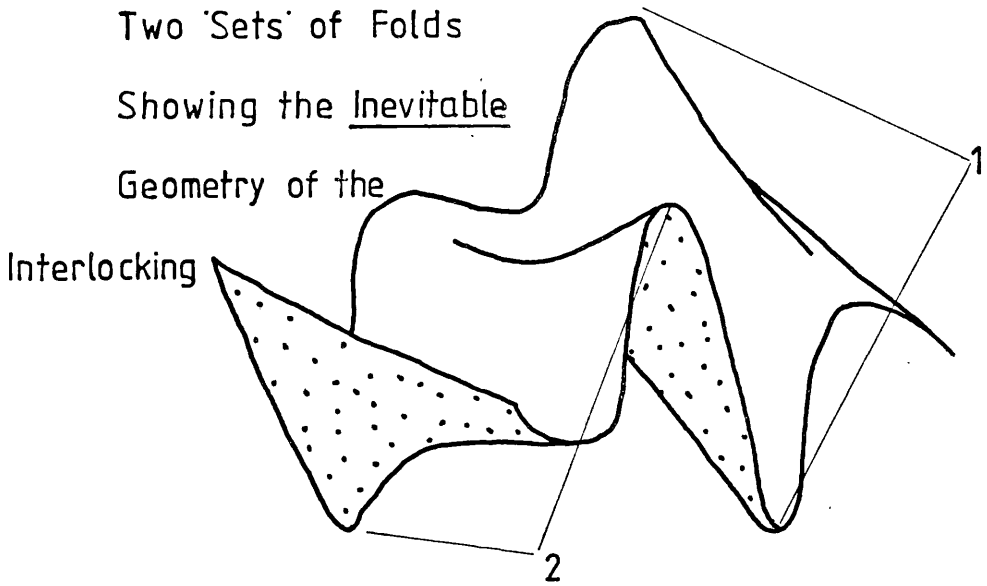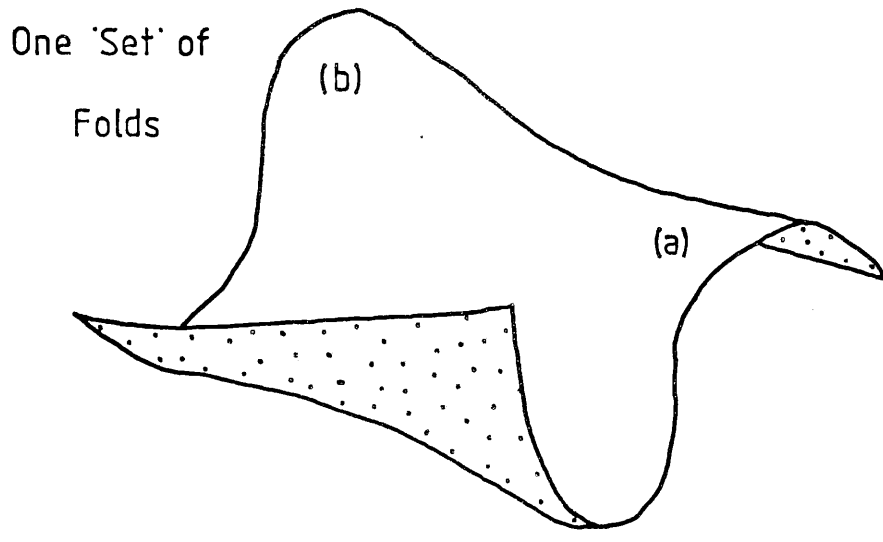
NOTE- While the Deformation is Only Buckling the Layer

Remains RECTANGULAR.

[Fold Culminations Must Therefore Form an En-échelon

Pattern]

Fig 71.

127

CYLINDRICAL AXIAL PLANE SECTION

All Classes of Fold ⟶

NON-CYLINDRICAL FOLDS LOOKED AT IN AXIAL PLANAR SECTION

PROFILE GEOMETRY ———— CORRESPONDING AXIAL GEOMETRIES

Class 1A

Class 1B

Class 1C

1B

Dip Isogons

Class 1 ⟶

Class 2

Class 1

Class 2

Class 3

3

1A

Class 2 ⟶ Class 2

Class 3 ⟶ Class 3

=

3

1A

1B

Note, 1B or (3 / 1A)

Fig 72.
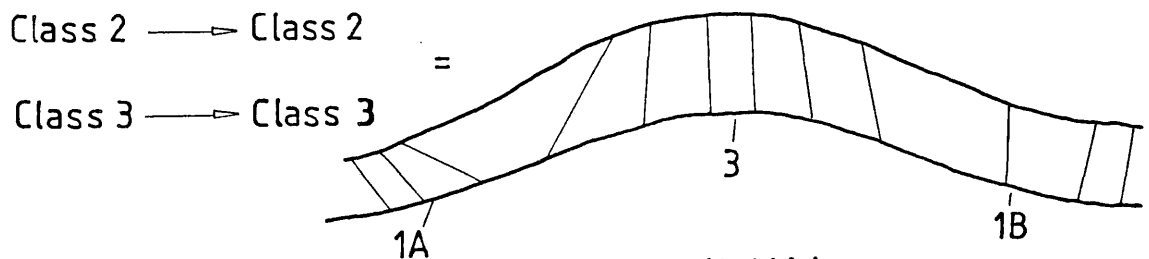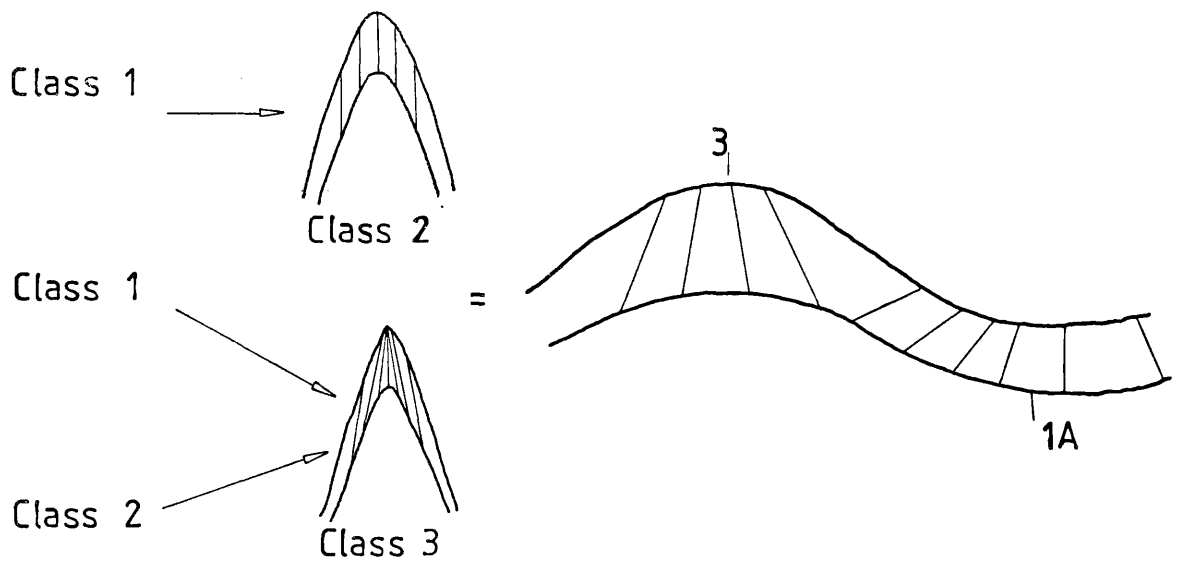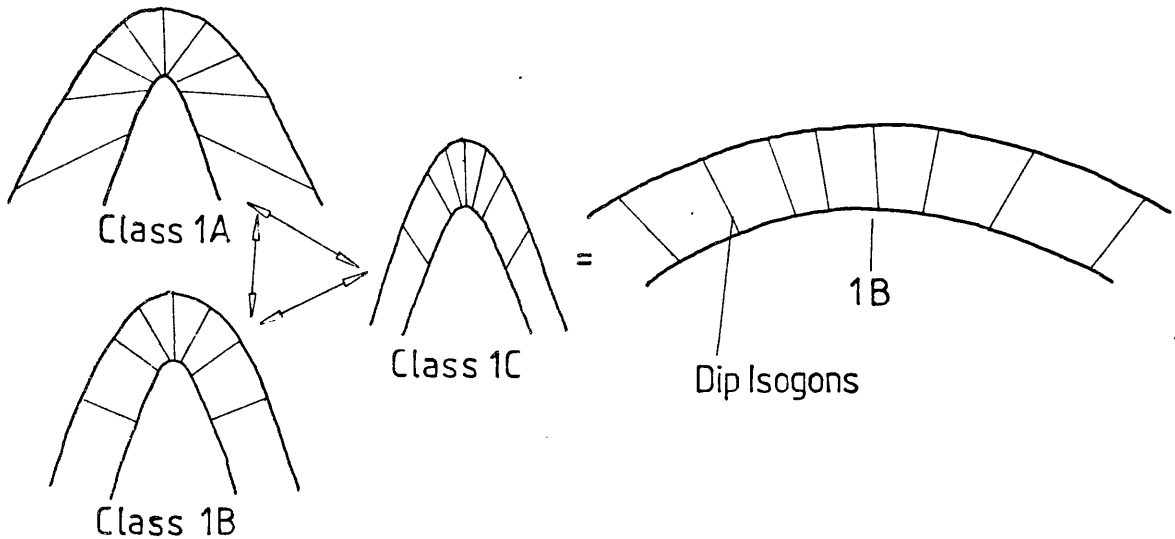
MOVEMENT OF MATERIAL DURING HETEROGENEOUS SIMPLE SHEAR

axial plane

Movement Parallel to the Axial Plane

apparent transport direction

Transport of Material From the Limb Regions to the Nose Region
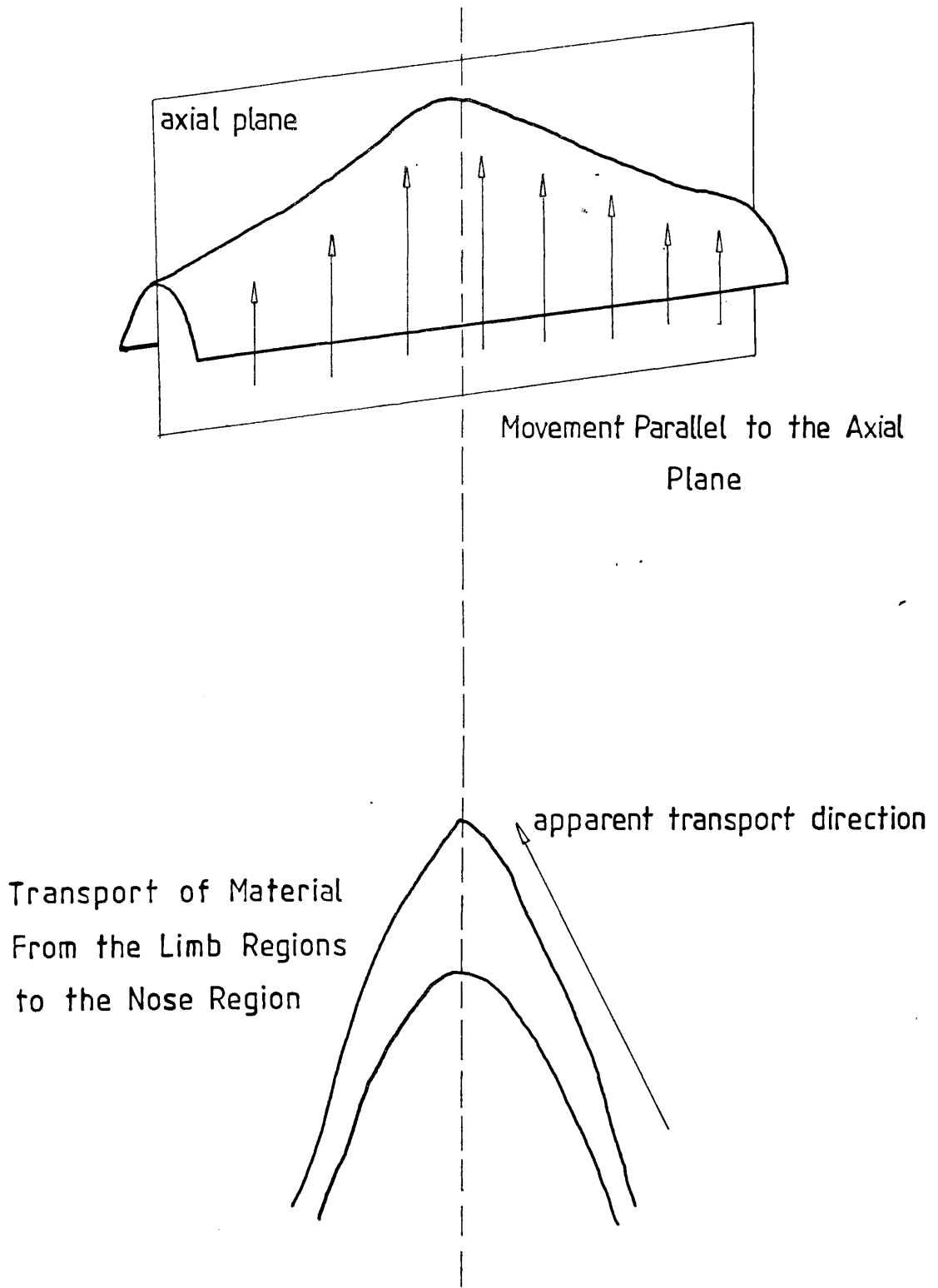
lies close to the long axis of the "spindles". This latter component is only strongly visible in thinner leucocratic layers showing extreme axial deviation.

As described by Ramsay and Sturt (1973), similar lineations can be interpreted as the product of layer parallel extension in the long axis of the sectional strain ellipse (x') for any particular foliation attitude.

The lineation then shows the direction of mass transport on any one plane, and when the geometry of the lineation is considered over-all it defines the direction of tectonic transport during the shearing (α) (fig.73). The geometry of this lineation on a fold is described by Ramsay and Sturt (1973). In their examples the lineation is not present in regions of the fold where the foliation is at a high angle to the (X) direction of the strain ellipsoid, (the regions of axial culmination). Ramsay and Sturt suggest that the lineation developed in a constrictional regime (K$>$1). As is seen from figure 73, the L2 lineation is present all round the F3 folds and forms a hinge parallel lineation along the entire length of the hinge. This suggests that during the production of L2 the deformation plane strain (K=1) was operative. The situation is, however, more complex than this since examples of F3 folds were found at (08.70,31.00) where L2 was refolded round the nose of minor F3 folds lying on the long limbs of larger F3 folds (fig.74). This implies that the development of F3 structures was long lived and multi-staged, once a fold was formed by flexural slip/tangential longitudinal strain (Ramsay, 1967), the deformation switched to a process of heterogeneous simple shear, while on the long limbs new folds were initiated. Similar observations have been made on the folds from Sørøy (Ramsay & Sturt,1973).

The development of non-cylindrical folds has also been described by Knill and Knill (1958), Voll (1960), Brynhi (1962) and Ramsay (1962,1967).

Fig 73.

RELATIONSHIP OF L2 TO THE F3 FOLDS

Non-cylindrical F3

L2

Tectonic 'a' Direction

L3

F3

S1/S2

Weak S3 in
Nose Region

L3 Turns Parallel to
The Hinge at the
Crest of the Fold

0   M   0.3

Fig 74.

131
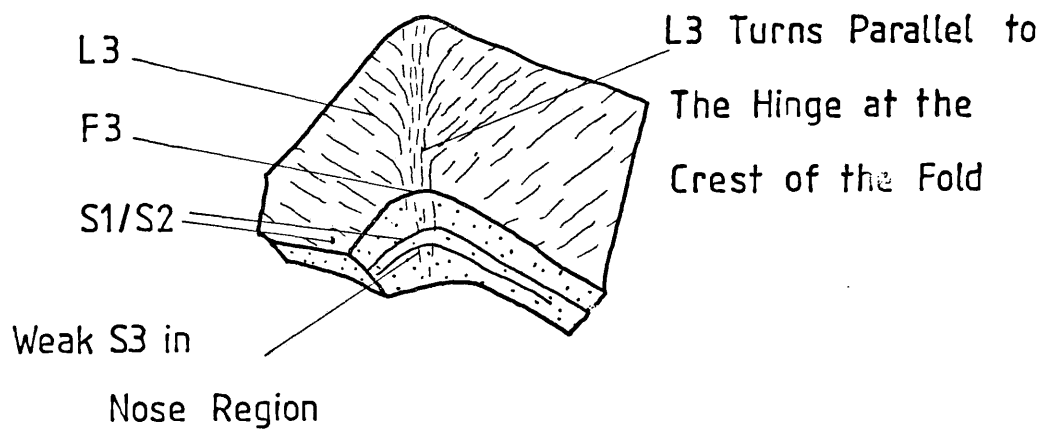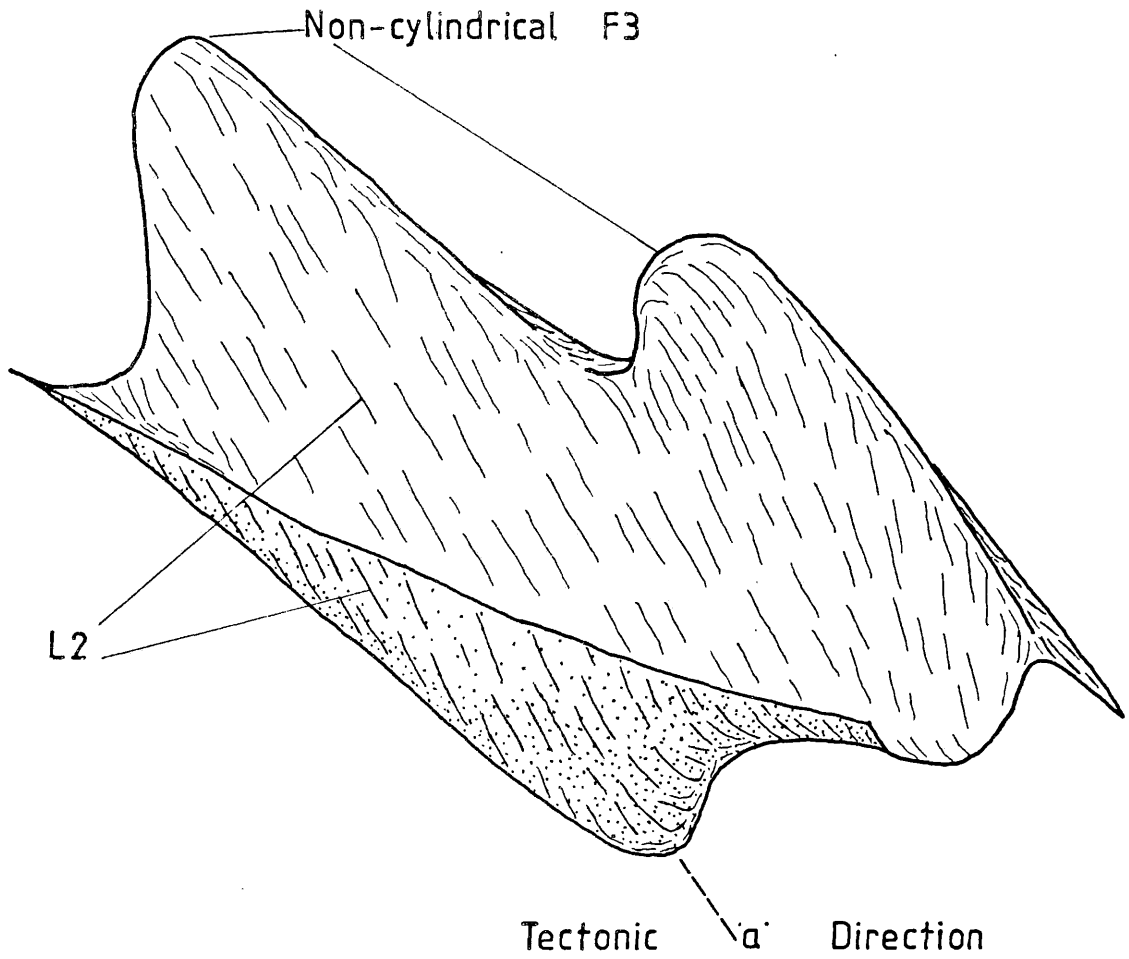
DIAGRAMS SHOWING HOW L2 IS FOLDED BY SOME LATE DEVELOPING F3 PARASITIC

FOLD

Deformed L2

L2

Late F3 Parasitic Folds

F3

0   M   1
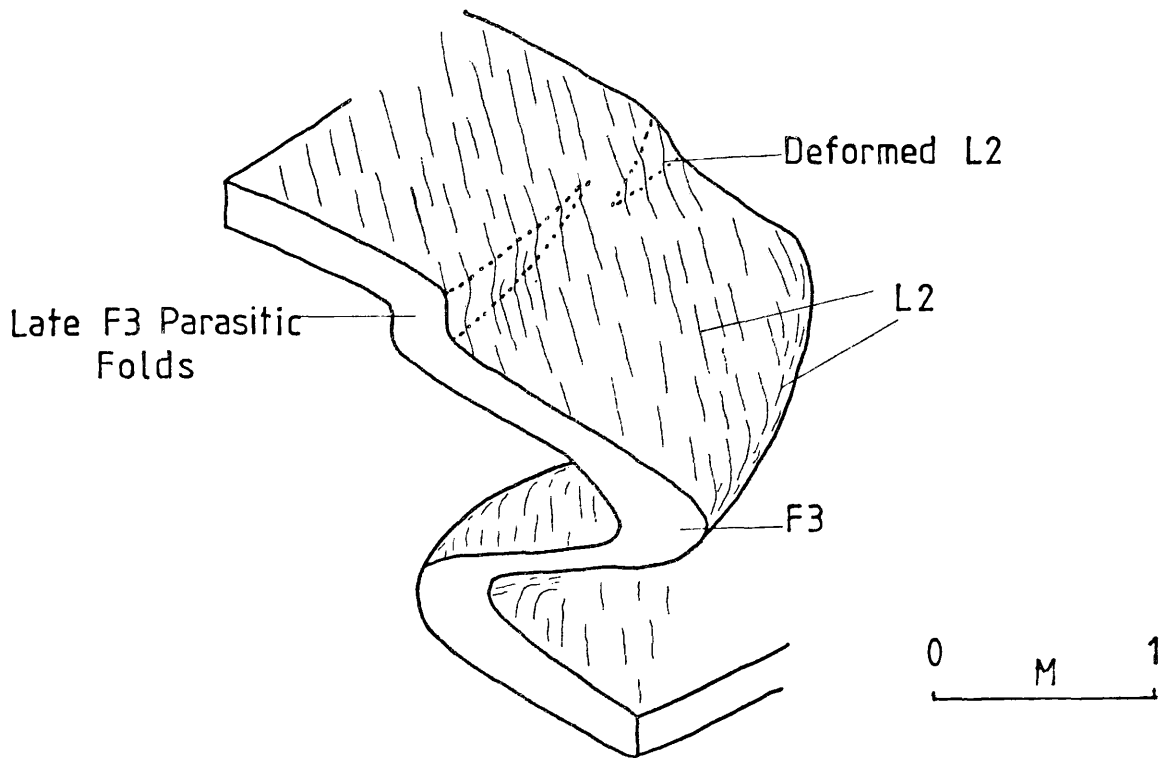
SIMPLIFIED GEOMETRY OF MODIFIED L2

140°

Shallow Limb of Late Parasitic Fold

Plots of L2.

L2 Trace

Steep Limb

S1/S2 Defining the Fold
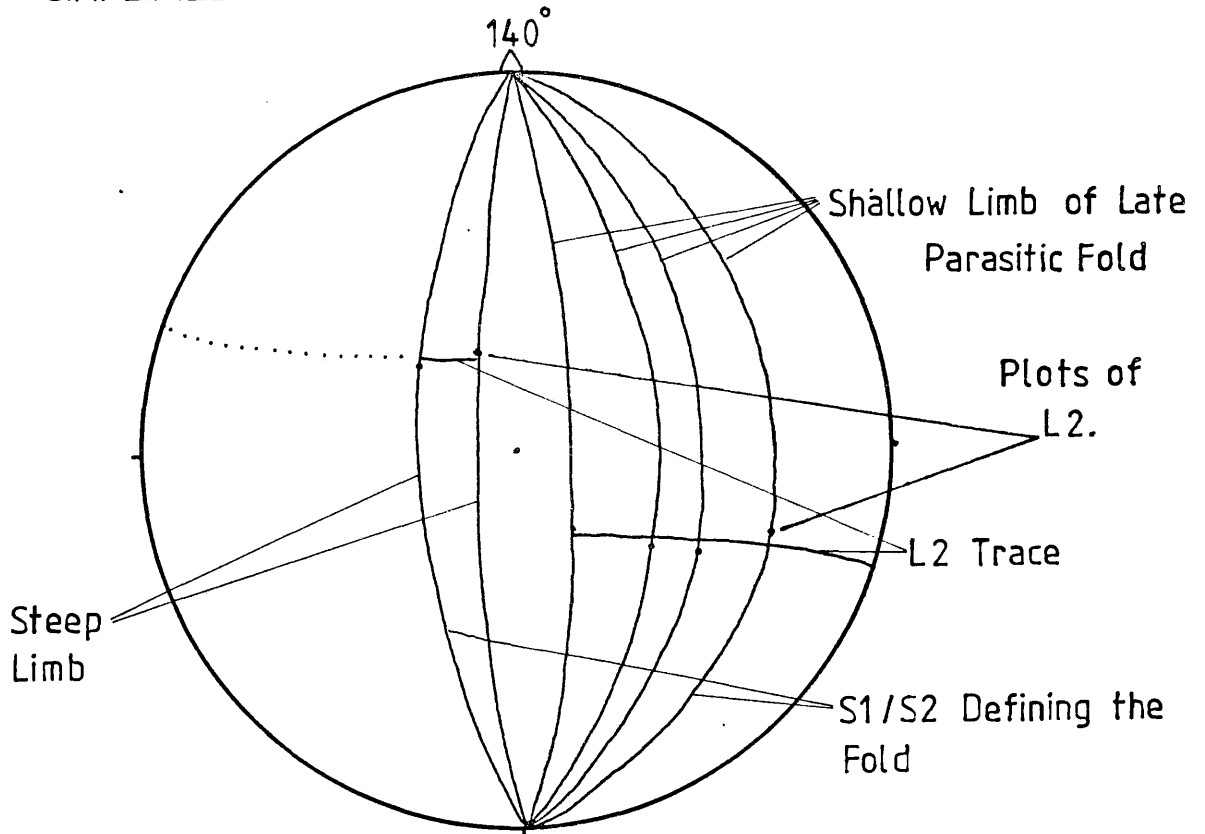
Note- Plunge of F3 Removed

There are four explanations as to their formation, summarised by Voll (1960):

1) Unequal stretching along the strike of the axial surface (internal rotation).

2) Passive rotation of detached hinges between discrete schistosity surfaces (external rotation).

3) Buckling of the layer prior to the development of the schistosity, which thus produces a curvilinear intersection with the layering.

4) Layering planes intersected by schistosity with different attitudes.

Ramsay and Sturt (1973) suggest that the range of complexity of structure observed can only be explained by non-uniform flow parallel to the axial surface between adjacent folds; they suggest that the non-uniform flow is the result of flattening $(K < 1)$ superimposed on folds initially formed in the constrictional field $(K > 1)$. Rhodes and Gayer (1977), suggest they are produced by layer parallel shearing during nappe translation. Fold hinges develop in the Y direction and rotate into X as the result of large strains at points of high cohesion.

It is considered that methods (3) and (4) are special situations and should be disregarded as not pertinent to the observed situation on Osterøy. Methods (1) and (2) are both possible but on the evidence from Osterøy, internal rotation (1) seems more likely because of the range of fold styles produced, the nature of L2 and the general geological context in which the folds form. The mechanism postulated, unlike that of Ramsay and Sturt, starts with a flexural flow tangential longitudinal strain deformation $(K < \text{or} = 1)$, which, after the folds "locked up" changes to a process of

heterogeneous simple shear (K=1), the greatest axial deviation occurring in the regions of highest strain, the "less competent" melanocratic layers deforming ahead of those which are leucocratic.

The hypothesis is further supported by the behaviour of L1 deformed round F3 folds. Figure 75 is a plot of L1 across the Southern gneisses, the pattern seen is interpreted as in figures 76 and 77. Stage 1 shows the original geometry of L1 (slightly disturbed by D2), Stage 2 shows L1 folded by F3, where the folds have a 1A-1C geometry. At this point the deformation could no longer proceed by flexural slip (flow)/tangential longitudinal strain, because the folds "locked up". The deformation process then switched to one of heterogeneous simple shear and the folds flattened. The Y axis at this stage had shifted so that the shear was oblique to the original fold axis (thus explaining the asymmetry in axial curvature), Stage 3. This produced a final distribution of L1 plunges as shown in Stage 4 (compare this with figs.75 & 78).

There is no evidence in the Southern gneisses to support Rhodes and Gayer's (1977) model of layer parallel shearing, indeed it is clear from the broad scale development of the major F3 folds that this model is untenable. The process must be fundamental to the deformation regime rather than a "special situation".

It is thus postulated that the non-cylindricity is the result of the mechanical state of the rock at the time of deformation and the mechanism by which it starts to deform. The rocks were at a metamorphic grade where there were marked mechanical (ductility) contrasts between layers of differing composition; the layering was very irregular and the rock locally extremely heterogeneous. The deformation started with folds initiating at points of heterogeneity, forming discrete buckles of the layering (pl.35), at numerous sites in the rock at one time. These folds

Fig 75.

PLOT OF L1 FROM THE SOUTHERN GNEISSES

PLOT OF SG.LINEATION

THIS PLOT HAS UNDERGONE -0- ROTATIONS

USING CORDINATE CARD   0

SAMPLING   2ACROSS/- 1DOWN   POLES PER   1PERCENT AREA   284 DATA   EQ AR

THE CONTOURS REPRESENT THE FOLLOWING PERCENTAGES

00.9<=1-2%>02.9<=3-4%>04.9<=5-6%>06.9<=7-8%>08.9<=9-10%>10.9<=11-12%>12.9
12.9<=13-14%>14.9<=15-16%>16.9<=17-18%>18.9<=19-20%>20.9<=21-22%>22.9
22.9<=23-24%>24.9<=25-26%>26.9<=27-28%>28.9<=29-30%>30.9<=31-32%>32.9
32.9<=33-34%>34.9<=35-36%>36.9<=37-38%>38.9<=39-40%>40.9<=41-42%>42.9
42.9<=43-44%>44.9<=45-46%>46.9<=47-48%>48.9<=49-50%>50.9<=51%+
NOTE A VALUE OF>0.5-0.9<=.LT.1%AND.GT.0%

Fig 76.

PROPOSED PATH FOR DEFORMATION OF L1, PART 1

STAGE 1

Original L1 Geometry
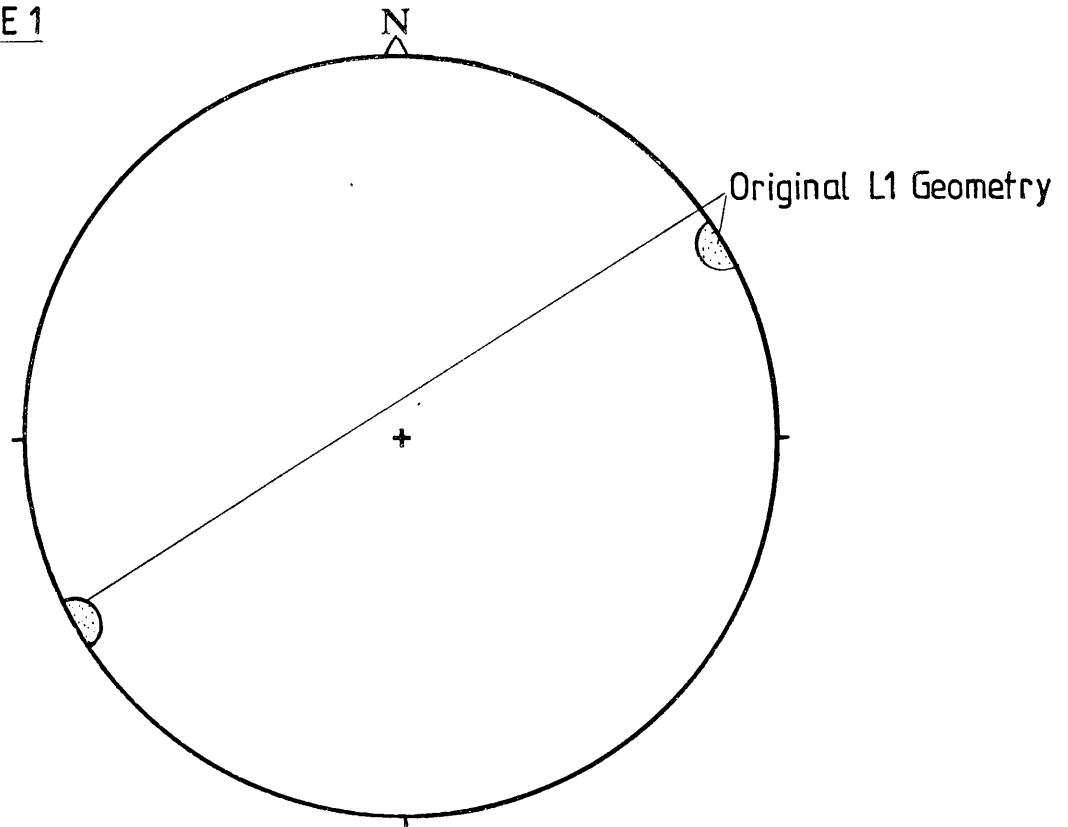
STAGE 2

Area Occupied by L1
After - Flexural Slip /
Tangential Longitudinal
Strain Deformation

Axial Plane [A P]

ΠGirdle of F3

(a)

(b)

AP

Shallow Limb

F3 Steep
Limbs, some
Overturned

a < b

Fig 77. 136
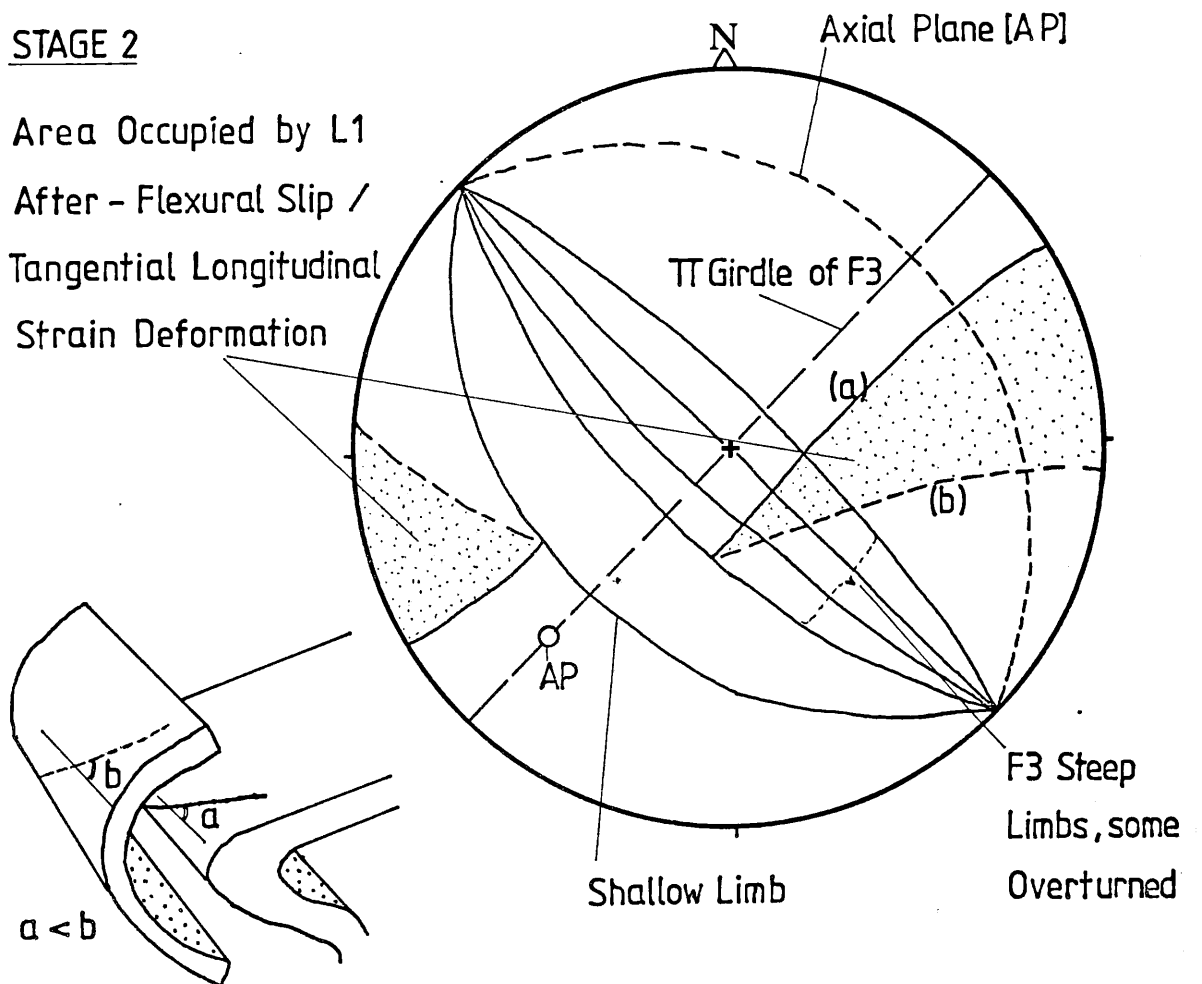
PROPOSED PATH FOR DEFORMATION OF L1, PART 2

STAGE 3

Lines of Movement Traced
by L1 During the Second
Stage of Deformation
by Simple Shear
Processes

L1 as it was at the
End of Stage 2

F3 Axial
Plane

'a' Direction of
Tectonic Tran-
-sport in
Simple
Shear
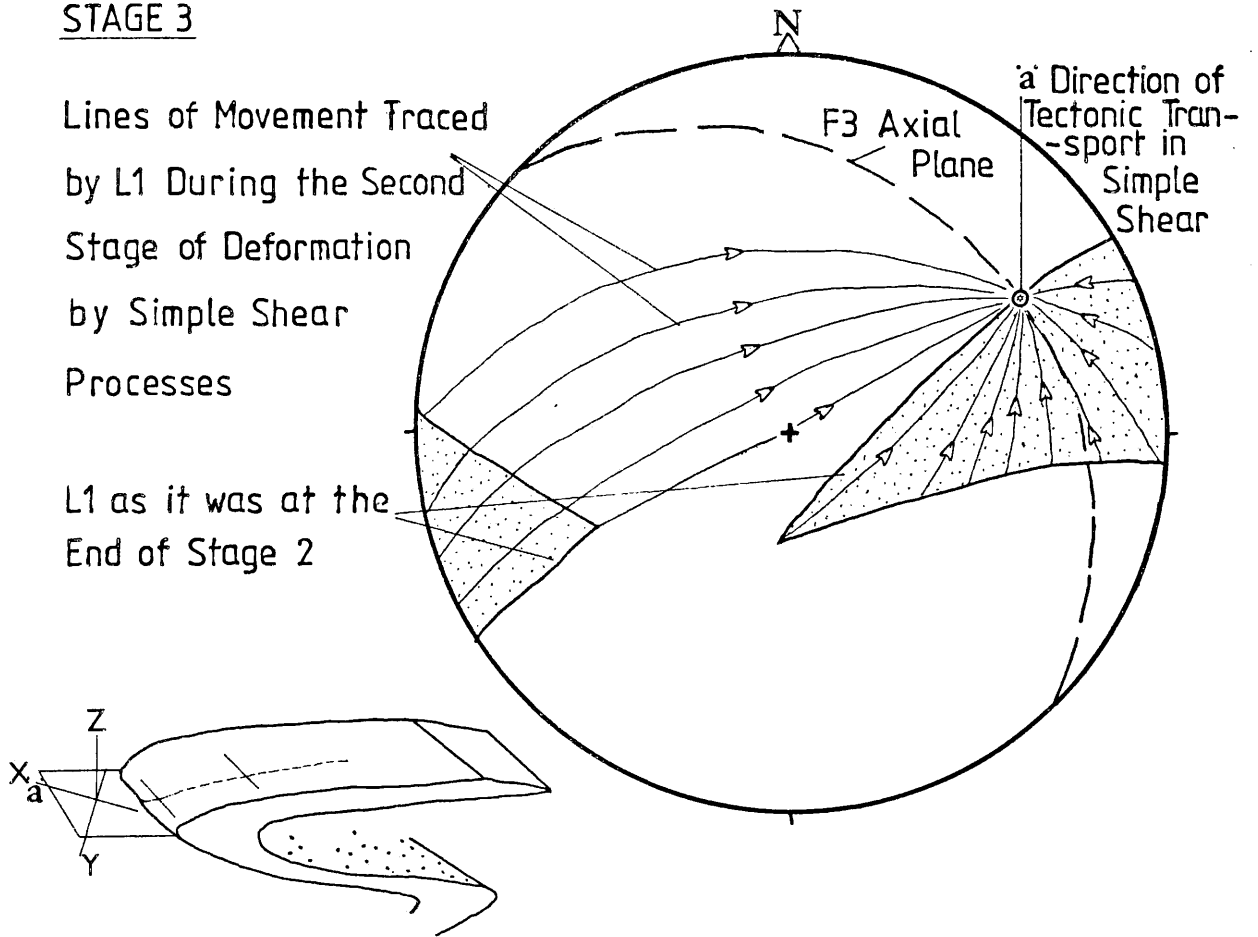
STAGE 4

THE SCATTER OF L1
WHICH WOULD
RESULT FROM
THESE PROCESSES
[Compare this
with the actual
scatter plotted
in Fig 75]
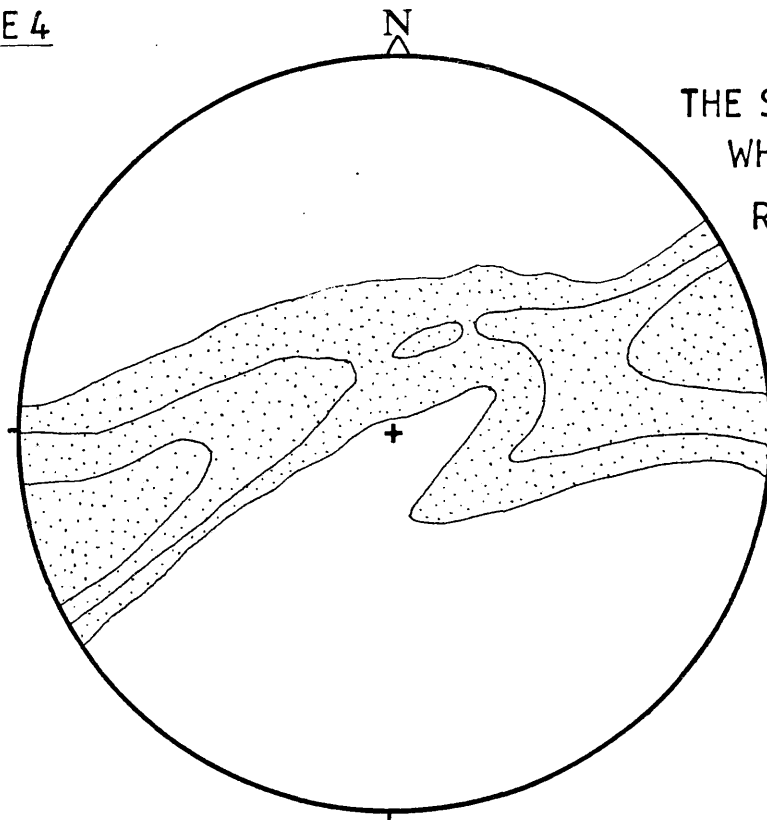
Fig 78.

SKETCH SHOWING HOW F3 WAS OBSERVED TO AFFECT

L1 IN THE SOUTHERN GNEISSES

F3 Fold Culmination

c

b

L1

a

Axis of F3

a > b > c
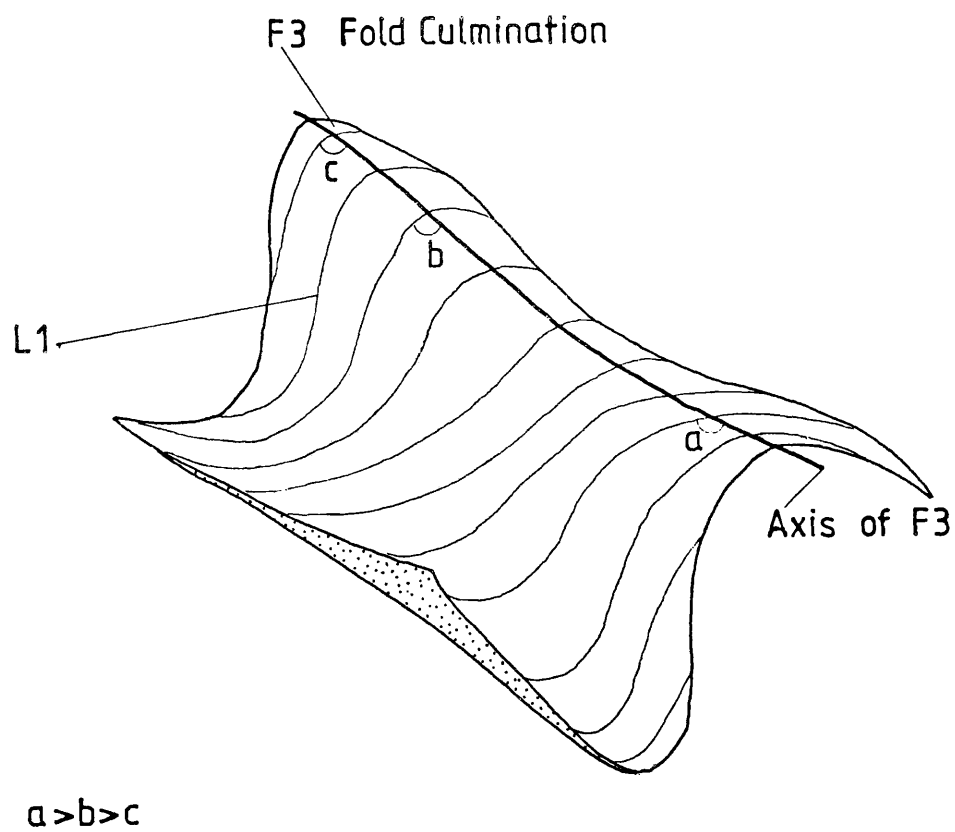
[This Geometry Supports the Deformation Path

Proposed in Figs 76 & 77]

amplified and extended axially from their points of formation until they met another fold and interlocked. Because the folds did not initiate regularly, it is unlikely that every crest would merge with a crest (Dubey & Cobbold,1977), and certain folds developed in advance of the rest to form an en-echelon pattern (pl.35). Smaller folds became parasitic on the larger folds and the buckling surface was first affected by a harmonic spectrum of developing folds with differing wavelengths and amplitudes, yet with constant wavelength/axial length/amplitude ratios. Thus preserving an identical "initial buckle" geometry throughout the layer. The layer, therefore remains rectangular at this stage (fig.70). Amplification continued until the folds "locked up"; this occurred first at the points of initiation as, at any one time these would be the most developed. The folds then had a primary non-cylindricity. At the point of "lock up" the deformation mechanism changed to one of heterogeneous simple shear, and the nose region extended even more, thus enhancing the primary non-cylindricity and causing the extreme axial deviations observed, L2, and the asymmetry along the fold axis. The lack of a well developed schistosity while there is a strong L2 lineation is taken to indicate that the shearing process occurs in a near plane strain regime. Because the process involves two mechanisms, there will be a relationship between "tightness" of the fold and the axial deviation (fig.63).

In the more micaceous lithologies, a weak new schistosity, S3, developed parallel to the axial plane of the F3 folds. It is marked by a crenulation cleavage and a parallel alignment of quartz deformation lamellae (pls.36 & 46). S3 forms a weak intersection lineation, L3, with S1/S2 in the noses of some F3 folds, which is parallel to L2. It is parallel to the average plunge of the F3 folds (fig.79).

Fig 79.

PLOT OF THE L3 INTERSECTION LINEATION

PLOT OF BERGEN ARC FOLD PLUNGE PARALLEL LINEATION

THIS PLOT HAS UNDERGONE -0- ROTATIONS

USING CORDINATE CARD   0

SAMPLING   2ACROSS/- 1DOWN   POLES PER   1PERCENT AREA   31 DATA   EQ AR

THE CONTOURS REPRESENT THE FOLLOWING PERCENTAGES

00.9<=1-2%>02.9<=3-4%>04.9<=5-6%>06.9<=7-8%>08.9<=9-10%>10.9<=11-12%>12.9

12.9<=13-14%>14.9<=15-16%>16.9<=17-18%>18.9<=19-20%>20.9<=21-22%>22.9

22.9<=23-24%>24.9<=25-26%>26.9<=27-28%>28.9<=29-30%>30.9<=31-32%>32.9

32.9<=33-34%>34.9<=35-36%>36.9<=37-38%>38.9<=39-40%>40.9<=41-42%>42.9

42.9<=43-44%>44.9<=45-46%>46.9<=47-48%>48.9<=49-50%>50.9<=51%+

NOTE A VALUE OF>0.5-0.9<=.LT.1%AND.GT.0%

Also associated with the D3 deformation are two varieties of fracture and quartz veining. The first is associated with the F3 folds, the middle limbs of which develop shears (figs. 58 & 80). In some cases the shearing has proceeded to the point of rupture, where two adjacent fold noses are separated along a local thrust. In the thrust plane quartz and quartz-microclase veins up to 30m long and 0.5m wide frequently develop; they are usually at a low angle to the S1/S2 foliation and axial planar to the F3 folds. The quartz veins are also seen to intrude the axial planes of folds formed by the reclosure of the D2 boudins (in both the Southern and Northern gneisses) during the D3 deformation (figs. 81 & 82). The displacement across the veins varies from 0.2m to 20m. These veins are the same as those developed in D4 in the Northern gneisses (cf. section 2.1.6).

The second variety of fracture occurs late in D3, and is seen at (17.70,11.50). Here there is a strike parallel band of rock bearing the S1/S2 foliation, folded by F3 and net veined with quartz and calcite. The veining is unaffected by F3 and the rock is completely shattered with rotated brecciated fragments set in a matrix of rock flour (pls. 47 & 50). There is no evidence of movement across the zone and it is interpreted as indicating the sight of rapid dewatering as the D3 stresses relaxed (pl. 37).

Discussion

F3 is responsible for the outcrop patterns seen in the Southern gneisses (map 1), the less resistant lithologies are eroded from the long limb regions back to the hinge region where the foliation is vertical. Thus, it is in the hinge regions that the variation in lithology is seen and because of the steep inclination of the foliation there is little expression of topographic effect on the outcrop patterns. The F3 hinges

Fig 80.

GENERAL F3 STRUCTURES VIEWED FROM THE
SOUTHEAST

F3

F1

S1 / S2

F3

D3 Thrusts
or Shears

F3

S1 / S2

F3

S1 / S2

F3

Small Band of
Mylonite

F1

Quartz Veins

F3 Shear with reverse transport

[From a Major Steep Limb (F3)]

Fig 81.
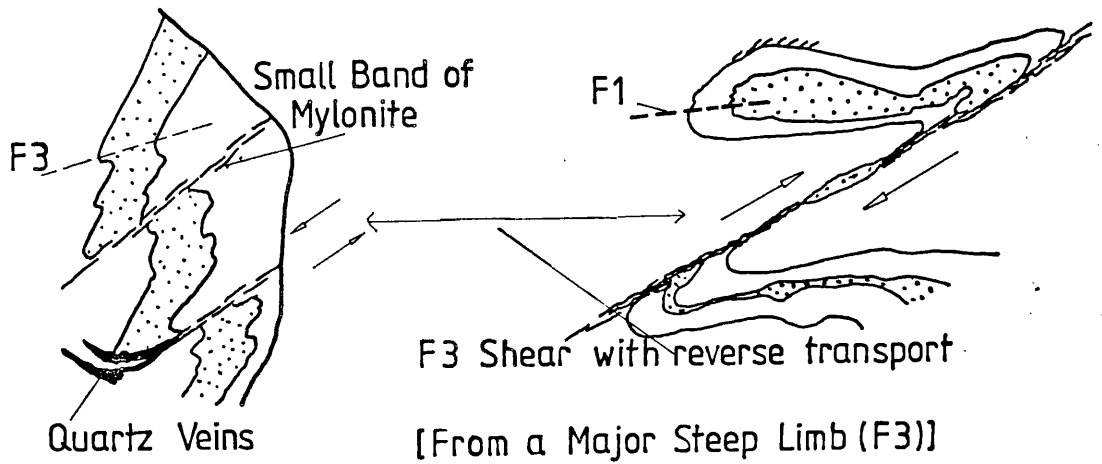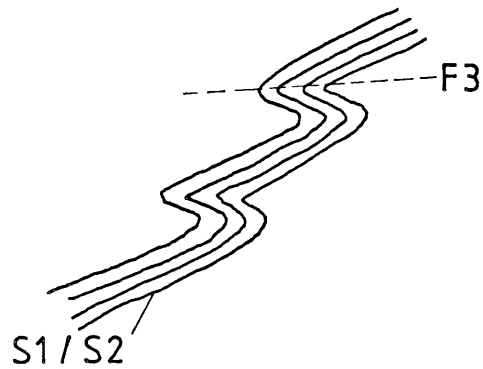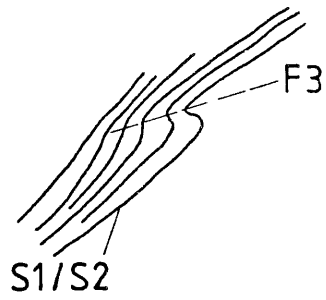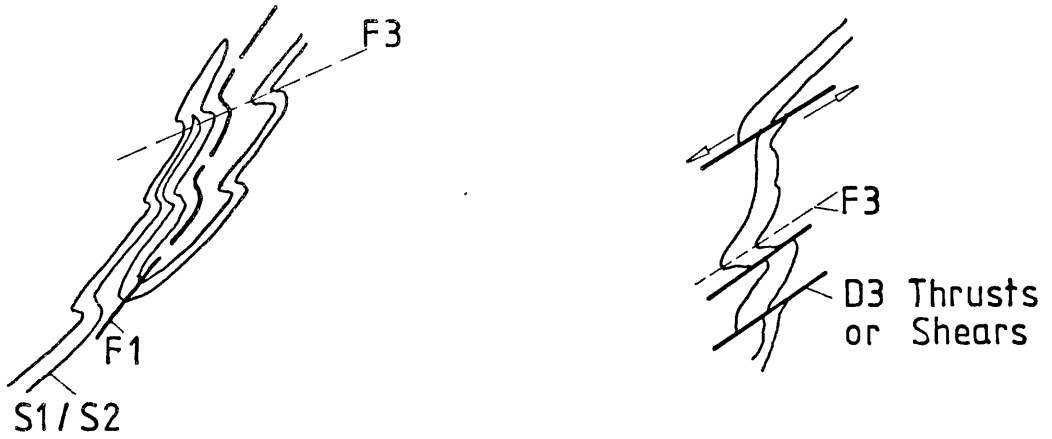
RECLOSED D2 VEIN BOUDIN. — SITE OF AN F3 FOLD

Granitic Vein

Quartz Vein

Gneiss

0 M 0.5
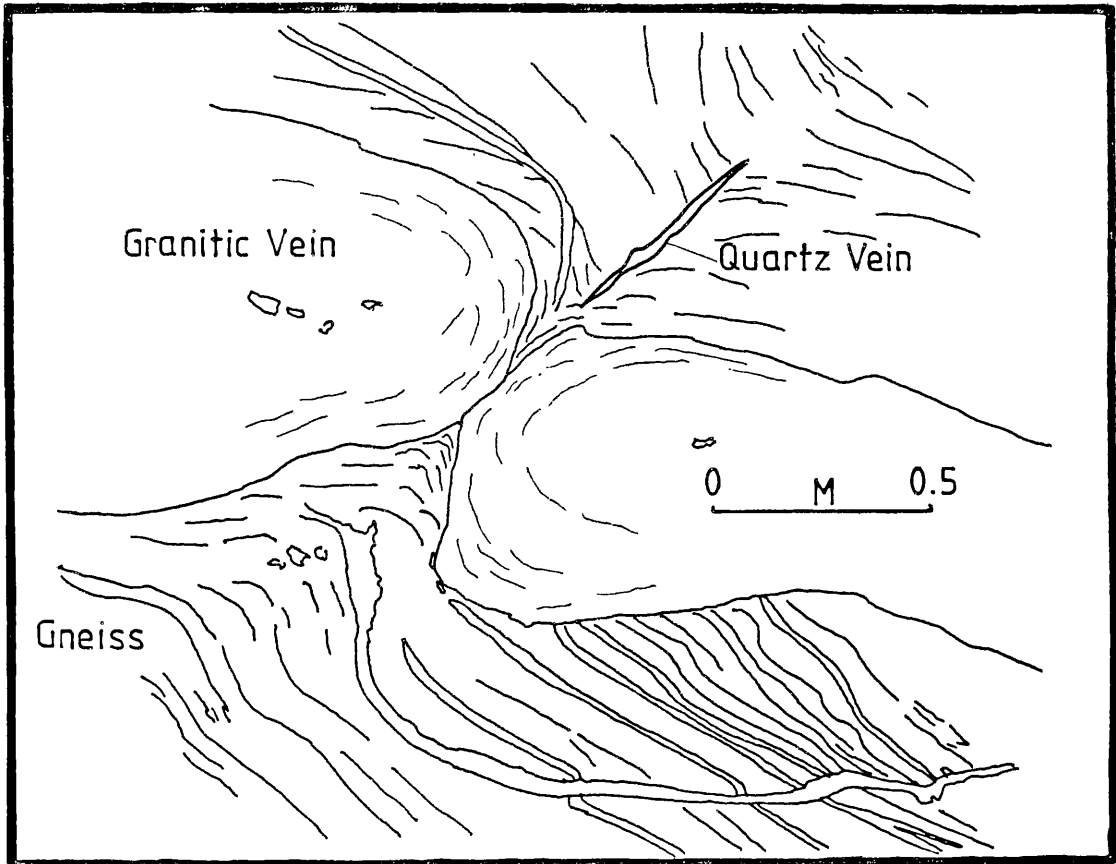
Fig 82.

F3 FOLD NUCLEATED ON A D2 BOUDIN

Basic Gneiss

Acid Gneiss

Quartz Vein
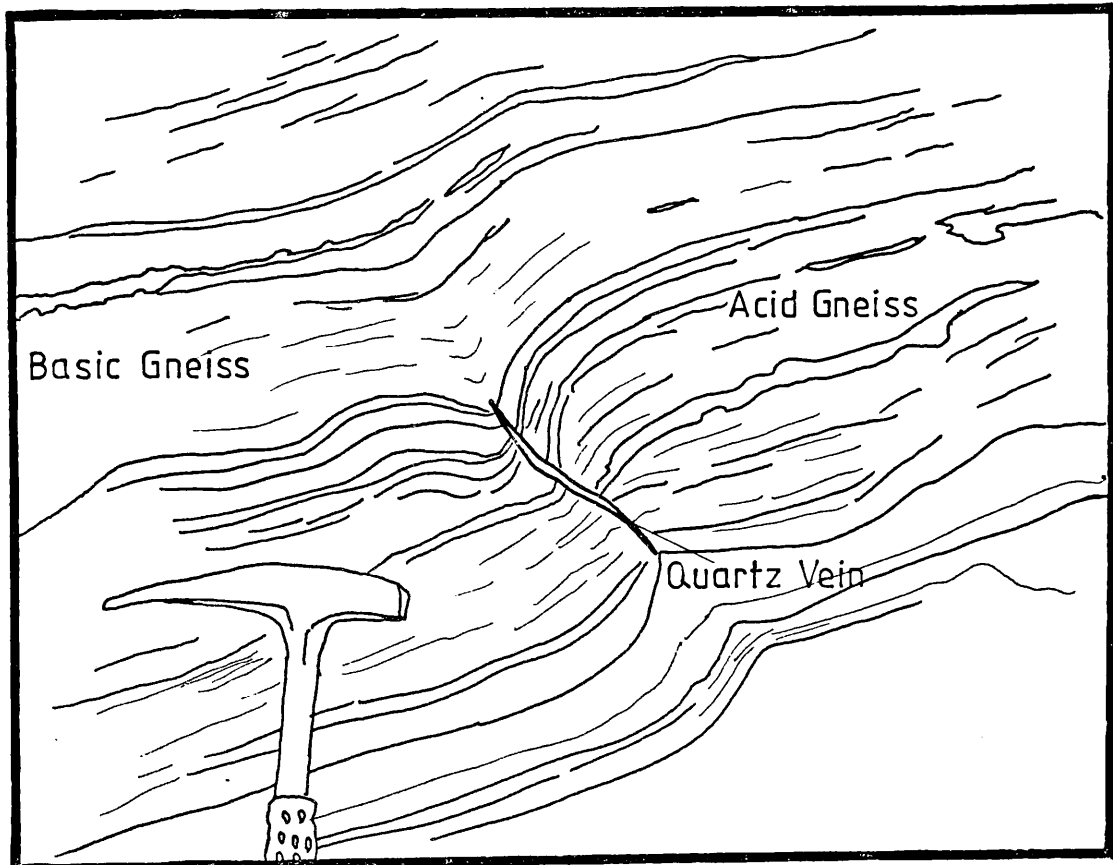
follow the trend of the Bergen Arcs, but it must be stressed that the "arc" of the Bergen Arcs is not responsible for the non-cylindricity of the F3 folds, it is a younger structure that reorientates the F3 hinges (F4 see below).

The sense of translation deduced from overturning of F3 folds (fig. 80) is from the north-east to the south-west. This is the first clear indication of folding producing folds with north-easterly trending axial traces and translation at right angles to the general trend of the Arcs across Osterøy, and probably represents the first phase in the formation of the Bergen Arc Structure.

On the basis of orientation and style of development this phase of deformation is correlated with D4 in the Northern gneisses; the contact between the two units is seen to be deformed by F3 folds. The difference in the effect of the deformation in the two units is that in the Northern gneisses the folds tend to have axial planes which are much steeper than in the Southern gneisses. In both units the structures developed pro-gressively (figs. 34 & 74); this is interpreted as indicating that the deformation was long lived.

The development of the D3 structures is summarised in figure 83.

2.2.5 D4, The Production of F4 and S4

The D4 deformation is not readily apparent in the Southern Gneiss Unit; its presence is mainly inferred from the progressive reorientation of older structures. The features produced in this deformation are:

    1)   F4 folds

    2)   S4 fracture cleavage

    3)   Thrusts.

Fig 83.

144

SIMPLIFIED GEOMETRY OF D3 STRUCTURES

Tectonic 'a'
[L2 forms a
Partial Ellipse
Round This]

F3 Axial Plane,
Quartz Veins &
S3

Plunge of F3 & L3

Shallow Limb

Overturned Steep Limb
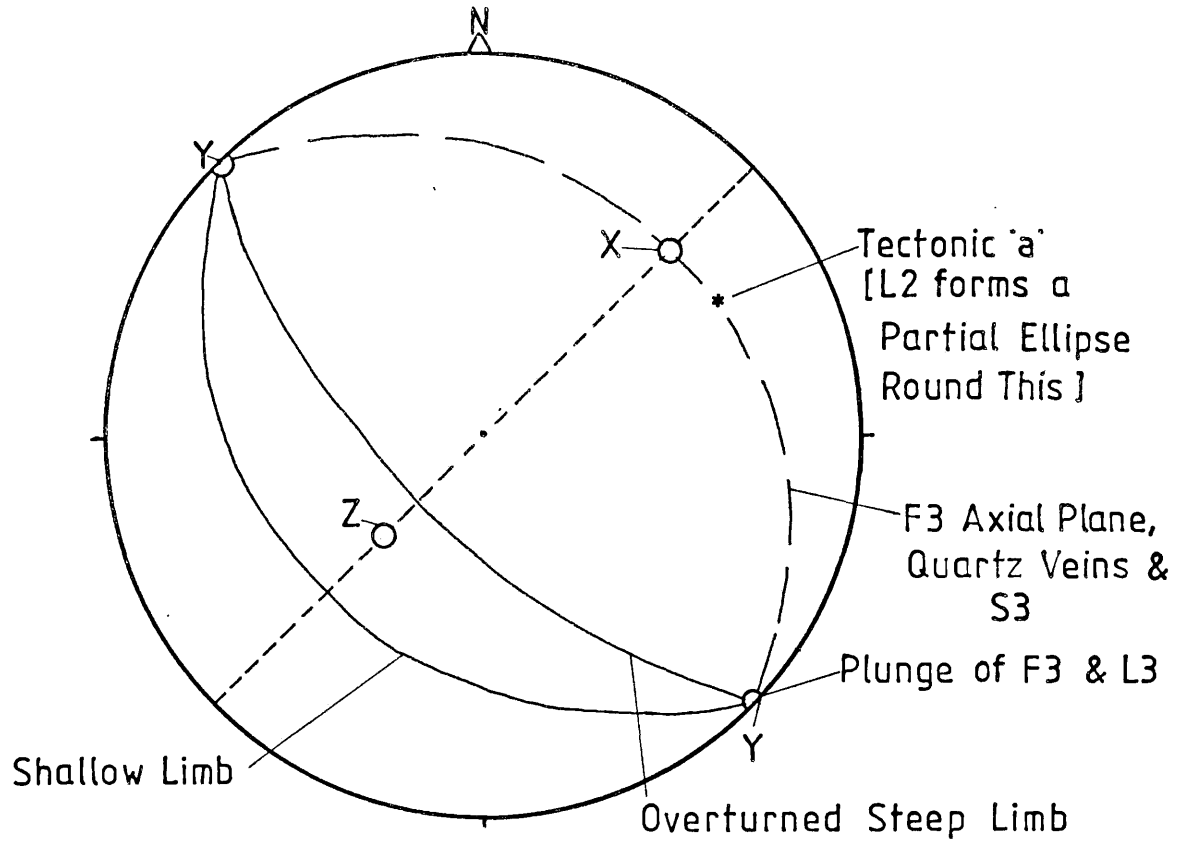
STRUCTURES ASSOCIATED WITH F3 FOLDS

L2

Axial Plane

Y Z

a

X

L3

F3

S1/S2

Weak S3

Quartz Vein
& Shear
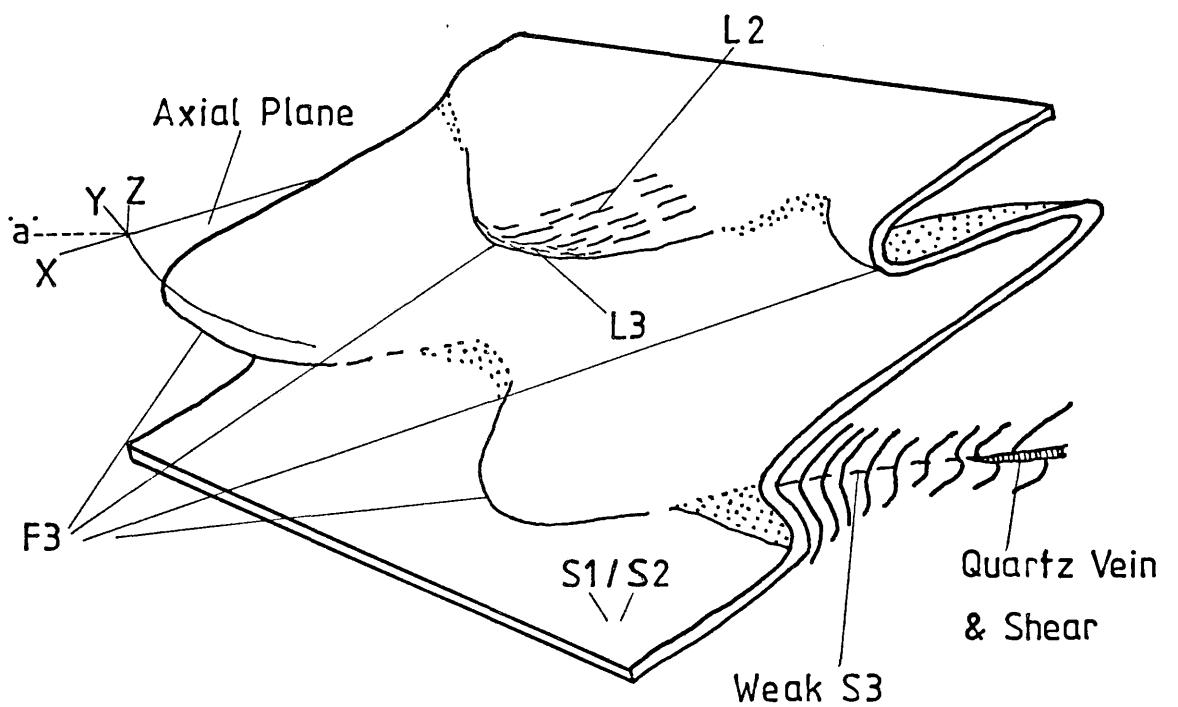
Regionally, that is in the Southern Gneiss Unit, the Northern Gneiss Unit and the Bergen Arcs, D4 has a profound effect on all earlier structures though in any one area its effects are cryptic. A very large scale synformal fold structure is present and best appreciated by examining its regional effects. Plate 38, taken from (19.00,23.00) in the Southern gneisses, looking across the Arcs to the north, clearly shows this large scale synform.

The axis of the structure passes through south Osterøy (fig.84), and it is this structure which is responsible for the preservation of the tectonically higher units seen in the Arcs; they have been eroded from the corresponding antiforms on either side. The axial trace of the fold is arcuate but whether this is a primary feature or the product of some later deformation cannot be ascertained from evidence on Osterøy. It is this arcuate form which is responsible for the "arc" of the Arcs.

In the Southern gneisses the F4 folding is not directly observable because the S1/S2 foliation is too highly disturbed by the F3 folding. If, however, the attitude of the F3 axial planes are examined, F3 folds become apparent. The F3 axial planes, as described above, were not originally planar, but described a non-cylindrical surface. In part this folding of the axial surface is primary but a large portion is due to superimposition of D4. Figure 85 is a plot of the F3 axial planes measured across the Southern gneisses. There is obviously a large scatter, reflecting the primary non-cylindricity of the surface. Two clusters which lie on a great circle defined by smaller concentrations are however the product of D4 and represent the limb regions of F4.

The general southerly dip of the dominant foliation in the Southern gneisses (the long limbs of the F3 folds), towards the axis of the F4 synform in the south-west is appreciated from figure 86, a plot of the

Fig.84

NORTH OSTERØY

D4

POSITION OF THE MAJOR F4 AXIAL TRACE

N

F4

0   2·5   5
Km

Fig 85.
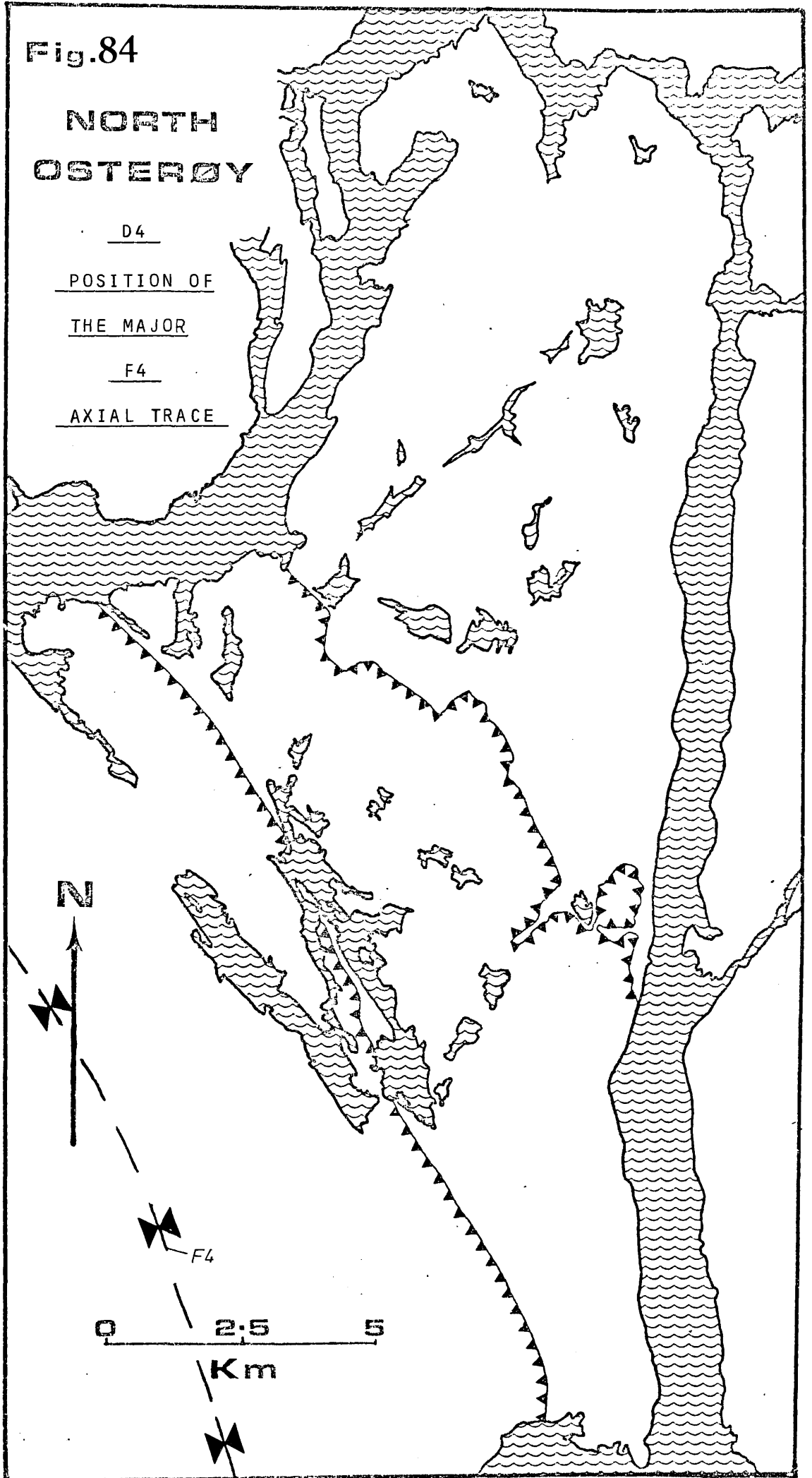
PLOT OF F3 AXIAL PLAINS WHICH DEFINES THE F4 FOLDS

PLOT OF BERGEN ARC FOLD AP.

THIS PLOT HAS UNDERGONE -0- ROTATIONS

USING CORDINATE CARD   0

SAMPLING   2ACROSS/- 1DOWN   POLES PER   2PERCENT AREA   81 DATA   EQ AR

THE CONTOURS REPRESENT THE FOLLOWING PERCENTAGES

00.9<=1-2%>02.9<=3-4%>04.9<=5-6%>06.9<=7-8%>08.9<=9-10%>10.9<=11-12%>12.9
12.9<=13-14%>14.9<=15-16%>16.9<=17-18%>18.9<=19-20%>20.9<=21-22%>22.9
22.9<=23-24%>24.9<=25-26%>26.9<=27-28%>28.9<=29-30%>30.9<=31-32%>32.9
32.9<=33-34%>34.9<=35-36%>36.9<=37-38%>38.9<=39-40%>40.9<=41-42%>42.9
42.9<=43-44%>44.9<=45-46%>46.9<=47-48%>48.9<=49-50%>50.9<=51%+
NOTE A VALUE OF>0.5-0.9<=.LT.1%AND.GT.0%

Fig 86.

PLOT OF S1/S2 FOLIATIONS FROM THE SOUTHERN GNISSES

PLOT OF SG.FOLIATION

THIS PLOT HAS UNDERGONE -0- ROTATIONS

USING CORDINATE CARD   0

SAMPLING   2ACROSS/- 1DOWN   POLES PER 1PERCENT AREA   1799 DATA   EQ AR

THE CONTOURS REPRESENT THE FOLLOWING PERCENTAGES

00.9<=1-2%>02.9<=3-4%>04.9<=5-6%>06.9<=7-8%>08.9<=9-10%>10.9<=11-12%>12.9
12.9<=13-14%>14.9<=15-16%>16.9<=17-18%>18.9<=19-20%>20.9<=21-22%>22.9
22.9<=23-24%>24.9<=25-26%>26.9<=27-28%>28.9<=29-30%>30.9<=31-32%>32.9
32.9<=33-34%>34.9<=35-36%>36.9<=37-38%>38.9<=39-40%>40.9<=41-42%>42.9
42.9<=43-44%>44.9<=45-46%>46.9<=47-48%>48.9<=49-50%>50.9<=51%+
NOTE A VALUE OF>0.5-0.9<=.LT.1%AND.GT.0%

composite foliation (S1/S2) across the Southern gneisses (the weak cluster

at the other end of the great circle reflects the steep limbs of F3.

The information used in plotting figure 86 is also plotted as for figure 40

(fig.87)).

The great circle described by the axial planes of the F3 folds,

figure 85, defines a plunge for the F4 structure at 140/15°.

At some localities within the Southern gneisses, (e.g.05.50,33.00)

a vertical close-spaced fracture cleavage, S4, is seen to cross cut the

F3 folds (fig.88); it strikes at 140°. Despite the absence of any

visible folds to which this cleavage might relate, consideration of its

attitude suggests that it is axial planar to F4.

Late thrusts, which cut the F3 folds, are to be found within the

Southern gneisses (18.00,15.00). These thrusts or reverse faults form

marked gullies in the Southern gneiss terrain, running parallel to the

strike of the S1/S2 foliation (fig.89). These thrusts persist into the

Northern gneisses (14.00,35.20). They are interpreted as having formed

during the F4 folding and representing conjugate shear planes on the inner

arc of the F4 synform (fig.90). The thrust planes contain rock flour.

Discussion

The effects of the D4 deformation are not apparent in the Osterøy

gneisses. Within the area generally the structure is best traced by

observing the attitude of the long limbs of the F3 folds which F4 refolds.

It is this effect which is visible in plate 38.

The D4 strain first developed with the generation of F4 folds. The

deformation occurred under lowest greenschist facies metamorphic conditions

(see section 3.5.4). Associated complementary shears in the limb regions

were then developed on favourably orientated long limbs of F3 structures

(fig.90). A new weak fracture cleavage developed in association with

Fig 87.

150

MAJOR [F3] FOLDS AFFECTING THE SOUTHERN GNEISS
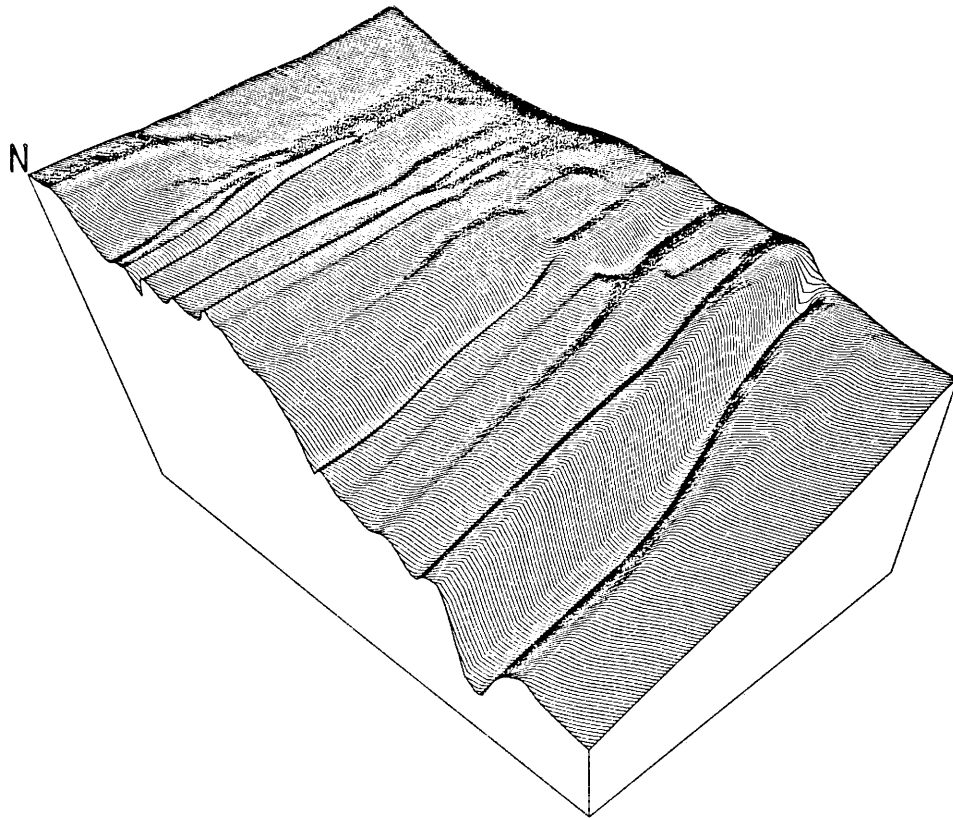

```
          PLOT OF THE FOLIATION IN THE SOUTHERN GNEISS UNIT US'ING - WDEPTH.
      AZIMUTH = 45              ALTITUDE = 55
      *WIDTH = 6.00            *HEIGHT = 5.00
      SMOOTHINGS = -1.00

      * BEFORE FORESHORTENING  22/11/78
```

Fig 88.

151
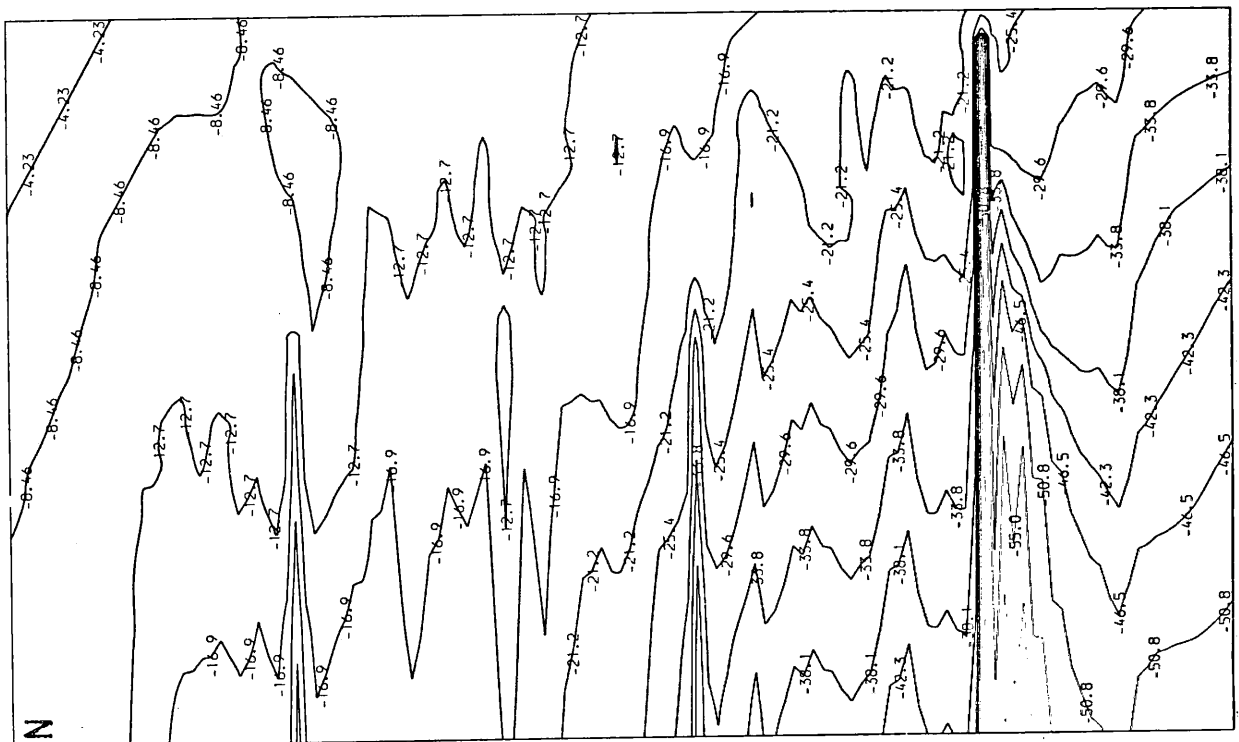
THE S4 FRACTURE CLEAVAGE CROSS-CUTTING F3 FOLDS
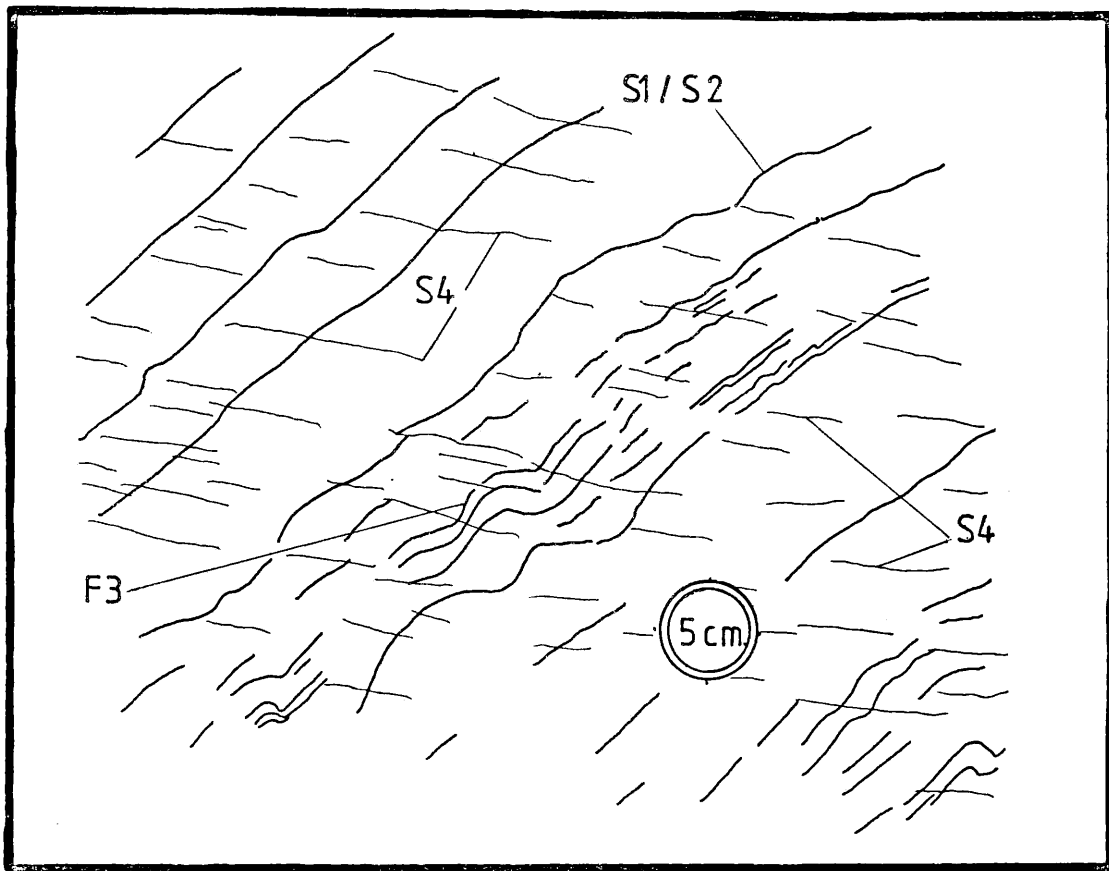
Fig 89.

A D4 THRUST
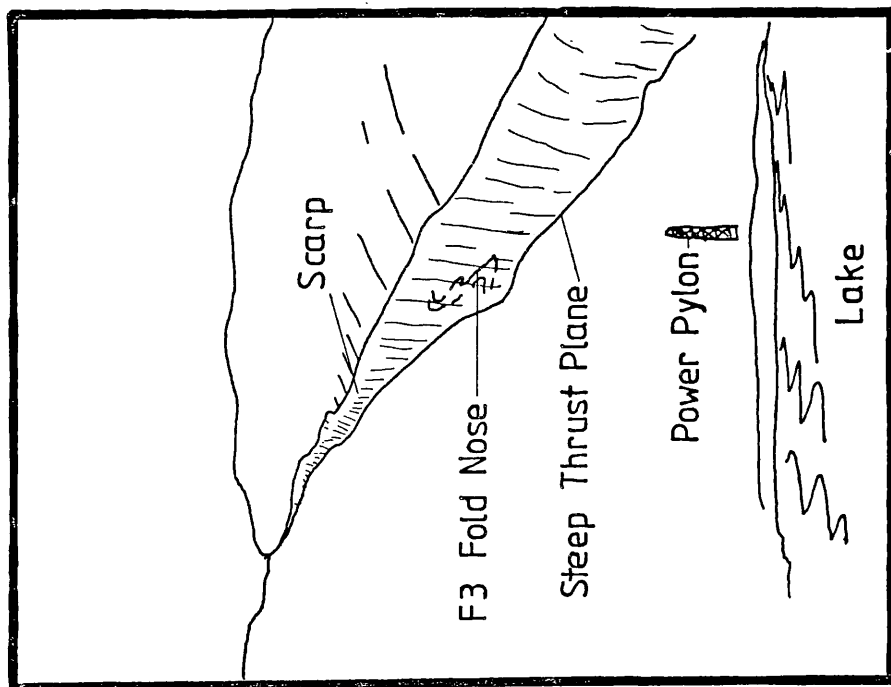
Fig 90.

EFFECTS OF THE D4 THRUSTING

[The Thrusts Affect
the Long Limbs of
the F3 Folds]

F3

D4 Thrusts

S1 / S2

F4

Median
Surface

?

D4 Thrusts Develop
In the Inner Arc
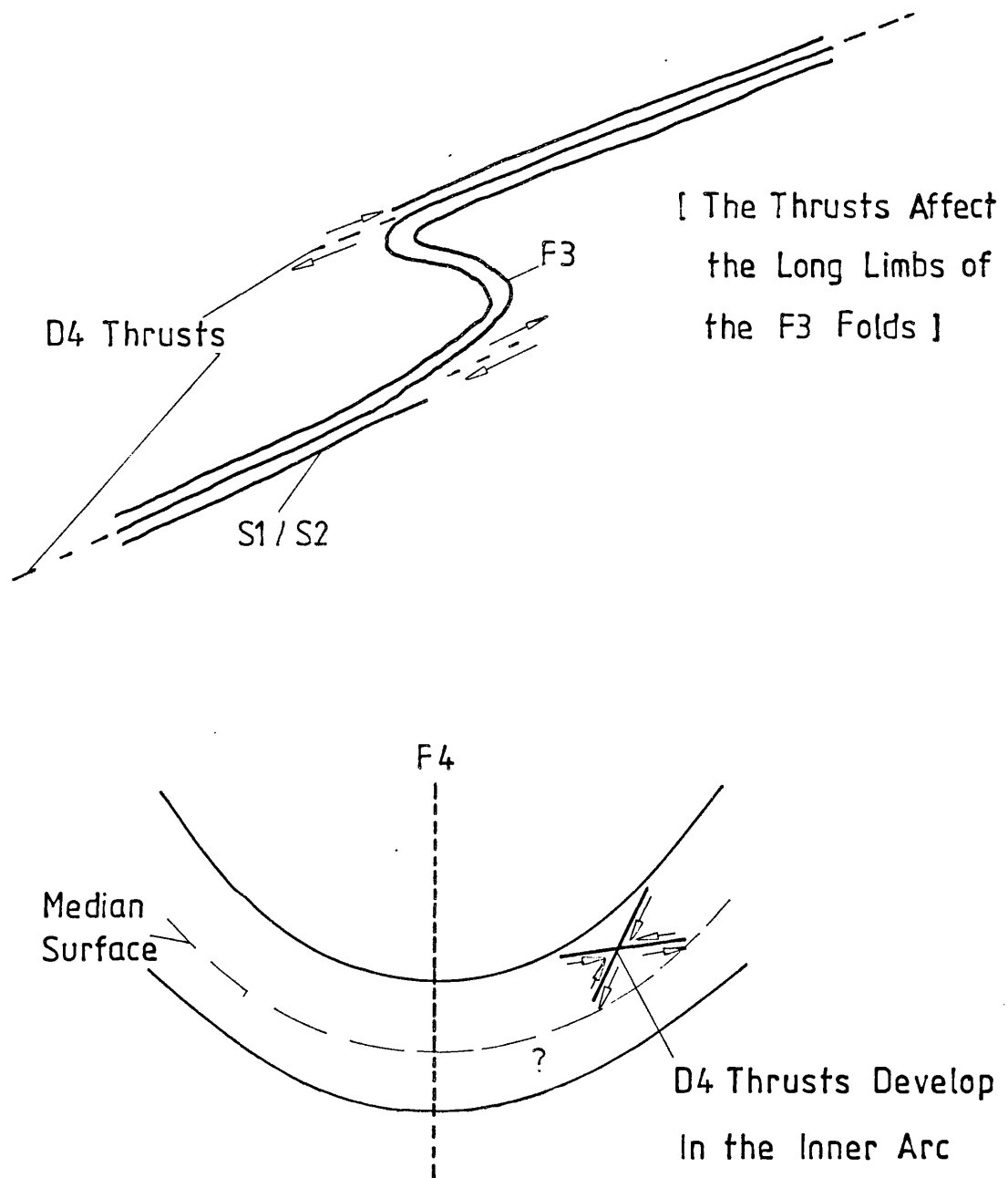
the F4 folds, orientated parallel to the a/b plane of the F4 folds, as eastblished from figure 85.

These relationships are summarised in figure 91.

2.2.6   D5, The Production of Late Joints

The topographic effects of the joints on Osterøy are seen in plate 39. The joints are important economically as they form the valleys in which agriculture is located and also control the directions of the fjords (Nilsen,1973).   There is very little displacement associated with any of these features, though they are frequently zones of intensive brecciation, hydraulic fracture and mineralisation.   The mineralisation is typically epidote, chlorite and calcite, which replaces and corrodes ,fragments of country rock found in the joint zones (pls.48 & 49), which frequently have plane boundaries (pl.40).

No detailed analysis of the joints on Osterøy has been attempted but a general analysis of lineaments on a macroscopic scale, based on air photographs and structures seen on map 1, is presented.

On Osterøy the joints seem to form three distinct sets (fig.92):

a)   Those which are radial to the Bergen Arc structure, orientated 020 to 050° with a concentration maxima at 045°.

b)   Those normal to the Bergsdalen front, orientated 320 to 335°.

c)   Those which parallel the fjord forming the east coast of Osterøy, orientated 355 to 005°.

All the joints are more or less vertical and the (a) and (b) sets have some small shear component (e.g. 10.00,31.00 and 20.90,33.70).

It is only in the Northern Gneiss Unit that all three sets are developed equally (fig.92).   To the south-west in the Southern Gneiss Unit and

Fig 91.

154

SIMPLIFIED GEOMETRY OF D4 STRUCTURES
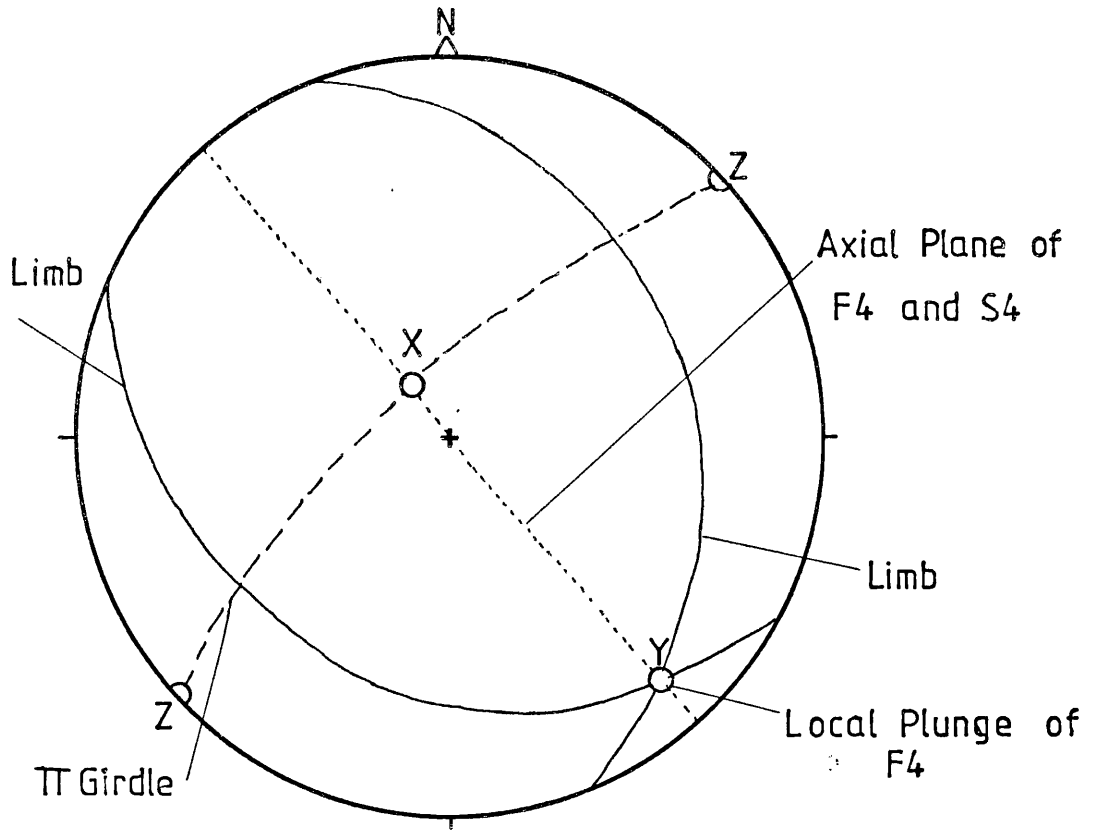
EFFECTS OF F4 FOLDING
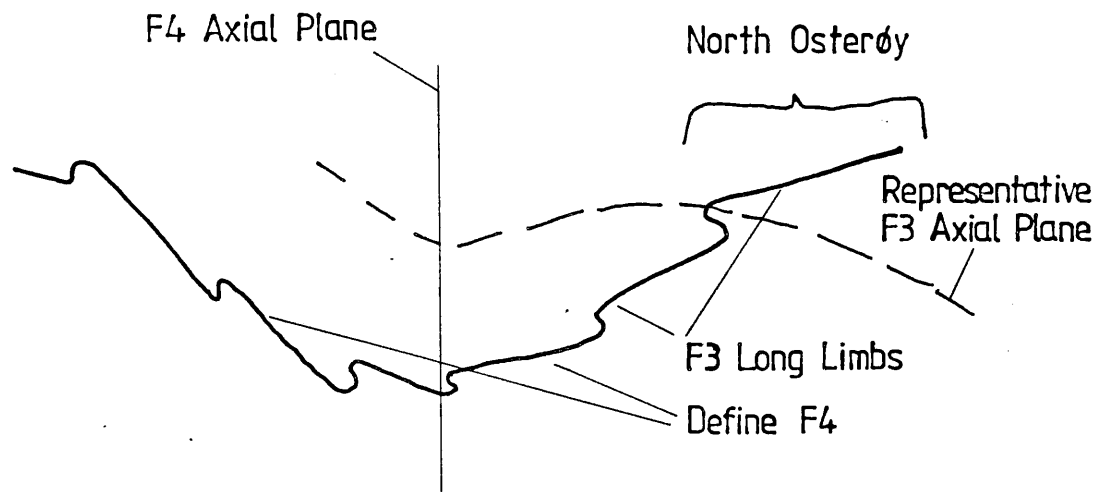
Fig. 92

NORTH
OSTERØY

D5

MAJOR JOINTS

320-335° Joint

045° Joint

355-005° Joint

N

0   2·5   5
Km
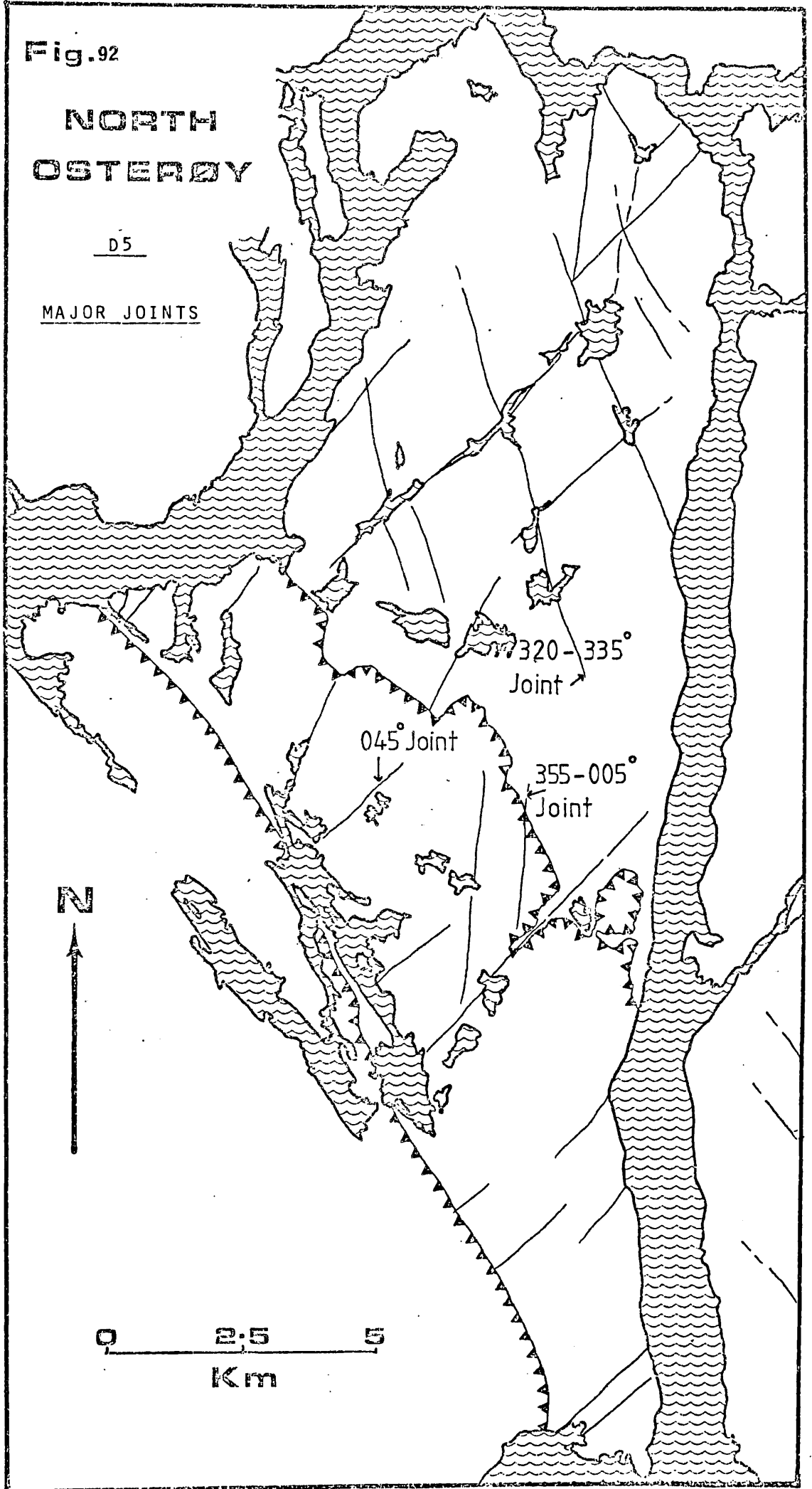
Bergen Arc, where the dominant foliation strikes 320°, the (b) set is not
seen; and to the south-east in the Bergsdalen, where the dominant foliation
strikes 045°, the (a) set is not seen. The absence of these two sets
in these areas may be either because they are lost in the foliation or
not developed there.

Figure 93 illustrates the distributions and this analysis of clustering
for the joints on Osterøy is also applicable to adjacent regions and conforms
well with the pattern found by Ramberg et al. (1977).

It is difficult to attempt meaningful analysis of jointing in
gneissose basement, as in gneissose terrains with complex deformation
histories it is thought that such analyses are unfruitful. At first sight
this is the case on Osterøy; the joint sets are not clearly relatable
to either the Bergen Arc or Bergsdalen structures, and do not fit patterns
described for joints situated at orogenic fronts. For example, Muecke
and Charlsworth (1966), who found that within the fold belt the joints
form wrench sets and away from it become normal to the fold axes.

A sensible analysis of patterns seen on Osterøy can however be made
by making two assumptions: firstly, that the joints are a phenomena of
stress relief and dewatering as the rocks are uplifted by erosion and
isostatic adjustment - dewatering is supported by the mineralisation and
the stress relief hypothesis is well established (Price,1966); secondly,
that elastic strain remains stored in the rocks and the orientation of
some of the joints probably reflects fossilised paleo-stress systems
induced in the rocks during earlier deformations - the fact that elastic
strain is stored in rocks is documented by Price (1966).

Examination of the structural development of the Osterøy gneisses
has established that during their early history the maximum principal
stress was probably horizontal, aligned at right angles to the Bergsdalen

Fig 93.

ORIENTATION OF JOINTS

Joint Orientation Expected
From Parallelogram
Solution

(a)=020-050° Joints
[⊞ = 045° Concentration]

(b)=320-335° Joints

(c)=355-005° Joints

σ1 For the Bergsdalen
Orogen

σ1
For the Bergen
Arc Orogen

σ1 Resolved For North Osterøy
Using The Parallelogram of
Forces

THE PARALLELOGRAM OF FORCES

225°, σ1
For Bergen Arc

σ1, 135° For Bergsdalen

180° = Resolved σ1 [a change in magnitude of
either vector will alter the
position of resolved σ1,
this will produce a scatter
of Joint orientations]

front (135°). Later, in D3 and D4, this switched to become orthogonal to the Bergen Arcs (locally 225°). The stresses stored as elastic strain in the gneisses must be the product of both of these, and assuming that one stress axis is vertical (gravity), the orientation of the maximum principal stress axis can be resolved using the parallelogram rule (fig. 93). The resolved maximum principal stress lies near 180°, given that the exact orientation depends on the relative magnitude of the two unresolved stresses at any one location; these will change the shape of the parallelogram, imparting a slight scatter to the resulting structures. Thus the expected orientations for shear joints would be 035 and 335° (normal to the Bergen Arcs and normal to the Bergsdalen (a) and (b) respectively).

A third set of joints (c) could develop along the acute bisectrix of conjugate set (a) and (b), parallel to the resolved maximum principal stress. This set could be interpreted as the result of progressive stress relief; after the initial formation of the shear joints, the maximum principal stress switched with the intermediate, and vertical dewatering joints developed in the 01/02 plane (fig. 94). These joints would be orientated 000° and in the field these are the most mineralised, reflecting a high Pp. H_2O involvement.

Discussion

The interpretation presented here fits very well with the pattern seen on Osterøy; it is however at variance with that proposed on a regional basis by Hobbs (1911).

2.2.7   Discussion on Deformation of the Southern Gneiss Unit

Figure 95 is a summary table of the observed deformation features affecting in this unit. It is not possible to detect a pattern in the deformation as it was for the Northern gneisses. There are several possible explanations for this:

Fig 94.

RELATIONSHIP OF JOINTS TO RESOLVED STRESS
FIELD

FIRST-Shear Joint
Formation
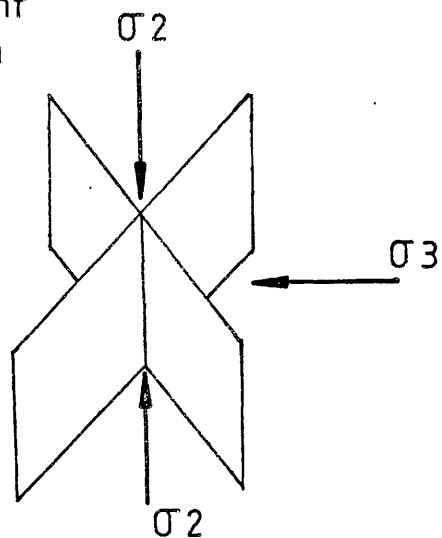
SECOND-The 355-005° Joint Formation
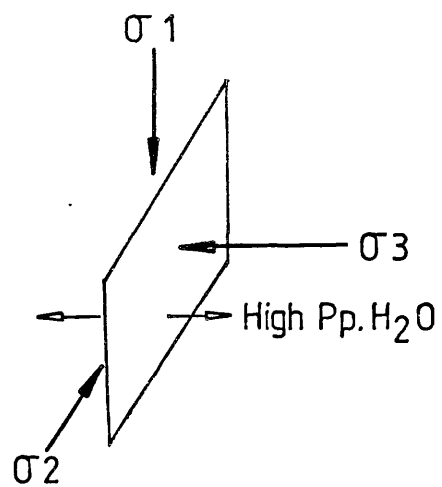
[the second Joints are extensively
mineralized with calcite & epidote]

Fig 95.

DEFORMATION IN THE SOUTHERN GNEISSES

D'Early'	D1	D2	D3	D4	D5
	F1	F2 S2	F3 L2 S3	Thrusting F4 S4	Jointing
	Acid Igneous Activity And Pegmatites [Minor Sediments]	Pegmatites	Qtz. Veining		
	Flattening L1 THRUSTING	Flattening Thrusting	L3		
S'Early'	Basic Igneous Activity				
Pegmatites	Pegmatites				

a) The mechanisms operating in the Southern gneisses were fundamentally different.

b) Any pattern is obscured by the deformation as it proceeds.

c) Only part of a "cycle" is developed.

It is likely that all three factors have been operative. In D1 the deformation took place at the highest metamorphic grade and was super-plastic (see section 4). Under such conditions folds would probably not develop serially, because layering would exert very little influence and thus the "cyclic" model postulated above could not operate. There is therefore no clear "flattening" (fig.37(F)) as a second stage to the D1 deformation as was so typical of the Northern gneisses. The pegmatite relationships then become much more confused; D1 involves axial planar parallel pegmatites but these seem to have developed contemporaneously with the formation of S1. The amount of deformation which D1 represents is, for any given portion of rock, much higher than that seen in the Northern gneisses. It is postulated that D1 represents deformation at a "higher level" in the basement, a para-autochthonous nappe formed further in towards the centre of tectonic activity than anything seen in the Northern gneisses (fig.38).

D2 on the other hand probably represents part of a "cycle". It is known, that at a higher level folding accompanied this deformation (see p.173), and these folds fold the layering and are isoclinal (Faerseth et al.,1977). Such folds would be formed in the first stages of a "cycle". In the second flattening stage, the deformation would progress to deeper and deeper levels of the crust, forming a new foliation (S2). It is interesting to note that while the D1 mylonitisation is homogeneous throughout, the D2 mylonitisation is heterogeneous, weakening as it descends the tectonic pile,eventually to die out just across the contact between the Northern

and Southern gneisses.   This suggests that these two units were "in place"
prior to D2.

D3, on the evidence presented, is clearly the same deformation as
D4 of the Northern gneisses.   It occurs at a much higher crustal level,
(structurally and metamorphically) than the preceding deformations,
and clearly shows how at higher levels the layering determines the geometry
of the developing structures.   The trend of the D3 structures and the
south-westerly transport is important as it is the first evidence seen
in the basement for the development of the Bergen Arc structure.

The effect of the D3 folding across all the north Osterøy gneisses
is seen on a computer generated block diagram of the foliation surface
across them (fig. 96).

The D4 structures show a continued development of the Arc structure,
folding the allochthon into a broad synform.

The question that thus arises is whether the Øygarden basement to
the west of the Arcs is the same as that on Osterøy, and is the arcuate
form of the synform primary or secondary?   More work is needed on the
western margin of the Arcs before these questions can be answered.

The D4 thrusts develop a different type of mylonite, more akin to
fault gouge (Gibson,1977), indicating that D4 operated at lower temperatures
and thus at a higher level in the crust then the preceding deformations
(see section 4).

D5 probably considerably postdates the earlier deformations, being
the product of uplift and stress relief during erosion, the stresses
responsible however seem to belong to the "earlier deformations", and as
such it must be grouped with them.

Fig 96.   163

COMBINED EFFECTS OF F4[N.Gneisses] & F3[S.Gneisses] ACROSS
NORTH OSTERØY.(These Folds Belong to the Same Deformation)
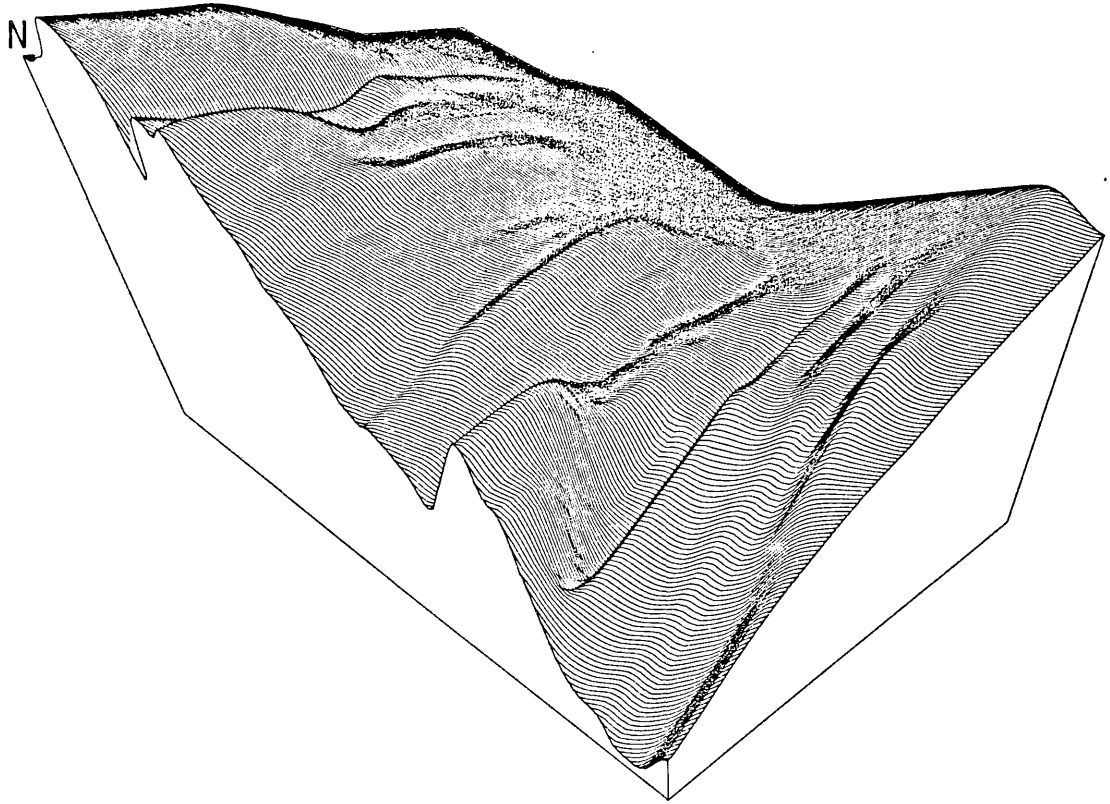
PLOT OF THE FOLIATION IN THE NORTH OSTEROY GNEISSES US ING - WDEPTH

AZIMUTH = 45   ALTITUDE = 55
*WIDTH = 6.00   *HEIGHT = 5.00
SMOOTHINGS = -1.00

* BEFORE FORESHORTENING 29/11/78
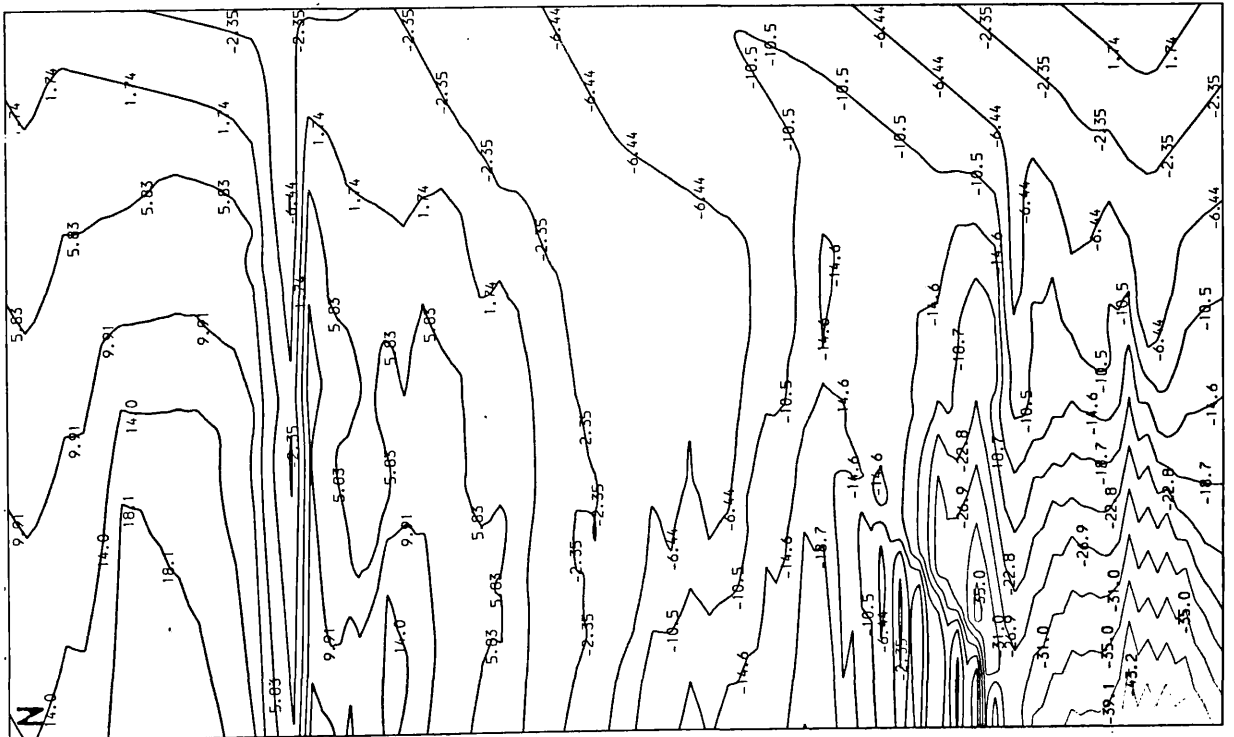
The deformation sequence in the Southern gneisses is interpreted as representing tectonic events occurring near a "centre of orogenic activity" (the allochthonous rocks of the Arcs are in contact with the Southern Gneiss Unit and both contain similar structures) at progressively lower and lower metamorphic conditions. The Southern gneisses were, therefore, originally the same as the Northern gneisses, but have suffered higher (structural) level deformation related to the emplacement of the higher nappes, and must therefore be grouped with these nappes on a structural basis.

2.3 CORRELATION OF DEFORMATIONAL EVENTS

2.3.1 The Northern and Southern Gneiss Units

The deformation phases in the Northern and Southern Gneiss Units are summarised in figures 36 and 95 respectively. All the deformations cannot be directly equated; the geometry of the folds and structures accompanying D1 (Northern gneisses) and D1 (Southern gneisses) are different.

In the following discussion deformations referring to the Northern gneisses will be denoted D^n, those of the Southern gneisses D^s and the suggested correlated events D^g (e.g. $D1^n$ refers to D1 of the Northern gneisses).

In any discussion of correlation of the deformation events in the units, the nature of the contact between them, the Tysse Thrust (fig.10), is of vital importance. It could be argued that this contact is a major plane of transport and that the Southern gneisses are entirely allochthonous. In this case no correlation can be made between the two units prior to emplacement. In the field the thrust is cryptic; it is not at all obvious as a definite boundary (pl.41). Its presence only begins to be suspected when foliation orientations are examined (figs.39 & 86) and on subdivision

of individual lithological units (map 1). It separates two regions in
which the dominant foliations strike at right angles to each other, and
its position becomes very clear on a computer generated block diagram
showing the variation of the northerly component of dip across the Osterøy
gneisses (fig. 99). Figure 99 and map 1 show that the 'strength' of the
feature increases towards its western end. This represents an increased
displacement on the thrust, in this region, with regard to the geometry
of the structures it is juxtaposing. These features indicate that the
Southern Gneiss Unit cannot be allochthonous or the displacement would
be equal across the entire outcrop; it must therefore represent a para-
autochthonous basement nappe derived by metamorphic and deformational
reworking from the Northern Gneiss Unit, a view supported by examination
of the petrology and metamorphic history of the two units.

To understand when the reworking and transport occurred, the deforma-
tions in the two units will be successively removed starting with the
youngest structures to affect both units $(D7^g)$, which is the late jointing.
The point at which the deformational histories divide will evidently give
the age of the Tysse Thrust.

The correlations between the two units are given in figure 97 and a
discussion of the basis for these correlations follows:

Figure 97.

THE NORTHERN AND SOUTHERN GNEISS DEFORMATION CORRELATION

NORTHERN GNEISS	SOUTHERN GNEISS	COMPOSITE		
D "Early	Not seen	D "Early"	)	
D1	Not seen	D1	)	PRECAMBRIAN
D2	D "Early"	D2	)	
D3	D1	D3 Tysse Thrust	)	
Not present	D2	D4	)	CALEDONIAN
D4	D3	D5	)	AND/OR
Not seen	D4	D6	)	LATER
(D5)	D5	D7	)	

Fig 99.

166

THE TYSSE THRUST IS APPARENT ON A DIAGRAM GENERATED ENHANCING THE NORTHERLY COMPONENT OF DIP.
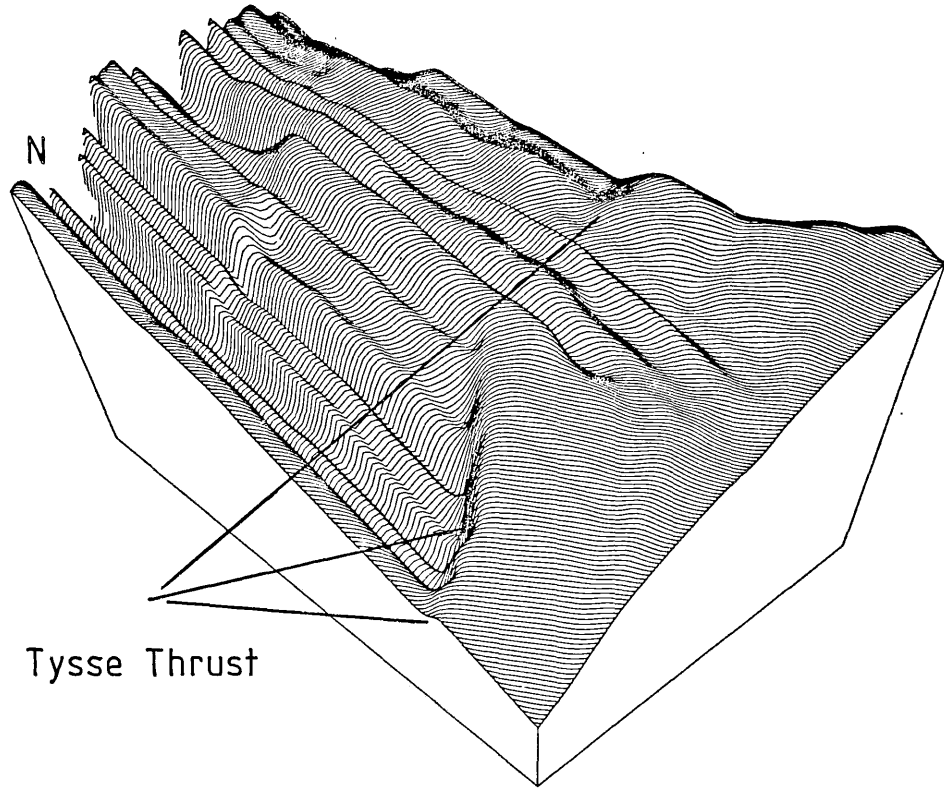
Tysse Thrust

PLOT OF THE FOLIATION IN THE NORTH OSTEROY GNEISSES US INO - NDEPTH
AZIMUTH = 45   ALTITUDE = 55
=WIDTH = 6.00   =HEIGHT = 6.00
SMOOTHINGS = -1.00

= BEFORE FORESHORTENING 27/11/78
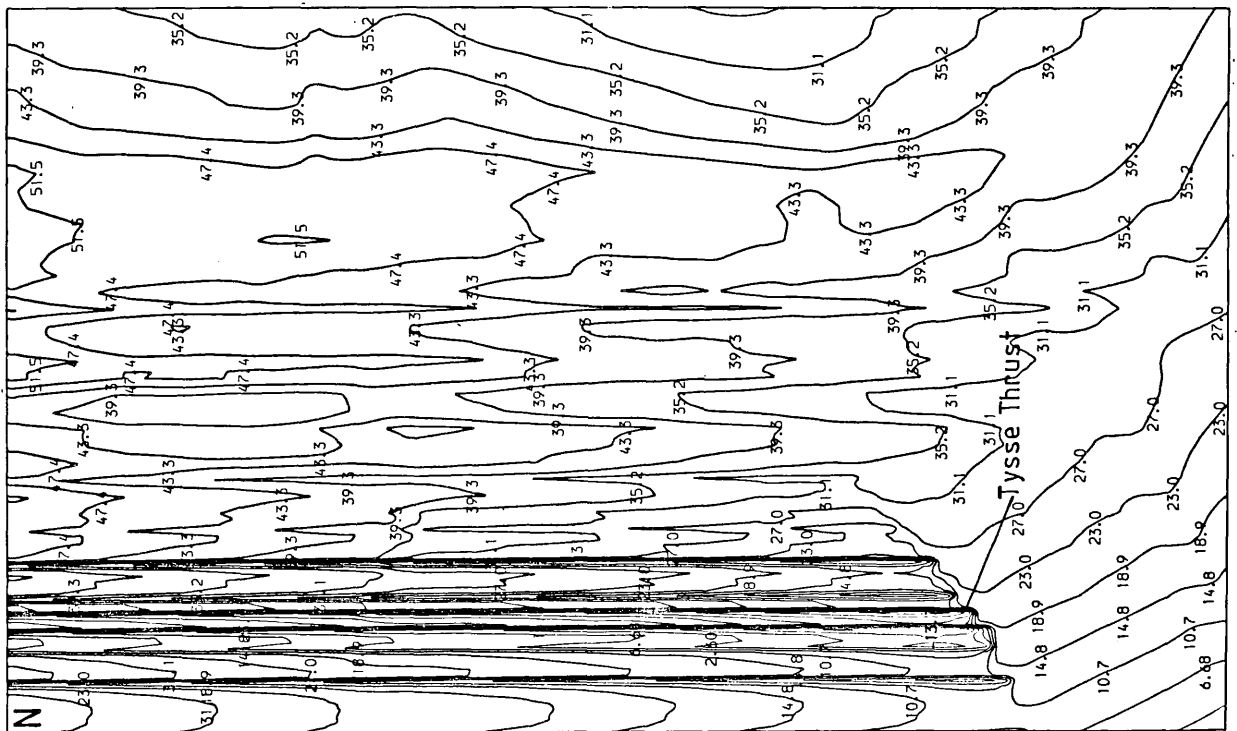
$\underline{D6^g}$: $F4^s$ is not visible in the Northern gneisses because the strike of these rocks is orthoganal to the $F4^s$ axial direction. However, because there is evidence that the two units were in place prior to $D6^g$, $F4^s$ must in fact affect them.

$\underline{D5^g}$: it has been proved (p.143) that $F3^s$ and $F4^n$ are the same folds; this is the first point of obvious structural similarity between the two units (fig.96).

$\underline{D4^g}$: this correlation presents more of a problem. However two points must be considered: a) $S2^s$ affects the Northern gneisses in a zone close to the Tysse Thrust. b) Moving up section in the Southern gneisses the effects of $D2^s$ increases and at the contact with the Bergen Arcs $S2^s$ is the dominant schistosity. It therefore finds a place between $D4^n$ and $D3^n$.

From this point back there is no immediate similarity in deformational events between the two units. The emplacement of the Southern Gneiss Unit must therefore be a $D3^g$ event and this therefore gives the relative age of the Tysse Thrust.

It is however proposed that $D1^s$ is the same event as $D3^n$. The bases for this proposition are seen in $D2^n$; development of $F2^n$ and $S3b^n$ is heterogeneous, as shown in figure 18. If $D3^n$ were similar, then the whole Southern Gneiss Unit could be explained as a slice of highly re-worked basement from the root of the Bergsdalen Nappes (fig.38), thrust over adjacent basement from the south-east, at the end of $D3^g$. $F3^n$ would then be the same as $F1^s$, S "Early"^{s} would be $S3b^n$ and $L3^n$ would equate with $L1^s$. Such an origin for the Southern gneisses would also explain the north-easterly alignment of the $F1^s$ fold axes and the way the Southern Gneiss Unit thins slightly to the north-west.

The structures seen in the Southern Unit are therefore interpreted as more developed equivalents of those in the Northern Unit. Because the structures seen in the Northern Unit young south-eastwards (fig.23), the Tysse Thrust brings together structures belonging to $D1^g$ and $D4^g$ in the west and $D3^g$ and $D4^g$ in the east, thereby explaining why its effects increase north-westwards. The thrust developed in two stages, first in $D3^g$ the Southern gneiss mylonites were formed. These mylonites represent "ductile thrusting" in the roots of an orogen (see section 4) and reflect the primary emplacement of the Southern Gneiss Unit. There is no sharp contact, rather the deformation is accommodated over a broad zone occupying the whole of the Southern Gneiss Unit.

Following this the $D3^g$ mylonites were reworked in $D4^g$, a second thrusting event which, while still ductile is more brittle than $D3^g$. For reasons given in section 4.2.3, the $D3^g$ mylonites absorb all the $D4^g$ strain so that little is transmitted to the underlying gneisses, explaining the absence of $D4^g$ in the Northern Gneiss Unit.

The Tysse Thrust is then a plane, separating rocks above which are strongly affected by two deformations that are only weakly represented in the rocks beneath. It is also a plane of transport (map 1) and is therefore best described as a plane of decollement, in some places "stuck" while in others "detached". $D3^g$ therefore is the point at which developmental histories of the two units converge.

2.3.2   The Osterøy Gneisses and the Bergen Arcs

The deformation sequence postulated for the Arcs by Faerseth et al. (1977) (fig.100), is based on observations of the rocks immediately to the west of the Southern Gneiss Unit, south-east of the area mapped. Extensive traverses were made in this area in an attempt to correlate the two. The following shortcomings in the sequence as presented by Faerseth et al.

Fig 100.

SUMMARY OF STRUCTURAL, METAMORPHIC AND INTRUSIVE EVENTS IN THE BERGEN ARC NAPPES, BASED ON OBSERVATIONS FROM THE SAMNANGER-OSTERØY AREA.

DEFORMATION PHASE	STRUCTURES	METAMORPHISM	INTRUSIVES
D_5	Conjugate wrench faults. Dextral movements along N60°E faults. Sinistral movements along N120°E faults.	Local thermal metamorphism	
D_4	Tight to open F_4 folds. Mainly located in the eastern part of the Samnanger area, close to the Bergsdalen nappes.	B 1.2.	Intrusion of quartz dioritic dykes
D_3	Close to tight major and minor F_3 folds. Development of S_3 crenulation cleavage. M_2	B 1.2./B 1.3.	
D_2	Tight to isoclinal major and minor F_2 folds. Development of S_2 foliation. Thrusting and imbrication accompanied by extensive cataclasis. Emplacement of serpentinite bodies along thrust planes.	Prograde in the Holdhus Group, varying from B 1.2. in the south to B 1.3. in the north. Retrograde in the Samnanger Complex B 1.2.–B 1.3.	Intrusion of quartz diorites
D_1	Large-scale recumbent folding giving an S_1 foliation. M_1	B 1.3. possibly B 2.1.	Intrusion of ultra-mafic, mafic and quartz dioritic material

POST-HOLDHUS GROUP

PRE-HOLDHUS GROP

AFTER :-
Færseth et al. 1977

were found. (References to Faerseth et al.'s sequence will be denoted D^f while the proposed correlation with the Osterøy gneiss sequence will be denoted D^g as before).

1) Their attempt to incorporate $D5^g$ from the Tysse area with $D4^f$ is rejected, as the style of the $F5^g$ folds clearly does not agree with their description of $F4^f$. It will be shown that the correct correlation is between $D5^g$ and $D3^f$.

2) There is no appreciation of the non-cylindricity of the $F3^f$, these folds are highly non-cylindrical over the whole Osterøy and Samnanger areas.

3) Their interpretation of the structures developed in $D4^f$ is questioned. Figures 9i and 10 of Faerseth et al. (1977) are supposed to show a dyke intruded along an $F3^f$ axial plane then folded by $F4^f$. In both cases the $F3^f$ axial planes are demonstrably not folded. Emplacement of the dyke across the $S2^f$ layering (in which $F2^f$ isoclines can be seen, p.44, fig.10) prior to $D3^f$ could equally explain these structures and would be in keeping with observations made in the gneisses, i.e. that the last stage of quartz diorite dyke intrusion was a late stage $D2^f$ or $D4^g$ event. Many of the other structures they attribute to $D4^f$ could equally be attributed to $D3^f$.

4) They interpret the "Osterøy Synform" (p.44, plate 1,AA, Faerseth et al.) as an $F3^f$ fold refolding an $F2^f$ fold. This interpretation is held to be incorrect partly because of the misinterpretations (1, 2 & 3) described above and for the following reasons:

a) Along strike from this synform, at Holdhus Fjell (plate 1, Faerseth et al.), similar structures are described as $F2^f$ folds (p.40).

b) The type 3 (Ramsay,1967) inteference pattern (p.42 and plate 1, Faerseth et al.) could be caused by original sedimentary variation, as shown in

figure 101, and is therefore, on the basis of the evidence presented, inconclusive.

c) The structural position of the "Osterøy Synform" relative to the major $D5^g$ fold is shown in figure 102. It is therefore clear that the "Synform" is a $D4^g$ structure.

On the basis of the points made above it is possible to make the following correlations between the deformations seen in the Arcs and the Osterøy basement.

Figure 98.

THE OSTERØY GNEISS AND BERGEN ARC DEFORMATION CORRELATION

NORTH OSTERØY GNEISSES	BERGEN ARCS	FINAL CORRELATION	
D "Early	Not present	D "Early"	)
D1	Not present	D1	)
D2	Not present	D2	) PRECAMBRIAN
D3	D1	D3	)
D4	D2	D4	)
D5	D3	D5	)
D6	D4	D6	) CALEDONIAN
Not present	D5	D7	) AND/OR LATER
D7	(D6)	D8	)

Faerseth et al. report only one deformation common to all the pre-Holdhus rocks of the Arcs $D1^f$. This deformation is also seen to affect the basement as it is possible to trace $L1^s$ into the rocks of the Arcs, across the Bergen Arc Thrust (fig. 10). Thus this thrust, like the Tysse Thrust, must be primarily a $D3^g$ structure, which means that the emplacement of the Bergen Arc Nappes is a $D3^g$ event. This $D3^g$ emplacement is supported by Faerseth et al., who describe $D1^f$ as "inverting major parts of the succession before the development of the later D2-D5 structures" (p. 37). Within the Arcs $D3^g$ will be imposed on rocks with various earlier histories because they are allochthonous nappes, and this is when the greater part of the tectonic transport occurred.

Fig **101.**

Pre- folding (F2)
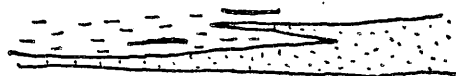
The "Osterøy Synform"

(F2)?

Schists
Marbles
Moberg conglomerate

S.W.   N.E.
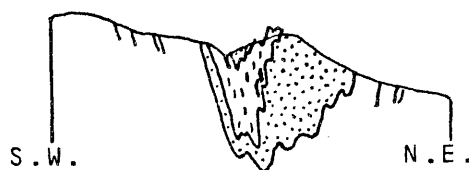
after Faerseth et al. 1977.

Fig **102.**

The Position of the "Osterøy Synform" Relative to
D5 of the Osterøy Gneisses.

F5

S.W.   N.E.

Arcs   Osterøy Gneisses

0   2 Km.
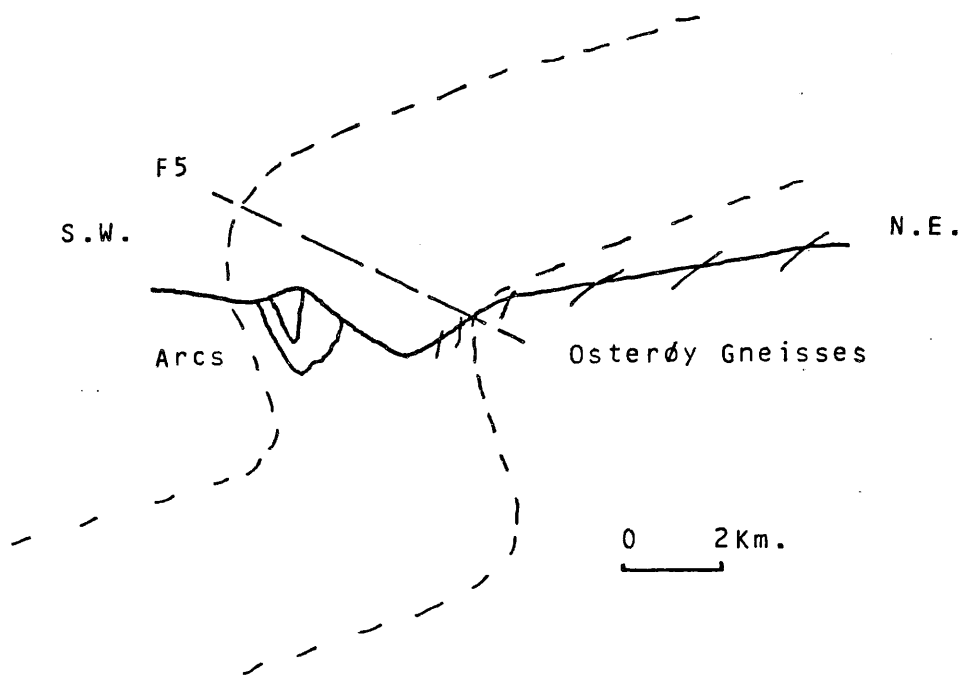
$D4^g$ thrusting and flattening on the basement is represented as the $D2^f$ folding, thrusting and imbrication in the Arcs, (4c above). This is the deformation in which $S2^s$ is imparted to the Osterøy Gneisses. As its effects increase up succession into the Arcs, and because the Bergen Arc Thrust is seen to cross-cut the lithologies of the Southern Gneiss Unit (map 1), it is suggested that the Bergen Arc Thrust is re-activated at this stage while the Tysse Thrust is not. This then is the second thrusting episode, in which the Holdhus rocks are now involved.

The evidence for the presence of $D5^g$ is conclusive (4c above), and thus $D5^g$ is correlated with $D3^f$; the small scale structures of $D5^g$ and $D3^f$ are identical as suggested (2 above).

The Bergen Arc Synform is clearly a $D6^g$ structure (pl.38). Some of the deformation structures described by Faerseth et al. as $D4^f$ (p.45, fig.11 c & g) could be attributed to this structure.

The $D5^f$ of Faerseth et al. comprises wrench faulting but such structures are not seen in the basement gneisses of Osterøy. The faulting probably occurred before the late jointing $D7^g$.

Thus at least eight deformations are required to explain the structural development of the area as a whole and these are summarised in figure 103.

Fig 103.

Deformation In The North Osterøy Gneisses

Deformation / Features Developed	Folding	Schistocity	Lineations	Thrusts	Basic Igneous Intrusions	Acid Igneous Intrusions
D8	Jointing					
D7	Wrench Faults					
D6	F6	S7		⟍		
D5	F5	S6	L4 L5			?
D4	F4	S5		⟍		⟍
	(Sediments)					
D3	F3	S4	L3	⟍	⟍	⟍
	NOT Important	Sediments				
D2	F2	S3	L2	⟍ ⟍	⟍	⟍
	S2	Sediments				
D1	F1	S1	L1		⟍	⟍
D 'Early'		S Early				?

3.   PETROLOGY

This section is divided into two parts; firstly, the description of

lithologies as seen on map 1, based on field and thin section observations;

secondly, a description of the metamorphic history of the rocks.   The

metamorphism is related to the structural elements as given in figure 103.

3.1.   COMPOSITION OF THE OSTERØY GNEISSES

The area is divided into Northern and Southern Gneiss Units, A and

B (fig.104), on the basis of tectonic history.   The units are very similar

in general composition, comprising gneissose acidic rocks with mappable

minor metasediments and intrusions of both acid and basic plutonics.

The minor lithological types provide an insight into the structural geometry

of the region.   The detailed variations in the background gneisses,

however, were not mapped as they could not be traced over any distance

at the scale of the map.   The Southern Unit is subdivided in more detail

than the Northern Unit and this is a reflection of tectonic condition.

In the Southern Unit the gneisses form traceable bands distinguishable

on the basis of outcrop morphology and colour, while remaining petrologically

very similar in hand specimen or thin section.   As the differences are

more of grain size and texture rather than of chemistry, these units

(map 1) must be regarded as litho/tectonic rather than lithological.

Quartz, albite, orthoclase plots (figs.105, 106 & 107), for the acid

gneisses collected from north Osterøy (Units A & B), show that the rocks

cannot be subdivided or grouped on a compositional basis.   There is no

clustering and the rock types identified in the field occupy overlapping

areas centred, with a wide scatter of points, around the minimum melting

eutectic composition for granite, at intermediate-high pressure (Winkler,

1974).   The scatter could be caused by the presence of metasedimentary

Fig 104.

LITHOLOGICAL DIAGRAM

(A) NORTHERN GNEISS UNIT	(B) SOUTHERN GNEISS UNIT

FLATTENED GNEISS AND MIGMATITE GROUP
 	
(contains flattened representatives of
all rock types present below)
 	
GNEISS AND MIGMATITE COMPLEX
 	
Sediments   Quartzites
              Mica Schists
              Quartzose Migmatites
 	
Migmatites
 	
Igneous Rocks
              Augen Gneiss
              Amphibolites
 	
UNFLATTENED GNEISS
 	
    Pink
    Grey
    Intermediate
    Basic
	METASEDIMENTARY ROCKS
	
	Micaceous Members Mica Schist (1)
	                        Mica Schist (2)
	                        Mica Schist (3)
	
	          Phyllonites
	    Quartzites
	          Quartz Mylonites
	
	IGNEOUS ROCKS
	
	    Augen Gneiss
	    Amphibolites Type 1
	                       Type 2
	                                Epidotite
	
	GNEISSOSE ROCKS
	
	    Helldalsefjell Gneiss
	    Pegmatite Rich Gneiss
	    Rispingen and Granitic Gneiss
	    Drangskollen Gneiss
	    Nonkletten Gneiss
	    Undifferentiated Gneiss (varieties)

ACID VEINS	ACID VEINS

Fig 105.

QUARTZ–ALBITE–ORTHOCLASE PLOT FOR
SOME ACID GNEISSES FROM NORTH
OSTERØY

100% AB

QTZ 100%

OR 100%

• Migmatized Quartz Rich Sediments

△ Flattened Gneiss and Migmatite

o Nonkletten Gneiss

(Modal % estimated, with Point Counted checking)
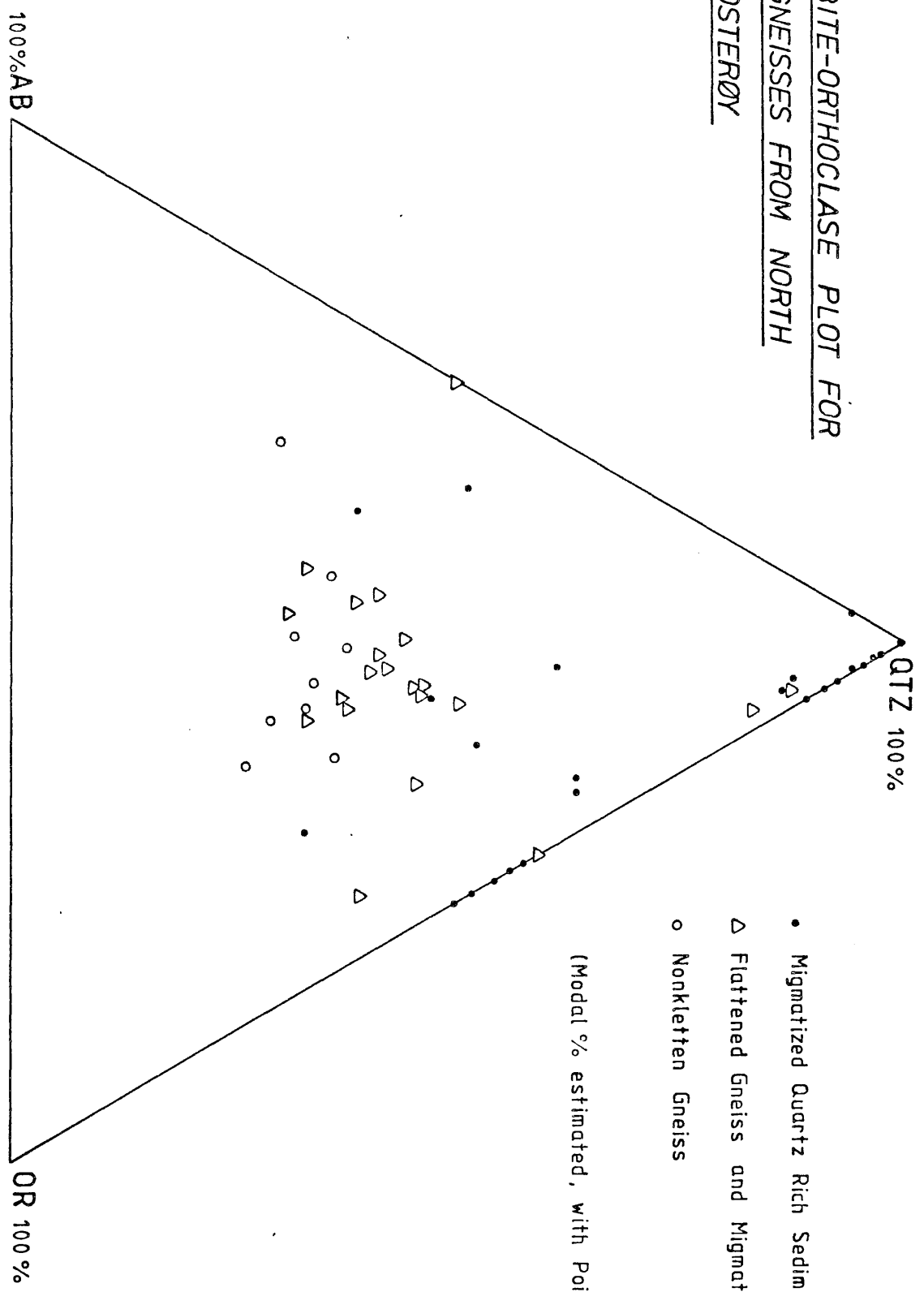
Fig 106.

QUARTZ–ALBITE–ORTHOCLASE PLOT FOR SOME ACID GNEISSES FROM NORTH
OSTERØY

△ Undifferentiated Gneiss

○ Unflattened Gneiss

□ Micaceous Metasediments

• Augen Gneiss

(Modal% estimated, with Point Counted checking & some Normative values from X.R.F. analyses)
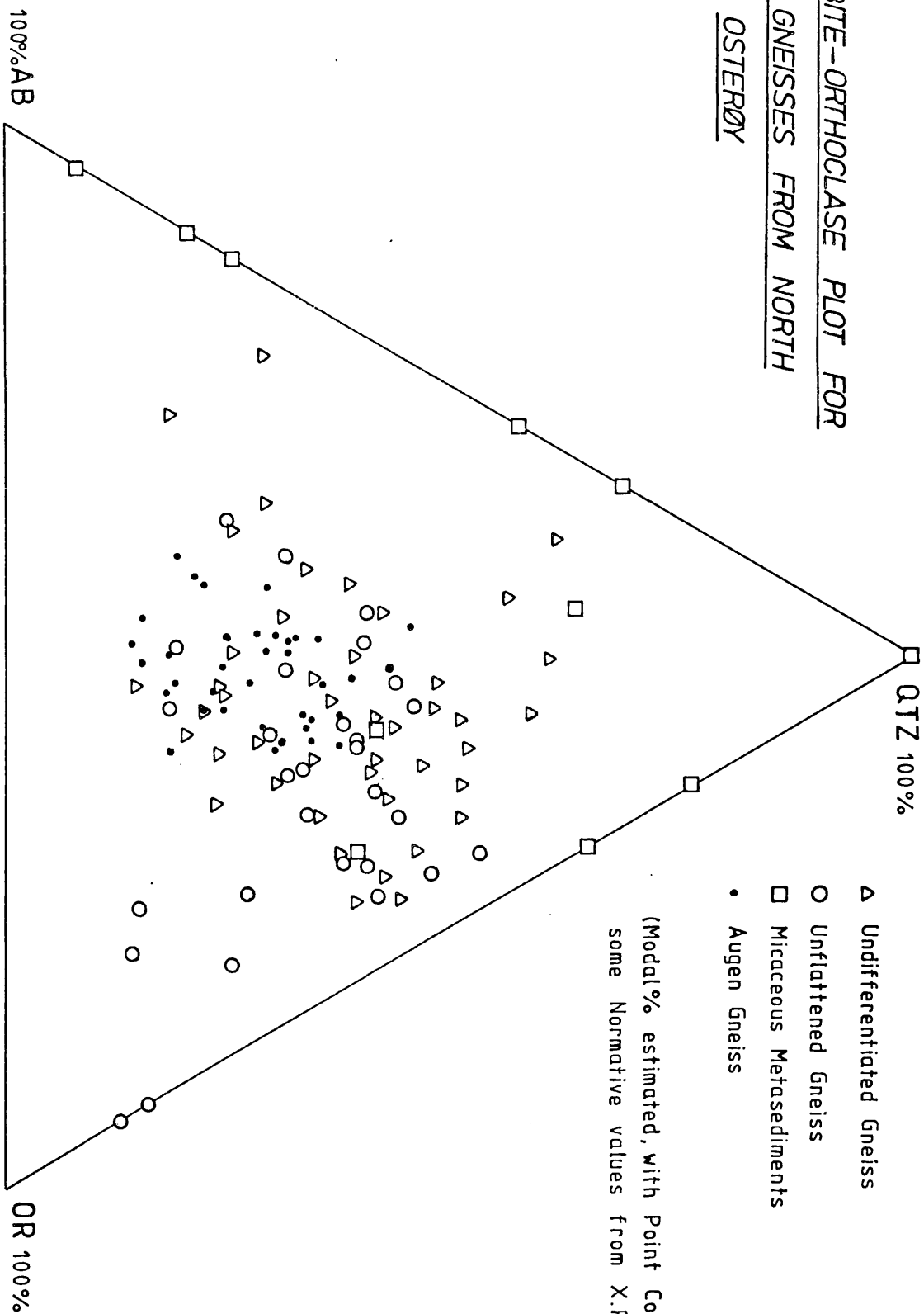
Fig 107.

QUARTZ-ALBITE-ORTHOCLASE PLOT FOR
SOME ACID GNEISSES FROM NORTH
ØSTERØY

- • Gneiss and Migmatite
- △ Drangskollen Gneiss
- ○ Pegmatite Rich Gneiss
- ■ Quartz Rich Gneiss
- ▲ Helldalsfjell Gneiss
- ▢ Granitic Gneiss

(Modal % estimated, with Point Counted
checking)

100% AB

QTZ 100%

OR 100%
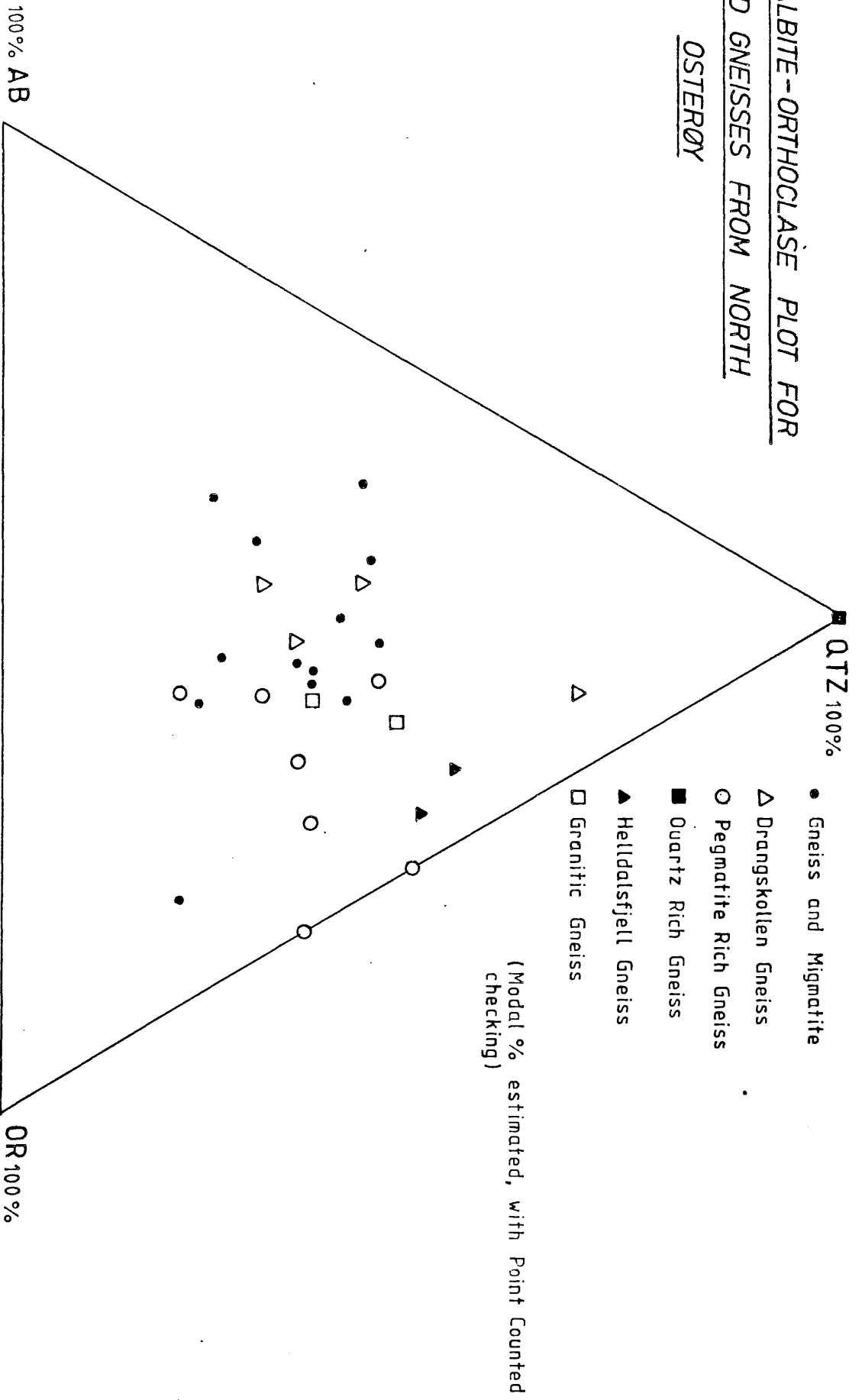
material, deformation and K-metasomatism during migmatisation. The augen gneisses, however, define a tight cluster round the granite melt eutectic region, supporting field evidence which indicates an igneous origin for these rocks.

The similarity in composition of these gneisses means that lithostructural mapping is the only means of classifying most of the rocks in the field.

The basic rocks in the gneisses (Units A & B) are divided on structural bases into three chronological groups. The structural observations point to an intrusive origin. A major element AFM plot (fig.108), of some of the basic rocks from all units suggests that they are basaltic in composition. This together with their structural field relationships and the presence of relict igneous textures in a clump of pigeonite crystals from one of the bodies, confirms an intrusive igneous origin for the basic rocks.

Trace element analyses of specimens collected from each of the three groups are plotted, following Pearce and Cann (1973), (fig.109) and Floyd and Winchester (1975), (fig.110). The scatter observed in figure 110 indicates that both "Tholeitic" and "Andesitic" rock types are present, but detailed plotting shows that rocks belonging to any one 'time unit' fall into both fields. A similar picture is presented in figure 109, where the points scatter across all the fields. This could indicate that the chronological subdivision is wrong or could be explained by a) the intrusive episodes being complex involving more than one suite in each phase, or b) deformation and protracted metamorphism at amphibolite and greenschist facies conditions having affected the trace element distribution in the rocks to the point where they can no longer be used, as Pearce and Cann (1973) suggest.

Fig 108.

A·F·M PLOT BASIC ROCKS FROM
THE OSTERØY GNEISSES
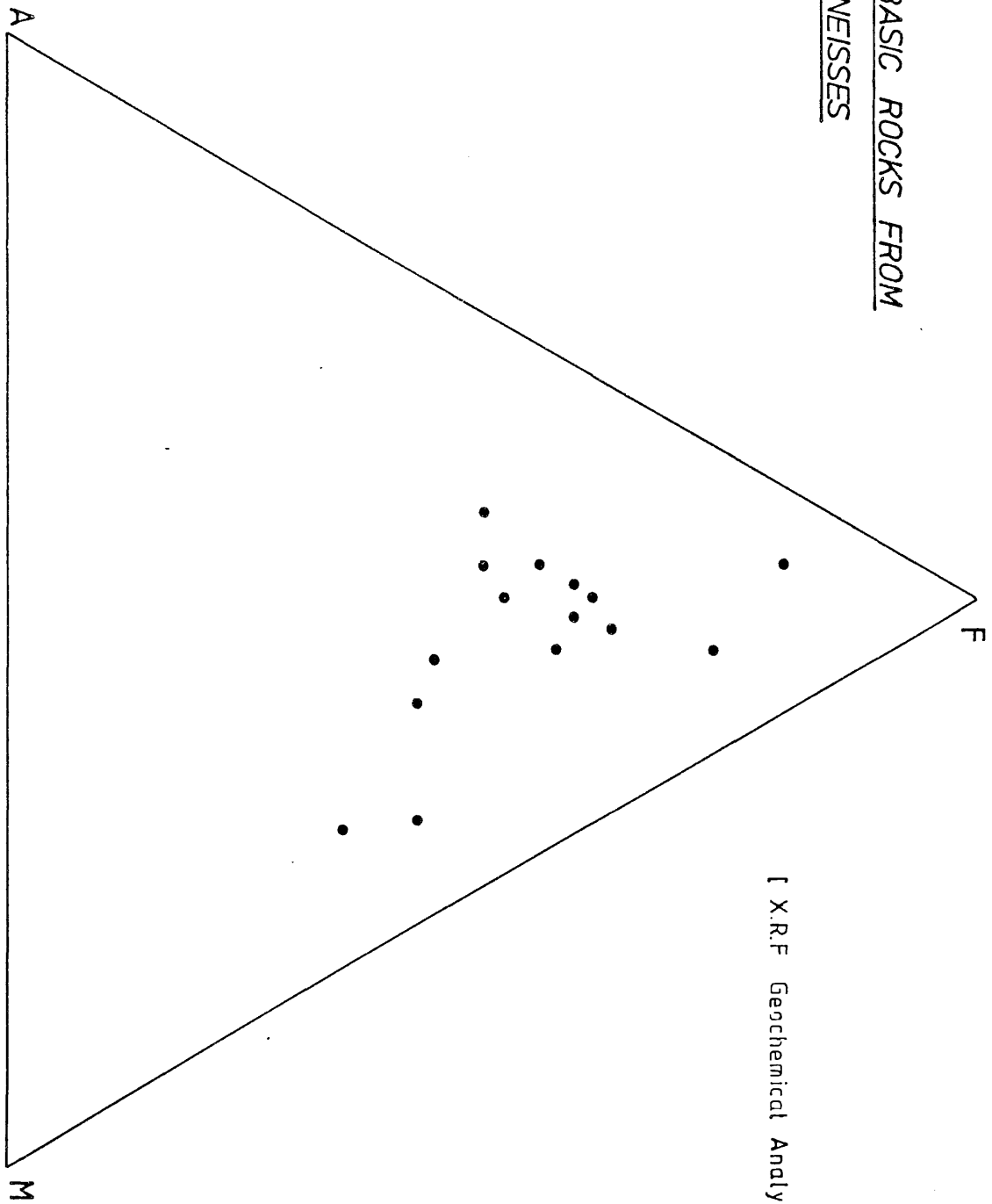
[X.R.F Geochemical Analyses]

Fig 109.

Ti-Zr-Y PLOT OF BASIC ROCKS
FROM NORTH OSTERØY

(X.R.F. Geochemical Analyses)
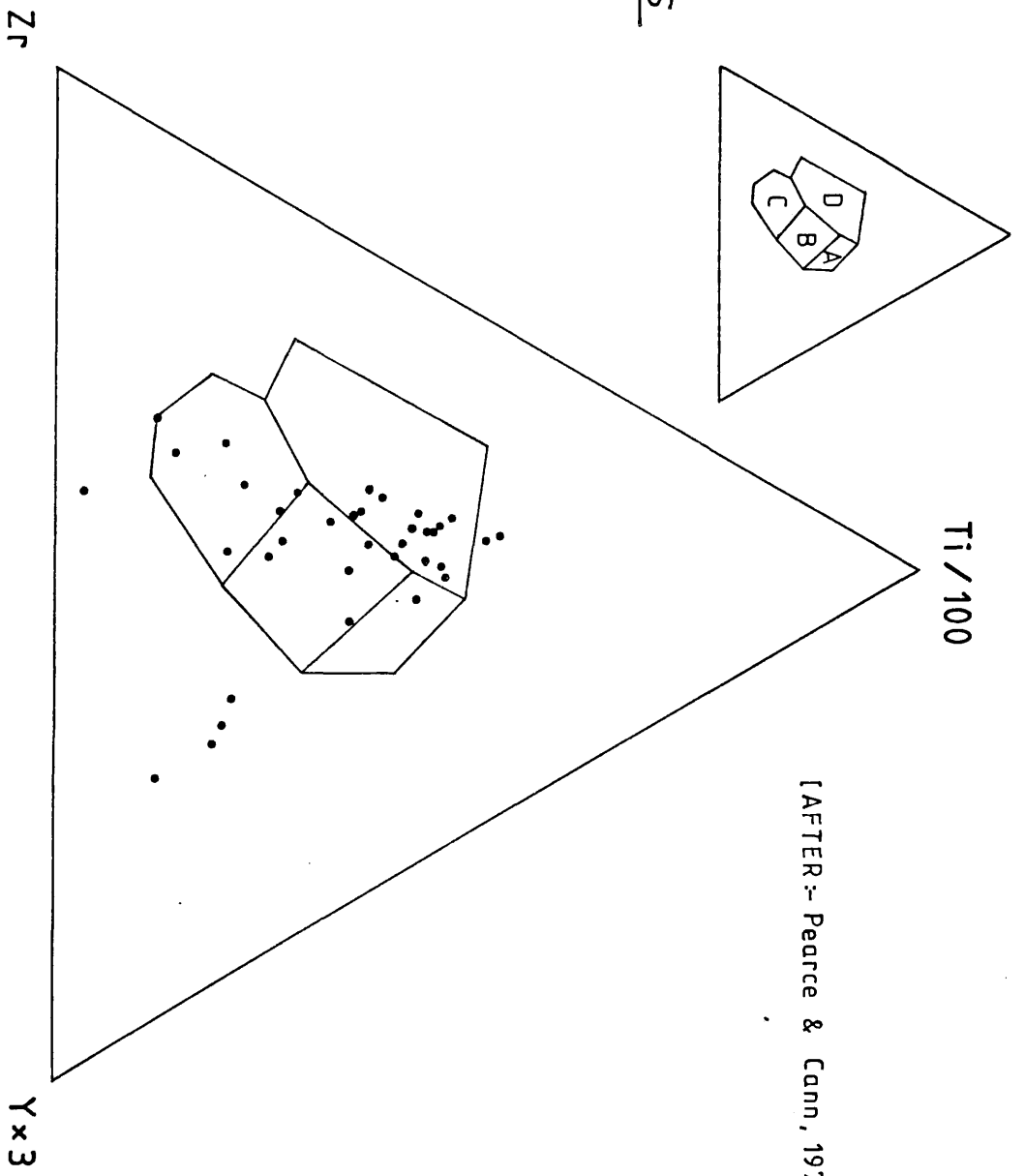
[AFTER:- Pearce & Cann, 1973]

Fig 110.

$TiO_2 - Zr/P_2O_5$ PLOT OF BASIC ROCKS FROM NORTH

OSTERØY

(X.R.F. Geochemical Analyses)

TiO_2

AB

TH

Zr/P_2O_5
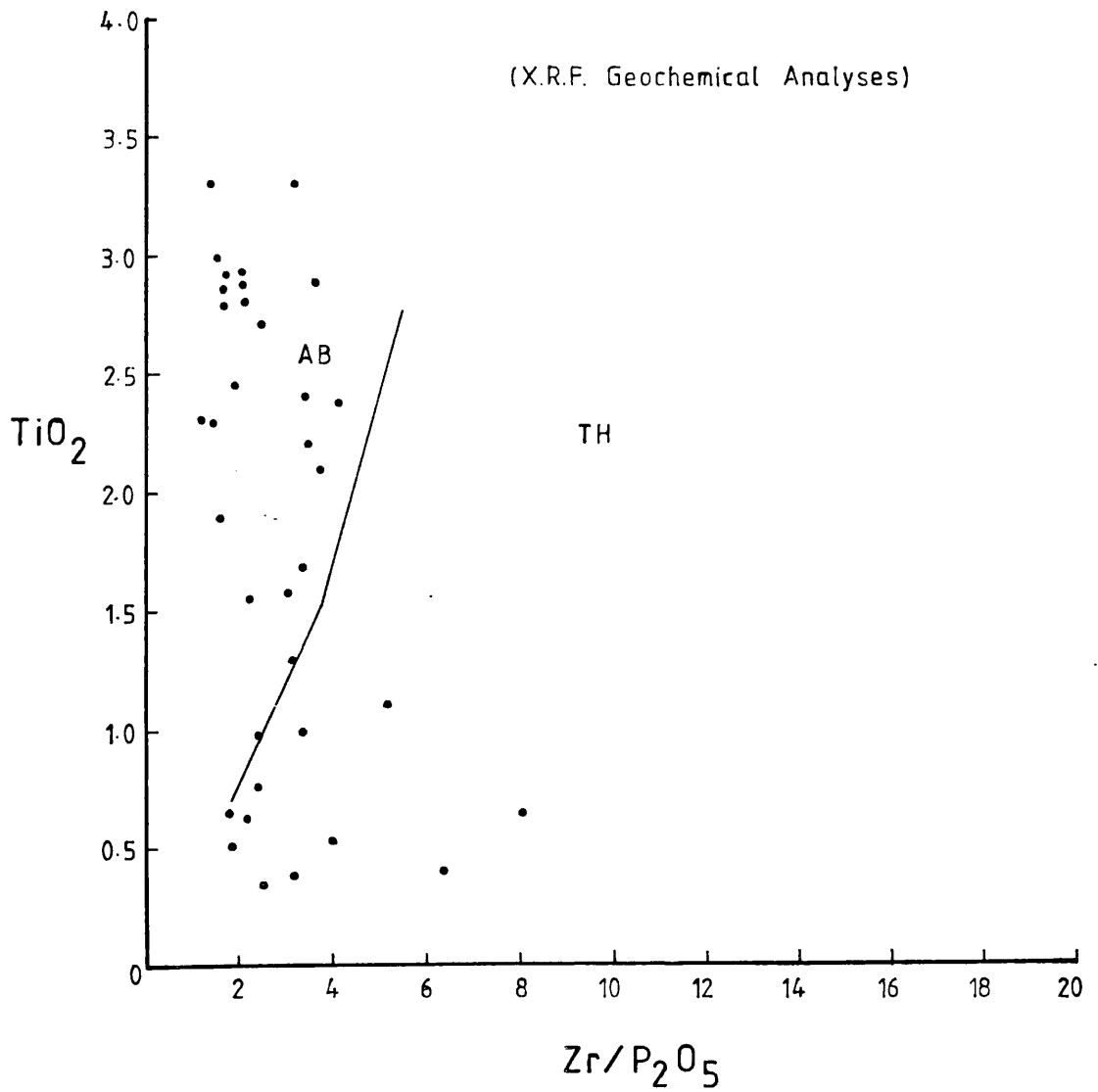
[AFTER :- Floyd & Winchester, 1975]

These observations are similar to those made for the Moine amphibolite suite of central and northern Sutherland, Scotland (Moorhouse & Moorhouse, 1979).

3.2   LITHOLOGIES OF THE NORTHERN GNEISS UNIT

The rocks comprising the Northern Unit (A) are subdivided into three groups (fig.104), using both petrological and tectonic characteristics. Within each group there is a wide variation in rock type and petrology.

TABLE GROUPING LITHOLOGIES OF THE NORTHERN GNEISS UNIT

3)   The Flattened Gneiss and Migmatite Group:

These are similar types of rocks to those of groups 1 and 2 below, but they are more deformed.   This group is distinguished on structural grounds only, and is structurally the highest   . member.

2)   The Gneiss and Migmatite Complex:

A suite of migmatised metasedimentary rocks, granites, granodiorites and amphibolites, tectonically involved with a suite of older (group 1) gneisses preserving structures of older deformations than those seen in the migmatised metasediments.   This unit, which is structurally at an intermediate level is therefore distinguished on both a structural and compositional basis.

1)   The Unflattened Gneisses:

These comprise a suite of granitic to granodioritic gneisses intruded by amphibolites.   They form the lowest structural unit and are distinguished on a structural basis, in that they contain a fold phase not seen in any other rocks.

3.2.1 The Unflattened Gneisses

These gneisses outcrop on the west coast of the island, are mainly granitic - granodioritic in composition, with small amounts of basic rocks.

They are usually very well compositionally banded, with a banding parallel schistosity. The acidic members can, on the basis of their colour in outcrop, be further subdivided into three main types: Pink Gneisses, Intermediate Gneisses and Grey Gneisses.

The Pink Gneisses are granitic in composition (fig.111, and analyses 1, 3 & 33 in appendix 2), coarse-to medium-grained (1-2mm) and well foliated. Augen of porphyroblastic potash feldspar up to 2cm across are common, together with segregational veins and lenses of quartzo-feldspathic material up to 10cm thick, bordered by selvedges of biotite and mafic constituents.

The biotite in the rocks defines a schistosity which parallels the banding in all areas except in the nose regions of intrafolial F1 folds of the banding (sections 2.1.1 & 2.1.2).

The Grey Gneisses are fine- to medium-grained (0.1-1mm) and granodioritic in composition (fig.111), richer in biotite and plagioclase and poorer in quartz and potash feldspar than the Pink Gneisses. Compositional banding is less evident and where segregational lenses are seen, they are thin, 1-3mm thick. In thin section the schistosity in these gneisses appears much more regular than in the Pink Gneisses and the mafic constituents are more evenly distributed throughout the rock.

The Intermediate Gneisses are more adamellitic in composition (fig.111), and consist of the Grey and Pink varieties interlayered in bands on the scale of 30cm or so in thickness.

The Basic Bodies

The mineralogy seen in these bodies depends on the size of the body sampled and its position on the D2 structures. In the largest (over 5m thick) examples, in the noses of F2 folds, relics of an original igneous mineralogy and texture are preserved. Towards the margins of

Fig 111. TABLE OF MINERAL CONTENT, MODAL RANGES.

ROCK TYPE / GROUP — RANGE of MODAL MINERAL (%)	UNFLATTENED GNEISS				GNEISS AND MIGMATITE COMPLEX			
	Pink Gneisses	Grey Gneisses	Intermediate Gneisses	Quartzites	Mica Schists	Quartzose Migmatite	Migmatites	Augen Gneiss
Quartz	30-40	20-30	15-35	60-95	30-50	55-70	25-45	20-35
Plagioclase	5-20	30-50	10-40	0-5	T	0-5	12-40	15-25
K-Feldspar	30-40	5-25	20-35	0-10	0-20	20-40	18-40	20-30
Biotite	5-15	15-25	15-20	1-15	5-23	0-10	0-25	8-20
Muscovite	0-10	–	T	1-10	20-50	0-30	0-2	–
Hornblende	–	T	T	–	–	–	0-15	1-20
Tremolite/Act.	–	–	–	–	–	–	–	–
Epidote	T	0-5	0-5	T	T	–	0-5	1-10
Sphene	T	T	0-5	T	–	–	0-3	1-2
Chlorite	T	T	T	T	T	T	0-10	0-2
Garnet	T	–	T	0-1	2-6	T	T	T
Apatite	T	T	T	T	–	T	T	0-1
Iron Ore	T	T	T	T	1-5	T	0-5	1-3
Zircon	T	–	T	T	–	–	T	–
Sericite	T	T	T	–	–	–	–	–
Tourmaline	–	–	–	–	–	–	–	–
Pyroxene	–	–	–	–	–	–	–	–
Kyanite	–	–	–	0-3	–	–	0-3	–
Staurolite	–	–	–	–	0-3	–	–	–
Graphite	–	–	–	–	–	–	–	–
Calcite	–	–	–	–	–	–	–	–

such bodies and in the F2 limb regions this igneous character is completely

overprinted and the rock is altered from a gabbro to an amphibolite.

In the smaller bodies the amphiboles are partly to completely re-

placed by biotite and epidote. The petrology of these bodies can there-

fore be comprehensively described in terms of three end members.

Gabbroic			Amphibolitic			Biotitic		
Diopside	5 per cent[*]		Hornblende	35-99 per cent[*]		Biotite	40 per cent.[*]	
Hornblende	30 "	"	Plag An 20	1-30 "	"	Epidote	25 "	"
Plag An25	50 "	"	Biotite	0-20 "	"	Quartz	10 "	"
Quartz	10 "	"	Quartz	0-10 "	"	Plag An20	15 "	"
Epidote	5 "	"	Iron ore	0-10 "	"	Sphene	5 "	"
Sphene	trace		Epidote	trace		Iron ore	2 "	"
Iron ore	"		Apatite	"		Apatite	trace	
Apatite	"		Sphene	"		Hornblende	"	
Chlorite	"		Chlorite	"		Chlorite	"	

---

[*] estimates in thin section.

In the least metamorphosed state, traces of what could be an original

igneous compositional layering are visible. It is probably this layering

which is responsible, in the metamorphosed state, for the more ultrabasic

compositions seen in some places. The plagioclase in these rocks is

frequently zoned, becoming more sodic in the outer regions. It is also

more sodic than the rest of the mineralogy would indicate, even where

pyroxene is still preserved. This is taken to be a feature of metamorphic

retrogression. The bodies are frequently cut by younger pegmatites;

close to these progress towards the retrograde biotitic mineralogy is

accelerated. In outcrop the rocks are well foliated though in the thicker,

coarse-grained (2-20mm) bodies this foliation is less apparent. Analyses

2, 27, 28, 29, 30, 31, 32, 72, 73, 75, 76, 77 and 78 in appendix 2 show

a range of compositions from these bodies.

Discussion

The Unflattened Gneisses are the oldest rocks in the area. Their

composition suggests a correlation with the Jostedal Complex of Bryhni (1966) and Carswell (1973).

The banding in the Intermediate gneisses consists of Pink and Grey gneiss interlayered. This banding at all scales is typical of the Unflattened gneisses regionally.

The origin of the Pink and Grey gneisses is obscure. The earliest textures seen are metamorphic but this does not preclude either a sedimentary or igneous origin. It is clear that some of the basic bodies are igneous intrusions into these gneisses and not metasediments or metavolcanics.

The basic intrusives show very clearly the extent of metamorphic retrogression these rocks have suffered (see section 3.5).

3.2.2 The Gneiss and Migmatite Complex

This group of rocks comprises portions of reworked Unflattened gneiss and a suite of migmatised metasedimentary rocks, which include quartzites, psammites and mica schists. Minor intrusive granitic and pegmatitic bodies and amphibolites are also found.

The amphibolites are basic in composition (fig.108) and field relationships show that they are intrusive into the sedimentary complex.

Sediments

Quartzites. Although similar to the gneisses (both weather grey), the quartzites have a restricted mineral assemblage (fig.111), are more massive and have a waxy appearance. A compositional layering paralleling the foliation in the surrounding gneisses is visible due to an increase in mafic content at certain horizons in the quartzites. Frequently these compositional variations appear gradational on one side and sharp on the other and this is tentatively interpreted as graded

bedding (Myres,1978). No consistent way up was determined from this because of the complexity of later folding. (The north-west "arm" of the major Quartzite outcrop at (22.00,38.00) appears to be right way up). These rocks preserve the most interesting metamorphic assemblages. The oldest are at the highest grade with the development of kyanite and garnet; younger assemblages show progressive retrogression to chlorite, accompanied by the development of new cross-cutting fabrics in the rocks (see section 3.5 below).

Mica Schists. These rocks are found as foliation-parallel lenses within the quartzites. The lenses are up to 1m thick and vary in quartz content (fig.111) from being a micaceous quartzite to a quartz mica schist. Characteristically the more micaceous varieties weather brick red due to secondary iron oxide, whereas the quartz-rich varieties green/yellow. The schists preserve more than one schistosity, one axial planar to tight folds paralleling the regional foliation and a crenulation cleavage at a high angle to this (fig.32). The schists contain staurolite and are interpreted as pelitic beds in the quartzite sequence.

Quartzose Migmatites. In outcrop these rocks are distinguished from the migmatites and gneisses by their lighter colour, (light grey with a pinkish hue) and their restricted mineralogy (fig.111). In hand specimen the rocks resemble the quartzites except that they do not develop the transluscent waxy appearence of the true quartzites. Feldspars and micas are more abundant than in the quartzites and are found in foliation parallel layers or lenses about 1-4 crystals thick, which are interpreted as being the product of the first stages of migmatisation. The rocks are frequently associated with the quartzites, but also occur separately, e.g. (14.00,45.00). They possibly had their origins as impure sandstones.

Unlike the quartzites no primary layering is detected in these rocks, though, in common with the country gneisses they are well foliated.

Migmatites

These rocks comprise the bulk of the Gneiss and Migmatite Complex. They are very similar in composition to the Unflattened gneisses (fig.111) and include reworked portions of these; the exact amount of Unflattened gneiss incorporated cannot be determined because the re-working ultimately destroys early structures, and without this control compositional differences cannot form a basis for subdivision of the migmatites. However, the metasedimentary portions of the migmatites occasionally contain kyanite and more hornblende is present in some of them than is seen in the Unflattened gneisses. There is also a further segregation of quartz from the feldspars in the metasedimentary leucocratic layers. The quartz forms anastomising, foliation parallel, polycrystalline ribbons of one crystal thickness. These three features, attributed to those portions of the migmatite suite that are of sedimentary origin, together with structural observations, do then provide some basis for separation of the older and younger portions of the Migmatite Complex. No attempt was made to delimit the exact extent of the metasediments on map 1; they are included in the migmatites and treated as one unit. Analyses 70 and 40 in appendix 2 are of two examples of the more mafic rock types in the Migmatite Complex.

Igneous rocks

Augen Gneisses. These are intrusive into the older Migmatite Complex, although they form bodies (not more than 30m thick) that are sub-parallel to the regional foliation; low angle cross-cutting relationships are seen and in some localities (12.50,35.70), the Augen gneisses are seen to surround and include portions of metasedimentary rocks. These

sediments were subsequently folded with the Augen gneisses in F2, and

for this reason they are thought to have been intruded at a late stage

in the migmatisation of the sedimentary complex, this event occurring

prior to F2.   Compositionally, the Augen gneisses are granitic (fig.111,

analysis 60, appendix 2), medium-grained (1-2mm) and dark grey in outcrop

with lensoidal segregation bands of white or pinkish feldspar and quartz,

frequently in the form of augen.   The augen may be made of single

microcline crystals or an aggregate of large feldspar crystals.

Myrmekite texture is common.   The plagioclase in the rock is albitic

(An 6-8), the iron ore is ilmenite and is frequently rimmed by sphene.

Amphibolites.   Within the Migmatite Complex there are sub-
stantial bodies of amphibolite (fig.112).   The origin of these rocks is

unclear, but the fact that they are found within the sedimentary complex,

are never deformed by F2 folds which fold the sediments and occur as

lenses (up to 8m thick) within the S3a foliation produced by these folds,

suggests they are of intrusive rather than sedimentary origin.   This

view is supported by geochemical analyses of these rocks (figs.108, 109

& 110) and analyses 41, 43, 62, 63, 64, 65, 66, 67, 68 and 71 in appendix

2, but attempts to distinguish them from their older counterparts in

the Unflattened gneisses proved to be unsuccessful.   In regions of high

strain and retrogression biotite replaces hornblende.   Mineralogically

then, there are two rock types representative of the basic bodies in

the Gneiss and Migmatite Complex:

Biotitic Amphibolite   and   Amphibolite

Hornblende	0-20 per cent.[*]	Hornblende	30-60 per cent.[*]
Plagioclase An 20	3-55 " "	Plagioclase An 30	20-50 " "
Biotite (brown)	30-40 " "	Biotite (brown)	0-30 " "
Quartz	3-8 " "	Quartz	0-5 " "
Epidote	0-25 " "	Chlorite	0-16 " "
Iron ore	2-4 " "	Iron ore	1-7 " "
Sphene	1-5 " "	Sphene	1-2 " "
Chlorite	trace	Apatite	1-2 " "
Apatite	"	Garnet	0-1 " "
		Epidote	trace

[*] thin section estimates.

Fig. 112.

NORTH OSTERØY

OUTCROPS OF AMPHIBOLITES
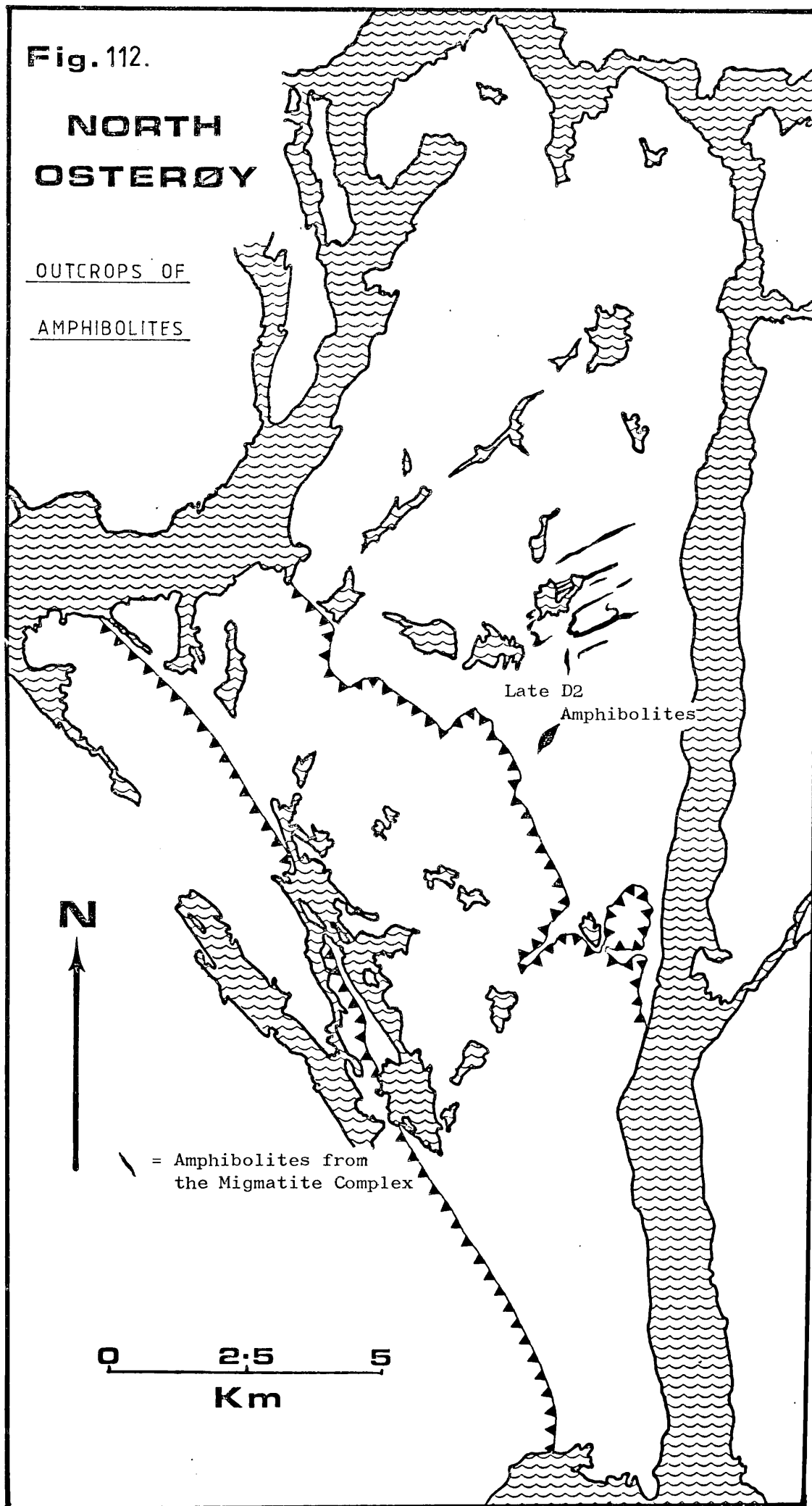
Late D2 Amphibolites

\ = Amphibolites from the Migmatite Complex

0   2.5   5
Km

The rocks are well foliated and while in the biotitic members the grain size is small (0.1-5mm), in the amphibolitic varieties the rocks are spotty in hand specimen; clumps of mafic minerals up to 10mm across made of crystals up to 2mm across are set as augen in a paler plagioclase-rich matrix. Frequently these knots of mafic minerals are centred round cores of allotriomorphic iron ore. As with the older amphibolites, the zoned plagioclase is sodic and is considered to reflect metamorphic retrogression.

Discussion

The rocks of the Gneiss and Migmatite Complex form a cover to the Unflattened gneisses. They appear to consist of more or less migmatised sediments and basic intrusions, and are tentatively correlated with the Fjordane Complex of Bryhni (1966) and Carswell(1973).

Early metamorphism at middle to upper amphibolite facies conditions was followed by metamorphism under progressively lower facies conditions. This is particularly well shown by the amphibolites, which developed chlorite in the final stage.

The early metamorphism represents the highest grade attained by any of the rocks of north Osterøy.

3.2.3   The Flattened Gneiss and Migmatite Group

There are two varieties included in this group of rocks, both are formed from the Unflattened gneisses and the gneiss and migmatites and are therefore compositionally very similar to them (fig.113), (spanning the range granite, adamellite, granodiorite) but in higher states of finite strain. The first of these varieties is found on the high ground in the Northern gneiss outcrop (map 1) and is recognised in the field by a strengthening of the (S4) foliation in the rock; it

Fig 113.　TABLE OF MINERAL CONTENT, MODAL RANGES.

ROCK TYPE / GROUP — RANGE of MODAL MINERAL (%)	FLATTENED GNEISS AND MIGMATITE	METASEDIMENTARY ROCKS					
		Micaceous Members			Phyllonites	Quartzites	
		Type 1	Type 2	Type 3		Quartz Mica Schist	Quartzite
Quartz	25-30	17-45	20-25	38-43	5-10	50-55	75-95
Plagioclase	15-35	0- 8	10-15	0-15	15-30	-	0-10
K-Feldspar	20-37	0- 5	-	10-20	0-40	1-15	-
Biotite	10-20	5-27	20-25	0- 5	5-45	0- 7	0- 4
Muscovite	0- 2	45-55	15-20	25-40	0-25	25-45	1- 7
Hornblende	0- 5	-	-	-	-	-	-
Tremolite/Act.	-	-	-	-	-	-	-
Epidote	0- 3	-	-	-	0- 5	1- 2	T
Sphene	0- 1	-	-	-	T	-	T
Chlorite	0- 3	0- 2	-	-	0- 2	-	-
Garnet	T	0-10	15-20	-	T	T	T
Apatite	-	T	T	-	T	0- 1	0- 1
Iron Ore	0- 5	0- 3	1- 3	1- 2	T	T	1- 2
Zircon	-	T	T	T	T	T	T
Sericite	-	-	-	-	0- 5	T	0- 2
Tourmaline	-	-	-	-	0- 5	-	-
Pyroxene	-	-	-	-	-	-	-
Kyanite	-	-	-	-	-	-	-
Staurolite	-	-	-	-	-	-	-
Graphite	-	T	-	-	-	-	-
Calcite	-	-	-	-	0-30	T	T

becomes apparent in outcrop (fig.19). There is also a general reduction in grain size when compared to the Gneiss and Migmatite equivalents. The latter are medium- to coarse-grained, while the flattened rocks are fine- to medium-grained (0.01-0.5mm). The more quartzose and basic units in the Flattened gneisses are correlated with the Quartzose Migmatites and amphibolites of the Gneiss and Migmatite Complex. Mineralogically the characteristic feature of these rocks is that biotite is the dominant mafic mineral with very little hornblende, and small euhedral crystals of inclusion-free garnet are common, dispersed in the rocks overgrowing the S4 foliation.

The second variety is found locally developed everywhere in the Northern Gneiss Unit, within zones of D5 shear. Entering these zones, there is a marked reduction in grain size and a strengthening in the schistosity (S6), which is rotated parallel to the walls of the zone.

3.3   LITHOLOGIES OF THE SOUTHERN GNEISS UNIT

The rocks comprising the Southern Unit (B) are broadly subdivided into three groups (fig.104). The rocks in the last two groups are found more to the south-western margin of the Southern gneiss outcrop, along the tectonic junction with the Arcs, while the rocks of the first group form the bulk of the outcrop. The rocks comprising the first group, while very well foliated, are, for the most part, extremely heterogeneous and have been lumped together as "Undifferentiated gneiss". However, traceable units are identified within these gneisses. These are not petrologically distinct and are distinguished more on the basis of their relative homogeneity, which shows them up from the surrounding gneiss, or by the fact that they are unusually rich in vein material. Such gneisses are given local names.

TABLE GROUPING THE LITHOLOGIES OF THE SOUTHERN GNEISS UNIT

3) Metasedimentary Rocks:

These rocks form a distinct suite comprising quartzites
and mica schists cropping out in a band along the contact
with the Bergen Arcs. Phyllonitic and mylonitic rocks
found in this band are also included here.

2) Igneous Rocks:

The rocks included in this group, the majority of the
amphibolites and some of the augen gneisses, form a
younger igneous suite. Most of the rocks involved are
found in the south-western half of the Southern Gneiss
outcrop.

1) Gneissose Rocks:

This group of rocks comprises lithologies very similar to
those found in the Northern Gneiss Unit. The group
includes the Nonkletten Gneiss, the Drangskollen Gneiss,
the Heldalfjell Gneiss, the Rispingen Gneiss, Granitic
Gneiss, Pegmatite-Rich Gneiss and Undifferentiated Gneisses.
The igneous rocks included here are part of the country rock
gneisses into which younger igneous rocks (2 above) were
emplaced.

3.3.1 Metasedimentary Rocks

Most of these rocks occur in a schuppen zone beneath the thrust
contact with the Bergen Arcs (map 1). There are two main rock types
present, mica schist and quartzite, but during the thrusting these were
tectonically interleaved with gneissose rocks belonging to group 1.
This process resulted in a mixing of the three lithologies, producing
thinly banded, fine-grained quartzose mylonites and phyllonites.

Micaceous Members

There are three varieties of mica schist present (fig.113), the first
of these crop out as long, thin (3m), foliation parallel lenses, grey

in colour with a silvery sheen on foliation surfaces. Garnet is present in places in this variety. The second variety is only found on Drangøy (06.00,32.00) and forms short thick lenses (150x30,). The rock is purplish when fresh, but weathers brown and is rich in garnets up to 3mm in diameter. The third variety of mica schist also has a restricted outcrop, being found as small pods in the gneisses at (21.30,17.00); it is the only variety to be found away from the schuppen zone. When fresh this variety has a silvery appearance and weathers to a pale green colour with gold tinges; garnet is not found in this variety. The mica schists are generally well foliated with large "oyster shell" muscovites up to 2cm across.

Feldspar and quartz in the rocks are mainly confined to thin iso-clinally folded layers. Crystal size usually does not exceed 1mm, except for garnet and potash feldspar which occur as porphyroblasts up to 5mm across, the former frequently showing snowball inclusion trails of quartz and graphite.

Phyllonites. Found as small lenses along strike from or beside type 1 mica schists in the schuppen zone (20.25,06.00); these rocks are distinguished from them by the higher proportion of non-micaceous minerals they contain (fig.113). The micaceous material in the phyllonites rather than forming bands in the rock, forms numerous "pip shaped" lenses, ranging in size from 3x5mm to 4x10cm. Within these pips grain size ranges from 0.1-2mm and the lenses are enwrapped by thin impersistent micaceous layers. The rocks are grey/green in colour and less silvery than the mica schists. They are also much richer in potash feldspar porphyroclasts than the mica schists and tend to show more late stage retrogression with the development of calcite and chlorite. In thin section muscovite is seen to occur as distorted books (fig.114), rather than as continuous sheets.

Fig 114.

DISTORTED MUSCOVITE BOOKS FROM A PHYLLONITE

0   mm   1

Matrix of Finer
Grained Quartz
and Feldspar

K-Feldspar

Muscovite

Iron Ore

Late Iron Stained
Shear Zone

K-Feldspar

Epidote
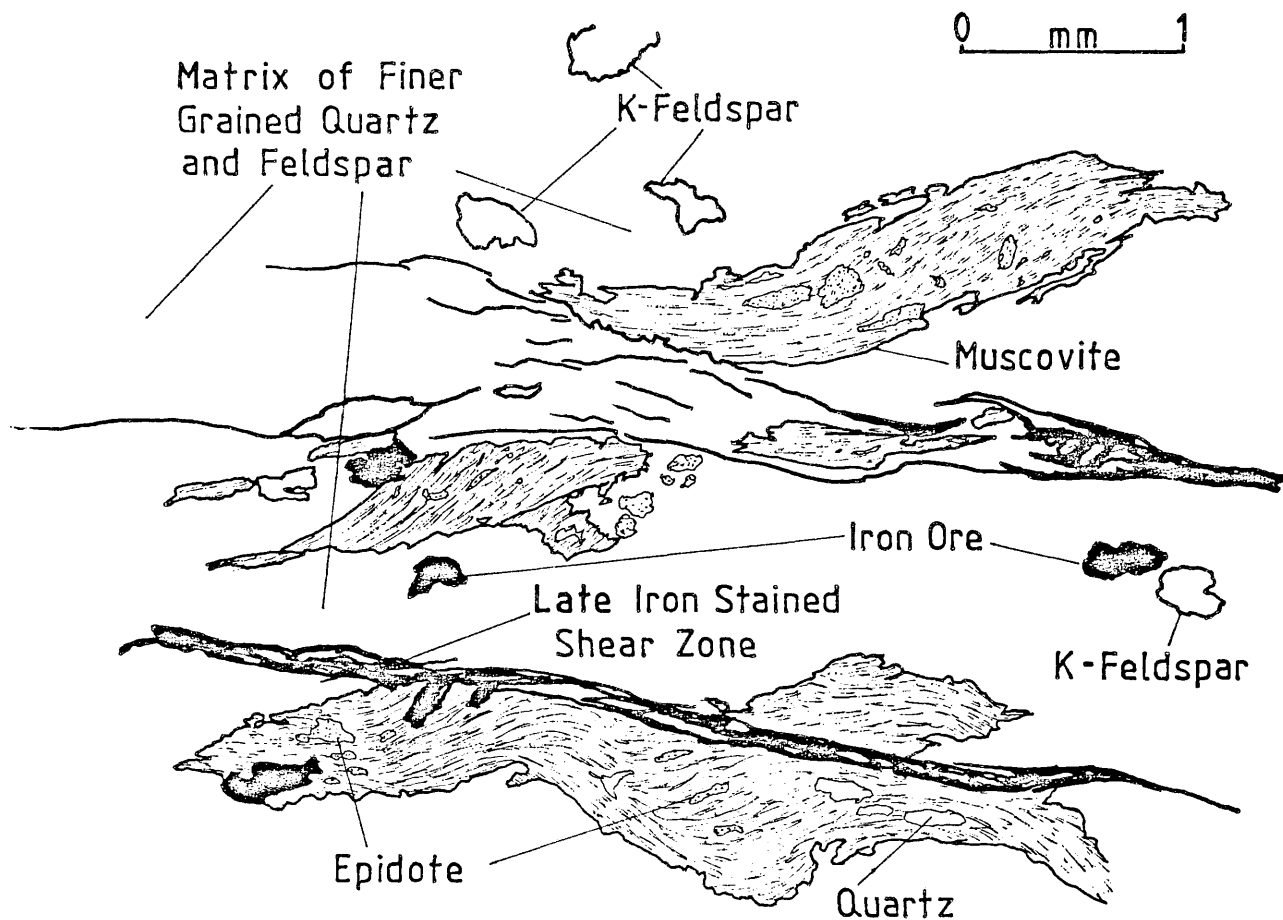
Quartz

Fig 115.

HORNBLENDE - QUARTZ - K-FELDSPAR   POD

Plane of Foliation

Knot of Quartz,
K-Feldspar &
Hornblende

Light Grey-Pink Gneiss

Pink K-Feldspar

Quartz

Hornblende

Foliation Wrapped
Round the Pod

Dark Grey Gneiss
Band
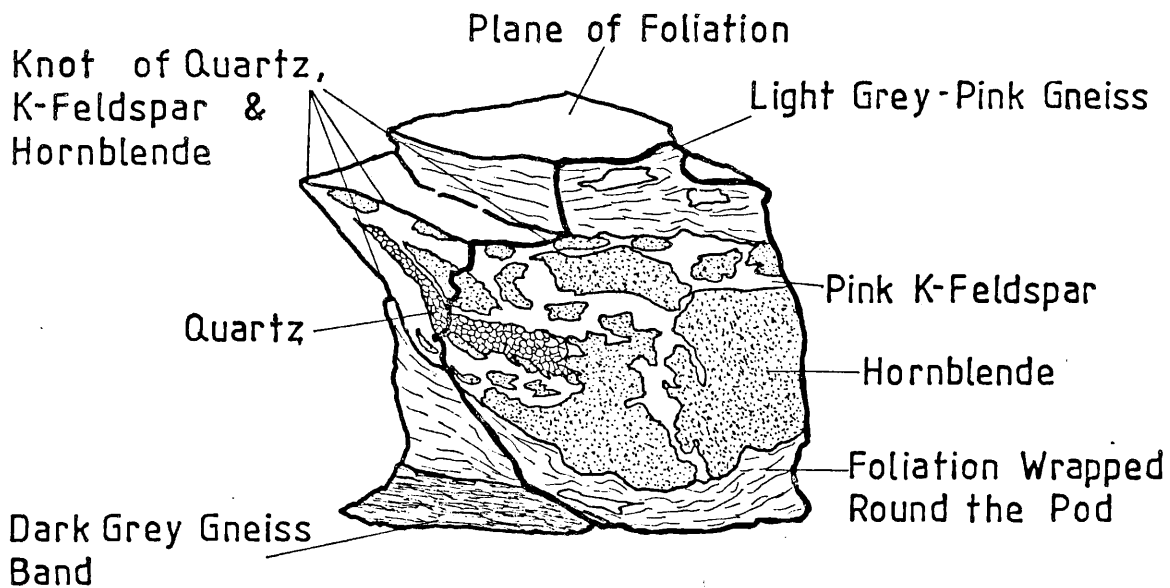
$\times \frac{1}{2}$

Quartzites

These form a very distinctive lithology in the schuppen zone with the type 1 mica schists, into which they frequently grade laterally. The bodies are never more than 6m thick, medium-grained and, when pure, milk white in colour, becoming green/grey as the mica content increases. Petrologically they fall between two end members, one a quartz mica schist and the other a pure quartzite (fig.113). These rocks preserve older fabrics very well; several generations of schistosity are seen, some depicted by the orientation of muscovite flakes, some by quartz lamellae and some by crystallographic lattice orientations (figs.123 & 124). The earliest fabric may be bedding, but this cannot be proved. The rocks are cut by several phases of quartz veins, some of these are isoclinally folded.

Quartzose Mylonites. These rocks differ from the 'normal' sediments in that they are richer in feldspar (fig.116, and analyses 5 and 10 in appendix 2). Characteristically the rocks are fine- to medium-grained, dark grey, with a strong foliation, numerous potash feldspar augen and porphyroclasts of coarsely crystalline rock fragments up to 1cm across. The lithology is associated with the schists, phyllonites and quartzites in the schuppen zone and forms a gradational rock type between the sediments and the group 1 gneisses. The most quartz-rich varieties are distinguished from the quartzites because they are fine-grained (0.1mm) and almost black in hand specimen. The difficulty in differentiating between these rocks and the gneisses other than in thin section means that this rock type is not distinguished on map 1, but the rock type is very important within the schuppen zone.

Discussion

The metasediments are the highest structural unit of the Osterøy gneisses. They have been included within the Bergen Arc lithologies by

Fig 116.

TABLE OF MINERAL CONTENT, MODAL RANGES.

ROCK TYPE / GROUP — RANGE of MODAL MINERAL (%)	METASEDIMENTARY ROCKS — Quartz Mylonites		IGNEOUS ROCKS	GNEISSOSE ROCKS		
	Quartz Rich	Quartz Poor	Augen Gneiss	Heildalsfjell Gneiss	Pegmatite Rich Gneiss	Rispingen/Granitic Gneiss
Quartz	90	30-50	15-35	35-64	20-33	35-45
Plagioclase	–	5-40	15-30	5-6	10-30	15-20
K-Feldspar	–	7-40	25-40	10-25	25-45	35-38
Biotite	2	0-8	5-20	10-14	1-10	3
Muscovite	7	0-10	0-3	6-15	0-15	–
Hornblende	–	–	0-5	–	–	T-4
Tremolite/Act.	–	–	–	–	–	–
Epidote	T	0-10	1-6	–	T	T
Sphene	–	0-4	1-10	–	T	T
Chlorite	–	1-6	–	–	1-4	–
Garnet	–	T	T	0-5	–	–
Apatite	–	T	T	T	T	–
Iron Ore	1	0-2	1-4	0-5	T	T-2
Zircon	–	–	–	–	–	–
Sericite	–	0-10	0-15	–	–	–
Tourmaline	–	–	–	–	–	–
Pyroxene	–	–	–	–	–	–
Kyanite	–	–	–	–	–	–
Staurolite	–	–	–	–	–	–
Graphite	–	–	–	–	–	–
Calcite	–	T	–	–	–	–

previous workers (Kolderup & Kolderup,1940). The implication is that these rocks formed a parautochthonous cover sequence, restacked and imbricated during the emplacement of the allochthonous Bergen Arc nappes.

No correlation is made between these rocks and the Northern Gneiss Metasedimentary Complex. The rocks are different in colour, composition and in the relationship of the mica schists to the quartzites. A minimum age of Ca.800 Ma. has been determined for the Southern gneiss metasediments (appendix 1). This correlates well with similar ages determined from xenolith-bearing granites within the Bergsdalen Nappes (Pringle et al.,1975). It is with these sediments and those of the Samnanger Complex (Faerseth et al.,1977), of the Bergen Arcs, that these rocks are correlated.

3.3.2   Igneous Rocks

There are two rock types involved in this group, augen gneisses and amphibolites, which occur as foliation parallel sheets in the gneisses. The augen gneisses are more extensively developed than the amphibolites. Both rock types are subdivided into two separate tectonic members, one set found in or close to the schuppen zone and the other found throughout the Southern gneisses.

Augen Gneisses

This quartz monzonitic-granitic rock type is perhaps the most distinctive in the Southern gneisses. It forms, for the most part, thick (50-400m) regional foliation concordant sheets up to 1400m long. Contacts with the surrounding gneisses are sharp and locally discordant with the local gneiss foliation; it is unclear whether this discordance is a product of deformation or an original intrusive feature. The rock appears rough and mottled in outcrop because it contains up to 40 per cent. large (up to 3cm across) augen porphyroblasts of potash feldspar.

These are set in a medium-grained (0.5-2mm) dark grey, mafic-rich matrix with a strong foliation. There is a considerable variation in augen content, from dark, augen-poor to pink, augen-rich portions. The variation occurs laterally both along and across the sheets. In the latter case the centres are seen to be richer in augen than the margins (pls.42-45); the augen at the margin are also smaller. Thin section work shows that this variation is the product of tectonism rather than a primary feature. There is also a tendency towards local migmatitic segregation of the matrix into leucocratic and melanocratic layers up to 1cm thick. The leucocratic layers often 'include' the augen to form long, thin, light coloured bands.

The general petrology of these rocks is given in figure 116 and analyses 21-26 and 51-60 (appendix 2), but the garnet-bearing examples come only from the easterly outcrops, while the main outcrops in the west are devoid of garnet. The feldspar porphyroblasts may be single micro-cline crystals or crystal aggregates, showing several phases of regrowth; they may be poikilitic (pls.51 & 52). Sphene in the rocks forms large euhedral crystals (2-3mm), while the epidotes, except for allanite, are smaller and anhedral. The plagioclase in the rocks, except for odd relics of normally zoned crystals with cores of An 30, is sodic (An 7-8) and forms small interstitial crystals in the matrix and exsolutions in perthitic augen. In general the darker varieties of the rock type are finer-grained than their pink counterparts.

Amphibolites

There appear to be two distinct varieties of amphibolite in the Southern gneisses. Type 1 is only found in the schuppen zone intruding the sediments. It occurs as foliation parallel dark green to black sheets with a strong internal foliation. The sheets range in size from 2x20m to 50x8000m, the longer bodies varying in thickness along their

length. The rocks are generally medium- to coarse-grained (0.5-5mm)
but they become fine- to medium-grained (0.01-1mm) in the thinner regions
and develop a paler green colour. The fine-grained rocks (08.20,30.20)
are serpentinitic and have a soapy feel in hand specimen.

MINERAL CONTENT:

Actinolite	25-80 per cent.[*]
Iron ore	0-10 " "
Sphene	0- 5 " "
Biotite (green)	0-60 " "
Chlorite (and talc)	0-40 " "
Apatite	0- 2 " "
Plag. albite-andesine	0-30 " "
Epidote (and clinozoisite)	0-20 " "
Quartz	0-23 " "
Sericite	0- 8 " "
Calcite	0- 2 " "
Garnet	0- 2 " "
Potash feldspar	trace
Dravite	"

---

[*] thin section estimates.

This range of composition is a response to a retrograde metamorphism and
deformation and to appreciate the mineralogies developed in individual
rocks, it is best to consider two end members, one biotite-rich, one
amphibole-rich.

Biotite-rich				Amphibole-rich		
Biotite	60 per cent.[*]			Actinolite	80 per cent.[*]	
Epidote	20 " "			Chlorite	5 " "	
Quartz	15 " "			Sphene	3 " "	
Sphene	3 " "			Plag. An 29-35	6 " "	
Iron ore	1 " "			Iron ore	2 " "	
Calcite	1 " "			Quartz	2 " "	
				Garnet	2 " "	

---

[*] point counted

Other examples of both end members are richer in plagioclase, which usually forms about 20 per cent. of the rock.

Type 2, again cropping out as foliation parallel sheets, differs from the first in that the bodies are much smaller (18.00,26.00), and found throughout the Southern gneisses. In outcrop they are dark green and frequently rich in biotite and relict garnet. The mafic minerals in these rocks tend to form clumps (up to 0.5cm across), imparting a coarse-grained appearance in hand specimen; foliation in these rocks is therefore apparently weaker.

MINERAL CONTENT:

Actinolite and hornblende	3-70 per cent.[*]
Biotite (green)	10-35 " "
Plag. (albite-oligoclase)	0-22 " "
Quartz	5-25 " "
Potash feldspar	0-15 " "
Sphene	1-4 " "
Iron ore	1 " "
Apatite	1 " "
Epidotes	0-1 " "
Garnet	0-5 " "
Calcite	trace

---

[*] thin section estimates.

A third rock type grouped with the amphibolites is found in the schuppen zone; epidote-rich pods up to 0.5m across are found scattered in the gneisses, enwrapped by the foliation. Contacts with the surrounding gneisses are sharp and the bodies do not seem to be aligned as boudins; their origin is unclear; they may be igneous or metasomatic. In hand specimen they are light green, fine-grained and comprise:

Hornblende	3 per cent.		*
Epidote	80	"	"
Clinozoisite	10	"	"
Quartz	4	"	"
Potash feldspar	1	"	"
Chlorite	1	"	"
Apatite	1	"	"
Iron ore	· trace		

---

* Point counted.

Discussion

Apart from the epidotites, the amphibolites are all basaltic and very similar in composition, analyses 4, 8, 9, 12, 13, 22, 23, 35, 38, 39, 48, 49, 61 and 68 (appendix 2). Subdivision of these and the augen gneiss rocks into two sub-varieties is done on the basis of minor variations in petrology and sometimes the type 2 amphibolites are less basic than those confined to the schuppen zone, and the augen gneisses in this zone contain no hornblende and less garnet. Moreover, type 1 amphibolites do not contain L3 and the augen gneisses outside the schuppen zone are more gradational with the country gneisses at their contacts. These factors when taken together with the igneous geochemistry (figs.108, 109 & 110), probably indicate that the two sub-varieties are separate intrusions.

The two-intrusion hypothesis is supported by independent structural evidence. The type 1 amphibolites and augen gneisses confined to the schuppen zone cut the sediments at (06.20,32.30), xenoliths of quartzite are found in the augen gneiss, while the rest of the augen gneisses and type 2 amphibolites are older than the sediments forming part of the old Southern Gneiss Complex, having deformed with it for a protracted period of its history. Thus not only are there two separate intrusions, but two intrusive episodes represented; this provides an insight as to the

composition and nature of the rocks from which the Southern Gneiss Unit was derived.

3.3.3   Gneissose Rocks

These form the bulk of the Southern gneiss outcrop.   For the most part they are well foliated, grey acid rocks with dispersed feldspar augen.   Occasionally layers rich in hornblende or quartz or feldspar or biotite are found, and while these variants are not volumetrically important individually, they do impart a great heterogeneity to the gneisses.   The more distinct units are mapped (map 1), because their stratigraphy 'proves' the thrust beneath the Bergen Arcs to be crosscutting. These distinct units are given suitable local place names, while the rest of the rocks are grouped as 'Undifferentiated Gneiss'.   The named units are distinguishable mainly on their weathering characteristics, a function of both composition and strain state, they are therefore not strictly lithological but lithotectonic divisions.

Helldalsfjell Gneiss

This forms a lensoid body 4000m long and up to 400m thick, best exposed at (15.00,29.50), on the top of Helldalsfjell.   The rock is distinguished by its brown weathering colouration and the high muscovite/biotite content seen in hand specimen (fig.116).   It is a paragneiss, probably originally an impure quartzite rich in quartz and micas.   It is well foliated, the micas distributed in schistosity parallel bands as well as disseminated throughout the rock.   Generally medium-grained (0-2mm), these rocks characteristically show F5 folds at all scales because of the banding and high mica content.

Pegmatite-Rich Gneiss

Both units of this gneiss type (one at (10.50,33.00) and the other at (18.00,22.00)), are distinguished by the large amounts of vein and

pegmatite material they contain.   The veins range up to 1m thick and crosscut the dominant foliation in the gneisses at a high angle, later to be folded with them, developing a new foliation sub-parallel to that in the host rocks.   Granitic in composition, these intrusives are coarse-grained (0.1-5cm) and rich in feldspar and quartz.   These pegmatites are seen throughout the Southern gneisses, but in the pegmatite-rich rocks they form up to 30 per cent. of the rock by volume.   A description of the intrusives will be given later; the petrology of the host rock is given in figure 116.   The gneisses are granitic, fine- to medium-grained (0.01-1mm) with a strong foliation, and rich in small augen of polycrystalline feldspar up to 1cm in diameter.

Rispingen and Granitic Gneisses

Forming very distinctive outcrops, clearly seen on air photographs at (20.80,15.00) and (21.00,10.50) respectively, these two rock types are grouped together because they are so similar.   They are hard weathering red/pink granites forming features of positive relief (fig.116).   The outcrops are about 3000m long and a maximum of 400m thick and well foliated. The Rispingen Gneiss is coarse-grained (0.5-3mm) and, in hand specimen, appears to be made of a mosaic of leucocratic augen separated by thin diastomosing mafic-rich layers.   The augen are generally pink, but may have white kernels.   The Granitic Gneiss, on the other hand, is fine-grained (0.01-1mm) and in hand specimen the leucocratic components, again separated by thin diastomosing mafic layers, form long thin lenses rather than augen.   Throughout the rock, irrespective of the layering, small (up to 1mm) crystals of iron ore are seen, while hornblende is absent. These features suggest that both rock types were probably originally ortho-gneisses.   The Granitic Gneiss in particular has been modified by later deformation and metamorphism which has destroyed hornblende, reducing grain size and producing iron ore.

Drangskollen Gneiss

This is a well-foliated, medium-grained (0.5-2mm), light grey weathering gneiss, best exposed on the highest point of Drangøy (05.80, 33.50), after which it is named. It is the clearest and most easily traceable of all the gneissose units, maintaining a homogeneous character right along the 10000m outcrop from one coast of Osterøy to the other; as such it forms a marker band. The width of the outcrop varies from 10m to 800m in some places. It is characteristically poorly banded, but with a strong schistosity, preserving L3 very well. D5 quartz veins are also very well developed in this lithology but few F5 folds are seen. Weathered surfaces frequently show ice chatter marks and rough surfaces expose small (1-2mm), spindle-shaped quartz crystals orientated with L3. Fresh surfaces are dark grey with small (0x3x1cm) white albite porphyroblasts lying in the schistosity defined by the micas.

The rock is adamellitic (fig.117), and largely recrystallised. The leucocratic minerals overgrow the mafics and albite porphyroblasts are seen to be late poikiloblastic developments. The restricted mineralogy and general uniformity of this lithology suggests it may have been an early intrusion into the gneisses, deformed, reworked and metamorphosed with them.

Nonkletten Gneiss

Named after the hill on which it is best seen (10.30,32.70), this gneiss type also crops out on the tip of Drangøy, forming a lensoid body 3000m long and up to 400m thick. The rocks are coarse-grained, well foliated hornblende gneisses (fig.117 and analyses 16 &18, appendix 2). The hornblende, while disseminated throughout the rock, is best developed along thin planes, which define the banding. These are frequently the sites on which pink, porphyroblastic feldspar augen, up to 3cm in diameter, nucleate. The hornblende is always anhedral, intergrown with almandine

Fig 117. TABLE OF MINERAL CONTENT, MODAL RANGES.

RANGE of MODAL MINERAL (%) / ROCK TYPE / GROUP	GNEISSOSE ROCKS				
	Drangskollen Gneiss	Nonkletten Gneiss	Undifferentiated Gneiss		
			Mafic	Quartz	Feldspar
Quartz	20-35	20-30	15-30	40-50	20-40
Plagioclase	20-25	15-25	5-45	5-25	15-30
K-Feldspar	20-30	25-30	5-40	7-40	30-45
Biotite	8-30	5-10	20-25	1-11	0-15
Muscovite	–	–	T	T	0-15
Hornblende	–	0-14	0-20	0-4	0-5
Tremolite/Act.	–	–	–	–	–
Epidote	5-8	0-7	5-15	0-7	0-5
Sphene	–	0-8	0-5	0-5	0-2
Chlorite	T	0-8	0-30	0-15	0-4
Garnet	–	T	0-20	–	–
Apatite	T	T	T	T	T
Iron Ore	1-2	0-5	0-10	0-3	0-10
Zircon	–	–	–	–	–
Sericite	–	0-10	–	–	–
Tourmaline	–	–	–	–	–
Pyroxene	–	–	–	–	–
Kyanite	–	–	–	–	–
Staurolite	–	–	–	–	–
Graphite	–	–	–	–	–
Calcite	–	–	–	–	–

and sphene and much replaced by biotite. The strong banding in these rocks means they show the F5 folding well at all scales and while they abut the Helldalsfjell paragneisses, there is no direct evidence that they are paragneisses themselves.

Undifferentiated Gneisses

These form the bulk of the Southern gneisses and show many compositional and textural variations. The rocks fall into three broad groupings: Mafic gneisses, rocks of all grain sizes, of dark colour with or without small infrequent feldspar augen and with the compositional range shown in figure 117; Quartz gneisses, which are lighter coloured except when fine-grained (when they can appear almost black), frequently with large (up to 2cm) feldspar augen and within the compositional range shown in figure 117; and Feldspar gneisses, frequently white or pale pink in outcrop with rarer light grey varieties. There is a broad range of grain size in the Feldspar gneisses and feldspar augen are common, similar to those found in the Quartz gneisses. The compositional range is given in figure 117.

The rocks are schistose and frequently well-banded with concentrations of mafic constituents. Members of the group may themselves be banded, alternating with each other locally across strike. None of the units comprising such a layering is very thick or laterally persistent. Plagioclase in these rocks is rather sodic, usually albitic (An 5-8) and never exceeding An 30. If the crystals are more than 0.1mm in diameter they are usually normally zoned too and large late albite crystals full of epidote and chlorite inclusions are common, but most of the augen in the rocks are single or polycrystalline microclines.

Two compositionally remarkable rock types were found within these gneisses. The first, best seen at (09.43,30.05) contains:

Quartz	25 per cent. *
Potash feldspar	20 " "
Sodic plag.	5 " "
Biotite (green)	1 " "
Chlorite	1 " "
Sphene	2 " "
Hornblende	50 " "
Apatite	trace

---

* Thin section estimates.

The rocks are found in pink or grey feldspathic gneiss as foliation parallel lenses up to 8cm thick (fig.115), which separate the gneisses into bands, some 15cm thick.   Knots of subhedral hornblende occur in these lenses, with crystals up to 5cm across.   These are set in a matrix of coarsely crystalline pink feldspars in which meandering polycrystalline quartz veinlets occur.

The second rock type is a quartzite, found outside the schuppen zone at (15.61,23.10), as a lens in a quartz gneiss;   it consists of 84 per cent. quartz, 15 per cent. muscovite and 2 per cent. kyanite.   The kyanite is found as small crystals sheared into the S4 schistosity, clearly from a paragneiss predating this structure and as it is the only kyanite-bearing rock found in the Southern gneisses it cannot be included with the rest of the Southern Gneiss Quartzites;   it may be a relic of an older assemblage.

Discussion

There is a great variety of rock types present in the gneissose unit, including rocks inferred to be of both igneous and sedimentary origin. Analyses 15-17, 20, 34, 36, 37, 45 and 47 (appendix 2), are of rocks from this group.

3.3.4   Origin of the Southern Gneisses

The Southern Gneisses form a thrust wedge.   It is inferred that they are a para-autochthonous nappe derived wholly from the northern "basement",

with a suite of igneous intrusives emplaced along thrust planes during deformation and reworking. All rock types present in the Southern gneisses have their counterparts in the Northern gneisses and they have both been metamorphosed at Amphibolite facies (kyanite grade) early in their development.

This explanation is also consistent with the interpretation of the structures. The differences between the two gneiss units are thought to be due to tectonism.

3.4   ACID VEINS IN THE OSTERØY GNEISSES

The Osterøy Gneisses are cut by numerous veins which show a great range in composition and texture. Varieties which crosscut the foliation are generally thicker, do not have selvedges and are interpreted as intrusions into the gneisses. It is recognised that this intrusive material may originate locally, from within the gneisses. Other varieties with selvedges are usually conformable with the local foliation and are interpreted as having generated locally during migmatisation. The veins are then, in Sederholm's (1967) terminology, arterites and/or veinites respectively.

Compositionally the varieties found are aplites, granites, pegmatites and trondhjemites. An example of granitic veining is seen at (11.00,34.60). This is a multi-stage intrusion, 1m thick, preserving xenoliths of earlier magma types. Trondhjemites, the least common vein type, are seen at (17.50,17.00). Aplites and pegmatites form the bulk of the veins, the latter predominating. Some of the pegmatites are virtually monomineralic composed of 80 per cent. microcline and 20 per cent. quartz. Some of these have the quartz segregated out into layers within the vein. In some pegmatites euhedral garnets are found. These veins are emplaced at many stages in the tectonic development of the gneisses. The garnetiferous pegmatites, because of the presence of garnets, are thought to be emplaced

during the thermal maxima.

The final type of vein comprises 99 per cent. quartz with occasional potash feldspar knots up to 5cm in diameter. Veins of this composition have been emplaced throughout the history of the gneisses, but by far the most important set were cognate with D5.

Most of the veins in the gneisses are highly deformed and are beginning to merge with the host rocks, which makes them difficult to study from a petrological viewpoint, but as they commonly preserve at least one tectonic fabric, they are useful as tectonic markers.

3.5 METAMORPHISM

A synopsis of the structural character of the north Osterøy gneisses is given in figure 103. Deformation across the area has been shown to be fundamentally heterogeneous (section 2), accounting for the preservation of old mineral assemblages which developed with the early deformation phases. The majority of the rocks in the area are acid in composition and the variations in mineral assemblages seen associated with the older structures are related to 'fossil' metamorphic events rather than variations in rock composition.

The metamorphic petrology and textural development of each metamorphic event will be discussed in conjunction with the deformation structure with which it is associated, starting with the oldest.

3.5.1 Possible Early Metamorphism (M "Early")

Establishment of the structural chronology indicates that the oldest rocks are the Unflattened Gneisses (fig.104); these preserve the oldest structure (S "Early"). Unfortunately, the mineral assemblages accompanying its formation were completely destroyed by later metamorphisms. In view of the mineralogical nature of S "Early" (section 2.1.1), it would appear

that the rocks were probably at Amphibolite facies conditions during its
formation.

3.5.2   First Metamorphism (M1)

Possible evidence for the next metamorphism is again found in the
Unflattened Gneisses.   In the nose regions of the F1 folds, relict crystals
of garnet are occasionally found, while in the limb regions of the same
folds these relics are absent.   In the basic rocks of this group,
hornblende is a relatively common mineral.   It could be argued that these
relics of Amphibolite facies mineralogy belong either to S "Early" or were
developed after D1 in a subsequent metamorphism.   However, the presence
of hornblende in the basic rocks, together with a relict igneous mineralogy,
points to the Amphibolite facies minerals having formed during D1.
Whether or not there was an intervening period of retrogression between
D "Early" and D1, or whether the minerals developed as the product of
a continuing metamorphic event cannot be determined.

Uplift

The next event affecting the environment of the Unflattened Gneisses
is determined by inference.   It is proved (section 3.2.2) that the Gneiss
and Migmatite Complex contains rocks, undeformed by F1, which were originally
sediments deposited on the Unflattened Gneisses.   At the time of deposition
therefore, the Unflattened Gneisses must have been at the surface.

Any mineral or textures which may have developed in response to this
uplift have, however, been completely masked by the effects of subsequent
metamorphic events.

3.5.3   Second Metamorphism (M2)

(M2a)

The second metamorphism is at Amphibolite facies, but is divided into

two stages on the basis of an intervening deformation which separates the thermal peak from the advent of its decline.

Following their deposition the sediments were migmatised and certain of the more micaceous members developed kyanite and staurolite, while a dark green hornblende (α yellowish green, β olive green, γ dark green), and almandine developed in the rest of the suite. The presence of these minerals indicates that the migmatisation occurred at conditions correspon- ding to the medium pressure subfacies of the Amphibolite facies, the equivalent to the kyanite and sillimanite zone in the Barrovian series (Miyashiro, 1973). The effects of the migmatisation were not solely confined to what is now the Gneiss and Migmatite Complex, but also locally affected the Unflattened Gneiss. At (11.20,34.60, fig.118), secondary potash feldspar overgrows the S1 layering, leaving a "ghost" outline of F1 fold noses.

In thin section all minerals, except quartz, sphene and iron ore can be seen to be progressively replaced by potash feldspar, so that K feldspar constitutes up to 60-70 per cent. of the rock. From this point quartz is progressively replaced. The potash feldspar crystals are anhedral and up to 2mm in diameter, forming a mosaic in which the quartz is left as an interstitial mineral. This is clear evidence for at least local mobility of elements, specially potassium.

Similar processes are seen to affect the sediments, e.g. the quartz migmatites and quartzites. Here, however, the effects are more widespread, presumably because their original mineralogical composition was unstable under Amphibolite facies conditions, while the Unflattened Gneisses already had a mineralogy stable at approximately these conditions. It is interesting to note that while the migmatisation is accompanied by fabric development (S2), it is not accompanied by folding; (S2 and the accompanying minerals are deformed by F2, which took place under Lower Amphibolitic facies

Fig 118.

SKETCH SHOWING THE EFFECTS OF THE M2a
METAMORPHISM ON THE UNFLATTENED GNEISSES

'Ghost' of S1

S1 in Sheared F1 Limb

Late Pegmatite

'Ghost' of S'Early'

(Pink)
Area of K-Feldspar
Metasomatism

S'Early', Fold by F1

0   M   3
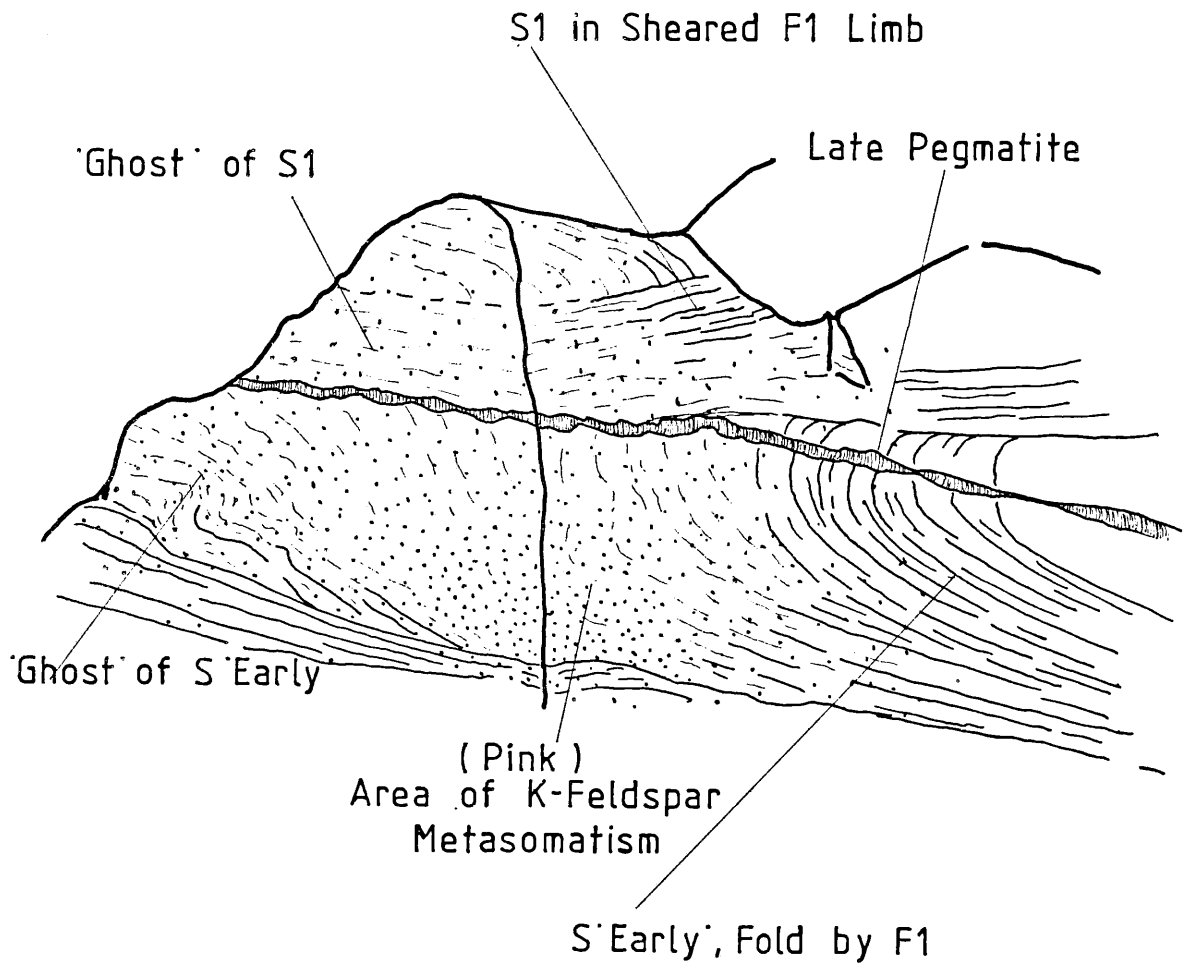
conditions). In circumstances where deformation and metamorphism occur together it is unusual for a metamorphic peak completely to precede the deformation (Fyfe et al.,1978, pp346-7).

(M2b)

The minerals which accompanied the development of S3 are again only poorly preserved but hornblende and almandine are found growing in relics of the S3a cleavage. Hornblende also developed as an essential mineral in those basic rocks intruded during D2: the hornblende is very similar to that grown during the main migmatisation. Most of the mineral growth occurred in the second stage of S3 development, the less flattened rocks show very little new mineral growth. The dominant mafic mineral to develop in M2b was biotite, and it is this which emphasises the strong S3b schistosity. All these features point to a continued stability under Amphibolite facies conditions during D2, with new mineral growth occurring only in regions of highest strain, where the S3b schistosity developed. There was however a slight retrogression from the conditions which prevailed during the migmatisation, as growth of kyanite and staurolite apparently stopped.

Uplift

Following D2 another return to near surface conditions is indicated by the presence of more sediments deposited on the gneisses. These are seen in the zone of imbrication beneath the Bergen Arcs. Any mineralogical changes that may have accompanied this uplift are again masked by younger events.

Discussion

The deposition of the second sedimentary sequence marks the penultimate event in the metamorphic development of the Osterøy gneisses. It was followed by another metamorphism at Amphibolite facies, terminating in a

long retrogession to Greenschist facies conditions. This last meta-morphism (described below), was largely responsible for the poor preservation of the mineralogical evidence for the metamorphic reactions involved in the earlier events. Discussion of this evidence has therefore been limited to the fabrics with which the paragneisses were associated. With these limited relict assemblages. any argument as to the reactions which produced them would be pure speculation; indeed without the structural evidence the metamorphic chronology of any specimen cannot be determined because the minerals produced in M1 and M2 are so similar.

Evidence for the early metamorphic events is taken entirely from the Northern gneisses; in the Southern gneisses the ultimate metamorphic event is too strong.

3.5.4. Third Metamorphism (M3)

The last metamorphism to affect the Osterøy gneisses, M3, reached its peak at Amphibolite facies and retrogressed through the Greenschist facies. It was responsible for the bulk of the mineral parageneses and was thus the most pervasive metamorphism. In the Northern gneisses its effects wax up succession south-eastwards and in the Southern gneisses, it virtually obliterated all evidence for earlier metamorphisms. It differs from M1 and M2 on two counts; firstly, a retrogression following the thermal peak can be proved, secondly, the thermal peak (and retrograde steps) are synchronous with deformation maxima. Four steps in the metamorphic retrogression are identified, all best developed in the Southern gneisses from where they will be described.

(M3a)

This event is seen in the gneisses, metasediments and Type 2 igneous rocks. The gneisses are banded so the mineral paragenesis must be examined in each component of this banding which is itself a product of D3.

In the mafic bands, an interlocking granoblastic texture between biotite (yellow green-dark green), hornblende (α green yellow, β bluish green, γ bluish green), allanite, quartz, plagioclase (A2 29-35), almandine, garnet and sphene are seen. The only minerals which are possibly a relic from an older paragenesis are sphene and quartz (pl. 53). These occur in two forms, as small crystals poikilitically enclosed by hornblende and as larger crystals which form part of the granoblastic texture. The crystals in the hornblende are interpreted as relics while the larger crystals are interpreted as relics on which a mimetic overgrowth has occurred during the metamorphism. The hornblende laths are aligned parallel to L3, while the biotite grows to define the S4 schistosity. The garnet is subhedral and the allanite is now metamict and virtually isotropic.

In the felsic bands the paragenesis is less well preserved, it consists of biotite (yellow green-dark green), quartz, sphene, allanite, plagioclase (An 29-35) and potash feldspar. The biotite again defines the S4 schistosity.

Microcline porphyroblasts forming augen are found throughout the rock. Also, lenses or "strings" of polycrystalline, coarse-grained microcline and quartz (pl. 54) are found, which have narrow biotite selvedges and are interpreted as products of a slight migmatisation which accompanied this metamorphism.

In the metasediments, the paragenesis of this metamorphism is less well preserved, but almandine porphyroblasts are common. Though presently enwrapped by a younger foliation, these crystals are internally zoned, the marginal zones are clear or contain minute graphite inclusions while the central zones are full of quartz inclusions which form rotational trails, "snowball structure" (pls. 55 & 56). The garnets are interpreted as having grown during M3a, and the rotational trails in the central zones

indicate this growth was syntectonic. The outer rims either grew very rapidly or postdate the deformation. The rotational inclusion trails are generally confined to garnets within the micaceous metasediments. In garnets in the quartzites the zoning is still seen and the inclusions of the central zones are still at an angle to the enveloping schistosity but they are not rotational. This is interpreted as a reflection of the difference in the response of the two rock types during deformation.

In Type 2 amphibolites hornblende (α green yellow, β bluish green, γ bluish green), almandine and plagioclase (An 30-35) are seen lying in S4, and the hornblendes are again aligned parallel to L3. The Augen Gneisses, which intrude the sediments, are similar to the host gneisses except the hornblende lacks sphene inclusions and the sphene forms very large (up to 2mm) crystals of typical lozenge shape. The microcline porphyroblasts too are different, showing a wide range of perthite exsolution textures (pls. 52, 58, 59, 64, 78 & 103).

Discussion

The alignment of the hornblende laths with L3, biotite with S4 and the rotational inclusion trails within the garnets, prove the syntectonic nature of this metamorphism. However, the garnets show at least three rims. The centres are full of quartz inclusions, while the outer rims show only minor graphitic trails which do not have rotational geometries. This indicates that the thermal event outlasted the tectonism.

The mineral paragenesis is similar to that developed in M2b. As a consequence of later metamorphisms it is incomplete, for example, the only mineral still preserved in the metasediments is garnet. It is therefore difficult to define exactly the metamorphic environment, but the blue/green colour of the hornblende and the An 25-30 content of the

plagioclase put it somewhere in the Amphibolite facies (Miyashiro,1973, p.299), probably somewhere between the low pressure and medium pressure type. A question then arises as to which K-feldspar polymorph formed during this event. The polymorph presently seen is microcline, but this is known to have been crystallised in the subsequent metamorphic "steps" and could therefore have replaced original orthoclase. A replacement like this would be consistent with the complex perthite textures observed, and it is inferred that perthites (e.g. Pls.52, 58, 59, 64, 78 & 103) are a part of the M3a paragenesis.

The metamorphic differentiation which produced the banding, selvedges, microcline porphyroblasts and K-feldspar and quartz segregation lenses (pl.54) prove a marked chemical mobility during this metamorphism. This mobility probably also explains the hornblende knots and lenses found in the Undifferentiated gneiss (fig.115). Allanite seems to be an essential mineral of the paragenesis. The crystals are large, euhedral and, as with sphene, it is present in both the mafic and felsic regions of the rock. It is also possible that apatite was a stable mineral, but this cannot be proved, as like microcline it is clearly recrystallised in subsequent metamorphic events. The presence of allanite is unusual; it is interpreted as forming as a 'house' for rare earths mobilised in the Amphibolite facies environment.

(M3b)

This event was responsible for the initial retrogression of the M3a paragenesis and is called the clinozoisite event.

In the gneisses, hornblende and biotite are replaced by secondary biotite (yellow green - dark green), defining a new schistosity, S5 (pl.60), at a slight angle to S4. Hornblende is also replaced by actinolite (α yellowish green, β green, γ dark green) and tremolite,

which sometimes rim hornblende crystals, leaving unaltered cores.

However, actinolite and tremolite have usually grown as a new mineral

during formation of S5. The early hornblende and biotite are also

corroded and embayed by quartz and feldspars (pls.60 & 61), so that they

become interstitial, anhedral relics in the new mineral paragenesis.

Clinozoisite formed both as anhedral, metamict rims round allanite nuclei

(pl.62), and as discrete euhedra.

Both K-feldspar and plagioclase replaced the mafic minerals partly

by enlargement of pre-existing crystals and by crystallisation at new

sites. The later plagioclase is albitic (An 6-8), while relict plagioclase

from the M3a paragenesis is strongly zoned (pl.63), with sodic rims.

The early plagioclase is also largely replaced by quartz and albite in

a similar way to the mafic minerals (pl.63). The zoning in the relics

is interpreted as a product of secondary leaching of calcium rather than

an original growth feature, because it is patchy. The M3a microcline

porphyroblasts are partially replaced by myrmekite (pl.64), but also

became clear as they recrystallised during the metamorphism. New porphyro-

blasts also formed in the S5 schistosity; in general these are less

perthitic than their M3a counterparts (pls.65, 51 & 59). Sphene continued

to crystallise in S5 by further nucleation on pre-existent cores and quartz

continued to segregate in the new banding forming 'ribbons' (pl.54) and

'strings' (pl.66). Similarly, potash feldspar forms segregation veins

and lenses, though these only have very weakly developed selvedges of

biotite.

In the amphibolites, similar reactions to those discussed above are

seen, but more clinozoisite forms and actinolite and tremolite become the

dominant amphiboles. In the Type 1 amphibolites, all the amphibole is

tremolite; it constitutes as the main mafic mineral in the rock, indicating

intrusion and crystallisation during the M3b event. This view is

supported by the fact that none of the minerals are aligned with L3 and

by the occurrence of relics of interstitial plagioclase, grown with the tremolite, with an An composition above An 20. After crystallisation these minerals were overgrown and poikilitically enclosed in dravite (watery yellow - straw yellow) porphyroblasts; no clinozoisite formed in this particular rock type, which distinguished it from the rest of the amphibolites. The Type 1 amphibolites were probably intruded towards the end of this stage of M3.

(M3c)

This event (the epidote event) is characterised by epidote growth and is concurrent with S5 and constitutes a retrogression of M3b. Tremolite and actinolite are replaced by a third growth of new biotite which is aligned with S5, while remnants of hornblende are replaced directly by biotite. The secondary biotite of M3b is overgrown by epidote, and epidote rims formed on clinozoisite grains. Epidote also formed rims on allanite and a third rim on allanites already rimmed by clinozoisite. The volume of epidote formed at this stage in the retrogression far exceeds the total volume of allanite or clinozoisite produced earlier. It constitutes the only epidote mineral in the Western Amphibolites, which supports the view that these were intruded during late M3b. In general the behaviour of the rest of the mineral paragenesis is a continuation of that seen in M3b, but myrmekite formation round microcline porphyroblasts is more noticeable (pl.67), and replacement textures, attributable to solution and replacement effects are better preserved (pl.55, fig.119). Otherwise microcline continued to form porphyroblasts and albite (An 5-6) is the dominant plagioclase.

(M3d)

This event is characterised by the development of muscovite. The mineralogical changes which characterise the event started during the formation of S5 and continued through D5 to accompany the formation of the S6 foliation.

Fig 119.

STRESS CONTROLLED CORROSION OF GARNET IN M3c

SECTION CUT PARALLEL TO S6

First Shell of
Garnet Full of
Inclusions

Garnet

Secondary Clear Rim

PROFILE SECTION THROUGH F5

[S5]

0 _ mm _ 1

F5

Garnet

Epidote

Remnant of Clear Rim
Here

Replacement by
Quartz Only
Occurs Parallel to
the F5 Axial Plane
[solution across the plane]
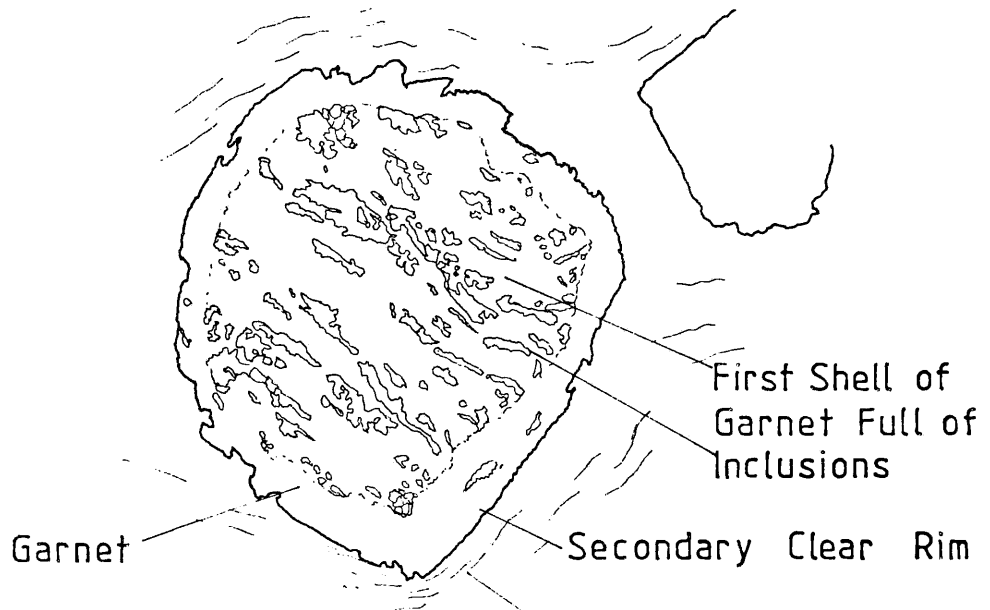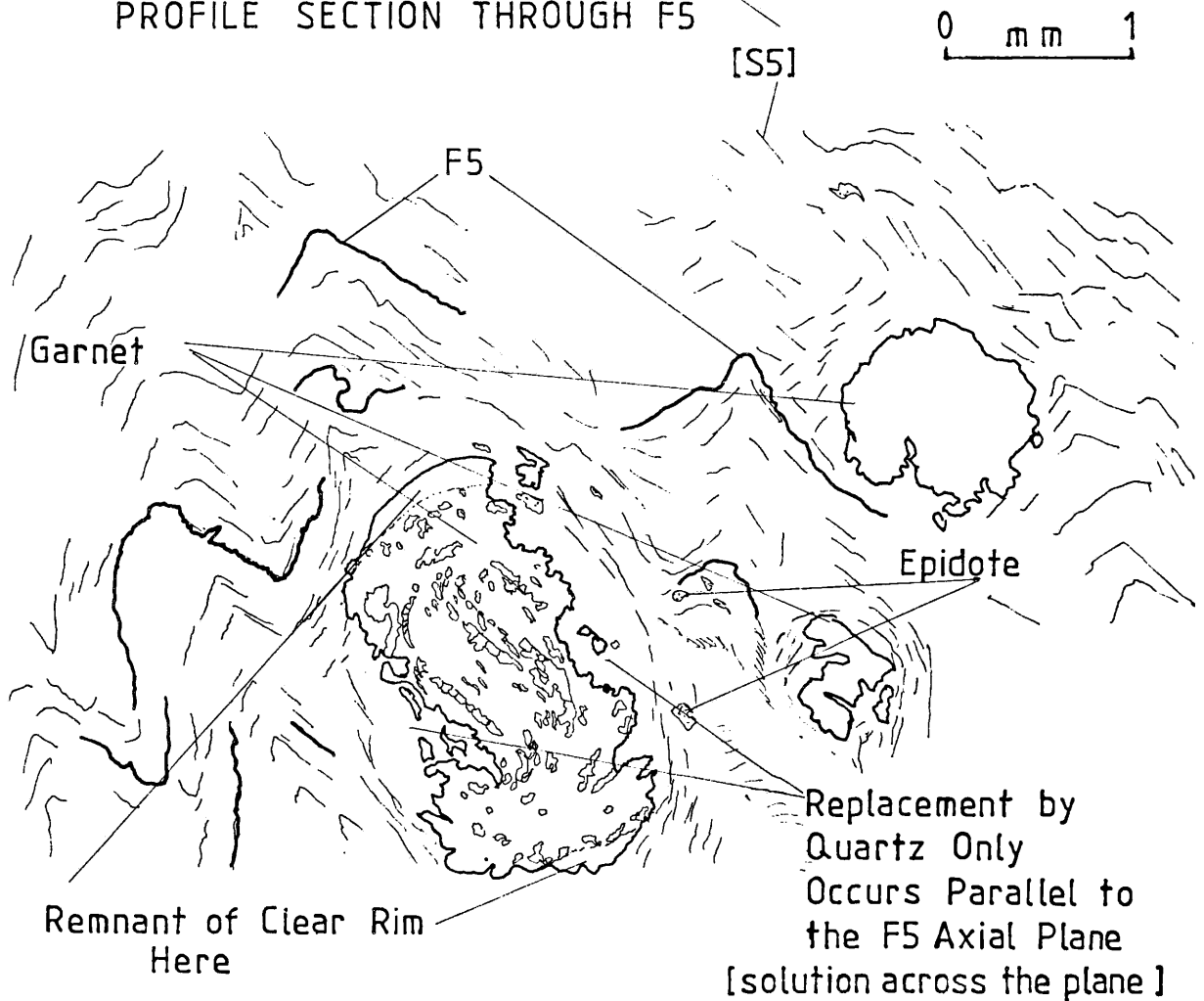
Epidote and biotite continued to crystallise, but in places, especially in the metasediments, biotite was replaced by muscovite with an accompanying exsolution of iron ore. The ore is of several varieties: skeletal ilmenite developed intergrown with sphene; magnetite and pyrite formed euhedral crystals dispersed through the rock; minute magnetite crystals formed in the cleavage planes of the developing muscovite as it replaced biotite, and there is much submicroscopic iron ore deposited along grain boundaries, especially along the axial planes of microscopic F5 folds. These ore crystals overgrow all except the S6 fabric.

There is evidence for the presence of mineralising solutions during M3d; shear zones formed along the axial planes of F5 folds are filled by vein quartz with accessory microcline. The sheared rock is annealed by recrystallisation of the felsic rock constituents. This recrystallisation caused embayment of the mafic constituents, which, realigned into S6 by the shearing, survive as anhedral interstitial relics in the new paragenesis. This mobility of acid material is also seen elsewhere; quartz in the meta-sediments annealed to form laths which define S6 (pl.46), microcline and albite both developed as porphyroblasts with markedly anhedral."amoeboid" outlines (pl.68). The An content of the albites is unknown because the crystals do not twin; characteristically they include laths of mica and epidote (pls.68,69,70 & 102). The inclusions are not always from the matrix because they are euhedral and crystals like these are not found in the matrix. Calcite also crystallised during this phase of the retrogression. Though it is seen in all rock types, it is best developed in the metasediments, where, augened by the S5 schistosity, it is distinguished from interstitial calcite of later age.

In the amphibolites this metamorphism finds expression not in muscovite development, but in the production of talc and epidote from the breakdown of tremolite and plagioclase (interstitial high An plagioclase). Schorlite (buff olive), also developed in these rocks and the micaceous metasediments.

The crystals are euhedral, zoned (with paler centres), and overgrow the S5 schistosity.

Discussion

The three metamorphic steps described above define a regime of declining temperature through the Greenschist facies (Miyashiro,1973). This thermal retrogression, overlapping several deformations, was obviously gradual and implies an accompanying reduction in hydrostatic pressure. A notable point is the close association of the new parageneses with the developing structural fabrics. The ability of the mineralogy to equilibriate with the retrogressive environment is closely controlled by tectonism. The reasons for this are discussed in section 4.2.1.

Chemically the retrogression is best described in terms of the movement of the cationic components of the minerals, especially 'Fe'+, 'Ca'+ and 'Al'+, though there must also have been some rearrangement of the 'Al - Si - O'- anions. The movement is accommodated through the processes of re-crystallisation and by movement of fluids through the rocks.

The original M3a paragenesis, developed throughout the rocks may be summarised:

(Hornblende + allanite + andesine + biotite + orthoclase + almandine + apatite + quartz). The fact that the plagioclase is in the andesine range means that with a reduction in temperature, the recrystallising plagioclase enters the peristerite field, yet only albite (An less than 10), is seen. The stages in the retrogression of the M3a paragenesis can therefore be summarised:

M3b

Andesine + hornblende $\longrightarrow$ Tremolite/actinolite + Clinozoisite + albite producing a new paragenesis which is:

(Tremolite/actinolite + clinozoisite + albite + biotite + microcline + apatite
+ quartz).

<u>M3c</u>

Andesine + hornblende ---> biotite + epidote + albite

Tremolite/actinolite + albite ---> biotite + epidote

producing a new paragenesis which is:

(Biotite + epidote + albite + microcline + apatite + quartz).

<u>M3d</u>

Andesine + hornblende ---> biotite + muscovite/talc + iron ore
+ epidote + calcite + albite

Tremolite/actinolite + albite ---> biotite + muscovite/talc + iron ore
+ epidote + calcite

Biotite ---> Muscovite + iron ore

producing a new paragenesis which is :

(Muscovite/talc + iron ore + albite + microcline + epidote + biotite
+ calcite + apatite + quartz).

For all the above reactions, there is no need to invoke any large-scale metasomatism in the rocks, the proportions of the ions involved in the reactions would appear to balance out. Also in the amphibolites, most of the reactions occurred at the contacts between the reacting phases. In the acid gneisses, however, the new minerals are not directly localised round nuclei of outgoing phases, the new minerals such as epidote, grow randomly in the rocks. This implies some local mobility of ions but not necessarily large-scale metasomatism.

This mobility of ions suggests the presence of a fluid phase in the rocks during metamorphism, allowing migration in an intergranular 'film'. The development of calcite/(dolomite) in M3d supports this view, for while the "Ca^{2+} can have origins from within the rocks, the "CO_3^{2-} must have come from a volatile phase because no minerals found in older parageneses contain the "CO_3^{2-} ion.

There is a problem with regard to apatite. Euhedral crystals are present in the parageneses right up to M3d and it is unclear whether they

are euhedral because they continually recrystallised or whether they are relics from the M3a paragenesis, unaffected by subsequent events.

(M3e)

Unlike the previous stages of the retrogression, this stage is not specifically associated with a developing schistosity and occurs throughout the rocks. The characteristic minerals formed, however, grew preferentially filling the planes of S7 fracture cleavage. These minerals are green chlorite (anomalous blue birefringence) and a grass green epidote. Away from these fractures, biotite and garnet are replaced by chlorite. In the garnet chlorite grew in random orientations, whereas in the biotite replacement started along the biotite cleavages from the ends of the 'books' and moved into the centre, producing a dumbell shape (fig.120). Hornblende and tremolite/actinolite are also replaced by chlorite to some extent both in the amphibolites and the acid gneisses and iron ore is exsolved as small euhedral laths along the cleavage planes. Calcite also crystallised in this metamorphic stage to form an interstitial mosaic in some of the rocks in the schuppen zone beneath the Major Arc. It was also deposited in hydraulic fractures formed at this time (pl.48). Any rock sheared in this stage of the retrogression (the D6 thrusts), did not anneal as in M3d, and remained as a friable rock flour.

Discussion

This metamorphism is interpreted as the last stage in the retrogression of the M3a paragenesis, the changes being the result of ground waters migrating through the gneisses, hydrating some of the minerals. The mineralisation of the S7 cleavage is the result of the passage of these solutions out of the rocks. The fact that there is no annealing in the shears suggests that at this stage the thermal environment is too low for activation of annealing in the felsic rock components.

Fig 120.

CHLORITE REPLACING BIOTITE WITH ACCOMPANYING EXOLUTION OF

IRON ORE, AN M3e PHENOMENON

(Deformation Predates Replacement)

Book of
Biotite, Bent with
Corroded Outlines

Chlorite Starts to Replace the Biotite
Along the Obvious Cleavages Especially
Where they are Bent

Exolved Iron

Chlorite

Uncorroded Outlines

0   mm   0.5
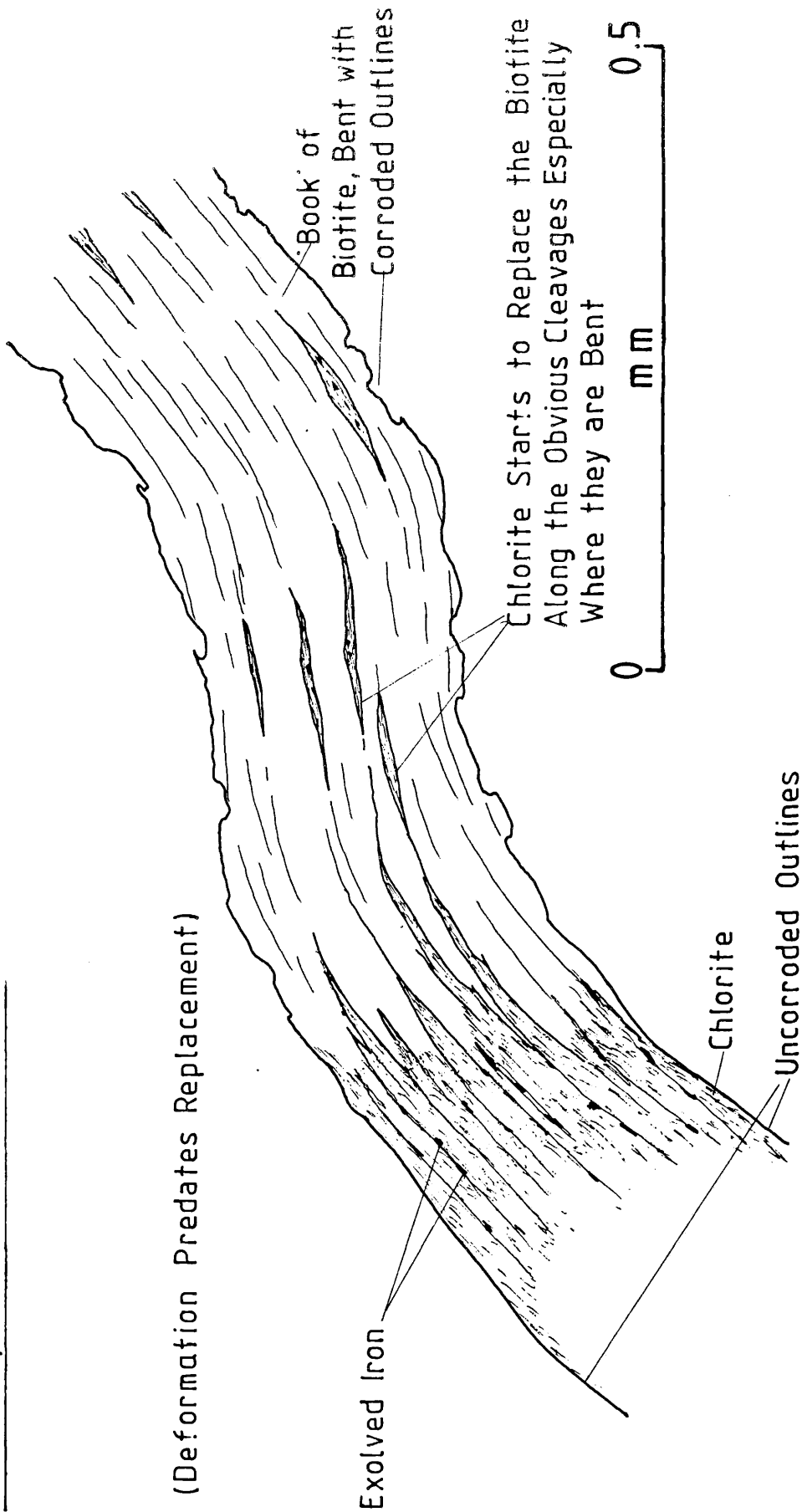
(M3f)

This metamorphism only affects the D8 joints and their wall rocks. Within the joint zones the rocks are shattered and form a breccia of rock fragments set in a matrix of fine crystal fragments. This matrix is extensively replaced by green epidote and calcite; in one instance crystals of stilbite were also found. For about twenty meters either side of the largest joints the feldspars and gneisses are red, because of the presence of minute hematite grains. These probably originated from solutions passing up the joints, for, although the gneisses are generally sericitized, it is only in association with the joints that this red colour is seen.

Discussion

The event is interpreted as a final dewatering of the rocks as they were uplifted to their present level. The mineralising solutions probably originated from below where the rocks were in an M3e type environment.

3.5.5 Conclusion

There are four distinct metamorphic events that have affected the Osterøy gneisses, the last and most important of which is best developed in the south of the area, but is also responsible for most of the mineral assemblages seen in the north.

These metamorphisms are not maxima in a continuing event because they are separated by periods of sedimentation. Therefore, there are at least three complete metamorphic cycles preserved, each widely separated in time. The gaps between the cycles and the duration of the metamorphisms themselves, except in the final case, are unknown but the cycles clearly relate to separate orogenies; the final metamorphism is Caledonian. These observations fit well with observations made as to the structural history of the area and together they are used in the formulation of the deformational

subdivisions outlined in the Structural section. Figure 149 provides a
summary of the metamorphic history of the North Osterøy gneisses.

4. MYLONITIC ROCKS OF OSTERØY

During the course of the present investigation it was realised that many of the rocks on Osterøy show features which match those described in the literature from mylonitic zones (Lapworth,1885; Holmquist,1910; Tiermier & Boussac,1911; Sander,1911; Sander,1912; Staub,1915; Quensel,1916; Horne,1930; Peach,1930; Christie,1960; Higgins,1971; Bell & Etheridge, 1973; Nicolas & Poirier,1976 and Sibson 1977). Whilst in places these are found in discrete zones and thus are interpretable as forming under classical conditions of mylonite formation, viz. (Lapworth,1885; Higgins, 1971; Sibson,1977 and figs. 121 & 122), large areas of gneisses (3 to 4km thick and 12 to 15km long) with similar characteristics cannot be thus interpreted because of their great thickness and regional development.

The occurrence of mylonitic features on such a large scale demands explanation beyond that normally given for mylonite formation and thus requires both a review of classical concepts and development of theoretical arguments. Thus the "mylonitic" rocks of Osterøy are described in terms of their modes of occurrence and characteristic megascopic, mesoscopic and microscopic features, and a broader theoretical consideration is given to their possible formation and that of classical mylonites.

4.1 THE OSTERØY MYLONITES

4.1.1 Description

The rocks in the area between the Tysse Thrust and the eastern boundary of the Major Bergen Arc, the Southern Gneisses (fig.10), have been affected by two major periods of deformation, each giving rise to foliations (sections 2.2.2 & 2.2.3). Where intensely developed, these deformations have resulted in an apparent structural simplicity despite the fact that the rocks are the most structurally evolved; D3 was coincident with an amphibolite facies metamorphism and produced a completely penetrative fabric

Fig 121.

TEXTURAL CLASSIFICATION OF FAULT ROCKS

[After:-SIBSON,1977]

		RANDOM - FABRIC	FOLIATED	
INCOHESIVE		*Fault Breccia* > 30% fragments	?	
		Fault Gouge < 30% "	?	
COHESIVE	GLASS OR DEVITRIFIED GLASS	*Pseudotachylyte*	?	
	FINE MATRIX WITH LITTLE OR NO RECRYSTALLISATION	*Crush Breccia* > 0,5 cm fragments / *Fine Crush Breccia* 0.1-0.5cm " / *Crush Microbreccia* < 0.1cm "		0-10% / MATRIX
		SERIES: *Protocataclasite* / CATACLASITE: *Cataclasite* / *Ultracataclasite*	*Protomylonite* / *Phyllonites* *Mylonite* / *Ultramylonite* — SERIES / MYLONITE	10-50% / 50-90% / 90-100% — PROPORTION OF
	RECRYSTALLISATION OBVIOUS	?	*Blastomylonite*	

Fig 122.

MODEL FOR THE PRODUCTION OF MYLONITES

[After :- SIBSON, 1977]
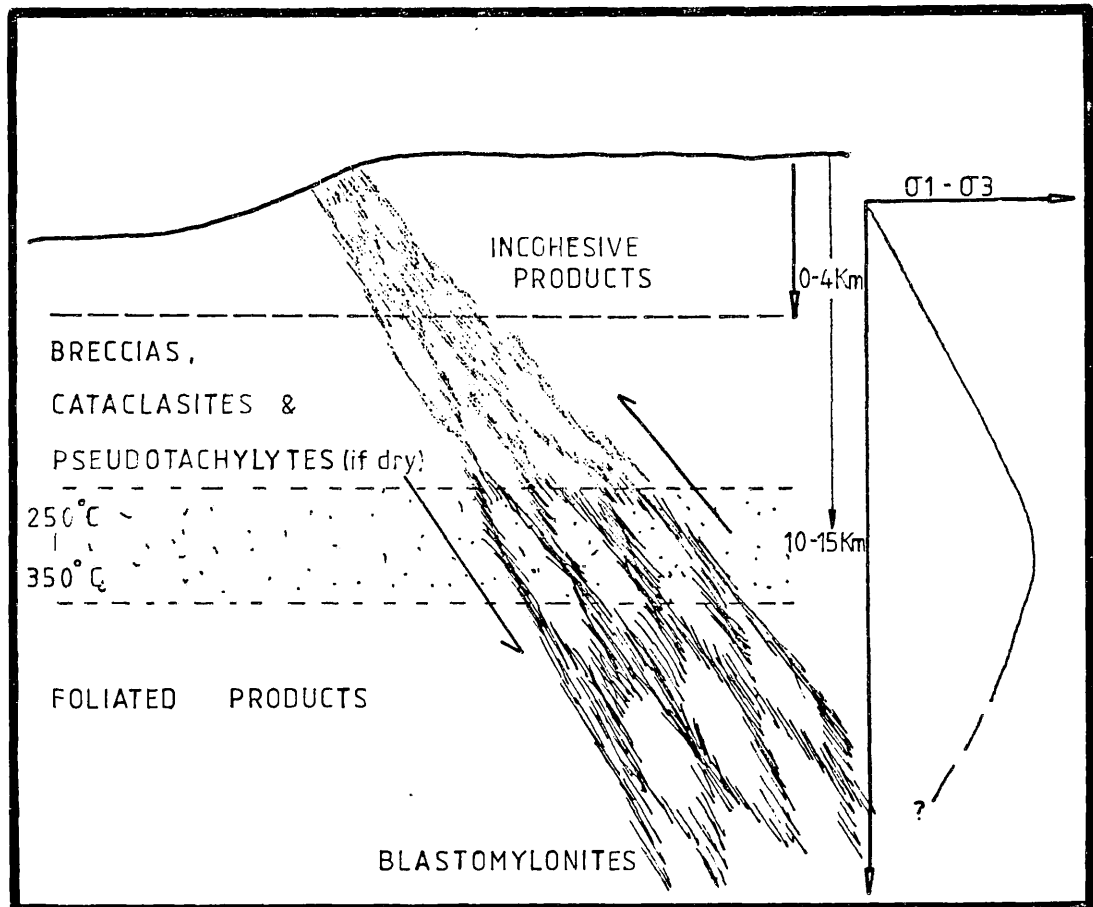
NOTE, The Overall Regime is One of SIMPLE SHEAR
[Faulting]

throughout the rocks (S4 & L3); D4 occurred under middle to upper green-schist facies conditions and produced discrete bands of new fabric (S5). Both deformations produced folds which became flattened into the developing foliations but the rock types produced in each event are quite distinct.

D3 Mylonites

D3 affects rocks which were very similar in character and composition to those described from the Northern gneisses (pl.71); it homogenises them metamorphically and texturally (pls.72, 73 & 74). Except in discrete lensoid bodies up to 30m long (tectonic pips), all the early characteristics of the rocks are lost and effectively a new rock type develops (pl.75).

The changes involved in D3 include a general reduction in grain size with accompanying growth of new minerals and formation of new textures from the decomposition of the old ones (pl.76). In detail, certain minerals, such as sphene, are seen to fragment and spread out in the plane of the developing foliation (pl.77) where the fragments act as nuclei for later sphene growth. Other minerals, such as biotite and hornblende, are destroyed in the margins of the "tectonic pips" (pl.60). They recrystallise with a deccusate texture in bands within the new schistosity; the new schistosity bears no causal relationship to that preserved in the pips because the schistosity within the pips cannot be traced into the new younger schistosity developed outside them (pl.75). Porphyroblastic minerals, which are often poikiolitic, including small crystals from the fine-grained matrix (pl.53), grow in the rock. In the case of garnet, the inclusions sometimes form rotational trails (pl.56).

As well as the relict "tectonic pips", at a microscopic level, porphyro-clasts of early minerals are occasionally seen enwrapped by the new schistosity. These occur as single crystals or polycrystalline aggregates which may be polymineralic. Feldspar frequently forms porphyroclasts,

early plagioclases are found with bent twin planes and undulose extinction and are much corroded by new, developing minerals (pls. 57 & 63). Frequently these are also fragmented. Potash feldspar often forms augen in the rocks, either as single crystals showing undulose extinction (pl. 79), or as many crystal fragments or subgrains of varying size (pls. 76, 80 & 81). In some cases subgrains recombine to develop a single crystal which may be smaller (pl. 82), of the same size (pls. 83 & 84), or larger (pls. 51, 85 & 86) than the original; the original size being determined from the deflection of the enveloping schistosity (pl. 84). In the last case the margins of the new crystals are crenulate (pls. 65, 86 & 87), extending out into the matrix like "pseudopodia" (pl. 85) enclosing matrix crystals (pl. 87) to form a poikiolitic texture (pls. 51, 85, 86 & 87). These augen are thus both porphyroclasts and porphyroblasts; in both cases the foliation is deflected round the nucleus (pls. 81, 82, 83 & 84). Recrystallisation effects are also accompanied by the complex perthite relationships described previously (pl. 58).

Coeval with the processes described above was the segregation of quartz into small ribbons parallel to the foliation, with very irregular margins clearly cross-cutting matrix minerals (pl. 54); their growth then was partially metasomatic because they are replacing other matrix minerals. The quartz in these ribbons and elsewhere in the rocks shows undulose extinction (pl. 88), subgrain development and annealing features similar to those described by White (1971, 1973a,b,c, 1975a,1976) and White and Treagus (1975), from rocks deformed at high strain rates. Where the rocks are composed of more than 80 per cent. quartz interlocking crenulated crystal margins develop (pl. 101). It is inferred that this texture is the product of annealing and recrystallisation of a rock in which the crystal size was much smaller because of the interlocking pattern of the crystal margins and the way in which isolated islands of crystals in one orientation

are found in a crystal with another orientation.   Where recrystallisation

occurred under stress, quartz laths showing undulose extinction developed

from the strained grains (pl.89).   The laths mostly lie in the plane of

the developing schistosity (pl.46).

During the development of the D3 mylonitic textures a crystallographic

orientation of quartz developed in the quartzites (best seen in thin section

using a sensitive tint).   Figure 123 illustrates that the orientation is

a monoclinic "c" axis fabric with the axis of symmetry around 030/40°.

This cluster of "c" axes coincides with a strong mesoscopic rodding fabric

(L3) seen in the field.   The quartz fabric has therefore persisted through

at least two later deformations and must have originally been much stronger.

A very weak girdle dipping at 170/30° is also present, which lies within the

plane of the schistosity.   On Osterøy the monoclinic fabrics are unique to

the quartzites, a plot of the quartz "c" axes of a granitic gneiss collected

a few yards away from the quartzite analysed above, shows no strong fabric

(fig.124), but there is again a weak girdle dipping at 265/20°, within the

plane of the schistosity.   Both these rocks contain the rodding fabric

and intrafolial fold structures equally developed, and both have the same

metamorphic and deformational histories.

In the polymineralic rocks, apart from the minerals described above,

the remaining minerals play a minor role in the development of distinctive

structures.   For the most part they form a fine-grained groundmass of

irregularly sized anhedral crystals (pl.90), but in some places the texture

becomes almost granoblastic (pl.91);   crystals of the same species in these

areas are usually of the same size.

D4 Mylonites

The over-all effect of D4 is a further reduction in grain size and an

enhancement of the banding or a development of platiness in the rocks

(pls.92, 93 & 94).   There is also a darkening in colour of rocks of all

Fig 123.

PLOT OF QUARTZ 'C-AXES', [Rock No FH A24]

QTZ 'C AXES' ROTATED TO FIELD POSITION (ROCK FHA24)

THIS PLOT HAS UNDERGONE -2- ROTATIONS

USING CORDINATE CARD   0

SAMPLING   2ACROSS/- 1DOWN   POLES PER   1PERCENT AREA   300 DATA   EQ AR

Plane of the Foliation

THE CONTOURS REPRESENT THE FOLLOWING PERCENTAGES

00.9<=1-2%>02.9<=3-4%>04.9<=5-6%>06.9<=7-8%>08.9<=9-10%>10.9<=11-12%>12.9
12.9<=13-14%>14.9<=15-16%>16.9<=17-18%>18.9<=19-20%>20.9<=21-22%>22.9
22.9<=23-24%>24.9<=25-26%>26.9<=27-28%>28.9<=29-30%>30.9<=31-32%>32.9
32.9<=33-34%>34.9<=35-36%>36.9<=37-38%>38.9<=39-40%>40.9<=41-42%>42.9
42.9<=43-44%>44.9<=45-46%>46.9<=47-48%>48.9<=49-50%>50.9<=51%+
NOTE A VALUE OF>0.5-0.9<=.LT.1%AND.GT.0%

Fig 124.

PLOT OF QUARTZ C-AXES, [Rock FH A73]

QTZ 'C AXES' ROTATED TO FIELD POSITION (ROCK FHA73)

THIS PLOT HAS UNDERGONE -0- ROTATIONS

USING CORDINATE CARD   0

SAMPLING   2ACROSS/- 1DOWN   POLES PER   1PERCENT AREA   300 DATA   EQ AR

Plane of the Foliation

THE CONTOURS REPRESENT THE FOLLOWING PERCENTAGES

00.9<=1-2%>02.9<=3-4%>04.9<=5-6%>06.9<=7-8%>08.9<=9-10%>10.9<=11-12%>12.9

12.9<=13-14%>14.9<=15-16%>16.9<=17-18%>18.9<=19-20%>20.9<=21-22%>22.9

22.9<=23-24%>24.9<=25-26%>26.9<=27-28%>28.9<=29-30%>30.9<=31-32%>32.9

32.9<=33-34%>34.9<=35-36%>36.9<=37-38%>38.9<=39-40%>40.9<=41-42%>42.9

42.9<=43-44%>44.9<=45-46%>46.9<=47-48%>48.9<=49-50%>50.9<=51%+

NOTE A VALUE OF>0.5-0.9<=.LT.1%AND.GT.0%

compositions resulting from a decrease in grain size and dispersion of micas.

As a consequence of D4, S4 and S5 lie very close to each other and the effects accompanying the increasing dominance of S5 are similar to those described above for D3 (S4). Under the microscope, bands of incipient D4 shear are seen to start in biotite-rich layers of S4, the biotites shearing and fragmenting along their cleavages. The fragments then act as nuclei for new biotite growth but the crystals never regain their former size. The zones of shear pass out of mafic regions into felsic bands, where they form discrete fine-grained bands containing biotite (pl.95).

Development of the D4 shear bands is accompanied by all the features which accompanied the development of the D3 mylonites with the following slight modifications:

Quartz segregations are frequent but tend to form "strings" along the S5 schistosity (pl.66). The cycle of destruction and regrowth of potash feldspar continued but now myrmekite formed round the augen (pls.64 & 67) and fragments of this became sheared into the matrix (pl.96). A poikiolitic form of albite joins potash feldspar as a porphyroblastic mineral forming augen in the S5 fabric (pls.68, 69, 70, 97 & 102). D3 quartz ribbons developed undulose extinction and deformation laths during D4 and in places recrystallised parallel to the plane of the new schistosity (pl.54).

The most striking features developed during D4 are found in association with the thrust contact with the Major Arc. At grid ref. (07.80, 29.80) augen gneiss is in contact with dark coloured metasediments (fig.129). At the top of the section, within the contact zone, augen shaped fragments of augen gneiss up to 20cm in diameter are suspended in dark schist characterised by large "oyster shell" muscovites lying along the planes of schistosity. Moving away from the contact the size of these fragments

Fig 129.

SKETCH OF THE CONTACT BETWEEN THE AUGEN GNEISS AND THE METASEDIMENTS IN THE THRUST ZONE BENEATH THE MAJOR ARC [A D4 MYLONITE ZONE]

AUGEN GNEISS
[K-FELDSPAR AUGEN]

DARK SCHIST WITH PORPHYROCLASTS OF K-FELDSPAR & AUGEN GNEISS

FINE GRAINED BLACK QUARTZOSE SCHIST WITH K-FELDSPAR AUGEN

DARK SCHISTOSE QUARTZITE

SCHISTOSE PSAMMITE

6.5M
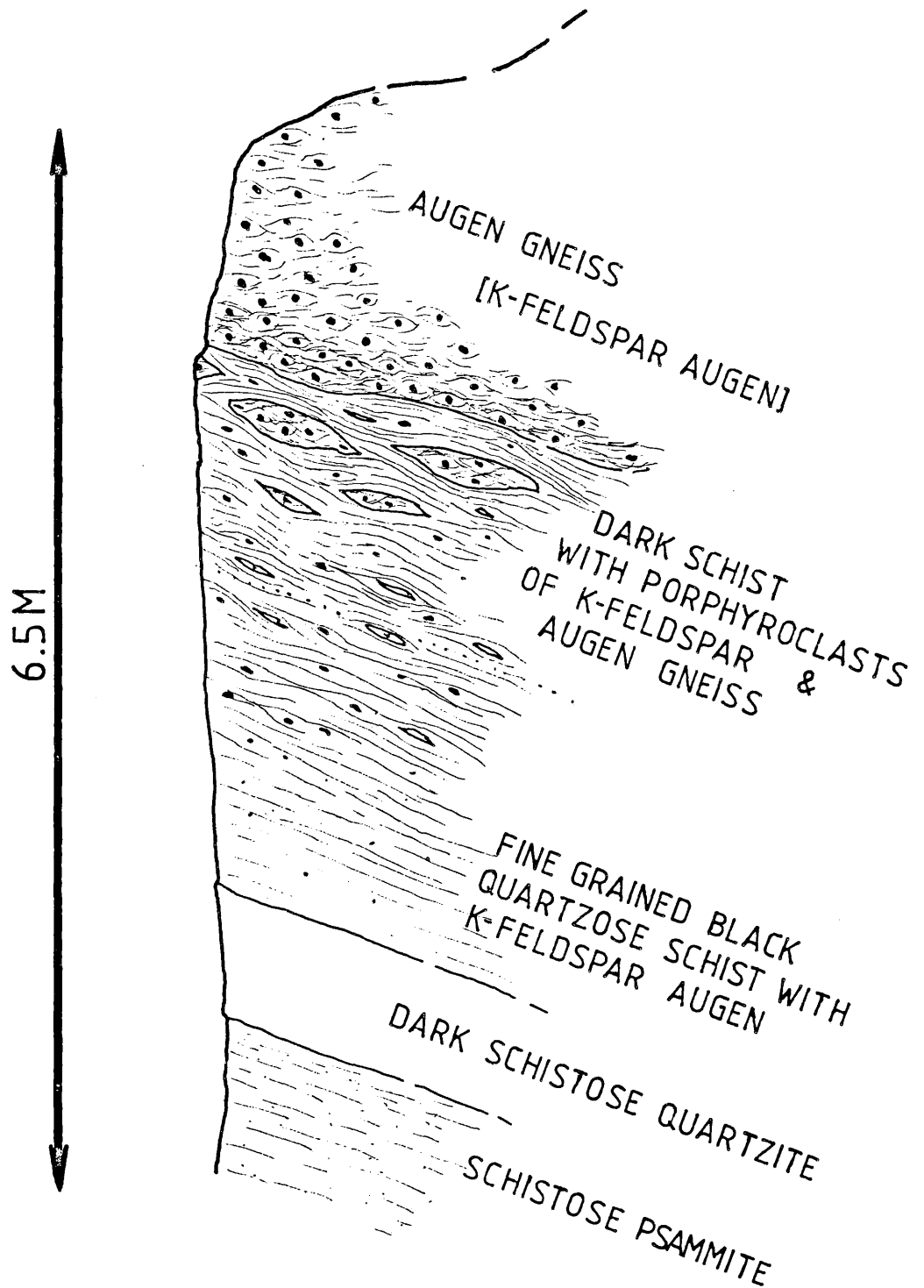
decreases until only isolated potash feldspar augen (2-3mm in diameter) remain. These contact rocks are interpreted as hybrid mylonites formed by the tectonic mixing of sediments and augen gneiss.

There is a relationship between the D3 and D4 folds and the locations of the mylonitic rock types; the new mylonitic fabrics are strongest in the limb regions of F3 folds, where the new schistosity parallels the old; the noses of F3 folds form "tectonic pips". During D4 the S5 schistosity was best developed where S4 was strongest and the grain size was smallest; it has thus in effect reactivated old F3 limbs. It is also developed along the short limbs of the F4 folds, (pl.23).

The effect of D4 on the rocks described above are therefore as widespread as those of D3 but only become dominant in some areas. Along the junction with the Major Arc, S5 is the dominant fabric, from here it dies out north-eastwards and is seen in the middle of the Southern gneiss outcrop as discrete bands of new schistosity. While these bands are found in the middle of homogeneous rocks, they tend to be preferentially sited along the contacts between gneiss types; D4 is thus responsible for the variation in grain size described approaching the margins of the augen gneisses (see section 3.3.2).

Other mylonitic rocks

Mylonitic rocks occur elsewhere in the gneisses in association with F5 folds. The middle limbs of these show a marked mechanical degradation of the minerals, but characteristically while the felsic minerals have annealed, maintaining the coherence of the rock, the biotites have not recrystallised, though they do define a new schistosity (S6). The D5 mylonites are therefore interpreted as having formed at a lower temperature than those of D4.

A second variety of mylonite is found along the D6 faults, where a fine-grained friable cream coloured rock which contains small angular fragments of rock and crystals, is interpreted as a rock flour formed during faulting. Mylonite is also associated with the D8 joints. Within the joint zones are rocks composed of gneiss and crystal fragments, set in a matrix of almost black isotropic powder (pl.50). This material occurs in sharp sided diastamosing bands (pl.47), and may contain voids into which drusy quartz has grown (pl.49). Calcite veins are common, especially in the larger rock fragments (pl.48) and their presence, together with voids, epidote and chlorite mineralisation, indicates formation by the explosive release of pore water during jointing. While such hydraulic pressure breccia is cohesive neither it nor the rock flour contain a foliation.

Discussion

Most of the features described above are characteristic of mylonites (Lapworth,1885). The Southern gneisses are thus a suite of mylonitic gneisses, though they do not conform to the usual description of mylonites in that they occur regionally rather than being confined to narrow zones.

Similar rocks seen elsewhere in the Bergen Arcs have also been called mylonites (Sinha Roy,1977c; Faerseth et al.,1977) and it is clear that mylonitic rocks form a considerable volume of rocks in the region.

Based on Sibson's 1977 classification of mylonites (fig.121), the rock types found on north Osterøy are: proto mylonite, mylonite, phylonite, blastomylonite, ultracataclasite and fault gouge. Most of the mylonites in the Southern Gneisses are blastomylonites.

4.1.2 Mode of Occurrence

The mylonites occur in three distinct situations and on this basis they may be grouped (figs. 130 & 131).

Fig 130.

ENVIRONMENTS IN WHICH ROCKS WITH MYLONITIC

TEXTURES WERE FOUND ON OSTERØY, (Part 1)

SIMPLE SHEAR MYLONITES

(Simple) SHEAR ZONE MYLONITES

A1
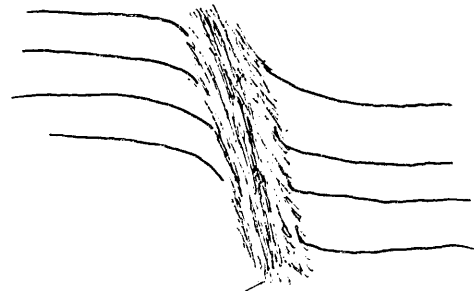
Mylonite

A2

THRUST ZONE MYLONITES

Thrust Zone

ABUTMENT MYLONITES

B1
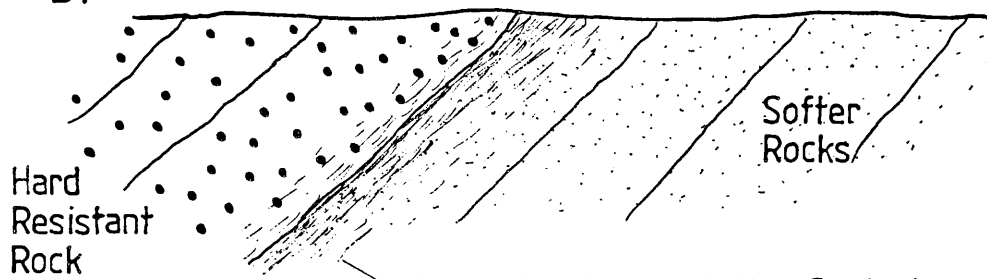
Softer Rocks

Hard Resistant Rock

Mylonite Forms at the Contact

B2

Tectonic Pip of Resistant Rock
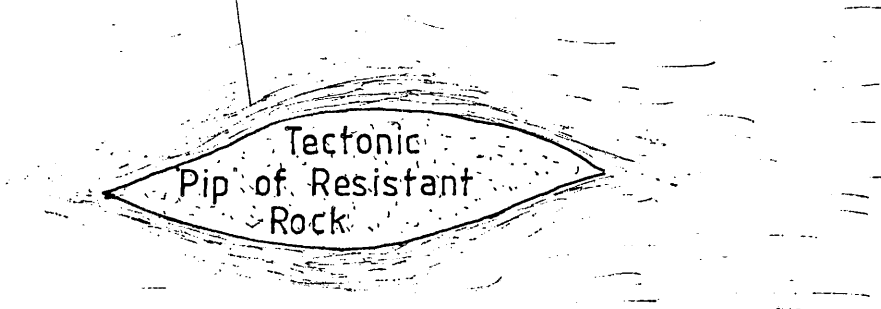
Fig 131.

ENVIRONMENTS IN WHICH ROCKS WITH MYLONITIC

TEXTURES WERE FOUND ON OSTERØY, (Part 2)

C1   FOLD ASSOCIATED MYLONITES

(Pure) SHEAR ZONE
MYLONITES

[tightening of folds]

Fold Train

Fold Nose
& Boudin Relics
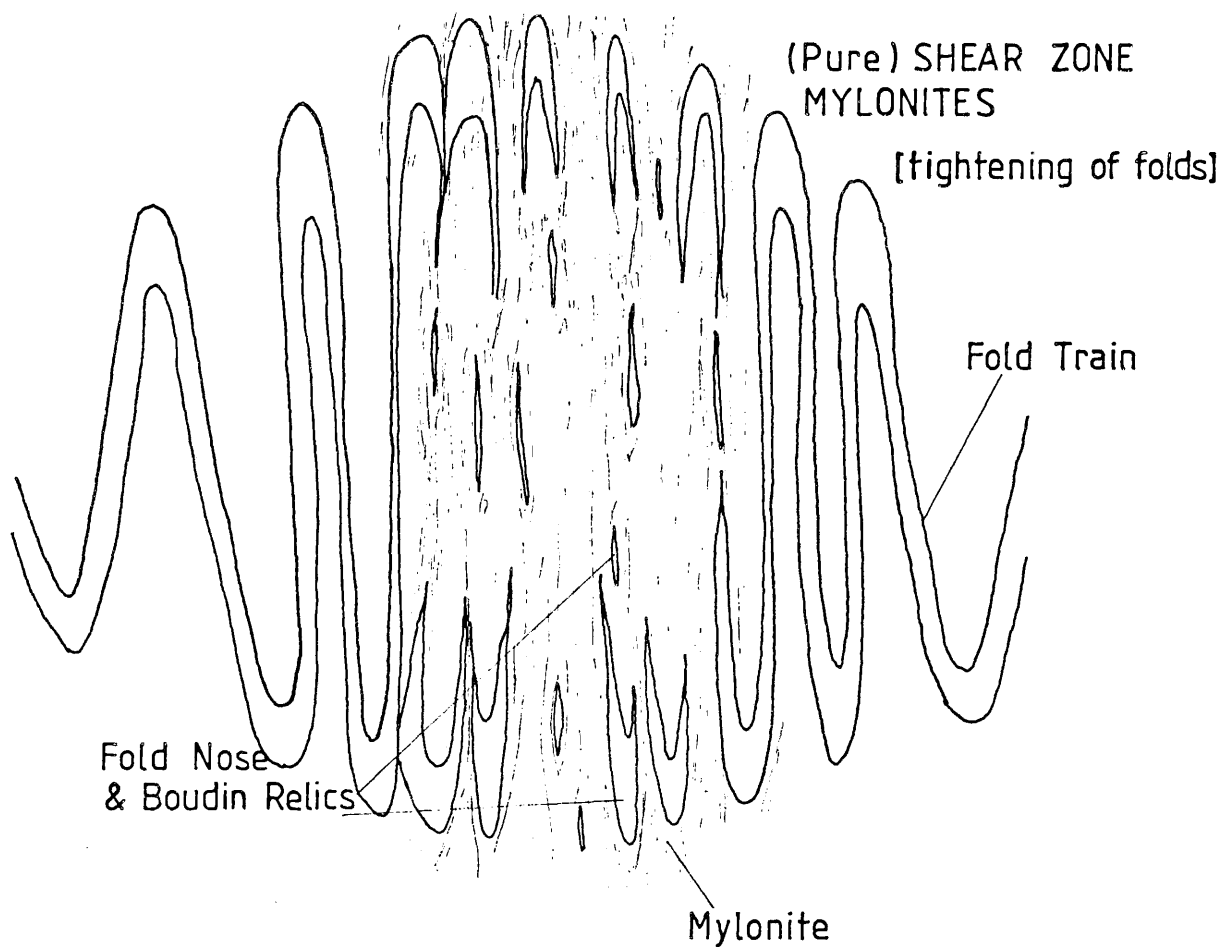
Mylonite

C2

MIDDLE LIMB MYLONITES
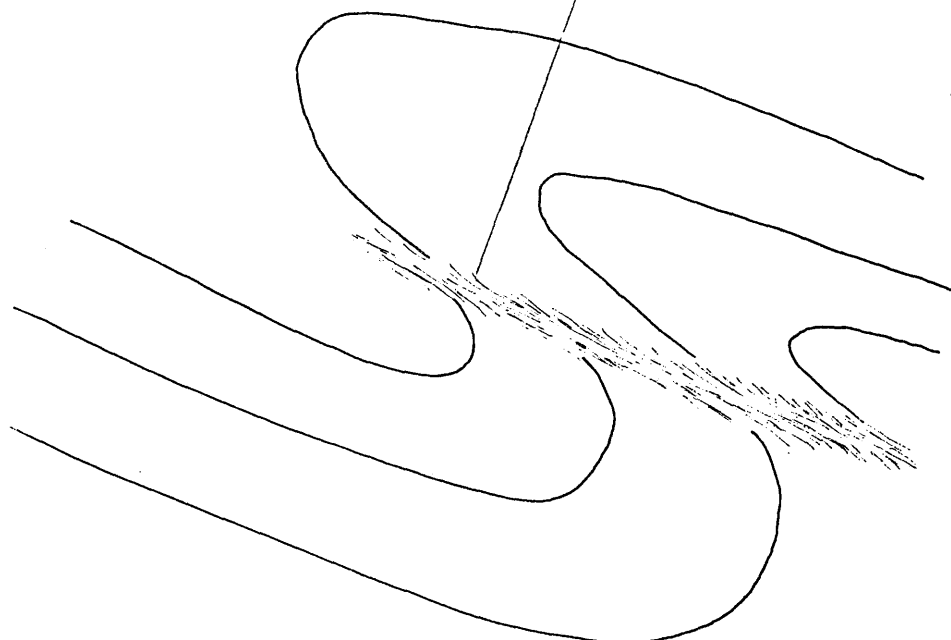
Fault Mylonites

These occur in close association with faults on Osterøy (fig.130,A2) and this variety is only represented by two rock types; the fault gouge and the D4 mylonite along the contact with the Major Arc.

Tectonic Abutment Mylonites

Most of the D4 and some of the D3 mylonites are of this type. The mylonites are found at the junction of two rock types of differing mechanical strength (fig.130, B1 & B2). The mylonitic rocks are better developed in the weaker member. Such locations of mylonitic rocks can be likened to a strain shadow round a porphyroclast where the schistosity is intensified across the layering at the points of maximum stress and reduced either side of the clast in the protected regions (Harker,1939; Simpson,1964). On Osterøy the strain effects are however on the kilometer scale. The "tectonic pips" appear to resist deformation and persist through succeeding deformations unaltered. During subsequent deformation it appears that the highly strained zones are the first to be reworked because veins cross-cutting early mylonites are most deformed in subsequent deformations, producing mylonites where the early mylonitisation was most intense (pl.23).

How the "tectonic pips" first form is problematic; some are remnants of early fold noses but others seem to form from the limb regions of the folds by a process akin to boudinage. Sinha Roy (1977b) suggests that small scale "tectonic pips" or porphyroclasts and high strain regions round them form by the intersection of sets of simple shear zones but this is considered unlikely on Osterøy because no evidence for simple shear zone arrays was found.

Regional Mylonites

These mylonites, which are the product of D3 and, to a lesser extent, D4 form the bulk of the Southern gneisses, which are therefore best described as a regional, flat lying mylonite belt. Characteristically these rocks are closely associated with folding and develop a strong "L" tectonite shape fabric. It has been·shown that the tightness of these folds decreases with depth (sections 2.1.5, 2.2.2 & 2.3.1 for D3 & 2.2.3 & 2.3.2 for D4) and since where the folds are open (section 2.1.5), no mylonite develops, it is apparent that mylonitisation is largely the product of "pure shear" flattening during the formation of the tight D3 and D4 folds (pl.99, fig.131-C1). In contrast the D5 mylonites are the product of "simple shear" in the short, middle limbs of asymmetric folds (pl.18, fig.131-C2) and are therefore akin to simple shear zone mylonites (fig.130-A1).

4.1.3   Pilot Geochemical Study

Thin section analysis of some of the mylonitic rocks in varying degrees of deformation suggested that apart from the development of new mineralogies and texture, there was a slight alteration of the bulk chemical composition with increasing deformation.   To examine this possibility a suite of samples was collected from an augen gneiss at locality (19.20,09.52), where it enters a D4 (abutment type) shear zone.   In the centre of the augen gneiss body the augen are 1.5 to 2cm in diameter but towards its southern contact the size of these decreases sharply.   At the contact the over-all grain size is considerably reduced and the augen eliminated; the rock also develops a new parallel banding.   Plates 42, 43, 44 and 45 show some of the textural variation among specimens.   No specimens were collected within a meter of the contact to avoid contamination due to mixing.

In thin section the principal mineralogical components of the rocks are quartz, potash feldspar, sodic plagioclase, biotite and accessory

chlorite, muscovite, epidote sphene and iron ore.   The chemical composition
of this suite of samples was determined, the lists of analyses are given
in appendix 2 (analyses 52-60).

There are problems in representing the variation in data across shear
zones in a way that clearly shows any geochemical trends that might be
present.   No such method exists in the literature;   Beach (1976) defines
his chemistry in classical two-component field plots;   Sinha Roy (1977b)
presents the raw data and states the broad trends.   Neither of these methods
is suitable because they do not show the details of the trends.

Herein data is presented on an Enrichment/Depletion plot, which is
constructed by plotting relative chemical enrichment or depletion against
degree of deformation.   The data must be plotted left and right of the
origin for symmetrical zones or on one side only, as in this case, for
asymmetrical zones.   The specimens may also be spaced evenly as in this
case or scaled to actual measured distances.

The enrichment/depletion value for each specimen is calculated by
subtracting the weight per cent. oxide for each element of the most deformed
rock from those for each of the specimens.   A scaling factor is employed
in some cases for the sake of clarity.

On such a plot any trend starting in the negative field and moving
towards the positive field represents a relative enrichment in that element
during deformation, and vice versa, especially if the slope is well defined.
The over-all behaviour of the lines compared with each other may define
patterns of behaviour amongst groups of elements.

Figures 125 to 128 present the analyses of major and trace elements
for two sets of samples.   It is clear that there is an over-all apparent
enrichment in SiO_2 accompanying the deformation and a corresponding
consistent pattern of apparent depletion in other major elements: MgO,
CaO, TiO_2, Fe_2O_3 and P_2O_5.

Fig 125.

MAJOR ELEMENT
ENRICHMENT / DEPLETION
DIAGRAM FOR THE FH B29
MYLONITE SUITE

(X.R.F. Geochemistry)

Fig 126.

TRACE ELEMENT
ENRICHMENT / DEPLETION DIAGRAM
FOR THE FH B29
MYLONITE SUITE

(X.R.F. Geochemistry)

Fig 127.

MAJOR ELEMENT
ENRICHMENT / DEPLETION
DIAGRAM FOR THE M1-3
MYLONITE SUITE
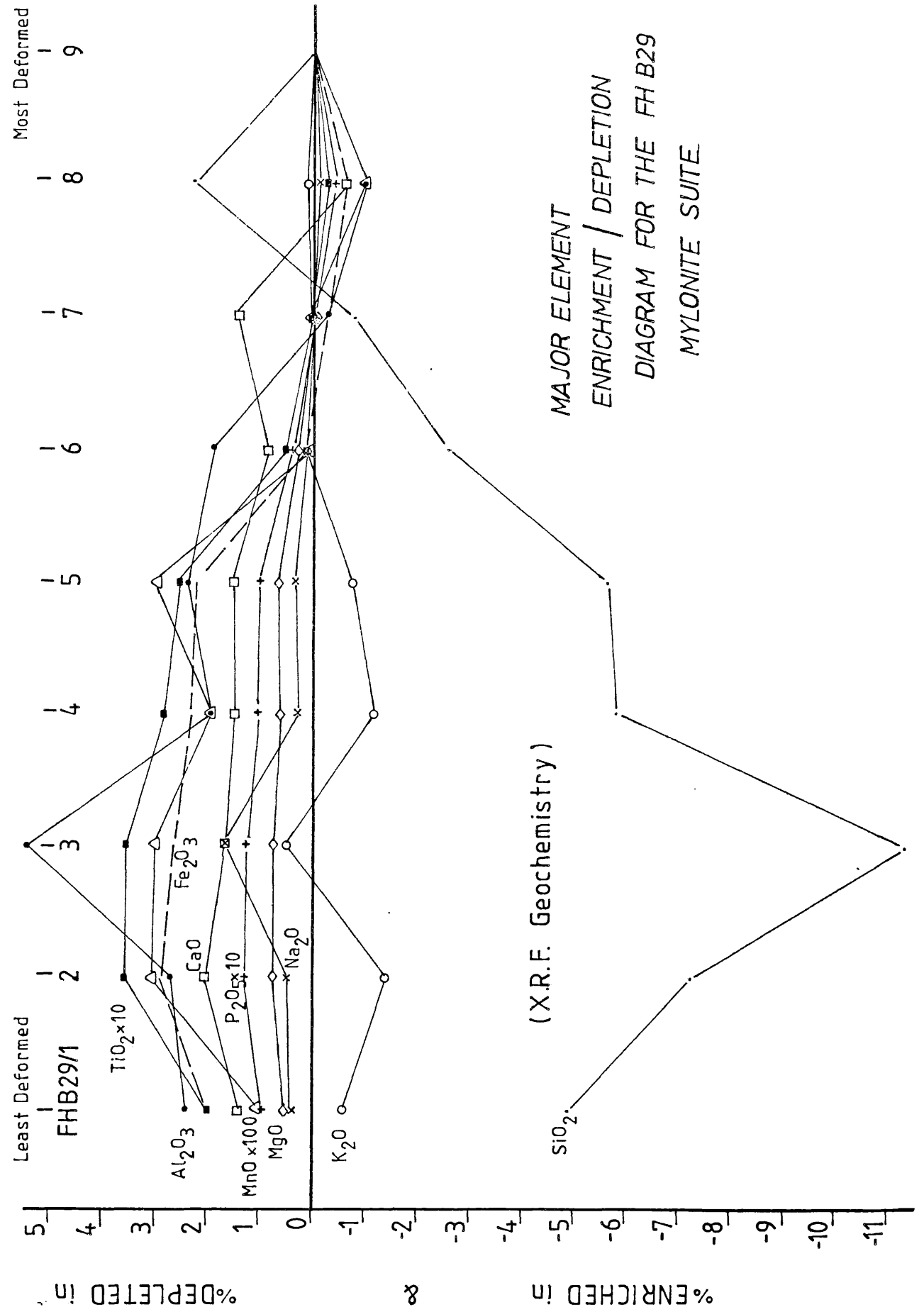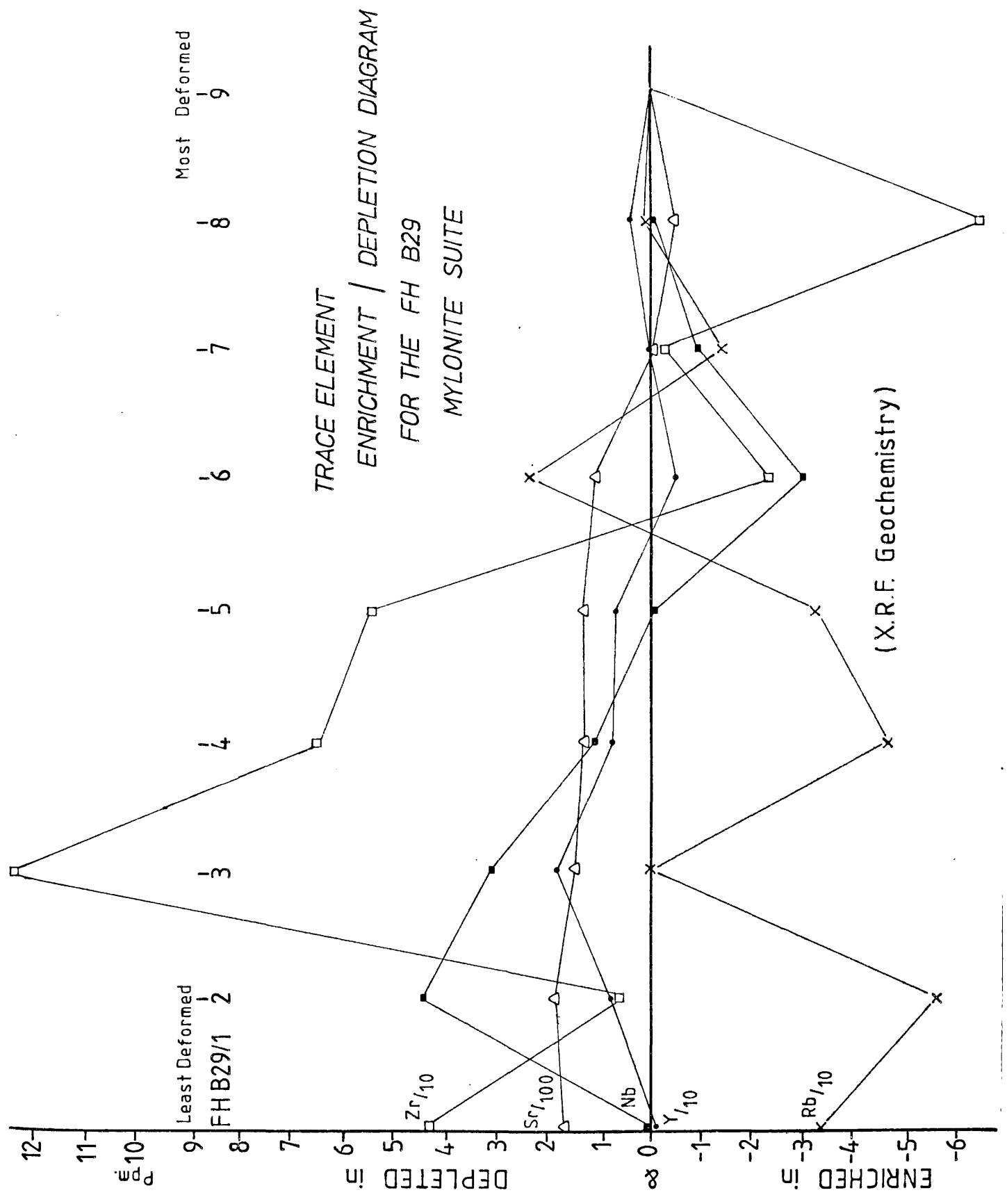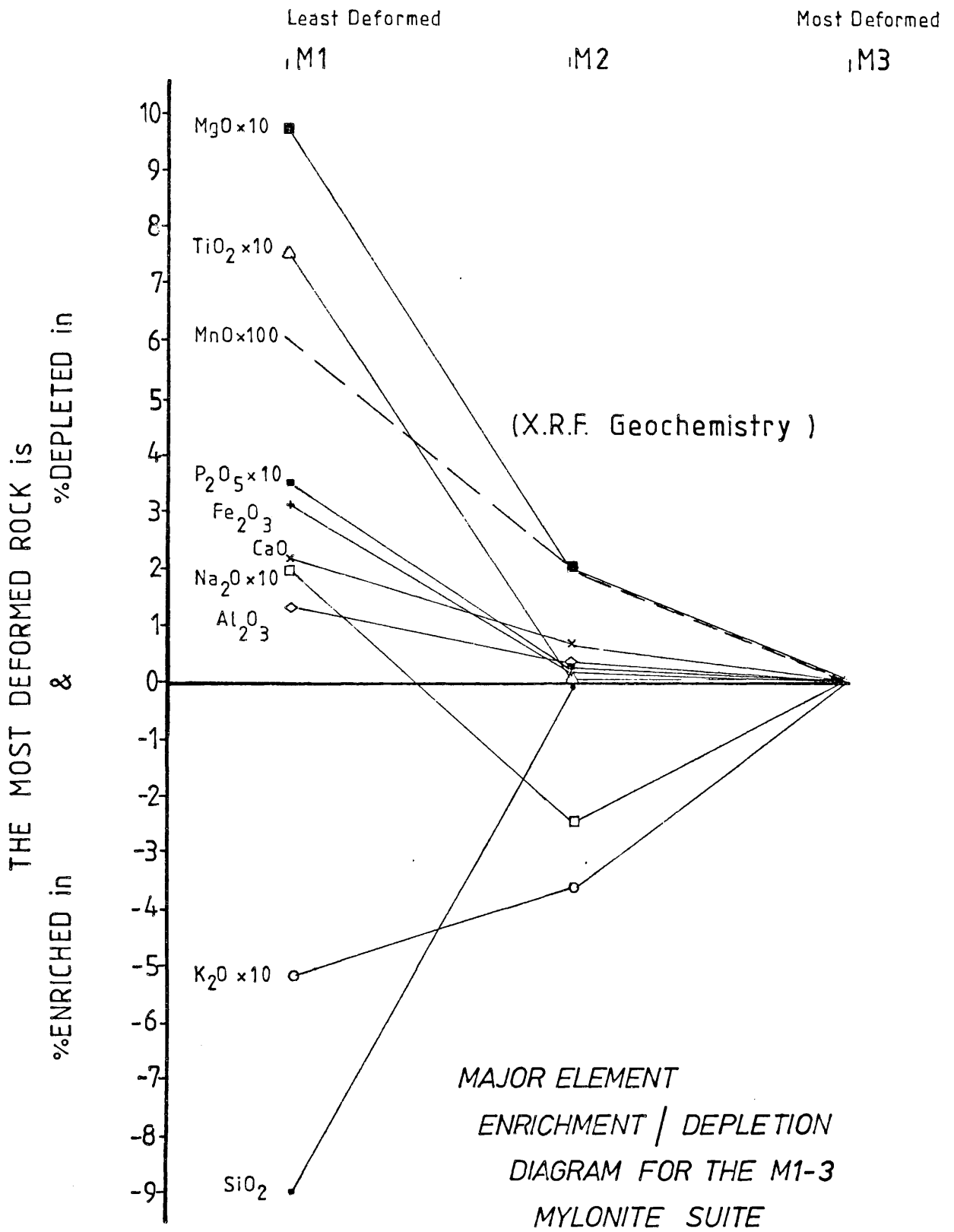
Fig 128.

TRACE ELEMENT ENRICHMENT / DEPLETION DIAGRAM FOR THE M1-3 MYLONITE SUITE

(X.R.F. Geochemistry)
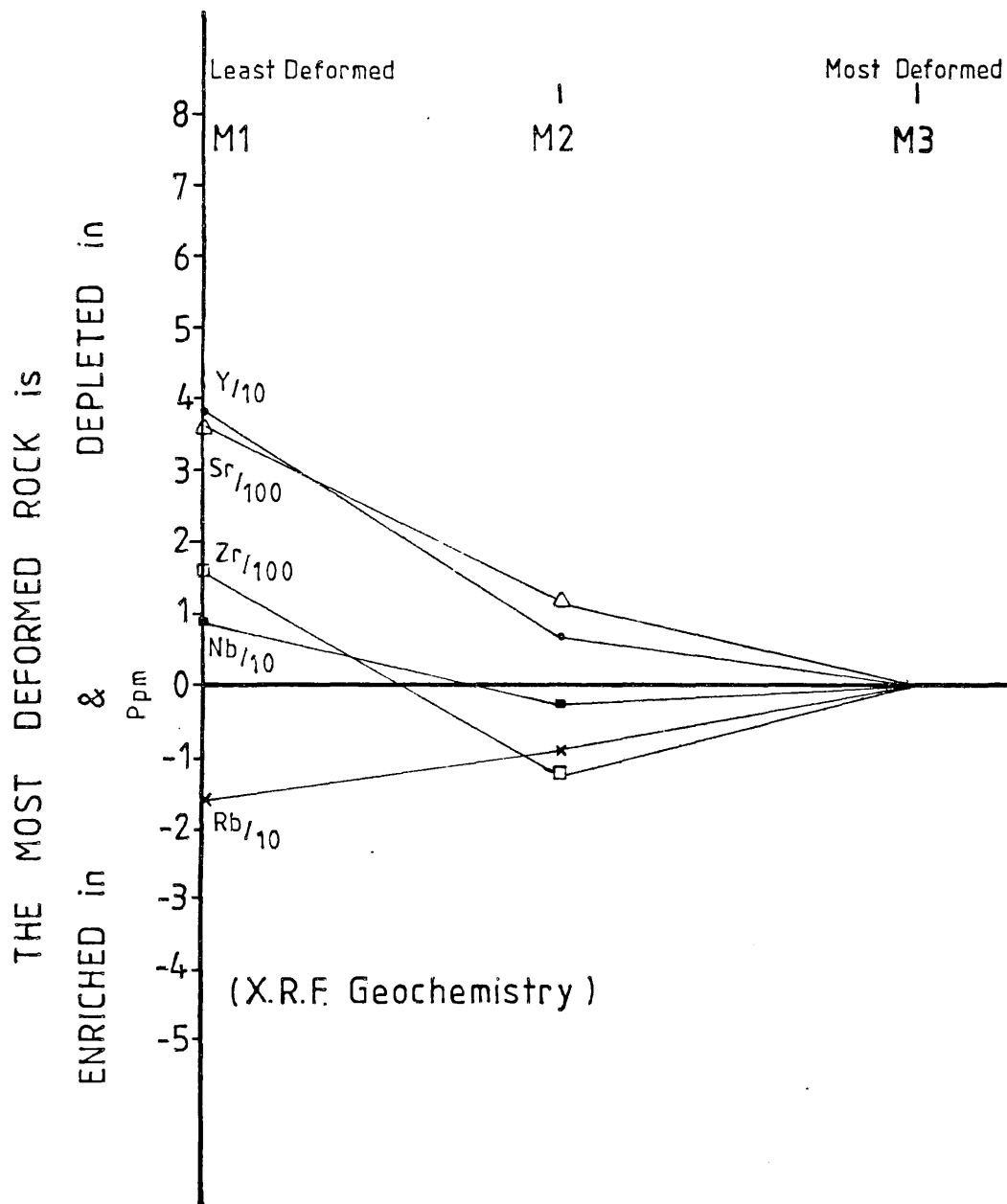
K_2O, Na_2O and Al_2O_3 do not follow either of the two trends described above, but rather define an over-all apparent enrichment in K_2O with increasing strain and an apparent depletion of Na_2O and Al_2O_3, yet the lines for all three when taken together form a pattern of their own.

Similarly, with the trace element plots, all except Rb are relatively depleted, Sr strongly so. The elements Rb and Zr define a trend pattern separate from the others; that for Rb is clearly similar to that described for K_2O.

Discussion

It is impossible to decide from the geochemical evidence alone whether the apparent SiO_2 enrichment is the result of addition of SiO_2 to the system or the subtraction of all other elements. However, thin section study reveals that the grain size of the mafic minerals decreases with increasing deformation, suggesting that their stability may have decreased because their surface area increased; thus subtraction may have caused the apparent silica enrichment.

A similar problem arises with the apparent K_2O enrichment. Thin section study reveals that microcline, the mineral most likely to carry K_2O, forms very large crystals in all the rocks. Thus during deformation microcline was stable and therefore its constituent elements are likely to have remained in the rock. However, it has been ascertained from the enrichment/depletion trends that K_2O, Na_2O and Al_2O_3 all behave in a related manner. As Na_2O and Al_2O_3 show depletion trends, it is inferred that while microcline was stable, plagioclase was unstable and was therefore removed. This conclusion is confirmed by the fact that plagioclase, rather than forming large crystals, is one of the small matrix minerals. The apparent K_2O enrichment is therefore similar to that shown by SiO_2, and is not, as classical interpretation would predict, the result of K-metasomatism.

The trace element plots show that Rb runs with the K_2O, and was therefore left behind whilst Sr in the rock was strongly depleted. This has important implications when considering ages based on Rb/Sr ratios.

The Y and Nb behave in a manner similar to the bulk of the mafic components. The Zr values must always be treated with caution in these plots, as large variations can be attributed to an uneven distribution of the mineral zirconium in the rock.

Thus the process of deformation is accompanied by the loss of the constituents of mafic minerals, aluminium and sodium.

4.1.4   Discussion on Possible Meaning of Textures

In thin section it is possible to subdivide the mineral textures seen in the Osterøy mylonites into sets. The presence, shape and size of any one crystal (especially plagioclase, K feldspar and quartz) is the result of the interaction of many processes (figs.134, 135 & 136), but it is possible in theory to determine the texture likely to result from the action of particular processes. The textures in any one rock are the product of two sets of these processes with diametrically opposed results; one set acting to increase crystal size, the other to decrease it. Assuming that any rock is the product of a dynamic equilibrium between these two sets and because the rocks are anisotropic it is possible, on the basis of the relative dominance of certain structures and textures, to identify individual processes responsible for any particular texture.

Textures resulting from processes causing grain size reduction

Textures from chemical processes. These textures are mainly the product of metamorphism which, apart from mechanical processes, is very important in determining the textures present in the rock.

a) Rim myrmekite (symplectites) (pls. 64 & 67)

b) Solution features (pl. 55): These features, because of their
       very nature are very difficult to identify and are therefore
       probably much more common than can be proved.

c) Relics (pls. 60 & 61).

Textures from mechanical processes. Textures produced by these
processes are further subdivided into those which result from high pore
fluid pressures and those formed as a result of high grain/grain contact
pressures.

d) High fluid pressure textures (pls. 47, 48, 49 & 50)
The mechanical pressure structures are again subdivided on the basis of
whether the stresses were applied at a rate faster or slower than, or equal
to the rate at which the mineral can accommodate the strain.

Faster:

e) Cataclastic textures (pls. 77, 96 & 100)

Slower or Equal:

f) Sub grains (pls. 76, 78, 79, 80, 81 & 82)

g) Undulose extinction (pls. 57, 79 & 88)

h) Quartz lamellae (pl. 46)

i) Augen and porphyroclasts (pls. 55, 76, 80, 83 & 84)

j) Shear bands (pl. 98)

k) Quartz strings (pl. 66).

Textures resulting from processes causing increase in grain size

There are two main processes by which mineral grains may increase in
size. The first involves the rearrangement of the crystal lattice so that
it conforms to, and merges with, adjacent grains of the same species.
The process results in reduction of the grain boundary surface area in the
rock. The second involves chemical reactions at adjacent crystal boundaries,

or redeposition of a mineral phase at a site of nucleation in the rock, while at other locations this phase is dissolving.

Lattice rearrangement structures

l) Crenulate crystal boundaries (pl.101)

m) Clearing features (pl.91)

n) Granoblastic texture (pl.91)

Chemically induced structures

o) Snowball garnets (pl.56)

p) Poikiloblasts (pls.53, 56, 70, 102 & 86)

q) Amoeboid growth (pls.51, 86, 85, 87 & 68)

r) Porphyroblasts (pls.55, 69, 70, 86, 97, 68 & 102).

These form in two ways, by recrystallisation of a grain originally porphyroclastic in nature, or by nucleation and growth of a new crystal.

s) Embayment and cross-cutting structures (pls.61 & 100)

t) Mimetic rims (pls.55 & 62)

u) Ribbons (pl.54).

Definition of Terms

The terms "crystallisation" and "recrystallisation" used in the following discussion are defined as follows:

Crystallisation: the appearance of a mineral at a site in the matrix for the first time; involves nucleation and growth of a new or similar phase.

Recrystallisation: A mineral is recrystallising if, following subgrain formation, it clears itself of strain and the subgrains reunite, reforming a discrete crystal; this may attain or exceed the size of the parent grain.

4.1.5   General Discussion

The Southern gneisses are unique because while there are other mylonite zones of equal thickness, for instance the Namtin and Namarodo mylonites from the south-west Nile region of Uganda (Hepworth,1964), the main foliation in the Southern gneisses is subhorizontal rather than steeply inclined or vertical.

There is also a fundamental difference between these thick tracts of mylonite, termed here "regional mylonites", and those typically described from fault zones, for example the Outer Isles Thrust (Sibson,1977), in that the genesis of regional mylonites is not clearly associated with major thrusts.   Indeed it is doubtful whether the term "mylonite" which was originally applied to rocks formed "where two superposed rock systems moved over each other as solid masses" (Lapworth,1885), is strictly applicable to regional mylonites where no overiding is seen.

A large body of opinion, led by Higgins (1971) regards mylonites as having a brittle, disruptive (cataclastic) origin and therefore diagnostic of fault zones.   Recently however it has been proved that the micro-structures seen in mylonites (polygonisation, subgrains, serrated grain margins, kink bands and grain aggregates) are equally attributable to ductile deformation, recovery and recrystallisation.   Therefore, in part, the processes responsible for mylonite generation can be plastic rather than brittle (Bell & Etheridge,1973;   Nicolas & Poirier,1976).

All the literature on the formation of mylonites regards the over-all deformation regime as one of simple shear because of the association with fault zones (viz. Higgins,1971;   Sibson,1977).   Whilst this regime is applicable to mylonite zones like the Outer Isles Thrust, it is inadequate in other cases where it is evident that there is a strong pure shear component in the generative deformation (Johnson,1967).

The Southern gneisses are an example of a pure shear mylonite zone.
Apart from the mechanical problems of generating mylonites of this thickness
over such a broad region by a simple shear mechanism, it is evident from
the mesoscopic structures (see section 2.2), that deformation accompanying
mylonite genesis is one of flattening without large-scale displacement
(the situation seen in fig.131-C1). ·

The geometry of the "mylonites" on Osterøy points to the conclusion
that mylonites are not a rock type specific to faulting regimes, but are
one aspect of a continuum of rock deformation and metamorphism.   The
theoretical basis for this conclusion and an explanation of the significance
and presence of the structures described above is given below.

4.2   THEORETICAL CONSIDERATIONS

It is generally agreed (e.g. Sibson,1977), that mylonites are produced
when the strain rate in a rock exceeds the annealing rate of its component
minerals.   It is usually thought that they are the product of a single
tectonic phase.   The rock is stressed, and strain is concentrated in a
band in which the rock develops a fine-grained texture and a foliation.
The unit so formed may then recrystallise to form a blastomylonite,
depending on its depth of burial (Sibson,1977).   (It is, however, understood
that subsequently the fault zone may reactivate (Christie,1960), thus
producing subsidiary mylonites which may incorporate portions of those
previously formed.)   Zones like this clearly exist;   the Outer Isles
Thrust described by Sibson (1977) being one of them.

The genetic origins of these mylonites are known, and it is possible
partially to quantify the strain rates appropriate to their production
(White,1975b; Price,1975).   Figure 132 shows a table of geologically
realistic strain rates and their associated structures.   Mylonites are
produced at strain rates between 10^{-1}/sec. and 10^{-8}/sec.

Fig 132.

GEOLOGICAL STRAIN - RATES
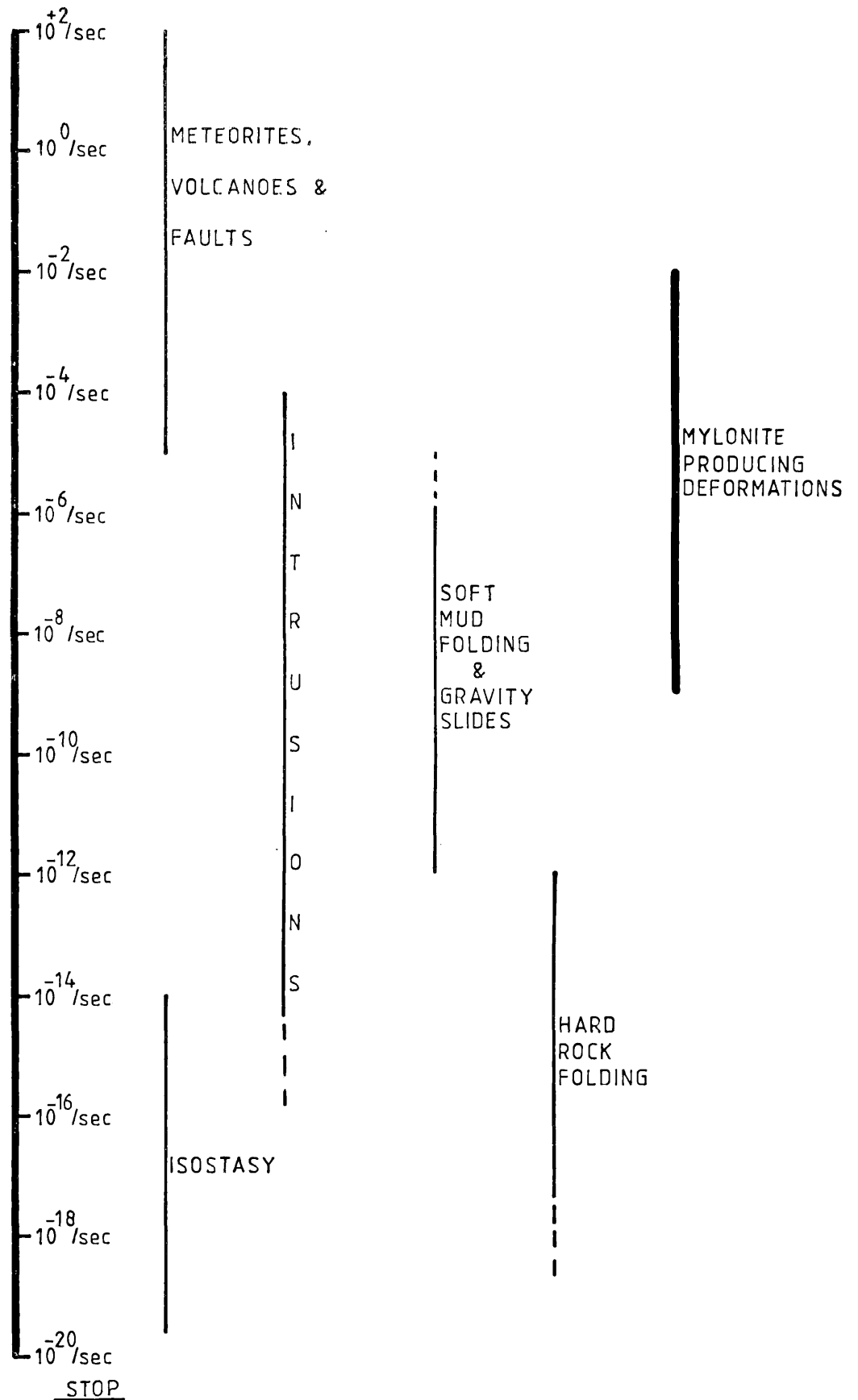
(After PRICE 1975)

The mylonites comprising the Southern gneiss unit on Osterøy do not
however fit Sibson's (1977) model, as it can be demonstrated that the
mylonites developed concurrently with regional folding in the gneisses, and
development continued through two phases of such folding; the metamorphic
grade during these processes waned from almandine amphibolite facies,
through to lower greenschist facies (section 3.5.4).

There is therefore a paradox, the tectonic facies (mylonites) indicate
high strain rates whilst the structural features associated with mylonite
formation (folding of hard rocks, i.e. gneisses), suggest the strain rate
should be in the order of 10^{-12}/sec. or less. The mode of occurrence is
also different: the Osterøy mylonites are not confined to a discrete band,
but are regional in extent.

Any model explaining mylonites must be based on the behaviour of its
component minerals and their reaction to stress. Recently advances have
been made in the understanding of molecular deformation paths, and a
review of these is necessary.

The deformation theory used in geology is based on that developed
for metallurgy and ceramics. Plates 104 and 105 model a plane through a
crystal. The areas (A) model ideal packing. The bands (E) model crystal
boundaries. Across the boundaries at which two crystals of different
orientations meet, is an area of mismatch; these areas are almost 50 per cent.
void space. The bands (F) model subgrain boundaries; here the mismatch
and void space are not so great. Areas (B) model strained crystal lattices;
microscopically these would be areas of undulose extinction (pl. 38).
Planes (C) model dislocation planes or stacking faults. The strain in
(B) areas can regularise to form (C) planes. Frequently in doing this a
hexagonal net structure develops (X, pl.105), (Wenk,1976; Nicolas &
Poirier,1976). Points (D) model vacancies or point defects. (Areas (E)

and (F) could be considered to be sites of accumulation of (D) type structures.) There is a dependence of vacancy density on grain size, as grain size decreases the proportion of vacancies per unit volume increases. The dependence is controlled by surface area and varies:

$$\frac{3A}{D} \ cm^2/cm^3 \qquad \cdots\cdots\cdots\cdots \ (1)$$

where D = average grain diameter
       A - the number of vacancies in a 1 cm length of crystal boundary.

Triaxial compression tests have yielded data on the conditions required to generate and mobilise dislocations (Heard,1960,1963; Serdengecti & Boozer,1961; Rutter,1972(a)). There are at least six independent distinguishable paths by which steady state deformation may be accommodated that have been discovered. All but one (Twinning) involve motion of defects through or around grains. These paths are:

(1)   Defectless flow (plastic flow without defect
        formation)   Plates 104 & 105

(2)   Glide (movement of edge or plane defect
        across lattice planes) $\cdots\cdots\cdots\cdots$ (C) & (B)

(3)   Creep (this occurs at elevated temperatures
        and includes the process called climb.
        It involves movement of an edge or plane
        defect by addition or subtraction of ions
        from the plane. The movement is there-
        fore confined within the plane). $\cdots\cdots\cdots\cdots$ (C) & (B)

(4)   Coble Creep (movement of point defects
        around grain and subgrain boundaries) $\cdots\cdots\cdots\cdots$ (F) & (E)

(5)   Nabbro Herring Creep (movement of point
        defects through the body of a crystal) $\cdots\cdots\cdots\cdots$ (D)

(6)   Twinning.

The basis of all deformation theory is Frick's first and second laws which describe the movement of point defects (vacancies, foreign or interstitial ions).

The first law governs the rate at which stresses anneal from crystals; it relates the flux of ions at right angles to a direction to the concentration gradient parallel to it.

$$J = -D \frac{dc}{dx} \qquad \ldots\ldots\ldots\ldots\ldots (2)$$

Where:

J = The flux of defects

D = The diffusive coefficient

$\frac{dc}{dx}$ = The concentration gradient along the axis.

The second law gives the profile of the gradient.

$$\frac{dc}{dt} = D \frac{d^2 c}{2} \qquad \ldots\ldots\ldots\ldots\ldots (3)$$

Where: t = time

Each mechanism can therefore be described mathematically (Elliot,1973; Wenk,1976; Nicolas & Poirier,1976) and Ashby (1972) proposed a composite diagram, "The Deformation Map" (fig.133), which expresses how rock would deform at steady state under any given environmental conditions. There are, therefore, five main processes by which rock may deform; only the last two readily achieve a steady state condition.

(1) Defectless flow (Ashby,1972). The rate controlling factor is the viscosity of the rock.

(2) Twinning, only significant in rocks composed of minerals which twin easily. Deformation is finite because a lattice cannot twin indefinitely in direction or amount.

(3) Cataclasis (fracture). Involves crystal breakdown, which is pressure dependent and frictional sliding between resultant fragments. A disruptive rather than continuous process. (This is the mechanism thought by Higgins (1971) to be responsible for mylonite geneses.)

Fig 133.

THE DEFORMATION MECHANISM MAP

[After :- ASHBY 1972 & RUTTER 1976]
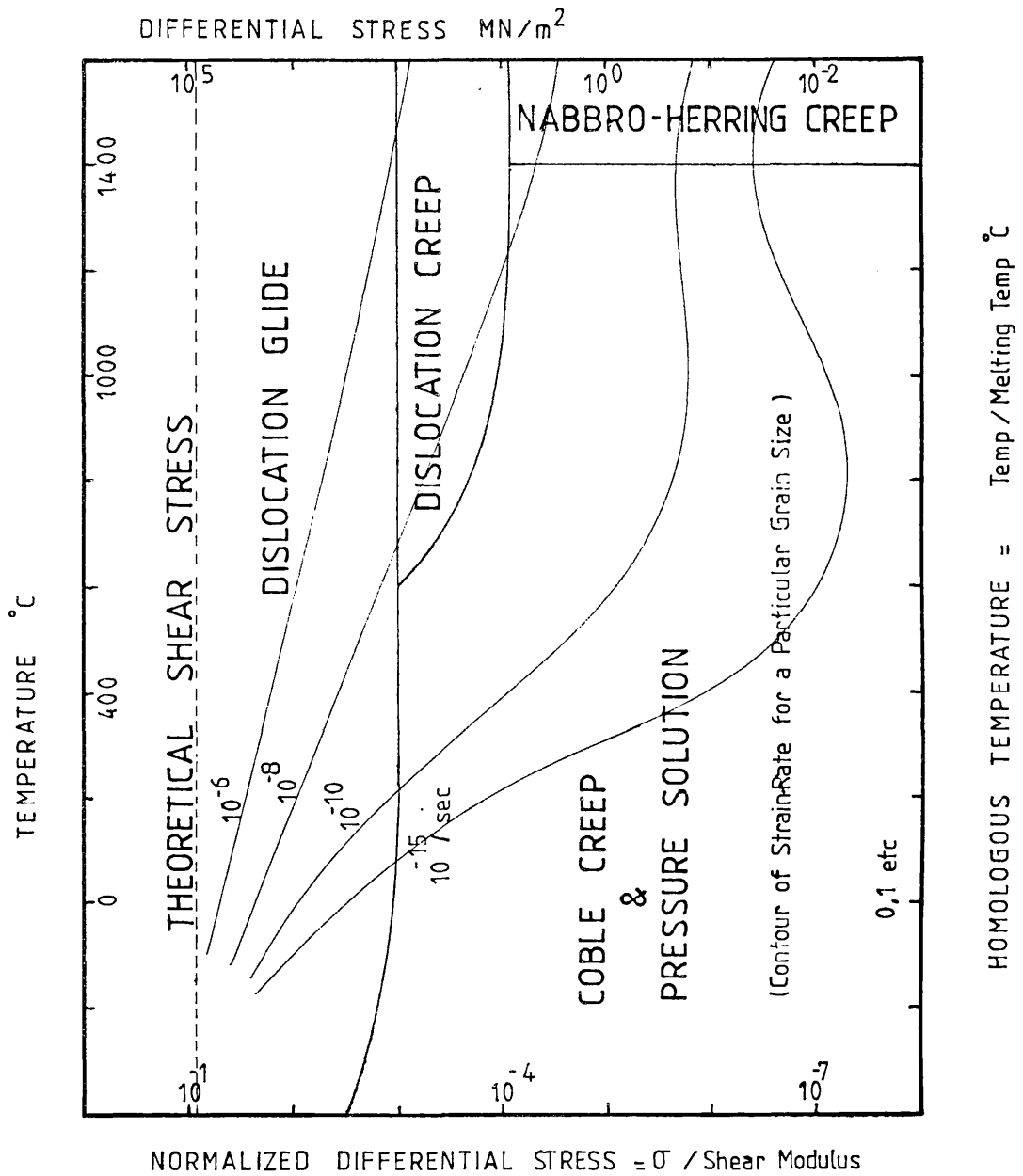
(4)   Intra-crystalline processes (Wenk,1976; Nicolas & Poirier,1976).
This involves the dislocation glide and climb mechanism described above.

(5)   Mass transfer or diffusive processes.   Included here are
coble creep, nabbro herring creep and pressure solution.   Deformation
is accommodated by migration of point defects (vacancies) from sites of
low stress to sites of high stress (to accommodate matter moves in the
opposite direction).

Rutter (1976) and McClay (1977 a & b) have added a new field to the
Ashby deformation map, that of pressure solution.   The mechanism is
basically one of the coble type, but the process is enhanced by a thin
film of fluid at the grain boundary.   The site of redeposition can therefore
in this instance be remote from the dissolving mineral.

There is some debate as to whether one or more mechanism at a time
can operate on a single mineral aggregate.   Mitra (1978) in contradiction
of Rutter (1976), concludes from his work on quartzite that a combined
flow law, composed of pressure solution and intra-crystalline processes
can operate.

Another process not considered by Ashby has recently been proposed.
Boullier and Gueguen (1975) in considering mylonite formation suggested
a process of "Superplastic Flow".   The process is quasi-viscous,
involving essentially grain boundary sliding, and allows unusually large
tensile deformation, without necking, at high strain rates.   Such a process
necessitates a marked reduction in viscosity during mylonite formation.
Calculations by S. White (pers. comm. 1977) for the viscosity of a quartz
mylonite suggesting viscosities similar to those for molten granite
(10^{-9} poise), support this.   Other work on superplasticity is reviewed
by Davies et al. (1970), Johnston (1970) and Edington et al. (1976).

The possible paths of deformation in rock are summarised in figures 134, 135 and 136. The processes can be further grouped on the basis of their effect on grain size:

DESTRUCTIVE	NO CHANGE	CONSTRUCTIVE
Dislocations	Coble creep	Pressure solution (b)
Pressure solution (b)	Pressure solution (a)	Chemical changes (as
Cataclasis	Dislocations	regards the stable
Chemical changes (as	Grain boundary sliding	phase)
regards the unstable	Nabbro herring creep	Annealing
phase)	Twinning	
	Annealing	

The Rate of Deformation Processes

The ease with which dislocations migrate is governed by the rate at which the largest ion can move. In rock the largest common ion (94% by volume of the Earth) is (O)2-, and the diffusion rate varies from mineral to mineral, depending on bond strengths. The mobility depends also on the ambient temperature. Thermal oscillations cause momentary breaks in these bonds. There is a temperature unique to every mineral (the Activation Temperature or Energy), however, below which the rate at which these breaks occur is insignificant. The variation in this activation temperature from mineral to mineral is seen in the Osterøy mylonites in the comparative amount to which minerals have recovered from deformational events. Gilletti, Semet and Yund (1977) investigated the diffusion of oxygen in feldspars; they concluded that these minerals have a low activation temperature and would therefore recrystallise in geological settings at comparatively low temperatures. This is confirmed in the Osterøy rocks, the feldspars are one of the first and last minerals to recrystallise in the mylonites.

The Grain Boundary

This acts as a plane of weakness in rock, it is the source and sink for dislocations and the plane at which chemical changes occur. It is

Fig 134.

265

POSSIBLE DEFORMATION PATHS IN POLYCRYSTALLINE
ROCKS, Part1

SINGLE CRYSTAL PATHS
DISLOCATION GLIDE & CREEP

σ1

undulose
extinction

crystal lattice

dislocations

strained lattice

CYCLES
OF
DEFORMATION

DEFORMATION

ANNEALING

ANNEALING & RECRYSTALL-
ISATION

enlarged
subgrains

subgrains

crystal reorganizes

subgrain walls

CATACLASIS

σ1

FRACTURE

Crystal fragments

(A High Strain Rate - Low Temperature Phenomenon)

Fig 135.
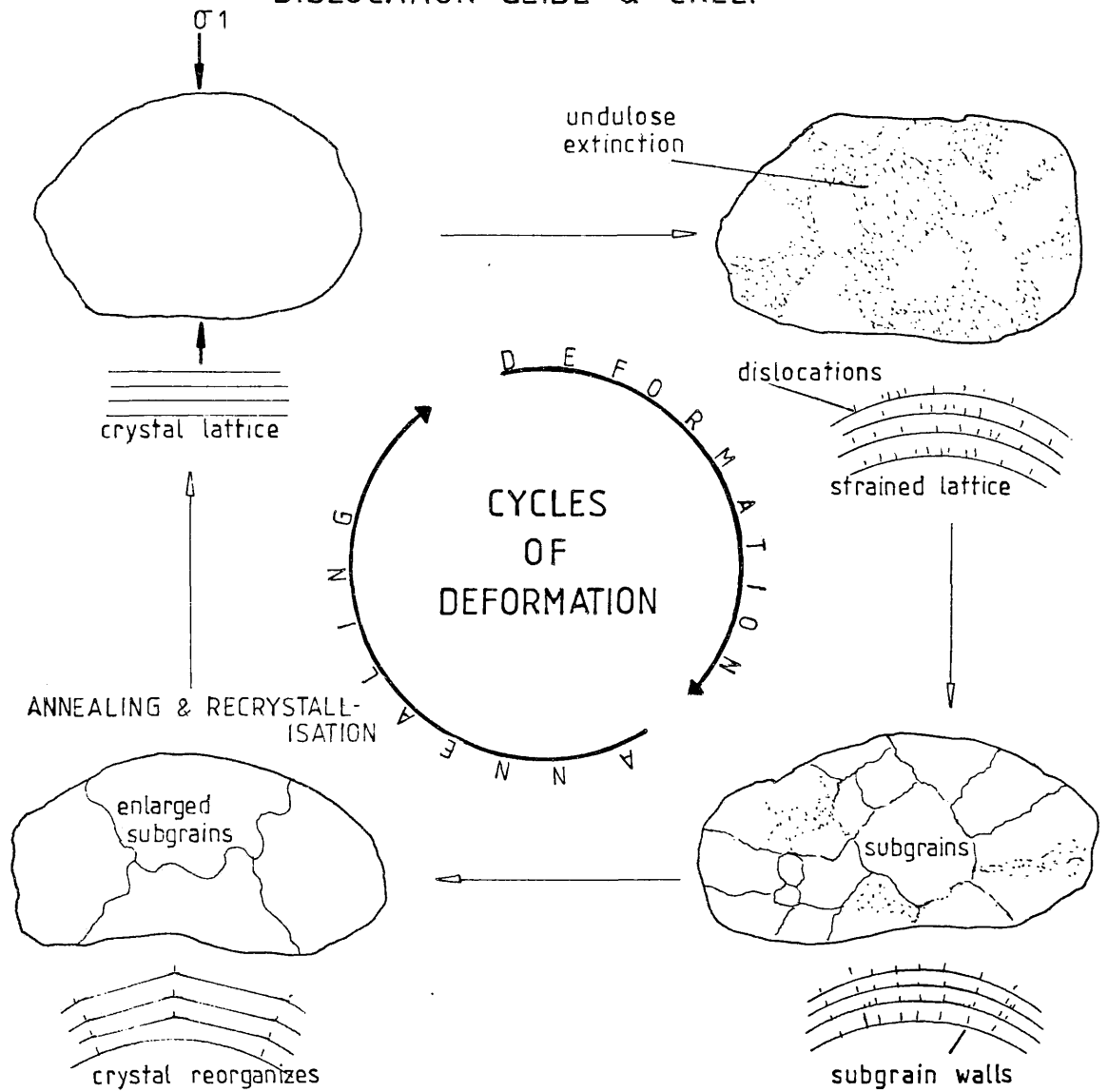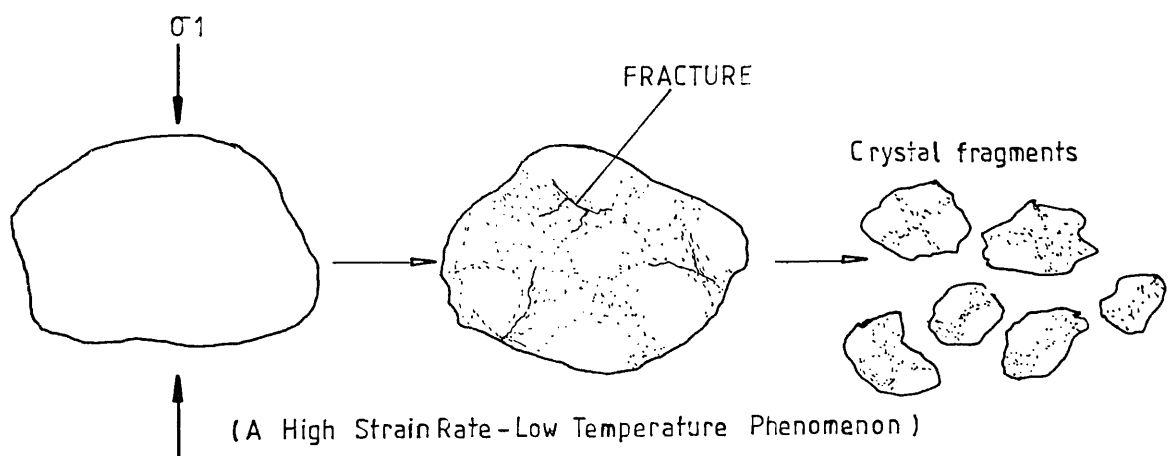
POSSIBLE DEFORMATION PATHS IN POLYCRYSTALLINE
ROCKS, Part 2

SINGLE CRYSTAL PATHS
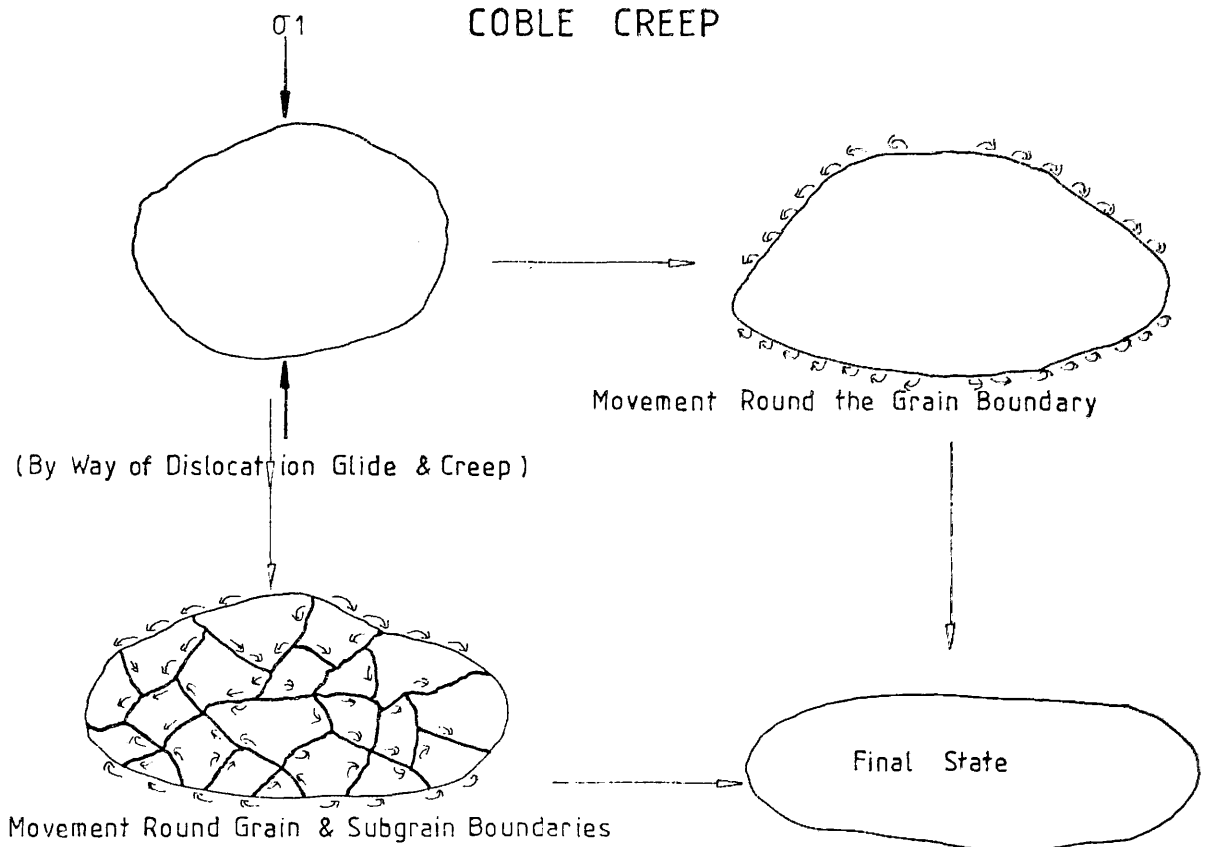
COBLE CREEP

σ1

Movement Round the Grain Boundary

(By Way of Dislocation Glide & Creep)

Movement Round Grain & Subgrain Boundaries

Final State

PRESSURE SOLUTION [COBLE CREEP] (a)

σ1

Material Dissolved

Material Deposited

NABBRO-HERRING CREEP

σ1

Final State

Movement Through the
Body of the Crystal
(A High Temperature Process)

Fig 136.
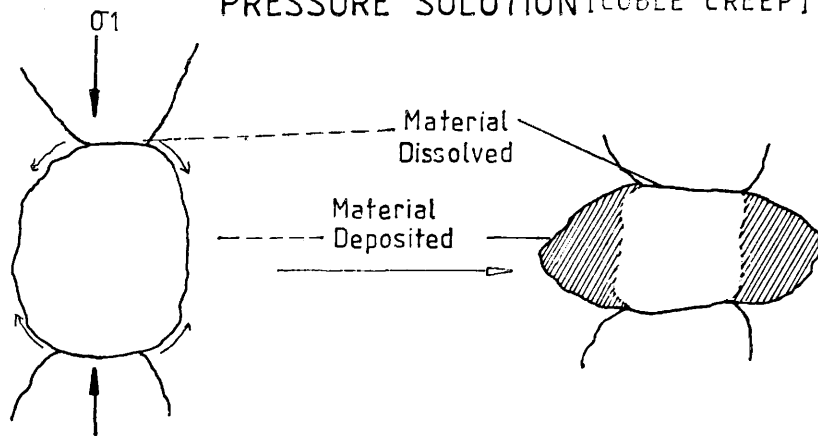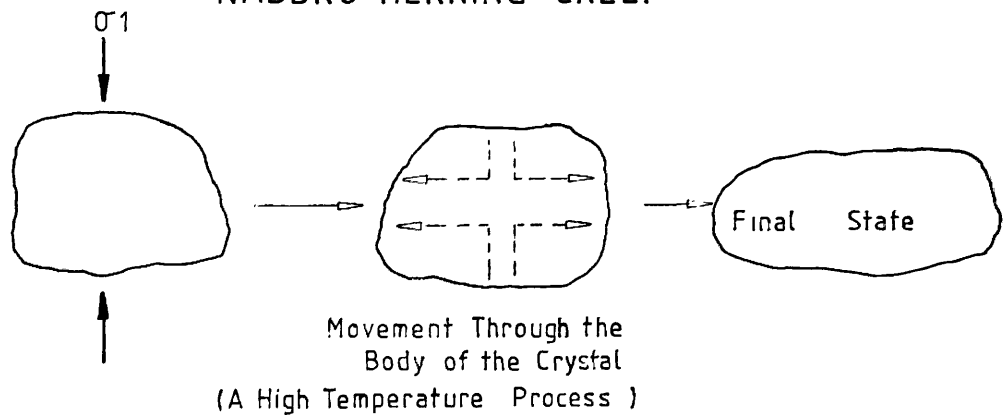
POSSIBLE DEFORMATION PATHS IN POLYCRYSTALLINE ROCKS, Part 3

POLYCRYSTALLINE MECHANISMS

PRESSURE SOLUTION [COBLE CREEP] **(b)**

$\sigma 1$

Solution

Finite State

Deposition

Finite State

(TRANSPORT OF MATERIAL IN SOLUTION)

GRAIN BOUNDARY SLIDING

$\sigma 1$

Marker

Slip on Grain Boundary

CHEMICAL CHANGES

$\sigma 1$

Hornblende

Hornblende

Biotite
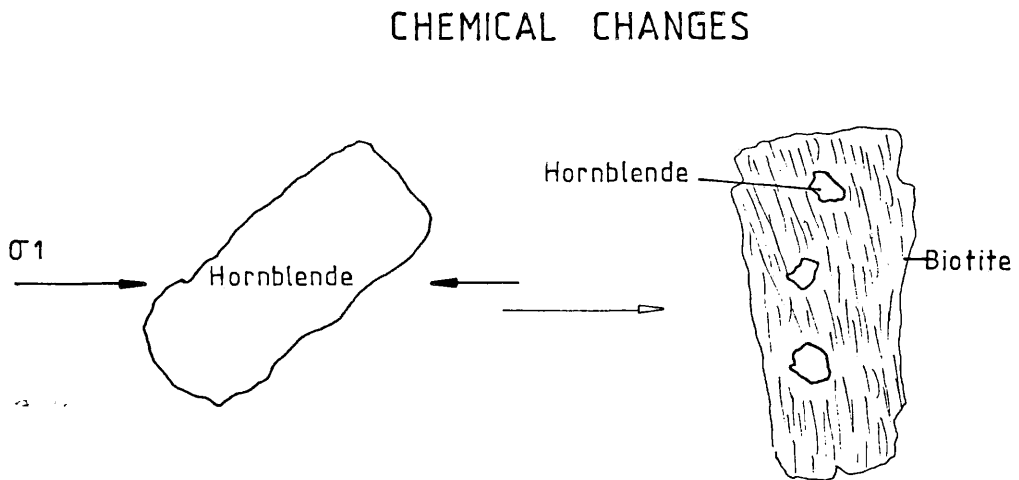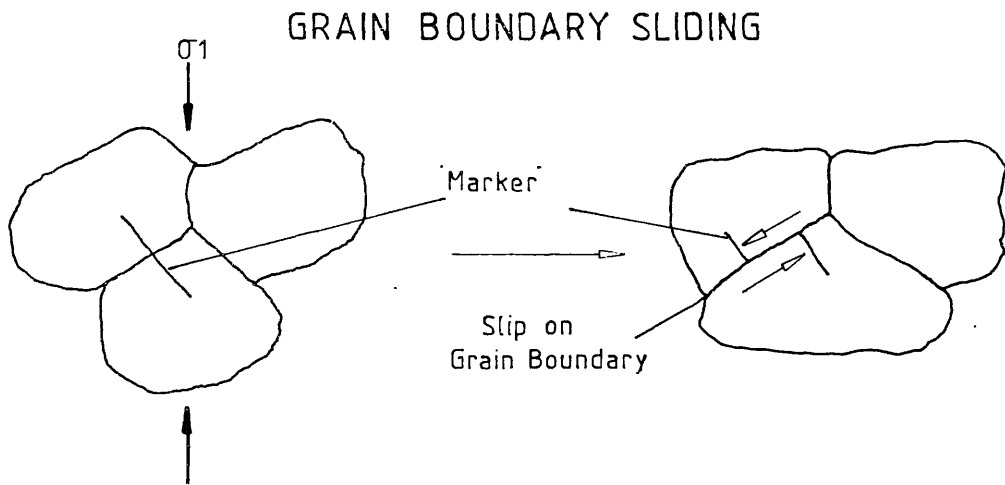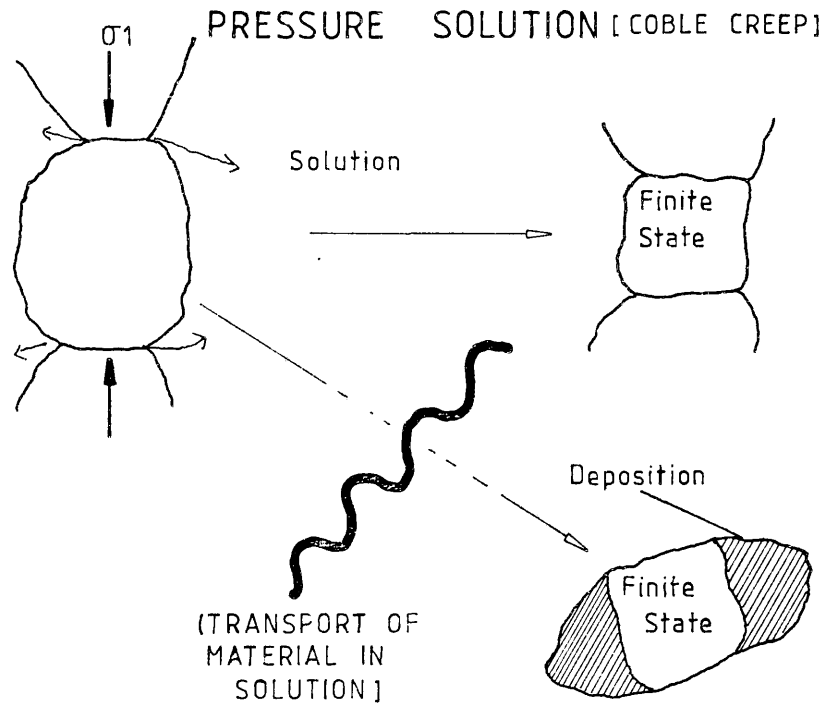
therefore fundamental in determining crystal size, shape and stability.

The surface energy properties of solids are discussed by Spry (1969) using analogies with liquids; the situation for solids is, however, more complex. There is a high state of order imposed in solid packing, bonds are of the strong ionic type rather than Van der Waals forces and this imposes symmetry and shape on the surfaces, increasing surface area above the theoretical ideal. Furthermore all non-cubic crystals are anisotropic; this anisotropy is reflected in the energies obtaining at the crystal faces. Faces with high energies are the smallest and straightest. In poly-crystalline rocks these considerations are of fundamental importance, as they determine which of two adjacent mineral phases will grow if both are stable and crystallising. The presence of defects in or near the grain boundary, because of the ionic nature of most minerals, will have significant effects on the surface energy.

The likely effects of grain boundary parameters on mylonites can therefore be summarised:

(1) Surface molecules are at a higher energy level than enclosed molecules; the surface of the mineral will therefore be the site of all chemical reactions.

(2) Similarly, unless this energy is partially satisfied by adjacent crystals (e.g. symplectite formation) or adsorbed material (e.g. pore fluid), any means by which the surface area may be reduced will be favoured. This can be achieved in two ways:

(a) Surfaces that are crenulate can become planar

(b) The volume of the mineral may be increased (grain growth).

4.2.1   Thermodynamics

It has been stated (2 above), that surface energies tend to minimise.
These energies, however, form only one component of the total energy
state of rock, the Gibbs Energy (G).

(G) complies with thermodynamic laws and tends always to a minimum
possible value.   A rock, then, should represent the minimum energy state
possible for matter in the conditions under which it was formed.   Should
the conditions change with time, then so will the state of the matter in
order to maintain the minimum possible (G),which we will call (Gm).   The
change in the state of matter, whilst obeying the equilibria laws will,
because matter does not behave as a continuous medium, go in a series of
steps.   (Gm) will therefore have stepped values too, while (G) will be
able to assume all intermediate positions because it is not directly
dependent on matter but also on other variables (Powell,1978).

We can, therefore, examine what happens to (G) as one of its component
variables changes.   The values of (Gm) as determined by the matter in the
rock can be mapped on the trace of the variation in (G).   For example,
let us consider the effect of varying the thermal energy of a system.
In the first instance there will be an addition of energy and in the second
a subtraction.   For simplicity this system can be represented as in
figure 137, a plot of (G) against time.

With the addition of thermal energy, two possible states of matter
can exist, phases A and B.   It can be seen, however, that the new (Gm) (Gm*)
for these phases is not reached by a direct route.   Rather (G) builds up
to a maximum then falls to the new equilibrium position.   Then, as more
heat is added and all the matter has swapped to its new state, it continues
to climb.   There are two reasons for this.   One, a small part, is caused
because the rate of supply of thermal energy exceeds the rate at which

Fig 137.

GENERAL PLOT OF GIBBS FREE ENERGY / TIME FOR A SIMPLE ROCK UNDERGOING METAMORPHISM

[PROGRADE METAMORPHISM]

Activation Energy

A State

B State

Original State

Point at which Thermal Energy began to be added to the system.

GIBBS FREE ENERGY OF THE SYSTEM [G]

TIME
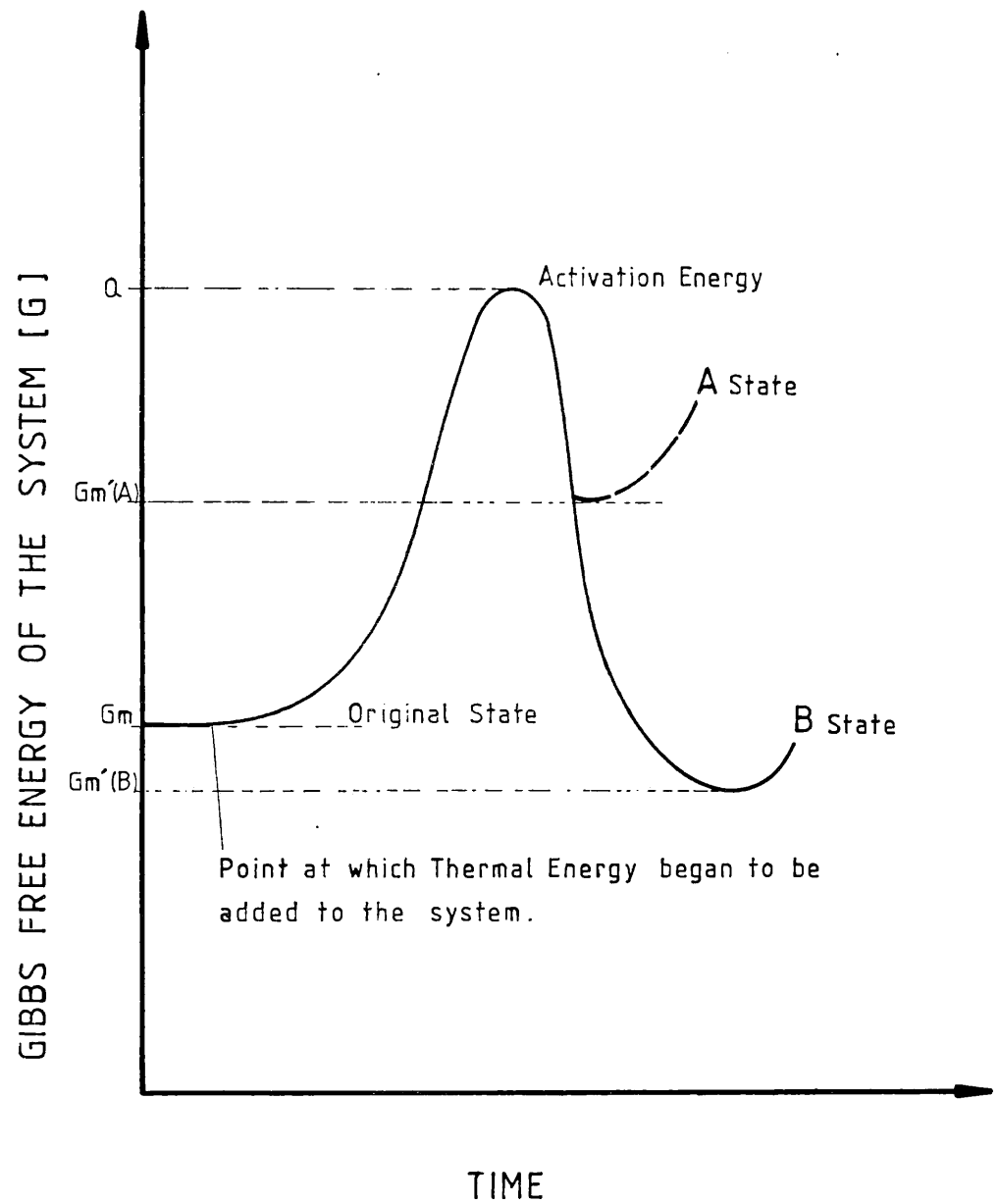
the matter can react to absorb it by shifting the equilibrium. At some
point though the excess energy speeds up the reaction, causing the graph
to dip rather than level out (a $10^{\circ}C$ increase doubles the rate of a
chemical reaction). The second part, and the more important, is caused
by the fact that before a shift in the state of matter is possible, the
original state has to be destroyed; this takes energy. The peak in the
graph, therefore, represents the activation energy (Q) required to do this.

The well-known Arrhenius equation expresses this and, in fact, is an
expansion of the (D) term in Frick's laws (2) (3).

$$D = Kr = A^{-Q/RT}$$

where:

D = the diffusion coefficient

Kr = the rate constant

A = the pre-exponential constant (the vibration of matter
because of its temperature)

R = the gas constant

T = temp. in $^{\circ}F$

Q = the activation energy.   .

The term (Q) can be subdivided Q = W + E, where (E) = enthalpy to form a
defect, and (W) = enthalpy to move a defect.

To explain his equation, Arrhenius suggested that in every system
an equilibrium existed between "normal" and "activated" molecules, and that
only the latter could take part in chemical reactions. Heat, he suggested,
increased the number of "activated" molecules, and therefore the rate at
which the reaction progressed. Point (B) would be the equilibrium position
selected by this system because the (Gm) value is less than for (A). The
attainment of the equilibrium position may involve an endothermic or
exothermic reaction; in a situation of prograde thermal variation the
former would be favoured.

Figure 138 shows the situation that develops when thermal energy is removed from the system. Here (G) never reaches the value (Q), so the rate at which the state of matter A or B is attained is infinitely slow. On a temperature basis alone then, retrogressive reactions in geological situations should be impossible. To some extent this is true; if conditions seen in figure 138 did not hold, then at the surface only minerals in equilibrium with surface pressure and temperature conditions would be found.

The fact that we do see retrogression reactions in geology means that the Arrhenius equation as first envisaged is only a partial solution to the attainment of equilibria. This is because there are terms other than temperature to be taken into consideration. Still accepting that molecules need to be "activated" in order that the reaction proceed at a reasonable rate, the most important variable other than temperature is the state of strain. It is possible mechanically to push a molecule from "non-activated" to "activated" condition.

Let us examine the system as shown in figure 139. Here the thermal variation is the same as that for figure 138, but the energy is applied to the system in the form of mechanical stress. (We see immediately that the value of (Q) remains the same, thus the term in the Arrhenius equation that changes or incorporates the stress function is (A).) Now the matter is given the requisite energy, the new state B is achieved and the rock will record the fact that (G) has passed that (Gm) value at some point in time. (Note: the rarer (Gm) states are likely to be utilised in these conditions.) A good example of just such a situation is that of the classical (Ramsay & Graham,1970) shear zone, where the phases present inside and outside the zone show different (Gm) values, simply because of the strain in the zone of shear. This sort of metamorphism is therefore stress dependent. It should not be confused with retrogression resulting

Fig 138.

GENERAL PLOT OF GIBBS FREE ENERGY / TIME FOR

A SIMPLE ROCK UNDERGOING METAMORPHISM

[RETROGRADE METAMORPHISM]

Q - - - - - - - - - - - Activation Energy

Gm˙(A) - - - - - - - - - - - A

Gm - - - Original State

Gm˙(B) - - - - - - - - B

Point at which
to be subtracted

Thermal Energy began
from the system

GIBBS FREE ENERGY OF THE SYSTEM [G]
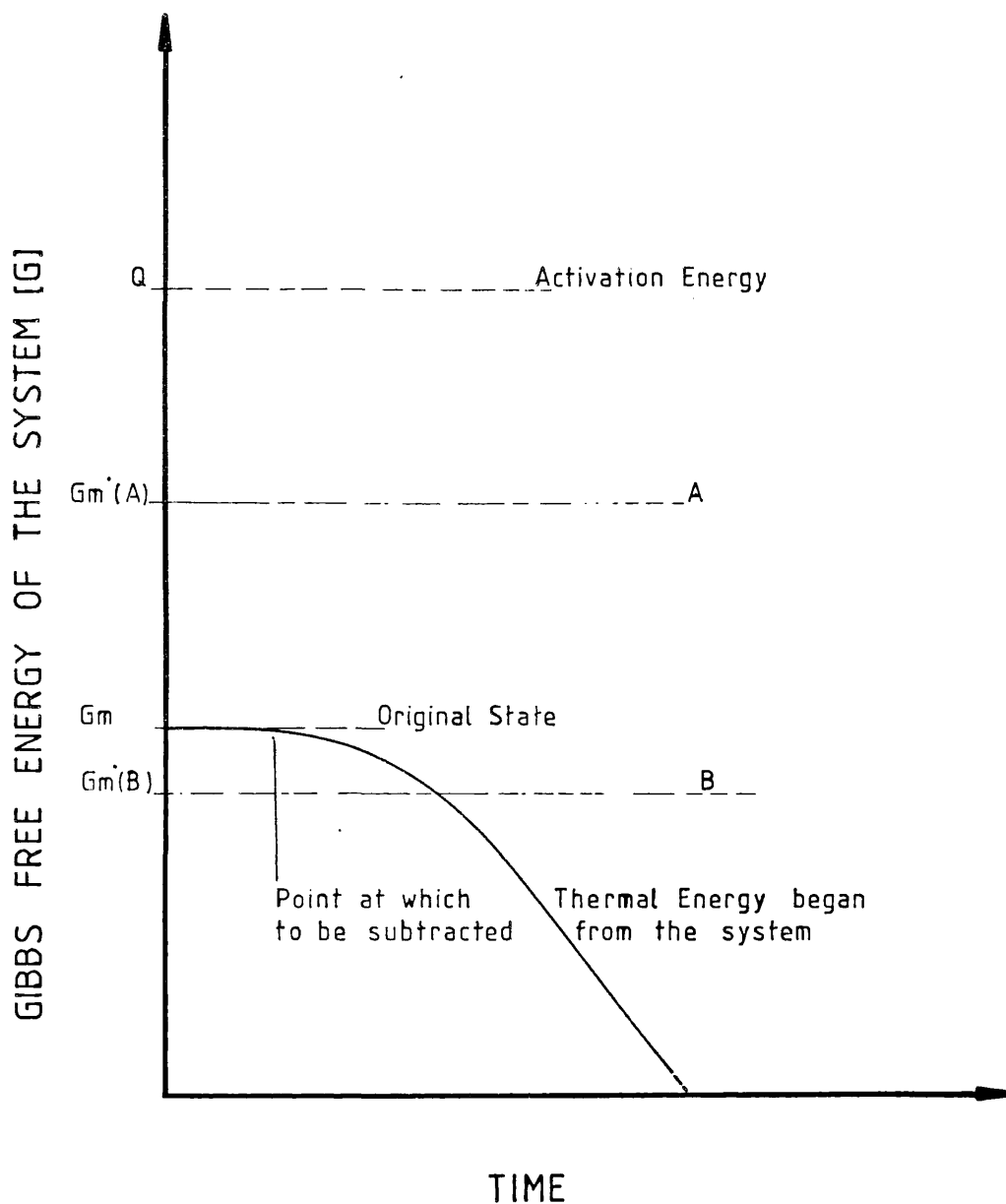
TIME

Fig 139.

GENERAL PLOT OF GIBBS FREE ENERGY / TIME FOR

A SIMPLE ROCK UNDERGOING METAMORPHISM

[DEFORMATION ACCOMPANYING THERMAL RETROGRESSION]
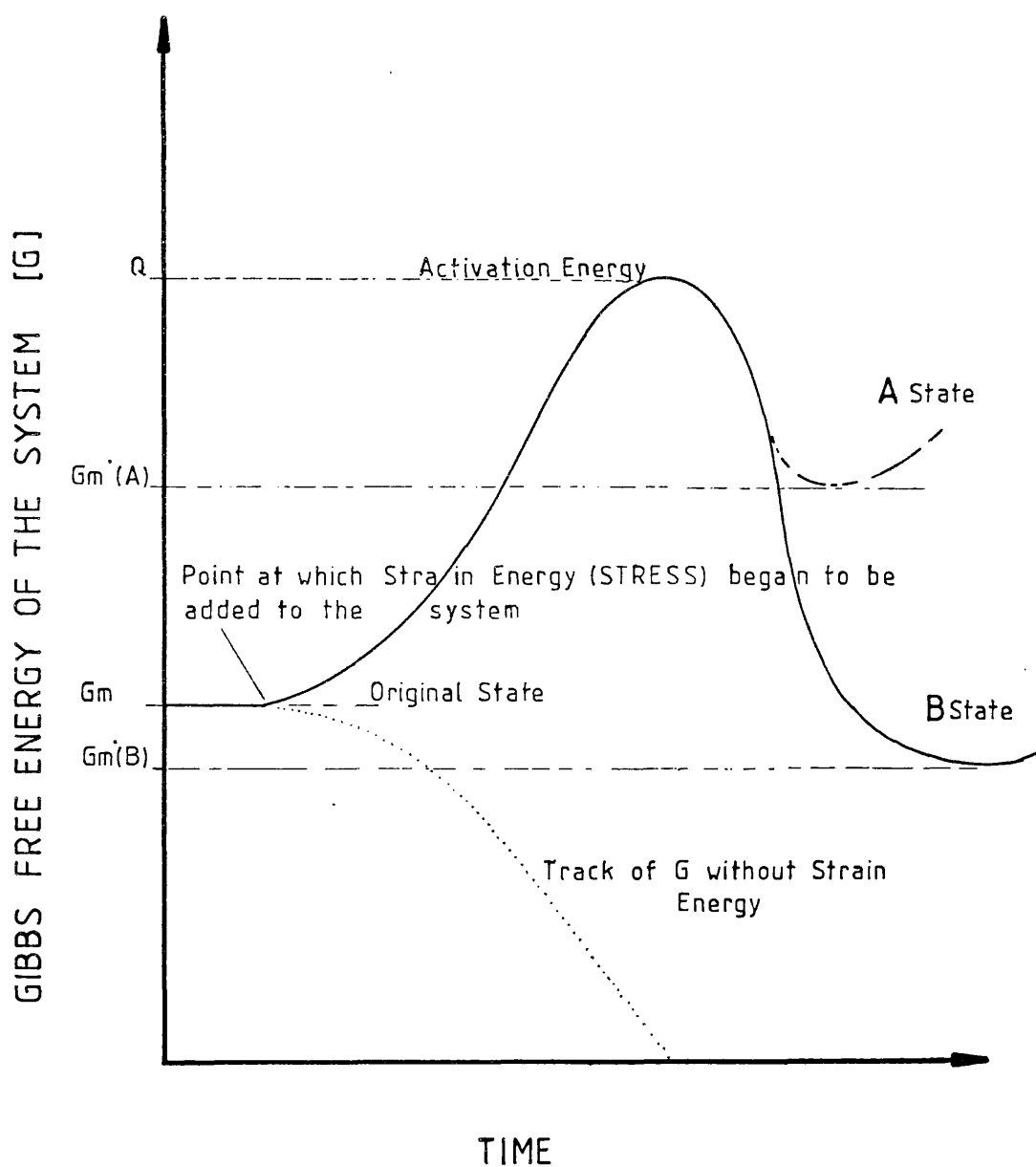
from subsequent prograde (thermal) phases, which do not progress to the level of those previously seen in the rock.

Confining the arguments to the situation where a mineral recrystallises in situ or at a site remote in the rock, a further understanding of the effects of strain is possible. The generalised plot for such a situation is seen in figure 140(a). It is clear from this, that no matter what the mechanism, (Q) for the mineral will remain constant, and that in this situation of recrystallisation chemical energies need not be considered.

Figure 140(b) shows the individual components of the system where the rock is stressed. For a fixed thermal value it is possible to increase (G) by the input of mechanical energy. If the product of the two exceeds (Q) for the mineral it will recrystallise PROVIDED the ambient thermal energy exceeds a critical value. This value is unique to every mineral species. Thus in a polymineralic rock some minerals will recrystallise while others will persist in the strained condition if the rock is subject to constant strain input at a fixed temperature. (The potash feldspar in the Osterøy mylonites is a good example of a recrystallising mineral while sphene remains deformed.) If, therefore, we know the absolute value of (Q) for a given mineral and the limits of its thermal environment, then, by examining the state of recrystallisation, estimates as to the strain rate should ultimately be obtainable.

The Critical Thermal Value

It is possible to attain (Q) virtually entirely by stress. In this case the return to the ground state will occur, but only over a long period. The gradient of the graph from (Q) to (Gm*) is therefore temperature dependent. Below a certain critical temperature (Tm), which varies from mineral to mineral, the rate of return to the ground state is infinitely slow.

Fig 140. 276

GENERAL PLOT OF GIBBS FREE ENERGY / TIME FOR A
MINERAL UNDERGOING RECRYSTALLISATION

(a)

Recrystallisation of the same
phase of a mineral

G

Q

Gm

TIME

(b)

G

Q

Strain
Energy portion
of G

Gt

Thermal level remains
constant

Thermal
portion of
G

Gm

TIME
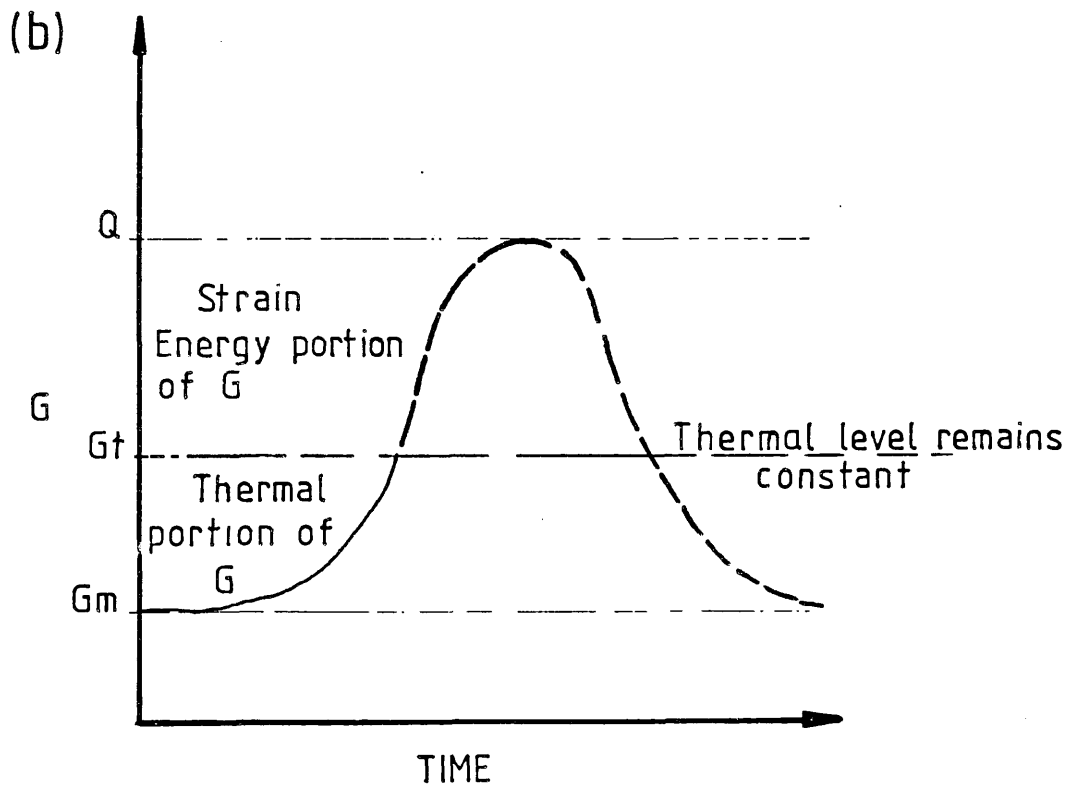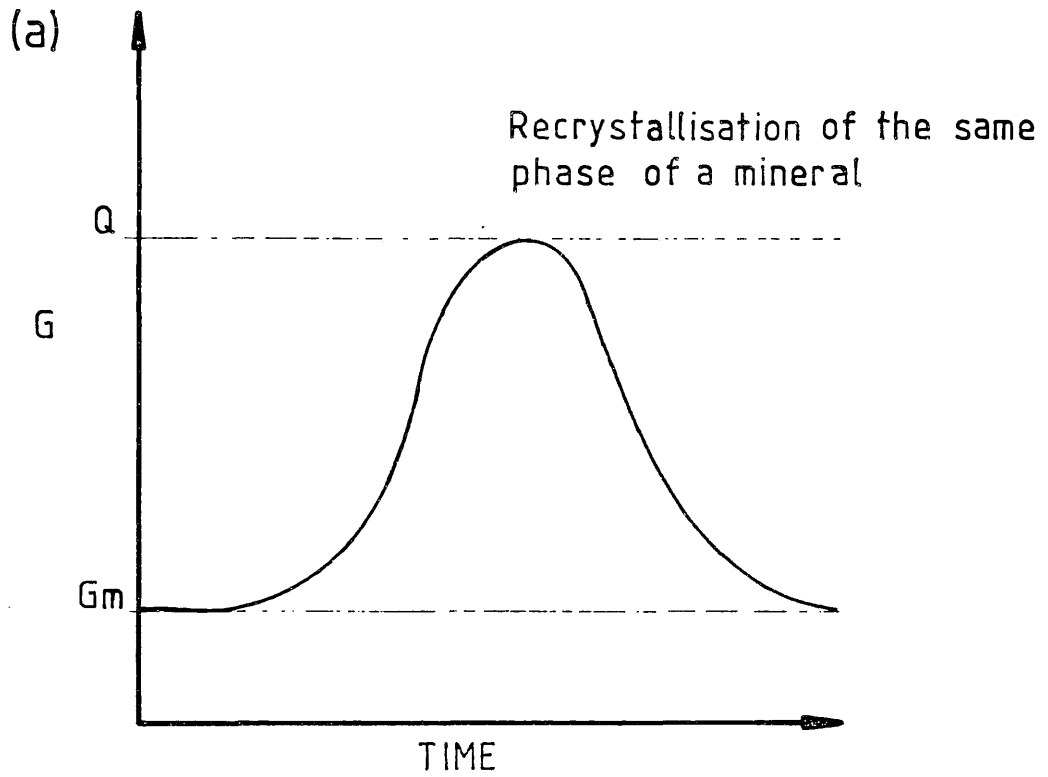
This means there is a threshold limit to the (T) term in the Arrhenius equation for single phase recrystallisation when strain alone is responsible for producing the "activated" state. Figure 141(a) shows the progress of the system when above (Tm). Figure 141(b) shows it when below (Tm).

It is therefore possible to define three new critical thermal positions:

(Tm) The "Mechanical" activation temperature, the point at which the entropy barrier caused by the rigidity of the crystal is overcome.

(Ti) The "Initiation" activation temperature, the point at which one or more of the phases present dissociate and recombine to produce one or more new phases. (Ti) is applied to the new phase.

(Tt) The "Termination" activation temperature, the point at which a mineral phase ceases to be stable and dissociates. ((Tt) of one mineral is therefore (Ti) of another.) There are two such points for each mineral, where $(Tt) < (Tm) < (Ti) < (Tt)$. This is because, as has been demonstrated, before a mineral can be "destroyed" (Q) must be reached. In the prograde situation this is achieved dominantly by thermal energy, in the retro-gressive by mechanical energy. In each case the new mineral formed is different, reflecting the nature of the metamorphism. (Pressure, too, is a relatively minor consideration here.)

From the observations made on the rocks of the Southern Gneiss Unit, which show a retrogressive metamorphism, it is possible to rank minerals on the basis of their order of "closure" (Tt) on the thermal decline:

(1)	Kyanite	(6)	Biotite
(2)	Garnet	(7)	Sodic feldspar
(3)	Hornblende	(8)	Chlorite
(4)	Actinolite	(9)	Potassic feldspar
(5)	Epidote	(10)	Quartz

In general minerals with a broad separation of their two (Tt)s, i.e. stable over a wide range of P T conditions, AND with a low (Tm) are likely to

Fig 141.

GENERAL PLOTS OF GIBBS FREE ENERGY / TIME FOR A STRAINED CRYSTAL IN TWO CONTRASTING THERMAL ENVIRONMENTS

(a)

Effect of Stress on a system where strain is the only increasing variable,& the system is above Tm.

G

Q
Gt
Tm
Gm

TIME

(b)

Strain Energy [Stress] stops being applied

Q

Effect of Stress on a system where strain is the only increasing variable & the system is below Tm.

Tm

G

Gm

Tm = Critical value for the Thermal component of G,[Gt] if recrystallisation is to proceed at a reasonable rate.

Gt

TIME

form the largest crystals in metamorphic terrains with a high tectonic component.

If the same minerals are now examined as to the degree of idiomorphy, then it is possible to rank them in order of decreasing idiomorphic tendency:

(1) Rutile, sphene, magnetite
(2) Tourmaline, kyanite, garnet
(3) Epidote
(4) Amphiboles
(5) Micas, chlorite
(6) Calcite
(7) Plagioclase, quartz
(8) Orthoclase, microcline.

This table, therefore, is a reflection of the energies developed at the grain boundaries as described above. (Note: all minerals will eventually develop the euhedral form given enough time above (Tt) and (Tm).)

It is also possible to observe how minerals of a given size resist stresses tending to reduce their size. They resist in two ways:
(1) Directly: here the crystal structure has high energy bonds, poor cleavage, dense packing in the lattice and high symmetry (e.g. garnet), making the crystal difficult to deform as compared to its neighbours.
(2) Passively: minerals can maintain their size and coherence by virtue of having a low (Tm). Stressing minerals below their (Tm) causes subgrain formation. Above (Tm), however, they anneal fast enough to maintain coherence, and in some cases maintain their original shape (e.g. potash feldspar).

At any one temperature the rate of grain growth decays with time as the surface area volume ratio increases. This means that for one strain rate there is an equilibrium grain size for every mineral. Two lists can be constructed grouping the same minerals in descending order of their ability to resist stress. The first deals with minerals that resist stress directly, the second with those which resist passively:

<div align="center">(1)   (2)</div>

```
. . . . . . . . . . . . . . . . . .(1)  Potash feldspar
 (9)  Garnet . . . . . . . . . . . . . . . . . . . . .
(10)  Sphene . . . . . . . . . . . . . . . . . . . . .
 (8)  Amphibole  . . . . . . . . . . . . . . . . . . .
. . . . . . . . . . . . . . . . . .(2)  Soda feldspar
. . . . . . . . . . . . . . . . . .(3)  Quartz
 (7)  Kyanite  . . . . . . . . . . . . . . . . . . . .
. . . . . . . . . . . . . . . . . .(4)  Muscovite
. . . . . . . . . . . . . . . . . .(5)  Biotite
. . . . . . . . . . . . . . . . . .(6)  Chlorite
```

(The numerics rank them in order of ease of annealing.)

In general, high bond strength and good symmetry etc. will tend to prolong the life of a crystal as a clast less well than the annealing mechanism when strains become extreme.   It is therefore the potash feldspar which forms the characteristic porphyroclasts in mylonites.

4.2.2   Processes in the Osterøy Mylonites

Crystallographic Orientation Fabrics

Crystallographic orientation fabrics are frequently described from mylonites.   The Osterøy mylonites are no exception.   The presence, strength and orientation of the fabric is dependent on, and relatable to, the dominant processes acting during the bulk deformation of the rock. Often these fabrics are accompanied by a strong shape fabric, visible on the mesoscopic and macroscopic scale.   The development of these fabrics is schematically represented in figure 142;   the likely process of formation and accompanying structure are tabulated in figure 143.   As can be seen the simplest and commonest path is a straightforward rotation and growth of inequidimensional grains into the X/Y plane of the strain ellipsoid; frequently the longest axis becomes aligned parallel to X (Spry,1969).

It is the crystallographic alignment of equidimensional minerals relative to macroscopic features that presents problems.   These alignments are not necessarily always in the X/Y plane, but may form an orthorhombic

Fig 142.

SCHEMATIC REPRESENTATION OF PATHWAYS BY WHICH

CRYSTALLOGRAPHIC FABRICS MAY DEVELOP

1) MECHANICAL ROTATION OF INEQUIDIMENSIONAL CRYSTALS
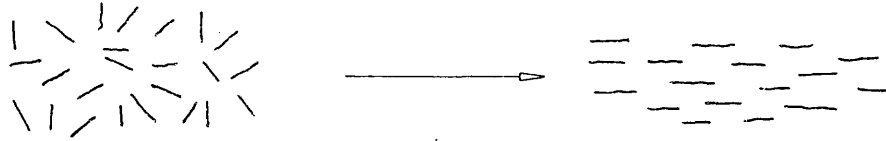
2) INTERNAL PLASTIC DEFORMATION OF EACH CRYSTAL
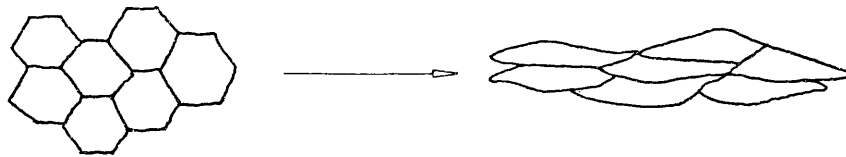
3) SLIDING OF CRYSTALS & SUBGRAINS WITH LITTLE INTERNAL DEFORMATION
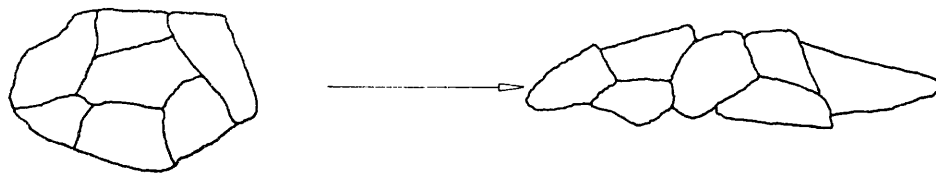
4) SOLUTION AND GROWTH OF CERTAIN GRAIN ORIENTATIONS
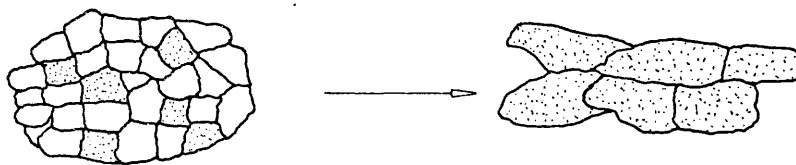
5) GROWTH OF PREFERENTIALLY ORIENTATED GRAINS DURING METAMORPHISM
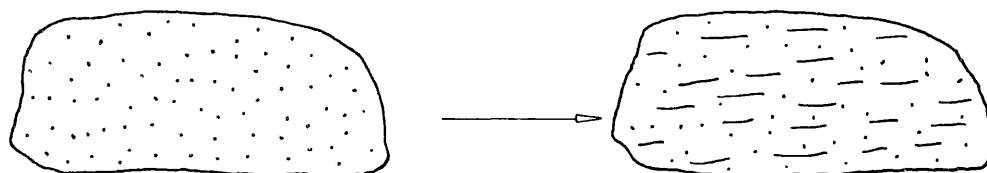
6) ENLARGEMENT & RECRYSTALLIZATION UNDER STRESS
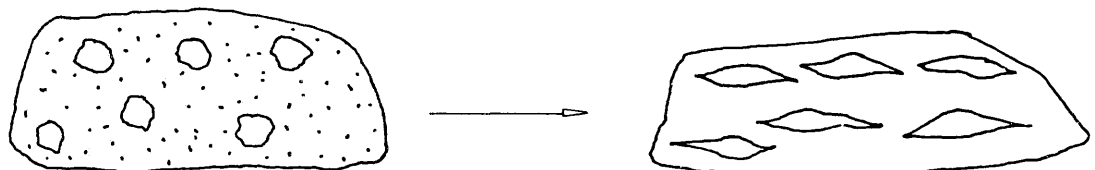
Fig 143.

TABLE OF LIKELY DEFORMATION MECHANISMS INVOLVED IN
THE PATHWAYS OF FIGURE 142 AND THE NATURE OF THE
FABRICS PRODUCED

Mechanism(s)	Fabric
1) Grain Boundary Sliding(+other processes)	Good Shape Fabric Poor Crystallographic Fabric.

2) Glide & Creep + GrainBoundary Sliding
      or Nabbro Herring Creep
      or Coble Creep
	Very Good Crystallographic Fabric
	if Glide &Creep were the Mechanisms
	but NOT if G.B.S. is important too.
	OTHERWISE,a Good Shape Fabric,

3) Grain Boundary Sliding (G.B.S.)	Only a weak Mesoscopic Shape Fabric.
4) Pressure Solution Coble Creep [+GBS][+Glide &Creep]	Good Shape Fabric & a weak to moderate Crystallographic Fabric depending on the amount of G.B.S. which may have occurred too.
5)Chemical Changes	Good Shape Fabric & ,with respect to the new mineral, probably a moderate Crystallographic Fabric.
6) Glide&Creep +Coble processes +Grain Boundary Sliding	Very Good Shape Fabric & possibly a very weak Crystallographic Fabric.

monoclinic or triclinic symmetry about one strain axis. Current theories explaining these fabrics are based on the work by March (1932) and sub-sequently Means and Patterson (1966). The process is essentially one of slip on suitably orientated planes of weakness in the lattices, causing rotation of the lattice without bodily rotation of the crystal. The process therefore is only possible when the rock is deforming dominantly in the area of the Deformation Map where climb and glide are the dominant processes.

The only other field of the Deformation Map where crystallographic orientation fabrics are likely to form, is that of pressure solution. It has been demonstrated above that anisotropic mineral grains have faces with varying surface energies. Following the principles described, crystals in the process of dissolving, nucleating and growing, which tend to be orientated so that the faces with the lowest energies will be normal to the maximum principal stress axis, are favoured. Crystals not so orientated will either dissolve faster or grow slower; the bulk of the crystals will therefore show a preferred alignment.

The Osterøy mylonites are different,as has been shown, in that only certain rock types have crystallographic orientation fabrics and as the only difference between the specimens is their mineralogy, it must be this that is responsible for their differing fabrics.

These observations shed light on the nature of the deformation of the mylonites. It is clear that processes other than those here described do not produce fabrics because the deformation paths for the rest are independent of crystal structure. Rock type, too, has an effect on fabric production, the homogeneity of monomineralic rocks regularises and restricts the deformation process, enhancing the fabric.

Thus fabrics form:

(a)   In conditions when glide, climb, pressure solution, coble creep and
crystallisation (twinning too to a certain extent), are the dominant
deformational processes, i.e. no other process acting in conjunction must
have proceeded at a rate which would negate or reverse the tendency towards
fabric development.

(b)   When the rock is composed of very few mineral species.

They do not form:

(a)   When grain boundary sliding is a process of deformation.

(b)   During deformations in which there have been rapid changes in the
grain size of some grains, the local volume adjustment causes rotations of
neighbouring minerals.

(c)   Where cataclasis or disaggregation of subgrains occurs, as the fragments
tend to rotate.

(d)   If recrystallisation, nucleation, or solution processes have proceeded
at a rate fast enough to overcome surface energy anisotropies.

(e)   If the stress field is short lived or rotating.

(f)   If the rock is polymineralic in composition because each mineral is
likely to deform by a different process.   (Even if these processes acting
alone would produce fabrics, they negate each other acting together.)

Polymineralic rocks are mechanically heterogeneous at the microscopic
level; they are therefore unlikely to fulfil any conditions except those
preventing fabric formation.

Thus in the quartzites on Osterøy, the deformational processes are
clearly defined (solution, climb and glide).   In the granite gneisses,
the processes are also clearly defined (grain boundary sliding; the result
of mechanical anisotropies, enhanced by volume change effects as the
mineralogy responded to the metamorphism).

These two rocks tell us that all processes (except perhaps nabbro herring creep) were operative simultaneously in the Osterøy gneisses during mylonitisation.

Changes in Bulk Chemistry

There is little published work on the geochemical changes accompanying mylonite genesis. Field evidence from known mylonite examples (e.g. the Moine thrust) clearly shows that as a rule, the rock product of intense mylonitisation is greatly enriched in quartz as compared to the parent rock. On a smaller scale there is evidence for the local chemical mobility in the production of the characteristic banding (Sclar,1965), though there are some who believe this is a deformational feature (Myres,1977; Vernon,1974). These observations may imply that there is some chemical mobility during mylonite production, on both the local and the "open system" scale. Work on shear zones by Beach (1976), where it was found that sodium and potassium were extremely mobile, supports this view. Beach also found that the shear zones were enriched in water, but he found no evidence for silica enrichment or depletion.

The pilot Enrichment/Depletion plots of the Osterøy augen gneiss however, proves mylonitisation of these gneisses was probably chemically an "open system" process, at least with respect to the size of the outcrops sampled. The deformation was accompanied by loss of mafics or femics, aluminium and sodium from the rocks. This proves that there were volume changes during mylonitisation and that surface active processes were operative.

Processes responsible for Mineral Textures

An understanding of the processes operative during the formation of the Osterøy mylonites is only possible after relating the textures observed to theoretical considerations and the deformation map. This should provide

information as to the significance of the mylonites as a unit in the context of their environment of formation.

Textures produced by Chemical Processes

This group of textures is the result of metamorphic changes, i.e. (Ti) and (Tt) effects. The changes often require mobility of ions in the rock for the reactions to progress. These ions are best transferred in solution; coble creep and pressure solution must therefore have been active during these changes. It is also reasonable to postulate that grain boundary sliding and mineral rotation would occur in the rock in response to local volume changes.

Rim Symplectites (Myrmekite)

Much is written as to the causes of this texture (Phillips,1974). In the Osterøy mylonites the structure is a product of the retrogression, and is chemically induced, because it works from the outside inwards. The reaction is not a solid/solid process as the texture forms regardless of the adjacent mineral species. This means the instability is the product of an external vector. An intergranular fluid must therefore be present, indicating that coble creep and pressure solution were active. The morphology of the texture indicates that at the time of formation the surface energies of quartz and sodic plagioclase were complementary. (The intergrowth as seen in these rocks is not actually worms but sinuous branching sheets of quartz in the plagioclase. This can be seen because no matter what the section through the intergrowth, it never shows a circular section.)

Solution features

Pressure solution is almost entirely responsible for these; the solution occurs at the points of highest stress. The process, while common, is difficult to detect except in the case where a marker is present,

287.

as in plate 55. There must always be grain boundary sliding accompanying
this process to accommodate the volume loss.

Relic structures

These are the product of metasomatic metamorphic reactions;
chemicals therefore need to be mobile through the body of the rock. The
transport of ions to and from the waxing and waning crystals must be via
an intergranular fluid; solid state ionic diffusion cannot alone explain
the texture. With the presence of an active intergranular fluid it is
reasonable to assume pressure solution is occurring elsewhere in the rock.
The feature, which characteristically shows little marked stress orienta-
tion, also indicates there could have been little grain boundary sliding
during formation. Indeed the local stress field during formation must
have been virtually isotropic; the feature therefore is the product of
a pause in tectonic development.

Clearing and Granoblastic texture

These are the product of annealing processes on strained rock.
Granoblastic texture represents the most stable configuration for the
minerals composing the rock. Internally each crystal approaches the
strain-free state (clearing) and develops equilibrium configurations with
its neighbours.

Given specific P T conditions each mineral present will attain a
constant size and shape according to the dictates of surface energy and
(Ti), (Tt) factors, provided no two minerals of the same species share a
common boundary. The absolute value of this grain size is dictated by the
extent to which the minerals have been ground in the first instance. Once
all the grains of one mineral in a rock are of equal size, the surface
energy ceases to be an important factor. A granoblastic texture can
therefore develop and be stable at all possible grain sizes. This means

that once a finer grained rock is generated from a coarse grained rock,
in the absence of subsequent P T and tectonic changes, it is difficult
to re-establish the original grain size.   The fine grained state is an
equilibrium condition; it can therefore develop during deformation and is
not only a post-deformational texture.

The processes operating are therefore two-fold:
Those acting at grain boundaries to relieve fossil stresses; grain and sub-
grain boundary migration, coble creep, solution, crystallisation (pressure
solution) and a little grain boundary sliding.

Those acting through the body of the mineral allowing re-ordering of the
lattice; glide and creep.

Crenulate Boundaries

These are seen in rocks with an essentially monomineralic composi-
tion.   They are features very like those seen in granoblastic texture, but
here two minerals of the same species share common boundaries.   The
ultimate grain size is therefore a function of time and temperature.   The
irregularity of the boundaries reflects the relative energies developed
at faces disposed at varying angles; the constant enlargement of the grains
results in   jigsaw-like junctions.

Processes operating in the formation of this structure are dislocation
glide and creep causing grain and subgrain boundary migrations.   The
process is driven by surface energy forces, thus the structure may form
during deformation or recovery.

Snowball Garnets

These are important structures, the mineral is obviously stable
in high strain rate conditions.   The growth pattern (Powell & MacQueen,1976)
indicates that they nucleate and grow during deformation.   This requires
there to be a mobility of chemicals, and points to a fluid phase present
during deformation.

The processes likely to be operating, as indicated by the structures preserved in this mineral are: grain boundary sliding, coble creep and pressure solution. As the mineral maintains coherence during rotation glide and creep must have been operative too.

Poikiloblastic Texture

The reason for the existence of inclusions in the body of a developing crystal is basically a surface energy phenomenon. The presence of the inclusions cannot unduly increase the surface energy equilibrium of the crystal. The inclusion must then satisfy the free bonds at the boundary between the two grains (a phenomenon akin to the "wetting" properties of liquids). The species of the inclusion, therefore, provide an insight into the properties of the including mineral. The usual inclusion in the Osterøy mylonites is quartz, though graphite can also be an inclusion in garnet.

Amoeboid Growth

This growth form is the result of regrowth of a crystal that has been mechanically dispersed into the matrix during deformation. On recrystallisation, the centre of nucleation approximates to the central portion of the original crystal, and moves out from this joining up the scattered pieces. Thus portions now separated by screens of matrix material produce pseudopodia-like extensions from the centre of nucleation. It is clear that these pseudopodia are the product of the migration of chemicals either in solution or by solid state diffusion around grain boundaries. Coble creep and pressure solution are therefore indicated, though the texture is mainly a chemical (Ti) product.

Porphyroblasts

These structures post-date the fabric of the rock in which they grow. In polymetamorphic terrains this relationship may be masked by

subsequent deformations. There are situations where the growth is syn-tectonic, whereupon the crystal displays both clastic and blastic features simultaneously. The processes are in the first instance nucleation of the mineral at a new site in the rock, a (Ti) effect requiring the presence of a fluid medium (coble creep and pressure solution could there-fore have been active). In the second instance, where the deformation continued during blastesis, glide, creep and grain boundary sliding must also be operative. The feldspar porphyroblasts/clasts in the Osterøy mylonites are of this second type. This means textural patterns developed at the margins of these structures (Sinha Roy,1977 a ; Ferguson & Harte, 1975) must be treated with extreme caution because they do not represent relics of the original rock.

Embayments

These features are produced in a manner similar to relic structures, a purely chemical process requiring transport of ions. Coble creep is therefore operative and if there is a significant fluid phase, pressure solution takes over.

Rims and Crystallisation

These are metamorphic features; the mobility of ions required in their formation indicates there was a fluid phase present. Pressure solution and coble creep were therefore active, as was grain boundary sliding.

Recrystallisation

This term covers all processes by which a mineral regains its original structure. The processes involved are: dislocation glide and creep; these are responsible for re-ordering the lattice and enlargement of the crystal by annexation of neighbouring grains. Coble creep and pressure solution; the mechanisms by which material is obtained from

non-adjacent grains. Implicit in any superplastic model explaining mylonites is that clearing and recrystallisation (annealing) operate during deformation, and not just in the post-tectonic period.

There is considerable controversy about the role of recrystallisation in the development of mylonitic banding (Vernon,1974; Myers,1978; Sclar, 1965). From the Osterøy mylonites it is clear that the banding results from shearing of once restricted pockets of mafic material into long streaks parallel to the foliation. The banding is then enhanced by migration of leucosome from areas rich in mafic fragments to the less mafic regions; selvedges develop. The scale of migration implied by the banding seen in the mylonites indicates the importance of the recrystallisation processes.

The movement of material from the mafic-rich regions happens because the energy for a mafic/leucocratic mineral grain boundary is less than that for a leucocratic/leucocratic mineral boundary. Rocks banded on the mesoscopic scale cannot then obey the granoblastic rule, the surface energies never equilibriate locally. It is by this process, too, that quartz ribbons form.

From these observations it is apparent that chemical effects, phase changes, metamorphic assembly changes (Ti/Tt effects) and the chemical transport component of recrystallisation, are extremely important when accommodating deformation. This view is supported by the recent work of White and Knipe (1978).

Mechanically formed Textures

Textures in this group are the product mainly of processes acting within the body of crystals. The tendency, contrary to most of the chemical processes, is always towards a diminution of grain size. Except at very high strain rates and pore fluid pressures, the grain size reduction

and shape change is achieved without the grain losing internal coherence. There is usually a substantial amount of grain boundary sliding and coble creep accompanying these shape changes. These processes continue after the internal processes stop.

Cataclasis

This is one of the high strain rate products; the grains lose internal coherence. Dislocations are generated in the lattice at a rate faster than glide and creep can dissipate them. The whole process of dislocation motion becomes more difficult as the dislocations get "tangled up"; this is work hardening. If stressing continues, brittle fracture occurs and the lattice fragments. These fragments are then strung out into the plane of the foliation; this is done by grain boundary sliding. There is another method for producing cataclasis in a rock, namely by high pore fluid pressures. The process is slightly different; the crystal is not work hardened before rupture, rather local pressure differences within and between crystals are responsible. These develop in areas where pore fluids escape from the rock; the rock and crystals are literally exploded apart. In the Osterøy mylonites, cataclasis of this last variety only occurs at a late stage in the tectonic history and produces the D8 mylonites. At this time the migratory fluids were rich in quartz, epidote and calcite, thus by inference pressure solution must also have been active somewhere in the rock.

Reduction of grain size by these methods is not a steady state process; cataclasis therefore has no place on the deformation map.

Undulose extinction

As dislocations build up in a lattice, distortions occur. Viewed optically these are seen as variations in extinction position in the crystal. The processes, therefore, are: defect formation and then migration by dislocation glide and creep.

Subgrains

Following on from undulose extinction, dislocation glide and creep carry defects through the lattice. In some areas bottlenecks occur; these define sub-areas in the original crystal. The subgrain boundaries, sites of high disorder, facilitate dislocation migration. Coble creep is therefore active in these regions. This process of grain size reduction differs from cataclasis, as a steady state is achieved. The diameter of the subgrains decreases (numbers of them increase) to a point where coble creep round the boundaries can dissipate the stress without initiation of new dislocations within the crystal.

Quartz Lamellae

These are subgrains and bands of undulose extinction that form in quartz. There is a definite alignment relative to the causative stress field. The processes involved are identical to those for undulose extinction and subgrain formation.

Augen and Porphyroclasts

In the Osterøy mylonites these can be divided into three types:

(1) Those which are seen to be unaffected by the stresses which have affected the matrix.

(2) Those in which the outer margin of the clast is strained like the matrix.

(3) Those in which there is extreme internal deformation.

In the case of varieties 2 and 3, there are further complications. The minerals can recrystallise concurrently with deformation, thereby obscuring strain that is seen elsewhere in the rock.

Type 1 porphyroclasts can only form from minerals with a "rigid" lattice stable at high strain rates, i.e. with little or no mechanical anisotropies and high bond strengths. The matrix flows round these crystals

by grain boundary sliding. The process for type 2 is grain boundary sliding too, but the crystal margins friction causes dislocation build-up and attrition occurs by glide and creep process. The subgrains are stripped off and there is no over-all change in axial ratio for the clast. Porphyroclasts formed by this method are unsuitable as markers for studies on the relative variation in strain ellipse across an area.

Type 3 clasts develop in the same way as the others, but glide and creep become more important, producing subgrains within the clast. The clast, therefore, changes shape during deformation. Once the aggregate of subgrains is formed, this then changes shape rapidly as the constituents rotate by grain boundary sliding. The clast becomes flattened into the plane of the foliation, but still remains an entity.

The porphyroclasts from Osterøy are of all three types; the commonest are made from potash feldspar which forms types 2 and 3 clasts. Type 1 clasts are best developed from garnets.

Shear Bands

The process of initiation of shear bands is important when discussing mylonites. In the Osterøy rocks, not as proposed by Sinha Roy (1977), it is clear that most of the shear zones that are distinctly seen in the rock are a relatively late phenomenon in the history of deformation.

All processes of grain boundary sliding involve simple shear at the grain boundaries. Thus, no matter the nature of the macroscopic deformation, it can be resolved in part into simple shear at the microscopic level. When the shear is between two grains of markedly differing mechanical properties, the "weaker" member (e.g. mica) will break up faster. Locally, therefore, the grain size of both components will be smaller as this region of the rock has acted to magnify the stress field. This grain size variation is obvious from the Osterøy mylonites. As has been

discussed above, reduction in grain size accelerates chemical effects.
It also provides more boundaries for coble creep, grain boundary sliding
etc. to work on. Once shearing of this sort starts on a microscopic
level, then it is a runaway process, and a large shear band develops.
It is the variation in mineralogy that is the primary reason for the initia-
tion of a shear band at any particular locus. When the confining pressure
is high the process happens at all such boundaries in the rock (sometimes
a body of rock can behave like a crystal - "tectonic pips"), it is only
as the confining pressure decays that the process becomes heterogeneous.
The main processes then are the grain boundary processes; these start and
continue after mechanical constraints have stopped glide and creep. Of
the grain boundary processes, it is grain boundary sliding that is most
important. All the boundary processes are accelerated by the presence
of a fluid phase (Westwood et al.,1967; Rutter,1972(b)), a Rebinder
effect. The chemical processes prove that there was a fluid phase through-
out the deformation.

4.2.3. Formation of the Osterøy Mylonites

The characteristics of the mylonites can be summarised:

(i) They are regional in development involving vast thicknesses
($>$ 3.5Km), of both allocthon and basement.

(ii) The internal structures and fabrics indicate superplastic
behaviour during their formation.

(iii) All the processes on the deformation map were operative during
deformation. (It is assumed that nabbro herring creep was operative too,
but never contributed significantly to any single textural development.)
In addition chemical changes, both types of cataclasis, and grain boundary
sliding were operative.

(iv) 99 per cent. of the mylonites are polymineralic rocks with at least four major mineral phases present. This means the rocks were strongly anisotropic, both mechanically and chemically, on the microscopic and mesoscopic scale.

(v) A fluid phase was present throughout the deformation, resulting in the acceleration of all surface operative processes. This reduced the mechanical strength of the rock significantly and also aided chemical movement.

With these conclusions it is possible to build a comprehensive model describing the nature of superplastic deformation as seen in the Osterøy mylonites. At the onset of deformation, the waxing stress field caused a build-up of dislocation density in the component crystals of the rock. The process proceeded, subgrains formed, and when the grain size reached the point where most of the deformation was accommodated by grain boundary processes (some coble creep but mostly grain boundary sliding, as is proven by observation of deformation structures in mafic areas and the porphyroclasts), a stable grain size was reached. Dislocations still formed within grains, but the grains were small enough, and surface processes active enough, for them to be few enough in number to migrate through the lattices without locking up. Then for a given mineral and strain rate there would be a unique stable grain size. Thus there is an equilibrium grain size state for any particular rock type and strain rate and the first response to stress is the generation of this state. Deformation then proceeded mainly by grain boundary sliding. This and other surface processes were accelerated by the presence of the fluid phase in the rock.

Part of the stress was stored in the rock when generating this fine-grained state, partly as "activated" molecules and partly as surface area energies. This then facilitated chemical reactions and recrystallisation, both of which provided "fresh" crystals to be deformed. This, too, accelerated the rate at which the stress was dissipated.

Superplasticity then is not a single process, but the utilisation of all possible processes, especially the surface active varieties, coble creep, pressure solution, chemical processes and grain boundary sliding. The most important factor for these surface processes is the grain boundary area in the rock. The amount of surface area is controlled by the activity of the internal processes, glide and creep. This means that superplasticity is a state of dynamic equilibrium between constructive and destructive processes, acting to dissipate the stresses.

The model can be expressed as a cybernetic loop relating: grain size, finite strain, strain rate and stress field (fig.144). This means we can consider two geological conditions. In both cases the rocks are of the same composition and in the same geological environment. The second body, however, has in it a zone in which the grain size is smaller than for the rest of the rock. On deformation the first body of rock will enter the loop, and as deformation proceeds will tend to deform homogeneously. The strain is accommodated by all parts of the rock, and the grain size achieves equilibrium evenly throughout the rock.

In the second instance, the presence of the inhomogeneity of grain size in one portion means that that portion starts deformation in a more "advanced" state than the rest of the rock. The rate of deformation in this area will therefore be high. This modifies the stress field which means the rest of the rock will remain undeformed, and all the deformation will be accommodated in the finger-grained portion. Should the rate of application of energy increase, two things can happen: either the grain size in the zone of shear can decrease to facilitate the operation of the surface active processes, and/or the volume of rock in the zone of shear can be increased by attrition from the margins. This, too, increases the total grain surface area present in the zone of shear. In reality both are likely to happen, the attrition process occurring first until the grain

Fig 144.

THE STRAIN-RATE / TEMPERATURE SYSTEM FOR THE
GENERATION OF THE OSTERØY MYLONITES

─────▶ =PRODUCES   ───▶ =CONTROLS   ─ ─▷ ─ =CONTRIBUTES TO
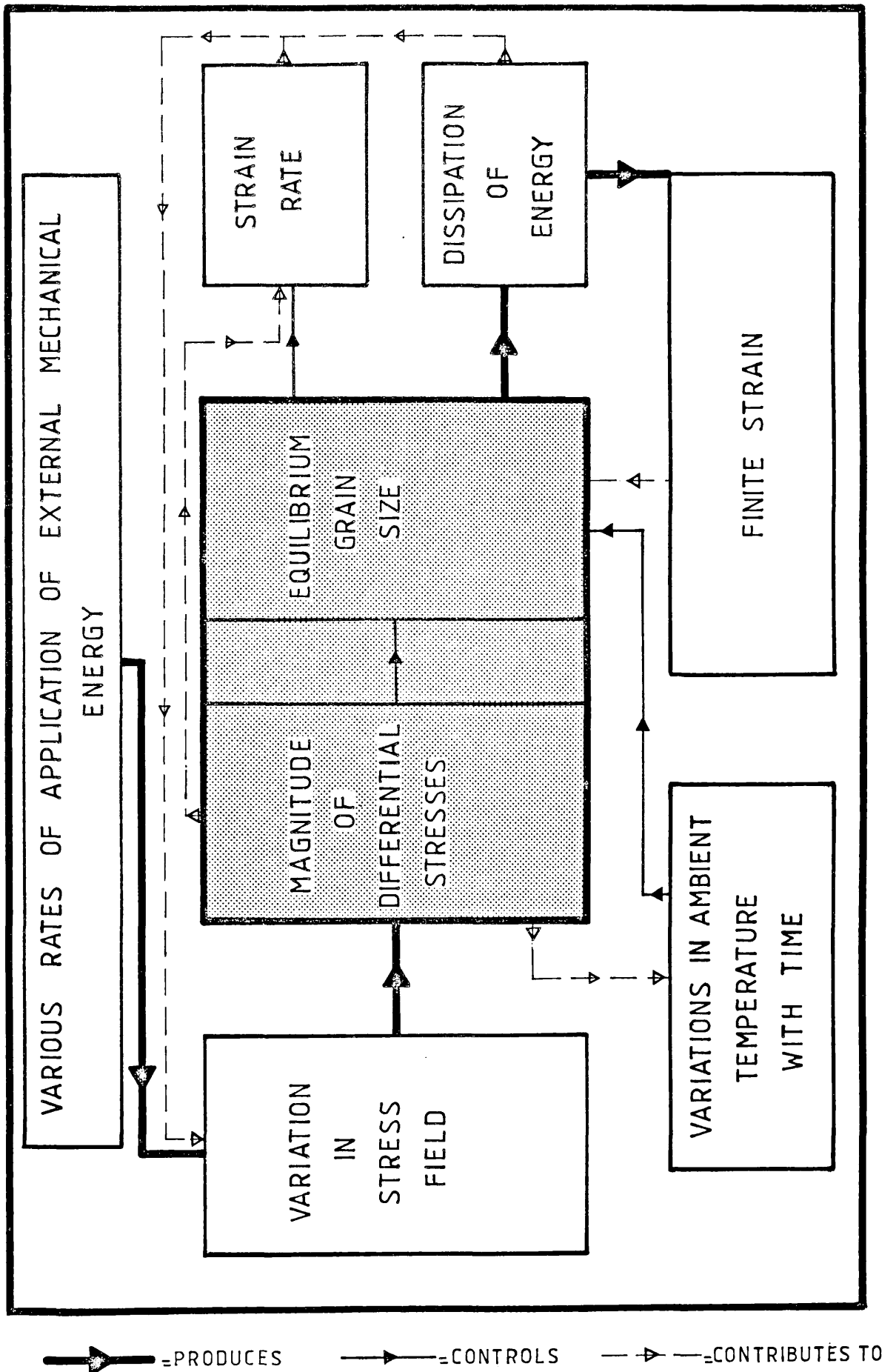
size in the zone has a chance to equilibriate. Then the only factor

tending to enlarge the zone will be the frictional resistance to sliding,

which will only cause a small amount of attrition.

In reality, rock is never homogeneous. When rocks deform super-

plastically they do so forming shear bands at the points of maximum

anisotropy (see previous description for modes of occurrence of the Osterøy

mylonites). The dynamic approach of the superplastic model explains why

restricted zones of shear develop and perpetuate; why sites of previous

shear are so frequently reactivated by later deformations rather than new

zones developing; how tectonic pips or pods of undeformed rock are created

and why, once formed, they persist unaffected by subsequent deformations.

Indeed all the above mentioned features are indicative of a superplastic

flow regime, where fine-grained rock acts as a "Strain Mop".

The relationship between differential stress, temperature and grain

size (the area defined by the stippled box in figure 144), can also be

described as shown in figure 145. The abscissa is the time axis, the

ordinate the grain size axis with the origin representing the original

grain size. All values below this represent reduction in grain size and

vice versa. The mechanism influencing grain size through time can be

described as a tensor with two major components, one of which can be

represented as $f(de/dt)$, the variation of strain rate with time, and the

other as $f(dT/dt)$, the variation of temperature with time. The solution

of this tensor determines the slope of the line for the variation of grain

size with time. A positive slope indicates grain growth, a negative slope

grain size reduction. When the gradient is vertical the rock has either

melted or fractured. A horizontal path indicates a steady state condition,

grain growth = grain size reduction. If the path is horizontal at a time

of deformation in the rock, the deformation process is likely to be

superplastic.

Fig 145.

SEPARATION OF METAMORPHIC ENVIRONMENTS ON A PLOT OF VARIATION IN GRAIN SIZE THROUGH TIME

A=Thermal metamorphism -[Melting]
B=Regional metamorphism
C=Osterøy mylonite type metamorphism
D=Traditional fault zone mylonite type metamorphism
E=Faulting
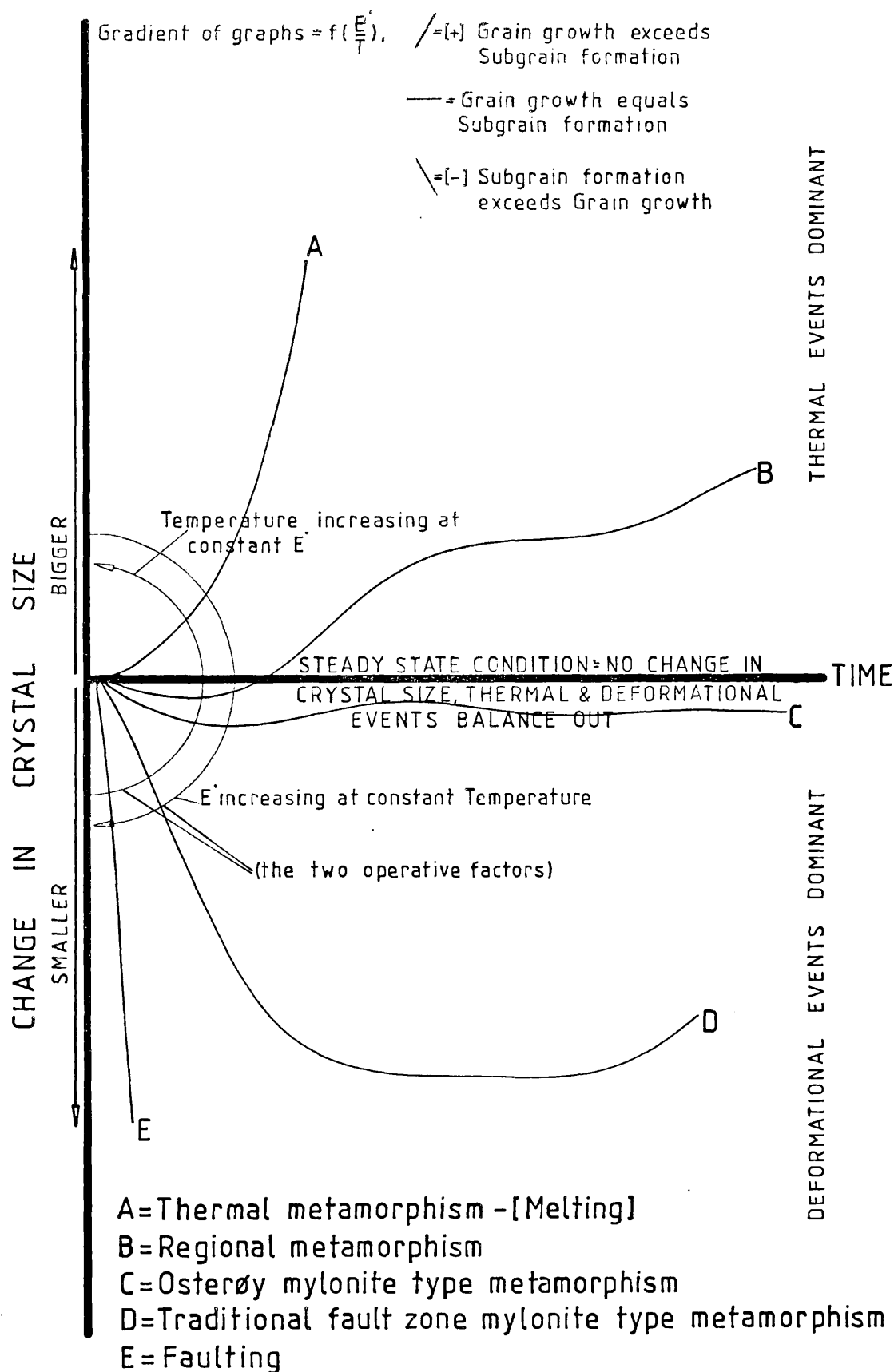
Examination of the paths for real rocks in this field enables different patterns to be distinguished which characterise the different possible metamorphic environments.

4.2.4 Implications of the Osterøy Mylonites

The Osterøy mylonites, therefore, describe a tectono/metamorphic system lying on a plane, defined by strain rate $(e^\cdot)$ and temperature, normal to the pressure axis of a diagram relating time (t), $(e^\cdot)$, temperature (T) and pressure (P). This diagram in fact describes completely the passage of rocks (metamorphic and structural history), through time (as opposed to the classical plots such as the PT diagram or the Deformation Map, which only describe one plane cut through it).

The three cartesian axes of this diagram are simplifications of parameters in an equation that defines the finite state of rock, its chemical composition and mineralogy as a function of what these variables were originally and how they have changed with time.

$$ECPh = f(d\ f(Eo.Co.Pho.)/dt)$$

where: E = finite strain $\qquad\cdot\qquad$ Eo = original strain state
$\qquad\quad$ C = finite chemistry $\qquad\qquad$ Co = original chemistry
$\qquad$ Ph = finite mineral phases Pho = original mineral phases.
$\qquad\quad$ f = some function

This equation can be expanded:

$$ECPh = f(d\ f(f(dCo/dCc).f(dPho/dPhc).f(dTo/dTc).f(dPo/dPc).f(d(d(\acute{O}1-\acute{O}3)/dt)o/$$
$$d(d(\acute{O}1-\acute{O}3)/dt)c))/dt)$$

where: Cc = the change in chemistry
$\qquad\quad$ Phc = the change in mineral phases
$\qquad\quad$ Tc = the change in temperature
$\qquad\quad$ Pc = the change in pressure
$\qquad\quad\acute{O}1$ = the maximum principal stress
$\qquad\quad\acute{O}3$ = the minimum principal stress
$\qquad\quad(d(\acute{O}1-\acute{O}3)/dt)o$ = the original strain rate
$\qquad\quad(d(\acute{O}1-\acute{O}3)/dt)c$ = the change in strain rate.

This can be more simply written as:

$$ECPh - f(d(f(C).f(Ph).f(T).f(P).f(d(\acute{O}1-\acute{O}3)/dt))/dt)$$

It is clear that this expression requires a large number of terms

for its solution, in fact the number approaches infinity when all possible

mineral phases are considered.   The equation would then be useless to

the geologist, but it can be simplified.   We know from field observations

that when the strain rate becomes excessively high, the rock fractures,

and that at slightly below this rate the chemistry alters by removal of all

material except quartz.   We know that above a certain temperature rock

melts, and we only need to consider geologically realistic pressures.

When considering the chemistry and mineral phases present, there are only

a finite number that are of geological importance.

Real geology, therefore, only occupies a small field within that space

theoretically possible.   Thus considering one moment in time it is

possible to write an equilibrium reaction to explain what is happening

in a rock:

$$(P_{eq} \cdot T_{eq} \cdot e^{\cdot}_{eq}) = G \ (P_{(to)} \cdot T_{(to)} \cdot e^{\cdot}_{(to)} \cdot A \cdot B)$$

where:

$$
\begin{aligned}
to &= \text{time at the start} \\
eq &= \text{time at equilibrium} \\
G &= \text{a function} \\
A &= \text{a function of the original chemistry at time zero} \\
B &= \text{a function of the original phases present at time zero.}
\end{aligned}
$$

This equation has a solution for the geologist;   this can be plotted on a

three-dimensional diagram constructed by adding a strain rate axis (similar

to that shown in figure 132) to the classical PT diagram (fig.146).

The equilibrium positions for the rock at given times can be joined

up.   The resulting line represents the behaviour of the rock with time,

the history of metamorphism and deformation as described by:

$$dEPh/dt = f \ (\ f \ (Ph) \cdot f \ (T) \cdot f \ (P) \cdot f(e^{\cdot}) \ )$$

This equation requires only twelve terms in its solution if the phases

present are known and the chemistry constant.

Fig 146.

THREE DIMENTIONAL STRAIN-RATE / PRESSURE /
TEMPERATURE DIAGRAM, ON WHICH METAMORPHIC
ROCKS ARE MORE ACCURATELY PLOTTED

VOLUME , in which metamorphic rocks
actually fall

STRAIN-RATE AXIS [/sec]

PRESSURE AXIS [Bars]

10^2

10^{-20}

P.T. PLANE of classical metamorphic
petrology

TEMPERATURE AXIS [°A]
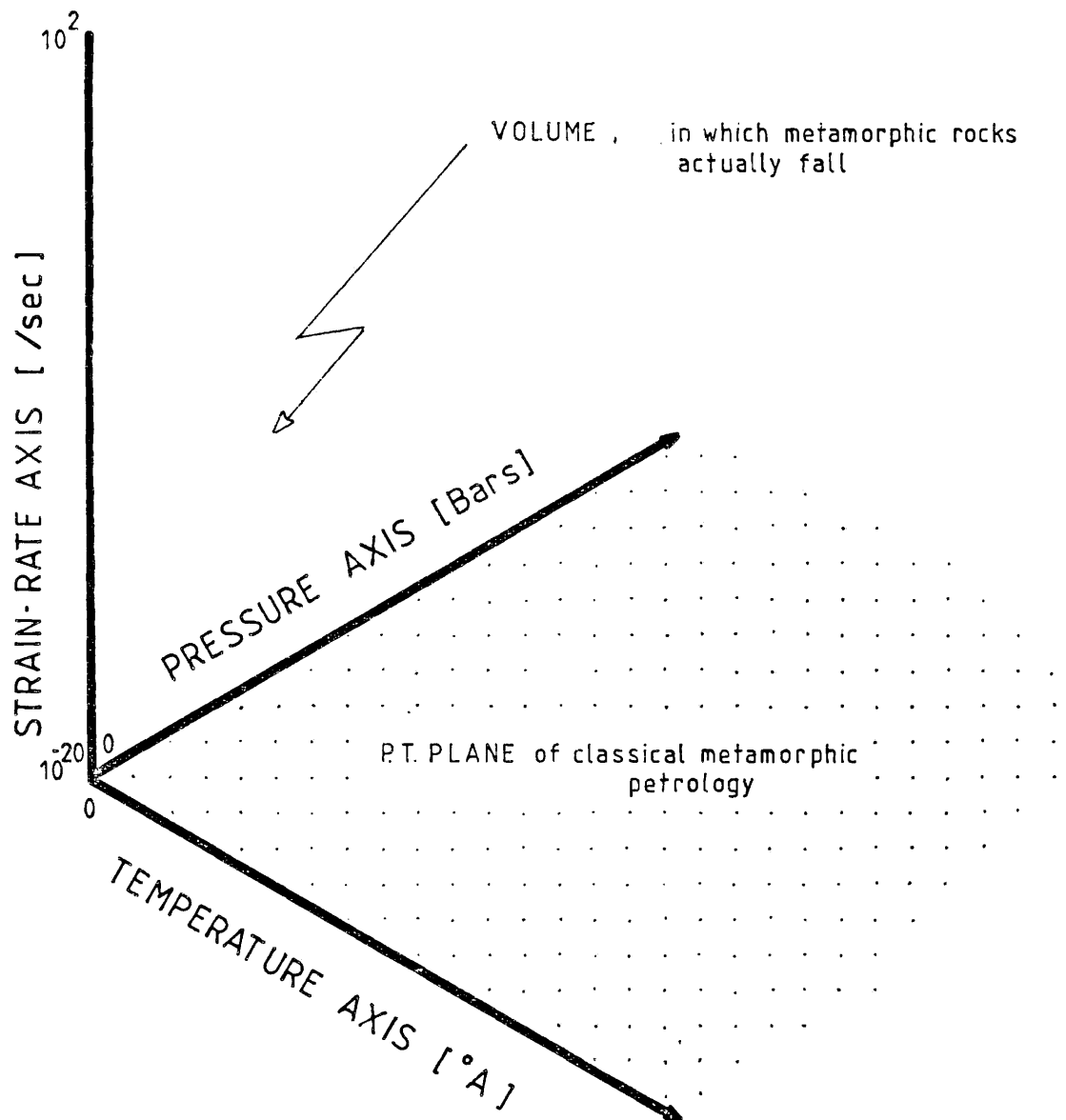
The Use of the e⁰ P T Diagram

The classical PT approach to metamorphic problems is useful and in general an adequate method for describing rocks. This approach has, however, virtually reached its limits with works such as Powell (1978) and Frazer (1977), and there are still inexplicable anomalies between theoretical and geological situations using this diagram and method (Hollister,1969). It does not take account of the texture in metamorphic rocks either.

There is therefore a need to be able to describe rocks in a more complete manner. This need is highlighted by the Osterøy mylonites, which define a plane at right angles to that of the classical PT diagram, while classical thrust mylonites and pseudotachylites like those described by Sibson (1975,1977) fall on a plane at right angles to both of these. It is clear, therefore, that any metamorphic event with a tectonic component will cause the rock to describe a path in the body of the cube defined by the e⁰, P, T axes. To project this path onto any one plane is deliberately to ignore an important part of the history of the rock. The e⁰ P T diagram, then, is the marriage of structural and metamorphic geology.

It is perhaps best to consider the effects of a third axis to the PT diagram by describing the effect it might have on one of the better known reactions, namely that of the aluminium silicate polymorphs.

The phase boundaries of this system will, with the addition of the e⁰ axis, describe a three-dimensional geometric form in the diagram. There are problems in determining the true form of this figure, as no specific experiments have been run to determine its shape as we move up the e⁰ axis. Fortuitously, many of the experiments that have been performed included significant proportions of effects that are attributable to e⁰. Indeed, authors have been aware for a long time that these effects

significantly alter the positions of the phase boundaries, and put much
effort into eliminating them.

Brown and Fyfe (1971) state: "Near equilibrium the Δs of the
andalusite-sillimanite reaction is only about 0.3 cal mol^{-1} deg^{-1}.
This means that if we wish to know the phase boundary with a certainty of
at least $\pm$50°C we must also use procedures which will give a free energy
with an accuracy of $\pm$15 cal mol^{-1}. For myanite reactions where Δs is
about 2 cal mol^{-1}deg^{-1}, again ΔG must be known within the limits of at
least $\pm$100 cal mol^{-1}. These are trivial quantities when it is noted that
the lattice energies of the three polymorphs are near 5 10^{5} cal mol^{-1}.

It is clear when these requirements are considered, that small effects,
strain energy, surface energy, impurity factors, will be critical in such
systems. If materials are ground to micron size range, surface energies
alone will be of the order of 100 cal mol^{-1}, and it is equally certain
that strain energies induced in grinding to such a size will greatly exceed
the surface energies. Thus it seems that the only experiments likely
to yield significant results will be those in which unstrained macro-
crystalline materials are used".

Similarly, Holdaway (1971) stated: "Intense grinding may shift phase
boundaries. Newton (1969) has shown that prolonged grinding of a kyanite-
sillimanite mixture preferentially degrades the kyanite as deduced by X-ray
line broadening. The result of such grinding could be to give a falsely
high pressure indication of the kyanite sillimanite phase boundary.
Newton's work indicates that a boundary 2kb above the equilibrium boundary
could result if grinding procedures similar to those of Althous (1967) are
used. Shearing squeezer results of Bell (1963) may also be in error for
this reason." "Fibrolite in sillimanite mineral samples has an effect
on the andalusite-sillimanite boundary. The boundary is raised by as

much as $200^{\circ}C$ for runs of short duration." Similar statements are made by Fyfe (1969).

When the field occurrence of the aluminium silicate polymorphs are examined, the literature is in the same confusion; apparent anomalies develop where one phase behaves metastabally and there are arguments as to whether all of the polymorphs seen to be present in the rock formed at the same time, or were the result of two phases in the metamorphic event.

It is possible that the introduction of the $e^{\bullet}$ axis returns an order to this confusion in both the natural and experimental situations. It should be recognised that the variation in the positions of the phase boundaries as described perhaps present a truer picture of geological situations than that presented by the positions of the boundaries actually on the base plane. Similarly, in the field apparent anomalies such as those described by Hollister (1969), who detected two distinct trends in the aluminium silicate polymorphs in what seemed to be a single phase event. In one trend kyanite pseudomorphed andalusite and was then replaced by sillimanite. In the other andalusite was replaced directly by fibrolite, or first replaced by kyanite then rimmed by fibrolite. To explain this he proposed a complex series of metastable paths. However, an examination of his descriptions and photographic plates of the two sorts of rock show clearly that those rocks in which the second trend was seen are sheared, while the remainder are not. Thus on the basis of the evidence presented above it is suggested that a more satisfactory explanation would be to state that the two trends represent identical PT conditions for both, but that the rocks of the second trend progressed along a vector with a larger component of $e^{\bullet}$ than did the other. It thus moved more into the body of the $e^{\bullet}$ P T cube and into an equilibrium situation that will be described below.

This field evidence, together with the experimental work, allows some very general conclusions to be drawn as to the shape of the polymorph diagram in three dimensions.

(1) The kyanite - sillimanite boundary plane curves towards the Pe* plane with an increasing component of e°.

(2) The andalusite - sillimanite boundary plane curves away from the e* axis with increasing component of e*.

(3) The triple point moves firstly towards the origin then curves away from it again, describing a spiral towards the Pe* plane with increasing e*.

(4) The kyanite - andalusite boundary plane seems to move towards the e*T plane with increasing e*.

(5) A new phase, fibrolite, develops some way up the e* axis. The phase comes in by branching the upward growth of both the kyanite - sillimanite and andalusite - sillimanite boundary planes. There therefore exists the possibility of a four-point junction at some specific e*.

Figure 147 embodies these ideas, and shows how Hollister's (1969) trends may plot on the diagram. The immediate objection to this proposal is that fibrolite is commonly described from the contact aureoles of granites which are believed to be passive intrusions. A set of teaching thin sections across one of these intrusions was studied. The FANAD Granite Pluton, outcropping on the three adjacent peninsulars of Rosynoll, Fanad and Inshowen in northern Donegal is a classical passive stoping intrusion (Pitcher & Berger,1972), yet it immediately became clear the minerals developed in the aureole are deformed. Andalusite, the first aluminium silicate to form, shows rotational inclusion trails (fig.148) and fibrolite, which replaces andalusite nearer the granite is deformed round andalusite nuclei, forming augen structure; some of the andalusite cores are even bent.

POSSIBLE STRAIN-RATE / PRESSURE / TEMPERATURE

DIAGRAM FOR THE ALUMINIUM-SILICATE

POLYMORPH SYSTEM

Fig 147.
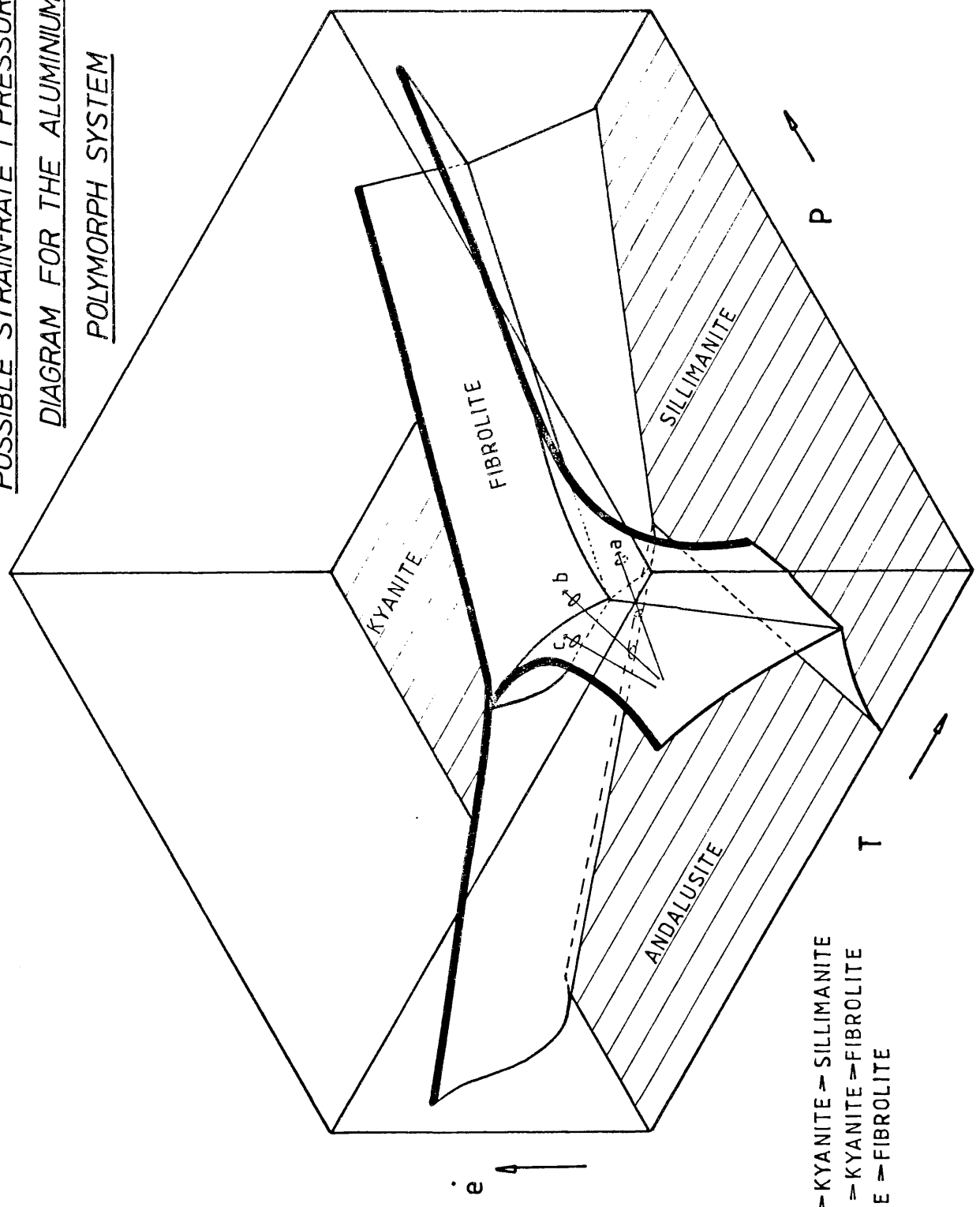
a) ANDALUSITE →KYANITE → SILLIMANITE
b) ANDALUSITE →KYANITE →FIBROLITE
c) ANDALUSITE →FIBROLITE

Fig 148.

TEXTURES IN ALUMINIUM SILICATE POLYMORPHS
FROM THE AUREOLE OF THE FANAD
GRANITE

ANDALUSITES SHOWING KINKED OR ROTATIONAL FABRICS

small crystal
nucleating
on a kink

small crystal keying a
kink

andalusite

muscovite

rotational inclusion
trails in a larger crystal
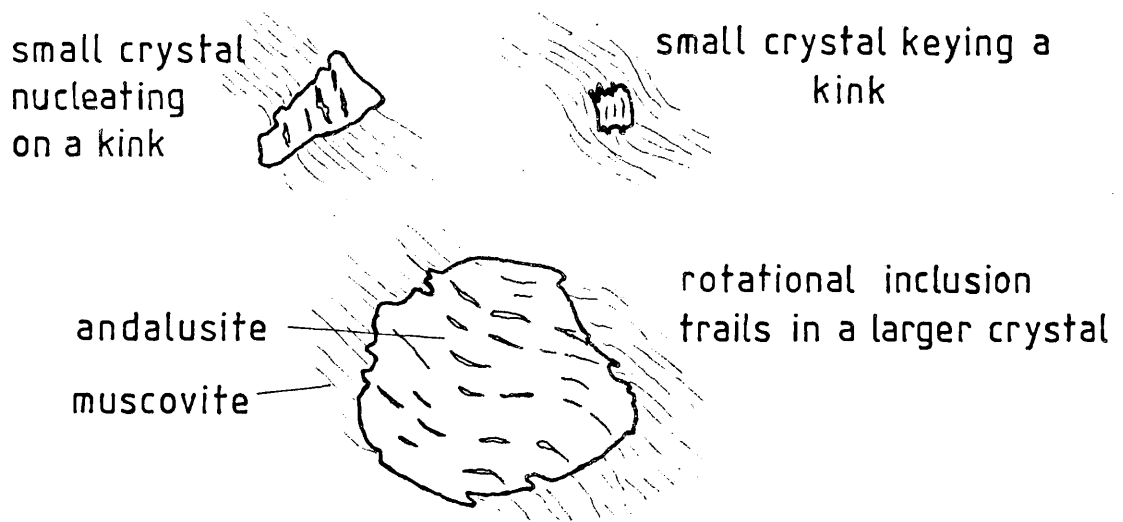
ANDALUSITE WITH FIBROLITE 'SHEATH'

fibrolite bends

late biotite

fibrolite 'sheath'
forming from the
andalusite

note augen
shape

andalusite

fibrolite

structure deformed during
or after the fibrolite
development

0   1   2mm
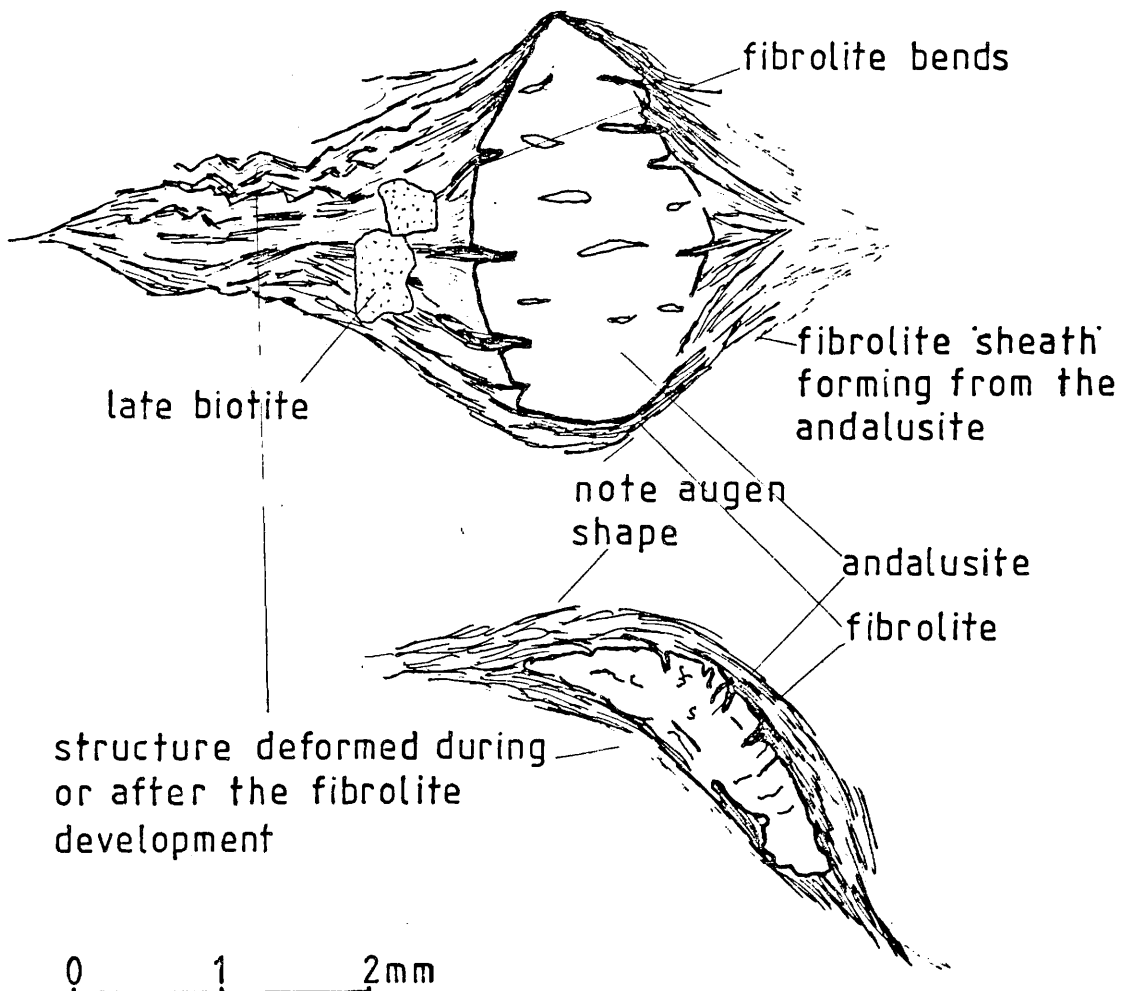
Admittedly these features do not amount to very high strains, but the rocks are deformed and it is not the amount of deformation but the strain rate that is important.

Another possible stress stable mineral may be chrysotile; this is always confined to cross fibre veinlets in serpentine. Read (1962) in his description of the mineral, notes that the veinlets are in fact zones of shear. Chrysotile, then, could be a polymorph of serpentine stable at high strain rates.

4.3 SIGNIFICANCE OF THE MYLONITES OF THE SOUTHERN GNEISSES

The Southern Gneiss Unit forms a belt of rock between a tectonically older complex of gneisses to the north-east and the Major Bergen Arc to the west. This rock unit shows features compatible with high strain rates and temperatures at virtually constant pressures. The rock types developed are similar to those seen in classical mylonite terrains. Their regional extent and vast thickness, however, preclude their development at the base of major thrusts, as the frictional forces required in their generation would make thrusting on the scale seen in the Bergen/ Jotunheim area impossible (Hubbert & Rubey,1959,1 & 2). One must therefore conclude that the period of plasticity and grain size reduction predated the brittle events, and that the mylonites of the Southern Gneiss Unit represent deformation occurring in the "root zone" of an orogenic belt, and were moved from this region as a basement nappe and given their flat attitude during the later brittle events.

The rocks do not conform to the original definition of mylonite (Lapworth,1885), in the sense that they are demonstrably not formed by the passage of two rigid plates past one another. They are more the product of a pure shear flattening. It is considered that mylonites of this type

are probably more common than hitherto recognised (Johnson,1967); that

the general confusion in the literature over their formation and the

plethora of terms for their description is due to workers trying to apply

Lapworth's original concept and description to related yet genetically

different rocks.   It is proposed, therefore, to remove confusion when

discussing rocks with a high strain rate component, to call all such rocks

"Tectonites".   By the addition of a prefix, "P" or "T" one could then

subdivide "P Tectonites", those defined by Lapworth, from "T Tectonites",

those discussed here.

5. GENERAL CONCLUSIONS

The conclusions are divided into three parts: a summary of the Osterøy gneisses and their formation; a regional synthesis; suggestions for further research.

5.1 THE HISTORY OF THE NORTH OSTERØY GNEISSES

5.1.1 Summary of Lithologies

The rocks forming the north-eastern part of Osterøy comprise portions of basement gneisses, migmatised metasediments, and acid and basic plutonics. The rocks are now all gneissose and preserve a complex history of meta- morphism and deformation. The gneisses belong to two major units: one autochthonous, the Northern Gneiss Unit; the other para-autochthonous, the Southern Gneiss Unit. A zone of translation, the Tysse Thrust Zone, separates the two units. The Southern gneisses are derived from and lie above the Northern gneisses.

The Northern gneisses are divided into three sub-units, primarily on a deformational basis, but the divisions also contain distinct lithologies. The oldest unit, the Unflattened Gneisses, consists of gneisses dated at 1855 ± 242 Ma. (Gray,1978), which resemble the Jostedal Complex (Bryhni, 1966). This is overlain by a sedimentary complex which has been extensively migmatised, possibly at 1509 ± 81 Ma (Gray,1978), and infolded with the basement prior to 1021 ± 84 Ma. (Gray,1978). This, the Gneiss and Migmatite Complex, resembles the Fjordane Complex (Bryhni,1966). Moving up the structural section the Gneiss and Migmatite Complex is reworked to form the Flattened Gneiss and Migmatite Complex.

The Southern gneisses are a 3 km thick sequence of mylonitic gneisses formed during two mylonite-producing deformations. The mylonitised rocks

are derived from the Northern gneisses, but the unit contains two suites

of rocks not found in the north. The first, a suite of mica schists

and quartzites is found in a schuppen zone beneath the allochthonous Bergen

Arc nappes. These rocks are correlated with those of the Samnanger

Complex (Faerseth et al.,1977; Kolderup & Kolderup,1940), within the Arcs

by tracing the continuous outcrops into the Samnanger region. The second

contains two groups of plutonic rocks, firstly amphibolites intruded into

the mylonites towards the end of their formation, and secondly, granitic

augen gneisses intruded into the mylonites, mica schists and quartzites

early in their deformation. The intrusive augen gneisses are dated

at 794.08 ± 18.82 Ma. (appendix 1) and contain xenoliths of the Samnanger

sediments from the schuppen zone. This implies that the Samnanger

sediments, and much of their deformation, are Precambrian and not Lower

Ordovician as has been hitherto assumed (Faerseth et al.,1977). This

discovery removes much of the basis of Sturt and Thon's (1976) criticism

of Gee and Wilson's (1974) claim that the Caledonian deformation and meta-

morphism in the major part of Scandinavia was a single late event and

that "there is no evidence of major unconformity within the Lower Paleozoic

sequence of the Scandinavian Caledonides". The major unconformity

between Samnanger and Holdhus (Faerseth et al.,1977) rocks described by

Sturt and Thon (1976), is therefore within the Lower Paleozoic, but

between rocks deformed in the Precambrian and fossiliferous, Ashgill

(Faerseth et al.,1977) sediments.

5.1.2 Summary of Metamorphic and Deformational History

There are four stages to the development of the North Osterøy Gneisses,

each stage a complete orogenic cycle punctuated by a period of sedimenta-

tion (fig.149). The first three stages were very similar and involved

a cyclic repetition of coaxial folding on a north-east - south-west axis,

with a sense of translation, given by the vergence of the folds, to the

Fig 149.

TABLE SUMMARIZING DEVELOPMENT OF THE NORTH OSTERØY GNEISSES

DEFORMATION PHASES	FOLDS	SCHISTOSITIES	LINEATIONS	BASIC INTRUSIONS	ACIDIC INTRUSIONS	METAMORPHISMS Lower Greenschist ⟷ Middle Amphibolite
D Early	?	S Early	?		✓	
D1	F1	S1	L1	✓	✓	
		S2	SEDIMENTS		✓	
D2	F2	S3a / S3b	L2	✓	✓ [T]	
			SEDIMENTS			
D3	F3	S4	L3	✓	✓ [T]	
			SEDIMENTS			
D4	F4	S5			✓ [T]	
D5	F5	S6	L4 / L5	(time)		
D6	F6	S7				
D7	FAULTING					
D8	JOINTING					[T =THRUSTING]

north-west.   At each stage the latest sediments became incorporated into the basement.

The first episode involved isoclinal folding of an early banding $(1855 \pm 242$ Ma., Gray,1978$)$ in an amphibolite facies environment, followed by uplift and sedimentation.

In the second episode the sediments were migmatised at middle amphibolite facies (at around 1509 ± 81 Ma., Gray,1978). This was followed by retrogression to lower amphibolite facies, accompanied by further isoclinal folding (prior to 1021 ± 84 Ma., Gray,1978), uplift and a new sedimentary cover.

The third stage differed from those preceding because the folding at amphibolite facies produced a thick sequence of mylonites $(794.08 \pm 18.82$ Ma., appendix 1$)$ and, at a late stage, translation of allochthonous and para-autochthonous nappes derived from sediments and the mylonites. These moved in a direction perpendicular to the north-east - south-west trend of the fold axes. The third suite of sediments was deposited on these nappes sometime during the Ashgill (Faerseth et al.,1977).

The final episode differed from the rest in that while deformation started more or less coaxial to the earlier structures, it later developed to produce north-west - south-east trending folds. There are several fold phases involved in the episode, each occurring in progressively lower greenschist facies environments. The thrusts formed in the preceding episode were reactivated, more mylonites were produced and new brittle thrusts developed in the nappes, cross-cutting the earlier structures. Translation was again perpendicular to a north-east - south-west axis.

Later folding on a north-west trend, folded these thrusts and was responsible for the Bergen Arc outcrop pattern.

This history, summarised in the cross sections (figs.158 & 150) is not immediately apparent from the outcrop patterns (map 1), which are controlled by major F2 and F5 folds. The linearity of outcrops is produced by erosion of the flat limbs to leave intervening steep limbs. The complete history is only deduced through detailed structural and litho-tectonic mapping. The key to the understanding of the history lies in appreciating that the main effect of deformation was flattening, and that the deformations were heterogeneous, increasing in intensity up the structural section to the south-east. The lowest part of the structural pile shows the oldest structures, which are flattened out of recognition at higher levels. The mylonitic para-autochthonous nappe being the highest structural unit, it therefore contains the largest number of deformations, but this is superficially the simplest unit because cumula-tive superposition of these flattenings has largely obliterated the early structures.

The mylonitic unit, once formed, 'cushioned' the underlying basement from further deformation by absorbing all the stresses in superplastic deformation, up to the point where metamorphic retrogression precluded further recrystallisation in the mylonite system (D5). The Tysse Thrust then acted as a plane of transport and is a structural boundary. The thrust separates the first two episodes, which may be regarded as separate Precambrian basement forming cycles, similar to those seen in Telemark (Torske,1977), from the last two. These, although chronologically separate are more closely related, a conclusion reached from a consideration of the morphology of the parental regional structures. Both are the result of metamorphism and deformation in a thermal environment of 400-500°C, at depths of 15-18 Km and of strain rates exceeding 10^{-11}/sec. These conditions are only attained in the root zones of orogens. The mylonites therefore can be regarded as a deep level ductile equivalent

Fig 150.

DIAGRAM SUMMARIZING DEVELOPMENT OF THE NORTH OSTERØY

GNEISSES

Episode 1

S Early

N

S1   L1

F1   D1

Episode 2

1. Sediments

S2

L2

F2   D2

S3a

S3b
(sediments [1]
mixed with basal
gneisses)

Episode 3

2. Sediments

L3

D3

F3   S4

S3

Episode 4

3. Sediments
[Ashgillian]

D4

S5

[S4+S5]

F4

Northern Gneiss
Unit

TYSSE THRUST

D2 THRUST

BERGEN ARC THRUST

D5

Bergen Arcs

Southern Gneiss
Unit

F5

F4
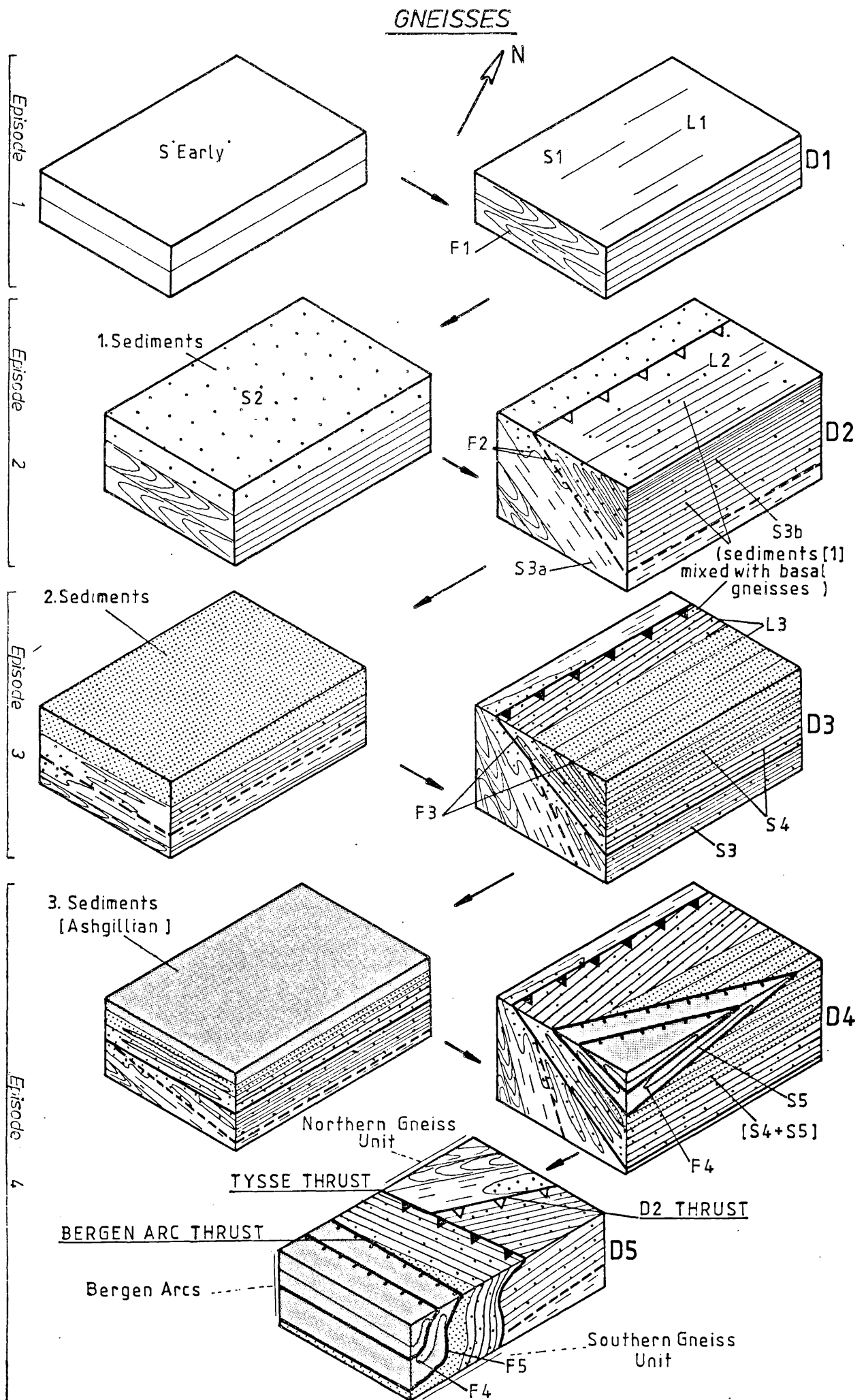
to brittle thrusting at the surface. The brittle thrusts cut the mylonites and are therefore later; they are considered to have formed after uplift (generated by ductile deformation at depth) and are responsible for the final removal and emplacement of the mylonitic unit.

5.2   REGIONAL SYNTHESIS

North Osterøy forms part of a triangle between the Bergen Arcs and Bergsdalen Nappes, and is ideally placed for the study of the response of the basement to the development of these structures. By detailed mapping across the basement/Arc contact on Osterøy and from the deformation history of the Arcs (Faerseth et al.,1977), correlative histories have been established for a protracted period of their history. This correlation is summarised in figure 151.

Assuming that the Northern gneisses are foreland and not part of a larger basement nappe, they can be used as a base line to which structures elsewhere may be related. It is proposed that the basement formed a permanent nucleus, which deformed in sympathy with its adjacent rocks. The cover rocks must therefore contain at least as many deformation phases, from the point of their sedimentary or tectonic emplacement, as the basement. A point of confluence in structures in the two areas is therefore a time of emplacement. On this basis it has been established that the Bergen Arc nappes were emplaced relatively early, during the third stage of development of the basement.

Folding before, during and after this emplacement, was on a north-east axis, and this must be significant in any consideration of an origin for the Bergen Arc nappes. The only major structure with a north-east trend is the Bergsdalen/Jotun mountain range. Unfortunately, the contact with the Bergsdalen nappes lies to the south-east of Osterøy, but based

Fig 151.

CORRELATED DEVELOPMENT HISTORIES FOR THE BERGEN ARCS & N.E. GNEISSES

BERGEN ARCS		N.E. GNEISSES
Bergen Arc Synform		(NS)
Non Cylindrical Folding on a N.W. Trend		
Folding and/or Flattening		Flattening
MINOR THRUSTING AND MYLONITE FORMATION		
Sediments and Pegmatites Isoclinally Folded on a N.N.E. Trend		Pegmatites Folded on a N.N.E. Trend
Ashgillian Holdus Sediments Deposited, Pegmatites Intruded		Pegmatites Intruded
MAJOR BRITTLE THRUSTING EVENT		
Ductile Thrusting, Mylonite Formation, Isoclinal Folding on a N.E. Trend with the Production of a Strong 'L' Tectonic Fabric (807 Ma)		
Samnanger Sediments Deposited		
Thick Cover (Volcanics)		Thin Cover (Quartzites)
SEPARATE PRE THRUSTING HISTORIES FOR EACH THRUST UNIT		Minor Thrusting
		Flattening
		Migmatization of Sediments and Folding on a N.E. Trend (1509 Ma)
		Sediments Deposited
		Intrafolial Isoclines, New Foliation Develops
		Oldest Detectable Foliation (1855 Ma)
		?

on the structures described from the Osterøy basement (this thesis),

Eksingedalen and the lower Bergsdalen Nappe (Gray,1978); the lower

Bergsdalen Nappe (fig.152), (Winter,1978; Evans,1978) and excursions

made from the basement into the Bergsdalen Nappes east of Osterøy, a

rudimentary deformation history for the Bergsdalen Nappes has been

established (fig.153).

There are several problems in this compilation:

1) There is good agreement with Gray on the Sequence of basement

   structures, but she does not integrate these with the deformations

   observed in the Bergsdalen Nappes.

2) Gray describes folding in the easternmost part of the Bergsdalen

   area on steep east - south-east plunging axes. These are not

   included in figure 153, because they are not seen further south and

   not understood in terms of deformation in the Osterøy basement.

3) In the Bergsdalen area, Gray, Evans and Winter describe their earliest

   folding as isoclinal, affecting quartzites and sediments and cut by

   syntectonic granite intrusions. These granites are dated at between

   1274 ± 48 Ma. (Pringle et al.,1977) and 971 ± 71 Ma. (Gray,1978).

   This situation is similar to that described from Osterøy (above).

   The isoclines are correlated with F3 on Osterøy, and the sediments

   with those in the Samnanger complex of the Bergen Arcs.

4) After the isoclines there are two phases of folding on a north-east

   trend before folding on a north-west axis. These latter north-west

   folds are correlated with F5 on Osterøy on the basis of their style

   and axial direction.

5) Gray would like to put the Lower Palaeozoic unconformity after the

   first of the two north-east trending fold phases on the basis that

   only the second affects the Palaeozoic sediments; Forster (per.comm.1979)

   however, describes a hidden intrafolial fold phase in these sediments.

Fig 152.

321

GENERALIZED GEOLOGICAL MAP OF THE BERGSDALEN QUADRANGLE
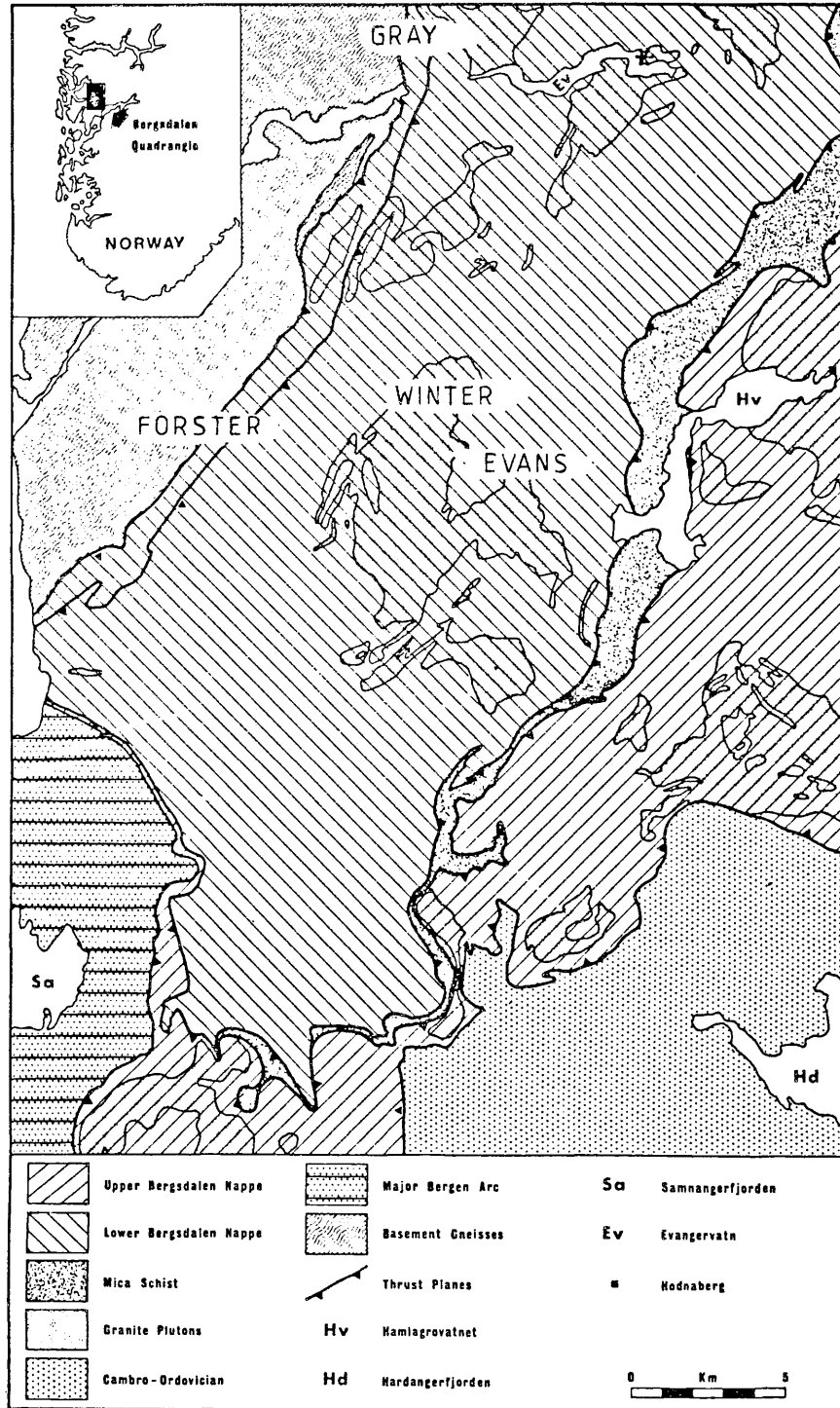
After :- KVALE (1964).

Fig 153. CORRELATED DEVELOPMENT HISTORIES FOR THE BERGEN ARCS, N.E. GNEISSES AND BERGSDALEN

BERGEN ARCS	N.E. GNEISSES	BERGSDALEN
Bergen Arc Synform (Thrusting Over Bergsdalen)		
Non Cylindrical Folding on a N.W. Trend		Much Weaker
Folding and/or Flattening	Flattening	Folding on a N.E. Trend and Flattening
MINOR THRUSTING AND MYLONITE FORMATION		
Sediments and Pegmatites Isoclinally Folded on a N.N.E. Trend	Pegmatites Folded on a N.N.E. Trend	Sediments and Pegmatites Folded in Tight to Isoclinal Folds on a N.N.E. Trend
Ashgillian Holdus Sediments Deposited, Pegmatites Intruded	Pegmatites Intruded	Fossiliferous Sediments of Bergsdalen/Jotun Deposited Pegmatites Intruded
MAJOR BRITTLE THRUSTING EVENT		
Ductile Thrusting Mylonite Formation, Strong 'L' Tectonic Fabric	Ductile Thrusting Mylonite Formation, Isoclinal Folding on a N.E. Trend with the Production of a (807 Ma ——1227 Ma)	
	Sumnunger and Bergsdalen Sediments Deposited	
Thick Cover	Thin Cover	Thick Cover
Separate Pre Thrusting Histories for Each Thrust Unit	Minor Thrusting	?
		Separate Pre Thrusting Histories for Each Thrust Unit
	Flattening	
	Migmatization of Sediments and Folding on a N.E. Trend (1509 Ma)	
	Sediments Deposited	
	Intrafolial Isoclines, New Foliation Develops	
	Oldest Detectable Foliation (1855 Ma)	
	?	

It is therefore suggested that the unconformity occurs immediately
after the early isoclinal folding, a sequence similar to that in
the Arcs (Faerseth et al.,1977).

6)   The first thrusts in the Osterøy basement were either late D2 or
early D3 and trend north-east (map 1, fig.1). They displaced the
early migmatised sediments and could be regarded as the first stages
in the development of the Bergsdalen Nappes.   This early thrusting
is however, regarded as separate from the deformation which produced
the Bergsdalen Nappes and as the product of pre-Bergsdalen tectonic
activity along the site in which the Bergsdalen sediments accumulated,
these early thrusts are brittle structures and it has been shown
that the early deformation accompanying emplacement of the Bergsdalen
Nappes was super-plastic rather than brittle.   This earlier tectonic
activity may have provided a source for some of the sediments
seen in the Bergsdalen Nappes.

The summary of deformation in the region presented in figure 153
serves as a common framework to be modified by later workers. The immediate
conclusion to be drawn from it is that the deformation sequence in the
Bergsdalen Nappes is very similar to that of the Bergen Arcs.   The Arcs,
however, continued to deform after the Bergsdalen Nappes with the formation
of the north-south aligned synform, with accompanying transport over the
Bergsdalen Nappes.   One might speculate, from the presence of tectonised
Devonian sediments north of the Arcs (Hoisaeter,1971), that this stage of
development may also be post-Devonian!

The conclusions drawn from the examination of the North Osterøy
basement are:

1.   The Northern Gneiss Unit forms a foreland to the Bergen Arcs and
Bergsdalen Nappes.

2.   From a structural point of view, the Southern Gneiss Unit is an integral part of the Bergen Arcs, thus the Tysse Thrust is the "basal thrust" to the Bergen Arc structure.

3.   The gneisses have to some extent deformed with the Bergsdalen and Bergen Arc lithologies and are good indicators as to when the nappes were emplaced.

4.   The gneisses have a long history of metamorphism, sedimentation and deformation, prior to their involvement with the Bergsdalen and Bergen Arc Nappes.

5.   The Bergen Arcs are a portion of the Bergsdalen/Jotun Nappes, affected by later local deformations.   It is the Bergen Arc Synform which is responsible for the marked change in trend between the Bergsdalen and Bergen Arc rocks.

6.   The Precambrian date on the granite from Osterøy and the granites in the Bergsdalen Nappes (e.g. Pringle et al.,1975), prove that much of the deformation in the nappes was in fact Precambrian,(Sveconorwegian, Andresen et al.,1974),and that, at least in the Bergen/Bergsdalen area, some of the sediments are also Precambrian.   The evolution of the Bergen Arc/Bergsdalen/Jotun structure was therefore in two stages, the first Sveconorwegian, the second Caledonian.

7.   The Sveconorwegian event involves more ductile deformation than the Caledonian, and in the Osterøy area is probably the more important of the two events.

5.2.1   Speculative Tectonic Reconstruction

The generally accepted view (e.g. Hossack,1978) as to the origin of the Bergen, Bergsdalen and Jotun nappes, is that they were rooted somewhere in the region now occupied by the North Sea, and travelled south-east over

the North Osterøy basement, to their present positions.   It is also
generally accepted (e.g. Sturt & Thon,1976;   Faerseth et al.,1977;
Pringle et al.,1975;   Hossack,1978) that nappe emplacement and accompanying
deformation was entirely Caledonian.

It has been shown above that the formation of the Bergsdalen Nappes
and Bergen Arcs was a two-stage process;   in the early Sveconorwegian
event, deformation occurred at deep crustal levels, whilst in the later
Caledonian event deformation occurred at shallower crustal levels.   In
both events the sense of transport, determined from the vergence of the
ductile structures which accompany the thrusting, was from south-east
to north-west.

These discoveries conflict with the generally accepted view, and
from the Osterøy viewpoint, a preferred model is one of a proximal root
for the nappes to the south-east.   This model is similar to that proposed
by Banham et al. (1979) for the Sygnefjell area along strike from Osterøy.
It implies the presence of a suture along the Bergsdalen/Jotun axis;
the arguments for and against this are discussed in Banham et al. (1979).
The difference here is that the suture is now regarded as Sveconorwegian-
Caledonian rather than just Caledonian.   The model for the development
of this suture is explained below.

Model

It is proposed that the present site of the Bergsdalen and Jotun
Nappes has acted as a "mobile zone" since 1800 Ma.   Its development
since then is summarised in a series of north-west - south-east sketch
sections across the suture (figs.154, 155 & 156).

Figure 154

a)   Situation at the time of the pre-D2 migmatisation.

b)   D2, F2 folding followed by thrusting to the north-west.

Fig 154.

MODEL FOR DEVELOPMENT OF THE
SVECONORWEGIAN - CALEDONIAN JOTUN SUTURE, PART 1

NW   SE

OSTERØY

1500Ma   ?FJODANE COMPLEX?

SEDIMENTS

MIGMATISATION   (a)

D Early /D1 Basement

? JOSTERDAL COMPLEX ?

D2

1020Ma

(b)

This symbol will be
used to refer to D2
basement from here on
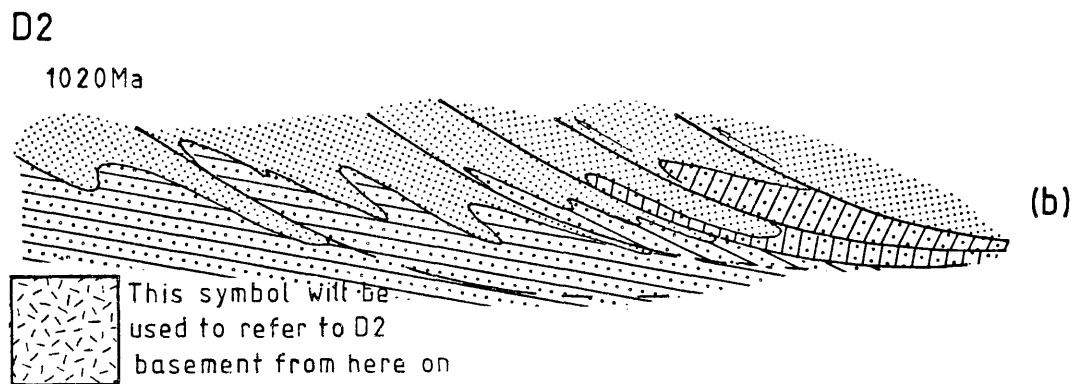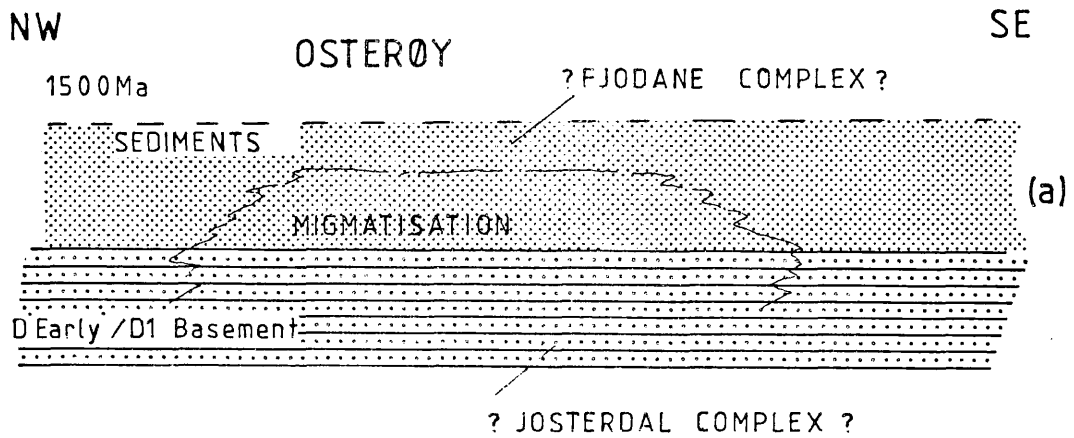
SITUATION FOR THE DEPOSITION OF THE SAMNAGER ROCKS

Erosion

Samnanger sediments
deposited   OCEAN

ANORTHOSITIC
toe to this continent
Activity starts
on this margin now

Psammitic

Gabbros &
Volcanics

Pelitic   (c)

ANORTHOSITES ⟶
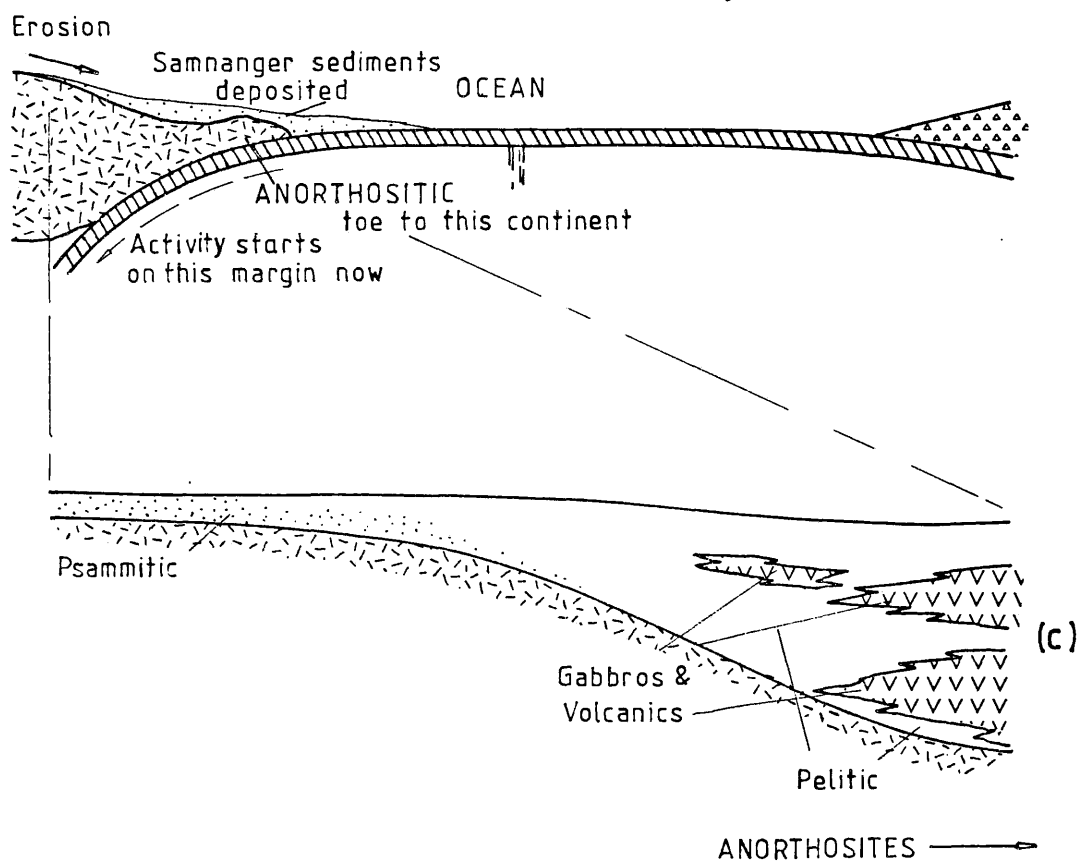
c)   Erosion and deposition of the Samnanger rocks, which included gabbros

and volcanics to the east.   At this stage an ocean existed south-

east of Osterøy.

Figure 155

d)   The ocean begins to close, deforming the sediments.   Granites are

intruded into the sediments and basement at this time.

e)   The deformation, which started at the toe of the continent in (d) has

now affected the foreland.   The nappes of Samnanger rocks are

emplaced and part of the continental toe (anorthositic) is pushed

over them.

f)   Activity on the northern margin now ceases, the new mountains are

eroded and Ashgillian sediments deposited over them, and in the

remains of the ocean which still existed south-east of Osterøy.

Figure 156

g)   The Caledonian orogeny finally closes the ocean by activity on the

southern margin, transporting the Palaeozoic nappes south over the

southern continent.   The southern continent underthrusts its northern

counterpart, reactivating the old thrusts and sending more Palaeozoic

nappes northwards, producing 'Ivrea type' flakes out of the older

nappes (see Gabrielsen et al.,1979).

h)   An east - west section through the Arcs and Bergsdalen shows the effects

of the later deformation, which also affects the Bergen region.

5.3   FURTHER RESEARCH

5.3.1   Suggestions for Further Research on Osterøy

Geochemistry: The geochemical study of the mylonites (section 4.1.3)

is incomplete;   more samples should be collected both across and along

strike to test the inferences drawn in the pilot study.   The geochemistry

Fig 155.   328

MODEL FOR DEVELOPMENT OF THE
SVECONORWEGIAN-CALEDONIAN JOTUN SUTURE, PART 2

NW   SE

D3 (ductile phase)   OSTERØY

1000Ma
still undeformed here

Diachronous Deformation
of sediments

(d)

1000Ma

800Ma

Granites   basement   900Ma   1100Ma

D3 (brittle phase)

800Ma

ANORTHOSITES (from continental toe)

[JOTUNHEIMEN]

(e)

Basement   reworked
basement nappes

sedimentary nappes

800-500Ma
SITUATION AT THE CLOSE OF THE FIRST PHASE OF ACTIVITY

erosion of mountain
chain

ANORTHOSITES [deposition of sediments
starts 'Sparagmites']

Cambrian shelf sea
sediments

sea

ocean

Southern continent

Activity on this margin now
ceases

DEPOSITION OF THE LOWER
PALAEOZOIC ROCKS

500Ma-Silurian ?

remnants of JOTUN
OCEAN

ANORTHOSITES
Holdhus sediments   volcanics

Northern
continent   pelitic sediments   Southern
continent   (f)

quiescent
margin   Activity starts on

the southern margin
now

Fig 156.

MODEL FOR DEVELOPMENT OF THE SVECONORWEGIAN-CALEDONIAN JOTUN SUTURE, PART 3

NW   SE

FINAL STAGE OF CLOSURE

D4

[Post Ashgillian]

reactivation of some D3 thrusts
& formation of some new ones

flat lying Palaeozoic
Nappes

unaffected D3
thrust

[steep
zone]

ANORTHOSITE forming
an Ivrea type flake

(g)

North-Eastern Gneiss
Basement

Telemark
Basement

Underthrusting of Northern
continent by the Southern continent

[OSTERØY]

LATE DEFORMATION ALONG THE AXIS OF THE SUTURE ENDS ACTIVITY

W   E

BergenArcs   Bergsdalen   Jotun

D5 + D6   (OSTERØY)

- Devonian ?

F6   F6

Øygarden basement

Late emplacement of the Arcs
over the Bergsdalen

ANORTHOSITE

(h)

F5

(for Map showing Lines of Section, see Fig 4.)

330.

of the migmatites merits more detailed future study, it may be possible to
separate the basement gneisses from the migmatised metasediments geochemically.

Geochronology: High strains in the gneisses make dating difficult.
However, a date on the veins cutting the F3 and F4 folds (pl.21) would
probably be feasible and useful because this would date the end of D3.

Structure: The study of mylonites began on Osterøy should be extended
to another area (e.g. a Laxfordian shear zone in Scotland), so that a com-
parative study of deformational styles may be made.

The F5 folds present an enigma; their style suggests they are the
top limb of a fold overturned to the west.   Why these late, non-cylindrical
folds should close towards the nappe pile with a sense of transport away
from the basement is not understood.

5.3.2   Suggestions for Further Research in the Region

The Øygarden basement and the area south-east of Osterøy, where the
Bergsdalen, basement and Bergen Arcs meet are being mapped as part of the
Bedford College project.   The mapping should be extended to the north-west
of Osterøy to trace the Tysse Thrust.   The rest of the North Eastern
Gneisses (fig.2) also need mapping to confirm that they are in fact
basement and not part of a larger nappe.

The work on the Bergen Arcs, basement and Bergsdalen Nappes should
be continued along the northern margin to tie in with the work at Sygnefjell
and extended into the nappes in an attempt to prove or disprove the
presence of a suture in this region.

REFERENCES

Aalstad, I., Åm, K., Habrekke, H. & Kihle, O., 1977. Aeromagnetic investigations along the Norwegian Geotraverse. In: Heier, K.S. (ed.), The Norwegian Geotraverse Project. Nor. geol. Unders., 77-99.

Abbey, S., 1978. Calibration Standards. X-Ray Spectr., 7, 2: 99-121.

Althous, E., 1967. The triple point andalusite-sillimanite-kyanite. Contrib. Mineral. Petrol., 16: 29-44.

Andresen, A., Heier, K.S., Jorde, K. & Naterstad, J., 1974. A preliminary Rb/Sr geochronological study of the Hardangervidda-Ryfylke Nappe System in the Røldal area south Norway. Nor. geol. Tidsskr., 54: 35-47.

Ashby, M.F., 1972. A first report of deformation mechanism maps. Acta Metall., 20: 887-97.

Banham, P.H., 1968. The basal gneisses and basement contact of the Hestbrepiggan area, north Jotunheimen, Norway. Nor. geol. Unders., 252: 77.

Banham, P.H. & Elliott, R.B., 1965. Geology of the Hestbrepiggan area, preliminary account. Nor. geol. Tidsskr., 45: 189-98.

Banham, P.H., Gibbs, A.D. & Hopper, F.W.M., 1979. Geological evidence in favour of a Jotunheimen Caledonian Suture. Nature, London, 277, 5694: 289-91.

Barth, T.F.W., 1938. Progressive metamorphism of sparagmite rocks of Southern Norway. Nor. geol. Tidsskr., 18: 54-65.

Battey, M.H. & McRitchie, W.D., 1975. The petrology of the pyroxene-granulite facies rocks of Jotunheimen, Norway. Nor. geol. Tidsskr., 55: 1-49.

Beach, A., 1976. The interactions of fluid transport, deformation, geochemistry and heat flow in early Proterozoic shear zones in the Lewisian. Philos. Trans. R. Soc. London, 280: 569-604.

Bell, P.M., 1963. Aluminium Silicate System: Experimental determination of the triple point. Science, 139: 1055-1056.

Bell, T.H. & Etheridge, M.A., 1973. Microstructure of Mylonites and their descriptive terminology. Lithos, 6: 337-48.

Biot, M.A., 1961. Theory of folding of stratified viscoelastic media and its implications in tectonics and orogenesis. Bull. geol. Soc. Am., 72: 1595-1632.

Biot, M.A., 1964. Theory of internal buckling of a confined multilayer sequence. Bull. geol. Soc. Am., 75: 563-8.

Bjørlykke, K., 1978. The eastern marginal zone of the Caledonide Orogen in Norway. In: I.G.C.P. Project 27, Caledonian-Appalachian Orogen of the North Atlantic Region. Geol. Surv. Canada, Paper 78-13.

Blay, P., Cosgrove, J.W. & Summers, J.M., 1977. An Experimental investigation of the development of structures in multilayers under the influence of gravity. J. geol. Soc. London, 133: 329-343.

Bott, M.H.P. & Dean, D.S., 1973. Stress diffusion from plate boundaries. Nature Phys. Sci., 243: 339-41.

Boullier, A.M. & Gueguen, Y., 1975. SP Mylonites: Origin of some mylonites by superplastic flow. Contrib. Mineral. Petrol., 50: 93-104.

Brown, E.H. & Fyfe, W.S., 1971. Kyanite-Andalusite Equilibrium. Contrib. Mineral. Petrol., 33: 227-231.

Brueckner, H.K., 1972. Interpretation of Rb-Sr ages from the Precambrian and Palaeozoic rocks of southern Norway. Am. J. Sci., 272: 334-358.

Brueckner, H.K., 1977. A structural, stratigraphic and petrologic study of anorthosites, eclogites and ultramafic rocks and their country rocks, Tafjord area, western south Norway. Bulletin NGU., 41, 332.

Brueckner, H.K., 1979. Precambrian ages from the Geiranger-Tafjord-Grotli area of the Basal Gneiss Region, west Norway. Nor. geol. Tidsskr., 59, 2: 141-155.

Brueckner, H.K., Wheeler, R.L. & Armstrong, R.L., 1968. Rb/Sr Isochron for older gneisses of the Tafjord area, Basal Gneiss Region, S.W. Norway. Nor. geol. Tidsskr., 48: 127-131.

Brynhi, I., 1962. Structural analysis of the Grøneheia area, Eikefjord, western Norway. Nor. geol. Tidsskr., 42: 331-69.

Bryhni, I., 1966. Reconnaissance studies of gneisses, ultrabasites, eclogites and anorthosites in outer Nordfjord, western Norway. Nor. geol. Unders., 241: 68.

Bryhni, I., 1973. Radiometriske dateringer av bergarter og mineraler i Gneisregionen. Naturen, Oslo, 97: 222-230.

Bryhni, I., 1977. The gneiss region west and northwest of Jotunheimen. In: Heier, K.S. (ed.) The Norwegian Geotraverse Project. Nor. geol. Unders.

Bryhni, I. & Grimstad, E., 1970. Supracrustal and Infracrustal rocks in the gneiss region of the Caledonides west of Breimsvatn. Nor. geol. Unders., 266: 105-140.

Bryhni, I., Fitch, F.J. & Miller, J.A., 1971. Ar^{40}/Ar^{39} dates from recycled Pre-Cambrian rocks in the gneiss region of the Norwegian Caledonides. Nor. geol. Tidsskr., 51: 391-406.

Carswell,D.A., 1973. The age and status of the Basal Gneiss Complex of north-west southern Norway. Nor. geol. Tidsskr., 53, 1: 65-79.

Chapple, W.M., 1968. A mathematical theory of finite-amplitude rock folding. Bull. geol. Soc. Am., 79: 47-68.

Christie, J.M., 1960. Mylonitic rocks of the Moine Thrust Zone in the Assynt region, north-west Scotland. Trans. geol. Soc. Edinburgh, 18: 79-93.

Cobbold, P.R., Cosgrove, J.W. & Summers, J.M., 1971. The development of internal structures in deformed anisotropic rocks. Tectonophysics, 12: 23-53.

Cosgrove, J.W., 1976. The formation of crenulation cleavage. J. geol. Soc. London, 132: 155-178.

Davies, G.J., Edington, J.W., Cutler, C.P. & Padmanaghan, K.A., 1970. Superplasticity - a review. J. Material. Sci., 5: 1091-102.

Dieterich, J.H. & Carter, N.L. 1969. Stress history of folding. Am. J. Sci., 267: 129-54.

Donath, F.A. 1962. Role of layering in geologic deformation. Trans. N.Y. Acad. Sci., 24: 236-249.

Dubey, A.K. & Cobbold, P.R., 1977. Non-cylindrical flexural slip folds in nature and experiment. Tectonophysics, 38: 223-239.

Edington, J.W., Melton, K.N. & Cutler, C.P., 1978. Superplasticity. Prog. Metal. Phys., 21: 63-170.

Elliot, D., 1973. Diffusion flow laws in metamorphic rocks. Bull. geol. Soc. Am., 84, 8: 2645-2664.

Eskola, P. 1921. On the eclogites of Norway. Skr. Nor. Vidensk. Akad. Oslo. KL. I, 8: 118.

Evans, J., 1978. Mapping project in the Småbrekk area, Bergsdalen, W. Norway. Geology Dept. Bedford College, University of London.

Faerseth, R.B., Thon, A., Larsen, S.G., Sivertsen, A. & Elvestad, L., 1977. Geology of the Lower Palaeozoic rocks in the Samnanger-Osterøy area, Major Bergen Arc, Western Norway. Bulletin NGU., 334: 19-58.

Ferguson, C.C. & Harte, B., 1975. Textural patterns at porphyroblast margins and their use in determining the time relations of deformation and crystallization. Geol Mag., 112: 467-80.

Flanagan, F.J., 1973. 1972 values for international geochemical reference samples. Geochim. cosmochim. Acta., 37: 1181-1201.

Floyd, P.A. & Winchester, J.A., 1975. Magma type and tectonic setting discrimination using immobile elements. Earth planet. Sci. Lett., 27: 211-18.

Fraser, D.G., 1977. Thermodynamics in Geology. D. Reidel Publishing Co.

Fyfe, W.S., 1969. Some second thoughts on Al_2O_3 - SiO_2. Am.J. Sci., 267: 291-296.

Fyfe, W.S., Price, N.J., Thompson, A.B., 1978. Developments in Geochemistry 1 Fluids in the Earths Crust. Fyfe, W.S., (ed.), Elsevier.

Gabrielsen, R.H., Naterstad, J. & Råheim, A., 1979. A Rb-Sr study of a possible Precambrian thrust zone, Hardangervidda - Ryfylke Nappe Complex, southwest Norway. Nor. geol. Tidsskr., 59, 3: 253-265.

Gee, D.G. & Wilson, M.R., 1974. The age of orogenic deformation in the Swedish Caledonides. Am. J. Sci., 274: 1-9.

Gee, D.G. & Wilson, M.R., 1976. Reply (To Sturt and Asbjorn 1976). Am. J. Sci., 276: 390-394.

Giletti, B.J., Semet, M.P. & Yund, R.A., 1977. Studies in diffusion - III. Oxygen in feldspars: an ion microprobe determination. Geochim. cosmochim. Acta.: 45-57.

Goldschmit, V.M., 1916. Geologisch - petrographische studien im Hochgebirge des sudlichen Norwegens iv. Ubersicht der Eruptivgesteine im Kaledonischen Gebirge zwischen Stavanger und Trondhjem. Skr. Nor. Vidensk. Acad. 2.

Gray, J., 1978. A structural history and Rb-Sr geochronology of Eksingedalen, W. Norway. Ph.D. Thesis, University of Aberdeen.

Griffin, W.L., 1971. Genesis of coronas in anorthosites of the Upper Jotun Nappe, Indre Sogn, Norway. J. Petrol., VII: 219-243.

Griffin, W.L., 1972. Formation of eclogites and the coronas in anorthosites, Bergen Arcs, Norway. Mem. geol. Soc. Am., 135: 37-63.

Griffin, W.L. & Bryhni, I., 1977. Corona reactions and the eclogite problem. In: Heier, K.S. (ed.), The Norwegian Geotraverse Project. Nor. geol. Unders.

Grubenmann, U. & Niggli, P., 1924. Die Gesteinsmetamorphose. Berntraeger, Berlin: 467pp.

Harker, A., 1939. Metamorphism. Methuen, London.

Heard, H.C., 1960. Transition from brittle to ductile behaviour in Solenhofen Limestone as a function of temperature, confining pressure and interstitial fluid pressure. Mem. geol. Soc. Am., 79: 193-226.

Heard, H.C., 1963. Effect of large changes of strain-rate in the experimental deformation of Yule Marble. J. geol. Chicago, 73: 162-195.

Hartshorne, N.H. & Stuart, A., 1970. Crystals and the Polarising Microscope. (4th Edition), Edward Arnold.

Heim, M., Schürer, U. & Milnes, G., 1977. The Nappe Complex in the Tyin-Bygdin-Vang region, central southern Norway. Nor. geol. Tidsskr., 57: 171-178.

Hepworth, J.V., 1964. Explanation of the geology of sheets 19, 20, 28 and 29. (southern West Nile). Rep. geol. Surv. Uganda, 10.

Hernes, I., 1967. The late Precambrian stratigraphic sequence in the Scandinavian Mountain chain. Geol. Mag., 104: 557-563.

Hernes, I., 1970. Tafjord-Grotli-området og grensen mellom det eldre prekambriske kompleks og den senprekambriske-eokambriske largrekke. Nor. geol. Tidsskr., 50: 261-268.

Higgins, M.W., 1971. Cataclastic Rocks. Prof. Pap. U.S. geol. Surv., 687.

Hiortdahl, T. & Irgens, M., 1862. Geologiske undersøkelser, Bergens omegn. Univ. program 2 halvar Christiana, 1-24.

Hobbs, W.H., 1911. Repeat patterns in the relief and in the structure of the land. Bull. geol. Soc. Am., 22: 123-176.

Hoisaeter, T., 1971. Thrust Devonian sediments in the Kvamshesten area, Western Norway. Geol. Mag., 108(4): 287-292.

Holdaway, M.J., 1971. Stability of andalusite and the Aluminium Silicate phase diagram. Am. J. Sci., 271: 97-131.

Hollister, L.S., 1969. Metastable paragenetic sequence of andalusite, kyanite and sillimanite, Kwoiek area, British Columbia. Am. J. Sci., 267: 352-370.

Holmquist, P.J., 1910. Die Hochgebirgsbildungen am Torne Trask in Lappland. Geol. Füren. Stockholm Forhandl., 32: 913-983.

Holtedahl, O., 1938. Geological observations in the Oppdal-Sunndal-Trollheimen district. Nor. geol. Tidsskr., 18: 29-53.

Horne, J., 1930. Chapters on the geology of Scotland. Oxford Univ. Press. London.

Hossack, J.R., 1972. The geological history of the Grønsennknipa Nappe, Valdres. Bulletin NGU., 281: 1-26.

Hossack, J.R., 1976. Geology and structure of the Beito Window, Valdres. Bulletin NGU., 327: 1-35.

Hossack, J.R., 1978. The correction of stratigraphic sections for tectonic finite strain in the Bygdin area, Norway. J. geol. Soc. London, 135: 229-241.

Hubbert, M.K. & Rubey, W.W., 1959. (1 & 2) Role of fluid pressure in mechanics of overthrust faulting. Bull. geol. Soc. Am., 70: (1) 115-166 (2) 167-206.

Jaeger, J.C., 1956. Elasticity, Fracture and Flow. Science Paperbacks, Methuen & Co. Ltd.

Johnson, M.W.R., 1967. Mylonite zones and mylonite banding. Nature, London, 213: 246-247.

Johnston, R.H., 1970. Superplasticity. Metall. Rev., 15: 115-35.

Kanestrøm, R., 1977. Seismic investigations of the crust and moho in southern Norway. In: Heier, K.S. (ed.) The Norwegian Geotraverse Project. Nor. geol. Unders.: 143.

Kanestrøm, R. & Haugland, K., 1971. Profile Section 3-4. In: Vogel, A. (ed.) Proceedings of the colloquium on Deep Seismic Sounding in N. Europe. Publ. Swedish Nat. Sci. Res. Council.

Keilhau, B.M., 1850. Von mehreren Verfassevn, Herausgegeben v. B.M. Keilhau. Christiania (Oslo).

Kjerulf, T., 1879. Udsigt over det sydige Norges geologi. Univ. program 2, halvar, Christiania (Oslo), 157.

Knill, J.C. & Knill, D.C., 1958. Some discordant fold structures from the Dalradian of Craignish, Argyll and Rosguile, Co. Donegal. Geol. Mag. 95: 497-510.

Kolderup, C.F., 1897. Et orienterende niveau i bergensskifrene. Bergens Mus. Aarsberet. 12: 1-10.

Kolderup, N.H., 1931. Oversikt over den kaledonske fjellkjede pa Vestlandet. Bergens Mus. Aarsberet., No11: 43.

Kolderup, N.H., 1960. The relationship between Cambro-Silurian schists and the gneiss complex in the deep-Caledonides of Sogn and Fjordane, west Norway. In: Dons, J.A. (ed.) Nor. geol. Unders. 212c.

Kolderup, C.F. & Moncton, H.W., 1912. The Geology of the Bergen Arc district, Norway. Proc. geol. Assoc. London. VXXII: 1-60.

Kolderup, C.F. & Kolderup, N.H., 1940. Geology of the Bergen Arc System. Bergens Mus. Skrifter. 20.

Krogh, E.J., 1977. Evidence of Precambrian continent - continent collision in western Norway. Nature, London, 167: 17.

Kvale, A., 1946. Petrologic and structural studies in the Bergsdalen quadrangle. Part I Petrography. Bergens Mus. Aarsberet.

Kvale, A., 1948. Petrologic and structural studies in the Bergsdalen quadrangle. Part II Structural geology. Bergens Mus. Aarsberet.

Kvale, A., 1960. The nappe area of the Caledonides in western Norway. In: Kvale, A. Guide to excursion A7 and C4. 21st Int. Geol. Cong. Nor. geol. Unders. 212e.

Lapworth, C., 1885. The highland controversy in British geology: its causes, course and consequences. Nature, London, 32: 558-559.

March, A., 1932. Mathematische theorie der regelung nach der Rorngestalt bei affiner deformation. Zietschr. Kristallographie, 81: 285-297.

Martins, J.A., 1969. The Precambrian rocks of the Telemark area, in the south central Norway. No.VII The Vradal area. Nor. geol. Unders. Arbok 1968, 258: 267-301.

Means, W.D. & Patterson, M.S., 1966. Experiments on preferred orientation of platy minerals. Contrib. Mineral. Petrol., 13: 108-133.

Mitra, S., 1978. Microscopic deformation mechanisms and flow laws in quartzites within the South Mountain Anticline. J. Geol. Chicago, 86: 129-152.

Miyashiro, A., 1973. Metamorphism and Metamorphic Belts. Publ. George Allen & Unwin.

Moorhouse, S.J. & Moorhouse, V.E., 1979. The Moine amphibolite suites of central and northern Sutherland, Scotland. Mineralog. Mag. London, 43: 211-25.

Muecke, G.K. & Charlesworth, H.A.K., 1966. Jointing in folded Cardium sandstones, along the Bow river, Alberta. Can. J. Earth Sci., 3: 579-96.

Myers, J.S., 1978. Formation of banded gneisses by deformation of igneous rocks. Precambrian Res., 6: 43-64.

McClay, K.R., 1977a. Pressure solution and Coble creep in rocks and minerals: a review. J. geol. Soc. London, 134: 57-70.

McClay, K.R., 1977b. Pressure solution and Coble creep in rocks. J. geol. Soc. London, 134: 71-75.

Naterstad, J., 1976. Comments on the Lower Paleozoic unconformity in west Norway. Am. J. Sci., 276: 394-397.

Naumann, C.F., 1824. Beytrage zur Kenntnisz Norwegens 1-2, Leipzig: 132-191.

Newton, R.C., 1969. Some high-pressure hydrothermal experiments on severely ground kyanite and sillimanite. Am. J. Sci., 267: 278-284.

Nicolas, A. & Poiriev, J.P., 1976. Crystalline Plasticity and Solid State Flow in Metamorphic Rocks. Publ. John Wiley and Sons.

Nilsen, T.H., 1973. The relation of joint patterns to the formation of fjords in western Norway. Nor. geol. Tidsskr., 53: 183-194.

Nilsen, T.H., 1976., Mesozoic rifting of the North Sea region and the formation of the joints on the west coast of Norway. Nor. geol. Tidsskr., 56: 455-456.

O'Nions, R.K. & Heier, K.S., 1972. A reconnaissance Rb-Sr geochronological study of the Kongsberg area, south Norway. Nor. geol. Tidsskr., 52: 143-150.

Peach, B.N., 1930. Chapters on the geology of Scotland. Oxford Univ. Press, London.

Pearce, A.J. & Cann, J.R., 1973. Tectonic setting of basic volcanic rocks determined using trace element analyses. Earth planet. Sci. Lett., 19: 290-300.

Phillips, E.R., 1974. Myrmekite - one hundred years later. Lithos, 7, 3: 181-194.

Pitcher, W.S. & Berger, A.R., 1972. The Geology of Donegal. Publ. John Wiley & Sons.

Powell, D. & Treagus, J.E., 1970. Rotational fabrics in metamorphic minerals. Min. Mag., 37: 801-814.

Powell, D. & MacQueen, J., 1976. Relationships between garnet shape, rotational inclusion fabrics and strain in some Moine metamorphic rocks of Skye, Scotland. Tectonophysics, 35: 391-402.

Powell, R., 1978. Equilibrium Thermodynamics in Petrology (an Introduction). Publ. Harper & Row.

Price, N.J., 1966. Fault and Joint Development in Brittle and Semi-brittle rock. Pergamon Press.

Price, N.J., 1970. Laws of rock behaviour in the Earth's crust. In: Somerton (ed.) Rock mechanics - theory and practice. Proc. 11th Symp. Rock Mech. Berkeley, A.I.M.M.: 1-23.

Price, N.J., 1975. Rates of Deformation. J. geol. Soc. London, 131: 533.

Price, N.J. & Hancock, P., 1972. Development of fracture cleavage and kindred structures. Proc. 24th Int. geol. Congr. Section 3: 584-92.

Priem, H.N.A., Boelrijk, N.A.I.M., Hebeda, E.H., Verdurmen, E.A.Th. & Verschure, R.H., 1973. A note on the geochronology of the Hestbrepiggan granite in west Jotunheimen. Bulletin NGU., 289: 31-35.

Pringle, I.R., Kvale, A. & Anonsen, L.B., 1975. The age of the Hernes Granite, Lower Bergsdalen Nappe, western Norway. Nor. geol. Tidsskr., 55: 191-195.

Quensel, P., 1916. Zur kenntnis der Mylonitbridung. Bull. geol. Instn. Univ. Upsala, 55: 91-116.

Ramberg, H., 1959. Evolution of ptygmatic folding. Nor. geol. Tidsskr., 39: 99-131.

Ramberg, H., 1963. Strain distribution and geometry of folds. Bull. geol. Instn. Univ. Upsala, 42: 3-20.

Ramberg, I.B., 1977. Gravity Interpretation of the Oslo Graben and associated Igneous rocks. Bulletin NGU., 325.

Ramberg, I.B., Gabrielsen, R.H., Larsen, B.T. & Solli, A., 1977. Analysis of fracture patterns in S. Norway. Geol. Mijbouw. 4: 295.

Ramsay, D.M. & Sturt, B.A., 1973. An analysis of noncylindrical and incongruous fold pattern from the Eo-Cambrian rocks of Sørøy, northern Norway. (Part 1 and 2). Tectonophysics, 18 (1) 81-107, (2) 109-121.

Ramsay, J.G., 1962. The geometry and mechanics of formation of 'similar' type folds. J. Geol. Chicago, 70: 309-27.

Ramsay, J.G., 1967. Folding and Fracturing of Rocks. Publ. McGraw-Hill, London.

Ramsay, J.G. & Graham, R.H., 1970. Strain variation in shear belts. Can. J. Earth Sci., 7: 786-813.

Read, H.H., 1962. Rutley's Elements of Mineralogy. Thomas Murby & Co. London.

Reusch, H., 1882. Silurfossiler og pressede konglomerater Bergensskifrene. Univer. program 1. halvar, Christiania (Oslo): 152.

Rhodes, S. & Gayer, R.A., 1977. Non-cylindrical folds, linear structures in the X direction and mylonite developed during translation of the Caledonian Kalak Nappe Complex of Finnmark. Geol. Mag., 114, 5: 329-408.

Rutter, E.H., 1972a. The effects of strain-rate changes on the strength and ductility of Solenhofen Limestone at low temperatures and confining pressures. Int. J. rock Mech. Ming Sci. Geomech. Abstr., 9: 183-189.

Rutter, E.H., 1972b. The influence of interstitial water on the rheological behaviour of calcite rocks. Tectonophysics, 14: 13-33.

Rutter, E.H., 1976, The kinetics of rock deformation by pressure solution. Philos. Trans. R. Soc. London, A283: 203-19.

Ryan, P.D. & Skevington, D., 1976. A re-interpretation of the Late Ordovician - early Silurian stratigraphy of the Dyvikvagen and Ulven-Vaktal areas, HordLand, western Norway. Bulletin NGU., 37, 324.

Sander, B., 1911. Uber Zusammenhange zwischen Teilbewegung und gefuge in Gesteinen. Tschermak's Miner. u. Petr. Mitt., 30: 281-314.

Sander, B., 1912. Uber einege Gesteinsgruppen des Tavernwestendes. Geol. Reichsanst. Jahrb., 62: 249-257.

Sclar, C.B., 1965. Layered mylonites and the process of metamorphic differentiation. Bull. geol. Soc. Am., 76: 611-612.

Sederholm, J.J., 1967. Selected Works, Granites and Migmatites. Publ. Oliver & Boyd, Edinburgh.

Sellevoll, M.A. & Warrick,R.E., 1971. A refraction study of the crustal structure in S. Norway. Bull. Seis. Soc. Am., 61: 457-471.

Serdengecti, S. & Boozer, G.H., 1961. The effects of strain-rate and temperature on the behaviour of rocks subjected to triaxial compression. Proc. 4th Symp. Roch. Mech. Pennsylvania State Univ. 83-98.

Sharma, R.P. & Sturt, B.A., 1977. Geology of the Fana-Krossnes area, west·coast of Norway. Sonderdruck aus der Geologischen Rundschau. Band 66, 1: 62-80.

Sibson, R.H., 1975. Generation of pseudotachylyte by ancient seismic faulting. Geophys. J. R. astron. Soc., 43: 775-94.

Sibson, R.H., 1977. Fault rocks and fault mechanisms. J. geol. Soc. London, 133, 3: 191-215.

Simpson, A., 1964. The metamorphism of the Manx Slate series, Isle of Man. Geol. Mag., 101: 20-36.

Sinha Roy, S., 1977a. Texture pattern at porphyroblast margins. Geol. Mag., 114(2): 147-149.

Sinha Roy, S., 1977b. Deformation and chemical processes in mylonite genesis. Geologiska Foreningens, Stockholm Forhandlingar., 99: 3-9.

Sinha Roy, S., 1977c. Mylonitic microstructures and their bearing on the development of mylonites - an example from deformed trondhjemites of the Bergen Arc region, S.E. Norway. Geol. Mag., 114(6): 445-458.

Skjerlie, F.J., 1968. The Pre-Devonian rocks in the Askvoll-Gaular area and adjacent districts, western Norway. Nor. geol. Unders. Arbok. 258: 325-359.

Smithson, S.B., Ramberg, I.R. & Grönlie, G., 1974. Gravity interpretation of the Jotun Nappe of the Norwegian Caledonides. Tectonophysics., 22: 205-222.

Southern Norway Tectonic Map., 1975. Norwegian Geotechnic Institute, Publ. Bloms Oppmåling A/s.

Spry, A., 1969. Metamorphic Textures. Pergamon Press.

Staub, R., 1915. Petrographische Untersuchungen im westichen Berninagebirge. Vjschr. Naturf. Ges. Zurich, 60: 71-91.

Strand, T., 1969. Geology of the Grotli Area. Nor. geol. Tidsskr., 49: 341-360.

Strand, T., 1972. The Norwegian Caledonides. In: Strand, T. & Kulling, O., Scandinavian Caledonides: 1-148. Publ. Wiley and Sons Ltd.

Sturt, B.A., Skarpenes, O., Ohanian, A.T. & Pringle, I.R., 1975. Reconnaissance Rb/Sr isochron study in the Bergen Arc System and regional implications. Nature, London, 253: 595-599.

Sturt, B.A. & Thon, A., 1976. The age of the orogenic deformation in the Swedish Caledonides, Discussion. Am. J. Sci., 276: 385-390.

Sturt, B.A. & Thon, A., 1978. Caledonides of southern Norway. In: I.G.C.P. Project 27, Norwegian Contribution No. 5E. Caledonian-Appalachian Orogen of the North Atlantic Region. Geol. Surv. Canada, Paper 78-13: 39-47.

Teall, J.J.H., 1918. Dynamic Metamorphism. Proc. geol. Assoc. London, 29: 1-15.

Termier, P. & Boussac, J., 1911. Sur les mylonites de la region de Savonne. C.r. Seances Acad. Sci. Paris, 152: 1550-56.

Torske, T., 1977. The south Norway Precambrian region - A Proterozoic cordilleran-type orogenic segment. Nor. geol. Tidsskr., 57: 97-120.

Vernon, R.H., 1974. Controls of mylonitic compositional layering during non-cataclastic ductile deformation. Geol Mag., VIII (2): 121-123.

Versteeve, A.J., 1975. Isotope geochronology in the high-grade metamorphic Precambrian of southwestern Norway. Bulletin NGU., 318: 1-50.

Voll, G., 1960. New work on petrofabrics. Liverpool Manchester geol. J., 2(3): 503-67.

Weiss, L.E., 1959. Geometry of superposed folding. Bull. geol. Soc. Am., 70: 91-106.

Wenk, R.H., 1976. Electron Microscopy in Mineralogy. Publ. Springer-Verlag.

Westwood, A.R.G., Goldheim, D.L. and Lye, R.G., 1967. Rebinder effects in MgO. Philos. Mag., 16: 505-19.

White, S., 1971. Natural creep deformation in quartzites. Nature (Phys. Sci.) 234: 175-77.

White, S., 1973a. The dislocation structures responsible for the optical effects in some naturally deformed quartzes. J. Mat. Sci., 8: 490-9.

White, S., 1973b. Syntectonic recrystallization and texture development in quartz. Nature, London, 244: 276-78.

White, S., 1973c. Deformation lamellae in naturally deformed quartz. Nature (Phys. Sci.) 245: 26-28.

White, S., 1975a. Effect of polyphase deformation on the defect structures in quartz II. Neues Jahrb. Mineral. Abhandlungen. 123: 237-252.

White, S., 1975b. Estimation of strain rates from microstructures. J. geol. Soc. London, 131(6): 577-585.

White, S., 1976. The effects of strain on the microstructures, fabrics and deformation mechanisms in quartzite. Philos. Trans. R. Soc. London, A283: 69-86.

White, S. & Treagus, J.E., 1975. Effect of polyphase deformation on the defect structures in quartz I. Neues Jahrb. Mineral. Abhandlungen. 123: 219-236.

White, S. & Knipe, R.J., 1978. Transformation - and reaction - enhanced ductility in rocks. J. geol. Soc. London, 135(5): 513-516.

Winkler, H.G.F., 1974. Petrogenesis of Metamorphic Rocks. Publ. Springer-Verlag.

Winter, D.A., 1978. Report on field mapping in Bergsdalen, W. Norway. Geology Department, Bedford College, University of London.

Zussman, J., 1967. Physical Methods in determinative mineralogy. Publ. Academic Press.

APPENDIX 1

RADIOMETRIC DATING

Two sets of samples from the North Osterøy Gneisses were selected for

Rb/Sr whole rock radiometric dating:

1		2	
AGII 3		FH 4	From
AGII 5	From	FH 5	the structurally
AGII 8	the	FH C	oldest portion of the
AGII 9	Southern Gneiss Unit	FH F	Northern Gneiss Unit
AGII 12		FH G	
AGII 13		FH N	

The second group was a suite of background gneisses and did not

provide any useful data.

The first group was taken from the augen gneiss body outcropping at

(10.30, 28.00) and this plotted as shown in figure 157. The plot does

not constitute an acceptable isocron but it does provide a rough indi-

cation of an age for the suite as shown. The high $^{87}Sr/^{86}Sr$ initial

ratio indicates the gneisses, which are determined to be of igneous

origin from their petrological and structural characteristics, must be

derived from Precambrian crustal material.

While the age obtained is meaningless by itself, it does correlate

with similar ages on similar bodies cropping out to the north-east of

Osterøy (Grey 1973), and furnishes an example of how difficult gneisses

can be to date. Even if it were an isocron it would be difficult to

decide whether the age represents the time of original intrusion or the

close of the last almandine amphibolite facies metamorphism affecting

the rocks.

Fig 157.

WHOLE ROCK Rb/Sr PLOT FOR THE FH, AG II

AUGEN   GNEISS GROUP

YORK-WILLIAMSON LEAST SQUARES FIT

A G II GROUP

Line	87Rb/86Sr	s.d.	87Sr/86Sr	s.d.	rho	Xres	Yres	Sample
1	1.542	.008	.72717	.00015	0.00	.00775	-.00024	AG II 13
2	1.611	.008	.72895	.00015	0.00	.03307	-.00096	A G 12
3	1.667	.008	.72706	.00015	0.00	-.03133	.00084	A G II 8
4	.716	.004	.71772	.00014	0.00	.00162	-.00023	A G II 9
5	1.226	.006	.72261	.00014	0.00	-.01062	.00052	A G II 3
6	1.502	.008	.72630	.00015	0.00	-.00188	.00006	A G II 5

No. of cycles 3
Centroid is   1.341   .72456
Slope   .011340 .000270
Intercept   .70935   .00020
MSWD=   32.56
Variance ratio (F)=   32.21
AGE   794.08+- 18.82 Ma (1-sigma)
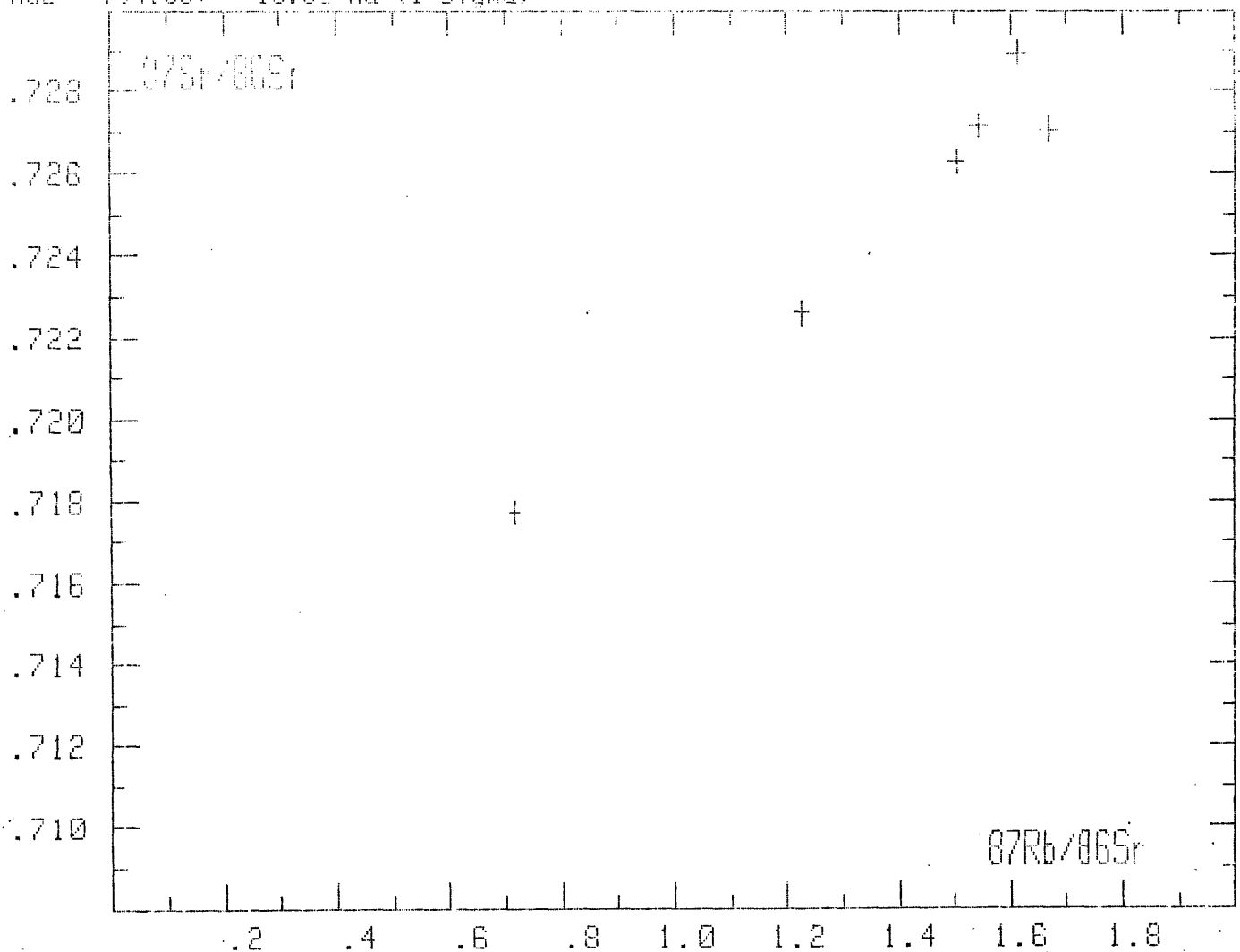
The total Rb/Sr ratios for these rocks were determined by XRF analysis at Bedford College and the isotopic ratios determined by mass spectrometry at Cambridge University. The wet chemistry for this was done by Mr H. Lloyd.

APPENDIX 2

GEOCHEMISTRY AND TECHNIQUES

Analyses were performed on the specimens listed below:

Rock No.	Grid References		
	X	Y	
FH 4	11.58	34.97	Pink banded acid gneiss
FH 8	11.27	34.76	Fine grained biotitic amphibolite
FH 9	11.85	35.13	Micaceous gneiss
FH 11	4.40	32.90	Fine grained amphibolite
FH 12	4.57	32.85	Mica schist
FH 12*SP	12.79	23.02	Fine grained amphibolite
FH 14	6.58	31.19	Fine grained acid gneiss
FH 16	6.00	31.71	Fine grained amphibolite
FH 19	8.13	30.24	Medium grained amphibolite
FH23	7.4	30.51	Garnetiferous mica schist
FH 27*SP	14.26	21.08	Medium grained amphibolite
FH 27	6.71	31.38	Medium grained amphibolite
FH 28	6.87	31.57	Medium grained amphibolite
FH 29	5.52	32.56	Medium grained amphibolite
FH 42	6.49	33.70	Intermediate gneisses
FH 43	6.31	33.72	Acid medium grained gneiss
FH 46	7.08	33.68	Intermediate gneiss
FH 60	7.98	29.92	Fine grained acid gneiss
FH 63	7.90	29.82	Fine grained acid gneiss
FH 69	7.90	29.82	Fine grained acid gneiss
FHAGII 12	9.4	28.83	Granodioritic augen gneiss
FH S1-2	7.87	30.62	Medium grained amphibolite
SH S1-6	5.93	32.34	Medium grained amphibolite
FH M1	5.14	32.30	Granodioritic augen gneiss mylonite
FH M2	"	"	" " " "
FH M3	"	"	" " " "
FH GM1	16.20	48.0	Coarse grained amphibolite
FH GM2	"	"	" " "
FH GM3	"	"	" " "
FH GM4	"	"	" " "
FH C	11.43	34.87	Fine grained amphibolite
FH E	11.45	34.90	Fine grained amphibolite
FH 3	11.74	35.06	Intermediate gneiss
FH A8	9.43	30.05	Microcline hornblendite
FH A11	9.48	29.26	Hornblendite
FH A14	14.41	30.87	Fine grained acid gneiss
FH A26	11.07	26.45	Fine grained acid gneiss
FH A28	10.74	25.74	Epidote
FH A29	12.02	24.73	Garnet bearing amphibolite
FH 39	12.62	38.34	Medium grained acid gneiss
FH A53	14.92	37.80	Coarse grained amphibolite
FH A56	15.15	33.24	Medium grained amphibolite

Rock No.	Grid Reference		Rock Type
	X	Y	
FH A56A	15.15	33.24	Medium grained amphibolite
FH A71	12.55	28.73	Medium grained amphibolite
FH A82	14.87	22.56	Intermediate gneiss
FH A83	15.28	22.81	Dark gneiss from quartz vein
FH A88	11.76	35.44	Acid medium grained gneiss
FH B14	15.40	18.00	Medium grained amphibolite
FH B21	20.20	12.80	Medium grained amphibolite
FH B23	21.70	3.95	Fine grained acid gneiss
FH B28	19.80	7.50	Garnetiferous mica schist
FH B29-9	19.20	9.25	High mylonitised intermediate gneiss
FH B29-8	19.20	9.25	Augen gneiss
FH B29-7	19.20	9.25	Augen gneiss
FH B29-6	19.20	9.25	Augen gneiss
FH B29-5	19.20	9.25	Augen gneiss
FH B29-4	19.20	9.25	Augen gneiss
FH B29-3	19.20	9.25	Augen gneiss
FH B29-2	19.20	9.25	Augen gneiss
FH B29-1	19.20	9.25	Intermediate augen gneiss
FH B34	17.03	13.98	Fine grained amphibolite
FH B49	21.30	33.80	Coarse grained amphibolite
FH B55	19.40	35.20	Medium grained amphibolite
FH B61	22.70	52.00	Medium grained amphibolite
FH B63	22.74	51.95	Coarse grained amphibolite
FH B65	22.53	51.70	Coarse grained amphibolite
FH B66	21.70	50.70	Pyritized amphibolite
FH B71	20.30	40.10	Medium grained amphibolite
FH B72	21.90	46.40	Augen gneiss intermediate
FH B74	23.60	43.40	Fine grained acid gneiss
FH B81	20.40	38.30	Medium grained amphibolite
FH B85	14.65	44.63	Medium grained amphibolite
FH B89	11.13	36.05	Medium grained amphibolite
FH C13	9.25	34.37	Medium grained acid gneiss
FH C24	11.45	34.90	Fine grained amphibolite
FH C25	11.45	34.90	Fine grained amphibolite
FH C26	11.74	35.06	Fine grained amphibolite
FH C27	11.75	35.10	Fine grained acid gneiss
FH C34	-	-	Mangerite

For a complete list of specimens considered and their locations see the microfiche included in Volume 2.

Specimens for Geochemical analysis were prepared using a roll jaw crusher and agate tema, these were thoroughly washed and dried between each specimen. The analytical method used was X-Ray Fluorescence Analysis on a Philips PW1212 X-Ray spectrometer. The powdered samples were prepared for analysis in two ways; for

restricted major element analysis and trace element analysis, 6 grams
of rock powder was mixed with 1 gram of PF Bakalite resin then pressed
into a pellet at 15 tons. The pellets were then hardened for 20
minutes at 105°C in an oven.

For major element analysis 0.4 grams of rock powder was weighed
with 2.4 grams of Johnson Matthey Spectraflux 104 in a Platinum Gould
crucible, and fused at 1000°C in a furnace. Duplicate samples were
weighed in each case. The fusion was then formed into a bead while
still molten, using a former and press heated to 200°C. As the beads
are hydroscopic, the samples were cooled in a desiccator and analysed
as soon as possible after preparation.

The Bedford College Spectrometer had no previous calibration for
rocks with silica contents as high as those for some of the specimens
from North Osterøy. A calibration therefore was erected using Pub-
lished standards (Abby, 1978; Flannagan, 1973) and a set of rocks
from the Osterøy Gneisses. These had been previously analysed (by
Mr H. Lloyd) using standard wet chemical techniques. Published stan-
dards were also analysed with my samples to check the calibration
and instrumental drift. The results on these checks (figs.159-163)
show good correlations between determined chemistry and the published
analyses.

The analyses determined from the samples listed above are given
in figures 164-169. Attempts at interpretation of the meaning of
these analyses in the Osterøy context did not prove fruitful so no
further analyses on the CO_2, F, H_2O+, H_2O- or FeO_2 contents of the
rocks were made. This accounts for the low totals seen in some of
the analyses.

Figure 159

TABLE OF ANALYSES CHECKS

	GSP-1 PUBLISHED	GSP-1 XRF	AGV-1 PUBLISHED	AGV-1 XRF	BCR-1 PUBLISHED	BCR-1 XRF	W-1 PUBLISHED	W-1 XRF	PCC-1 PUBLISHED	PCC-1 XRF
ROCK NAME										
SiO_2	-	-	-	-	-	-	-	-	-	-
TiO_2	0.66	0.69	1.05	1.06	2.22	2.18	1.07	1.02	0.015	0.04
Al_2O_3	-	-	-	-	-	-	-	-	-	-
Fe_2O_3	4.33	4.18	6.84	6.74	13.52	12.92	11.11	10.20	8.28	11.83
MnO	-	-	-	-	-	-	-	-	-	-
MgO	-	-	-	-	-	-	-	-	-	-
CaO	2.02	2.06	5.00	4.86	6.98	7.14	10.98	11.00	0.53	0.35
Na_2O	-	-	-	-	-	-	-	-	-	-
K_2O	5.53	5.52	2.93	2.91	1.68	1.86	0.64	0.70	0.0	0.00
P_2O_5	0.28	0.26	0.50	0.48	0.33	0.38	0.14	0.19	0.00	0.03
TOTAL	12.82	12.71	16.32	16.05	24.73	24.48	23.94	23.11	8.795	12.25
Zr	500	509	225	212	185	161	105	82		
Y	30.4	34	21.3	18	37.1	37	25	22		
Rb	254	243	67	69	47	44	21	19		
Nb	29	17	13	14	12	12	9.5	6		
Sr	233	236	657	667	330	318	190	186		

Figure 160

TABLE OF ANALYSES CHECKS

	ROCK NAME SY 1		ROCK NAME G2		ROCK NAME 5081 NIMP		ROCK NAME 5088 NIMN		ROCK NAME 5079 NIMG	
	PUBLISHED	XRF	PUBLISHED	XRF	PUBLISHED	XRF	PUBLISHED	XRF	PUBLISHED	XRF
SiO_2	-	-	69.19	69.25	51.04	50.57	52.55	52.89	75.72	76.17
TiO_2	0.49	0.35	0.50	0.51	0.20	0.20	0.20	0.21	0.09	0.10
Al_2O_3	-	-	15.35	15.32	4.19	4.30	16.54	16.67	12.09	12.25
Fe_2O_3	8.21	7.14	2.67	2.64	12.76	11.67	8.91	8.85	2.02	2.00
MnO	-	-	0.04	0.04	0.22	0.21	0.18	0.17	0.02	0.02
MgO	-	-	0.77	0.74	25.29	24.95	7.48	7.66	0.04	0.03
CaO	10.2	9.11	1.98	1.88	2.69	2.59	11.46	11.46	0.78	0.76
Na_2O	-	-	4.06	4.12	0.37	0.35	2.46	2.40	3.30	3.32
K_2O	2.67	2.62	4.52	4.35	0.09	0.11	0.25	0.27	5.00	4.96
P_2O_5	0.22	0.26	0.14	0.12	0.03	0.07	0.03	0.10	0.02	0.01
TOTAL	21.79	19.48	99.22	98.97	96.88	95.02	100.07	100.68	99.08	99.62
Zr			300	308						
Y			12	14						
Rb			168	164						
Nb			13.5	11						
Sr			479	486						

Figure 161

TABLE OF ANALYSES CHECKS

ROCK NAME	5078 NIMD		5077 W5		FHAGII 12		FH E		FH J	
	PUBLISHED	XRF	PUBLISHED	XRF	WET CHEMISTRY	XRF	WET CHEMISTRY	XRF	WET CHEMISTRY	XRF
SiO_2	38.88	39.32	55.35	55.53	65.65	55.67	57.67	57.81	76.07	76.00
TiO_2	0.02	0.02	1.46	1.41	0.70	0.70	1.33	1.29	0.09	0.05
Al_2O_3	0.32	0.44	15.52	14.99	16.16	16.08	14.23	14.41	12.80	12.70
Fe_2O_3	16.96	17.17	10.32	10.38	3.33	3.32	9.50	9.52	0.67	0.68
MnO	0.22	0.22	0.23	0.23	0.087	0.07	0.22	0.20	0.16	0.02
MgO	43.56	43.35	3.80	3.92	0.75	0.71	4.22	4.27	0.16	0.11
CaO	0.28	0.33	4.70	4.57	1.30	1.31	4.92	4.81	0.94	0.94
Na_2O	0.05	0.08	5.52	5.34	4.31	4.28	2.30	2.25	2.65	2.57
K_2O	0.01	0.04	3.28	3.29	5.92	6.01	3.26	3.22	6.04	6.01
P_2O_5	0.02	0.01	0.19	0.30	0.18	0.15	0.50	0.40	0.011	0.00
TOTAL	100.32	101.01	100.37	99.96	98.387	98.30	98.15	98.18	99.447	99.08

Figure 162

TABLE OF ANALYSES CHECKS

	ROCK NAME FH 4		ROCK NAME FH 9		ROCK NAME FH 14		ROCK NAME FH 23		ROCK NAME FH 29	
	WET CHEMISTRY	XRF	WET CHEMISTRY	XRF	WET CHEMISTRY	XRF	WET CHEMISTRY	XRF	WET CHEMISTRY	XRF
SiO_2	67.52	67.67	77.68	77.59	79.61	79.41	57.67	58.05	52.28	52.36
TiO_2	0.40	0.42	0.10	0.08	0.38	0.40	1.06	1.05	1.03	0.99
Al_2O_3	17.04	16.73	11.84	11.93	9.81	9.95	20.62	20.79	14.66	14.81
Fe_2O_3	2.08	2.11	0.76	0.77	1.95	1.95	8.71	8.66	9.20	9.25
MnO	0.056	0.05	0.017	0.01	0.023	0.02	0.098	0.08	0.18	0.16
MgO	0.56	0.55	0.26	0.23	0.33	0.33	1.98	2.11	7.50	7.63
CaO	1.95	1.93	0.53	0.52	0.35	0.36	0.78	0.80	8.17	8.18
Na_2O	3.99	4.06	2.72	2.67	1.45	1.46	0.85	0.89	3.36	3.34
K_2O	5.73	5.70	5.04	5.06	5.33	5.34	4.98	4.98	1.78	1.75
P_2O_5	0.10	0.07	0.007	0.00	0.067	0.05	0.27	0.23	0.13	0.17
TOTAL	99.426	99.29	98.954	98.86	99.300	99.27	97.018	97.64	98.29	98.64

Figure 163

TABLE OF ANALYSES CHECKS

	ROCK NAME FH 42		ROCK NAME FH 43		ROCK NAME FH 50	
	WET CHEMISTRY	XRF	WET CHEMISTRY	XRF	WET CHEMISTRY	XRF
SiO_2	75.86	76.05	68.58	68.96	43.41	43.14
TiO_2	0.28	0.28	0.44	0.43	1.65	1.65
Al_2O_3	12.17	12.21	15.96	15.89	18.48	18.61
Fe_2O_3	1.91	1.94	2.84	2.85	13.92	13.88
MnO	0.024	0.02	0.057	0.05	0.26	0.25
MgO	0.20	0.17	0.94	0.85	8.30	8.30
CaO	0.72	0.70	3.45	3.51	8.19	8.18
Na_2O	4.04	4.06	4.70	4.76	2.29	2.29
K_2O	4.11	4.16	2.02	1.99	0.99	1.00
P_2O_5	0.023	0.01	0.13	0.11	0.21	0.22
TOTAL	98.617	99.60	99.117	99.40	97.70	97.52

Figure 164

MAJOR ELEMENT ANALYSES

	1	2	3	4	5	6	7	8	9	10	11	12	13	14
SiO_2	67.67	54.80	77.59	.00	.00	46.29	79.41	46.29	.00	58.05	.00	.00	43.20	52.36
TiO_2	.42	1.57	.08	2.21	.31	2.09	.40	2.53	.50	1.05	2.93	2.71	2.41	.99
Al_2O_3	16.73	10.65	11.93	.00	.00	13.31	9.95	15.74	.00	20.79	.00	.00	14.27	14.81
Fe_2O_3	2.11	14.02	.77	14.67	10.37	15.38	1.95	13.06	7.48	8.66	16.36	17.24	15.52	9.25
MnO	.05	.29	.01	.00	.00	.18	.02	.18	.00	.08	.00	.00	.19	.16
MgO	.55	4.58	.23	.00	.00	5.41	.33	6.33	.00	2.11	.00	.00	5.78	7.63
CaO	1.93	7.71	.52	8.59	7.21	7.68	.36	5.88	9.70	.80	7.65	7.50	8.69	8.18
Na_2O	4.06	2.29	2.67	.00	.00	1.84	1.46	4.03	.00	.89	.00	.00	.07	3.34
K_2O	5.70	2.20	5.06	1.77	5.78	5.31	5.34	2.11	.30	4.98	5.03	1.43	4.90	1.75
P_2O_5	.07	.46	.00	.42	.19	.55	.05	.49	.10	.23	3.46	.56	.67	.17
TOTAL	99.29	98.57	98.86	27.66	24.86	98.04	99.27	96.64	18.08	97.64	35.43	29.44	95.70	98.64
F/F+M	.793	.754	.770	※	※	.740	.855	.574	※	.804	※	※	.729	.548

TRACE ELEMENT ANALYSES PPM

	1	2	3	4	5	6	7	8	9	10	11	12	13	14
ZR	245	140	209	145	73	198	227	169	19	247	694	136	226	57
Y	32	39	5	34	19	61	25	33	6	66	132	30	48	16
RB	181	281	149	100	178	266	253	80	8	176	369	43	255	61
NB	14	8	1	11	6	16	10	20	1	30	18	15	6	2
SR	412	385	194	347	345	67	67	439	723	103	77	344	242	334
TI/ZR	10	67	2	91	107	63	10	89	157	25	25	119	63	104
Y/ZR	.13	.28	.02	.23	.26	.31	.11	.20	.32	.27	.19	.22	.21	.28

1	FH4
2	FH8
3	FH9
4	FH11
5	FH12
6	FH12※
7	FH14
8	FH16
9	FH19
10	FH23
11	FH27※
12	FH27
13	FH28
14	FH29

TABLE OF GEOCHEMICAL LISTINGS

Figure 165

MAJOR ELEMENT ANALYSES

	15	16	17	18	19	20	21	22	23	24	25	26	27	28
SIO2	76.05	68.96	.00	43.14	.00	.00	65.67	44.75	.00	63.66	72.65	72.75	.00	.00
TIO2	.28	.43	2.15	1.42	3.04	1.93	.70	.64	.63	1.06	.32	.31	.33	.38
AL2O3	12.21	15.89	.00	18.61	.00	.00	16.08	19.10	.00	14.80	13.83	13.55	.00	.00
FE2O3	1.94	2.85	13.60	13.88	16.63	11.80	3.32	7.58	9.35	4.90	1.98	1.77	9.80	10.10
MNO	.02	.05	.00	.25	.00	.00	.07	.10	.00	.09	.05	.03	.00	.00
MGO	.17	.85	.00	8.30	.00	.00	.71	11.74	.00	1.21	.44	.24	.00	.00
CAO	.70	3.51	7.62	8.18	5.50	6.29	1.31	8.56	7.92	2.57	1.06	.41	12.81	11.21
NA2O	4.06	4.76	.00	2.29	.00	.00	4.28	2.30	.00	4.13	3.68	3.93	.00	.00
K2O	4.16	1.99	1.78	1.00	5.04	3.39	6.01	.47	.63	4.93	5.08	5.45	.55	1.06
P2O5	.01	.11	.65	.22	.57	.44	.15	.13	.12	.38	.05	.03	.10	.09
TOTAL	99.60	99.40	25.80	97.52	30.78	23.90	98.30	95.37	18.65	97.73	99.14	98.47	23.59	22.84
F/F+M	.919	.770	*	.626	*	*	.824	.392	*	.802	.818	.881	*	*

TRACE ELEMENT ANALYSES PPM

	15	16	17	18	19	20	21	22	23	24	25	26	27	28
ZR	407	151	110	88	176	166	631	23	26	470	196	318	25	29
Y	48	14	31	23	38	40	73	8	8	70	38	32	21	19
RB	169	59	29	20	231	100	173	14	29	149	156	165	11	48
NB	17	4	4	9	19	10	34	2	-0	31	9	12	4	7
SR	40	540	694	331	240	335	291	699	553	428	170	62	67	46
TI/ZR	4	17	117	112	103	71	6	166	145	13	9	5	79	78
Y/ZR	.12	.09	.28	.26	.22	.24	.12	.35	.31	.15	.19	.10	.84	.66

15	FH42
16	FH43
17	FH46
18	FH60
19	FH63
20	FH69
21	FHAG2
22	FHSI2
23	FHSI6
24	FHM1
25	FHM2
26	FHM3
27	FHGM1
28	FHGM2

TABLE OF GEOCHEMICAL LISTINGS

Figure 166

TABLE OF GEOCHEMICAL LISTINGS

MAJOR ELEMENT ANALYSES

	29	30	31	32	33	34	35	36	37	38	39	40	41	42
SIO2	52.25	.00	.00	57..1	76.00	.00	.00	.00	.00	39.95	47.36	.00	44.48	.00
TIO2	.76	.53	1.78	1.29	.05	1.52	2.38	2.27	.92	1.55	2.89	1.37	2.88	2.30
AL2O3	12.72	.00	.00	14.41	12.70	.00	.00	.00	.00	20.53	12.15	.00	16.02	.00
FE2O3	9.30	9.74	11.03	9.52	.68	14.38	16.50	14.44	7.04	12.11	18.84	8.50	15.38	13.21
MNO	.17	.00	.00	.20	.02	.00	.00	.00	.00	.12	.23	.00	.17	.00
MGO	8.86	.00	.00	4.27	.11	.00	.00	.00	.00	.98	4.65	.00	5.62	.00
CAO	9.42	5.66	6.82	4.81	.94	8.00	9.04	6.59	3.81	18.48	9.38	3.92	7.99	8.67
NA2O	2.89	.00	.00	2.25	2.57	.00	.00	.00	.00	1.44	.93	.00	3.47	.00
K2O	1.56	1.47	3.57	3.22	6.01	2.25	.85	4.35	2.27	.33	1.53	4.56	.71	.70
P2O5	.18	.10	.38	.40	.00	.50	.43	.38	.23	.35	.47	.53	.47	.62
TOTAL	98.11	17.50	23.58	98.18	99.08	26.65	29.20	28.03	14.17	95.84	98.43	18.88	97.19	25.50
F/F+M	.512	*	*	.690	.861	*	*	*	*	.925	.802	*	.732	*

TRACE ELEMENT ANALYSES PPM

	29	30	31	32	33	34	35	36	37	38	39	40	41	42
ZR	43	40	118	126	88	291	176	145	173	77	169	435	95	84
Y	94	30	27	31	2	94	44	45	33	34	56	84	26	35
RB	100	75	189	230	172	58	27	173	135	6	57	137	5	17
NB	35	12	28	8	-0	26	6	5	9	10	5	38	8	8
SR	29	356	659	316	264	46	221	383	406	1102	64	603	611	613
TI/ZR	105	79	90	61	3	31	81	93	28	120	102	18	181	164
Y/ZR	2.19	.75	.23	.25	.02	.32	.25	.31	.19	.44	.33	.19	.27	.42

29	FHGM3
30	FHGM4
31	FHC
32	FHE
33	FHJ
34	FHA8
35	FHA11
36	FHA14
37	FHA26
38	FHA28
39	FHA29
40	FHA39
41	FHA53
42	FHA56*

Figure 167

MAJOR ELEMENT ANALYSES

	43	44	45	46	47	48	49	50	51	52	53	54	55	56
SIO2	52.93	.00	.00	.00	.00	75.82	.00	80.90	.00	72.47	74.60	71.66	69.85	66.85
TIO2	.64	1.10	2.41	2.02	.84	.18	2.45	.18	3.20	.31	.21	.28	.38	.56
AL2O3	7.75	.00	.00	.00	.00	12.44	.00	7.55	.00	13.54	13.21	13.40	15.45	15.94
FE2O3	11.46	9.63	14.09	9.75	10.13	1.07	15.45	1.12	15.59	1.72	1.15	1.44	1.89	4.01
MNO	.39	.00	.00	.00	.00	.04	.00	.04	.00	.05	.04	.05	.05	.08
MGO	13.56	.00	.00	.00	.00	.03	.00	.80	.00	.24	.12	.20	.46	.89
CAO	8.25	5.19	7.98	6.35	5.50	.48	8.37	1.36	7.96	1.02	.49	2.49	1.85	2.54
NA2O	.62	.00	.00	.00	.00	3.60	.00	.39	.00	3.92	3.88	3.97	4.02	4.29
K2O	2.02	3.60	1.26	2.02	3.63	5.04	3.25	4.97	.96	5.01	5.11	5.08	5.20	4.22
P2O5	.10	.28	.60	2.89	.20	.00	.92	.02	.76	.04	.01	.04	.08	.14
TOTAL	97.72	19.80	26.34	23.03	20.30	98.70	30.44	97.33	28.47	98.32	98.82	98.61	99.23	99.52
F/F+M	.458	※	※	※	※	.973	※	.583	※	.878	.906	.878	.804	.818

TRACE ELEMENT ANALYSES PPM

	43	44	45	46	47	48	49	50	51	52	53	54	55	56
ZR	80	145	94	635	83	180	227	266	129	253	189	250	230	307
Y	24	31	20	29	29	43	45	26	35	40	44	40	35	46
RB	56	142	32	92	254	186	127	117	18	169	170	155	192	137
NB	5	8	8	18	6	11	8	7	8	12	12	1-	9	12
SR	274	278	615	329	241	38	174	101	588	99	52	88	204	225
TI/ZR	47	45	153	19	60	5	64	4	148	7	6	6	9	10
Y/ZR	.30	.21	.21	.05	.35	.24	.20	.10	.27	.16	.23	.16	.15	.15

43	FHA56
44	FHA71
45	FHA87
46	FHA83
47	FHA88
48	FHB14
49	FHB21
50	FHB23
51	FHB28
52	FHB29
53	FHB29
54	FHB29
55	FHB29
56	FHB29

TABLE OF GEOCHEMICAL LISTINGS

Figure 168

MAJOR ELEMENT ANALYSES

	57	58	59	60	61	62	63	64	65	66	67	68	69	70
SIO2	66.73	61.10	65.27	67.52	52.73	44.96	.00	.00	.00	.00	.00	.00	.00	.00
TIO2	.59	.66	.66	.53	1.68	2.46	1.90	2.31	2.99	3.30	1.12	2.79	.98	1.09
AL2O3	15.45	19.02	16.25	15.90	14.69	16.26	.00	.00	.00	.00	.00	.00	.00	.00
FE2O3	4.07	4.35	4.54	3.64	10.60	15.10	14.02	14.18	15.09	16.35	10.94	14.85	6.02	9.56
MNO	.07	.08	.08	.06	.13	.18	.00	.00	.00	.00	.00	.00	.00	.00
MGO	.80	.97	.96	.74	3.81	6.80	.00	.00	.00	.00	.00	.00	.00	.00
CAO	2.49	2.66	3.04	2.42	5.94	7.86	8.06	7.97	6.58	7.94	4.01	8.27	3.41	4.21
NA2O	4.21	5.09	4.39	4.28	3.10	3.50	.00	.00	.00	.00	.00	.00	.00	.00
K2O	3.83	5.47	3.87	4.37	4.11	1.01	1.41	2.81	3.68	1.20	3.77	1.10	2.97	1.98
P2O5	.14	.17	.17	.13	.81	.41	.58	.94	.98	.62	.28	.73	.33	.40
TOTAL	98.38	99.57	99.23	99.59	97.60	98.54	25.97	28.21	29.32	29.41	20.12	27.74	13.71	17.24
F/F+M	.836	.818	.825	.831	.736	.689	*	*	*	*	*	*	*	*

TRACE ELEMENT ANALYSES PPM

	57	58	59	60	61	62	63	64	65	66	67	68	69	70
ZR	317	377	347	295	271	77	90	110	143	197	370	120	279	124
Y	47	58	47	39	47	20	28	28	40	42	61	31	39	31
RB	123	169	111	135	242	25	44	64	117	42	187	24	85	82
NB	13	15	16	12	16	5	4	3	10	7	21	6	10	8
SR	225	247	277	258	334	641	443	676	353	257	832	588	403	642
TI/ZR	11	10	11	10	37	191	126	125	125	100	18	139	21	52
Y/ZR	.15	.15	.14	.13	.17	.26	.31	.25	.28	.21	.16	.26	.14	.25

57	FHB29
58	FHB29
59	FHB29
60	FHB29
61	FHB34
62	FHB49
63	FHB55
64	FHB61
65	FHB63
66	FHB65
67	FHB66
68	FHB71
69	FHB72
70	FHB74

TABLE OF GEOCHEMICAL LISTINGS

Figure 169

MAJOR ELEMENT ANALYSES

	71	72	73	74	75	76	77	78	79
SIO2	45.27	.00	.00	67.44	.00	.00	.00	.00	.00
TIO2	2.80	.40	2.10	.47	2.92	2.86	3.30	1.75	1.52
AL2O3	15.70	.00	.00	14.72	.00	.00	.00	.00	.00
FE2O3	15.27	9.59	14.77	4.20	14.65	14.52	16.00	13.04	8.64
MNO	.18	.00	.00	.07	.00	.00	.00	.00	.00
MGO	5.28	.00	.00	1.53	.00	.00	.00	.00	.00
CAO	7.27	9.74	9.40	2.19	7.55	7.64	7.92	5.53	4.12
NA2O	3.71	.00	.00	4.36	.00	.00	.00	.00	.00
K2O	1.95	1.05	1.26	2.88	2.62	1.71	1.50	5.06	4.25
P2O5	.56	.08	.36	.16	.73	.76	1.04	.73	1.17
TOTAL	97.99	20.86	27.89	98.02	28.47	27.49	29.76	26.11	19.70
F/F+M	.743	*	*	.733	*	*	*	*	*

TRACE ELEMENT ANALYSES PPM

	71	72	73	74	75	76	77	78	79
ZR	115	51	134	129	121	120	146	141	342
Y	30	46	31	26	28	30	38	47	30
RB	47	52	40	92	64	34	40	313	80
NB	6	9	11	10	8	10	10	6	21
SR	613	41	316	364	473	576	512	358	1517
TI/ZR	145	47	93	21	144	142	135	74	26
Y/ZR	.26	.90	.23	.20	.23	.25	.26	.33	.09

71 FHB81
72 FHB85
73 FHB89
74 FHC13
75 FHC24
76 FHC25
77 FHC26
78 FHC27
79 FHC34

TABLE OF GEOCHEMICAL LISTINGS

APPENDIX 3

MINERAL IDENTIFICATION AND TECHNIQUES

Most minerals were identified using standard transmitted light techniques on rock slices (0.03 mm thick) using a Leitz polarising microscope. The relative abundance of mineral species was largely estimated visually, with regular checks on the accuracy of estimation using a mechanical stage and point counter.

Where difficulty was found in identifying minerals, alternative techniques were employed: if a sample of the pure mineral was not easily obtainable from the crushed rock, the Universal Stage was used to determine the precise optical characteristics; where a pure sample could be obtained, by magnetic separation or heavy liquid separation and hand picking, the RI of the mineral was determined using RI liquids, an Abbe Refractometer and spindle stage; if enough of the sample was obtained, an X-Ray Powder Photograph, from which the "d" spacings were calculated, was made of the finely powdered sample. The photographs were taken with a Phillips 14.6 mm radius Debye-Scherrer camera with a Straumanis film mounting, in Ni filtered $Cu(K\alpha)$ radiation.

The Universal stage was also used to determine the optical orientation of quartz crystals, this being done to determine whether there be any crystallographic fabric present in the rocks. The technique was applied to three right angle sections cut from field oriented specimens.

Details of the techniques used are to be found in (Hartshorne and Stuart, 1970), (Zussman, 1967).

APPENDIX 4

STRUCTURAL ANALYSIS

The nature of the project and the volume of readings made manual manipulation of structural data impractical. It was therefore decided to employ the aid of a computer to process it. To this end a data base was created, and stored on file in the computer. This contained all the structural information on a grid referenced basis (see program instructions below).

A fortran program (Sort 2) was then written to handle and sort this data on the basis of either structural type or grid reference and structural type.

The data were then plotted onto a stereo net, programs to do this have already been written, and to avoid duplication, one of these was obtained from Dr W. Owen (University of Birmingham). It was found that this program was unable to handle the quantity of data to be pro- cessed, it did not contour on a percentage basis, and the rotational facilities were inoperative. The program was therefore rewritten to correct these shortcomings (Program Sterio 2). Further modifications were made to enable it to handle "c" axis data obtained from universal stage work, (Program Sterio 3).

The University of London computer has a microfilm facility, this is ideal for geological computing. A program (Draw) was written there- fore using these facilities. This produces an output on film which is a contoured stereonet. This can be used as a transparency for pro- jection, or can be enlarged and printed.

All these programs were loaded onto a library in the computer for public use; instructions as to the use of this library are given below.

The computer was also used when calculating and plotting the geochemical data.

Note. In the listings given below certain symbols have been transliterated.

e.g. : has become O

Reference as to what these transliterated symbols should be can be found in the ULCC Microfilm documentation.

```
C     STATISTICAL STEREONET CONTOURING PROGRAM,MICROFILM OUTPUT.
C     --------------------------------------------------------------
C
C
C     THIS PROGRAM PACKAGE STATISTICALLY MANIPULATES AND DISPLAYS
C     NUMERICAL STRUCTURAL DATA 'PRESENTED IN VARIOUS FORMS'
C     ONTO 35 MM BLACK AND WHITE FILM. THE OUTPUT IS IN THE FORM
C     OF A CIRCLE,FILLED WITH LINEAR CONTOURS OF VARYING INTENSITY,
C     A LEGEND,AND KEY.
C
C
C          THE PHILOSOPHY BEHIND THE CONSTRUCTION OF THE PACKAGEO-
C          ----------------------------------------------------------
C
C     THERE ARE THREE PROGRAMS,
C       (1). SORT2    (F.W.M.HOPPER,1977)
C       (2). STERIO2   (DR.W.OWEN,MODIFIED BY F.W.M.H,1977)
C       (3). DRAW    (F.W.M.HOPPER,1977)
C
C     (1)     TAKES DATA FROM A RANDOM 'PILE' ,JUST AS IT WAS TAKEN IN
C     THE FIELD,AND SORTS IT INTO 'BLOCKS' ON THE BASIS OF STRUCTURAL TYPE
C     OR ON STRUCTURAL TYPE AND LOCALITY.TO THE 'BLOCKS THE PROGRAM ADDS A
C     STRING OF 'STEERING' PARAMETERS,SPECIFIED BY THE USER.
C     THUS IN ONE RUN VARYING FORMS OF DATA CAN BE DEALT WITH. THE DATA
C     'BLOCKS' ARE WRITTEN ON TO A TAPE WHICH IS THEN IMMEDIATELY USED BY
C     THE SECOND PROGRAM.
C
C     (2) CALCULATES AND WRITES THE DATA ON TO ANOTHER TAPE WHICH IS THEN
C     IMMEDIATELY USED BY THE THIRD PROGRAM. ALL OTHER OUTPUT FROM THE
C     SECOND PROGRAM IS SUPPRESSED.
C
C     (3) CALCULATES AND MANIPULATES THE DATA, AND USING DIMFILM,
C     (U.L.C.C) , DRAWS A PAGE WITH TITLEING, KEY AND CIRCLE. IT THEN
C     FITS THE MATRIX CONTAINING THE DATA OVER THE CIRCLE AND CONTOURS IT
C     IN ACCORDENCE WITH LIMITS PRESET WITHIN THE PROGRAM. THE OUTPUT IS
C     IN THE FORM OF A ROLE OF NEGATIVE FILM,
C     THE OUTPUTS ARE SELF EXPLANITORY.
C
C
C               USING THE PACKAGE.
C               ================================
C               ================================
C
C
C     THE USER MUST READ THESE INSTRUCTIONSO-
C     THE PACKAGE IS DESIGNED SO THAT THE 'WORKS' OF BOTH PROGRAMS SHOULD
C     NOT NEED TO BE ALTERED.THE PACKAGE IS FLEXIBLE ,THE FLEXIBILITY IS
C     ACHIEVED BY A SET OF STEERING CARDS EXTERNAL TO THE PROGRAM,
C     FED IN AS DATA. THUS A SENSIBLE USER,KNOWING WHAT HE WANTS,
C     AND FOLLOWING THE INSTRUCTIONS GIVEN BELOW,
C     NEED NOT KNOW HOW IT WORKS.
C
C     THERE ARE 4 SECTIONS OF INSTRUCTIONSO-
C     I
C     THE JOB CONTROL LANGUAGE (ORANGE CARDS) 'A SPECIMEN OF WHICH IS GIVEN'
C
C     II
C     THE STEERING CONTROLS FOR THE FIRST PROGRAM
C
C     III
C     THE FORM OF THE STRUCTURAL DATA INPUT.
C
C     IV
C     CONSTRUCTION OF THE WHOLE PACKAGE 'SPECIMEN GIVEN'.
```

```
C
C
C        = '= '= '= '= '= '= '= '= '= '= '= '= '= '= '= '= '= '= '= '= '= '= '= '= '= '= '= '= '= '= '= '= '= '=
C
C
C
C        [I].    JOB CONTROL
C                ----------------
C
C
C            AS THE PACKAGE IS THREE PROGRAMS,ONE MUST BE COMPILED
C        (USE MNF) AND RUN WITH THE DATA ;THEN THE NEW DATATAPE(SCRATCH)
C        IS PASSED ON TO THE SECOND PROGRAM WHICH MUST BE COMPILED (MNF) RUN.
C        SIMILALY,THE THIRD PROGRAM MUST BE COMPILED (MNF),AND RUN USING
C        THE NEW DATA TAPE (FILMPUT).
C        THE FOLLOWING 4 LISTS SHOW THE JOB CONTROL STRUCTURE POSSIBILITES.
C        A,  PROGRAM + DATA FED IN AS CARDS
C        B,  PROGRAM ON FILE + DATA AS CARDS
C        C,  PROGRAM + STRUCTURAL DATA ON FILE +STEERING DATA ON CARDS
C        D,  PROGRAM +STEERING DATA ON CARDS + STRUCTURAL DATA ON FILE
C
C        THE PROGRAM STORED ON FILE AT BEDFORD IS ALREADY COMPILED
C        IT IS THEREFORE ALREADY IN BINARY ;THE TWO SETS OF
C        JOB CONTROL INSTRUCTIONS REFER TO (1)THE COMPILED FILE,
C        (2)THE CARD DECK.
C
C        IT IS ASSUMED THAT SITUATIONS A,OR B, ABOVE,WILL BE THOSE MOST
C        COMMONLY USED (B=RELEVANT TO BEDFORD, A=GENERAL).
C        A
C        JOB (.........,J9,T120,M7600)    ***(NAME)***
C        ATTACH(DIMFILM,DIMFILM,ID=PUBLIC)
C        ATTACH(MFILM,MICROFILM,ID=PUBLIC)
C        LIBRARY(DIMFILM,MFILM)
C        MNF (E=2,R=0,L=0.I=INPUT)
C        LGO(INPUT)
C        RETURN(LGO)
C        MNF.
C        LGO(SCRATCH)
C        RETURN(LGO)
C        MNF.
C        LGO(FILMPUT)
C         (E O R)
C
C
C
C
C        JOB (.........,J9,T120,M7600)    ***(NAME)***
C        ATTACH(PLOTST,ID=LIBBED)
C        ATTACH(DIMFILM,DIMFILM,ID=PUBLIC)
C        ATTACH(MFILM,MICROFILM,ID=PUBLIC)
C        LIBRARY(PLOTST,DIMFILM,MFILM)
C        SORT2(INPUT)
C        STERIO2(SCRATCH)
C        (*********************** SEE BELOW ********************)
C        DRAW(FILMPUT)
C         (E O R)
C
C        (*********** IF YOU WANT A PAPER OUTPUT AS WELL ***********)
C        INSERT HERE O- -------
C        STERIO1(SCRATCH)
C        ------------------------
C
C
C
C
C        AT U.L.C.C. RUN THE JOB ON THE 7600. COMPUTER.
C        OTHER COMPUTERS MUST BE LARGE ENOUGH TO HANDLE ARRAYS OF THE SIZE THE
C        JOB REQUIRES (A L.C.M.IS NEEDED).
```

```
C     OTHERWISE REDUCE THE SIZE OF THE ARRAYS IN PROGRAM (1) FROM 5000-1000
C     THIS STILL PROVIDES ROOM FOR 1000 READINGS (DATA CARDS).
C     THE JOB TAKES 75,000 WORDS OF MEMORY FOR THE 1ST PROGRAM AS IT STANDS;
C     THIS REQUIREMENT ENDS WHEN THE FIRST PROGRAM STOPS; THE DATA IS
C     THEN BACK ON TAPE.
C     NOTE....THE THIRD PROGRAM UTILISES THE MICROFILM PLOTTING PACKAGE
C     CALLED 'DIMFILM'. THUS IT CAN ONLY BE RUN ON COMPUTERS WHERE THIS
C     LIBRARY IS AVALABLE.
C
C
C          = '= '= '= '= '= '= '= '= '= '= '= '= '= '= '= '= '= '= '= '= '= '= '= '= '= '= '= '=
C
C     [II].  STEERING.
C            ------------
C
C
C     THE FIRST PROGRAM READS THE INFORMATION FROM YOUR DATA CARDS.
C     IT THEN COMPARES THIS WITH INFORMATION FROM THE STEERING CARDS AND
C     MANIPULATES IT ACCORDING TO YOUR INSTRUCTIONS. THE STEERING CARDS ARE
C     PLACED BEFORE THE DATA CARDS AND ARE SEPARATED FROM THEM BY AN (E O R)
C      THERE ARE IN ALL  136  STEERING CARDS,AND THEY ARE ARRANGED IN
C     'BLOCKS' THUS O-
C
C     CORD.    30 CARDS     FORMAT(F5.2,1X,F5.2,1X,F5.2,1X,F5.2)
C
C     THESE CARDS ARE USED WHEN THE GRID SEARCHING FACILITY OF THE PROGRAM
C     IS TO BE UTILISED .THIS FACILITY ENABLES THE USER TO SPECIFY
C     SUB AREAS OUT OF THE TOTAL AREA HIS DATA COVERS AND TO PLOT ONLY
C     THAT DATA WITHIN THESE SUB AREAS.
C     THE 'CORD'CARDS SPECIFY ONE GRID AREA YOU WISH SEARCHED PER CARD.
C     IE. EACH CARD DEFINES ONE SQUARE. X,X,FIRST. Y,Y,SECOND, USING 5
C     FIGURE NUMBERS, THE MIDDLE ONE OF WHICH IS A DECIMAL POINT.
C     EG.01.10 10.01 01.10 10.01 DEFINES A GRID SQUARE.
C     SHOULD THIS FACILITY NOT BE REQUIRED THEN THE FIRST 30 CARDS CAN
C     BE BLANK (BLANK FILLED).
C
C
C     TITLE    17 CARDS     FORMAT(5A10,A4)
C
C     ON THESE CARDS IN COLUMNS 1-54 YOU CAN WRITE WHAT YOU WANT TO CALL EACH
C     TYPE OF STRUCTURAL READING YOU HAVE MEASURED AND WILL BE PLOTTING.
C     NOTE.
C     THE ORDER IN WHICH THESE CARDS ARE STACKED MUST BE THE SAME AS THAT
C     IN WHICH YOU STACK ALL THE SUBSEQUENT STEERING CARDS.
C     IF YOU ARE NOT USING 17 DIFFERENT TYPES OF READING THEN MAKE UP THE
C     NUMBERS OF TITLE CARDS WITH BLANKS.
C     TO GET A NEAT TITLEING,THE TITLE SHOULD BE CENTERED IN THE
C     54 SPACES AVALABLE ON THE TITLE CARD.
C
C
C     RAMAX    17 CARDS     FORMAT(4A5)
C
C     INSERT THE INFORMATION IF NECESSARYO-
C     (AS SPECIFIED IN THE COMMENTS FOUND AT THE TOP OF THE SECOND
C     PROGRAM (STERIO2)) IN THE FIRST 20 COLUMNS.
C     NOTE.
C     THE PLAGERISING FACILITY OF DR. OWENtS PROGRAM HAS NOT BEEN TESTED
C     BY F.W.M.H.
C     BLANK FILL UP TO 17 IF ALL THE CARDS ARE NOT USED.
C
C
C     SYMB     17     FORMAT(A2)
C
C     IN THE FIRST TWO COLUMNS OF THE CARD WRITE TWO LETTERS UNIQUELY
C     IDENTIFYING EACH TYPE OF READING YOU WANT PLOTTED. EG. BD FOR BEDDING,
```

```
C      FP FOR PLUNGE  , LA FOR LINEATION 1, LB FOR LINEATION 2,ETC.
C      MAKE SURE YOU  STACK THE CARDS SO THAT IF BD IS AT THE TOP, THEN THE
C      1ST 'TITLE CARD' REFERS TO THE BEDDING TOO,
C      AND SHOULD RAMAX BE USED THEN THE FIRST RAMAX CARD IS THE RIGHT ONE
C      FOR THIS,AND SO ON FOR THE FOLLOWING STEERING CARDS.
C      IF ALL 17 CARDS ARE NOT IN USE BLANK FILL.
C
C
C      EDOCN      17 CARDS      FORMAT(I1)
C
C      THE CORRECT NUMBER FOR THE TYPE OF READING, EG. BEDDING,
C      LINEATION,TO BE COMPUTED MUST BE PLACED IN COLUMN 1 HERE.
C      FOR THE CORRECT NUMBER IE. (1,2,3,4,OR 5),SEE SECTION
C      [III] BELOW.
C      (BLANK FILL IF NECESSARY).
C
C
C      NR      17 CARDS      FORMAT(I1)
C
C      THIS REFERS TO THE NUMBER OF COMPOUND ROTATIONS TO BE MADE.
C      (SEE COMMENTS IN DR.OWENS PROGRAM(STERIO)). IF ROTATION IS UNUSED
C      THEN O SHOULD BE PLACED IN THE 1ST COLUMN OF ALL 17 CARDS.
C      IF ↑NR↑ IS NOT O AND ROTATIONS ARE TO BE MADE, THEN THE
C      ↑DECR,DIPR,ANR↑ CARDS MUST BE FILLED ,SEE BELOW.
C
C
C      NPC      17 CARDS      FORMAT(I1)
C
C      THIS REFERS TO THE PERCENTAGE AREA OF THE STEREONET YOU WISH TO
C      SAMPLE AT. IT IS DIRECTLY EQUIVALENT TO THE SIZE OF THE HOLE IN
C      THE POINT COUNTER WHEN CONTOURING MANUALLY. NORMALLY THIS IS BEST SET
C      AT 1 OR 2 PERCENT; THUS,1 OR 2 SHOULD BE PLACED IN THE FIRST COLUMN
C      OF EACH NPC CARD .BLANK FILL TO MAKE UP NUMBERS.
C
C
C      PASS,DEVIDE      1 CARD      FREE FORMAT
C
C      TWO VALUES ARE REQUIRED ON ONE CARD, EACH SEPARATED BY A ',' AND
C      STARTING IN COLUMN 1.
C      BEFORE THE ',' = PASS
C          PASS SHOULD BE SET TO 10  IF THE CO-ORDINATE GRID SEARCH
C      IS TO BE OPERATIVE. IF IT IS NOT REQUIRED ANY NO. EXCEPT 10 EG.1,
C      SHOULD BE PLACED THERE INSTEAD.
C      AFTER THE ',' =DEVIDE
C              ON THE 'STRUCTURAL' DATA CARDS YOU MAY HAVE WRITTEN
C      AN 'N' OR 'S' IN THE 7TH. COLUMN SHOULD YOU WISH TO USE THE DATA
C      DIVIDING PROCESS DESCRIBED BELOW, SECTION [III]. THENO-
C      TO GATHER AND USE ONLY CARDS WITH ONE OR THE OTHER OF N/S, ON THEM
C      YOU SHOULD PLACE AFTER THE ',' O-
C      1= FOR USING ALL THE DATA. THE N/S FACILITY IS IGNORED THIS IS THE
C      DEFAULT NUMBER PLACED AFTER THE ','.
C      2= FOR GATHERING TOGETHER ALL THOSE CARDS WITH 'S' ON THEM,
C      AND USING THEM ONLY.
C      3= FOR GATHERING TOGETHER ALL THE CARDS WITH 'N' ON THEM,
C      AND USING THEM ONLY.
C
C
C      DECR,DIPR,ANR      3 CARDS      FREE FORMAT
C
C      THESE CARDS ARE USED WHEN A ROTATION OR COMPOUND ROTATION
C      IS TO BE MADE ON ONE OR ALL OF THE DATA SETS PRODUCED,
C      (YOU CAN↑T DO DIFERENT ROTATIONS ON DIFERENT DATA SETS,
C      BUT YOU CAN ROTATE ONE AND NOT THE REST,OR TWO THE SAME
C      AND NOT THE REST.
```

```
C        SET THE ↑NR↑ OF THE RELEVANT DATA SET(S) TO
C        (1-3) DEPENDING ON HOW MANY OF THE DECR,DIPR,ANR CARDS
C        YOU HAVE FILLED, THIS WILL CAUSE THE ROTATION OF
C        THAT DATA SET(S)).
C        EACH CARD PRODUCES ONE ROTATION 0-
C        DECR= 3 FIGURE NUMBER FOR THE COMPASS BEARING OF THE ROTATION
C        AXIS.
C        DIPR= 2 FIGURE NUMBER FOR THE INCLINATION OF THE AXIS FROM
C        THE HORIZONTAL.
C        ANR= UP TO 3 FIGURE NUMBER FOR THE AMOUNT OF ROTATION ABOUT
C        THE AXIS.
C        ALL THE NUMBERS ARE SEPERATED BY ↑,↑S.
C        ROTATION OCCURS ONLY IN THE CLOCKWISE SENSE, THUS
C        360 DEGREES OF ROTATION ARE POSSIBLE.
C        IF THE CARDS ARE TO BE UNUSED,THEY SHOULD BE FILLED WITH 3↑O↑S.
C        IE.0,0,0.IF THIS IS NOT DONE THE.PROGRAM WILL FAIL.
C
C
C        ------------------------------------------------------------
C        NOTE.
C        ----
C        DO NOT INCORPORATE INTO YOUR (STRUCTURAL DATA), CARDS WHICH DO
C        NOT HAVE A MATCHING 'SYMB' ON THEM IN THE (STEERING CARDS).
C        IF THIS HAPPENS THE FIRST PROGRAM WILL TREAT THESE CARDS AS
C        PUNCHING ERRORS AND TERMINATE THE PROGRAM.
C        THE STEERING CARD 'BLOCKS' MUST BE PLACED IN THIS ORDERO-
C        CORD              (30)
C        TITLE             (17)
C        RAMAX             (17)
C        SYMB              (17)
C        EDOCN             (17)
C        NR                (17)
C        NPC               (17)
C        PASS,DEVIDE       (1)
C        DECR,DIPR,ANR     (3)
C
C        SHOULD YOU HAVE TOO FEW OR TOO MANY STEERING CARDS
C        THEN THE PROGRAM WILL BE STOPPED AND A MESSAGE TO THE
C        EFFECT GIVEN.
C
C            = '= '= '= '= '= '= '= '= '= '= '= '= '= '= '= '= '= '= '= '= '= '= '= '= '=
C
C
C        [III].      STRUCTURAL DATA.
C                    ---------------------------
C
C
C        DATA IS FED IN ON CARDS, ONE READING PER CARD.
C        THE CARDS ARE IN THE FORMATO-
C        (A5,1X,A1,1X,I3,1X,I2,1X,A2,1X,F5.2,1X,F5.2)
C        SUBDIVIDED.
C        STRUCTURAL READING= (8X,I3,1X,I2)
C        THE STRUCTURAL READINGS ARE PLACEDO-
C        DIP/STRIKE COLUMNS 9-11.
C        AMOUNT OF DIP COLUMNS 13 14.
C        N/S DIVIDER= (6X,A1)
C        SYMB= (15X,A2)
C        GRID REFERENCE CO-ORDINATES=X,Y,= (18X,F5.2,1X,F5.2)
C        THE FIRST 5 COLUMNS ARE FOR THE LOCALITY NO. FOR YOUR REFERENCE,
C        AND LIKEWISE COLUMNS 30 ONWARDS CAN BE USED FOR YOUR COMMENTS
C        OR SPECIMEN NO. FROM THAT LOCALITY.
C        COLUMNS 6,8,12,15,18,24,MUST BE LEFT BLANK.
C
C
```

```
C           THE FORM OF THE DATA, STRUCTURAL READINGSO-
C     4 TYPES OF READING ARE ACCEPTABLE.
C     (A),PLAGIARISED DATA - USED FOR POLE PLOTS WHERE THE DIP IS
C     EXPRESSED AS THE RADIAL DISTANCE FROM THE CENTRE,IN THE
C     RADIAL DIRECTION (SEE COMMENTS AT START OF PROGRAM STERIO) .
C     (B),DATA IN THE FORM OF COMPASS DIRECTION AND DIP FROM HORIZONTAL
C     IN THAT DIRECTION, IE.AS DEC,DIP OF LINES OR POLES IN SPACE
C     EG. 090/45
C     (C),READINGS FOR PLANAR ELEMENTS MEASURED AS DIRECTION OF DIP
C     AND AMOUNT OF DIP IN THAT DIRECTION.IE.DEC=AZIMUTH OF DIP.
C     EG. 090/45 ,NOTE PLANES MUST BE TREATED DIFFERENTLY FROM LINES
C     WHEN PLOTTING THUS THIS READING IS NOT THE SAME AS IN (B).
C     (D),READINGS ON PLANAR ELEMENTS USING THE STRIKE DIRECTION AS
C     THE COMPASS BEARING.ALWAYS ARRANGING IT SO THAT THE DIP IS 90
C     DEGREES CLOCKWISE FROM THE STRIKE DIRECTION QUOTED.IE.DEC=
C     STRIKE AND(AZIMUTH OF DIP=STRIKE+90).EG. 000/45 =
C     (090/45 ,(C))=(000E45 OR 180E45) .
C
C     IN ORDER THAT THE COMPUTER UNDERSTAND WHICH OF THE 4 SORTS
C     OF DATA INPUT YOU ARE USING IT IS NECESSARY FOR THE USER
C     TO TELL IT . THIS IS DONE BY SETTING SPECIFIC VALUES INTO AN ARRAY
C     CALLED EDOCN, HOW THIS IS DONE IS EXPLAINED ABOVE. HOWEVER,
C     THE VALUES ARE O-
C     (A) , EDOCN=4(IF THE PLOT IS OF EQUAL AREA)
C           EDOCN=5(IF THE PLOT IS OF EQUAL ANGLE)
C     (B) , EDOCN=1
C     (C) , EDOCN=2
C     (D) , EDOCN=3
C           USER SET PARAMETERS
C
C
C     THE DIVIDER.
C     SHOULD THE USER HAVE SAMPLED TWO AREAS, THEN HE MAY WISH
C     TO COMPARE OVERALL READINGS FROM THE TWO . FOR THIS PURPOSE A
C     SYMBOL (N) IS DESIGNATED TO ALL READINGS FROM ONE AREA, AND
C     (S) TO ALL THE READINGS FROM THE OTHER. THUS N/S IS PLACED
C     IN COLUMN 7 OF THE DATA CARD. SHOULD THIS FACILITY NOT BE
C     REQUIRED THEN THE COLUMN MAY BE LEFT BLANK,OTHERWISE IT MUST
C     BEAR ONE OR THE OTHER.
C
C
C     THE SYMB (STRUCTURAL TYPE IDENTIFIER).
C     AS HAS BEEN EXPLAINED ABOVE (SECTION [II]) YOU MUST DECIDE ON TWO
C     LETTERS WHICH IDENTIFY EACH SORT OF STRUCTURAL READING YOU HAVE BEEN
C     MEASURING. THESE ARE THEN PLACED IN COLUMNS 16 17 OF THE DATA CARD FOR
C     THAT READING.
C     THE PROGRAM CAN HANDLE UP TO 17 DIFFERENT TYPES OF STRUCTURE AT ONCE.
C
C
C     THE GRIDS.
C     THE PROGRAM HAS THE ABILITY (WHEN PASS IS SET TO 10, SEE ABOVE)
C     TO SEARCH FOR READINGS INSIDE SPECIFIED AREAS WHICH YOU HAVE COVERED
C     (SEE 'CORD' ABOVE [II]).
C     YOU CAN LOOK AT 30 DIFFERENT GRID AREAS ON ONE RUN SHOULD YOU WISH TO,
C     THESE MAY BE SUB AREAS OF EACH OTHER OR SEPARATE AREAS. THEY MAY BE OF
C     ANY SIZE.
C     ALL DATA FROM EACH AREA ARE SORTED INTO THE DIFFERENT STRUCTURAL TYPES
C
C     (SYMB.),AND A STEREONET FOR EACH IS PRODUCED, TELLING YOU WHICH (1-30)
C     CO-ORDINATE CARD WAS USED (SEE [II] ABOVE)
C     WARNING  XXXXXXXXXXXX
C     THE PROGRAM CAN TAKE UP TO 17 DIFFERENT 'SYMB'S ,SHOULD THESE OCCUR
C     IN ALL 30 OF THE REQUESTED GRID SQUARES THEN, THE RESULT WILL
C     BE 510 STEREONETS IE. NO.OF 'SYMB'XNO.OF 'CORD'=MAX NO OF STEREONETS.
```

```
C
C       THE GRID REFERENCE OF THE LOCALITY WHERE A PARTICULAR READING IS MADE
C       IS PLACED IN COLUMNS 19-23=X,  25-29=Y.
C       IF NO USE IS TO BE MADE OF THIS GRID SEARCH PROCESS LEAVE  THE
C        COLUMNS BLANK
C       THE 1ST 1-5 COLUMNS ARE FOR LOCALITY NOS. THE PROGRAM IGNORES THEM.
C       SIMILALY WITH COLUMNS 30 ONWARDS.
C       *****WHEN PUNCHING DATA ASK THE ADVISOR ABOUT PROGRAMMING A DRUM CARD.
C       THIS WILL HELP ELIMINATE ERRORS AND SPEED PUNCHING*****
C
C
C          ='='='='='='='='='='='='='='='='='='='='='='='='='='='='='='=
C
C
C
C
C
C       [IV].      CONSTRUCTION
C                  ----------------
C
C
C
C       ALL 4 OF THE POSSIBILITIES FOR CONSTRUCTION REFERRED TO IN SECTION
C       [I] ABOVE WILL BE DEALT WITH. <E O R> =END OF RECORD.
C                                     <E O F> =END OF FILE.
C                                     JC =JOB CONTROL CARDS.
C                                     P1 =PROGRAM SORT2.
C                                     P2 =PROGRAM STERIO2.
C                                     P3 =PROGRAM DRAW.
C                                     D =DATA CARDS.
C                                     S =STEERING CARDS.
C       THUSO-
C          A=  JC         B=  JC         C=  JC         D=  JC
C              <E O R>        <E O R>        <E O R>        <E O R>
C              P1             S              S              P1
C              <E O R>        <E O R>        <E O R>        <E O R>
C              S              D              <E O F>        S
C              <E O R>        <E O R>                       <E O R>
C              D              <E O F>                       P2
C              <E O R>                                      <E O R>
C              P2                                           P3
C              <E O R>                                      <E O R>
C              P3                                           <E O F>
C              <E O R>
C              <E O F>
C
C
C          ='='='='='='='='='='='='='='='='='='='='='='='='='='='='='='=
C
C       ADDITIONAL FEATURES AVAILABLE IN THE LIBRARY.
C       ---------------------------------------------------
C       ---------------------------------------------------
C
C
C       THERE ARE TWO MORE PROGRAMS AVAILABLE IN THE LIBRARY
C       STERIO3 ...PRODUCING A LINE PRINTER OUTPUT
C       STERIO5 ...PRODUCING MICROFILM OUTPUT
C       THEY ARE USED TO PLOT AND ROTATE DATA OBTAINED
C       FROM THREE RIGHT-ANGLE SECTIONS CUT THROUGH A
C       ROCK. EG. 'C AXIS' FABRIC DATA.
C       ONLY ONE ROCK CAN BE DEALT WITH PER RUN
C       OF THE PROGRAM.
C
C       THE PROGRAMS ARE USED THUS O-
C
C       NOTE --(+++) CARD NEEDED FOR PAPER OUTPUT.
C            --(***) CARD NEEDED FOR MICROFILM OUTPUT.
C
```

```
C       JOB (         ,J6,T120,M7600)              ***  +++
C       ATTACH (PLOTST,ID=LIBBED)                  ***  +++
C       ATTACH (DIMFILM,DIMFILM,ID=PUBLIC)         ***
C       ATTACH (MFILM,MICROFILM,ID=PUBLIC)         ***
C       LIBRARY (PLOTST,DIMFILM,MFILM)    ***
C       LIBRARY (PLOTST)                       +++
C       STERIO3 (INPUT)                        +++
C       STERIO4 (INPUT)                        ***
C       DRAW (FILMPUT)                         ***
C       (E 0 R)
C       THEN COMES THE DATA THUS 0-
C       FIRST THE STEERING CARDS.
C       STARTING IN COLUMN 1 0-
C       3
C       0            ........................
C       (INTEGER (I4) THE NUMBER OF READINGS TO BE USED IN THIS
C                                DATA SET) RIGHT ADJUSTED  ..
C       12111*TITLE OF DATA UP TO 55 CHARACTERS LONG
C            *=THE NO. OF ROTATIONS THIS DATA SET IS TO UNDERGO.
C                         A MAX OF 3. THUS *=0,1,2 OR 3.
C       THE NEXT CARD HAS THE ROTATION DATA IN 9F5.1 FORMAT
C       DECLINATION OF ROTATION AXIS /DIP OF ROTATION AXIS /
C       AMOUNT OF ROTATION (CLOCKWISE ONLY)/ ETC.UP TO 3 TIMES.IE
C        230.  90. 124. 360.  30. 555. 042. 20.  80.
C       THE NEXT CARDS ARE THE DATA CARDS WITH THE DATA ON
C       THEM IN 5 SETS OF DIRECTION OF DIP / AMOUNT OF DIP.
C       FORMAT 10F4.0
C       WHEN THE DATA IS FINISHED FOR THIS FACE TYPE 1000 IN
C       THE NEXT SPACE MEANT FOR THE DIRECTION OF DIP.
C       (THE DATA IS RIGHT ADJUSTED IN THE FORMAT SPACE).
C
C
C       THE NEXT TWO FACES NEED THE SAME SORT OF DATA SET STARTING
C       AT THE CARD MARKED   ................ ...... ABOVE
C
C
C       NO MORE THAN THREE DATA SETS CAN BE HANDLED IN A RUN
C       IE. 1 ROCK A RUN.
C       THE OUTPUT IS 4 NETS, DATASET1,2,3, THEN NET 4 WHICH
C       IS THE SUM OF THE ROTATED FORMS OF 1+2+3; BUT IS ITSELF
C       UNROTATED ABOVE THE ROTATIONS THAT HAVE GONE INTO 1,2 3 .
C       THE DECK IS TERMINATED BY AN (E 0 R) CARD, FOLLOWED BY
C       AN (E 0 F) CARD.
C
C
C       THE PROGRAMS ARE A FURTHER MODIFIED FORM OF DR OWENS
C       PROGRAM (MODIFIER,F.W.M.H)
C
C       MISCELLANEOUS.
C       ————————————————
C       THE PROGRAM IS AT PRESENT SET TO TAKE 5000 DATA CARDS.
C       INTX/INTY THESE SHOULD NOT BE TOUCHED
C       IWS.
C       THE PROGRAM WILL CALCULATE TO EQUAL AREA OR ANGLE OUTPUT.
C       IWS=1 FOR =AREA (PRESENT SETTING)
C       IWS=2 FOR =ANGLE
C       THE PROGRAM ON FILE AT BEDFORD IS IN BINARY FORM-IE. COMPILED.
C
C       NOTE............
C       ——————————————————
C       ——————————————————
C
C
C       THE CIRCLE DESCRIBED ARROUND THE CONTOURS IS NOT THE TRUE
```

```
C      PRIMITIVE. IT COINCIDES WITH THE PRIMITIVE NEAR THE CARDINAL
C      POINTS,BUT ELSEWHERE LIES SLIGHTLY OUTSIDE IT.
C      DATA FALLING EXACTLY ON THE PRIMITIVE IN THESE AREAS CAN BE
C      RECOGNISED AS THEY WILL BE EXACTLY MIRRORED ACROSS THE NET,
C      AND THE CONTOURS WILL CONVERGE TO FORM A STEEP ↑CLIFF↑
C      ON THE OUTER SIDE.
C      DATA PLOTTING NEAR THE PRIMITIVE WILL NOT BE MIRRORED,
C      AND WILL NOT HAVE SUCH A STEEP ↑CLIFF↑.
C      WHERE ONLY SOME OF THE DATA FALL ON THE PRIMITIVE, THIS
C      PORTION CAN BE DETECTED BY LOOKING FOR MIRRORED PEAKS AT
C      THE EDGE, WHICH ARE AT THE SAME ↑HEIGHT↑ ACROSS THE NET.
C      THIS EDGE EFFECT IS AN UNAVOIDABLE PART OF (DIMFILM)
C      CONTOURING ROUTINES.
C
C      NOTE ALSO... CONTOUR LABELS ARE SUPPRESSED IF THE CONTOURS
C      ARE CLOSE; VALUES FOR THEM MAY BE DETERMINED BY COUNTING
C      ↑UP SLOPE↑ FROM THE ↑LOWEST↑ WHICH WILL ALWAYS BE (0.50).
C
C
C      WHEN PAPER OUTPUT IS REQUESTED, 10' DIAMETER NETS
C      FILLED WITH ALPHA-NUMERICS ARE PRINTED ONTO THE
C      LINE PRINTER. THEY HAVE A KEY PRINTED WITH THEM
C      AND ARE THUS SELF EXPLANATORY.
C      IT IS RECOMMENDED THAT INITIALY WHEN LOOKING AT
C      YOUR NETS ONLY PAPER OUTPUT IS USED .
C      THEN, WHEN YOU ARE SURE YOU WANT THEM, RUN
C      THE JOB TO PRODUCE MICROFILM.
C        XXXXXXXXXXXXXXXXXXXXXXXXXXXXXXXXXXXXXXXXXXXXXXXXXX
C
C
```

```
          PROGRAM SORT2 (DATA,OUTPUT,INPUT,SCRATCH,TAPE10=DATA,
         -TAPE6=OUTPUT,TAPE5=INPUT,TAPE7=SCRATCH)
C         DATA SORTING PROGRAM
C         ALL OUTPUT SUPPRESSED,PROGRAM WRITES TO TAPE 7,EXCEPT WHEN
C         AN ERROR IS FOUND IN THE DATA INPUT.
C         F.W.M.HOPPER.
C         SET UP ARRAY DIMENSIONS.
          INTEGER CDEC (5000) ,CDIP (5000) ,DCEC (5000) ,DCIP (5000) ,DADEC (5000) ,
         -DADIP (5000)
          INTEGER DEC,PO,TESN,A,GRID,PASS,B,C,D,E,DEVIDE
          INTEGER SYMB (17) ,EDOCN (17) ,NR (17) ,NPC (17)
          DIMENSION IDENT (5000) ,XCORD (5000) ,YCORD (5000) ,NS (5000) ,IDEN (5000)
          DIMENSION CORD (30,4) ,DECR (3) ,DIPR (3) ,ANR (3)
          DIMENSION TITLE (17,6)
          DIMENSION RAMAX (17,4)
          COMMON IDENT,XCORD,YCORD,NS,IDEN,CDEC,CDIP,DCEC,DCIP,DADEC,DADIP
          LEVEL2,IDENT,XCORD,YCORD,NS,IDEN,CDEC,CDIP,DCEC,DCIP,DADEC,DADIP
C
C
C         READ IN CO-ORDINATE DATA. STEERING.
          DO 1 I=1,30
          READ (5,2) (CORD (I,J) ,J=1,4)
          WRITE (6,1111)
1111      FORMAT (1HN)
          IF (EOF (5) .NE.0.0) GO TO 6050
2         FORMAT (F5.2,1X,F5.2,1X,F5.2,1X,F5.2)
1         CONTINUE
C
C
C         D=THE SIZE OF SYMB ARRAY,=THE SIZE OF THE EDOCN ARRAY
          D=17
C         READ IN THE REST OF THE STEERING DATA.
          DO 3 I=1,D
          READ (5,4) (TITLE (I,J) ,J=1,6)
          IF (EOF (5) .NE.0.0) GO TO 6050
4         FORMAT (5A10,A4)
3         CONTINUE
          DO 34 I=1,D
          READ (5,5) (RAMAX (I,J) ,J=1,4)
          IF (EOF (5) .NE.0.0) GO TO 6050
5         FORMAT (4A5)
34        CONTINUE
          DO 35 I=1,D
          READ (5,6) (SYMB (I))
          IF (EOF (5) .NE.0.0) GO TO 6050
6         FORMAT (A2)
35        CONTINUE
          DO 36 I=1,D
          READ (5,7) (EDOCN (I))
          IF (EOF (5) .NE.0.0) GO TO 6050
7         FORMAT (I1)
36        CONTINUE
          DO 40 I=1,D
          READ (5,41) (NR (I))
          IF (EOF (5) .NE.0.0) GO TO 6050
41        FORMAT (I1)
40        CONTINUE
          DO 50 I=1,D
          READ (5,51) (NPC (I))
          IF (EOF (5) .NE.0.0) GO TO 6050
51        FORMAT (I1)
50        CONTINUE
          READ (5,*) PASS,DEVIDE
          IF (EOF (5) .NE.0.0) GO TO 6050
```

```
        DO 71 I=1,3
        READ(5,*) (DECR(I),DIPR(I),ANR(I),
71      CONTINUE
        IF(EOF(5).NE.0.0)GO TO 6050
C
C       CHECK TO SEE IF NEXT CARD IS (E O R). IF NOT
C       STOP AND SAY SO,TOO MANY STEERING CARDS.
        READ(5,9000)DUMMY
9000    FORMAT(A1)
        IF(EOF(5).NE.0.0)GO TO 7000
        WRITE(6,8000)
8000    FORMAT('1',25X,' YOU HAVE TOO MANY STEERING CARDS,CHECK THEM ')
C       TO STOP ENTIRE JOB. I CALL NON EXISTANT ROUTINE.
        CALL ABNORML
        STOP
C       (E O R) WAS REACHED TOO SOON WHEN READING IN THE STEERING CARDS.
C       WRITE THIS FACT OUT.
6050    WRITE(6,6000)
6000    FORMAT('1',25X,' YOU HAVE TOO FEW STEERING CARDS,CHECK THEM ')
C       TO STOP ENTIRE JOB. I CALL NON EXISTANT ROUTINE.
        CALL ABNORML
        STOP
7000    CONTINUE
C
C       FIXED PARAMETERS AND COUNTERS.
        AA=0
        TESN=510
        JOHN=1
        NDSET=0
        INTX=1
        INTY=2
        IR=1
        IWS=1
        NSET=D
        GRID=30
        DEC=1000
C
C
C       READ IN STRUCTURAL DATA.
        DO 8 PO=1,5000
        READ(10,9) (NS(PO),DADEC(PO),DADIP(PO),IDENT(PO),XCORD(PO),
       -YCORD(PO))
9       FORMAT(6X,A1,1X,I3,1X,I2,1X,A2,1X,F5.2,1X,F5.2)
        IF(EOF(10).NE.0)GO TO 10
C       CHECK FOR (EOF) AND COUNT NO OF DATA CARDS.
        NDSET=NDSET+1
8       CONTINUE
10      CONTINUE
C
C
C       SEARCH FOR GROSS PUNCHING ERRORS
        CALL ERROR(IDENT,DADIP,DADEC,SYMB,PO,D)
C
C
C       JUMP INTO LOOP IF GRID SEARCHING IS NOT REQUIRED.
        IF(PASS.NE.10)GO TO 15
C
C
C       GRID SEARCHING LOOP CYCLE =30
11      DO 12 A=1,GRID
        AA=A
        K=0
C       SEARCH USING ALL DATA AND ONE GRID CARD.
        DO 13 B=1,NDSET
```

```
C          IF CO-ORDINATE CARD BLANK, SKIP TO END OF LOOP.
           IF (CORD(A,2).EQ.-0.0)GO TO 12
           IF (XCORD(B).LE.CORD(A,1).OR.XCORD(B).GE.CORD(A,2))GO TO 13
           IF (YCORD(B).LE.CORD(A,3).OR.YCORD(B).GE.CORD(A,4))GO TO 13
           K=K+1
C          CONDITIONS SATISFIED FILL ARRAYS.
           DCEC(K)=DADEC(B)
           DCIP(K)=DADIP(B)
           IDEN(K)=IDENT(B)
13         CONTINUE
C          LEAP OVER THE NON CO-ORDINATE BASED ARRAY FILLER ROUTINE.
           GO TO 14
C
C
15         K=0
C          FILL ARRAYS.
           DO 16 C=1,NDSET
           K=K+1
           DCEC(K)=DADEC(C)
           DCIP(K)=DADIP(C)
           IDEN(K)=IDENT(C)
16         CONTINUE
C
C
C          START THE COMPARATIVE AND ASSIGNMENT ROUTINES.
14         DO 17 NUM=1,NSET
           CALL SET(NUM,D,SYMB,IDEND)
C          SETS UP THE IDEND TO TEST FOR A CERTAIN IDENTIFIER
C
C
C          START TESTING
           CALL TEST(K,IDEND,IDEN,CDEC,CDIP,DCEC,DCIP,J,DEVIDE,NS)
C
C          IF TEST HAS FOUND NOTHING GO TO NEXT CYCLE OF THE LOOP.
           IF (J.EQ.0)GO TO 17
C
C          FIND THE CORRECT NCODE FOR THE SYMB FUNCTION
           CALL FINDE(D,IDEND,SYMB,NUM,NCODE,EDOCN)
C
C          MAKE SURE IDEND IS CLEARED OR IT WILL REPEAT THE LAST LOOP.
           IDEND=2H
C
C
C          START THE COMPLEX PROCESS OF WRITING OUT PROCESSED DATA.
           IF (JOHN.GT.1)GO TO 20
C          WRITE TOTAL NO OF DATA SETS TO BE EXPECTED USING CO-ORDINATES.
           IF (PASS.EQ.10)WRITE(7,21)TESN
C          WRITE NORMAL (17) NO OF DATA SETS TO BE EXPECTED.
           IF (PASS.NE.10)WRITE(7,21)NSET
21         FORMAT(I3)
20         JOHN=JOHN+1
C          IF CO-ORDINATE CARDS WERE USED GO AND PRINT WHICH ONE.
           IF (AA.NE.0)GO TO 30
           E=0
C          NO CO-ORDINATES WERE USED PRINT 0.
           WRITE(7,27)E
C          LEAP OVER CO-ORDINATE PRINTING BIT.
           GO TO 29
C          PRINT THE NO OF THE CO-ORDINATE CARD IN USE.
30         WRITE(7,27)A
29         CONTINUE
27         FORMAT(I3)
C          WRITE TOTAL NO OF DATA TO BE PRINTED.
           WRITE(7,19)J
```

```
19        FORMAT(I4)
C         PRINT THE TITLE CARD FOR THE NEXT PROGRAM WITH ALL PARAMETERS
C         RELEVANT TO THIS CYCLE OF THE LOOPS.
          WRITE(7,22) (INTX,INTY,NCODE,NPC(NUM),IWS,NR(NUM),(TITLE(NUM,I),
         -I=1,6),(RAMAX(NUM,I),I=1,4))
22        FORMAT(6I1,5A10,A4,4A5)
C         WRITE OUT THE ROTATION DATA IF NR IS NOT O
          IF(NR(NUM).EQ.0)GO TO 84
          WRITE(7,85)  (DECR(II),DIPR(II),ANR(II),II=1,3)
85        FORMAT(9F5.1)
84         L=1
          M=5
C         WRITE OUT THE SORTED DATA,5 TO A LINE, CHECK TO SEE IF THE LINE
C         IS FILLED, IF SO GO TO NEXT IF NOT WRITE OUT PORTION THEN TERMINATE
C         DATA BY WRITING 1000.
23        WRITE(7,24) (CDEC(I),CDIP(I),I=L,M)
          IF(M.EQ.J)WRITE(7,25)DEC
          IF(M.EQ.J)GO TO 17
          M=M+5
          L=L+5
          IF(M.LT.J)GO TO 23
          WRITE(7,24) (CDEC(I),CDIP(I),I=L,J),DEC
24        FORMAT(10I4)
25        FORMAT(I4)
17        CONTINUE
12        CONTINUE
C         WRITE TOTAL NO OF DATA CARDS.
          WRITE(7,25)NDSET
C         PREPARE TAPE (SCRATCH) FOR NEXT PROGRAM.
          REWIND 7
          REWIND 5
          REWIND 10
          STOP
          END
C
C
C
C         THIS ROUTINE CHECKS THE DATA FOR 'IMPOSSIBLE ERRORS', TELLS
C         YOU WHAT THEY ARE AND STOPS THE PROGRAM.
          SUBROUTINE ERROR(IDENT,DADIP,DADEC,SYMB,PO,D)
          INTEGER DADIP(PO),DADEC(PO),SYMB(D),PO,D
          DIMENSION IDENT(PO)
          LEVEL2,IDENT,DADIP,DADEC
          LOGICAL FOUND
          NO=1
          IP=PO-1
C
1112      FORMAT(1HZ)
          WRITE(6,34)
34        FORMAT('1',25X,'ERRORS IN YOUR DATA (IF ANY) WILL BE LISTED BELOW'
         -,/)
C
          DO 31 I=1,IP
          FOUND=.FALSE.
          DO 32 J=1,D
          IF(IDENT(I).NE.SYMB(J))GO TO 32
          FOUND=.TRUE.
32        CONTINUE
          IF(.NOT.FOUND.OR.DADEC(I).GT.360.OR.DADIP(I).GT.90)WRITE(6,33)
         -I,IDENT(I),DADEC(I),DADIP(I)
          IF(.NOT.FOUND.OR.DADEC(I).GT.360.OR.DADIP(I).GT.90)NO=3
33        FORMAT(25X,' CARD ',I4,5X,' IDENT= ',A2,5X,' DADEC= ',I3,5X,
         -' DADIP= ',I2)
31        CONTINUE
```

```
        IF (NO.NE.3) WRITE (6,35)
35      FORMAT(5(/),25X,'WELL DONE - NO ERRORS WERE FOUND IN YOUR DATA.')
        IF (NO.NE.3) RETURN
        WRITE (6,100)
100     FORMAT('0',10X,'THE PROGRAM WAS TERMINATED BECAUSE YOUR DATA HAD T
       -HE ABOVE ERROR(S) IN IT.  TERMINATION OCCURED IN SUBROUTINE ERROR.
       -',/,'1')
        WRITE (6,1112)
        CALL ABNORML
        STOP
        END
C
        SUBROUTINE SET(NUM,D,SYMB,IDEND)
C       SETS IDEND TO THE CORRECT IDENT
C
        INTEGER SYMB(D),D
        IDEND=SYMB(NUM)
        RETURN
        END
C
        SUBROUTINE TEST(K,IDEND,IDEN,CDEC,CDIP,DCEC,DCIP,J,DEVIDE,NS)
C
C       TESTS THE IDEND AGAINST THE IDENT AND STORS IT IF CORRECT
C
        INTEGER CDEC(K),CDIP(K),DCEC(K),DCIP(K),DEVIDE
        DIMENSION IDEN(K),NS(5000)
        LEVEL2,CDEC,CDIP,DCEC,DCIP,NS,IDEN
        J=0
C       SET DEVIDE TO ITS DEFAULT VALUE OF 1
        IF (DEVIDE.EQ.-0.0) DEVIDE=1
C       CREATE THE ARRAYS OF SORTED DATA.
        DO 18 I=1,K
        IF (DEVIDE.EQ.1) GO TO 1
        IF (DEVIDE.EQ.2) GO TO 2
        IF (NS(I).NE.1HN) GO TO 18
        GO TO 1
2       IF (NS(I).NE.1HS) GO TO 18
1       CONTINUE
        IF (IDEN(I).NE.IDEND) GO TO 18
        J=J+1
        CDEC(J)=DCEC(I)
        CDIP(J)=DCIP(I)
18      CONTINUE
        RETURN
        END
C
        SUBROUTINE FINDE(D,IDEND,SYMB,NUM,NCODE,EDOCN)
C
C       FINDS THE NCODE CORRESPONDING TO THE IDEND
C
        INTEGER SYMB(D),EDOCN(D),D
        IF (IDEND.EQ.SYMB(NUM)) NCODE=EDOCN(NUM)
        RETURN
        END
            IDENT  ABNORML
*            SUBROUTINE ABNORML
*            THIS ROUTINE IS SPECIFIC TO THE ULCC.7600,AND WILL ABORT
*            THE WHOLE JOB SHOULD IT BE CALLED
            ENTRY  ABNORML
 ABNORML    BSS    1                      .ENTRY/EXIT
            MESSAGE STARS,,1
            MESSAGE MESAGE,,1
            MESSAGE STARS,,1
            ABORT  ,NODUMP
```

```
STARS     DATA     CO****  ***  ***  ***  ***  ***  ***  ***  ***  ***  ***  ***0
MESAGE    DATA     C*ERROR IN YOUR DATA, SEE OUTPUT FILE FOR DETAILS*
          END
```

```
        PROGRAM STERIO2 (INPUT,OUTPUT,FILMPUT,TAPE5=INPUT,TAPE6=OUTPUT,
      -TAPE8=FILMPUT)
C       PROGRAM SET FOR A 66 LINE/PAGE PRINTER,BUT WITH ALL OUTPUT
C       SUPPRESSED EXCEPT THAT WRITEN TO TAPE 8,THIS GOES TO THE
C       NEXT PROGRAM FOR PLOTTING.
        INTEGER A,TND
        DIMENSION ALPH(27),STER(81),TITLE(55),S(3,3),DCR(3),ARAN(2)
        DIMENSION SR(3,3),ST(3,3),DECR(3),DIPR(3),ANR(3)
        DIMENSION ND(49,41),DADEC(10),DADIP(10),NND(49,41)
C       DIMENSION ND(65,41),DADEC(10),DADIP(10),NND(65,41)
C USE ND(49  FOR 6 LI/IN, ND(65  FOR 8 LI/IN
C DIMENSION COSINE ARRAYS
        DIMENSION QL(65,41),QM(65,41),QN(65,41)
        DATA ALPH(1),ALPH(2),ALPH(3),ALPH(4),ALPH(5),ALPH(6),ALPH(7),
       1ALPH(8),ALPH(9),ALPH(10),ALPH(11),ALPH(12),ALPH(13),ALPH(14),
       2ALPH(15),ALPH(16),ALPH(17),ALPH(18),ALPH(19),ALPH(20),
       3ALPH(21),ALPH(22),ALPH(23),ALPH(24),ALPH(25),ALPH(26),ALPH(27)/
       41H ,1HA,1HB,1HC,1HD,1HE,1HF,1HG,1HH,1HI,1HJ,1HK,1HL,1HM,1HN,1HO,
       51HP,1HQ,1HR,1HS,1HT,1HU,1HV,1HW,1HX,1HY,1HZ/,STAR/1H*/,
       6ARAN(1),ARAN(2)/5HEQ AR,5HEQ AN/
        DATA IX1/23/,RX1/23.62/,IX2/49/,RX2/1.38/,RX3/48.62/,
       1RX4/1.6667/,IX3/25/
C       DATA IX1/31/,RX1/31.52/,IX2/65/,RX2/1.48/,RX3/64.52/,
C       1RX4/1.25/,IX3/33/
C FOR 6 LI/IN USE  23   23.62   49   1.38   48.62   1.6667   25
C        8               31   31.52   65   1.48   64.52   1.25     33
        PI=3.1415926536
        DEGTOR=PI/180.0
        INTXL=0
        INTYL=0
        IWSL=0
        READ (5,487)NSET
        WRITE(8,487)NSET
  487 FORMAT(I3)
C
C
        DO 71 ISET=1,NSET
        READ(5,344)A
        IF(EOF(5).NE.0.0)GO TO 7
  344   FORMAT(I3)
        READ(5,343)TND
        IF(EOF(5).NE.0.0)GO TO 7
  343   FORMAT(I4)
        READ(5,14) INTX,INTY,NCODE,NPC,IWS,NR,(TITLE(I),I=1,55),
       -RAMAX
        IF(EOF(5).NE.0.0)GO TO 7
  14    FORMAT(6I1,55A1,4F5.2)
        IF(INTY.LT.2) INTY=2
C
C PRELIMINARIES FOR SET
C CANORM IS COSINE OF ANGLE, ALPHA, OF CONE OF SAMPLING (I.E. SEMI-ANGLE)
C FOR  1 PERCENT AREA (OR SOLID ANGLE) CANORM=0.99
        CANORM=1.0-0.01*FLOAT(NPC)
        SANORM=SQRT(1.0-CANORM*CANORM)
C FORM SIN(ALPHA+5)  - SEE BELOW
        SA5=SANORM*COS(36.0*DEGTOR)+CANORM*SIN(36.0*DEGTOR)
        LTOT=0
C CALCULATE ARRAY LIMITS FOR ND
        NIX=IX1/INTX
        NIY=39/INTY
C ND IS ND(2*NIX+3,2*NIY+3)
C CENTRE IS (NIX+2,NIY+2)
C CALCULATE LOCAL GRID LIMITS
        LGY=IFIX(FLOAT(NIY)*SANORM+1.5)
```

```
        LGX=IFIX(FLOAT(NIX)*SANORM+1.5)
C  CLEAR ND, NUMERICAL OUTPUT ARRAY
201     N2X=2*NIX+3
        N2Y=2*NIY+3
        DO 1030 I=1,N2X
        DO 1030 J=1,N2Y
1030    ND(I,J)=0
C  BUILD DIRN COSINE ARRAYS - SKIP IF ALREADY DONE
        IF(IWS.NE.IWSL) GO TO 1033
        IF(INTX.EQ.INTXL.AND.INTY.EQ.INTYL) GO TO 1032
1033    DO 1031 I=1,N2X
        DO 1031 J=1,N2Y
        X=FLOAT((NIX+2-I)*INTX)/RX1
        Y=FLOAT((J-NIY-2)*INTY)/39.37
        CALL ERECT(X,Y,IWS,DCL,DCM,DCN)
        QL(I,J)=DCL
        QM(I,J)=DCM
1031    QN(I,J)=DCN
1032    CONTINUE
        WRITE(8,342)A
        WRITE(8,727)NR
5012    FORMAT(14H1INPUT DATA - ,55A1,3X,9HSTEERING ,5I1,3X,8HRAMAX = ,
     1F5.2//)
C  IF DATA ARE TO BE ROTATED, CALCULATE ROTATION MATRIX,S.
        IF(NR.EQ.0) GO TO 1009
        READ(5,1107) (DECR(IR),DIPR(IR),ANR(IR),IR=1,3)
1107    FORMAT(9F5.1)
727     FORMAT(I1)
        DO 1100 I=1,3
        DO 1101 J=1,3
1101    S(I,J)=0.0
1100    S(I,I)=1.0
        DO 1102 IR=1,3
        CALL ROTDAT(DECR(IR),DIPR(IR),ANR(IR),SR)
        CALL PROMAT(SR,S,ST)
        DO 1103 I=1,3
        DO 1103 J=1,3
1103    S(I,J)=ST(I,J)
1102    CONTINUE
1009    CONTINUE
C
C  READ AND PROCESS DATA
 1007 READ (5,1001) (DADEC(I),DADIP(I),I=1,5)
 1001 FORMAT(10F4.0)
5013    FORMAT(5(F10.2,F7.2))
        DO 1003 I=1,5
        I2END=1
        ENDEC=DADEC(I)
        IF(ENDEC.EQ.1000.0) GO TO 1002
        IF(ENDEC.EQ.2000.0) GO TO 1007
        IF(DADIP(I).GE.0.0) GO TO 800
        DADIP(I)=-DADIP(I)
        ENDEC=ENDEC+180.0
        IF(ENDEC.GT.360.0) ENDEC=ENDEC-360.0
800     CONTINUE
        LTOT=LTOT+1
        ENDEC=DEGTOR*ENDEC
        IF(NCODE.LT.4) GO TO 1500
C  PLAGIARISED DATA
        X=DADIP(I)*COS(ENDEC)/RAMAX
        Y=DADIP(I)*SIN(ENDEC)/RAMAX
        IWS2=NCODE-3
        CALL ERECT(X,Y,IWS2,DCLA,DCMA,DCNA)
        GO TO 2030
```

```
C   OTHER CASES    CHANGE TO CONFORM WITH NCODE = I
1500  ENDIP=DPSTR*RADIP(I)
      IF(NCODE-2) 1502,1503,1504
1504  ENDEC=ENDEC+0.5*PI
1503  ENDEC=ENDEC+PI
      IF(ENDEC.GT.2.0*PI) ENDEC=ENDEC-2.0*PI
      ENDIP=0.5*PI-ENDIP
1502  CONTINUE
C
C   CALCULATE DIRECTION COSINES
      DCLA=COS(ENDIP)*COS(ENDEC)
      DCMA=COS(ENDIP)*SIN(ENDEC)
      DCNA=SIN(ENDIP)
2030  IF(NR.EQ.0) GO TO 3000
C   ROTATE DATA IF REQD.  TAKE OTHER END OF AXIS IF OUT OF LR HEMIS.
      DO 3001 IC=1,3
3001  DCR(IC)=S(IC,1)*DCLA+S(IC,2)*DCMA+S(IC,3)*DCNA
      DCLA=DCR(1)
      DCMA=DCR(2)
      DCNA=DCR(3)
      IF(DCNA.GE.0.0) GO TO 3000
2003  DCNA=-DCNA
      DCLA=-DCLA
      DCMA=-DCMA
3000  CONTINUE
C   FIND LOCAL ZERO - NEAREST ND LOCN TO DATA POINT
      CALL PJECT(DCLA,DCMA,DCNA,IWS,XCOMP,YCOMP)
      ILZ=-IFIX(FLOAT(NIX)*XCOMP+0.5)+NIX+2
      JLZ=IFIX(FLOAT(NIY)*YCOMP+0.5)+NIY+2
C   SCAN OVER LOCAL GRID
      ILL=ILZ-LGX
      ILU=ILZ+LGX
      JLL=JLZ-LGY
      JLU=JLZ+LGY
      IF(ILL.LT.1) ILL=1
      IF(JLL.LT.1) JLL=1
      IF(ILU.GT.N2X) ILU=N2X
      IF(JLU.GT.N2Y) JLU=N2Y
      DO 2001 IL=ILL,ILU
      DO 2001 JL=JLL,JLU
C   FIND DIRN COSINES OF ARRAY LOCN - FIND CORRESP TRUE SPACE POINT
C   AND CALL ERECT
      DCL=QL(IL,JL)
      DCM=QM(IL,JL)
      DCN=QN(IL,JL)
C   IGNORE GRID POINTS IF MORE THAN 5 DEGREES BEYOND PRIMITIVE
      IF(DCN.LT.-0.087) GO TO 2001
C   ADD ONE TO CELL IF APPROPRIATE
      IF((DCLA*DCL+DCMA*DCM+DCNA*DCN).GE.CANORM) ND(IL,JL)=ND(IL,JL)+1
2001  CONTINUE
C   CHECK WHETHER POINT LIES WITHIN ALPHA+5 OF PERIMETER - IF SO, REPEAT
C   CALCULATION FOR OTHER END OF AXIS
      IF(DCNA.GT.SA5.OR.I2END.LT.0) GO TO 1003
      I2END=-1
      GO TO 2003
1003  CONTINUE
      GO TO 1007
C   WRITE TABLE OF CALCULATED VALUES
1002      WRITE(8,2014) (TITLE(I),I=1,55)
2014  FORMAT(1H ,55A1)
      WRITE(8,2113) INTY,INTX,NPC,LTOT,ARAN(IWS)
2113  FORMAT(1H ,'  SAMPLING   ',I3,'ACROSS/-',I3,'DOWN ',15X,'POLES PER
     -  ',I2,'PERCENT AREA ',5X,I4,' DATA ',5X,A5)
2004  FORMAT(1H0,55A1//12H SAMPLING - ,I3,8H ACROSS/,I3,5H DOWN,
```

```
          15X,10HPOLES PER ,I2,13H PERCENT AREA,5X,I4,5H DATA,5X,A5)
5001   FORMAT(12HOROTATED BY ,F6.1,13H ABOUT DEC = ,F6.1,8H   DIP = ,
       1F6.1)
7000   FORMAT(19H ROTATION MATRIX    ,3F10.4/(19X,3F10.4))
       CALL CENT(ND,TND,NND,N2X,N2Y)
C      DO 2005 IX=1,N2X
       WRITE(8,3777)N2X
       WRITE(8,3777)N2Y
3777   FORMAT(I2)
       DO 3333 IX=1,N2X
3333   WRITE(8,2006) (NND(IX,IY),IY=1,N2Y)
2006   FORMAT(1H ,41I3)
2015   FORMAT(1H1)
C   ALPHANUMERIC OUTPUT
342    FORMAT(1H , '  USING CORDINATE CARD   ' ,I3)
2013   FORMAT(60X,1HN)
       IX=1
       DO 2007 ISX=1,IX2
C   CLEAR STER AND PUT IN LIMITING STARS
       DO 2008 ISY=1,81
2008   STER(ISY)=ALPH(1)
       CSQ=(FLOAT(ISX)-RX2)*(RX3-FLOAT(ISX))
       IF(CSQ.LT.0.0) GO TO 2020
       IDIFY=IFIX(RX4*SQRT(CSQ)+0.5)
       IYLR=41-IDIFY
       IYUR=41+IDIFY
       STER(IYLR)=STAR
       STER(IYUR)=STAR
C   IDENTIFY CORRESPONDING LOCNS OF STER AND ND
2020   IF(ISX.NE.((IX-NIX-2)*INTX+IX3)) GO TO 2009
       DO 2010 IY=1,N2Y
       ISY=41+(IY-NIY-2)*INTY
       IF(ISY.LT.1.OR.ISY.GT.81) GO TO 2010
C   SET CORRECT ALPHANUMERIC VALUE IN STER
C      ID=ND(IX,IY)+1
C      IF(ID.GT.27) ID=27
       ID=(NND(IX,IY)+1)/2+1
       IF(ID.GT.26) ID=27
       IF(ID.EQ.0) ID=1
       STER(ISY)=ALPH(ID)
       IF(NND(IX,IY).EQ.-1)STER(ISY)=1H.
2010   CONTINUE
       IX=IX+1
       IF(ISX.EQ.IX3) STER(1)=ALPH(24)
       IF(ISX.EQ.IX3) STER(81)=ALPH(6)
2011   FORMAT(20X,81A1)
2009   CONTINUE
2007   CONTINUE
902    FORMAT(60X,1HS//)
910    FORMAT(25X,*NUMERICS = THE PERCENTAGE INTERVAL THE LETTERS COVER*
       -/25X           *A=1-2  B=3-4  C=5-6  D=7-8  E=9-10  F=11-12   *
       -/25X           *G=13-14  H=15-16  I=17-18  J=19-20  K=21-22   *
       -/25X           *L=23-24  M=25-26  N=27-28  0=29-30  P=31-32   *
       -/25X           *Q=33-34  R=35-36  S=37-38  T=39-40  U=41-42   *
       -/25X           *V=43-44  W=45-46  X=47-48  Y=49-50  Z=50+     *
       -/25X           * . REPRESENTS A VALUE.GT.0,BUT.LT.1 PERCENT  *)
C      910   FORMAT(25X,50HKEY  A=1  B=2  C=3  D=4  E=5  F=6  G=7  H=8  I=9
C      119HJ=10 K=11 L=12 M=13//30X,30HN=14 0=15 P=16 Q=17 R=18 S=19 ,
C      235HT=20 U=21 V=22 W=23 X=24 Y=25 Z=26+)
C   STORE PARAMETERS FOR COMPARISON WITH NEXT SET
       INTXL=INTX
       INTYL=INTY
       IWSL=IWS
   71 CONTINUE
```

```
C
      READ (5,333) NDSET
333   FORMAT (I4)
8107  FORMAT (20X,I4,5X,I3)
C
7     CONTINUE
      REWIND 8
      REWIND 5
      STOP
      END
      SUBROUTINE PJECT (DCL,DCM,DCN,IWS,X,Y)
C GIVEN DEC,DIP IN RADIANS CALCULATES PROJECTED POINT (X UP,Y RIGHT)
C AS FRACTION OF PLOTTING CIRCLE RADIUS, FOR EQUAL AREA (IWS=1) OR
C EQUAL ANGLE (IWS=2).
      SIND=ABS (DCN)
      IF (IWS.EQ.1) GO TO 1
      R=SQRT ((1.0-SIND)/(1.0+SIND))
      GO TO 2
1     R=SQRT (1.0-SIND)
2     IF (DCM.EQ.0.0.AND.DCL.EQ.0.0) GO TO 3
      DEC=ATAN2 (DCM,DCL)
      GO TO 4
3     DEC=0.0
4     X=R*COS (DEC)
      Y=R*SIN (DEC)
      RETURN
      END
      SUBROUTINE ERECT (X,Y,IWS,DCL,DCM,DCN)
C FROM COORDINATES X,Y (FRACTIONS OF PLOTTING CIRCLE RADIUS) CALCULATES
C DIRECTION COSINES ASSUMING EQUAL AREA (IWS=1) OR EQUAL ANGLE (IWS=2)
C PROJECTION.
      R=SQRT (X*X+Y*Y)
      IF (R.GE.1.41) RETURN
      IF (R.LT.1.0E-9) GO TO 1
      IF (IWS.EQ.1) DCN=1.0-R*R
      IF (IWS.EQ.2) DCN=COS (2.0*ATAN2 (R,1.0))
      STHOR=SQRT (1.0-DCN*DCN)/R
      DCL=X*STHOR
      DCM=Y*STHOR
      RETURN
1     DCL=0.0
      DCM=0.0
      DCN=1.0
      RETURN
      END
      SUBROUTINE ROTDAT (DECR,DIPR,ANGROT,S)
C CALCULATES ROTATION MATRIX,S.
      DIMENSION S(3,3),R(3,3),T(3,3)
      DEGTOR=0.01745329252
      DO 3000 I=1,3
      DO 2999 J=1,3
2999  S(I,J)=0.0
3000  S(I,I)=1.0
      DO 3001 IRPT=1,5
      I=1
      ANG=-DEGTOR*DIPR
      IF (IRPT.NE.3) GO TO 3002
      I=2
      ANG=DEGTOR*ANGROT
3002  J=3
      IF (IRPT.EQ.1.OR.IRPT.EQ.5) J=2
      IF (IRPT.EQ.1) ANG=-DEGTOR*DECR
      IF (IRPT.EQ.5) ANG=DEGTOR*DECR
      IF (IRPT.EQ.4) ANG=DEGTOR*DIPR
```

```
      DO 3003 K=1,3
      DO 3006 L=1,3
3006  R(K,L)=0.0
3003  R(K,K)=1.0
      R(I,I)=COS(ANG)
      R(J,J)=R(I,I)
      R(I,J)=-SIN(ANG)
      R(J,I)=-R(I,J)
      DO 3005 K=1,3
      DO 3005 L=1,3
      T(K,L)=0.0
      DO 3005 M=1,3
3005  T(K,L)=T(K,L)+R(K,M)*S(M,L)
      DO 3004 K=1,3
      DO 3004 L=1,3
3004  S(K,L)=T(K,L)
3001  CONTINUE
      RETURN
      END
      SUBROUTINE PROMAT(XM1,XM2,XMP)            PMAT  1
C   FORMS MATRIX PRODUCT (XMP) = (XM1)(XM2).
      DIMENSION XM1(3,3),XM2(3,3),XMP(3,3)      PMAT  2
      DO 1 I=1,3                                PMAT  3
      DO 1 J=1,3                                PMAT  4
      XMP(I,J)=0.0                              PMAT  5
      DO 1 K=1,3                                PMAT  6
    1 XMP(I,J)=XM1(I,K)*XM2(K,J)+XMP(I,J)       PMAT  7
      RETURN                                    PMAT  8
      END                                       PMAT  9
C
      SUBROUTINE CENT(ND,TND,NND,N2X,N2Y)
C
C     CENT CONVERTS ALL COMPONANTS OF ARRAY TO  O/O OF TOTAL NO OF DATA
C     -FED INTO THE CONSTRUCTION OF THE ARRAY.
C
      INTEGER TND
      DIMENSION ND(49,41),NND(49,41)
C     DIMENSION ND(65,41),NND(65,41)
C     USE(49) FOR 6 LI/IN AND (65) FOR 8 LI/IN
      DO 1 I=1,N2X
      DO 2 K=1,N2Y
      NND(I,K)=(ND(I,K)*100)/TND
      IF((NND(I,K).EQ.0).AND.(ND(I,K).NE.0))NND(I,K)=-1
2     CONTINUE
1     CONTINUE
      RETURN
      END
C
C
C
C
C
```

```
              PROGRAM STERIG3 (INPUT,OUTPUT,FILMPUT,TAPE5=INPUT,TAPE6=OUTPUT,
              -TAPE8=FILMPUT)
C             PROGRAM SET FOR A 66 LINE/PAGE PRINTER,BUT WITH ALL OUTPUT
C             SUPPRESSED EXCEPT THAT WRITEN TO TAPE 8,THIS GOES TO THE
C             NEXT PROGRAM FOR PLOTTING.
C             THE PROGRAM IS MODIFIED TO RUN 3 SETS OF CRYSTALLOGRAPHIC DATA
C             ROTATE THESE ONTO A SINGLE PLANE AND SUM THEM.
C             THE OUTPUT IS 4 PLOTS, 1 FOR EACH SET AND THE SUM LAST.
C             IE. THE PROGRAM HANDLES UNIVERSAL STAGE DATA
              INTEGER A,TND,TND1
              DIMENSION ALPH(27),STER(81),TITLE(55),S(3,3),DCR(3),ARAN(2)
              DIMENSION SR(3,3),ST(3,3),DECR(3),DIPR(3),ANR(3)
              DIMENSION ND(49,41),DADEC(10),DADIP(10),NND(49,41),NNND(49,41)
C             DIMENSION ND(65,41),DADEC(10),DADIP(10),NND(65,41),NNND(61,41)
C     USE ND(49  FOR 6 LI/IN, ND(65  FOR 8 LI/IN
C     DIMENSION COSINE ARRAYS
              DIMENSION QL(65,41),QM(65,41),QN(65,41)
              DATA ALPH(1),ALPH(2),ALPH(3),ALPH(4),ALPH(5),ALPH(6),ALPH(7),
             1ALPH(8),ALPH(9),ALPH(10),ALPH(11),ALPH(12),ALPH(13),ALPH(14),
             2ALPH(15),ALPH(16),ALPH(17),ALPH(18),ALPH(19),ALPH(20),
             3ALPH(21),ALPH(22),ALPH(23),ALPH(24),ALPH(25),ALPH(26),ALPH(27)/
             41H ,1HA,1HB,1HC,1HD,1HE,1HF,1HG,1HH,1HI,1HJ,1HK,1HL,1HM,1HN,1HO,
             51HP,1HQ,1HR,1HS,1HT,1HU,1HV,1HW,1HX,1HY,1HZ/,STAR/1H*/,
             6ARAN(1),ARAN(2)/5HEQ AR,5HEQ AN/
              DATA IX1/23/,RX1/23.62/,IX2/49/,RX2/1.38/,RX3/48.62/,
             1RX4/1.6667/,IX3/25/
C             DATA IX1/31/,RX1/31.52/,IX2/65/,RX2/1.48/,RX3/64.52/,
C            1RX4/1.25/,IX3/33/
C     FOR 6 LI/IN USE   23   23.62   49   1.38   48.62   1.6667   25
C             8              31   31.52   65   1.48   64.52   1.25     33
              PI=3.1415926536
              DEGTOR=PI/180.0
              INTXL=0
              INTYL=0
              IWSL=0
              TND1=0
              III=0
              READ (5,487)NSET
              NSET1=NSET+1
              WRITE(8,487)NSET1
          487 FORMAT(I3)
C
C
              DO 71 ISET=1,NSET
              READ(5,344)A
              IF(EOF(5).NE.0.0)GO TO 7
          344 FORMAT(I3)
              READ(5,343)TND
              IF(EOF(5).NE.0.0)GO TO 7
          343 FORMAT(I4)
              READ(5,14)INTX,INTY,NCODE,NPC,IWS,NR,(TITLE(I),I=1,55),
             -RAMAX
              IF(EOF(5).NE.0.0)GO TO 7
          14  FORMAT(5I1,55A1,4F5.2)
              IF(INTY.LT.2) INTY=2
C
C     PRELIMINARIES FOR SET
C     CFNORM IS COSINE OF ANGLE, ALPHA, OF CONE OF SAMPLING (I.E. SEMI-ANGLE)
C     FOR 1 PERCENT AREA (OR SOLID ANGLE) CANORM=0.99
              CANORM=1.0-0.01*FLOAT(NPC)
              SANORM=SQRT(1.0-CANORM*CANORM)
C     FORM SIN(ALPHA+5) - SEE BELOW
              SA5=SANORM*COS(36.0*DEGTOR)+CANORM*SIN(36.0*DEGTOR)
              LTOT=0
```

```
C  CALCULATE ARRAY LIMITS FOR ND
       NIX=IX1/INTX
       NIY=39/INTY
C  ND IS ND(2*NIX+3,2*NIY+3)
C  CENTRE IS (NIX+2,NIY+2)
C  CALCULATE LOCAL GRID LIMITS
       LGY=IFIX(FLOAT(NIY)*SANORM+1.5)
       LGX=IFIX(FLOAT(NIX)*SANORM+1.5)
C  CLEAR ND, NUMERICAL OUTPUT ARRAY
201    N2X=2*NIX+3
       N2Y=2*NIY+3
       DO 1030 I=1,N2X
       DO 1030 J=1,N2Y
       IF(III.GT.0)GO TO 1030
       NNND(I,J)=0
1030   ND(I,J)=0
       III=III+1
C  BUILD DIRN COSINE ARRAYS - SKIP IF ALREADY DONE
       IF(IWS.NE.IWSL) GO TO 1033
       IF(INTX.EQ.INTXL.AND.INTY.EQ.INTYL) GO TO 1032
1033   DO 1031 I=1,N2X
       DO 1031 J=1,N2Y
       X=FLOAT((NIX+2-I)*INTX)/RX1
       Y=FLOAT((J-NIY-2)*INTY)/39.37
       CALL ERECT(X,Y,IWS,DCL,DCM,DCN)
       QL(I,J)=DCL
       QM(I,J)=DCM
1031   QN(I,J)=DCN
1032   CONTINUE
       WRITE(8,342)A
       WRITE(8,727)NR
5012   FORMAT(14H1INPUT DATA - ,55A1,3X,9HSTEERING ,5I1,3X,8HRAMAX = ,
      1F5.2//)
C  IF DATA ARE TO BE ROTATED, CALCULATE ROTATION MATRIX,S.
       IF(NR.EQ.0) GO TO 1009
       READ(5,1107) (DECR(IR),DIPR(IR),ANR(IR),IR=1,3)
1107   FORMAT(9F5.1)
727    FORMAT(I1)
       DO 1100 I=1,3
       DO 1101 J=1,3
1101   S(I,J)=0.0
1100   S(I,I)=1.0
       DO 1102 IR=1,3
       CALL ROTDAT(DECR(IR),DIPR(IR),ANR(IR),SR)
       CALL PROMAT(SR,S,ST)
       DO 1103 I=1,3
       DO 1103 J=1,3
1103   S(I,J)=ST(I,J)
1102   CONTINUE
1009   CONTINUE
C
C  READ AND PROCESS DATA
 1007 READ (5,1001) (DADEC(I),DADIP(I),I=1,5)
 1001 FORMAT(10F4.0)
5013   FORMAT(5(F10.2,F7.2))
       DO 1003 I=1,5
       I2END=1
       ENDEC=DADEC(I)
       IF(ENDEC.EQ.1000.0) GO TO 1002
       IF(ENDEC.EQ.2000.0) GO TO 1007
       IF(DADIP(I).GE.0.0) GO TO 800
       DADIP(I)=-DADIP(I)
       ENDEC=ENDEC+180.0
       IF(ENDEC.GT.360.0) ENDEC=ENDEC-360.0
```

```
 800     CONTINUE
         LTOT=LTOT+1
         ENDEC=DEGTOR*ENDEC
         IF (NCODE.LT.4) GO TO 1500
C  PLAGIARISED DATA
         X=DADIP(I)*COS(ENDEC)/RAMAX
         Y=DADIP(I)*SIN(ENDEC)/RAMAX
         IWS2=NCODE-3
         CALL ERECT(X,Y,IWS2,DCLA,DCMA,DCNA)
         GO TO 2030
C  OTHER CASES - CHANGE TO CONFORM WITH NCODE = 1
1500     ENDIP=DEGTOR*DADIP(I)
         IF (NCODE-2) 1502,1503,1504
1504     ENDEC=ENDEC+0.5*PI
1503     ENDEC=ENDEC+PI
         IF (ENDEC.GT.2.0*PI) ENDEC=ENDEC-2.0*PI
         ENDIP=0.5*PI-ENDIP
1502     CONTINUE
C
C  CALCULATE DIRECTION COSINES
         DCLA=COS(ENDIP)*COS(ENDEC)
         DCMA=COS(ENDIP)*SIN(ENDEC)
         DCNA=SIN(ENDIP)
2030     IF (NR.EQ.0) GO TO 3000
C  ROTATE DATA IF REQD.  TAKE OTHER END OF AXIS IF OUT OF LR HEMIS.
         DO 3001 IC=1,3
3001     DCR(IC)=S(IC,1)*DCLA+S(IC,2)*DCMA+S(IC,3)*DCNA
         DCLA=DCR(1)
         DCMA=DCR(2)
         DCNA=DCR(3)
         IF (DCNA.GE.0.0) GO TO 3000
2003     DCNA=-DCNA
         DCLA=-DCLA
         DCMA=-DCMA
3000     CONTINUE
C  FIND LOCAL ZERO - NEAREST ND LOCN TO DATA POINT
         CALL PJECT(DCLA,DCMA,DCNA,IWS,XCOMP,YCOMP)
         ILZ=-IFIX(FLOAT(NIX)*XCOMP+0.5)+NIX+2
         JLZ=IFIX(FLOAT(NIY)*YCOMP+0.5)+NIY+2
C  SCAN OVER LOCAL GRID
         ILL=ILZ-LGX
         ILU=ILZ+LGX
         JLL=JLZ-LGY
         JLU=JLZ+LGY
         IF (ILL.LT.1) ILL=1
         IF (JLL.LT.1) JLL=1
         IF (ILU.GT.N2X) ILU=N2X
         IF (JLU.GT.N2Y) JLU=N2Y
         DO 2001 IL=ILL,ILU
         DO 2001 JL=JLL,JLU
C  FIND DIRN COSINES OF ARRAY LOCN - FIND CORRESP TRUE SPACE POINT
C  AND CALL ERECT
         DCL=QL(IL,JL)
         DCM=QM(IL,JL)
         DCN=QN(IL,JL)
C  IGNORE GRID POINTS IF MORE THAN 5 DEGREES BEYOND PRIMITIVE
         IF (DCN.LT.-0.087) GO TO 2001
C  ADD ONE TO CELL IF APPROPRIATE
         IF ((DCLA*DCL+DCMA*DCM+DCNA*DCN).GE.CANORM) ND(IL,JL)=ND(IL,JL)+1
2001     CONTINUE
C  CHECK WHETHER POINT LIES WITHIN ALPHA+5 OF PERIMETER - IF SO, REPEAT
C  CALCULATION FOR OTHER END OF AXIS
         IF (DCNA.GT.SA5.OR.I2END.LT.0) GO TO 1003
         I2END=-1
```

```
         GO TO 2003
1003  CONTINUE
         GO TO 1007
C  WRITE TABLE OF CALCULATED VALUES
1002       WRITE (8,2014) (TITLE(I),I=1,55)
2014  FORMAT(1H ,55A1)
         WRITE (8,2113) INTY,INTX,NPC,LTOT,ARAN(IWS)
2113  FORMAT(1H ,' SAMPLING  ',I3,'ACROSS/-',I3,' DOWN ',15X,' POLES PER
     - ',I2,'PERCENT AREA ',5X,I4,' DATA ',5X,A5)
2004  FORMAT(1H0,55A1//12H SAMPLING - ,I3,8H ACROSS/,I3,5H DOWN,
     15X,10HPOLES PER ,I2,13H PERCENT AREA,5X,I4,5H DATA,5X,A5)
5001  FORMAT(12HOROTATED BY ,F6.1,13H ABOUT DEC = ,F6.1,8H  DIP = ,
     1F6.1)
7000  FORMAT(19H ROTATION MATRIX    ,3F10.4/(19X,3F10.4))
         IF (III.LE.3) CALL CENT(ND,TND,NND,N2X,N2Y)
         IF (III.EQ.3) GO TO 7676
6767  CONTINUE
         IF (III.EQ.3) III=8
         TND1=TND1+TND
         IF (III.EQ.8) WRITE (8,342) A
         IF (III.EQ.8) NR=0
         IF (III.EQ.8) WRITE (8,727) NR
         IF (III.EQ.8) WRITE (8,2014) (TITLE(I),I=1,55)
         IF (III.EQ.8) WRITE (8,2113) INTY,INTX,NPC,TND1,ARAN(IWS)
         DO 7579 NAX=1,N2X
         DO 7578 NAY=1,N2Y
         NNND(NAX,NAY)=NNND(NAX,NAY)+ND(NAX,NAY)
7578  CONTINUE
7579  CONTINUE
         IF (III.EQ.8) CALL CENT1(NNND,TND1,NND,N2X,N2Y)
7676  CONTINUE
C        DO 2005 IX=1,N2X
         WRITE (8,3777) N2X
         WRITE (8,3777) N2Y
3777  FORMAT(I2)
         DO 3333 IX=1,N2X
3333  WRITE (8,2006) (NND(IX,IY),IY=1,N2Y)
2006  FORMAT(1H ,41I3)
2015  FORMAT(1H1)
C  ALPHANUMERIC OUTPUT
342   FORMAT(1H , ' USING CORDINATE CARD  ' ,I3)
2013  FORMAT(60X,1HN)
         IX=1
         DO 2007 ISX=1,IX2
C  CLEAR STER AND PUT IN LIMITING STARS
         DO 2008 ISY=1,81
2008  STER(ISY)=ALPH(1)
         CSQ=(FLOAT(ISX)-RX2)*(RX3-FLOAT(ISX))
         IF (CSQ.LT.0.0) GO TO 2020
         IDIFY=IFIX(RX4*SQRT(CSQ)+0.5)
         IYLR=41-IDIFY
         IYUR=41+IDIFY
         STER(IYLR)=STAR
         STER(IYUR)=STAR
C  IDENTIFY CORRESPONDING LOCNS OF STER AND ND
2020   IF (ISX.NE.((IX-NIX-2)*INTX+IX3)) GO TO 2009
         DO 2010 IY=1,N2Y
         ISY=41+(IY-NIY-2)*INTY
         IF (ISY.LT.1.OR.ISY.GT.81) GO TO 2010
C  SET CORRECT ALPHANUMERIC VALUE IN STER
C        ID=ND(IX,IY)+1
C        IF (ID.GT.27) ID=27
         ID=(NND(IX,IY)+1)/2+1
         IF (ID.GT.26) ID=27
```

```
         IF(ID.EQ.0) ID=1
         STER(ISY)=ALPH(ID)
         IF(NND(IX,IY).EQ.-1)STER(ISY)=1H.
2010     CONTINUE
         IX=IX+1
         IF(ISX.EQ.IX3) STER(1)=ALPH(24)
         IF(ISX.EQ.IX3) STER(81)=ALPH(6)
2011     FORMAT(20X,81A1)
2009     CONTINUE
2007     CONTINUE
902      FORMAT(60X,1HS//)
910      FORMAT(25X,*NUMERICS = THE PERCENTAGE INTERVAL THE LETTERS COVER*
         -/25X          *A=1-2   B=3-4   C=5-6   D=7-8   E=9-10  F=11-12  *
         -/25X          *G=13-14 H=15-16 I=17-18 J=19-20 K=21-22  *
         -/25X          *L=23-24 M=25-26 N=27-28 O=29-30 P=31-32  *
         -/25X          *Q=33-34 R=35-36 S=37-38 T=39-40 U=41-42  *
         -/25X          *V=43-44 W=45-46 X=47-48 Y=49-50 Z=50+    *
         -/25X          * . REPRESENTS A VALUE.GT.0,BUT.LT.1 PERCENT  *)
C        910    FORMAT(25X,50HKEY  A=1  B=2   C=3  D=4  E=5  F=6  G=7  H=8  I=9  ,
C        119HJ=10 K=11 L=12 M=13//30X,30HN=14 O=15 P=16 Q=17 R=18 S=19 ,
C        235HT=20 U=21 V=22 W=23 X=24 Y=25 Z=26+)
C  STORE PARAMETERS FOR COMPARISON WITH NEXT SET
         INTXL=INTX
         INTYL=INTY
         IWSL=IWS
         IF(III.EQ.3)GO TO 6767
   71 CONTINUE
C
         READ(5,333)NDSET
333      FORMAT(I4)
8107     FORMAT(20X,I4,5X,I3)
C
7        CONTINUE
         REWIND 8
         REWIND 5
         STOP
         END
         SUBROUTINE PJECT(DCL,DCM,DCN,IWS,X,Y)
C  GIVEN DEC,DIP IN RADIANS CALCULATES PROJECTED POINT (X UP,Y RIGHT)
C  AS FRACTION OF PLOTTING CIRCLE RADIUS, FOR EQUAL AREA (IWS=1) OR
C  EQUAL ANGLE (IWS=2).
         SIND=ABS(DCN)
         IF(IWS.EQ.1) GO TO 1
         R=SQRT((1.0-SIND)/(1.0+SIND))
         GO TO 2
1        R=SQRT(1.0-SIND)
2        IF(DCM.EQ.0.0.AND.DCL.EQ.0.0) GO TO 3
         DEC=ATAN2(DCM,DCL)
         GO TO 4
3        DEC=0.0
4        X=R*COS(DEC)
         Y=R*SIN(DEC)
         RETURN
         END
         SUBROUTINE ERECT(X,Y,IWS,DCL,DCM,DCN)
C  FROM COORDINATES X,Y (FRACTIONS OF PLOTTING CIRCLE RADIUS) CALCULATES
C  DIRECTION COSINES ASSUMING EQUAL AREA (IWS=1) OR EQUAL ANGLE (IWS=2)
C  PROJECTION.
         R=SQRT(X*X+Y*Y)
         IF(R.GE.1.41) RETURN
         IF(R.LT.1.0E-9) GO TO 1
         IF(IWS.EQ.1) DCN=1.0-R*R
         IF(IWS.EQ.2) DCN=COS(2.0*ATAN2(R,1.0))
         STHOR=SQRT(1.0-DCN*DCN)/R
```

```
        DCL=X*STHOR
        DCM=Y*STHOR
        RETURN
1       DCL=0.0
        DCM=0.0
        DCN=1.0
        RETURN
        END
        SUBROUTINE ROTDAT(DECR,DIPR,ANGROT,S)
C   CALCULATES ROTATION MATRIX,S.
        DIMENSION S(3,3),R(3,3),T(3,3)
        DEGTOR=0.01745329252
        DO 3000 I=1,3
        DO 2999 J=1,3
2999    S(I,J)=0.0
3000    S(I,I)=1.0
        DO 3001 IRPT=1,5
        I=1
        ANG=-DEGTOR*DIPR
        IF(IRPT.NE.3) GO TO 3002
        I=2
        ANG=DEGTOR*ANGROT
3002    J=3
        IF(IRPT.EQ.1.OR.IRPT.EQ.5) J=2
        IF(IRPT.EQ.1) ANG=-DEGTOR*DECR
        IF(IRPT.EQ.5) ANG=DEGTOR*DECR
        IF(IRPT.EQ.4) ANG=DEGTOR*DIPR
        DO 3003 K=1,3
        DO 3006 L=1,3
3006    R(K,L)=0.0
3003    R(K,K)=1.0
        R(I,I)=COS(ANG)
        R(J,J)=R(I,I)
        R(I,J)=-SIN(ANG)
        R(J,I)=-R(I,J)
        DO 3005 K=1,3
        DO 3005 L=1,3
        T(K,L)=0.0
        DO 3005 M=1,3
3005    T(K,L)=T(K,L)+R(K,M)*S(M,L)
        DO 3004 K=1,3
        DO 3004 L=1,3
3004    S(K,L)=T(K,L)
3001    CONTINUE
        RETURN
        END
        SUBROUTINE PROMAT(XM1,XM2,XMP)                               PMAT 1
C   FORMS MATRIX PRODUCT (XMP) = (XM1)(XM2).
        DIMENSION XM1(3,3),XM2(3,3),XMP(3,3)                         PMAT 2
        DO 1 I=1,3                                                   PMAT 3
        DO 1 J=1,3                                                   PMAT 4
        XMP(I,J)=0.0                                                 PMAT 5
        DO 1 K=1,3                                                   PMAT 6
1       XMP(I,J)=XM1(I,K)*XM2(K,J)+XMP(I,J)                          PMAT 7
        RETURN                                                      PMAT 8
        END                                                         PMAT 9
C
        SUBROUTINE CENT(ND,TND,NND,N2X,N2Y)
C
C       CENT CONVERTS ALL COMPONANTS OF ARRAY TO  O/O OF TOTAL NO OF DATA
C       -FED INTO THE CONSTRUCTION OF THE ARRAY.
C
        INTEGER TND
        DIMENSION ND(49,41),NND(49,41)
```

```
C          DIMENSION ND(65,41),NND(65,41)
C          USE(49) FOR 6 LI/IN AND (65) FOR 8 LI/IN
           DO 1 I=1,N2X
           DO 2 K=1,N2Y
           NND(I,K)=(ND(I,K)*100)/TND
           IF((NND(I,K).EQ.0).AND.(ND(I,K).NE.0))NND(I,K)=-1
2          CONTINUE
1          CONTINUE
           RETURN
           END
C
C
           SUBROUTINE CENT1(NNND,TND1,NND,N2X,N2Y)
C
C          THIS PERCENTAGES THE SUMED MATRIX NNND WHICH IS
C          RUN 1+2+3= THE OUTPUT NET NO 4
           INTEGER TND1
C          DIMENSION NNND(65,41),NND(65.41)
           DIMENSION NNND(49,41),NND(49,41)
C          USE (49) FOR 6 LI/IN,AND (65) FOR 8 LI/IN.
           DO 1 I=1,N2X
           DO 2 K=1,N2Y
           NND(I,K)=(NNND(I,K)*100)/TND1
           IF((NND(I,K).EQ.0).AND.(NNND(I,K).NE.0))NND(I,K)=-1
2          CONTINUE
1          CONTINUE
           RETURN
           END
```

```
      PROGRAM DRAW(INPUT,OUTPUT,TAPE3=INPUT,TAPE4=OUTPUT)
C     THE PURPOSE OF THIS PROGRAM IS TO CONSTRUCT A PAGE CONTAINING A
C     CIRCLE, IN WHICH IS FITTED A TWO DIMENSIONAL ARRAY (ND), HOLDING
C     THE DATA FROM PROGRAM STERIO.
C     THIS ARRAY IS THEN CONTOURED AT PRESET VALUES.
C     THESE VALUES CAUSE CONTOURS AT TWO PERCENT INTERVALS FROM 0-50
C     PERCENT, WITH INCREASING CONTOUR DENSITY WITH ASCENT.
C     THE PROGRAM READS FROM A TAPE CREATED BY STERIO,AND USES INFORMATION
C     FROM THIS, AS WELL AS ARRAYS OF DATA WITHIN ITSELF TO CONSTRUCT TITLING,
C     AND A KEY FOR THE PAGE, WHICH IS DRAWN BY THE PROGRAMME ON FILM.THUS
C     THE PROGRAMME TO RUN AT ALL WITHOUT MODIFICATION, MUST RUN WITH STERIO,
C     WHICH IN TURN IN ITS PRESENT FORM MUST RUN WITH SORT2.........
C                     SET UP DIMENSIONS
      INTEGER X(3),TITLE(6),STRR(10),P,NRR(3),NR(1),N(1),ICVALS(27)
      INTEGER S(1),E(1),W(1),SP(1),PS(1),NRS(2),GUFG(5)
      INTEGER GUFA(5),GUFB(9),GUFC(8),GUFD(8),GUFE(8),GUFF(8)
      REAL ND(41,49),CVALS(27)
      DIMENSION NND(49,41)
C               COMMON BLOCK WITH A DIMFILM SUBROUTINE
C               CONTROLLING THE SIZE OF CONTOUR PLOTTING
C               AREA IN A WINDOW.
      COMMON/DIMCONS/A(18)
C               DATA STATEMENTS CONTAINING LABELING THAT
C               DO NOT NEED TO CHANGE INSIDE THE PRGRAMME.
      CALL DATA(NRR,'THIS PLOT HAS UNDERGONE -',3)
      CALL DATA(NRS,'- ROTATIONS ',2)
      DATA N/1HN/
      DATA S/1HS/
      DATA E/2H-E/
      DATA W/2HW-/
      DATA SP/1H↑/
      DATA PS/1H./
C         ARRAY HOLDING CONTOUR LEVEL VALUES.
      DATA CVALS/00.5,00.9,02.9,04.9,06.9,08.9,                         .
     -10.9,12.9,14.9,16.9,18.9,20.9,
     -22.9,24.9,26.9,28.9,30.9,32.9,
     -34.9,36.9,38.9,40.9,42.3,44.9,
     -46.9,48.9,50.9/
C          DATA FOR THE KEY.
      CALL DATA(GUFA,'THE CONTOURS REPRESENT THE FOLLOWING PERCENTAGES'
     -,5)
      CALL DATA(GUFB,'00.9<=1-20 :0>02.9<=3-40 :0>04.9<=5-60 :0>06.9<=7-80:
     -0>08.9<=9-100:0>10.9<=11-120:0>12.9'.9)
      CALL DATA(GUFC,'12.9<=13-140:0>14.9<=15-160 '0>16.9<=17-180:0>18.9<
     -=19-200 '0>20.9<=21-220:0>22.9',8)
      CALL DATA(GUFD,'22.9<=23-240:0>24.9<=25-260:0>26.9<=27-280:0>28.9<
     -=29-300:0>30.9<=31-320:0>32.9',8)
      CALL DATA(GUFE,'32.9<=33-340:0>34.9<=35-360:0>36.9<=37-380:0>38.9<
     -=39-400 '0>40.9<=41-420:0>42.9',8)
      CALL DATA(GUFF,'42.9<=43-440:0>44.9<=45-460:0>46.9<=47-480:0>48.9<
     -=49-500:0>50.9<=510:0+',8)
      CALL DATA(GUFG,'NOTE A VALUE OF>0.5-0.9<=.LT.10:0AND.GT.00'0',
     -5)
C               ARRAY CONTROLLING LEVELS OF CONTOUR INTENSITY.
      DATA ICVALS/10,11,12,13,14,15,16,17,18,19,20,21,22,23,24,25,25,
     -26,26,27,27,28,28,29,29,30,30/
C             READ IN NUMBER OF DATA SETS TO BE DEALT WITH.
      READ(3,1)NSET
1     FORMAT(I3)
C             SET UP FOR PLOTTING ON DIMFILM.
      CALL CAM35MM
      A(1)=1.0
      A(2)=0.0
      CALL CINE
```

```
        CALL BOUNDS(0.0,100.0,0.0,150.0)
        CALL SYMHT(1.666666)
        DO 2 I=1,NSET
C           START READING DATA FROM PREVIOUS PROGRAMME.
        READ(3,3) (X(J),J=1,3)
        IF(EOF(3).NE.0)GO TO 4
3       FORMAT(1X,2A10,A7)
        READ(3,5)NR
5       FORMAT(A1)
        READ(3,6) (TITLE(J),J=1,6)
6       FORMAT(1X,5A10,A5)
        READ(3,7) (STRR(J),J=1,10)
7       FORMAT(1X,9A10,A8)
        READ(3,8)N2X
        READ(3,8)N2Y
8       FORMAT(I2)
        N3X=N2X
        N3Y=N2Y
C          READ IN MATRIX OF DATA TO BE CONTOURED.
        DO 9 IX=1,N2X
        READ(3,10) (NND(IX,IY),IY=1,N2Y)
10      FORMAT(1X,41I3)
9       CONTINUE
C          CONVERT IT TO A REAL ARRAY, STAND IT ON END,
C          AND TURN IT UPSIDE DOWN. SO THAT IT FITS THE CINE
C          MODE OF THE FILM AND IS STILL CORRECT N,S,E,AND W.
        N2X1=N2X+1
        DO 11 P=1,N2X
        DO 12 K=1,N2Y
        ND(K,P)=NND(N2X1-P,K)
C          EQUATION TO GATHER 0-1 PERCENT LEVEL.
        IF(ND(K,P).EQ.-1)ND(K,P)=0.51
12      CONTINUE
11      CONTINUE
C          FIND LARGEST CIRCLE THAT CAN BE FITTED INTO A
C          MATRIX N3X,N3Y. NOTE, N3X CAN BE <,>,=, N3Y
C          ALL VALUES OUTSIDE ARE THEN SET TO EXTREME VALUES TO
C          FORCE INTERPOLATION DURING CONTOURING TO REMAIN
C          WITHIN THE CIRCLE.
        CALL ZIRCLE(ND,N3Y,N3X,-10.0)
        CALL OUTLINE
C          START LABELING
        CALL OFFTOXY(36.5,134.0)
        CALL SYMTEXT(X,27)
        CALL OFFTOXY(31.0,138.0)
        CALL SYMTEXT(NRR,25)
        CALL OFFTOXY(56.25,138.0)
        CALL SYMTEXT(NR,1)
        CALL OFFTOXY(57.5,138.0)
        CALL SYMTEXT(NRS,11)
        CALL WINDOW(21.5,77.5,142.0,148.0)
        CALL WINDFRM
        CALL ENDWIND
        CALL OFFTOXY(22.0,144.5)
        CALL HVYTYPE
        CALL UNLIN
        CALL SYMTEXT(TITLE,55)
        CALL NOUNLIN
        CALL NRMTYPE
        CALL OFFTOXY(1.0,130.0)
        CALL SYMTEXT(STRR,98)
        CALL OFFTOXY(50.0,124.5)
        CALL SYMTEXT(N,1)
        CALL OFFTOXY(50.0,123.0)
```

```
      CALL HVYTYPE
      CALL SYMTEXT(SP,1)
      CALL SYMTEXT(SP,1)
      CALL NRMTYPE
      CALL OFFTOXY(0.0,75.0)
      CALL SYMTEXT(W,2)
      CALL OFFTOXY(98.0,75.0)
      CALL SYMTEXT(E,2)
      CALL OFFTOXY(50.0,26.0)
      CALL SYMTEXT(SP,1)
      CALL OFFTOXY(49.0,25.0)
      CALL SYMTEXT(S,1)
      CALL OFFTOXY(50.0,75.0)
      CALL HVYTYPE
      CALL SYMTEXT(PS,1)
      CALL NRMTYPE
C           DRAW CIRCLE TWICE TO MAKE IT DARK.
      CALL CIRCLE(50.0,75.0,48.0)
      CALL CIRCLE(50.0,75.0,48.0)
C             DRAW KEY BOX AND KEY.
      CALL WINDOW(10.0,90.0,2.0,24.0)
      CALL WINDFRM
      CALL ENDWIND
      CALL OFFTOXY(26.0,22.0)
      CALL UNLIN
      CALL SYMTEXT(GUFA,48)
      CALL NOUNLIN
      CALL ROMGRK(1RO)
      CALL OFFTOXY(14.0,18.0)
      CALL SYMTEXT(GUFB,85)
      CALL OFFTOXY(15.5,15.2)
      CALL SYMTEXT(GUFC,79)
      CALL OFFTOXY(15.5,12.4)
      CALL SYMTEXT(GUFD,79)
      CALL OFFTOXY(15.5,9.6)
      CALL SYMTEXT(GUFE,79)
      CALL OFFTOXY(19.0,6.8)
      CALL SYMTEXT(GUFF,72)
      CALL OFFTOXY(30.0,4.0)
      CALL SYMTEXT(GUFG,44)
      CALL DEFALTS
C     WINDOW AREA TO CONTAIN CONTOUR ARRAY.
      CALL WINDOW(0.6,99.4,27.1,122.8)
C        TURN ON INTERPOLATION,A CUBIC EQUATION.
      CALL CINTERP(10)
C        SET CONTOURING LABLE SIZE.
      CALL CLABHT(0.5,0)
C        CONTOUR.
      CALL CONTR1(ND,N3Y,N3X,27,CVALS,ICVALS)
C        TURN EVERYTHING OFF.
      CALL NOCINT
      CALL ENDWIND
      CALL NEWFRAM
2     CONTINUE
4     CONTINUE
      CALL ENDFILM
      STOP
      END
      SUBROUTINE DATA(ARRAY,STRING,LENTH)
C        PUTS DATA STRINGS INTO 10H WORD BLOCKS.
      IMPLICIT INTEGER(A-Z)
      DIMENSION ARRAY(LENTH),STRING(LENTH)
      IF(LENTH.GT.0)GO TO 10
      CALL DISPLA('*** WARNING0-SILLY ARRAY SIZEO',LENTH)
```

```
        RETURN
10      DO 20 I=1,LENTH
        IF (STRING(I).EQ.0) RETURN
20      ARRAY(I)=STRING(I)
        IF (STRING(LENTH+1).NE.0) CALL DISPLA
      -('*** WARNING-ATTEMPT TO EXCEED BOUNDS',LENTH+1)
C              NOTE DISPLA PRINTS OUT ONTO THE DAY FILE.
        RETURN
        END
        SUBROUTINE ZIRCLE (ARRAY,NX,NY,SPECVAL)
C         GENERAL CIRCLE FITTING ROUTINE,ALTERS VALUES OUTSIDE
C         CIRCLE TO SPECIFIED VALUE.
        IMPLICIT INTEGER (A-Z)
        REAL ARRAY(NX,NY)
        REAL XYRATIO,SPECVAL,R
C                               FIND RADIUS IN TERMS OF Y
        R=NY/2.0
        IR=R+0.51
C                               FIND RADIUS IN TERMS OF X
        IRX=NX/2.0 + 0.51
        IRSQ=R*R + 0.51
C                               FIND RATIO OF AXIS SCALES
        XYRATIO=FLOAT(NX)/FLOAT(NY)
C                               CALC ODD/EVEN CENTERING ADJUSTMENTS
        IXCENT=0
        IF ((IRX+IRX).EQ.NX) IXCENT=1
        IYCENT=0
        IF ((IR +IR ).EQ.NY) IYCENT=1
        DO 800 IY=1,IR
C                               FIND Y DISPLACEMENT FROM CENTRE
        ITABY=IR-IY
C                               CALC X DISPLACEMENT FROM CENTRE
        ITABX=SQRT(FLOAT(IRSQ-(ITABY*ITABY))) * XYRATIO
C                               FILL IN LEFT HAND SPECIAL VALUE
        ITAB=IRX-ITABX
C                               JUMP IF CIRCLE REACHES LEFT BOUND
        IF (ITAB.LT.1) GO TO 350
        DO 300 IX=1,ITAB
C                               ABOVE EQUATOR
        ARRAY(IX,IR-ITABY)=SPECVAL
C                               BELOW EQUATOR
        ARRAY(IX,IR+ITABY+IYCENT)=SPECVAL
300     CONTINUE
C                               FILL IN RIGHT HAND SPECIAL VALUES
350     ITAB=IRX+ITABX+IXCENT
C                               JUMP IF CIRCLE REACHES RIGHT BOUND
        IF (ITAB.GT.NX) GO TO 800
        DO 400 IX=ITAB,NX
C                               ABOVE EQUATOR
        ARRAY(IX,IR-ITABY)=SPECVAL
C                               BELOW EQUATOR
        ARRAY(IX,IR+ITABY+IYCENT)=SPECVAL
400     CONTINUE
800     CONTINUE
        RETURN
        END
```

```
DOC SOURCE
 FORMATTER ↑WITH↑ ALL ↑FROM↑ BEDFORDALBUM
↑BEGIN↑
↑MODE↑↑FILEPROC↑ = ↑PROC↑ (↑REF↑↑CHARPUT↑) ↑VOID↑;
↑OP↑ ⋇ = (↑INT↑ N, ↑FILEPROC↑ FILEPROC) [] ↑FILEPROC↑O
     ↑BEGIN↑
     [1ON] ↑FILEPROC↑ ARRAY;
     ↑FOR↑ I ↑TO↑ N ↑DO↑ ARRAY [I] O= FILEPROC;
      ARRAY
     ↑END↑;
[] ↑CHAR↑ A='NF', B='SF'; [102] ↑CHAR↑ C;
↑REAL↑ X,Y; ↑INT↑DIR,AMT;
 PRINT ('FRAMING.....');
 PRINT ((NEWLINE, '⋇⋇⋇FRAMEOO=/CD257.16.ALGOL2', NEWLINE));
↑WHILE↑ READ ((NEWLINE, 8 ⋇ SPACE, DIR, AMT,SPACE,C, X, Y));
       C ↑NE↑ 'XX'
↑DO↑↑BEGIN↑
     ↑IF↑ C=A ↑OR↑ C=B
     ↑THEN↑ OUTF(STANDOUT, 6X2D '.',3D '.',2D.2D,2D.2DL , (AMT,DIR,X,Y))
     ↑FI↑
     ↑END↑;
 PRINT ((':⋇⋇⋇FRAMEOSO-', NEWLINE))
↑END↑
↑FINISH↑
⋇⋇⋇
```

THE PLOTST EXTENSION, BLOCK — D — .
_____

THIS EXTENSION TO THE PLOTST LIBRARY WAS WRITTEN BY —
  F. W. M. HOPPER AND C. J. COOKSON   1978

THE LIBRARY ALSO UTILISES THE ULCC. DIMFILM AND MICROFILM
ROUTINES, AND THE SYMAP AND SYMVU PACKAGES, AS AVAILABLE AT ULCC.

_____

BLOCK —D—
THIS PART OF THE PLOTST LIBRARY IS A SET OF FORTRAN
PROGRAMS WHICH TAKE GRID REFERENCED FOLIATION READINGS,
MEASURED AS AZIMUTH OF DIP AND AMOUNT OF DIP.
FROM THEM IT CONSTRUCTS A THREE DIMENSIONAL BLOCK DIAGRAM
OF THE AVERAGE FOLIATION SURFACE ACROSS THE AREA FROM WHICH
THE READINGS WERE TAKEN.

THE PHILOSOPHY BEHIND THE PACKAGE.

THE DATA IS TAKEN,READ IN AS BINARY (THE DEFAULT) OR
IN A USER SPECIFIED FORMAT. (WHERE THE INFORMATION IS
PRESENTED — DIP, AZIMUTH, X COORDINATE, Y COORDINATE,
X IS ALONG THE BOTTOM AXIS OF THE MAP WITH 0.0 IN
THE BOTTOM LEFT CORNER.)
FROM THIS INFORMATION, THE APPARENT DIP ALONG THE E—W GRID
LINES ARE CALCULATED AND WRITTEN OFF TO A FILE FOR FURTHER USE.
LIKEWISE FOR THE APPARENT DIPS MEASURED ALONG THE N—S
GRID LINES .
TWO FILES ARE THEREFORE MADE (WRITTEN IN BINARY) WITH THE
INFORMATION ON THEM AS — APPARENT DIP (+ OR —, DEPENDING
ON WHETHER THE DIP WAS DOMINANTLY TO THE E=+,W=—,N=+,S=—
THE VALUES RANGING FROM +90.0 TO —90.0 DEGREES),
X COORDINATE AND Y COORDINATE, (ONE SET OF READINGS PER LINE).
NEXT THESE TWO DATA FILES MUST BE PROCESSED BY A PROGRAM
THAT PREPARES THEM FOR SYMAP. THIS IS NECESSARY BECAUSE
SYMAP WILL ONLY ACCEPT 1000 DATA POINTS (SO THE DATA MUST BE
'SHRUNK' IF THERE ARE TOO MANY). THIS IS DONE BY FITTING THE
DATA ONTO A COARSER GRID AND AVERAGING POINTS THAT HAPPEN
TO FALL ON THE SAME INTERSECTIONS.
SYMAP ALSO EXPECTS THE 0.0 POSITION TO BE IN THE TOP LEFT
CORNER, AND THE X (FIRST) COORDINATE TO BE THE NUMBER OF ROWS
DOWN FROM THIS. THE PROGRAM SORTS ALL THIS OUT; THE DATA ARE
ARRANGED IN SYMAP FORMAT AND TO THIS DATA A SET OF DEFAULT
SYMAP STEERING INSTRUCTIONS ARE ADDED.
THE USER MAY OVERRIDE THE PROGRAM, REQUESTING THE DATA BE 'SHRUNK'

TO LESS THAN 1000 , HE MAY ALSO SUPPLY HIS OWN SYMAP INSTRUCTIONS
AT THIS POINT.

THEN, AT THIS STAGE IN THE PROGRESS OF RUNNING THE LIBRARY ,
THERE ARE STILL TWO DATA FILES, ONE OF EASTERLY APPARENT DIPS
AND ONE OF NORTHERLY APPARENT DIPS, ONLY NOW THESE FILES ARE IN A
FORM ACCEPTABLE TO SYMAP, (SEE ULCC. PUBLICATIONS).

THE SYMAP PACKAGE IS NOW USED TO INTERPOLATE APPARENT DIP
VALUES FOR GRID POSITIONS FOR WHICH NO INFORMATION WAS
SUPPLIED.
THIS IS DONE IN TURN FOR EACH DATA FILE.

IT IS IMPORTANT TO UNDERSTAND HOW SYMAP WORKS.-
IT MOVES TO EACH GRID INTERSECTION AND IF THERE IS NO VALUE
FOR THAT INTERSECTION, IT LOOKS ROUND TO THE NEAREST 3 OR 4
FILLED INTERSECTIONS, AVERAGES THEIR VALUES AND STORES THE
AVERAGE AS THE VALUE FOR THAT INTERSECTION. IT USES THIS VALUE IF
NECESSARY FOR FUTURE AVERAGINGS.
SYMAP THUS TENDS TO MODEL A SOAP FILM (LYING) OVER A SET OF PEGS
ARRANGED AT ABSOLUTE HEIGHTS DEPENDING ON THE VALUES OF THE
'READINGS' AT INTERSECTIONS WITH VALUES, IT CLINGS TO THE GIVEN
VALUES IN THE SMOOTHEST POSSIBLE WAY, NEVER MOVING TO A VALUE
ABOVE OR BELOW THEM, 'BETWEEN PEGS'.
WITH DATA IN THIS PROGRAM LIBRARY IT IS BEING ASKED TO
INTERPOLATE BETWEEN APPARENT DIPS WHICH VARY BETWEEN 90.0
AND -90.0. THIS IT DOES FAITHFULLY, HOWEVER, THE NATURE OF
AN APPARENT DIP MEANS THAT AS THE VALUE GIVEN ON ONE DATA FILE
APPROACHES 90 THE CORRESPONDING VALUE ON THE OTHER APPROACHES
0.0 . THIS IS FINE FOR SINGLE OR SIMPLE STRUCTURES WITH A LARGE
WAVELENTH RELATIVE TO THE MAP AREA, BUT IF THE STRUCTURES ARE SMALL
SCALE AND THERE ARE A LOT OF THEM ACROSS THE MAP OR IF THERE
IS AN INTERFERENCE PATTERN, THEN WE HAVE THIS SITUATION. -
CONSIDER, A SITUATION WHERE TWO ORTHOGONAL UPRIGHT FOLD TRAINS
INTERFERE, THEN, THE DIP-AZIMUTH DATA WILL BE SUCH THAT WHEN THE
APPARENT DIPS ARE CALCULATED; ON A ROW OF READINGS WITH HIGH
E-W COMPONENTS TO THEIR DIPS, (AND THEREFORE LOW N-S
COMPONENT ON THE OTHER FILE), THERE MIGHT BE A POINT AT WHICH
THERE IS A LOW E-W COMPONENT AND A CORRESPONDING HIGH N-S
COMPONENT.
ON INTERPOLATION THE EFFECT OF THE ONE LOW (NEAR 0.0) VALUE
ON THE FILE FULL OF HIGH VALUES WILL BE NEGLIGIBLE, BUT THE
EFFECT OF THE ONE HIGH VALUE ON THE TAPE FULL OF LOW VALUES
WILL BE MARKED.
INTERPOLATION, IN THESE CIRCUMSTANCES, HAS THE AFFECT OF
PARTIALLY STRIPPING ONE FOLD TRAIN FROM THE OTHER .
ONE PHASE IS 'EXAGGERATED' ON EACH FILE.
THE PERIODICITY AND OVERALL GEOMETRY OF EACH PHASE, WILL HOWEVER
BE FAITHFULLY REPRODUCED ACROSS THE MAP. A METHOD THEREFORE EXISTS
FOR MAXIMIZING THE EFFECTS OF ONE COMPONENT OF DEFORMATION IN A POLY
PHASE TERRAIN AND STUDYING ITS COMPONENT IN A N-S OR E-W
DIRECTION, (WITHIN THE LIMITS OF THE ORIGINAL FIELD SAMPLING).
AT THE END OF THE SYMAP RUNS THERE ARE STILL TWO FILES,
ONLY NOW THEY CONTAIN COMPLETE INFORMATION AS TO THE VARIATION
IN THE N-S AND E-W APPARENT DIPS AT ALL POINTS OVER THE AREA.
THE FILES ARE IN STANDARD SYMAP BINARY FORMAT.

THE PROBLEM NOW IS TO RECOMBINE THE APPARENT DIPS TO
GENERATE THE ACTUAL SURFACE WHICH THEY REPRESENT.
THIS PRESENTS A PROBLEM BECAUSE THE PROCESS OF INTERPOLATION,
DESCRIBED ABOVE MEANS THAT THE DATA CANNOT NECESSARILY BE MERGED
TO PRODUCE A UNIQUE OUTPUT; THE OUTPUT WILL VARY AS TO WHICH FILE
IS DOMINANTALY USED TO CONSTRUCT THE OUTPUT.
SEVERAL (5) PROGRAMS WERE WRITTEN TO RECOMBINE THE APPARENT DIP
FILES, SO THAT THEY MAY BE LOOKED AT IN MANY POSSIBLE WAYS, THUS
ALLOWING A FULLER UNDERSTANDING AS TO THE GEOMETRY OF THE STRUCTURES

IN THE AREA. WHERE THE FORM OF THE FOLIATION SURFACE IS SIMPLE,
ALL THESE PROGRAMS WILL GIVE THE SAME RESULT; IT IS ONLY WHERE
THE INFORMATION ON THE TWO DATA FILES IS AFFECTED BY THE INTERPOLATION

AFFECT, THAT ANY DIFFERENCE IN OUTPUT IS SEEN.
WHAT THESE PROGRAMS DO IS TO SET ONE CORNER OF THE AREA TO A HEIGHT
OF 0.0. THEN STARTING FROM THIS THEY WORK OUT THE FIRST EDGE
OF THE AREA USING THE DATA FROM ONE FILE. (THE ALGORITHM IS-
ONE KNOWS THE SPACING BETWEEN GRID POINTS AND THE APPARENT DIP
AT THE POINT, SO USING PYTHAGORAS THE RELATIVE HEIGHT OF THE NEXT
POINT MAY BE CALCULATED).
NEXT THIS IS DONE USING DATA FROM THE OTHER FILE FOR ALL POINTS
ON THE AREA RUNNING AT RIGHT ANGLES TO THE FIRST EDGE. (THE CORRECT
E-W,N-S FILE USED IN EACH CASE).
ONE PROGRAM DOES A SIMILAR PROCESS ON THE NE DIAGONAL, HAVING
FIRST WORKED OUT TRUE DIP FROM BOTH APPARENT DIP FILES.
THE PRODUCT OF RUNNING THESE PROGRAMS IS ONE NEW DATA FILE THAT IS

TWO DIMENSIONAL MATRIX (129*129) OF ABSOLUTE HEIGHT VALUES.
THE OUTPUT IS IN A FORM EXACTLY LIKE THAT SYMAP WOULD PRODUCE.

THE NEW DATA FILE MUST NOW BE TURNED INTO A VISUAL PICTURE
THIS CAN BE DONE IN TWO WAYS.
1) BY PASSING IT TO SYMVU AND GETTING A THREE D BLOCK DIAGRAM ON
   MICROFILM. IF THIS IS DONE THE USER MUST SUPPLY THE
   SYMVU STEERING ELECTIVES.

2) BY PASSING IT TO YET ANOTHER PROGRAM IN THE LIBRARY (WHICH
   WILL ACCEPT ANY SYMAP TYPE OUTPUT AND IS THEREFORE OF GENERAL
   USE AS A GOOD ALTERNATIVE TO USUAL LINE PRINTED SYMAP OUTPUT).
   THIS PROGRAM USES THE ULCC DIMFILM ROUTINES AND DRAWS A NORMAL
   GEOGRAPHIC CONTOUR MAP OF THE SURFACE ONTO MICROFILM.

           PROGRAM SPECIFICATIONS
    _____

THE APPARENT DIP GENERATOR-

SURFACE (DATAIN,NORDIP,EASDIP,INPUT,OUTPUT)
DATAIN- DATA FILE, EACH RECORD CONTAINS DIP,AZIMUTH,X,Y.
        FORMAT TO READ DATA LOOKED FOR ON INPUT, IF NOT FOUND
        IT DEFAULTS TO A BINARY READ.
NORDIP
EASDIP- BINARY OUTPUT FILES OF APPARENT DIPS (RESPECTIVELY)
        EACH RECORD CONTAINS X,Y,VALUE (REAL NOS)
        FILES REWOUND AFTER WRITING.
INPUT - IF NO FORMAT DIRECTIVE IS TO BE SUPPLIED, SUBSTITUTE
        A DUMMY FILE FOR INPUT, OR PUT TWO (EOR) CARDS TOGETHER
        ON THE INPUT STREAM. IF A FORMAT IS TO BE SUPPLIED, A
        CARD - (FORMAT) - SHOULD BE PLACED BETWEEN THEM.
        NB PROGRAM EXPECTS REAL NOS.
OUTPUT- ERROR MESSAGES AND INFORMATION AS TO NUMBER OF RECORDS
        READ ON DATAIN, PASSED TO USER.

THE SYMAP PREPARING PROGRAM, THIS IS A GENERAL PURPOSE PROGRAM
AND MAY BE USED TO PREPARE ANY GEOGRAPHIC DATA FOR SYMAP IN
ISOLATION FROM THE REST OF THE LIBRARY, SO A USER FORMAT IS
SUPPLIED HERE TOO.

SYMPREP (TAPE1,TAPE2,INPUT,OUTPUT)
TAPE1 - SOURCE FILE FOR DATA, EACH RECORD CONTAINS X,Y,VALUE
        FORMAT LOOKED FOR ON INPUT, BINARY DEFAULT.
        SOURCE NOT REWOUND BEFORE OR AFTER READING
        TAPE1 SHOULD BE SUBSTITUTED FOR NORDIP OR EASDIP
        WHEN RUNNING THE PACKAGE.
TAPE2 - SYMAP DATA FILE PRODUCED BY PROGRAM.

THE FILE SHOULD BE SUBSTITUTED FOR A DIFFERENT FILE NAME
AS THE PROGRAM MUST BE RUN TWICE ONCE FOR EACH APPARENT
DIP FILE.
TAPE2 IS REWOUND AFTER WRITING.
INPUT— READS DIRECTIVES FROM THE INPUT STREAM, MAY BE SUBSTITUTED
FOR A DUMMY FILE IF DEFAULT PARAMETERS ARE TO BE USED, (AS
WITH INPUT FOR SURFACE).
AVAILABLE DIRECTIVES—
1)   LIMIT — DEFAULTS TO 1000, BUT MAY BE SET BETWEEN 1 AND 1000,
              CONTROLS THE NO. OF RECORDS PUT ONTO TAPE2.
2)   FORMAT — DEFAULTS TO BINARY, BUT A CARD FORMAT (.....), WILL
              CAUSE READING IN THAT FORMAT , REAL NOS.
3)   F—MAP   — A DEFAULT SET OF F—MAP DIRECTIVES ARE INCLUDED
              IN THE PROGRAM, THESE MAY BE CHANGED BY THE USER.
              SHOULD ONE BE CHANGED THEY MUST ALL BE SET.
              THE USER SHOULD SUPPLY CARDS—
               F—MAP

               .
               . ELECTIVES (SEE ULCC. SYMAP PUBLICATIONS)
               .
              99999   =REQUIRED TERMINATOR
OUTPUT— MESSAGES AND ERRORS ROUTED TO HELP USER.

THE INTERPOLATOR

SYMAP, SEE ULCC. PUBLICATIONS.
          IF SYMAP IS CALLED WITH A DUMMY FILE AS THE SECOND FILE,
          THE MAP OUTPUT IS DIVERTED, THIS SAVES PAPER AS IT IS NOT
          NEEDED FOR THE RUNNING OF THE PROGRAM.
          THE SYMAP OUTPUT PRODUCED IS TAPE8. THIS IS IN SYMAP
          BINARY FORMAT.
          TAPE 8 SHOULD BE REWOUND AND COPIED TO A LOCAL FILE
          THEN RETURNED (THE TAPE8 FILE NAME WILL BE REQUIRED LATER)
          SUGGESTED LOCAL FILE NAMES ARE INDIP, AND IEDIP, RESPECTIVELY
          THEY NEED NOT BE REWOUND.

RECOMBINATION OF THE TWO APPARENT DIP FILES.

THERE ARE 5 WAYS OF DOING THIS.
DIAG— WORKS ON N—E DIAGONAL WITH 0.0 IN BOTTOM LEFT.
NDEPTH—WORKS SOUTH TO NORTH 0.0 IN BOTTOM LEFT.
SDEPTH—WORKS NORTH TO SOUTH 0.0 IN TOP RIGHT.
WDEPTH—WORKS EAST TO WEST 0.0 IN TOP RIGHT.
EDEPTH—WORKS WEST TO EAST 0.0 IN BOTTOM LEFT.
        (INDIP,IEDIP,TAPE8,TAPE7,OUTPUT)
INDIP—
IEDIP— APPARENT DIP FILES IN SYMAP FORMAT (SEE ULCC. PUB)
TAPE8— FINAL MATRIX FILE OF RECONSTRUCTED SURFACE, IN SYMAP
       TYPE BINARY FORMAT (REWOUND AFTER WRITING)
TAPE7— FILE FOR LOCAL USE WITHIN PROGRAM, SHOULD NOT BE TAMPERED
       WITH.
OUTPUT—MESSAGES TO USER, AS TO — NATURE OF THE RESULTS OF THE
       CALCULATIONS AND AS TO POSSIBLE PROBLEMS.

THE DRAWING OF THE BLOCK DIAGRAM

SYMVU, SEE ULCC. PUBLICATIONS (MICROFILM MUST BE ATTACHED AND
                                LIBRARIED, SEE ULCC.PUB)
INPUT— READS TAPE8 IN SYMAP FORMAT, BUT ALSO REQUIRES A SET
       OF STEERING ELECTIVES SUPPLIED BY THE USER, THESE ARE
       PUT ON THE INPUT STREAM. THE USER IS REFERED TO THE
       ULCC. BULLETINS , BUT A SAMPLE SET IS SUPPLIED BELOW.
OUTPUT—TO MICROFILM + INFORMATION TO USER.

THE GEOGRAPHIC CONTOURING PROGRAM (AN ALTERNATIVE TO SYMVU)
THIS DRAWS A NORMAL CONTOUR MAP, IT IS A GENERAL PURPOSE
PROGRAM AND WILL HANDLE ANY SYMAP TYPE MATRIX. DIMFILM AND
MICROFILM MUST BE ATTACHED IN A LIBRARY FORM FOR OUTPUT TO
BE PRODUCED ON MICROFILM (SEE ULCC. PUBLICATIONS).

GRID (TAPE5,PARM,OUTPUT)
TAPE5- USED AS INPUT (SUBSTITUE FOR SYMAP TAPE8, OR TAPE8
                    PRODUCED BY ONE OF THE '5' PROGRAMS).
        TAPE5 IS REWOUND BEFORE AND AFTER READING.
PARM-   THE WORD 'NOLABEL' OR 'LABEL', SUBSTITUTED HERE WILL TURN
        LABELING OF THE CONTOURS ON OR OFF RESPECTIVELY, THE DEFAULT
        IS FOR LABELS TO BE PRODUCED.
OUTPUT-MICROFILM AND INFORMATION TO THE USER AS TO PROGRESS OF AND
        ERRORS IN EXECUTION.

THERE IS AN ALTERNATIVE GRID PROGRAM WHICH ALLOWS THE USER TO
SPECIFY THE NUMBER AND LEVEL OF THE CONTOURS

GRID2 (TAPE8,INPUT,PARM,OUTPUT)
TAPE8- USED AS INPUT (THIS IS SYMAP TAPE8, OR TAPE8
                    PRODUCED BY ONE OF THE '5' PROGRAMS).
        TAPE8 IS NOT REWOUND IN THE PROGRAM
INPUT- THIS IS DEFAULTED TO READ FROM THE INPUT STREAM, ON
        IT THERE SHOULD BE TWO CARDS . THE FIRST, STATING
        AS AN INTEGER NUMBER (N) HOW MANY CONTOURS ARE TO BE
        DRAWN, WHERE (N) < OR = 18.
        THE SECOND CARD SHOULD CONTAIN (N) CONTOUR LEVELS, REAL
        NOS. SEPERATED BY (,)S.
        IF TAPE8 HAS MORE THAN ONE MAP ON IT THESE CARDS MUST
        BE SUPPLIED EACH TIME GRID2 IS CALLED, THE SETS OF CARDS
        SEPARATED BY (EOR) CARDS.
PARM-   THE WORD 'NOLABEL' OR 'LABEL', SUBSTITUTED HERE WILL TURN
        LABELING OF THE CONTOURS ON OR OFF RESPECTIVELY, THE DEFAULT
        IS FOR LABELS TO BE PRODUCED.
OUTPUT-MICROFILM AND INFORMATION TO THE USER AS TO PROGRESS OF AND
        ERRORS IN EXECUTION.

                    JOB CONTROL
        ——

TO RUN THE LIBRARY ONE MUST SET UP THE JOB CONTROL CARDS
AS IN THE SPECIMEN DECK BELOW.
NOTE. IT IS ASSUMED THAT ONLY THE FIRST LOT OF DATA IS NOT
IN BINARY FORMAT THUS ONLY ONE FORMAT IS SUPPLIED.
THE SPECIMEN SYMVU ELECTIVES WILL PRODUCE A SATISFACTORY
OUTPUT, THESE ARE AT THE BOTTOM OF THE JOB CONTROL CARDS.

```
JOB,........,J6,T59,M7600.      **  YOUR NAME  **
ATTACH,PLOTST,ID=LIBBED.
ATTACH,SVU,SYMVU,ID=PUBLIC.
ATTACH,SYMAP,ID=PUBLIC.
ATTACH,DIMFILM,ID=PUBLIC.
ATTACH,MFILM,MICROFILM,ID=PUBLIC.
LIBRARY,PLOTST,DIMFILM,MFILM.
SURFACE.     GENERATES NORDIP AND EASDIP
SYMPREP,NORDIP,SYMNORT,INPUT.  GENERATES SYMNORT
SYMPREP,EASDIP,SYMEAST,INPUT.  GENERATES SYMEAST
SYMAP,SYMNORT,RUBISH.  GENERATES TAPE8
REWIND,TAPE8.
COPY,TAPE8,INDIP.
```

```
RETURN,TAPE8.
SYMAP,SYMEAST,RUBBISH.   GENERATES TAPE8
REWIND,TAPE8.
COPY,TAPE8,IEDIP.
RETURN,TAPE8.
WDEPTH. GENERATES TAPE8        (USE ONE OF THE '5' PROGRAMS HERE)
GRID,TAPE8,LABEL.
REWIND,TAPE8.
LIBRARY,SVU,MFILM.
SYMVU.
 <EOR>
(YOUR FORMAT SPECIFICS)
YOUR DATA IN THE ABOVE FORMAT
 .
 .
 .
 .
 .
 <EOR>
LIMIT 1000
 <EOR>
LIMIT 1000
 <EOR>
      A TITLE TO YOUR PLOT CAN BE PUT IN HERE ———————————————————————.
 129 129   2   4   2       4        1              6                    1
 55.0 45.0  6.0     5.0      -300.0     200.0                                    .75
 <EOR>
 <EOF>
            ———————— GOOD LUCK —————————
```

```
        PROGRAM SURFACE(DATAIN, NORDIP, EASDIP, INPUT, OUTPUT,
       + TAPE1=NORDIP, TAPE2=EASDIP, TAPE4=INPUT, TAPE5=DATAIN )
C
C
C          RPOGRAM WRITTEN BY C.COOKSON AND F.W.M. HOPPER   1978.
C          --------------------------------------------------
C  A PROGRAM TO READ IN DIP AND AZIMUTH DATA, CALCULATE FROM THEM THEIR
C  NORTHERLY AND EASTERLY COMPONENTS, AND WRITE OUT THOSE COMPONENTS
C  (ALONG WITH THEIR X- AND Y-COORDINATES) TO THE FILES EASDIP AND
C  NORDIP.
C  FORMATS - THE DATA INPUT FILE WILL BY DEFAULT BE CALLED DATAIN,
C            AND IS THE FIRST FILE ON THE PROGRAM CARD. THE DATA
C            ON THAT FILE MUST CONTAIN 4 VALUES ON EACH RECORD (LINE),IN
C            THE ORDER   -  DIP, AZIMUTH, X-COORD, Y-COORD .
C            THESE ARE ALL REAL NUMBERS.
C            A SINGLE RECORD READ FROM THE FILE 'INPUT' WILL BE USED
C            AS THE FORMAT SPECIFIER TO BE APPLIED TO THE INFORMATION ON
C            THE FILE 'DATAIN'.   IF 'INPUT' IS EMPTY THE PROGRAM WILL
C            DEFAULT TO ASSUMING A FREE-FORMAT READ.
C            ('INPUT' MAY BE MADE TO APPEAR EMPTY BY SUBSTITUTING THE NAME
C            OF A DUMMY FILE IN THE 4TH PARAMETER POSITION ON THE PROGRAM
C            CALL CARD).
C            READING WILL CONTINUE UNTIL END-OF-FILE IS ENCOUNTERED.
C
C            THE OUTPUT FILES EASDIP AND NORDIP WILL BE WRITTEN IN BINARY
C            FORMAT WITH THREE VALUES PER RECORD, IN THE ORDER
C                 X, Y, EASTERLYDIP             X, Y, NORTHERLYDIP
C            ON THE APPROPRIATE FILE.
C            BOTH OUTPUT FILES ARE REWOUND AT START AND FINISH OF THE
C            PROGRAM O THE DATA INPUT FILE IS NOT REPOSITIONED BEFORE OR
C            AFTER READING.
C     N.B.  SINCE NO ARRAYS ARE USED IN THIS PROGRAM  (NO, NOT ONE)   THERE
C            IS NO LIMIT ON THE SIZE OF THE DATA SET TO WHICH IT MAY BE
C            APPLIED - UNTIL YOU RUN OUT OF DISC SPACE, OF COURSE.

        INTEGER FNAME, FORM(8)
        LOGICAL FIXFORM
C                          ------ STATEMENT FUNCTIONS ------
        SIND ( ARG ) = SIN ( ARG * 0.0175 )
        COSD ( ARG ) = COS ( ARG * 0.0175 )
        TAND ( ARG ) = TAN ( ARG * 0.0175 )
        ATAND ( ARG ) = ATAN ( ARG ) * 57.143

C                                      INITIALISE...
        NPTS = 0
        PRINT 1
    1   FORMAT('0',T22,17('*'),' PROGRAM SURFACE ',17('*') )
        FIXFORM = .T.
C
C                      SEE IF THERE IS A FORMAT IN INPUT FOR US.
        READ(4,7) FORM
        FIXFORM = EOF(4).EQ.0.0
C                      AND ECHO IT IF THERE WAS.
        IF (FIXFORM) PRINT 8 , FORM
C                      AND TELL HIM IF THERE WAS NOT
        IF (.NOT.FIXFORM) PRINT 9
    9   FORMAT('0',T22,'DEFAULT FREE-FORMAT DATA ASSUMED.')
C
C                      GO.
C
    7   FORMAT (8A10)
    8   FORMAT('0',T22,'INPUT FORMAT READ AS - ',8A10 )
C
C                                      NPTS WILL COUNT THE NO OF POINTS...
```

```
   10    IF(FIXFORM) READ (5,FORM) DIP, AZIMUTH, X, Y
         IF(.NOT.FIXFORM) READ(5,*) DIP, AZIMUTH, X, Y
C                                          SEE WHERE TO STOP
         IF(EOF(5).NE.0.0) GO TO 20
         NPTS = NPTS+1
C                     DO THE SUMS ------FIRST NORTHERLY
C
C
         DIPNORT = ATAND ( TAND ( DIP ) * COSD ( AZIMUTH ) )
C
C
C                                        THEN EASTERLY
C
C
         DIPEAST = ATAND ( TAND ( DIP ) * SIND ( AZIMUTH ) )
C
C
C                                          OK .
C
C
C                                NOW WRITE THEM TO OUT FILES...
         WRITE (1) X, Y, DIPNORT
         WRITE (2) X, Y, DIPEAST
C
C                                AND ROUND FOR THE NEXT
         GO TO 10

   20    PRINT 4,NPTS
C                                WELL - WE MAY AS WELL PRINT SOMETHING
         REWIND 1      REWIND 2
         STOP 'OK'

    4    FORMAT('O',T22,'NO. OF DATA POINTS READ FROM SOURCE FILE - ',
        +I5,     /, 'O',T22, '*********************************************
        +*****  ',/, 'O                         END OF SURFACE RUN.',/ )
         END
```

```
            PROGRAM SYMPREP (TAPE1, TAPE2, INPUT, OUTPUT, TAPE5=INPUT)
C
C                  WRITTEN BY C.J. COOKSON 1978.
C                  ================================
C
C
C      TO FUDGE A LARGE DATA SET ( >1000 POINTS ) INTO AN INPUT
C      FORMAT ACCEPTABLE TO SYMAP.
C      DATA MUST BE AS RECORDS OF THREE VALUES - X CO-ORD, Y CO-ORD,
C      VALUE, ON THE FILE SUBSTITUTED FOR TAPE1.
C      THE FORMAT OF THE DATA SHOULD BY DEFAULT BE BINARY, BUT IF REQUIRED
C      A DIRECTIVE ON FILE INPUT MAY SPECIFY A FORTRAN FORMAT STATEMENT WHICH
C      WILL BE USED INSTEAD FOR READING THE DATA.
C      ( SEE DOCUMENTATION )
C      THE X AND Y CO-ORDS ARE EXPECTED IN ↑CONVENTIONAL↑ GEOGRAPHICAL
C      RELATIONSHIP - I.E. ↑X↑ IS THE FIRST VALUE REPRESENTING HORIZONTAL
C      DISPLACEMENT FROM THE LEFT EDGE OF THE AREA, Y IS VERTICAL
C      DISPLACEMENT FROM THE BOTTOM EDGE.  ( SYMAP, OF COURSE, EXPECTS
C      SOMETHING DIFFERENT O THIS IS DEALT WITH BY THE PROGRAM. )

            COMMON / FREDF1 / DATA
            COMMON / FREDF2 / FLAGS
            REAL DATA(191,191)
            INTEGER FLAGS(191,191), FMAPDIR(73,8), INP(8), FMT(8)

            INTEGER UNRECOG, FMAPNO
            LOGICAL ENDFIL, FINISHD, FIXFORM
            LEVEL 2, DATA, FLAGS


            ENDFIL(K) = EOF(K) .NE. 0.0

            REWIND 2

            FIXFORM = .F.     FMAPNO = 0     LIMIT = 0  ·  UNRECOG = 0
C                                  CHECK FOR INPUT DIRECTIVES
 2000 READ(5,2001) INP
 2001 FORMAT(8A10)
            IF(ENDFIL(5))GO TO 2990
C                                  SO WE WANT A DUMMY RECORD IF HE LETS
C                                  EVERYTHING DEFAULT
C                                  F-MAP O
 2002 IF((INP(1).AND.MASK(30)).NE.5LF-MAP) GO TO 2010
C                                  F-MAP - HAVE WE BEEN HERE BEFORE ·
            IF(FMAPNO.NE.0)CALL SYSTEM(52,'1*** DUPLICATE F-MAP DIRECTIVE FOUN
           +D - PROGRAM ABANDONED ***')
C                                  COPY ACROSS TOP LINE
            DO 2003 I=1,8
            FMAPDIR(1,I) = INP(I)
 2003 CONTINUE
            FMAPNO = 1
C                                  AND KEEP READING THE REST OF THEM
 2005 READ(5,2001) (FMAPDIR(FMAPNO+1,J),J=1,8)
            IF(ENDFIL(5))GO TO 2990
C                                  WATCH FOR THE END OF F-MAPS
            IF((FMAPDIR(FMAPNO+1,1).AND.MASK(6)).EQ.1L )GO TO 2007
C                                  SEE IF HES GIVEN US A 99999
            IF((FMAPDIR(FMAPNO+1,1).AND.MASK(6)).EQ.1L9) GO TO 2008
C                                  YES (PROBABLY )
            FMAPNO = FMAPNO+1     IF(FMAPNO.GT.73)GO TO 2009
            GO TO 2002
C                                  ELSE COPY THIS LINE BACK TO INP -
 2008 DO 2006 I=1,8
            INP(I) = FMAPDIR(FMAPNO+1,I)
```

```
      2006 CONTINUE
C                                 AND GO BACK TO THE TOP TO TEST IT AGAIN....
           GO TO 2002
C                                 BUT FOR LEGITIMATE F-MAP DIR,
      2007 FMAPNO = FMAPNO+1
      2009 IF(FMAPNO.GT.73)CALL SYSTEM(52,'1**** TOO MANY FMAP DIRECTIVES - PR
          +OGRAM ABANDONED ****')
C                                 ELSE GET THE NEXT
           GO TO 2005

C                                 NOT AN F-MAP O TRY LIMIT
      2010 IF((INP(1).AND.MASK(30)).NE.5LLIMIT) GO TO 2020
C                                 YES - SEEN BEFORE .
           IF(LIMIT.NE.O)CALL SYSTEM(52,'1**** DUPLICATE LIMIT DIRECTIVE FOUND
          + - PROGRAM ABANDONED ****')
C                                 OK - CONVERT TO INTEGER
C                                 REMOVE THE TEXT WORD -
           INP(1) = INP(1).AND.(.NOT.MASK(30))
C                                 LEFT JUSTIFY THE REST OF THE LINE -
           CALL SHUNT(INP,8)
C                                 WHICH SHOULD PUT THE INTEGER CHARS IN WORD
C                                 1 - SO ITS NOW OK TO INTIFY IT
           IFAIL = 1   LIMIT = INTIFY(INP(1),IFAIL)
           IF(IFAIL.EQ.1 .OR. LIMIT.LT.1 .OR. LIMIT.GT.1000)
          +CALL SYSTEM(52,'1**** BAD LIMIT DIRECTIVE - PROGRAM ABANDONED ****')
C                                 ELSE OK
           GO TO 2000

C                                 SO MAYBE ↑TWAS A FORMAT -
      2020 IF((INP(1).AND.MASK(36)).NE.6LFORMAT)GO TO 2030
C                                 YES - HAD ONE ALREADY .
           IF(FIXFORM)CALL SYSTEM(52,'1**** DUPLICATE FORMAT DIRECTIVE FOUND
          +- PROGRAM ABANDONED ****')
           FIXFORM = .T.
C
C                                 COPY ACROSS
           FMT(1) = INP(1).AND.(.NOT.MASK(36))  .OR. 6L
           DO 2021 I=2,8
           FMT(I) = INP(I)
      2021 CONTINUE
           GO TO 2000

C                                 HERE FOR UNRECOGNISED DIRECTIVE
      2030 CONTINUE
           PRINT 2989,INP
           UNRECOG = UNRECOG+1
           IF(UNRECOG.GT.50) CALL SYSTEM (52,'1**** TOO MANY UNRECOGNISED DIRE
          +CTIVES - PROGRAM ABANDONED ****')
           GO TO 2000
      2989 FORMAT('0**** UNRECOGNISED DIRECTIVE - IGNORED O ',8A10)

C                                 HERE AT END OF I/P FILE
      2990 PRINT 2992
      2992 FORMAT('0',T22,17('*'),' PROGRAM SYMPREP ',17('*') )
           IF(FIXFORM)PRINT 2993,FMT
      2993 FORMAT('0**** FIXED FORMAT SPECIFIED AS O ',8A10)
           IF(LIMIT.NE.O)PRINT 2994, LIMIT
           IF(LIMIT.EQ.O)  PRINT 2995
      2994 FORMAT('0**** MAXIMUM NO OF POINTS REQUIRED IS ',I4)
      2995 FORMAT('0     DEFAULT MAXIMUM NO OF POINTS (1000) USED')
           IF(LIMIT.EQ.O)LIMIT=1000
C                                 DONE
C                                 START READS...
           IF(.NOT.FIXFORM)  READ(1) XMAX,YMAX,ZMAX
```

```
          IF (FIXFORM)        READ(1,FMT) XMAX,YMAX,ZMAX
          IF (ENDFIL(1)) CALL SYSTEM(52,'1**** EMPTY SOURCE FILE ****')
          NPTS = 1

          XMIN = XMAX    YMIN = YMAX    ZMIN = ZMAX

C                                        AND GO ON TO EOF
    1     IF (.NOT.FIXFORM)   READ(1) X, Y, Z
          IF (FIXFORM)        READ(1,FMT) X, Y, Z
          IF (ENDFIL(1)) GO TO 5
C                                KEEP COUNT OF NO OF POINTS
          NPTS = NPTS + 1

          IF (X.GT.XMAX) XMAX = X    IF (X.LT.XMIN) XMIN = X
          IF (Y.GT.YMAX) YMAX = Y    IF (Y.LT.YMIN) YMIN = Y
          IF (Z.GT.ZMAX) ZMAX = Z    IF (Z.LT.ZMIN) ZMIN = Z

          GO TO 1

    5     PRINT 7, NPTS, XMAX, XMIN, YMAX, YMIN, ZMAX, ZMIN
    7     FORMAT('0',T7,I8,' DATA FIELDS ON SOURCE FILE',/,
         +        '0',T11,'X CO-ORDINATE RANGE - ',2F20.10,/,
         +        '0',T11,'Y CO-ORDINATE RANGE - ',2F20.10,/,
         +        '0',T8,'INPUT DATA VALUE RANGE - ',2F20.10 )

C                                  CHECK FOR NON-SILLY RANGES
          IF (XMAX.EQ.XMIN) CALL SYSTEM(52,'1**** ZERO X CO-ORDINATE RANGE ****'
         +)
          IF (YMAX.EQ.YMIN) CALL SYSTEM(52,'1**** ZERO Y CO-ORDINATE RANGE ****'
         +)
C                                  NOW START THE MATRIX FITTING.
C     WE WANT TO LOOP ROUND SQUASHING THE WHOLE DATA SET INTO A MATRIX
C     WHICH STARTS SMALL AND GETS BIGGER ON EACH PASS O THE BIGGER IT GETS,
C     THE MORE DEFINED DATA POINTS WILL SURVIVE THE SQUEEZE.
          LO = SQRT(FLOAT(LIMIT))    IHI = 191   ISTEP = 20   FINISHD = .F.

  900 DO 1000 IMAT = LO, IHI, ISTEP

          DO 8 I=1,IMAT
          DO 8 J=1,IMAT
          FLAGS(I,J)=0
    8     CONTINUE

          XFACT = (FLOAT(IMAT)-1.0) / (XMAX-XMIN)
          YFACT = (FLOAT(IMAT)-1.0) / (YMAX-YMIN)
C                                  NOW PLUG THE DATA VALS INTO OUR ARRAY,
C                                  KEEPING TRACK OF THE NUMBER OF MULTIPLE
C                                  ASSIGNMENTS TO ANY POINT.
          NMULTS = 0
          REWIND 1
                NASS = 0
   10     READ(1) X,Y,Z
          IF (ENDFIL(1)) GO TO 20
C                                  CONVERT CO-ORDS
          IX = IFIX( (X-XMIN) * XFACT ) + 1
          IY = IFIX( (Y-YMIN) * YFACT ) + 1
          IF (FLAGS(IX,IY).EQ.0) GO TO 12
C                              NOT THE FIRST VALUE AT THIS POINT - AVERAGE
          DATA(IX,IY) = ( DATA(IX,IY) + Z ) / 2.0
          NMULTS = NMULTS+1
          GO TO 10

   12     DATA(IX,IY) = Z
          FLAGS(IX,IY) = 1
```

```
       NASS = NASS+1

       GO TO 10


  20   CONTINUE

       IF(FINISHD)PRINT 101,IMAT,IMAT,NASS,NMULTS
 101   FORMAT('0',T10,' AT MATRIX SIZE',I4,' BY',I4,',',I5,' POINTS REMAI
      +NED AFTER',I5,' REPEATED ASSIGNMENTS')
C                                       IS THAT GOOD ENOUGH.
       IF(NASS.GT.LIMIT) GO TO 1010
C                                       OR DO WE NEED TO CONTINUE...
       IF(NASS.EQ.NPTS .OR. FINISHD)GO TO 1030
1000   CONTINUE               .
C                                       IF WE GET HERE, THEN OUR
C                                       MATRIX IS NOT BIG ENOUGH...
       PRINT 1005
1005 FORMAT('0XXXXXXXX WARNING XXXXXXXX LESS THAN OPTIMAL DATA PACKING AT
      + LIMIT OF THIS PROGRAM XXXXXXXX',/,
      + '0                        THE DATA SET SUPPLIED WOULD YIELD GREATER
      + ACUITY IF APPLIED DIRECTLY',/,
      + '                        TO SYMAP.',/,
      + '0XXXXXXXXXXXXXXXXXXXXXXXXXXXXXXXXXXXXXXXXXXXXXXXXXXXXXXXXXXXXXXXX
      +XXXXXXXXXXXXXXXXXXXXXXXXXXXXXXXXXXX',/)
       PRINT 1006,IHI,LO,NASS,NPTS
1006   FORMAT('0IHI=',I5,' LO=',I5,' NASS=',I5,' NPTS=',I5)
       IMAT = IHI   GO TO 1030


C                                       RESET THE CONTROL PARAMETERS
1010 LO = IMAT - ISTEP
       IHI = IMAT
       FINISHD = ISTEP.EQ.1
       IF(.NOT.FINISHD) ISTEP = ISTEP / 4          .
C                                       AND GO ROUND AGAIN
       GO TO 900



C                                NOW FOR SYMAP SATISFACTION
1030 WRITE(2,30)
  30   FORMAT('B-DATA POINTS         X')

C                                       WRITE MATRIX CO-ORDS IN SYMAP FORMAT IF
C                                       THE MATRIX POINTS CONTAIN VALUES

       DO 40 IX = 1,IMAT
C                                       FLOAT BACK TO ORIGINAL INPUT RANGE
       X = ( FLOAT(IX-1) / XFACT ) + XMIN
       DO 40 IY = 1,IMAT
C                                       A VALUE HERE .
       IF(FLAGS(IX,IY).EQ.0)GO TO 40
C                                       YUP. CONVERT THE Y CO-ORD ( INCLUDING
C                                       SYMAP FIX
       Y = YMAX - ( ( FLOAT(IY-1) / YFACT ) + YMIN )
       WRITE(2,50) Y, X
  40   CONTINUE

  50   FORMAT(10X,2F10.4)


C                                END THE B-DATA
       WRITE(2,55)
  55   FORMAT('99999')
C                                NOW REPEAT THE EXERCISE FOR THE VALUES...
       WRITE(2,60)
```

```
   60   FORMAT('E-VALUES                    X')
C                                  GET MODIFIED ZMAX, ZMIN ON THE WAY
       ZMAX = ZMIN = ( ZMAX+ZMIN ) / 2.0
       DO 70 IX = 1,IMAT
       DO 70 IY = 1,IMAT
       IF(FLAGS(IX,IY).EQ.0) GO TO 70
       IF(DATA(IX,IY).GT.ZMAX) ZMAX = DATA(IX,IY)
       IF(DATA(IX,IY).LT.ZMIN) ZMIN = DATA(IX,IY)
C                                  AND WRITE IT OUT
       WRITE(2,75) DATA(IX,IY)
   70   CONTINUE
   75   FORMAT(10X,F10.4)
C                                  AND CLOSE THEM OFF
       WRITE(2,80)
   80   FORMAT('99999')
C                                  NOW FOR THE F-MAP ELECTIVES...
       IF(FMAPNO.EQ.0)GO TO 95
C                                  HERE WHEN HE HAS GIVEN THEM
       WRITE(2,82) ((FMAPDIR(I,J),J=1,8),I=1,FMAPNO)
   82   FORMAT(8A10,/)
C                                  AND TERMINATE IN CASE HE FORGOT
       WRITE(2,85)
   85   FORMAT('999999')
       GO TO 99
C                                  HERE FOR DEFAULTS
   95   WRITE(2,100)
  100   FORMAT('F-MAP                   X ', / ,
      +                              , / ,
      +                              , / ,
      +                              , / ,
      +            '    1      21.6      13.0'; / ,
      +            '    3      10.0         '; / ,
      +            '   17                   '; / ,
      +            '   21                   '; / ,
      +            '   22                   '; / ,
      +            '   24                   '; / ,
      +            '99999                 '   )
C                                  WRAP IT UP
   99 WRITE(2,85)
       ENDFILE 2
       REWIND 2
C                                  AND TELL HIM THE GOOD NEWS
       PRINT 102
  102 FORMAT('0                    XXXXXXXXXXXXXXXXXXXXXXXXXXXXXXXXXXXXXXXXXX
      +XXXXXXXXXXXXXX ',/,
      +            '0                  END OF SYMPREP.',/ )
       STOP 'OK'
       END
```

```
        PROGRAM WDEPTH (INDIP,IEDIP,TAPE8,TAPE7,OUTPUT,TAPE1=INDIP,
       -TAPE2=IEDIP,TAPE6=OUTPUT)
C
C       PROGRAM WRITTEN BY F.W.M.HOPPER   1978
C       --------------------------------------------
C
C
C       THIS PROGRAM RECOMBINES TWO INTERPOLATED APPARENT DIP
C       FILES AND GENERATES THE THEORETICAL FOLLIATION SURFACE
C       FROM THEM, TO BE PASSED TO SYMVU.
C       THE ONLY OTHER OUTPUT IS INFORMATION AS TO THE SIZE OF THE
C       MATRIX AND THE MAXIMUM / MINIMUM VALUES GENERATED.
C       CALCULATED FROM THE EAST TO THE WEST WITH 0.0 IN THE
C       TOP RIGHT CORNER.
C
C       ARRAYS.
C       =======
C                       ROW      - CONTAINS CURRENT ROW DIP VALUES.
C                       COL      - CONTAINS LAST COLUMN FROM INDIP
C                       DROP     - CONTAINS DEPTHS OF THE SURFACE FROM AN
C                                  ORDNANCE DATUM LEVEL IN THE CURRENT ROW.
C                       SCALES   - CONTAINS THE CONTROL VALUES FOR SYMVU.
C                       DUM      - A DUMMY ARRAY NOYHING USED FROM IT .
C
C       VARIABLES.
C       ============
C                       NROW     - NUMBER OF ROWS ( = SCALES(1) ).
C                       NCOL     - NUMBER OF COLUMNS ( = SCALES(2) ).
C                       ROWDIST  - DISTANCE BETWEEN THE ROWS(=SCALES(3)).
C                       COLDIST  - DISTANCE BETWEEN THE COLUMNS(=SCALES(4)).
C                       MIN      - MINIMUM VALUE OF INTERPOLATED DIP VALUES(=SCALES(5)).
C                       MAX      - MAXIMUM VALUE OF INTERPOLATED DIP VALUES(=SCALES(6)).
C                       SCALES 7-24 ARE REDUNDANT BUT MUST BE PRESENT.
C
C
C       DIMENSION SCALES(24), DUM(200), COL(200), ROW(200), DROP(200)
C
C
C       THE ARRAY SCALES WILL FORWARD THE 24 VALUES NEEDED FOR THE
C       SYMVU ROUTINE.
C
C
C       EQUIVALENCE (NROW,SCALES(1)), (NCOL,SCALES(2))
C
C               STATEMENT FUNCTIONS ---------------------------------------
C                 TAND ( ARG ) = TAN ( ARG * 0.0175 )
C
C       REWIND THE TAPES TO BE USED AS INPUT, WHICH ARE 'INDIP'
C       (INTERPOLATED NORTHERLY DIPS ) AND 'IEDIP' ( INTERPOLATED
C       EASTERLY DIPS ), AND HAVE BEEN COPIED FROM TAPE 8.
C
        REWIND 1
        REWIND 2          .
        READ(1) (SCALES(K),K=1,24)
C       'DISTROW' AND 'DISTCOL' ARE THE DISTANCES BETWEEN THE GRID
C       POSITIONS OF THE INTERPOLATED MATRIX.
C
        DISTROW = 1.0 / SCALES(3)
        DISTCOL = 1.0 / SCALES(4)
C       READ 1ST CARD OF (2) WITH SCALES ON.
        READ (2)
C       READ FROM TAPE(1) THE LAST COLUM FROM EACH ROW.
        NN=NCOL-1
        WRITE(6,133)
```

```
133     FORMAT(5X, 'XXXXXXXXXXXXXXXXXXXXXXXXXXXXXXXXXXXXXXXXXXXXX ',/////,
       +5X,'        --- PROGRAM WDEPTH ---        ',/////,
       +5X, 'XXXXXXXXXXXXXXXXXXXXXXXXXXXXXXXXXXXXXXXXXXXXX ',)
        DO 88 I=1,NROW
        READ(1)  (DUM(K),K=1,NN),ROW(I)
88      CONTINUE
C
C
C       WORK OUT THE DROP AT EACH POINT ALONG THE LAST COL OF THE MATRIX
C       FROM THE INTERPOLATED NORTHERLY DIPS, ASSUMING THE DROP IN THE TOP
C       RIGHT CORNER TO BE 0.0 AND WRITE THEM TO COL AS AN INTERMEDIATE
C       STORE.
C
C
        COL(1)=0.0
        DO 451 K=2,NROW
             R=ROW(K)
             ROW(K) = ABS (ROW(K))
             COL(K)=COL(K-1) + DISTROW * (SIGN (TAND (ROW(K)) , R ))
  451 CONTINUE
C
C
        DROPHI=DROPLO=COL(1)
C       NOW WORK OUT THE DROP AT ALL OTHER GRID POINTS USING THE
C       INTERPOLATED EASTERLY DIPS, EXEPT THE LAST WORD ON THE ROW,
C       WHICH WE ALREADY KNOW FROM WHAT WE HAVE IN COL.
C
C
        DO 452 L=1,NROW
        READ(2)  (ROW(K),K=1,NCOL)
        DROP(NCOL)=COL(L)
             DO 453 N=2,NCOL
                  K=NCOL-N+1
                  R=ROW(K)
                  ROW(K) = ABS(ROW(K))
             DROP(K) = DROP(K+1) + DISTCOL * (SIGN (TAND (ROW(K)) , R ))
453          CONTINUE
C
C
        DO 74 I=1,NCOL
        IF (DROP(I) .GT.DROPHI) DROPHI=DROP(I)    IF (DROP(I) .LT.DROPLO)
       -DROPLO=DROP(I)
74      CONTINUE
C
C
C       WRITE VALUES TO TAPE 7 AS AN INTERMEDIATE STOR.
             WRITE(7)  (DROP(K),K=1,NCOL)
  452 CONTINUE
        ENDFILE 7
C
C
C
C       WE NOW HAVE THE MINIMUM AND MAXIMUM DROP VALUES AND THESE ARE
C       PUT IN SCALES(5) AND SCALES(6)-(24) RESPECTIVELY.
C
C
        DO 454 K=6,24
             SCALES(K) = DROPHI
  454 CONTINUE
        SCALES(5) = DROPLO
        REWIND 7
        WRITE(8) SCALES
        DO 700 I=1,NROW
        READ(7)  (DROP(J),J=1,NCOL)
        WRITE(8)  (DROP(J),J=1,NCOL)
```

```
700     CONTINUE
        ENDFILE 8
        REWIND 8
        WRITE(6,777) NROW,NCOL,(SCALES(K),K=3,6)
777     FORMAT(5X, 'ROWS ',5X,I5,/,5X, 'COLUMNS ',5X,I5,/,
       -5X, 'ROWSPACING ',5X,G22.11,/,5X, 'COLUMNSPACING ',5X,G22.11,/,
       -5X, 'LOWEST VALUE ',5X,G22.11,/,5X, 'HIGHEST VALUE',5X,G22.11)
C          FIND OUT IF THERE ARE GOING TO BE ANY SCALING
C          PROBLEMS WHEN SYMVU GETS THE FILE.
        IF(DROPHI.EQ.0.0)GO TO 771
        IF((DROPHI+DROPLO)/DROPHI.GT.2/3) PRINT (6,778)
771     CONTINUE
778     FORMAT (20X, 'XXXXXXXXXXXXXXX   W A R N I N G   XXXXXXXXXXXXXXX '/
       +//,5X, 'YOU HAVE A SCALING PROBLEM   YOUR SYMVU PLOT MAY '/
       +,5X, 'LOOK FLAT.   YOU HAVE EITHER A VERY HIGH (HIGHEST '/
       +,5X, 'VALUE) OR A VERY LOW (LOWEST VALUE), tSEE ABOVEt.'/
       +,5X, 'IF YOUR WHOLE DATA IS NOT EVENLY SPREAD BETWEEN THEM, '/
       +,5X, 'DURING SCALING THE VARIATION IN THE SURFACE MAY BE '/
       +,5X, 'LOST.'/
       +,5X, 'THIS MAY BE OVERCOME BY CAREFUL SELECTION OF THE '/
       +,5X, 'APPROPRIATE SYMVU ELECTIVES - SEE MANUAL- , OR '/
       +,5X, 'YOU MAY HAVE TO OPERATE ON YOUR MATRIX.  TO DO THIS'/
       +,5X, '--FIRST EXAMINE IT, BY LOOKING AT THE TAPE8 PRODUCED'/
       +,5X, 'BY THIS PROGRAM, WITH PROGRAM GRID IN THIS LIBRARY'/
       +,5X, '-SEE DOCUMENTATION-. THIS WILL SHOW YOU THE LOCATION'/
       +,5X, 'OF THE TROUBLE. WITH THIS KNOWLEDGE YOU CAN START TO '/
       +,5X, 'PRUNE OUT THE OFFENDING READINGS.  GET HELP DOING THIS '/
       +//,5X, 'XXXXXXXXXXXXXXXXXXXXXXXXXXXXXXXXXXXXXXXXXXXXXXXXXXXX ')
        STOP
        END
```

```
      PROGRAM EDEPTH  (INDIP,IEDIP,TAPE8,TAPE7,OUTPUT,TAPE1=INDIP,
     -TAPE2=IEDIP,TAPE6=OUTPUT)
C
C            PROGRAM WRITTEN BY F.W.M. HOPPER 1978
C            -----------------------------------------
C
C
C       THIS PROGRAM RECOMBINES TWO INTERPOLATED APPARENT DIP
C       FILES AND GENERATES THE THEORETICAL FOLLIATION SURFACE
C       FROM THEM TO BE PASSED TO SYMVU.
C       THE ONLY OTHER OUTPUT IS INFORMATION AS TO THE SIZE OF THE
C       MATRIX AND THE MAXIMUM / MINIMUM VALUES GENERATED.
C       CALCULATED FROM THE WEST TO THE EAST WITH 0.0 IN THE
C       BOTTOM LEFT CORNER.
C
C       ARRAYS.
C       =======
C                   ROW       - CONTAINS CURRENT ROW DIP VALUES.
C                   COLL      - CONTAINS FIRST COLUMN FROM INDIP
C                   DROP      - CONTAINS DEPTHS OF THE SURFACE FROM AN
C                               ORDNANCE DATUM LEVEL IN THE CURRENT ROW.
C                   SCALES    - CONTAINS THE CONTROL VALUES FOR SYMVU.
C
C       VARIABLES.
C       ==========
C                   NROW      - NUMBER OF ROWS ( = SCALES(1) ).
C                   NCOL      - NUMBER OF COLUMNS ( = SCALES(2) ).
C                   ROWDIST   - DISTANCE BETWEEN THE ROWS (=SCALES(3)).
C                   COLDIST   - DISTANCE BETWEEN THE COLUMNS (=SCALES(4)).
C                   MIN    - MINIMUM VALUE OF INTERPOLATED DIP VALUES (=SCALES(5)).
C                   MAX    - MAXIMUM VALUE OF INTERPOLATED DIP VALUES (=SCALES(6)).
C                   SCALES 7-24 ARE REDUNDANT BUT MUST BE PRESENT.
C
C
C       DIMENSION SCALES(24) , COL (200) , ROW(200) , DROP(200)
C
C
C       THE ARRAY SCALES WILL FORWARD THE 24 VALUES NEEDED FOR THE
C       SYMVU ROUTINE.
C
C
C       EQUIVALENCE (NROW,SCALES(1)) , (NCOL,SCALES(2))
C
C        STATEMENT FUNCTIONS ============================
C        TAND ( ARG ) = TAN ( ARG * 0.0175 )
C
C       REWIND THE TAPES TO BE USED AS INPUT, WHICH ARE 'INDIP'
C       (INTERPOLATED NORTHERLY DIPS ) AND 'IEDIP' ( INTERPOLATED
C       EASTERLY DIPS ), AND HAVE BEEN COPIED FROM TAPE 8.
C
        REWIND 1
        REWIND 2
        READ(1)  (SCALES(K) ,K=1,24)
C       'DISTROW' AND 'DISTCOL ' ARE THE DISTANCES BETWEEN THE GRID
C       POSITIONS OF THE INTERPOLATED MATRIX.
C
        DISTROW = 1.0 / SCALES(3)
        DISTCOL = 1.0 / SCALES(4)
C       READ 1ST CARD OF (2) WITH SCALES ON.
        READ (2)
C       READ FROM TAPE (1) THE FIRST COLUM FROM EACH ROW.
        WRITE (6,133)
133     FORMAT (5X, '******************************************* ',////,
     +5X,'          --- PROGRAM EDEPTH ----          ',////,
```

```
      +5X, 'XXXXXXXXXXXXXXXXXXXXXXXXXXXXXXXXXXXXXXXXXX ',)
        DO 88 I=1,NROW
        READ(1) ROW(I)
88      CONTINUE
C
C
C       WORK OUT THE DROP AT EACH POINT ALONG THE FIRST COL OF THE MATRIX
C       FROM THE INTERPOLATED NORTHERLY DIPS, ASSUMING THE DROP IN THE BOTTOM
C       LEFT CORNER TO BE 0.0 AND WRITE THEM TO COL AS AN INTERMEDIATE
C       STORE.
C
C
        COL(NROW)=0.0
        DO 451 J=2,NROW
        K = NROW - J + 1
        R=ROW(K) * (-1.0)
        ROW(K) = ABS(ROW(K))
        COL(K)=COL(K+1)+DISTROW*(SIGN(TAND(ROW(K)),R))
451 CONTINUE
C
C
        DROPHI=DROPLO=COL(1)
C       NOW WORK OUT THE DROP AT ALL OTHER GRID POINTS USING THE
C       INTERPOLATED EASTERLY DIPS, EXEPT THE FIRST WORD ON THE ROW,
C       WHICH WE ALREADY KNOW FROM WHAT WE HAVE IN COL.
C
C
        DO 452 L=1,NROW
        READ(2) (ROW(K),K=1,NCOL)
        DROP(1)=COL(L)
            DO 453 K=2,NCOL
          R=ROW(K) * (-1.0)
          ROW(K) = ABS(ROW(K))
          DROP(K)=DROP(K-1)+DISTCOL*(SIGN(TAND(ROW(K)),R))
453         CONTINUE
C
C
        DO 74 I=1,NCOL
        IF(DROP(I).GT.DROPHI)DROPHI=DROP(I)   IF(DROP(I).LT.DROPLO)
       -DROPLO=DROP(I)
74      CONTINUE
C
C
C       WRITE VALUES TO TAPE 7 AS AN INTERMEDIATE STOR.
            WRITE(7) (DROP(K),K=1,NCOL)
452 CONTINUE
        ENDFILE 7
C
        ENDFILE 7
C
C
C       WE NOW HAVE THE MINIMUM AND MAXIMUM DROP VALUES AND THESE ARE
C       PUT IN SCALES(5) AND SCALES(6)-(24) RESPECTIVELY.
C
C
        DO 454 K=6,24
            SCALES(K) = DROPHI
454 CONTINUE
        SCALES(5) = DROPLO
        REWIND 7
        WRITE(8) NROW,NCOL,(SCALES(K),K=3,24)
        DO 700 I=1,NROW
        READ(7) (DROP(J),J=1,NCOL)
        WRITE(8) (DROP(J),J=1,NCOL)
```

```
700    CONTINUE
       ENDFILE 8
       REWIND 8
       WRITE(6,777) NROW,NCOL,(SCALES(K),K=3,6)
777    FORMAT(5X,'ROWS ',5X,I5,/,5X,'COLUMNS ',5X,I5,/,
      -5X,'ROWSPACING ',5X,G22.11,/,5X,'COLUMNSPACING ',5X,G22.11,/,
      -5X,'LOWEST VALUE',5X,G22.11,/,5X,'HIGHEST VALUE',5X,G22.11)
C        FIND OUT IF THERE ARE GOING TO BE ANY SCALING
C        PROBLEMS WHEN SYMVU GETS THE FILE.
       IF(DROPHI.EQ.0.0)GO TO 771
       IF(( DROPHI+DROPLO)/DROPHI.GT.2/3) PRINT (6,778)
771    CONTINUE
778    FORMAT (20X,'XXXXXXXXXXXXXXXX   W A R N I N G   XXXXXXXXXXXXXXXXX'/
      +//,5X,'YOU HAVE A SCALING PROBLEM   YOUR SYMVU PLOT MAY'/
      +,5X,'LOOK FLAT.    YOU HAVE EITHER A VERY HIGH (HIGHEST '/
      +,5X,'VALUE) OR A VERY LOW (LOWEST VALUE), ↑SEE ABOVE↑.'/
      +,5X,'IF YOUR WHOLE DATA IS NOT EVENLY SPREAD BETWEEN THEM,'/
      +,5X,'DURING SCALING THE VARIATION IN THE SURFACE MAY BE'/
      +,5X,'LOST.'/
      +,5X,'THIS MAY BE OVERCOME BY CAREFUL SELECTION OF THE '/
      +,5X,'APPROPRIATE SYMVU ELECTIVES - SEE MANUAL- , OR '/
      +,5X,'YOU MAY HAVE TO OPERATE ON YOUR MATRIX.  TO DO THIS'/
      +,5X,'--FIRST EXAMINE IT, BY LOOKING AT THE TAPE8 PRODUCED'/
      +,5X,'BY THIS PROGRAM, WITH PROGRAM GRID IN THIS LIBRARY'/
      +,5X,'-SEE DOCUMENTATION-. THIS WILL SHOW YOU THE LOCATION'/
      +,5X,'OF THE TROUBLE. WITH THIS KNOWLEDGE YOU CAN START TO'/
      +,5X,'PRUNE OUT THE OFFENDING READINGS.  GET HELP DOING THIS '/
      +//,5X, 'XXXXXXXXXXXXXXXXXXXXXXXXXXXXXXXXXXXXXXXXXXXXXXXXXXX ')
       STOP
       END
```

```
      PROGRAM SDEPTH (INDIP,IEDIP,TAPE7,TAPE8,OUTPUT,TAPE1=INDIP,
     1TAPE2=IEDIP,TAPE6=OUTPUT)
C
C
C
C                     PROGRAM WRITTEN BY F.W.M. HOPPER 1978.
C                     _____
C
C
C
C         THIS PROGRAM RECOMBINES TWO INTERPOLATED APPARENT DIP
C         FILES AND GENERATES THE THEORETICAL FOLLIATION SURFACE
C         FROM THEM, TO BE PASSED TO SYMVU.
C         THE ONLY OTHER OUTPUT IS INFORMATION AS TO THE SIZE OF THE
C         MATRIX AND THE MAXIMUM / MINIMUM VALUES GENERATED.
C         CALCULATED FROM NORTH TO SOUTH WITH 0.0 IN THE TOP RIGHT
C         CORNER.
C
C
C
C       ARRAYS.
C       =======
C                     ROW       - CONTAINS CURRENT ROW DIP VALUES.
C                     DROP      - CONTAINS DEPTHS OF THE SURFACE FROM AN
C                                 ORDNANCE DATUM LEVEL IN THE CURRENT ROW.
C                     SCALES    - CONTAINS THE CONTROL VALUES FOR SYMVU.
C
C       VARIABLES.
C       ==========
C                     NROW      - NUMBER OF ROWS ( = SCALES(1) ).
C                     NCOL      - NUMBER OF COLUMNS ( = SCALES(2) ).
C                     DISTROW   - DISTANCE BETWEEN THE ROWS.
C                     DISTCOL   - DISTANCE BETWEEN THE COLUMNS.
C                     MAX       - MAXIMUM VALUE OF INTERPOLATED DIP VALUES.
C                     MIN       - MINIMUM VALUE OF INTERPOLATED DIP VALUES.
C
      DIMENSION SCALES(24), ROW(200), DROP(200)
C
C
C       THE ARRAY SCALES WILL FORWARD THE 24 VALUES NEEDED FOR THE
C       SYMVU ROUTINE.
C
C
      EQUIVALENCE (NROW,SCALES(1)), (NCOL,SCALES(2))
C
C             STATEMENT FUNCTIONS _____
C
C         TAND ( ARG ) = TAN ( ARG * 0.0175 )
C
C
C
C       REWIND THE TAPES TO BE USED AS INPUT, WHICH ARE 'INDIP'
C       (INTERPOLATED NORTHERLY DIPS ) AND 'IEDIP' ( INTERPOLATED
C       EASTERLY DIPS ), AND HAVE BEEN COPIED FROM TAPE 8,SYMAP OUTPUT.
C
C
      REWIND 1
      REWIND 2
C
C
C       THE FIRST 24 WORDS CONTAIN THE CONTROL INFORMATION FROM SYMAP.
C             SCALES(1) - (NROW) - NUMBER OF ROWS.
C             SCALES(2) - (NCOL) - NUMBER OF COLUMNS.
C             SCALES(3) - NUMBER OF ROWS TO AN INCH.
C             SCALES(4) - NUMBER OF COLUMNS TO AN INCH.
C             SCALES(5) - MINIMUM VALUE OF INTERPOLATED DIP VALUES.
```

```
C               SCALES (6) - (24)  - MAXIMUM VALUE OF INTERPOLATED DIP VALUES.
C

        READ (1)  (SCALES (K) ,K=1,24)
C
C        'DISTROW' AND 'DISTCOL ' ARE THE DISTANCES BETWEEN THE GRID
C        POSITIONS OF THE INTERPOLATED MATRIX.
C
C

        DISTROW = 1.0 / SCALES (3)
        DISTCOL = 1.0 / SCALES (4)
        READ (2)
C         HAVING RED OF THE SCALES ON 2 READ THE FIRST ROW.
        READ (2)  (ROW (I) ,I=1,NCOL)
C
C
C        WORK OUT THE DROP AT EACH POINT ALONG THE TOP ROW OF THE MATRIX
C        FROM THE INTERPOLATED EASTERLY DIPS, ASSUMING THE DROP IN THE TOP
C        RIGHT CORNER TO BE 0.0 AND WRITE THEM TO TAPE 7 AS AN
C        INTERMEDIATE STOR.
C
C

        DROP (NCOL) =0.0
        WRITE (6,133)
133     FORMAT (5X, 'XXXXXXXXXXXXXXXXXXXXXXXXXXXXXXXXXXXXXXX ',////,
       +5X,'         ---- PROGRAM SDEPTH ----         ',////,
       +5X, 'XXXXXXXXXXXXXXXXXXXXXXXXXXXXXXXXXXXXXXX ',)
        DO  451 J=2,NCOL
        K=NCOL-J+1
        R=ROW (K)
        ROW (K) = ABS (ROW (K) )
        DROP (K) =DROP (K+1) +DISTCOL*(SIGN (TAND (ROW (K) ) ,R) )
   451 CONTINUE
        WRITE (7)  (DROP (K) ,K=1,NCOL)
C
C
C        INITIALISE 'DROPHI ' AND 'DROPLO '
C
C

        DROPHI=DROPLO=DROP (1)
        DO  79 I=2,NCOL
        IF (DROP (I) .GT.DROPHI) DROPHI=DROP (I)   · IF (DROP (I) .LT.DROPLO) DROPLO=
       -DROP (I)
79      CONTINUE
C
C
C        NOW WORK OUT THE DROP AT ALL OTHER GRID POINTS USING THE
C        INTERPOLATED NORTHERLY DIPS, AND WRITE THESE TO TAPE 7 TOO.
C
C

        READ (1)
        DO  452 L=2,NROW
        READ (1)  (ROW (K) ,K=1,NCOL)
            DO  453 J=1,NCOL
        K=NCOL-J+1
        R=ROW (K)
        ROW (K) =ABS (ROW (K) )
        DROP (K) = DROP (K) +DISTROW*(SIGN (TAND (ROW (K) ) ,R) )
   453      CONTINUE
C
C

        DROPHI=DROPLO=DROP (1)
        DO  73 I=2,NCOL
        IF (DROP (I) .GT.DROPHI) DROPHI=DROP (I)    IF (DROP (I) .LT.DROPLO) DROPLO=
```

```
      -DROP(I)
73    CONTINUE
C
C
          WRITE(7) (DROP(K),K=1,NCOL)
  452 CONTINUE
C
      ENDFILE 7
      ENDFILE 7
C
C     WE NOW HAVE THE MINIMUM AND MAXIMUM DROP VALUES AND THESE ARE
C     PUT IN SCALES(5) AND SCALES(6)-(24) RESPECTIVELY.
C
C
      DO 454 K=6,24
          SCALES(K) = DROPHI
  454 CONTINUE
      SCALES(5) = DROPLO
      REWIND 7
      WRITE(8) NROW,NCOL,(SCALES(K),K=3,24)
      DO 700 I=1,NROW
      READ(7) (DROP(J),J=1,NCOL)
      WRITE(8) (DROP(J),J=1,NCOL)
700   CONTINUE
      ENDFILE 8
      REWIND 8
      WRITE(6,777) NROW,NCOL,(SCALES(K),K=3,6)
777   FORMAT(5X,'ROWS',5X,I5,/,5X,'COLUMNS',5X,I5,/,
     -5X,'ROWSPACING',5X,G22.11,/,5X,'COLUMNSPACING',5X,G22.11,/,
     -5X,'LOWEST VALUE',5X,G22.11,/,5X,'HIGHEST VALUE',5X,G22.11)
C     FIND OUT IF THERE ARE GOING TO BE ANY SCALING
C     PROBLEMS WHEN SYMVU GETS THE FILE.
      IF(DROPHI.EQ.0.0)GO TO 771
      IF(( DROPHI+DROPLO)/DROPHI.GT.2/3) PRINT (6,778)
771   CONTINUE
778   FORMAT (20X, 'xxxxxxxxxxxxxxxx  W A R N I N G  xxxxxxxxxxxxxxxx '/
     +//,5X, 'YOU HAVE A SCALING PROBLEM   YOUR SYMVU PLOT MAY'/
     +,5X, 'LOOK FLAT.    YOU HAVE EITHER A VERY HIGH (HIGHEST '/
     +,5X, 'VALUE) OR A VERY LOW (LOWEST VALUE), ↑SEE ABOVE↑.'/
     +,5X, 'IF YOUR WHOLE DATA IS NOT EVENLY SPREAD BETWEEN THEM,'/
     +,5X, 'DURING SCALING THE VARIATION IN THE SURFACE MAY BE'/
     +,5X, 'LOST.'/
     +,5X, 'THIS MAY BE OVERCOME BY CAREFUL SELECTION OF THE '/
     +,5X, 'APPROPRIATE SYMVU ELECTIVES - SEE MANUAL- , OR '/
     +,5X, 'YOU MAY HAVE TO OPERATE ON YOUR MATRIX.   TO DO THIS'/
     +,5X, '-FIRST EXAMINE IT, BY LOOKING AT THE TAPE8 PRODUCED'/
     +,5X, 'BY THIS PROGRAM, WITH PROGRAM GRID IN THIS LIBRARY'/
     +,5X, '-SEE DOCUMENTATION-. THIS WILL SHOW YOU THE LOCATION'/
     +,5X, 'OF THE TROUBLE. WITH THIS KNOWLEDGE YOU CAN START TO'/
     +,5X, 'PRUNE OUT THE OFFENDING READINGS.  .GET HELP DOING THIS '/
     +//,5X, 'xxxxxxxxxxxxxxxxxxxxxxxxxxxxxxxxxxxxxxxxxxxxxxxxxxxxxxxxxxx ')
      STOP
      END
```

```
      PROGRAM NDEPTH (INDIP,IEDIP,TAPE8,TAPE7,OUTPUT,TAPE1=INDIP,
     -TAPE2=IEDIP,TAPE6=OUTPUT)
C
C     PROGRAM WRITTEN BY F.W.M.HOPPER 1978
C     ------------------------------------------
C
C
C     THIS PROGRAM RECOMBINES TWO INTERPOLATED APPARENT DIP
C     FILES AND GENERATES THE THEORETICAL FOLIATION SURFACE
C     FROM THEM, TO BE PASSED TO SYMVU.
C     THE ONLY OTHER OUTPUT IS INFORMATION AS TO THE SIZE OF THE
C     MATRIX AND THE MAXIMUM / MINIMUM VALUES GENERATED.
C     CALCULATION DONE FROM SOUTH TO NORTH WITH 0.0 IN THE BOTTOM
C     LEFT CORNER.
C
C     ARRAYS.
C     =======
C                   ROW      - CONTAINS CURRENT ROW DIP VALUES.
C                   DROP     - CONTAINS DEPTHS OF THE SURFACE FROM AN
C                              ORDNANCE DATUM LEVEL IN THE CURRENT ROW.
C                   SCALES   - CONTAINS THE CONTROL VALUES FOR SYMVU.
C
C     VARIABLES.
C     ==========
C                   NROW     - NUMBER OF ROWS ( = SCALES(1) ).
C                   NCOL     - NUMBER OF COLUMNS ( = SCALES(2) ).
C                   ROWDIST  - DISTANCE BETWEEN THE ROWS(=SCALES(3)).
C                   COLDIST  - DISTANCE BETWEEN THE COLUMNS(=SCALES(4)).
C                   MIN      - MINIMUM VALUE OF INTERPOLATED DIP VALUES(=SCALES(5)).
C                   MAX      - MAXIMUM VALUE OF INTERPOLATED DIP VALUES(=SCALES(6)).
C                   SCALES 7-24 ARE REDUNDANT BUT MUST BE PRESENT.
C
C
C     DIMENSION SCALES(24) , ROW(200) , DROP(200)
C
C
C     THE ARRAY SCALES WILL FORWARD THE 24 VALUES NEEDED FOR THE
C     SYMVU ROUTINE.
C
C
C     EQUIVALENCE (NROW,SCALES(1)) , (NCOL,SCALES(2))
C
C           STATEMENT FUNCTIONS ------------------------
C                   TAND ( ARG ) = TAN ( ARG * 0.0175 )
C
C     REWIND THE TAPES TO BE USED AS INPUT, WHICH ARE 'INDIP'
C     (INTERPOLATED NORTHERLY DIPS ) AND 'IEDIP' ( INTERPOLATED
C     EASTERLY DIPS ), AND HAVE BEEN COPIED FROM TAPE 8.
C
      REWIND 1
      REWIND 2
      READ(1) (SCALES(K),K=1,24)
C     'DISTROW' AND 'DISTCOL' ARE THE DISTANCES BETWEEN THE GRID
C     POSITIONS OF THE INTERPOLATED MATRIX.
C
      DISTROW = 1.0 / SCALES(3)
      DISTCOL = 1.0 / SCALES(4)
C     READ ALL CARDS ON 2 EXEPT THE LAST.
      WRITE(6,133)
133   FORMAT(5X, 'xxxxxxxxxxxxxxxxxxxxxxxxxxxxxxxxxxxxxxxxxxxx ',/////,
     +5X,'        --- PROGRAM NDEPTH ---        ',/////,
     +5X, 'xxxxxxxxxxxxxxxxxxxxxxxxxxxxxxxxxxxxxxxxxxxx ',)
      DO 37 K=1,NROW
      READ (2)
37    CONTINUE
```

```
      READ(2) (ROW(I),I=1,NCOL)
C
C
C     WORK OUT THE DROP AT EACH POINT ALONG THE BOTTOM ROW OF THE MATRIX
C     FROM THE INTERPOLATED EASTERLY DIPS, ASSUMING THE DROP IN THE BOTTOM
C     LEFT CORNER TO BE 0.0 AND WRITE THEM TO TAPE 7 AS AN INTERMEDIATE
C     STORE.
C
C
      DROP(1)=0.0
      DO 451 K=2,NCOL
           R=ROW(K)*(-1.0)
           ROW(K) = ABS(ROW(K))
           DROP(K)=DROP(K-1) + DISTCOL * (SIGN (TAND (ROW(K)) , R ))
  451 CONTINUE
      WRITE(7) (DROP(K),K=1,NCOL)
C
C
      DROPHI=DROPLO=DROP(1)
      DO 73 I=2,NCOL
      IF(DROP(I).GT.DROPHI)DROPHI=DROP(I)  IF(DROP(I).LT.DROPLO)DROPLO=
     -DROP(I)
 73   CONTINUE
C
C
C     NOW WORK OUT THE DROP AT ALL OTHER GRID POINTS USING THE
C     INTERPOLATED NORTHERLY DIPS.
C
C     READ TO END OF 1 THEN WORK BACKWARDS THROUGH IT.
      DO 93 I=1,NROW
      READ(1)
 93   CONTINUE
      DO 452 L=2,NROW
      BACKSPACE 1
      BACKSPACE 1
      READ(1) (ROW(K),K=1,NCOL)
           DO 453 K=1,NCOL
                R=ROW(K) * (-1.0)
                ROW(K) = ABS(ROW(K))
              DROP(K)=DROP(K) + DISTROW * (SIGN (TAND (ROW(K)) , R ))
 453       CONTINUE
C
C
      DO 74 I=1,NCOL
      IF(DROP(I).GT.DROPHI)DROPHI=DROP(I)  IF(DROP(I).LT.DROPLO)
     -DROPLO=DROP(I)
 74   CONTINUE
C
C
           WRITE(7) (DROP(K),K=1,NCOL)
  452 CONTINUE
      ENDFILE 7
C
C
C     WE NOW HAVE THE MINIMUM AND MAXIMUM DROP VALUES AND THESE ARE
C     PUT IN SCALES(5) AND SCALES(6)-(24) RESPECTIVELY.
C
C
      DO 454 K=6,24
           SCALES(K) = DROPHI
  454 CONTINUE
      SCALES(5) = DROPLO
      BACKSPACE 7
      WRITE(8) SCALES
```

```
      DO 700 I=1,NROW
      READ(7)  (DROP(J),J=1,NCOL)
      WRITE(8) (DROP(J),J=1,NCOL)
      BACKSPACE 7
      BACKSPACE 7
700   CONTINUE
      ENDFILE 8
      REWIND 8
      WRITE(6,777) NROW,NCOL,(SCALES(K),K=3,6)
777   FORMAT(5X,'ROWS',5X,I5,/,5X,'COLUMNS',5X,I5,/,
     -5X,'ROWSPACING',5X,G22.11,/,5X,'COLUMNSPACING',5X,G22.11,/,
     -5X,'LOWEST VALUE',5X,G22.11,/,5X,'HIGHEST VALUE',5X,G22.11)
C     FIND OUT IF THERE ARE GOING TO BE ANY SCALING
C     PROBLEMS WHEN SYMVU GETS THE FILE.
      IF(DROPHI.EQ.0.0)GO TO 771
      IF(( DROPHI+DROPLO)/DROPHI.GT.2/3) PRINT (6,778)
771   CONTINUE
778   FORMAT (20X,'xxxxxxxxxxxxxx   W A R N I N G   xxxxxxxxxxxxxxxx'/
     +//,5X,'YOU HAVE A SCALING PROBLEM . YOUR SYMVU PLOT MAY'/
     +,5X,'LOOK FLAT.   YOU HAVE EITHER A VERY HIGH (HIGHEST '/
     +,5X,'VALUE) OR A VERY LOW (LOWEST VALUE), ↑SEE ABOVE↑.'/
     +,5X,'IF YOUR WHOLE DATA IS NOT EVENLY SPREAD BETWEEN THEM,'/
     +,5X,'DURING SCALING THE VARIATION IN THE SURFACE MAY BE'/
     +,5X,'LOST.'/
     +,5X,'THIS MAY BE OVERCOME BY CAREFUL SELECTION OF THE '/
     +,5X,'APPROPRIATE SYMVU ELECTIVES - SEE MANUAL- , OR '/
     +,5X,'YOU MAY HAVE TO OPERATE ON YOUR MATRIX.  TO DO THIS'/
     +,5X,'—FIRST EXAMINE IT, BY LOOKING AT THE TAPE8 PRODUCED'/
     +,5X,'BY THIS PROGRAM, WITH PROGRAM GRID IN THIS LIBRARY'/
     +,5X,'-SEE DOCUMENTATION-. THIS WILL SHOW YOU THE LOCATION'/
     +,5X,'OF THE TROUBLE. WITH THIS KNOWLEDGE YOU CAN START TO'/
     +,5X,'PRUNE OUT THE OFFENDING READINGS.  GET HELP DOING THIS.'/
     +//,5X, 'xxxxxxxxxxxxxxxxxxxxxxxxxxxxxxxxxxxxxxxxxxxxxxxxxxx ')
      STOP
      END
```

```
      PROGRAM DIEPTH (INDIP,IEDIP,TAPE8,TAPE7,OUTPUT,TAPE1=INDIP,
  -TAPE2=IEDIP,TAPE6=OUTPUT)
C
C     PROGRAM WRITTEN BY F.W.M.HOPPER 1978
C     ───────────────────────────────────────
C
C
C     THIS PROGRAM RECOMBINES TWO INTERPOLATED APPARENT DIP
C     FILES AND GENERATES THE THEORETICAL FOLIATION SURFACE
C     FROM THEM, TO BE PASSED TO SYMVU.
C     THE ONLY OTHER OUTPUT IS INFORMATION AS TO THE SIZE OF THE
C     MATRIX AND THE MAXIMUM / MINIMUM VALUES GENERATED.
C     THIS IS THE BEST PROGRAM TO USE AS IT COMBINES THE VALUE
C     FOR THE POINT FROM EACH TAPE TO GENERATE THE SURFACE. THIS
C     ELIMINATES THE REMANDER EFECT WHEN THE FOLIATION SURFACE IS
C     AN INTERFERANCE PATTERN.
C     THE 0.0 POINT IS IN THE BOTTOM LEFT CORNER.
C
C     ARRAYS.
C     =======
C                 ROW      - CONTAINS CURRENT ROW DIP VALUES.
C                 DROP     - CONTAINS DEPTHS OF THE SURFACE FROM AN
C                            ORDNANCE DATUM LEVEL IN THE CURRENT ROW.
C                 SCALES   - CONTAINS THE CONTROL VALUES FOR SYMVU.
C                 EDGE     - HOLDS THE VALUES FOR THE LEFT EDGE OF
C                            THE MATRIX.
C                 COL      - THIS HOLDS THE ROW FROM TAPE 1 AND FOR
C                            A TIME THE LEFT EDGE VALUES.
C                 DROPP    - AN INTERMEDIATE STORE OF DROPS.
C
C     VARIABLES.
C     ==========
C                 NROW     - NUMBER OF ROWS ( = SCALES(1) ).
C                 NCOL     - NUMBER OF COLUMNS ( = SCALES(2) ).
C                 ROWDIST  - DISTANCE BETWEEN THE ROWS (=SCALES(3)).
C                 COLDIST  - DISTANCE BETWEEN THE COLUMNS (=SCALES(4)).
C                 MIN      - MINIMUM VALUE OF INTERPOLATED DIP VALUES (=SCALES(5)).
C                 MAX      - MAXIMUM VALUE OF INTERPOLATED DIP VALUES (=SCALES(6)).
C                 SCALES 7-24 ARE REDUNDANT BUT MUST BE PRESENT.
C
C
      DIMENSION SCALES(24), ROW(200), DROP(200),EDGE(200),COL(200),
  -DROPP(200)
C
C
C     THE ARRAY SCALES WILL FORWARD THE 24 VALUES NEEDED FOR THE
C     SYMVU ROUTINE.
C
C
      EQUIVALENCE (NROW,SCALES(1)), (NCOL,SCALES(2))
C
C           STATEMENT FUNCTIONS ─────────────────────────
C                 TAND ( ARG ) = TAN ( ARG * 0.0175 )
C                 ATAND (ARG) = ATAN (ARG) * 57.143
C                 SIND (ARG) = SIN (ARG * 0.0175)
C                 COSD (ARG) = COS (ARG * 0.0175)
C
C     REWIND THE TAPES TO BE USED AS INPUT, WHICH ARE 'INDIP'
C     (INTERPOLATED NORTHERLY DIPS ) AND 'IEDIP' ( INTERPOLATED
C     EASTERLY DIPS ), AND HAVE BEEN COPIED FROM TAPE 8.
C
      REWIND 1
      REWIND 2
      READ(1) (SCALES(K),K=1,24)
C     'DISTROW' AND 'DISTCOL' ARE THE DISTANCES BETWEEN THE GRID
```

```
C       POSITIONS OF THE INTERPOLATED MATRIX.
C
        DISTROW = 1.0 / SCALES(3)
        DISTCOL = 1.0 / SCALES(4)
        DIAG = SQRT ( DISTROW*DISTROW + DISTCOL*DISTCOL )
        ANG = ATAND (DISTCOL/DISTROW)
C       READ ALL CARDS ON 2 EXEPT THE LAST.
        WRITE(6,133)
133     FORMAT (5X, 'XXXXXXXXXXXXXXXXXXXXXXXXXXXXXXXXXXXXXXXXXX ',////,
       +5X,'          --- PROGRAM DIEPTH ---        ',////,
       +5X, 'XXXXXXXXXXXXXXXXXXXXXXXXXXXXXXXXXXXXXXXXXX ',)
        DO 37 K=1,NROW
        READ(2)
37      CONTINUE
C       READ LAST ROW FROM TAPE 2
        READ(2) (ROW(I),I=1,NCOL)
C
C
C       WORK OUT THE DROP AT EACH POINT ALONG THE BOTTOM ROW OF THE MATRIX
C       FROM THE INTERPOLATED EASTERLY DIPS, ASSUMING THE DROP IN THE BOTTOM
C       LEFT CORNER TO BE 0.0 AND WRITE THEM TO TAPE 7 AS AN INTERMEDIATE
C       STORE.
C
C
        DROP(1)=0.0
        DO 451 K=2,NCOL
            R=ROW(K)*(-1.0)
            ROW(K) = ABS(ROW(K))
            DROP(K)=DROP(K-1) + DISTCOL * (SIGN (TAND (ROW(K)) , R ))
    451 CONTINUE
        WRITE(7) (DROP(K),K=1,NCOL)
C
C
        DROPHI=DROPLO=DROP(1)
        DO 73 I=2,NCOL
        IF (DROP(I).GT.DROPHI) DROPHI=DROP(I)    IF (DROP(I).LT.DROPLO) DROPLO=
       -DROP(I)
73      CONTINUE
C
C       GET TO SECOND LAST ROW OF 2
        BACKSPACE 2
        BACKSPACE 2
        READ(2) (ROW(I),I=1,NCOL)
C
C
C       NOW GET THE VALUES FOR THE LEFT EDGE FROM 1 , READ THEM TO COL
C       AND STORE THE VALUES IN EDGE.
C
C
        DO 333 I = 1,NROW
        J = NROW -I +1
        READ(1) COL (J)
333     CONTINUE
        EDGE(1) = DROP(1)
        DO 334 I = 2,NROW
        R = COL(I) * (-1.0)
        COL(I) = ABS(COL(I))
        EDGE(I) = EDGE(I-1) + DISTROW * (SIGN (TAND (COL(I)) , R ))
334     CONTINUE
C       NOW GET THE VALUES FOR THE SECOND LAST ROW OF 1 INTO COL.
        BACKSPACE 1
        BACKSPACE 1
        READ(1) (COL(K),K=1,NCOL)
C
```

```
C        NOW WORK OUT ALL THE OTHER GRID POINTS USEING THE
C        INFORMATION FROM BOTH TAPES TO FIND OUT THE DROP
C        ALLONG THE DIAGONAL.
C
C
         DO 337 J = 2,NROW
         IF (J.EQ.2) GO TO 338
         BACKSPACE 1
         BACKSPACE 1
         READ(1) (COL(L),L=1,NCOL)
         BACKSPACE 2
         BACKSPACE 2
         READ(2) (ROW(L),L=1,NCOL)
338      CONTINUE
         DO 336 K = 2,NCOL
         A = ABS (COL(K))
         B = ABS (ROW(K))
         FIE = ATAND (TAND(B)/TAND(A))
         DIP = ATAND (TAND(B) * (1/COSD(FIE)))
         IF (COL(K).GE.0.0.AND.ROW(K).GE.0.0)AZIMUTH = 90.0-FIE
         IF (COL(K).GE.0.0.AND.ROW(K).LT.0.0)AZIMUTH = 270.0+FIE
         IF (COL(K).LT.0.0.AND.ROW(K).GE.0.0)AZIMUTH = 90.0+FIE
         IF (COL(K).LT.0.0.AND.ROW(K).LT.0.0)AZIMUTH = 270.0-FIE
C
C        THIS HAS GIVEN US THE AZIMUTH AND TRUE DIP OF THE PLANE AT
C        THIS POINT AS DEFINED BY THE TWO APPARENT DIPS.
C
C        FROM THE AZIMUTH THE STRIKE WILL BE FOUND ON THE EAST END
C        OF THE AXIS.
C
         IF(AZIMUTH.LT.90.0)STRIKE = AZIMUTH + 90.0
         IF(AZIMUTH.GE.90.0.AND.AZIMUTH.LT.270.0)
        +STRIKE = AZIMUTH - 90.0
         IF(AZIMUTH.GE.270.0)STRIKE = AZIMUTH - 270.0
C
C        NOW FIND THE TWO LIMITING AZIMUTH DIRECTIONS WHICH DEFINE
C        WEATHER THE COMPONENT OF DIP IS DOMINENTLY TO THE NE. OR SW.
C        AND HENCE WEATHER THE FINAL DIP WILL BE (+) OR (-).
C
         XNTH = 270.0 + ANG
         XSTH = 90.0 + ANG
C        NOW WORK OUT THE ANGLE BETWEEN THE STRIKE IN THE E. QUADRENT
C        AND THE DIRECTION OF THE DIAGNAL TO THE NE.
C
C
         GAP = ABS ( STRIKE - ANG )
C
C
C        NOW FIND THE APPARENT DIP ALLONG THE NE. DIAGNAL.
C
C
         DIDIP = ATAND ( TAND (DIP) * SIND (GAP) ) * (-1.0)
C
C
C        IF THE AZIMUTH WAS IN THE RIGHT DIRECTION ( TO THE SW. )
C        MAKE THE DIDIP (+).
C
C
         IF(AZIMUTH.LE.XNTH.AND.AZIMUTH.GT.XSTH)
        +DIDIP = DIDIP * (-1.0)
C
C
C        NOW WORK OUT THE DROPS FROM THESE WITH REFERENCE TO
C        THE LAST DROPS FOUND, STORE THE DROPS IN DROPP UNTIL
```

```
C        THE END THEN REPLACE THE OLD DROPS WITHE THE VALUES
C        FROM DROPP.
C
C
         DROPP(K) = DROP(K-1) + DIAG * (TAND(DIDIP) )
336      CONTINUE
         DROP(1) = EDGE(J)
         DO 575 I = 2,NCOL
         DROP(I) =DROPP(I)
575      CONTINUE
C
C
         DO 74 I=1,NCOL
         IF(DROP(I).GT.DROPHI)DROPHI=DROP(I)   IF(DROP(I).LT.DROPLO)
        -DROPLO=DROP(I)
74       CONTINUE
C
C
C
C        NOW WRITE OUT THE VALUES ONTO 7 AND CONTINUE
C
            WRITE(7)  (DROP(K),K=1,NCOL)
337      CONTINUE
         ENDFILE 7
C
C
C
C        WE NOW HAVE THE MINIMUM AND MAXIMUM DROP VALUES AND THESE ARE
C        PUT IN SCALES(5) AND SCALES(6)-(24) RESPECTIVELY.
C
C
         DO 454 K=6,24
            SCALES(K) = DROPHI
   454   CONTINUE
         SCALES(5) = DROPLO
         BACKSPACE 7
         WRITE(8) NROW,NCOL,(SCALES(K),K=3,24)
         DO 700 I=1,NROW
         READ(7)  (DROP(J),J=1,NCOL)
         WRITE(8)  (DROP(J),J=1,NCOL)
         BACKSPACE 7
         BACKSPACE 7
700      CONTINUE
         ENDFILE 8
         REWIND 8
         WRITE(6,777) NROW,NCOL,(SCALES(K),K=3,6)
777      FORMAT(5X,'ROWS ',5X,I5,/,5X,'COLUMNS ',5X,I5,/,
        -5X,'ROWSPACING',5X,G22.11,/,5X,'COLUMNSPACING',5X,G22.11,/,
        -5X,'LOWEST VALUE',5X,G22.11,/,5X,'HIGHEST VALUE',5X,G22.11)
C        FIND OUT IF THERE ARE GOING TO BE ANY SCALING
C        PROBLEMS WHEN SYMVU GETS THE FILE.
         IF(DROPHI.EQ.0.0)GO TO 771
         IF(( DROPHI+DROPLO)/DROPHI.GT.2/3) PRINT (6,778)
771      CONTINUE
778      FORMAT (20X,'************** W A R N I N G **************'/
        +//,5X,'YOU HAVE A SCALING PROBLEM   YOUR SYMVU PLOT MAY'/
        +,5X,'LOOK FLAT.   YOU HAVE EITHER A VERY HIGH (HIGHEST '/
        +,5X,'VALUE) OR A VERY LOW (LOWEST VALUE), ↑SEE ABOVE↑.'/
        +,5X,'IF YOUR WHOLE DATA IS NOT EVENLY SPREAD BETWEEN THEM,'/
        +,5X,'DURING SCALING THE VARIATION IN THE SURFACE MAY BE'/
        +,5X,'LOST.'/
        +,5X,'THIS MAY BE OVERCOME BY CAREFUL SELECTION OF THE '/
        +,5X,'APPROPRIATE SYMVU ELECTIVES - SEE MANUAL- , OR '/
        +,5X,'YOU MAY HAVE TO OPERATE ON YOUR MATRIX.  TO DO THIS'/
        +,5X,'--FIRST EXAMINE IT, BY LOOKING AT THE TAPE8 PRODUCED'/
        +,5X,'BY THIS PROGRAM, WITH PROGRAM GRID IN THIS LIBRARY'/
```

```
+,5X,'-SEE DOCUMENTATION-. THIS WILL SHOW YOU THE LOCATION'/
+,5X,'OF THE TROUBLE. WITH THIS KNOWLEDGE YOU CAN START TO'/
+,5X,'PRUNE OUT THE OFFENDING READINGS.  GET HELP DOING THIS '/
+//,5X,'*************************************************')
 STOP
 END
```

```
      PROGRAM GRID  (TAPE5,PARM,OUTPUT,
-TAPE6=OUTPUT)
C
C         PROGRAM WRITTEN BY F.W.M.HOPPER 1978.
C
C     ----------------------------------------------------
C
C
C     THE PROGRAM IS WRITTEN SO THAT A PARAMETER SUPPLIED
C     IN THE CALL TO THE PROGRAM MAY BE USED IN THE PROGRAM.
C     THIS PARAMETER (PARM) ENABLES LABELING OF THE CONTOURS
C     TO BE TURNED OFF.
C     THE DEFAULT IS FOR LABELS TO BE PRINTED.
C     THE WORD †LABEL† USED AS SHOWN BELOW ALSO PRODUCES
C     LABELS
C     THE WORD †NOLABEL† STOPS LABELS APPEARING.
C
C     THE PROGRAM SHOULD BE CALLED WITH LIB6000,ID=LIBBED
C     ATTACHED, IF LABELS ARE TO BE TURNED OFF.
C     THE PROGRAM CALL SHOULD HAVE AS ITS SECOND PARAMETER
C     (IF INPUT IS SUBSTITUTED, OTHERWISE THE ONLY PARAMETER.)
C     ONE OF THESE WORDS. EG O-
C     GRID(NOLABEL)
C     ANY UNKNOWN PARAMETER WILL DEFAULT TO PRODUCTION OF LABELS.
C
C
C     THE PROGRAM TAKES A MATRIX ARRAY FROM OUR FILLIN
C     OR SYMAP AND CONTOURS IT . THIS REPLACES TRADITIONAL
C     SYMAP OUTPUT (LINE PRINTED) .
C     THE OUTPUT MUST RELATE TO THE USERS ORIGINAL CO-ORDINATES
C     THUS ※※ O-
C
C     IF THE GRID WAS CONSTRUCTED O-
C     Y
C     I
C     I
C     I
C     I   A
C     I----------------X          THE GEOGRAPHIC WAY .
C
C        WHERE A IS A VALUE AT REF X,Y
C
C
C     THEN IT MUST BE TRANSLATED BY ALTERING THE  X,Y ASSIGNMENTS
C     WITHOUT ALTERING THE POSITION OF THE DATA.
C     THIS CAN BEST BE DONE BY WRITEING OUT THE MATRIX ,THEN
C     READING IT IN AGAIN.
C     MA=THE MATRIX
C     XM=MAX X VALUE
C     YM=MAX Y VALUE
C              DO 1 I=1,YM
C              IK=YM+1-I
C              WRITE(8)  (MA(IK,J),J=1,XM)
C         1    CONTINUE
C              REWIND 8
C              DO 2 I=1,YM
C              READ(8)  (MA(I,J),J=1,XM)
C         2    CONTINUE
C              NDX=YM
C              NDY=XM
C
C     MA=THE NEW MATRIX WHICH IS THUSO-
C
```

```
C
C
C            _____NDY (XM)
C
C        I
C        I
C        I
C        I
C        I
C        I
C        I    A
C        NDX(YM)       THE WAY SYMAP WANTS IT   (NOTE.. THE ACTUAL -
C        - POSITION OF THE DATA IN THE MATRIX HAS NOT MOVED AT ALL,
C        WHAT WAS IN THE BOTTOM LEFT CORNER IS STILL THERE
C        WE ARE JUST CALLING THE BOTTOM LEFT CORNER SOMETHING
C        DIFFERENT NOW . IE. THE VALUE A IS NOW AT NDX,NDY.
C        THESE TRANSPOSITIONS SHOULD BE DONE AS A SEPARATE
C        PROGRAM AND THE OUTPUT PASSED TO MY PROGRAM
C        WITH THE ADDITIONAL INFORMATION AS SPECIFIED BELOW.
C
C
C        _____
C        IN THE PROGRAM, O-
C        THE FIRST WORD READ (NDX)
C        IS   -NUMBER OF ROWS IN THE GRID
C        THE SECOND  O-   (NDY)
C        IS  -NUMBER OF COLUMNS IN THE GRID
C        THE THIRD   O-    (NDC)
C        IS   -SCALING HOW MANY ROWS IN EACH UNIT
C        THE FOURTH  O-   (NDD)
C        IS   -SCALING HOW MANY COLUMNS IN EACH UNIT
C
C
C        ND IS THE ARRAY TO BE PLOTTED IN THE SYMAP
C        FORM AS DESCRIBED ABOVE.
C
C        THE PROGRAM IS WRITTEN TO UTILISE THE ULCC. DIMFILM ROUTINES.
C
C        _____
         REAL ND(200,200)
         INTEGER FNAME
         REAL NDC,NDD,NDA,NDB
C        READ IN FIRST CARD OF CONTROL INFO.
C
C
         REWIND 5
         WRITE(6,133)
133      FORMAT(5X, '*************************************************',/////,
        +5X,'       --- PROGRAM GRID ---         ',/////,
        +5X, '*************************************************',)
         READ(5) NDX,NDY,NDC,NDD
C        WORK OUT SCALING FOR 'BOX' SIZE
C
C
         NDA=NDX/NDC
         NDB=NDY/NDD
C        CALL THE PLOTTING SUBROUTINE
C
C
         CALL CCCC(ND,NDX,NDY,NDA,NDB)
         REWIND 5
         STOP
         END
C
C
         SUBROUTINE CCCC  (ND,NDX,NDY,NDA,NDB)
```

```
C          THIS ROUTINE ACTUALLY DOES THE PLOTTING.
C
C
           INTEGER ICVALS(18) , FNAME
C          SET UP
C
C
           REAL ND(NDY,NDX) ,CVALS(18) ,MIN,MAX
           REAL NDA,NDB,NDC,NDD
           COMMON/DIMCONS/A(18)
           DATA ICVALS/5,7,9,11,13,15,17,19,21,22,23,24,25,26,27,28,29,30/
           NDX1=NDX
           NDY1=NDY
           NTP=0
C          READ IN MATRIX ND  CHECK FOR ERRORS INFORM IF ANY.
C          NDX1= THE NUMBER OF COLUMNS IN THE MATRIX TO BE CREATED, AND THE
C          NUMBER OF LINES IN THE MATRIX BEING READ IN.
C          NDY1= THE NUMBER OF LINES IN THE MATRIX TO BE CREATED, AND THE
C          NUMBER OF COLUMNS IN THE MATRIX BEING READ IN.
C
C
           DO 13 JJ=1,NDX1
           J=NDX1+1-JJ
           READ(5)  (ND(I,J),I=1,NDY1)
           IF(EOF(5).NE.0)GO TO 50
 13        NTP=NTP+1
           GO TO 100
 50        WRITE(6,55) NDX1,NDY1,NTP
   55      FORMAT('0*** ERROR ***',/,'  MATRIX DIMENSIONS FROM FILE HEADER WERE
          + ',I5,' LINES BY ',I4,' COLUMNS O ',/,'  END-OF-FILE ENCOUNTERED AF
          +TER READ OF LINE ',I4,/,'*** ERROR ***',/)
           GO TO 56
 100       READ(5)
           IF(EOF(5).NE.0)GO TO 150
           WRITE(6,58) NDX1,NDY1
   58      FORMAT('0*** WARNING ***',/,'   MATRIX SIZE FROM FILE HEADER WAS ',
          +I4,' LINES BY ',I4,' COLUMNS O ',/,'   BUT MORE DATA THAN THIS EX
          +ISTS ON YOUR INPUT FILE. CONTOUR MAP IS THEREFORE BASED ON ONLY P
          +ART OF YOUR INFORMATION',/,' *** WARNING ***',/)
 56        RETURN
 150       CONTINUE
C          FIND OUT THE MAX AND MIN VALUES OF THE DATA
C
C
           MIN=MAX=ND(1,1)
           DO 10 I=1,NDY1
           DO 10 J=1,NDX1
           IF(MIN.GT.ND(I,J)) MIN=ND(I,J)
           IF(MAX.LT.ND(I,J)) MAX=ND(I,J)
 10        CONTINUE
C          FIND OUT THE RANGE THE DATA COVERS
C
C
           RANGE=MAX-MIN
C          DIVIDE THE RANGE INTO 17 STEPS
C
C
           STEP=RANGE/17.0
C          ASSIGN TO CVALS EACH OF THE STEPPED CONTOUR VALUES
C          FOR THE COMPLETE RANGE CONTOURING WILL OCCUR AT
C          THESE VALUES.
C
C
           CVALS(1)=MIN
```

```
        DO 12 I=2,18
        CVALS(I) = CVALS(I-1) + STEP
12      CONTINUE
C       START THE DIMFILM PROCESS AND ACTUALLY PLOT THE THING.
C
C
        CALL CAM35MM
        A(1)=1.0
        A(2)=0.0
        IF(NDA.GT.NDB) CALL CINE
        CALL BOUNDS(0.0,NDB,0.0,NDA)
        CALL CHECK(-2)
        CALL MARGIN(0.0)
        CALL WINDOW(0.0,NDB,0.0,NDA)
        CALL WINDFRM
        CALL CINTERP(10)
        IPAR = FNAME(4LPARM)
        IF(IPAR.EQ.4LPARM.OR.IPAR.EQ.5LLABEL) GO TO 1000
        IF(IPAR.EQ.7LNOLABEL)GO TO 1001
        CALL REMARK('*** UNRECOGNISED PARAMETER ***')
        CALL REMARK(IPAR)
        GO TO 1000
1001    CALL NOCLAB
1000    CONTINUE
        CALL CONTR1(ND,NDY,NDX,18,CVALS,ICVALS)
        CALL ENDWIND
        CALL ENDFILM
        RETURN
        END
C       SUBROUTINE CALCMP(X,Y,I,J)
C       DATA NFRAM/0/
C       IF(J.LT.0)GO TO 1
C       IF(J.EQ.2)NFRAM=NFRAM+1
C       RETURN
C1      IF(J.EQ.-2)  I=NFRAM
C       X=Y=0.0
C       ENTRY STARTF
C       ENTRY FINISHF
C       RETURN
C       END
```

THE STRUCTURAL AND METAMORPHIC DEVELOPMENT

OF THE BERGEN ARC/BERGSDALEN FORELAND

GNEISSES OF OSTERØY, S.W. NORWAY

by

Frederick William Metcalfe HOPPER

VOLUME 2

Thesis submitted for the Degree of

Doctor of Philosophy

Bedford College (University of London)   February 1980

CONTENTS

VOLUME 2

Plate 1

NORTHERN GNEISSES

D "Early", S "Early" and its accompanying banding. Note
how it is sheared and crosscut by two younger, sub-
horizontal pegmatitic veins.

Plate 2

NORTHERN GNEISSES
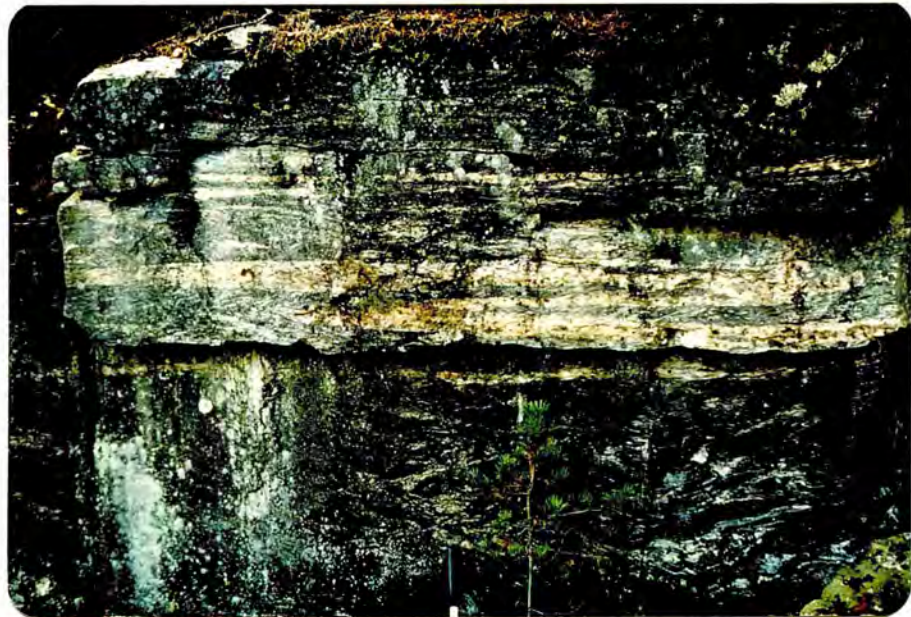
D1, tight intrafolial F1 isoclines. Usually the limbs of
these folds cannot be seen as they are sheared out. In
this case the exposure is formed from M shaped parasitic
folds in a larger nose region.

Plate 3

NORTHERN GNEISSES

D1, an early D1 pegmatitic vein which crosscuts the composite layering at a high angle yet is slightly folded by later D1 deformation.

Plate 4

NORTHERN GNEISSES

D1, S "Early" folded by an F1 fold. Note that by the hand a zone of shear has developed in limb of a small paracitic fold. An early D1 pegmatite occupies this zone of displacement. The larger veins are younger still.

Plate 5

NORTHERN GNEISSES

Post D1 veins which crosscut the main composite foliation
at a high angle and are then folded in D2. Note it is
crosscut by a younger vein running sub parallel to the
foliation.

Plate 6

NORTHERN GNEISSES
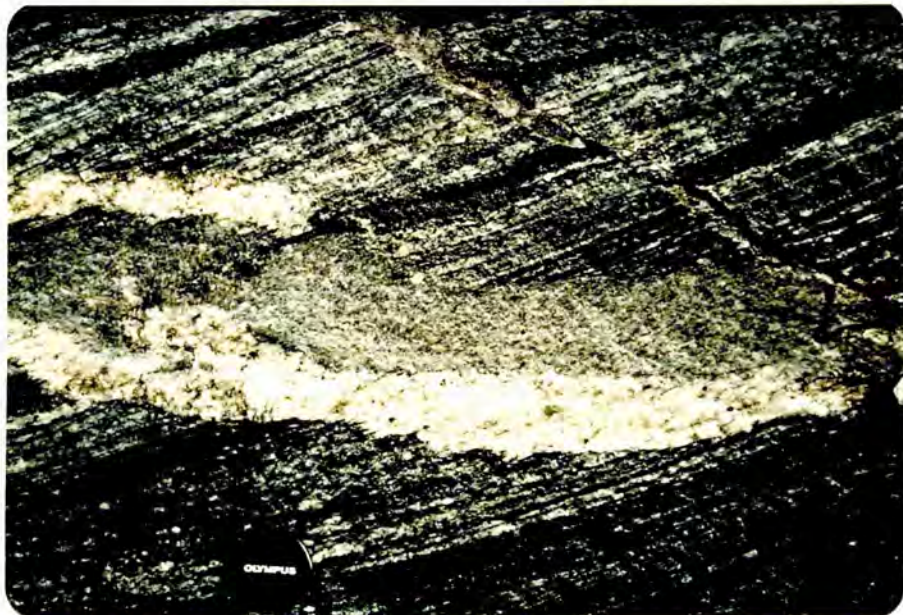
Two generations of post D1 and pre D2 veining. Note they
crosscut the earlier composite foliation yet display a
younger schistosity (S3) internally, indicating subsequent
deformation. They are also garnetiferous.

Plate 7

NORTHERN GNEISSES
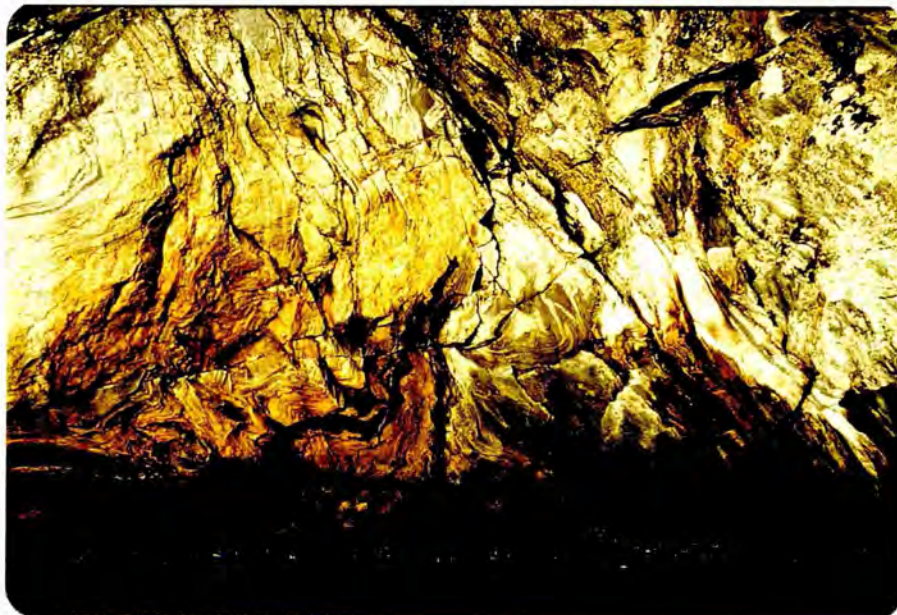
D2, F1 isoclines and D1 basic bodies folded round the nose of a relatively open F2 fold.

Plate 8

NORTHERN GNEISSES

D2, A quartzite exposure showing S2 folded round in an F2 fold with the start of a very weak axial planar schistosity (S3) developing. Note that the F2 folds are tighter in this exposure than in plate 7. The obvious fold is 1.5 metres high.

Plate 9

NORTHERN GNEISSES

D2, L2 exposed on an S1 foliation plane, outcrop 1.5 metres long.

Plate 10

NORTHERN GNEISSES

D2, F1 folds refolded in an F2 nose. Note axial planar pegmatitic vein in the F2 fold and the fact that these folds are tighter than in plates 7 or 8.

Plate 11

NORTHERN   GNEISSES

D2, Close up of a refolded F1 fold from plate 10. Note
the new schistosity (S3) running parallel to the late
axial plane pegmatitic vein which crosscuts the F1 fold
and the typical "limb region" pegmatitic veins either
side of the F1 closure.

Plate 12

NORTHERN   GNEISSES

D2, a large F2 closure folding S1 and S2 and a set of cross-
cutting pegmatites which intersect the composite foliation
at a low angle. These pegmatites are attributed to the pre
D2 migmatitic episode.

Plate 13

NORTHERN GNEISSES

D2, late D2 pegmatitic vein cutting a paracitic F2 fold and the composite foliation it deforms, at a high angle. Note this vein is itself slightly folded in the D2 flattening.

Plate 14

NORTHERN GNEISSES
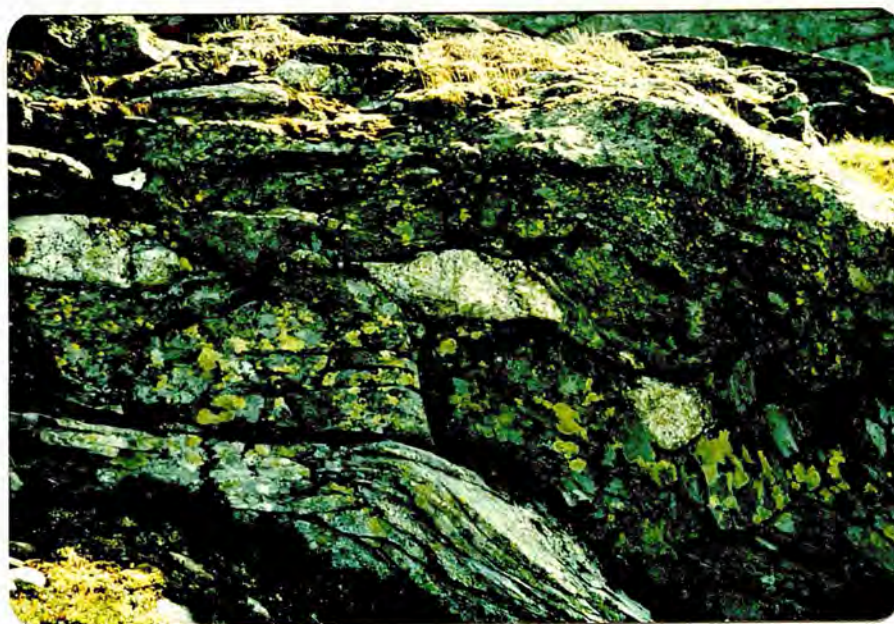
D2-D3, a post F2 amphibolite cut by a late pegmatite which has boudinaged in D2b and is subsequently folded by F3.

Plate 15

NORTHERN GNEISSES

D3, a large scale, open F3 fold affecting S3b from the highest
ground on Osterøy. These folds are the only large scale folds
visible in the Northern Gneisses.

Plate 16

NORTHERN GNEISSES

D3, Open F3 folds producing a strong large scale mullion
rodding, L3. The regularity of L3 proves the cylindrical
nature of the folds in this area.

Plate 17

NORTHERN
GNEISSES

D3, A profile view of F3, showing the open geometry which is typical over most of Osterøy. Note these folds are only seen where S3b is well developed.

Plate 18

NORTHERN   GNEISSES

D4, A shear zone formed in the middle limb of an F4 fold, in which the new S5 schistosity is well developed.
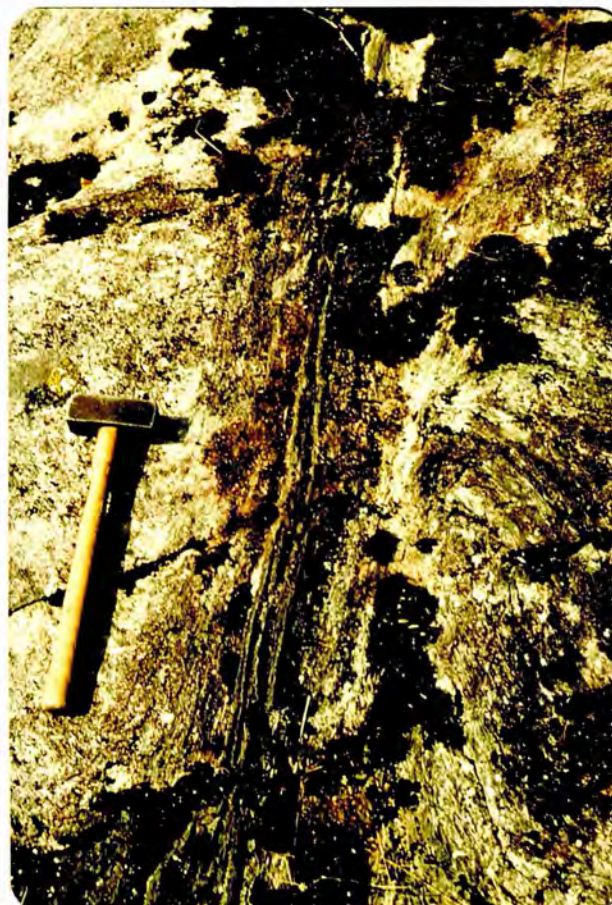
Plate 19

NORTHERN
  GNEISSES

D4, A large scale example of a D4 shear zone from the north of
the island. Note how the layering is contorted on entering
the zone yet regular in the middle, only now vertical rather
than horizontal.

Plate 20

NORTHERN   GNEISSES

D4, Profile view of a D4 shear
zone, demonstrating how they
form in the middle limbs of
poorly developed F4 folds.

Plate 21

NORTHERN GNEISSES

A D4 quartz vein in a D4 shear zone. The quartz veins are sub-axial planar to the F4 folds.

Plate 22

NORTHERN GNEISSES
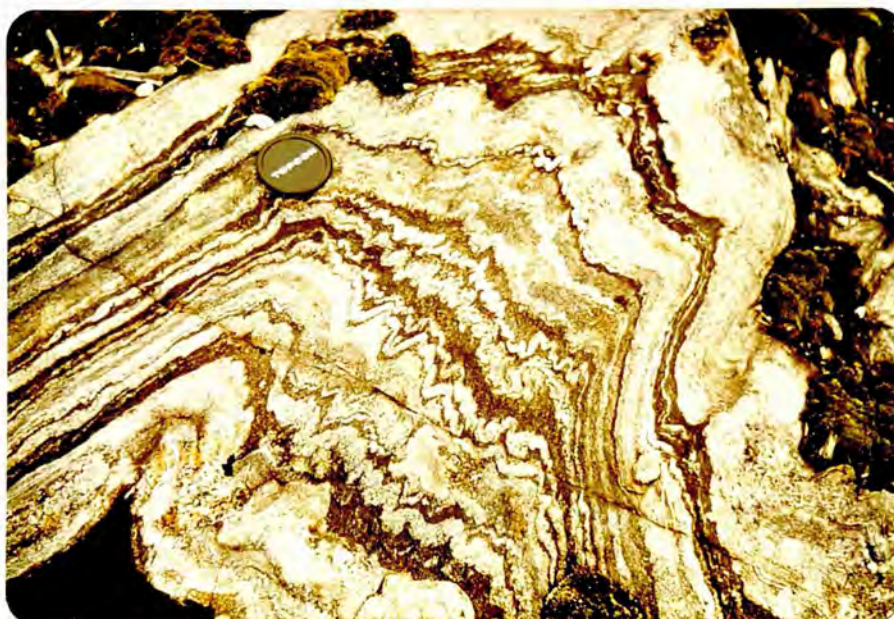
D4, Nose region of an F4 fold. Note that the wavelength of the paracitic folds varies with the thickness of the layer folded and that the folds in one layer do not force a fold in the next layer provided there is a separation of one fold wavelength between the layers.

Plate 23

SOUTHERN
GNEISSES
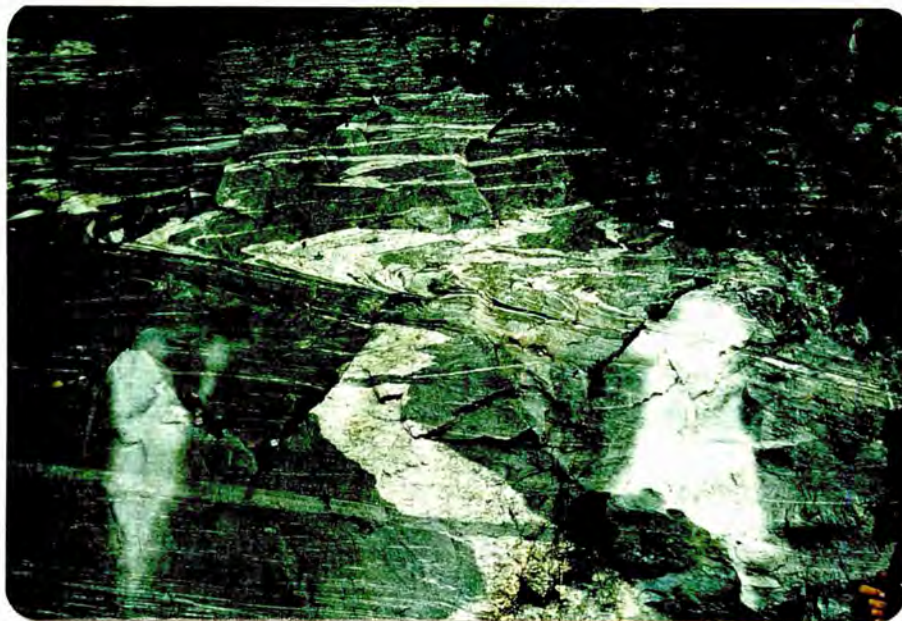
D "Early", Dl & D2, An Fl fold folding S "Early". This is
then crosscut by a pegmatitic vein which is then folded by F2.
Note the F2 fold has a sheared limb which started as one limb
of the Fl fold. The shear zone is a band of secondary mylonite.
Note also that there is a secondary trondhjemite vein intruded
horizontally, crosscutting the S2 schistosity.

Plate 24

SOUTHERN
GNEISSES

D "Early" & Dl, the general shape of an Fl fold folding S "early"
showing a thinned limb & a pegmatitic vein which crosscuts
S "Early" at a shallow angle (The leucocratic layers defining
S "Early" may also once have been intrusive veins, some of these
are now boudins and the whole texture of the gneiss in the Fl
limbs is mylonitic).

Plate 25

SOUTHERN
GNEISSES

D "Early" -D1, S "Early" folded round an F1 fold. Note the fold
is crosscut by an axial planar pegmatitic vein and that S "Early"
itself contains pegmatitic veins, some of which are boudinaged.
There is also a small F3 fold represented in the top right corner
and the rocks are generally mylonitic, the mylonite produced
during D1.

Plate 26

SOUTHERN
GNEISSES

D1, Intrafolial, isoclinal F1 folds just depicted by subtle
changes in the composition of S "Early". Note the spindle shape
of the quartz grains on the weathered surface. These are the
product of S2 crosscutting the rodded shape fabric L1 produced
by the interaction of D1 with S "Early". This rock is a blasto-
mylonite.

Plate 27

SOUTHERN GNEISSES
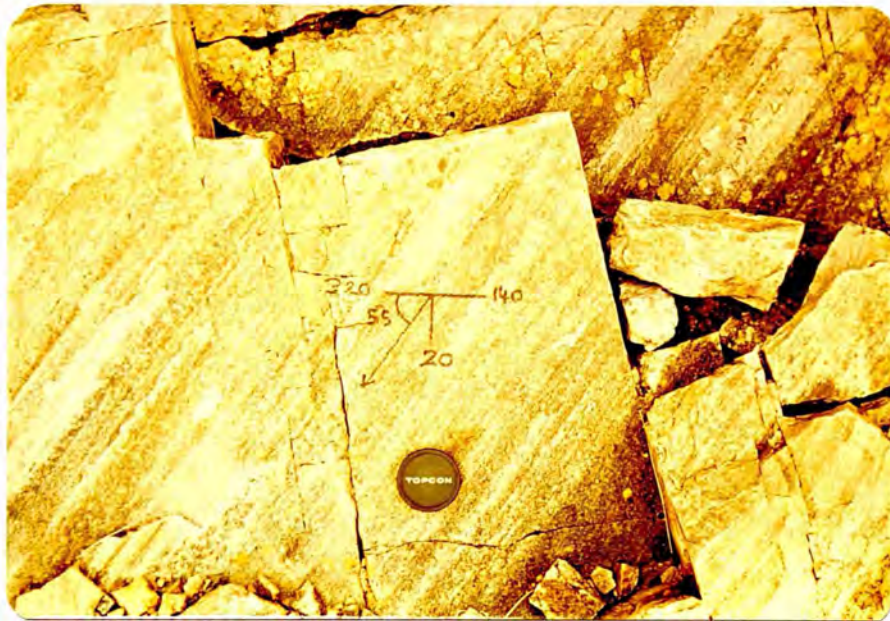
D1, The L1 lineation as exposed on planes of S1 schistosity.

Plate 28

SOUTHERN GNEISSES

D1, K-feldspar porphyroclasts in the gneisses. Seen in three
dimensions it can be seen that these define an L tectonite
rodding structure, the expression of an extreme prolate strain
ellipsoid. The lineation this defines is L1.

Plate 29

SOUTHERN
    GNEISSES
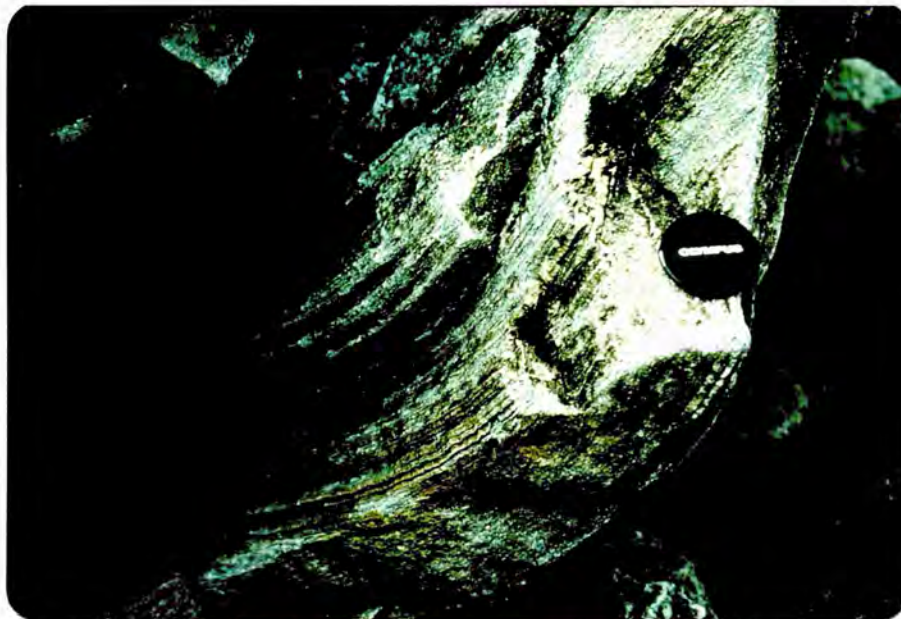
D1-D3, The L1 lineation, here refolded by an F3 fold, is seen
to be a mullion structure as well as a shape fabric, plates
27 & 28.

Plate 30

SOUTHERN GNEISSES

D1-D2, Dissociated F1 fold noses
shredded into an amphibolite by
the D2 shearing. The leucocratic
portion formed strings and veins
in the amphibolite prior to F1.
Note: compare this plate with that
of a similar mylonite described by
Higgins 1971.
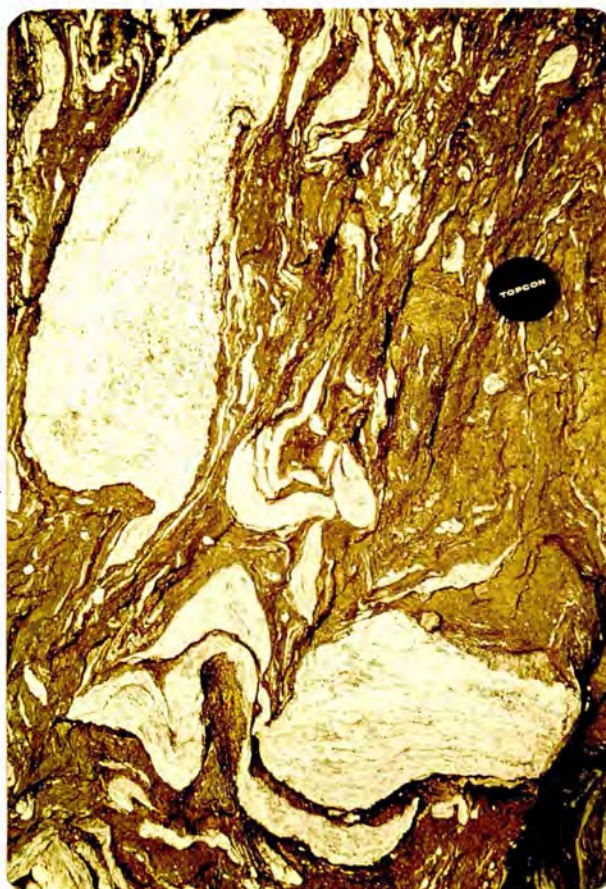
Plate 31

SOUTHERN GNEISSES

D1-D3, Type 3 interference pattern (Ramsay 1967), produced by
the interplay of F1 refolded by F3.

Plate 32

SOUTHERN GNEISSES

D3, A fine scale banding between amphibolitic and quartzo-
feldspathic material displaying highly non-cylindrical F3
folds very well. Note the axial directions vary by as much
as 120° over 10 cm. distances along the hinges.

Plate 33

SOUTHERN   GNEISSES

D3, An S1 foliation plane folded by F3, showing the non-cylindrical nature of these folds, the relationship of the paracitic folds to the main fold and to each other.

Plate 34

SOUTHERN   GNEISSES

D3, The truncated nose of a non-cylindrical F3 fold which could be misinterpreted as a Type 1 interference pattern (Ramsay 1967). Note L1 running from top right to bottom left, is folded round the nose.

Plate 35

SOUTHERN GNEISSES
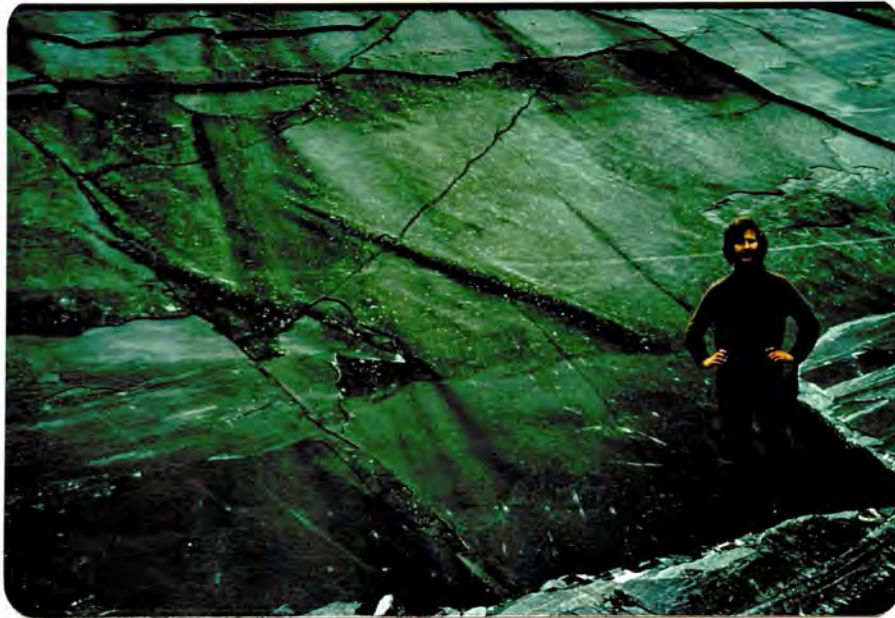
D3, A broad S1/S2 foliation plane on which small F3 buckles are seen in an enechelon pattern. Note that each fold is nucleating quite separately, spaced out in the layer, and that all the folds are non-cylindrical.

Plate 36

SOUTHERN GNEISSES
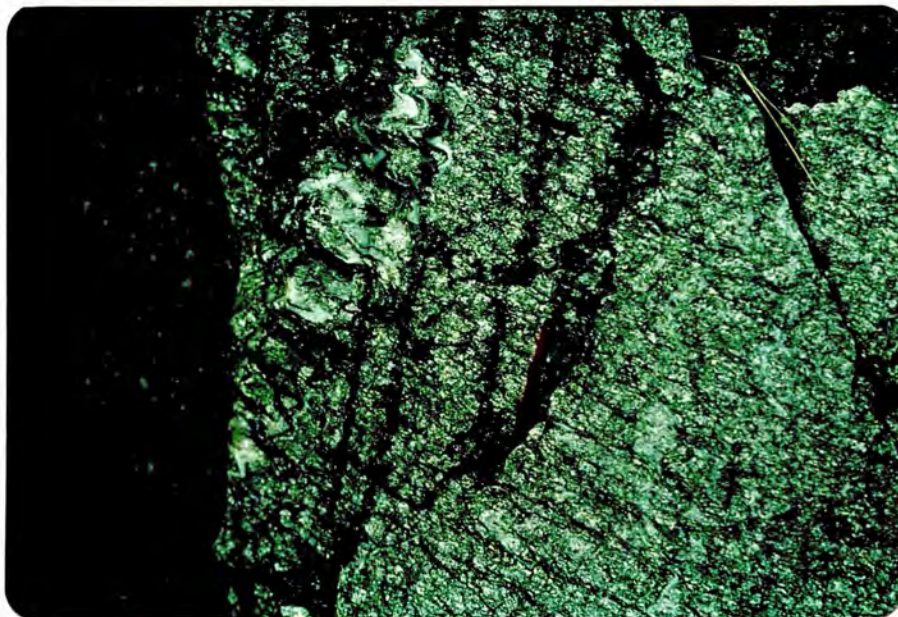
D3, The S3 crenulation cleavage developed in a mica schist, the only lithology in which it is seen. This is axial planar to the F3 folds and its outcrop on the S1/S2 foliation planes in the noses of the F3 folds defines L3.

Plate 37

SOUTHERN GNEISSES

D3, Hydraulic fracture network filled with calcite. It is
developed in a D1 mylonite band with an excellent F1 fold
nose exposed in the middle.

Plate 38

SOUTHERN GNEISSES
AND BERGEN ARCS

D4, A view across the Northern part of the Bergen Arcs from
Osterøy showing the large scale broad synformal F4 fold, which
affects the dominant foliation planes as seen from the dip
slopes of the distant hills.

Plate 39

NORHTERN   GNEISSES
& SOUTHERN   GNEISSES

D5, A view showing the scale and importance of the late jointing
affecting the North Osterøy gneisses.

Plate 40

SOUTHERN   GNEISSES

D5, A North-South joint, showing the mineralisation developed
along these structures. Note the calcite veins, general epi-
dotization and sharp planar walls. It is their alteration
that causes them to weather out as such marked gullies.

Plate 41

NORTHERN   GNEISSES
& SOUTHERN   GNEISSES

A view from the slopes of Hogafjell south across the Northern
and Southern Gneisses, showing the best and most obvious
exposure of the Tysse thrust, the contact between them.

Plate 42

Least deformed specimen in a sequence (Pl.42-45) of mylonitized
augen gneiss showing reduction in porphyroclast size with
increasing deformation.

Plate 43

Second specimen in the (Pl42-45) sequence of mylonitized augen gneiss.

Plate 44

Third specimen in the (Pl.42-45) sequence of mylonitized augen gneiss.

Plate 45
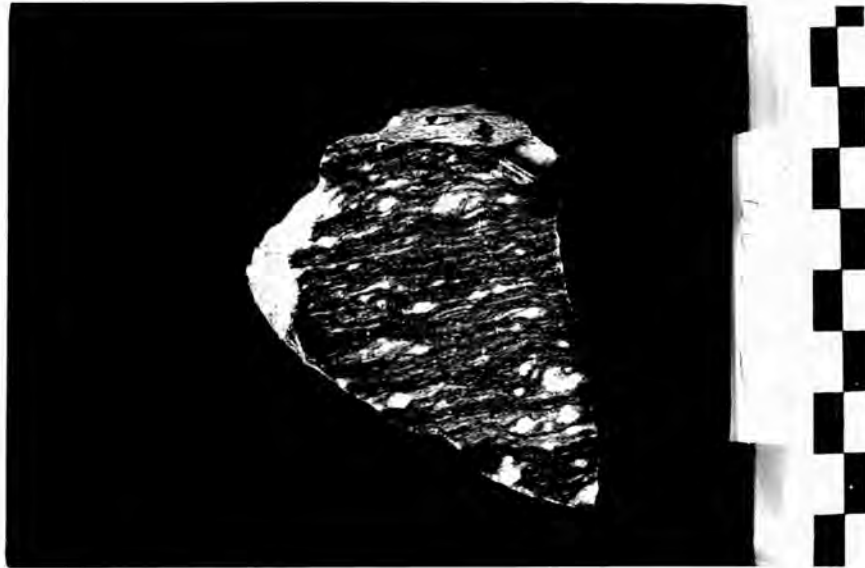
Most deformed specimen in the sequence (Pl.42-45) mylonitized augen gneiss showing reduction in porphyroclast size with increasing deformation.

Plate 46   x 10
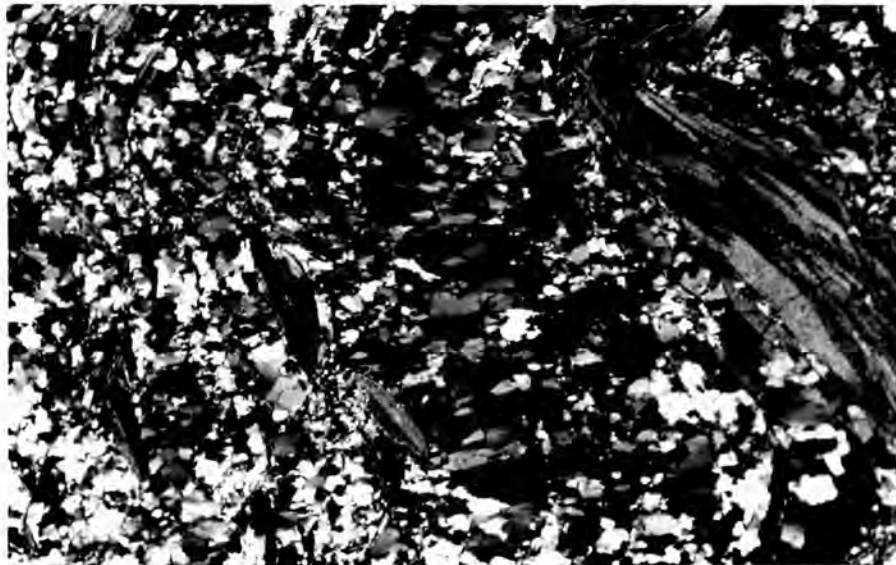
Quartz laths or deformation lamellae subgrains which define a new axial plane schistosity to the folds in the mica layers.

Plate 47   x 10
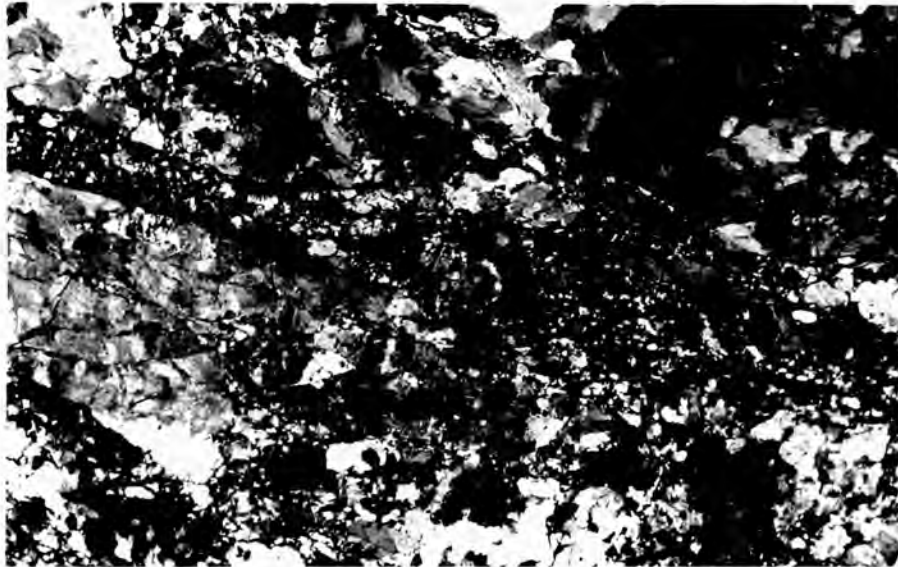
Hydraulic fractures filled with rock flour produced during the
escape of the fluid phase. <u>Note</u> angular fragments of rock and
crystals set in an isotropic matrix; and sharp sides to the
bands of mylonitic material.

Plate 48   x 10
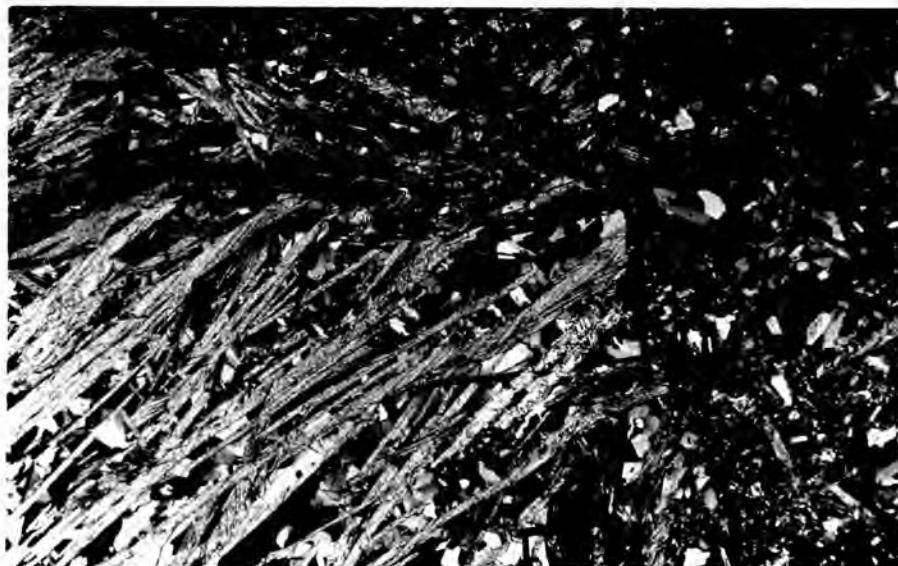
Fragments of rock in a breccia cut through by calcite veins,
formed by hydraulic fracture, set in a matrix of hydraulic
cataclasite with a vast range of fragment size.

Plate 49   x 10
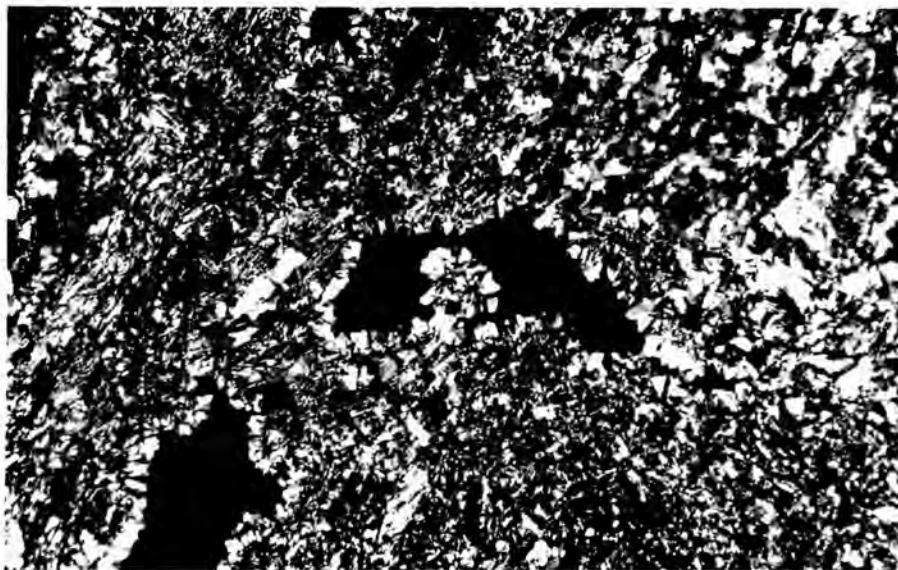
Part of a late breccia zone from a joint. Note the voids rimmed
by radially grown drusy mosaics of quartz crystals. The presence
of the voids in the rock indicates the pp. H_2O exceeded or equal-
led the load pressure.

Plate 50   x 10
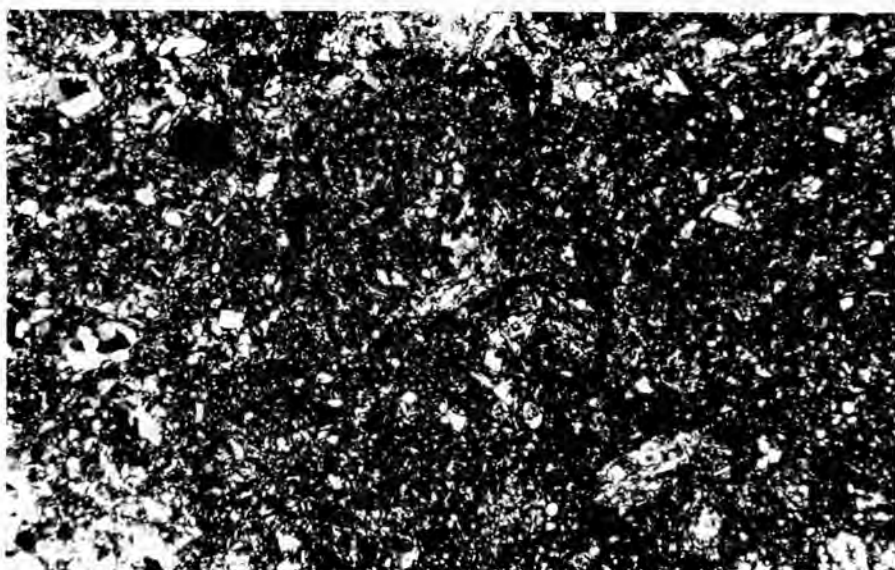
A hydraulic cataclasite, note that there is no foliation while
the rock is annealed, with angular crystal and rock fragments set
in an isotropic dusty matrix.

Plate 51   x 23
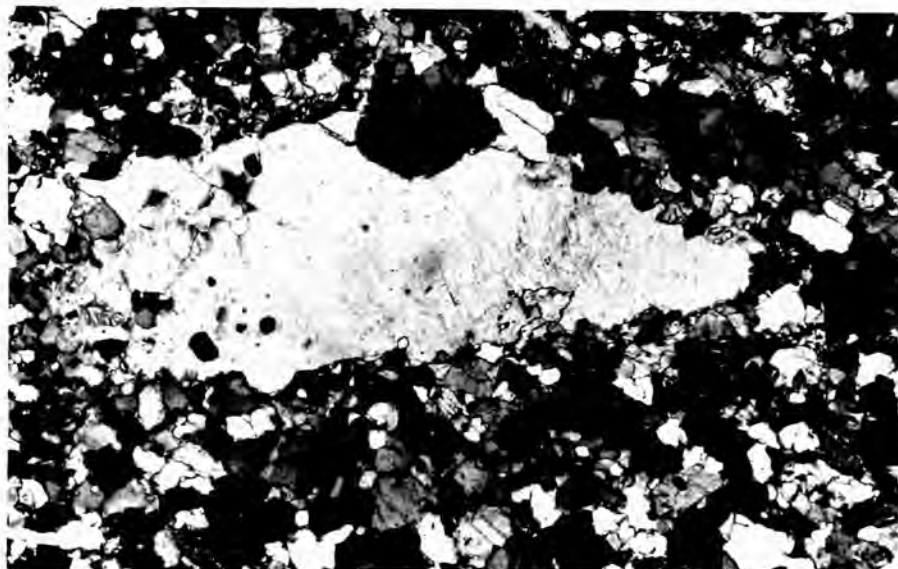
A good example of a K-feldspar overgrowing its surrounding matrix
in an "amoeboid" manner. The poikilolitic margins of the porphyro-
blast prove secondary growth of the K-feldspar. The feldspar is
not perthitic indicating it developed late in the metamorphism.

Plate 52   x 10
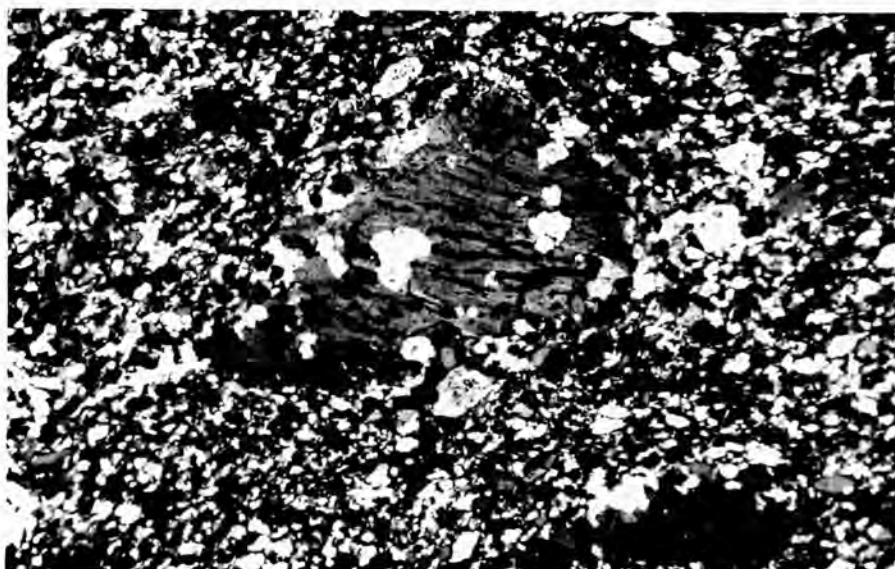
A braid perthite with poikilolitic inclusions of quartz, proving
that this K-feldspar is a secondary feature in the rock, which
crystallised over pre-existing matrix minerals.

Plate 53   x 23
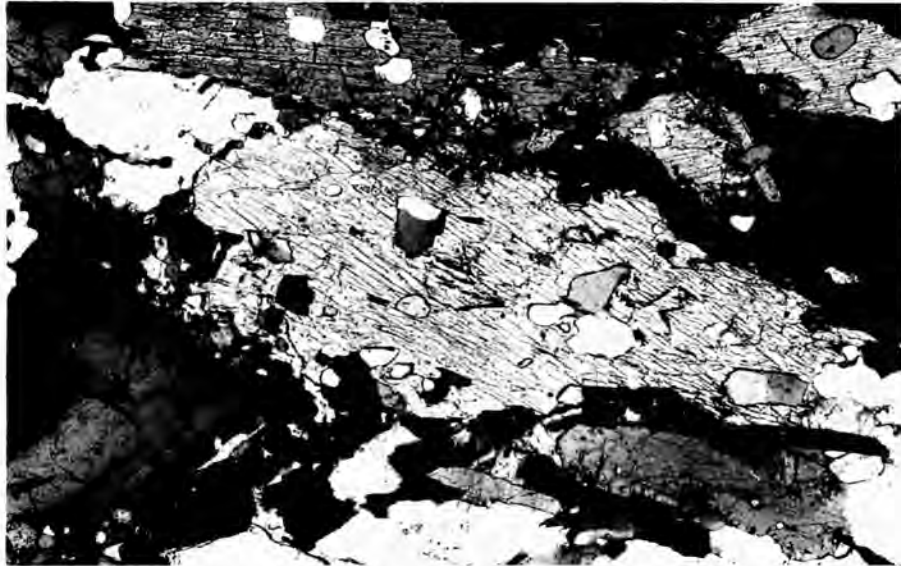
A poikilolitic hornblende crystal; the inclusions of quartz and
sphene are not portions of a single crystal and the hornblende
must therefore replace a pre-existent mineralogy which was finer
grained than that presently seen.

Plate 54   x 10
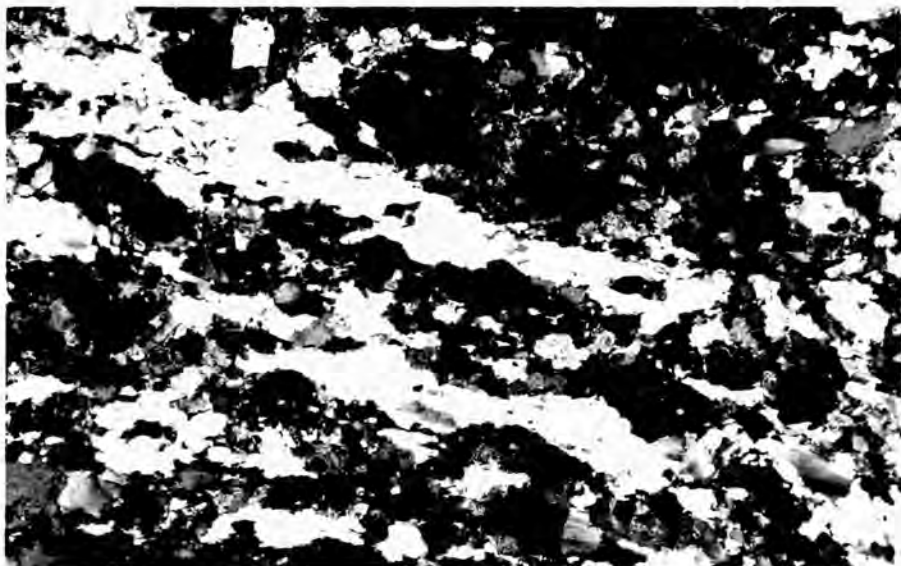
Quartz segregation ribbons with secondary (D4) deformation lamellae
at an angle to them. Note the ribbons lie sub-parallel to the
foliation and have sharp margins which cut across matrix crystals -
they are therefore a secondary development.

Plate 55   x 10

A zoned garnet containing inclusions of quartz and graphite. A
large distorted knot of graphite shows where pressure solution
(of matrix) has occurred as the schistosity was flattened round
the garnet.

Plate 56   x 10
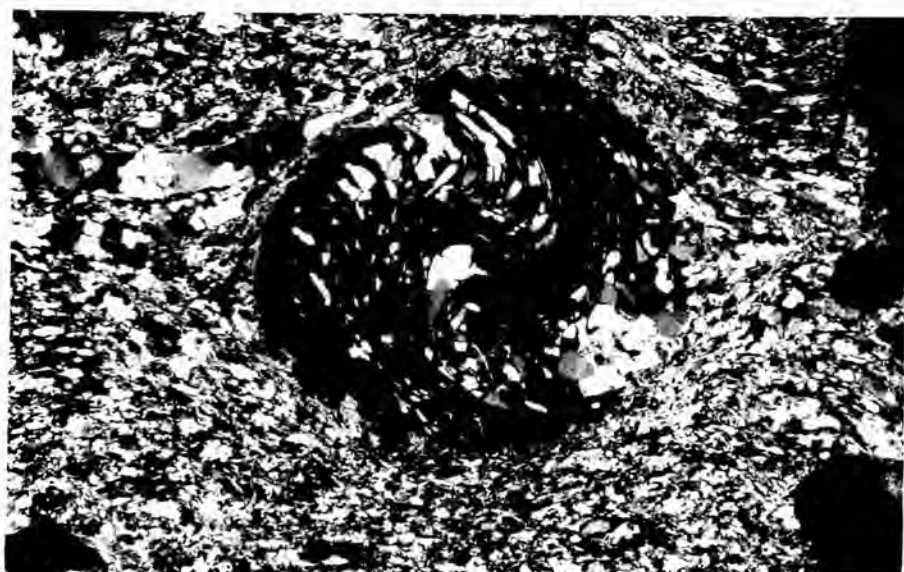
A rotated garnet crystal, enveloped by matrix with a strong later
schistosity.

Plate 57   x 23

Undulose extinction in a plagioclase crystal. Note the slight
bending of the twin lamellae.

Plate 58   x 10
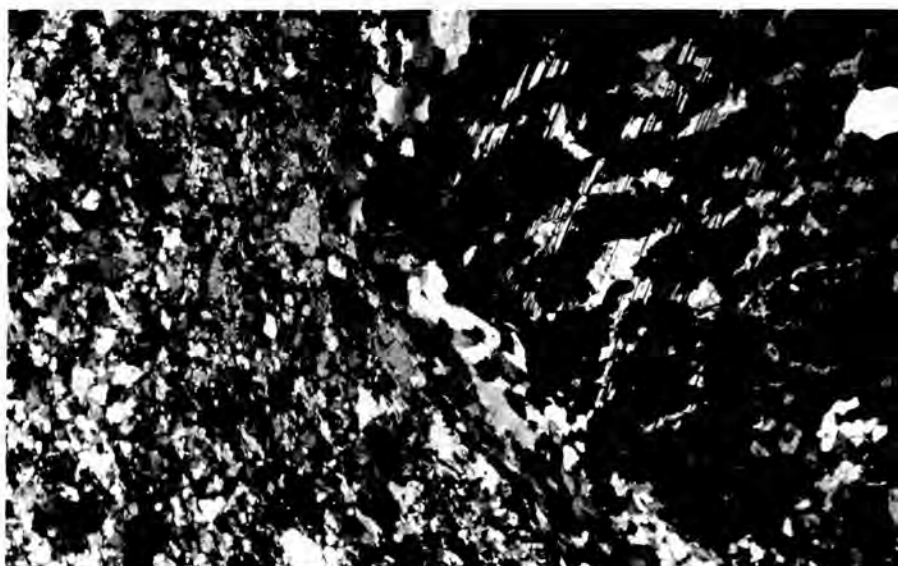
A microcline porphyroclast with a rim of coarser crystalline matrix
in its pressure shadow.   Note the patch perthite texture.

Plate 59   x 10
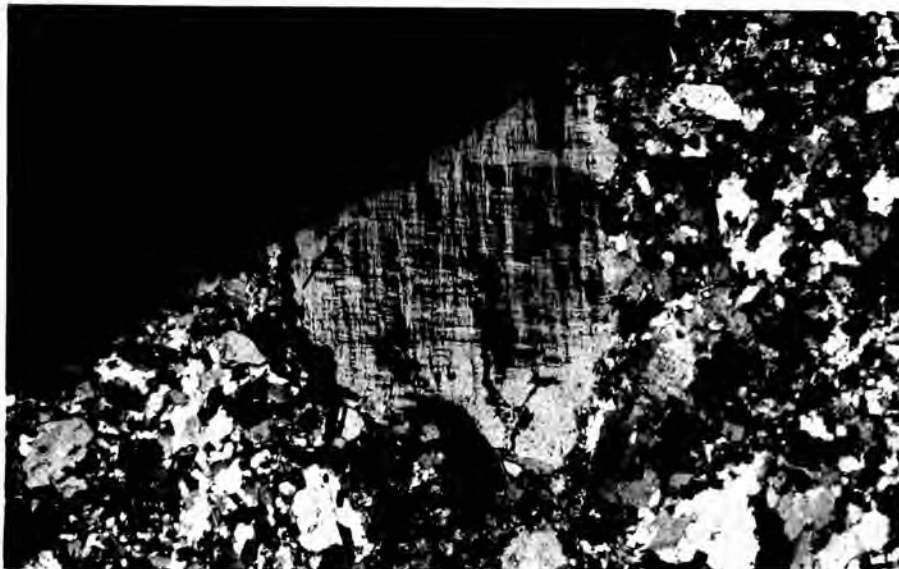
Microperthitic microcline. The fact that this microcline is not
coarsely perthitic is taken to indicate that it grew later in
the metamorphism than those which are.

Plate 60   x 93

In the bottom of the plate relict biotite crystals are seen over-
grown by the leucocratic minerals; this area forms the margin of
a small "tectonic pip." The top portion of the plate shows later
recrystallised biotites which overgrow the leucocratic matrix.

Plate 61　x 23
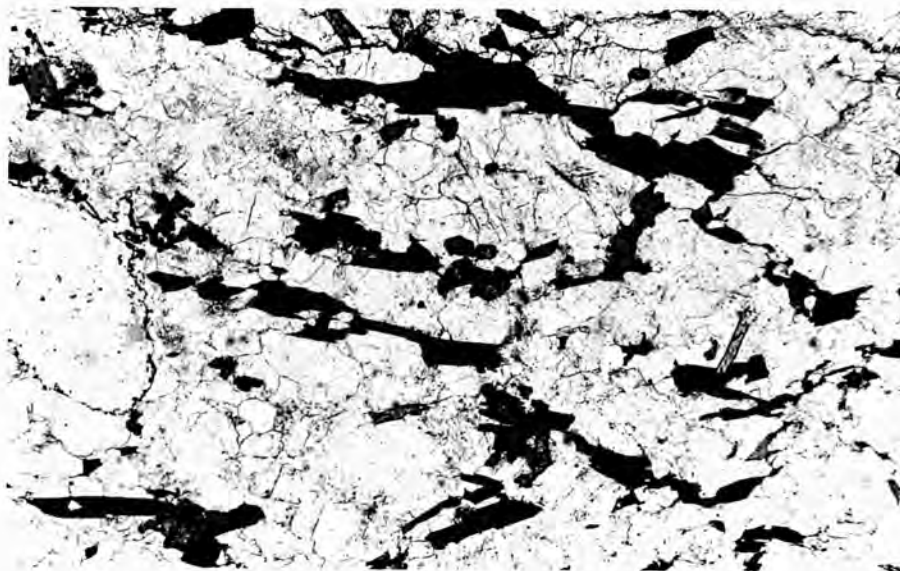
Embayed biotite - biotite cut, overgrown and embayed by the
leucocratic portions of the rock, leaving interstitial relics
of the biotite.

Plate 62　x 10

Epitaxy - rimming of allenite by clinozoicite and epidote.　In
proximity to the metamict allenite the epitaxial epidotes are
also metamict.

Plate 63   x 93
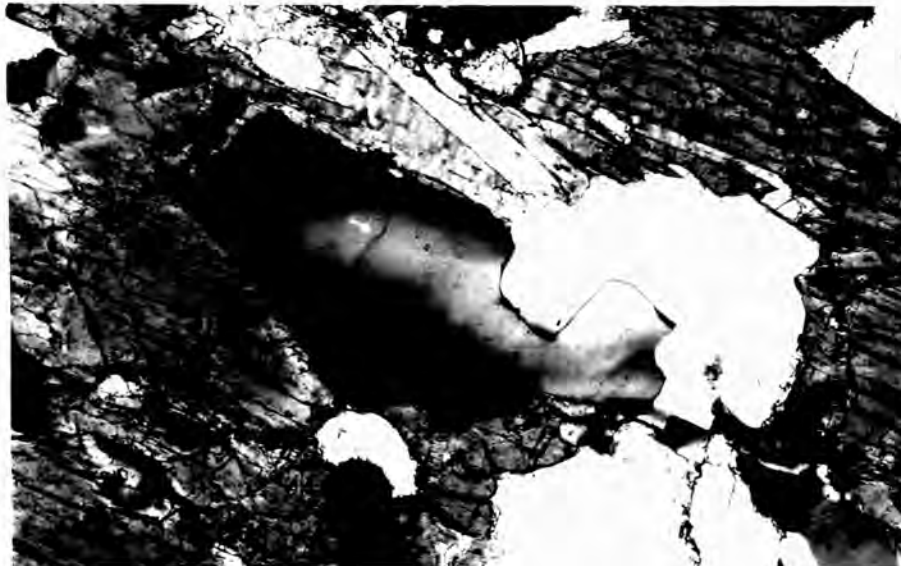
A relict plagioclase crystal associated with an amphibole knot -
now overgrown by quartz and strongly normally zoned (Na rich rims).

Plate 64   x 23
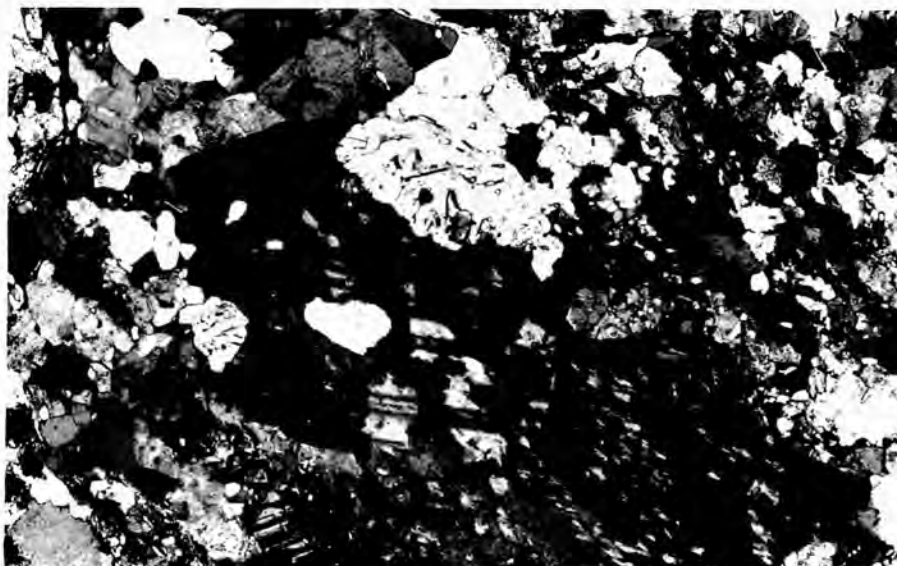
Myrmekite corrosion. The rims of K-feldspar crystals are invaded
by myrmekite (these may be stripped off during deformation, leaving
isolated fragments of myrmekite in the matrix, as in Plate 95).

Plate 65   x 93
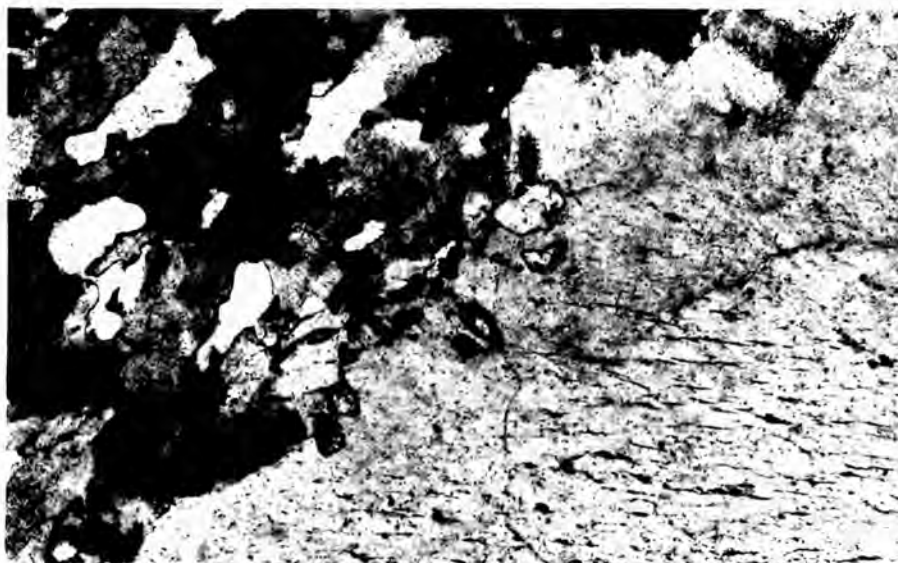
A large recrystallized K-feldspar which has enclosed crystals of
the matrix at its margins. The margin is crenulate with "pseudo-
podia" growing out from it into the matrix. Note this K-feldspar
is not particularly perthitic, indicating that it was formed late
in the metamorphism.

Plate 66   x 10
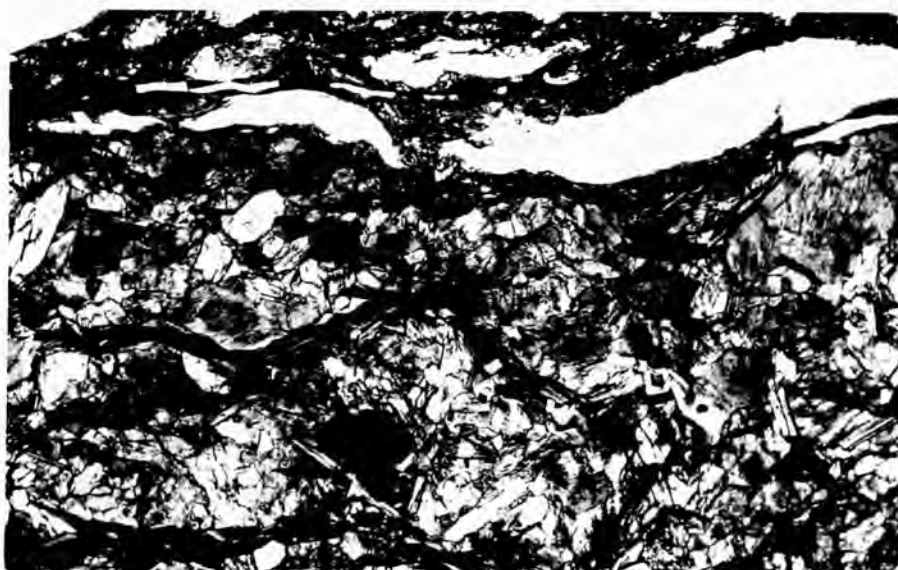
A small scale shear zone in an amphibolite. Note the sharp red-
uction in crystal size in the zone and the presence of "strings"
of quartz in them.   These were segregation "ribbons" which are
deformed during shear to form sinuous "strings".

Plate 67   x 120
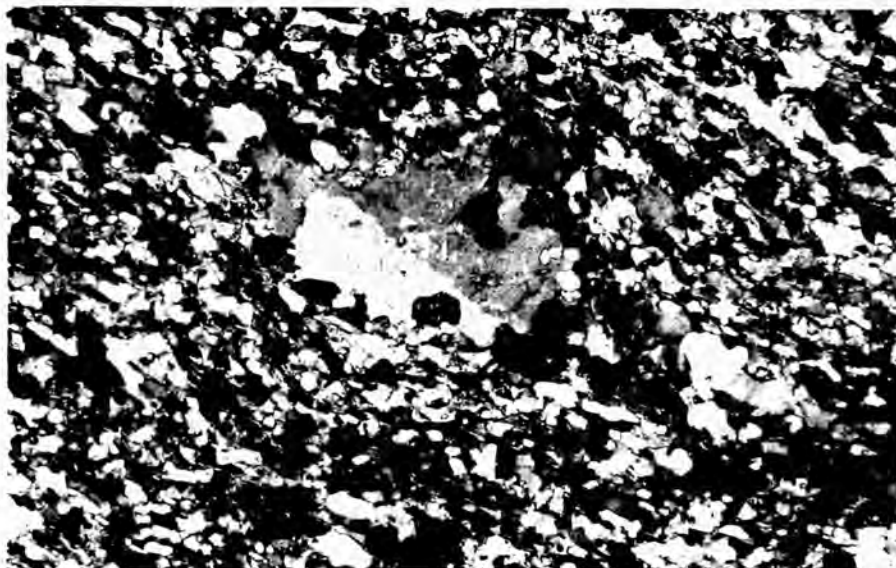
A K-feldspar strongly corroded by myrmekite round the margins.
This myrmekite rimming increases through the M3 retrogression.
Note characteristic "cauliflower" growth form of the myrmekite
centred at numerous sites round the margin.

Plate 68   x 10
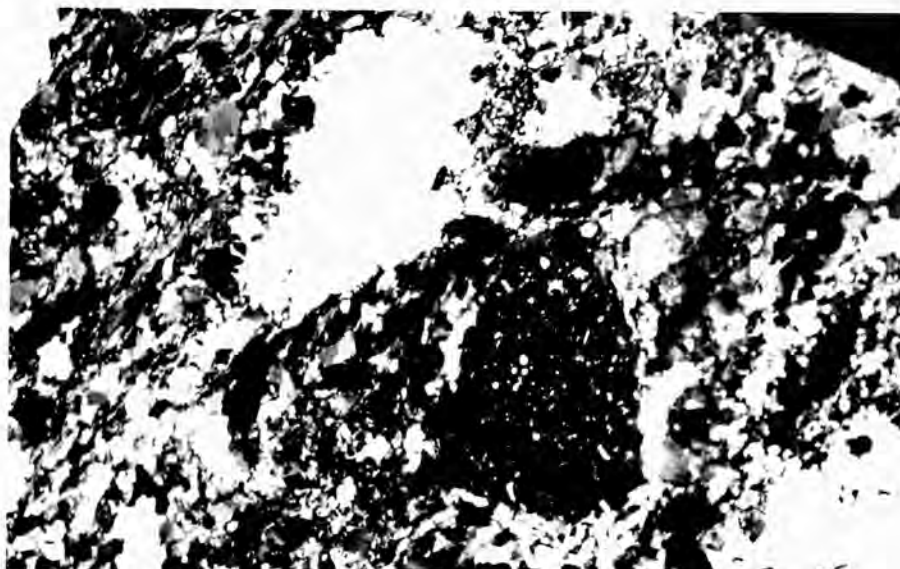
A K-feldspar (top) and a late Na-feldspar (bottom) showing the
difference between the two. The K-feldspar has an amoeboid
growth form and shows myrmekite invasion, while the Na-feldspar
is full of chlorite and epidote inclusions. Both crystals are
porphyroblasts.

Plate 69   x 23
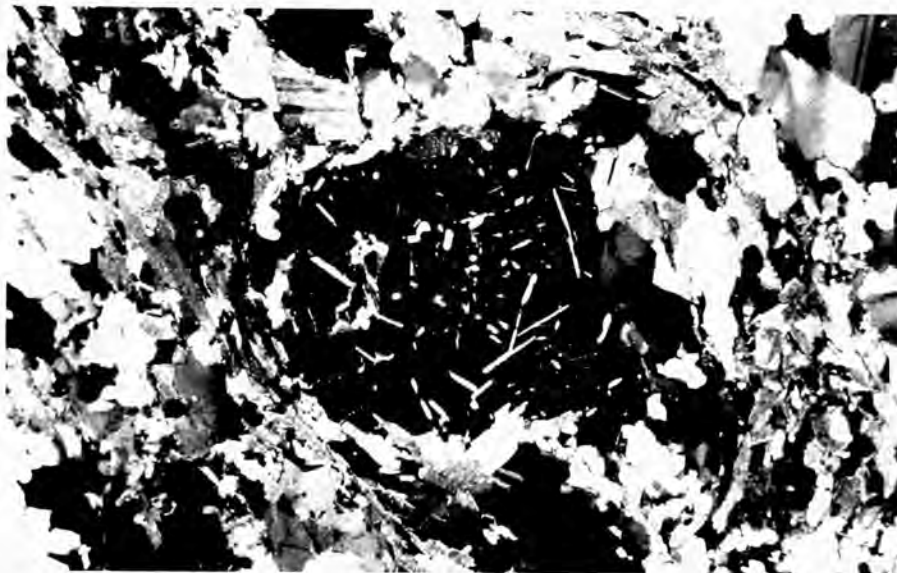
A late Na-feldspar (albite) porphyroblast showing typical inclusion
of unorientated mica, chlorite and epidote. Such crystals are typ-
ically, a late product of the M3 metamorphism.

Plate 70   x 23
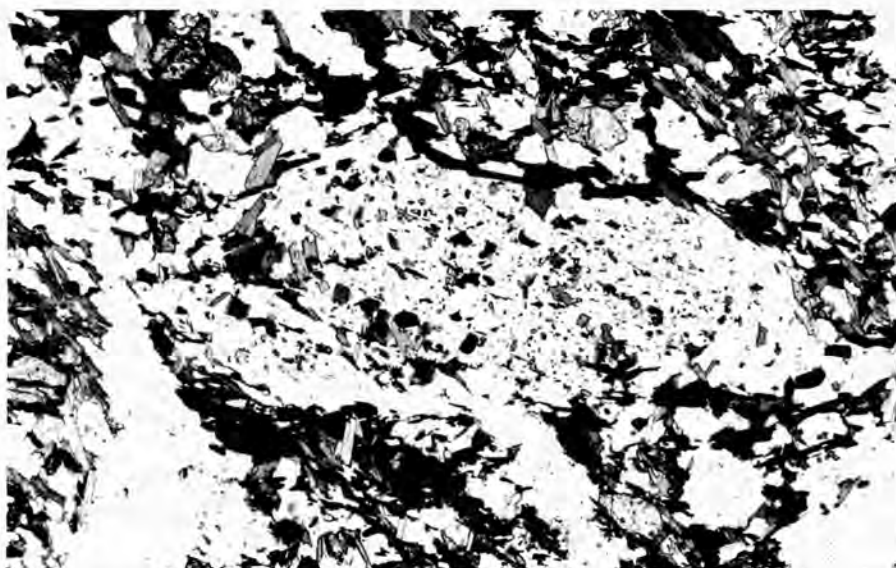
A late albite porphyroblast full of epidote and chlorite inclusions,
overgrowing biotite and hornblende in an amphibolite.

Plate 71
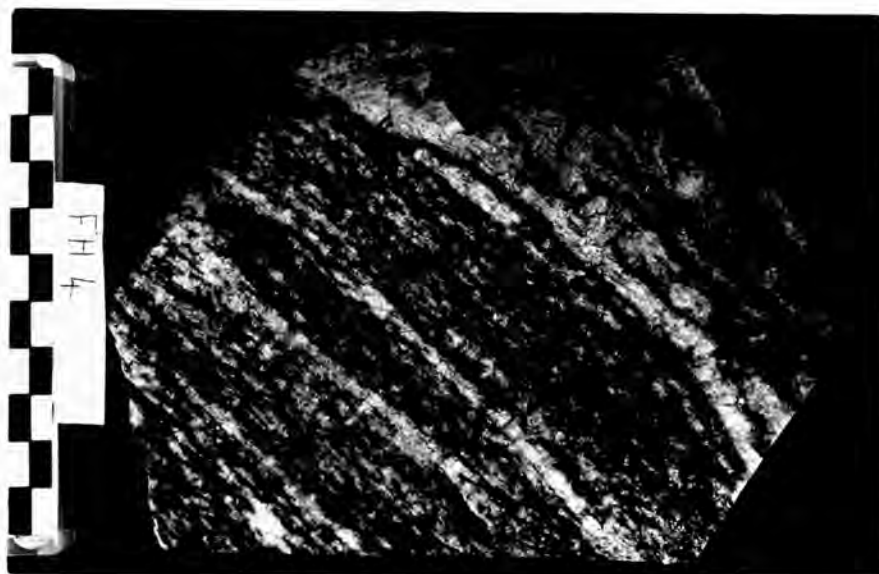
An example of typical un-mylonitized acid gneiss from the Northern Gneiss Unit.

Plate 72
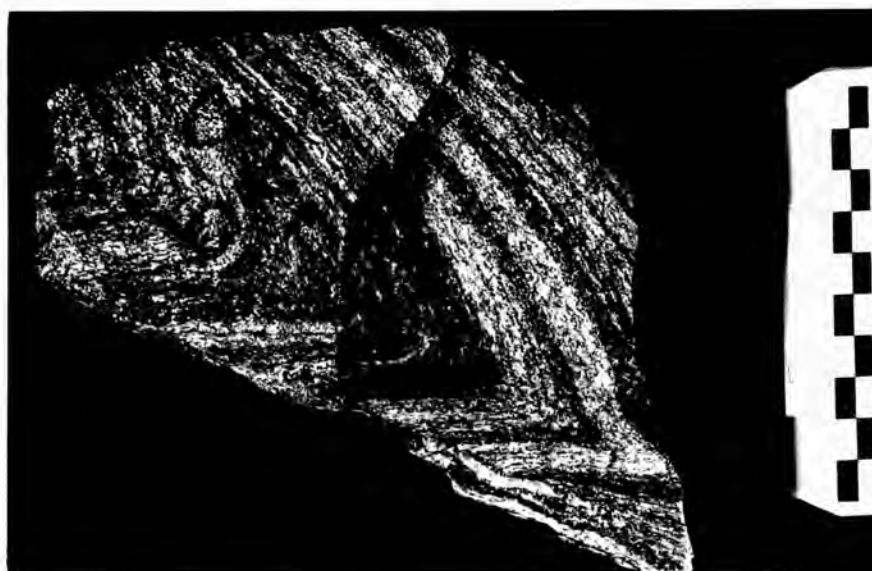
Example of moderately mylonitized acid gneiss from the Southern Gneiss Unit. Note the F5 fold has no accompanying schistosity.

Plate 73

Highly mylonitized gneiss from the Southern Gneiss Unit showing
characteristic banding and development of K-feldspar augen.
This rock would be called a blastomylonite.

Plate 74
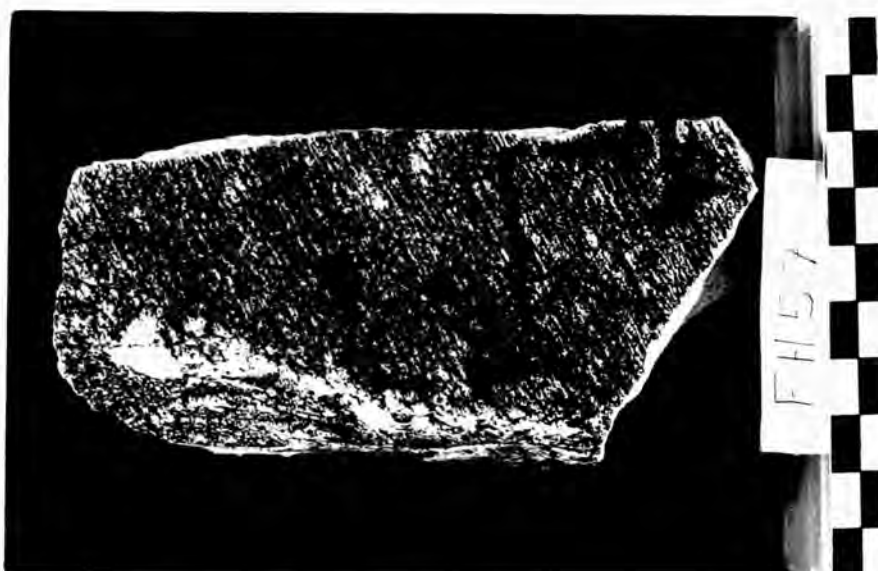
Highly mylonitized gneiss from the Southern Gneiss Unit, showing
the characteristic strong linear fabric seen on the schistosity
surfaces (L1).

Plate 75

A "pip" of unmodified gneiss set in a younger mylonitized matrix.
The "pip" contains an old texture and banding that shows no
causal relationship to the younger texture and banding developed
in the matrix surrounding it.

Plate 76   x 10
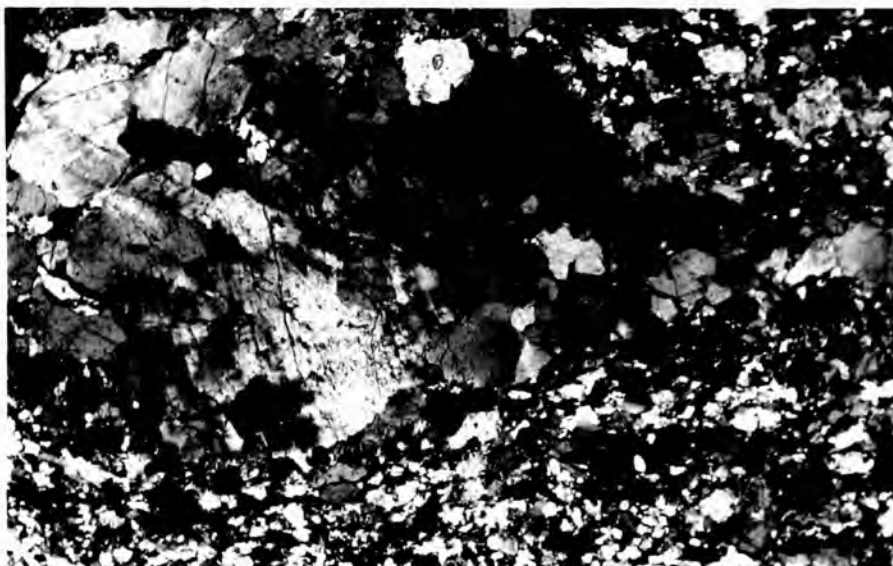
A K-feldspar broken up by stresses which have produced undulose
extinction, sub grain formation and rotation of some of the sub
grains.   This is an example of the start of the process of def-
ormation of K-feldspar porphyroblasts that is completed in Plates
80 and 81.

Plate 77   x 10
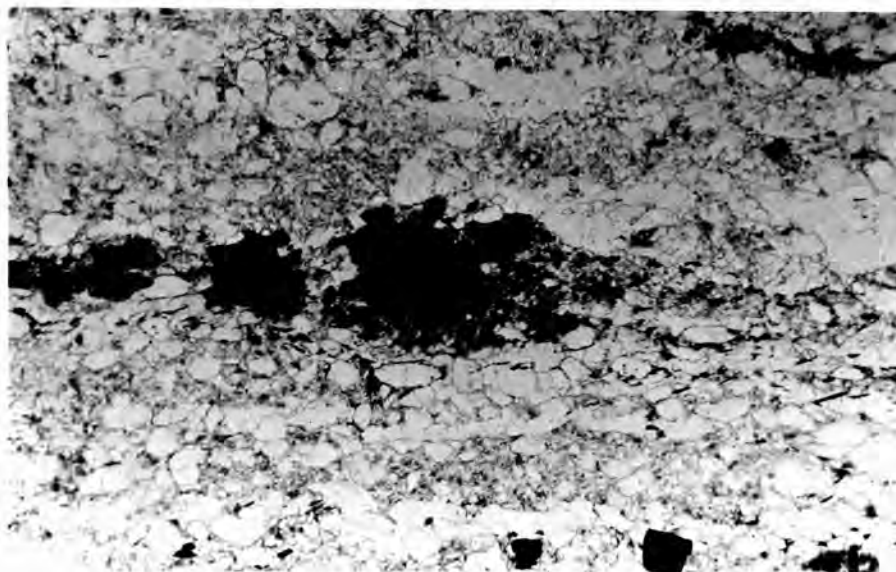
A crushed and boudinned sphene crystal, now much replaced by FeO and spread out in the plane of the schistosity.

Plate 78   x 10

An example of rod perthite. Once this was a large crystal that was deformed in a manner similar to that shown in Plate 76 so that the sub grains were rotated. Subsequently however, the sub grains have regrown to form 3 larger sub grains in slightly differing orientations. Eventually these will reunite to form a new crystal equal or larger in size than the original. Note that the crystals are poikilolitic.

Plate 79   x 15
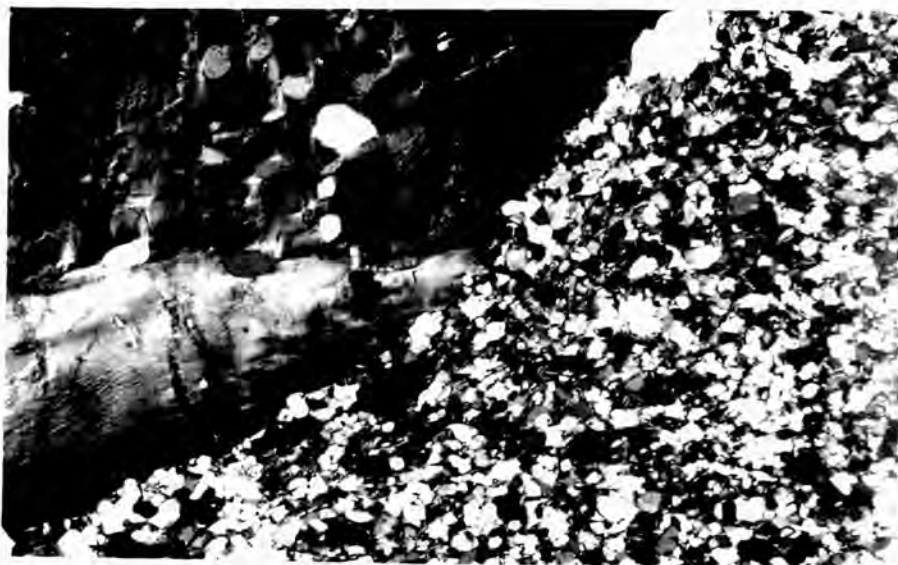
An example of a K-feldspar crystal showing undulose extinction.
This is the first stage of sub grain formation in a porphyroclast
and precedes the stage shown in Plate 76.

Plate 80   x 10
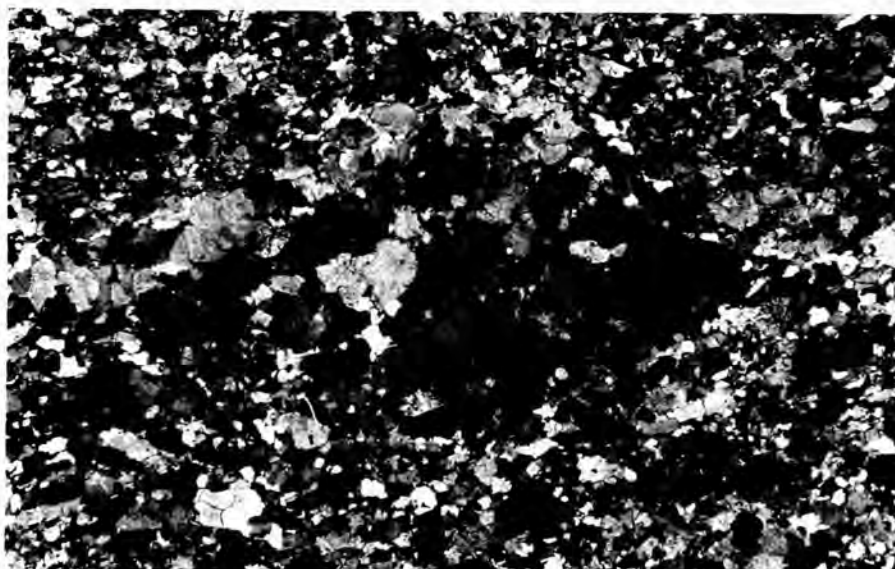
An augen of K-feldspar composed of numerous sub grains all in
differing orientations. Note that the augen is beginning to be
spread into the plane of the schistosity and that the K-feldspar
crystals are still much larger than the crystals comprising the
matrix. This Plate represents a more advanced stage of deformation
of what was originally a single crystal than that shown in Plate 76.

Plate 81   x 10
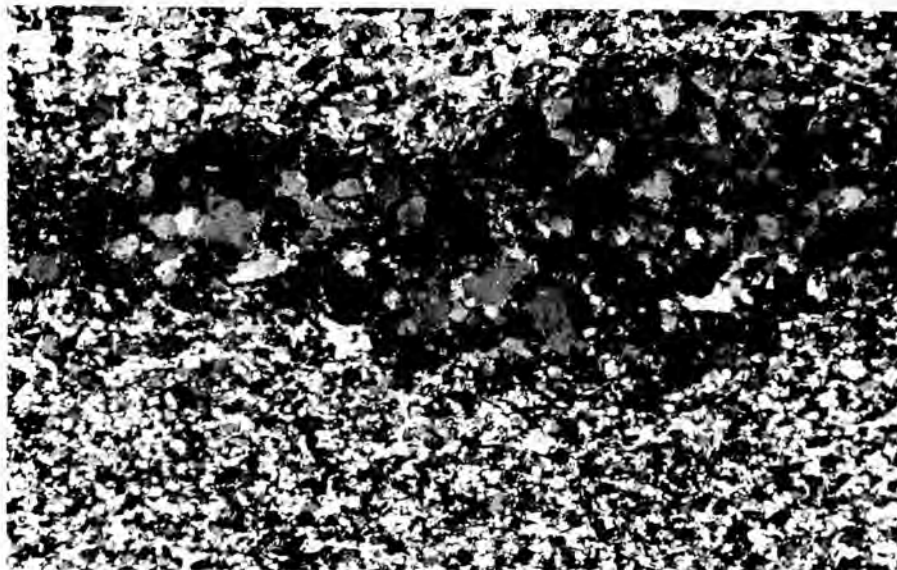
An aggregate of K-feldspar crystals forming a very thin augen
spread in the plane of the dominant schistosity. This lens shape
is a further advancement of the processes described in Plates 79,
76, and 80 respectively and represents the remnants of a very
strained porphyroclastic crystal of K-feldspar.

Plate 82   x 10
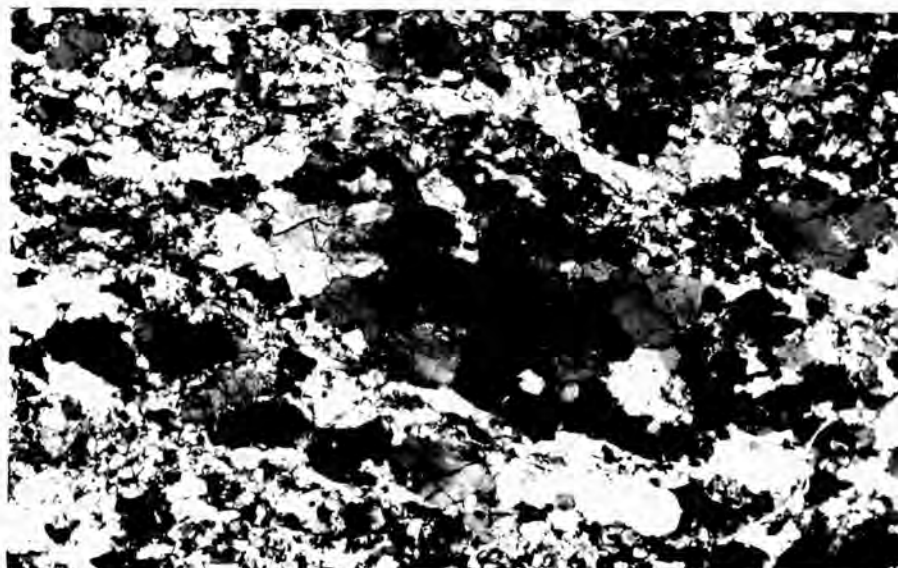
A deformed K-feldspar porphyroclast such as that described in Plate
80 or 81 which has subsequently started to recrystallize. The large
black portion in the middle of the augen is the re-crystallising
portion and is overgrowing the surrounding sub grains as seen from
the crosscutting relationships it has with them. Eventually the
crystals will grow to be as large or larger than the original K-
feldspar as shown in Plate 83.

Plate 83   x 23
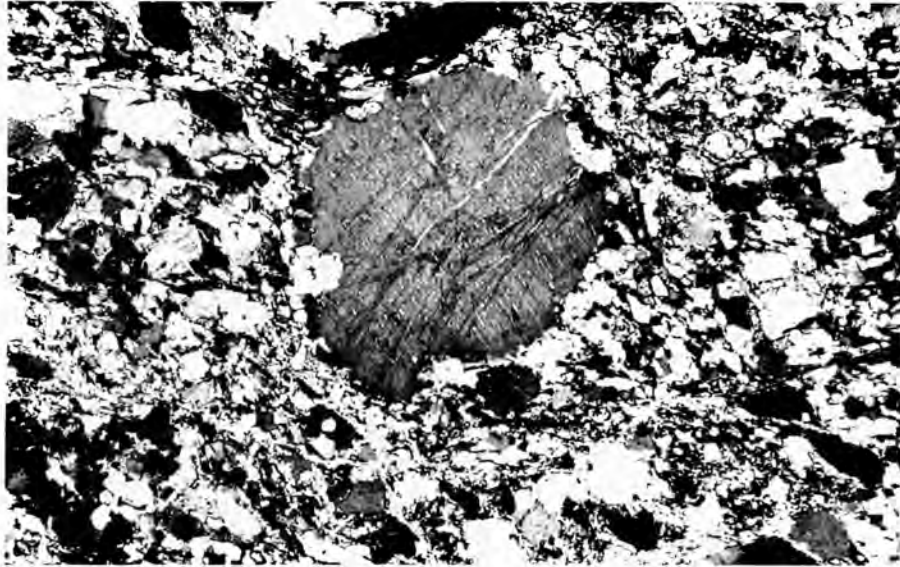
A perthitic microcline which has recrystallized from an aggregate
of sub grains (such as in Plate 82), to form a new crystal which
is of the same size as that which occupied the site prior to the
deformation producing the strains seen in the matrix (augen struc-
ture round the crystal - Plate 84).   The fact that this is a re-
crystallization product is deduced from the lack of internal strain
features and the manner in which the crystal crosscuts and over-
grows its marginal neighbours.   Note the large hydraulic fractures
across the crystal.

Plate 84   x 23
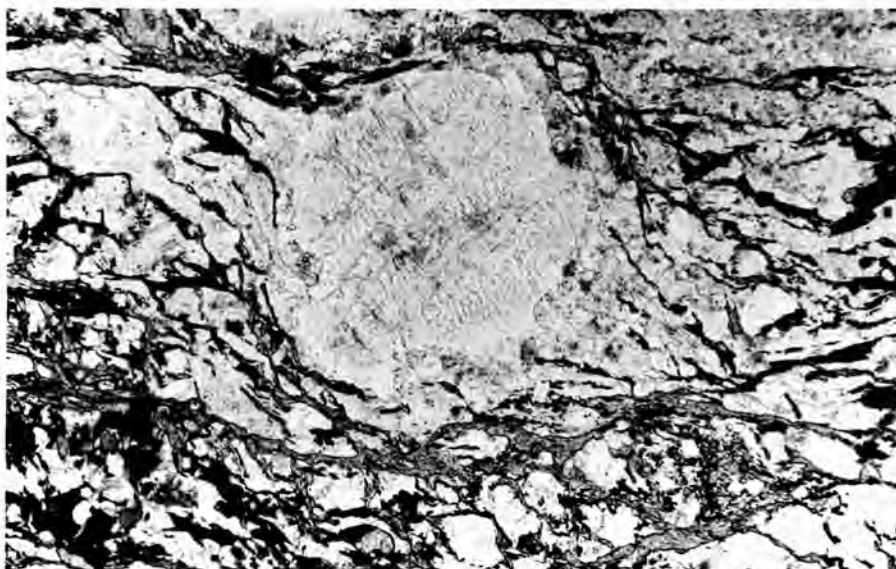
A p.p.l view of the crystal shown in Plate 83, showing how the
schistosity enveloping the porphyroblast is in fact overgrown,
proving secondary recrystallization.

Plate 85   x 93
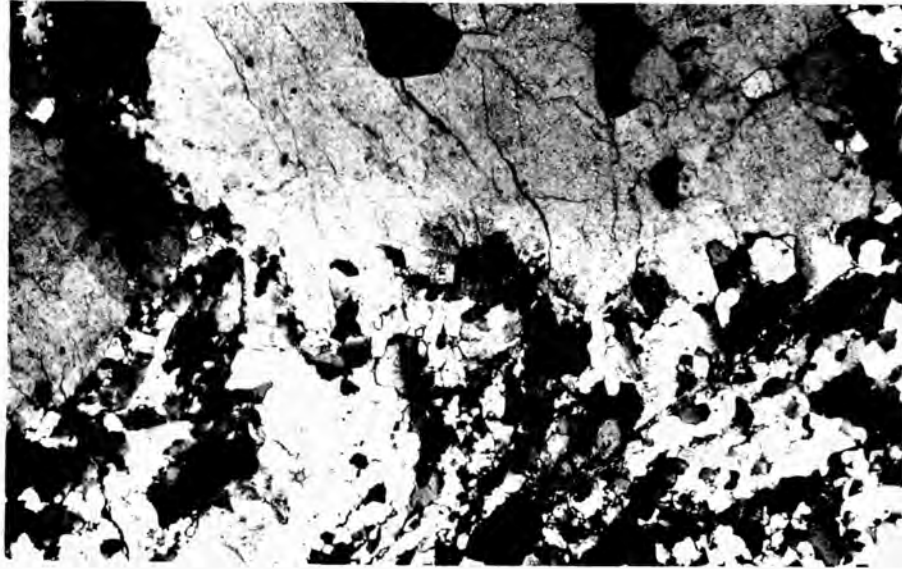
A K-feldspar porphyroblast which has overgrown its matrix during
recrystallization. Note inclusions of individual matrix crystals,
the crenulate margin and the extension "pseudopodia" of the K-
feldspar crystals into the matrix. Such a growth form is said to
be ameboid and is characteristic of a porphyrobalstic crystal.

Plate 86   x 15
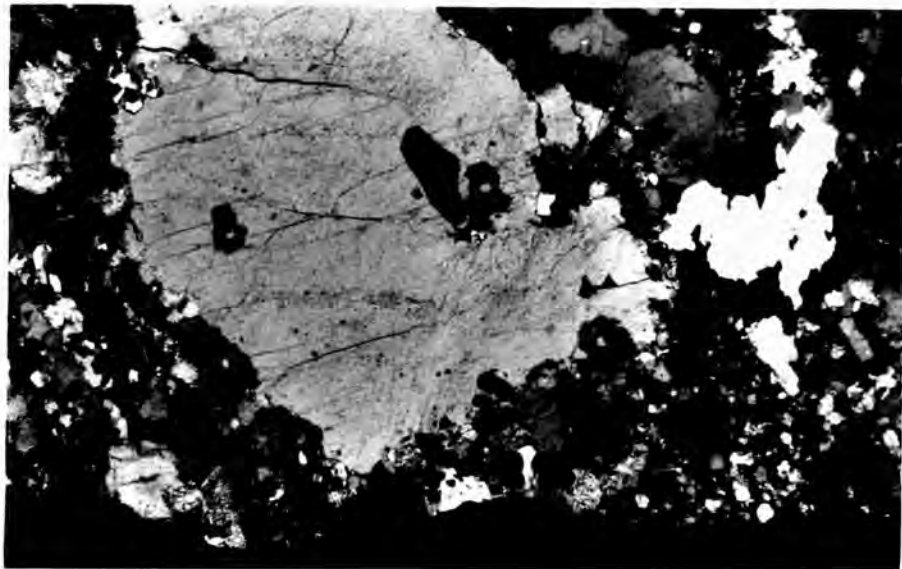
A K-feldspar porphyroblast which has enlarged during re-crystal-
lization, overgrowing its matrix "sheath". Note the "amoeboid"
outlines and poikilolitic nature. The large quartz grain to the
right forms part of the old strain shadow.

Plate 87   x 93
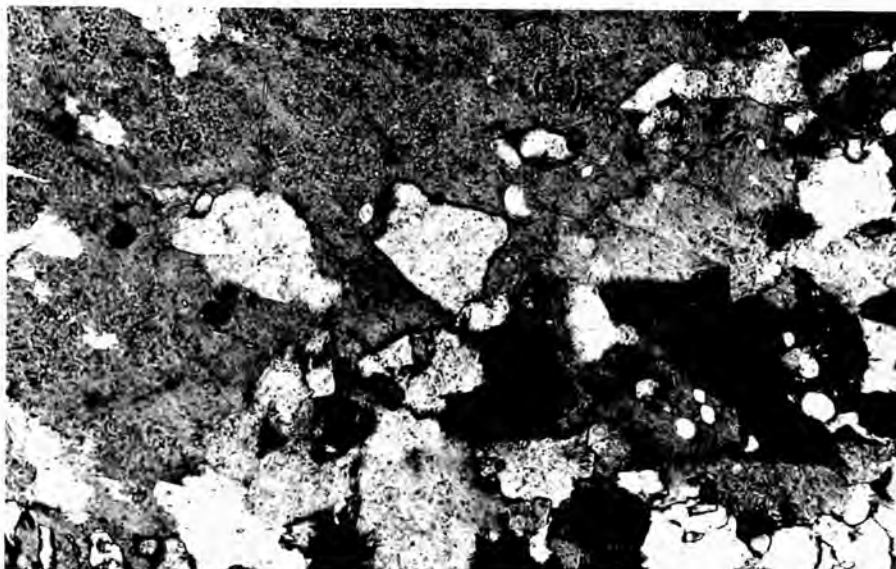
An "amoeboid" margin to a K-feldspar porphyroblast, showing the
process of inclusion of matrix grains during recrystallization.
Note these grains are discrete crystals, not like a crystal inter-
growth (symplectite texture).

Plate 88   x 30

Undulose extinction in quartz (This is a precursor to sub grain
formation).

Plate 89   x 10
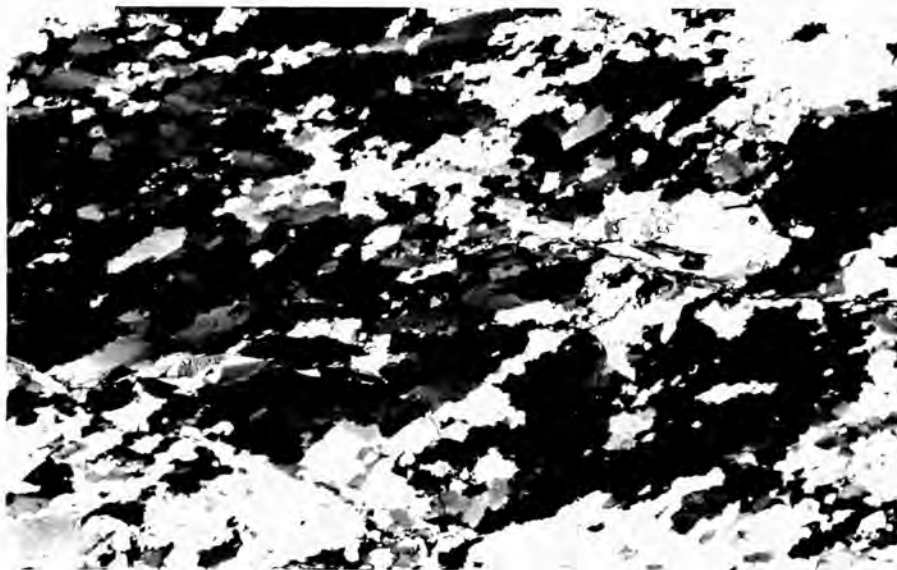
Quartz laths defining a strong schistosity which runs at a shallow
angle diagonally across the plate. The laths were produced from
older strained (Plate 88) quartz grains, by annealing and re-
crystallization processes.

Plate 90   x 93
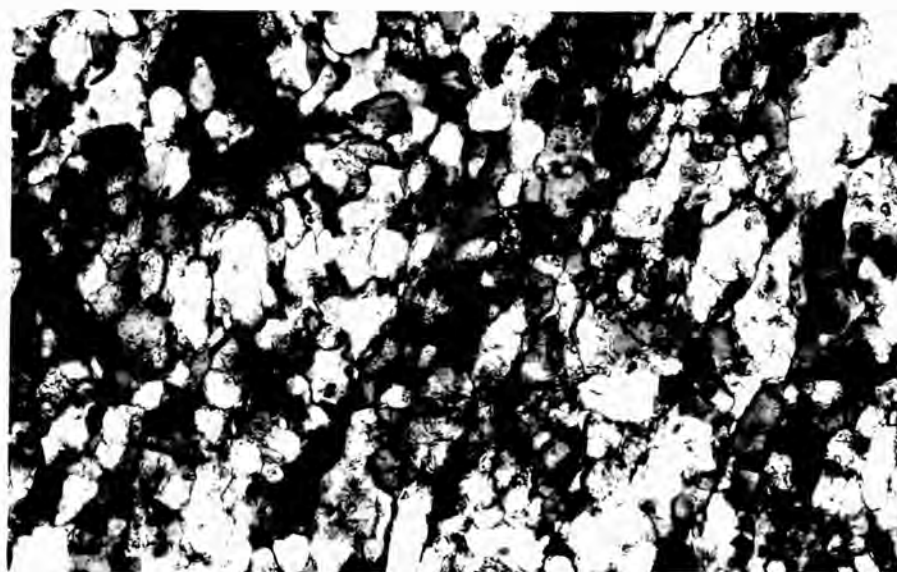
Example of matrix from the mylonitic gneissic rocks. Note the
irregular grain size, irregular crystal morphology and the lack
of good 120° junctions (Though these can be seen to be beginning
to form in places).

Plate 91   x 10

Recrystallized matrix of a mylonitic gneiss, compared to Plate 90
this matrix is now relatively strain free, the crystal size is
larger, the crystals are more regular and 120° junctions are
common.   An annealed matrix.

Plate 92

Mylonitic banding, typical of the Southern Gneiss Unit rocks.

Plate 93

Gneiss in which mylonitization is extreme, from a D4 mylonitic band. Note virtually all the K-feldspar augen are destroyed.

Plate 94
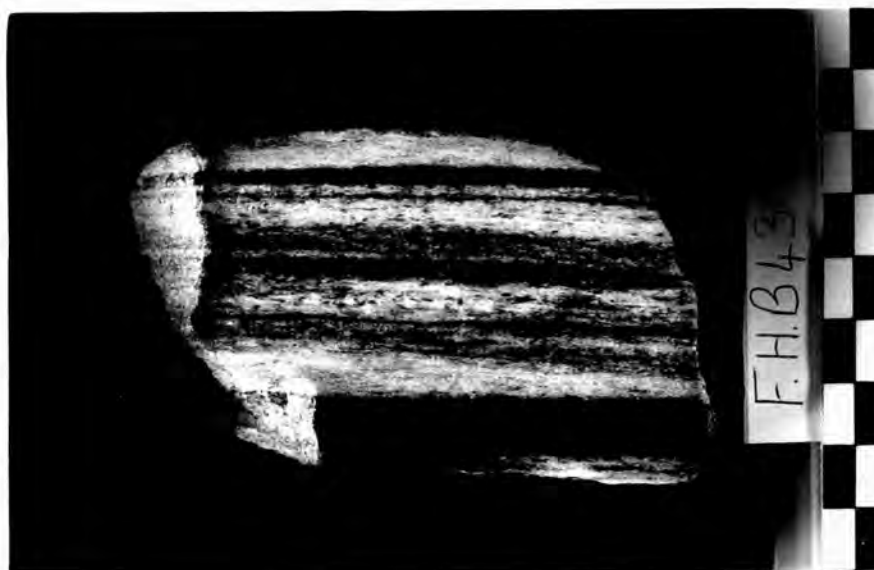
Typical hand specimen of mylonitized gneiss from the Southern Gneiss Unit.

Plate 95   x 10
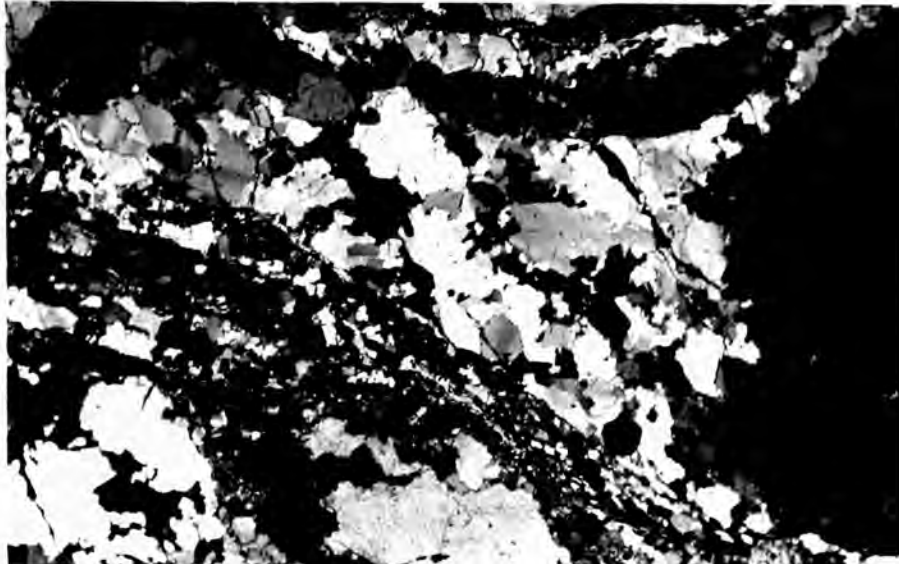
Thin bands of mylonite forming in a biotite rich layer adjacent
to a porphyroblast. Note sharp margins and grain size contrast
between the more leucocratic minerals inside and outside the
zone of shear.

Plate 96   x 120

Myrmekite shredded from the rim of a K-feldspar augen. This
myrmekite cannot have formed in situ because it is surrounded
by minerals other than fledspar. Note it is overgrown by a
late apatite crystal.

Plate 97   x 10
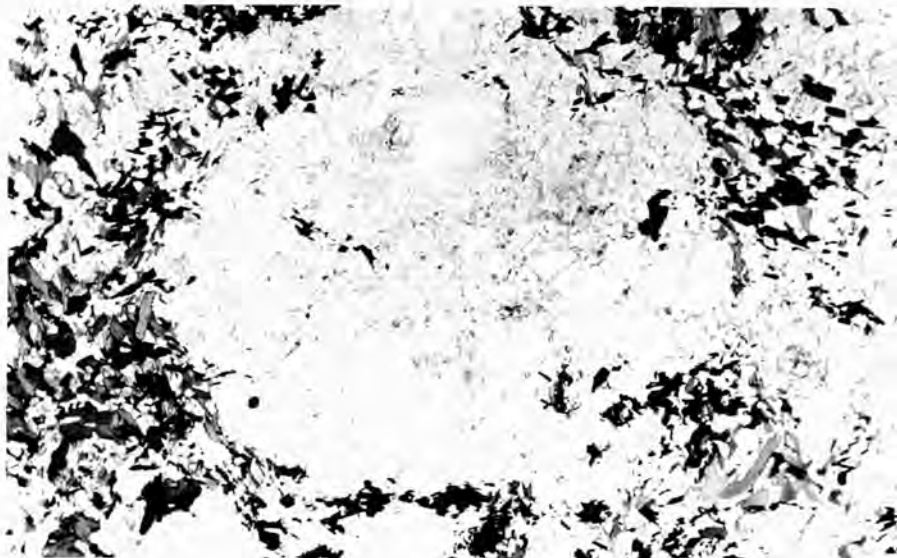
An albite porphyroblast overgrowing a fine grained micaceous
groundmass. Note it is poikilolitically including relics of
the micas.

Plate 98   x 15
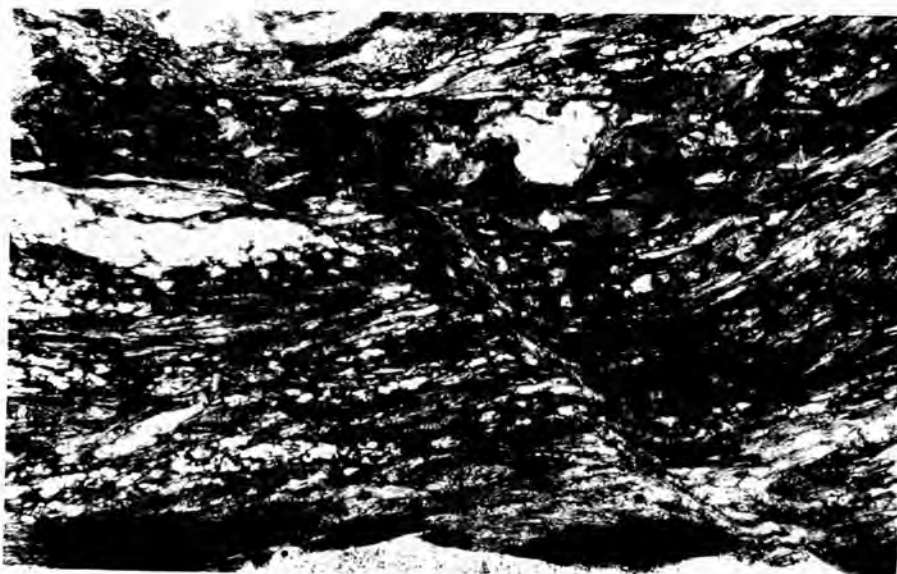
A shear band cutting across the dominant schistosity at a high
angle. Such bands, which reveal extreme local deformation, are
not disruptive. They must therefore have formed by plastic
deformation. This band is a zone of simple shear similar to
those described by Ramsay and Graham 1970.

Plate 99

A fold train from Osterøy. Note the progressive tightening of the folds from left to right and the accompanying development of a mylonitic banding as the folds get tighter.

Plate 100   x 10

A relict garnet porphyroblast now overgrown by feldspar. Note that the garnet is fractured with numerous fracture planes prior to the feldspar growth. This fracturing is interpreted as a cataclastic texture resulting from very high strain rates. Note too the later inclined fractures which cut the feldspar.

Plate 101   x 10
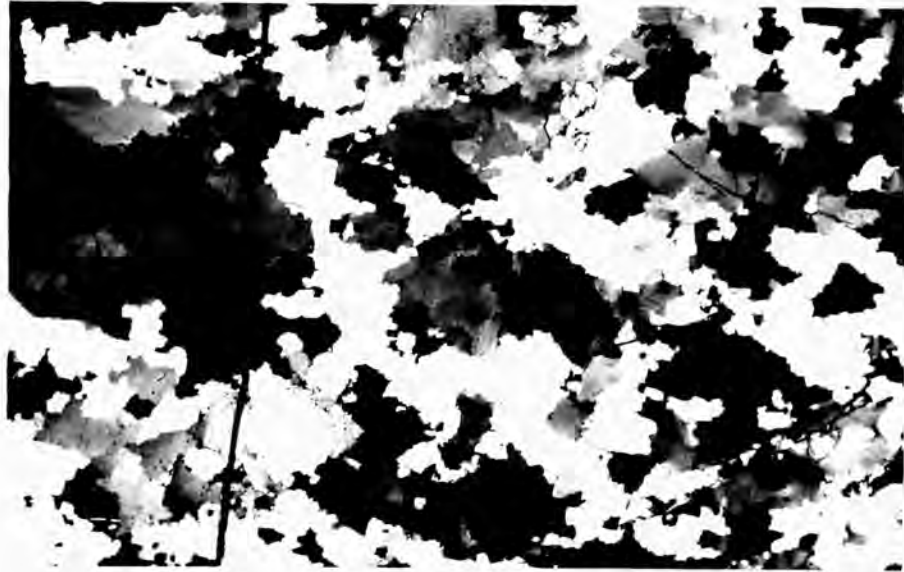
Quartzite showing crenulated crystal margins which are the result
of annealing and recrystallisation of what was a finer grained
and more highly strained rock. The large surface areas of the
crystals are possible because the adjacent crystals are of the
same species and the surfaces are therefore of lower energy than
they would otherwise be.

Plate 102   x 10
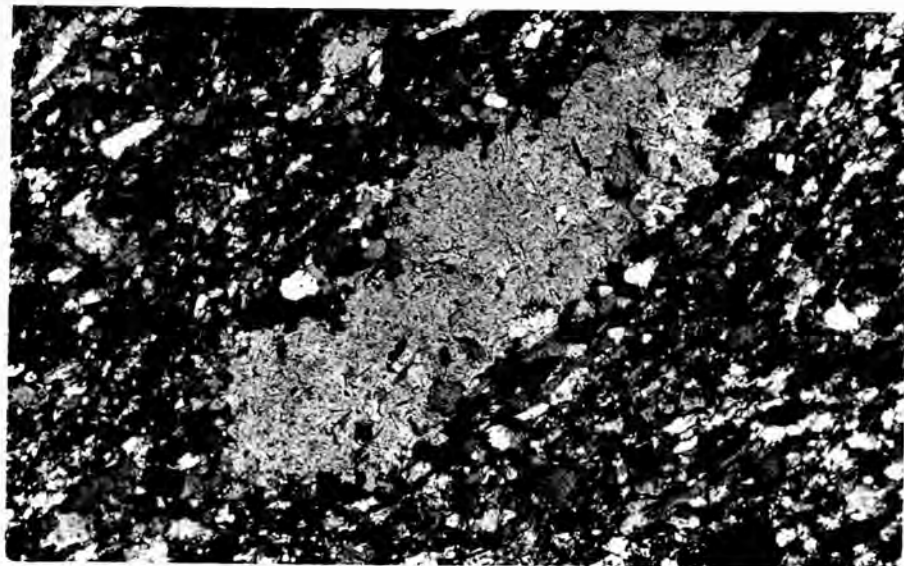
A late albite porphyroblast overgrowing a fine grained matrix
but aligned with the long axis parallel to the dominant schist-
osity (S5). Note it is poikilolitic, full of inclusions from
the matrix (which it has included by a process similar to that
for Pl.78) and epidote and chlorite laths. Note too its amoeboid
crenulated outlines.

Plate 103   x 10
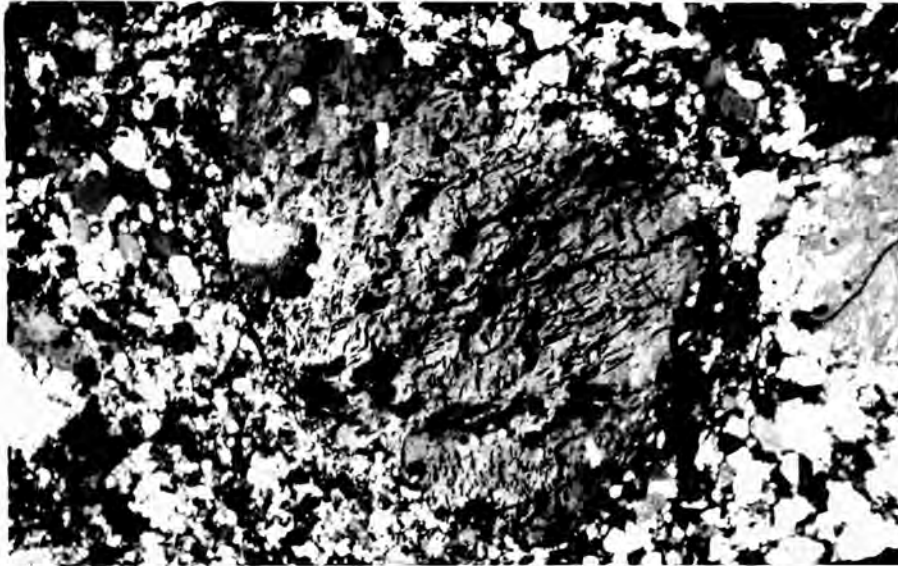
A perthite showing compound texture. Note that this crystal
shows none of the crenulated marginal textures which indicate
that it overgrew the present matrix; indeed the margins are
sharp. The augen is therefore a porphyroclast and is inter-
preted as a relic of the M3a paragenesis.

Plate 104
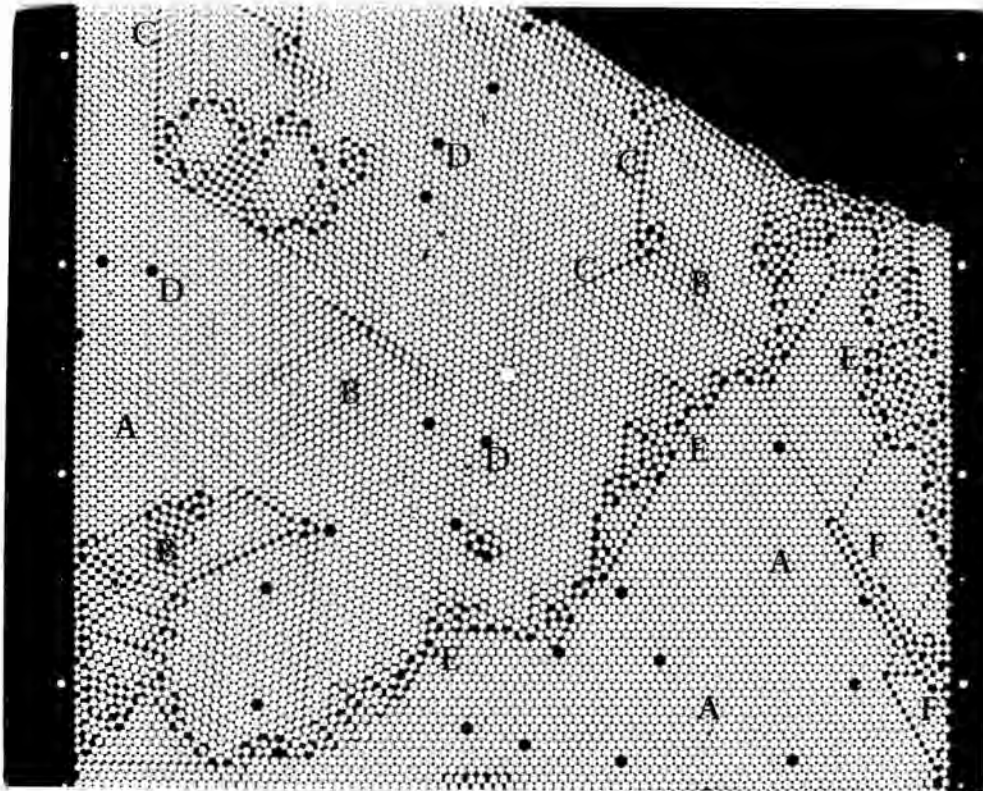
Ball bearing box model, modelling a plane through a crystal(s).
In this case the crystals are relatively unstrained and the
model represents an annealed rock which has been slightly re-
strained.

Plate 105
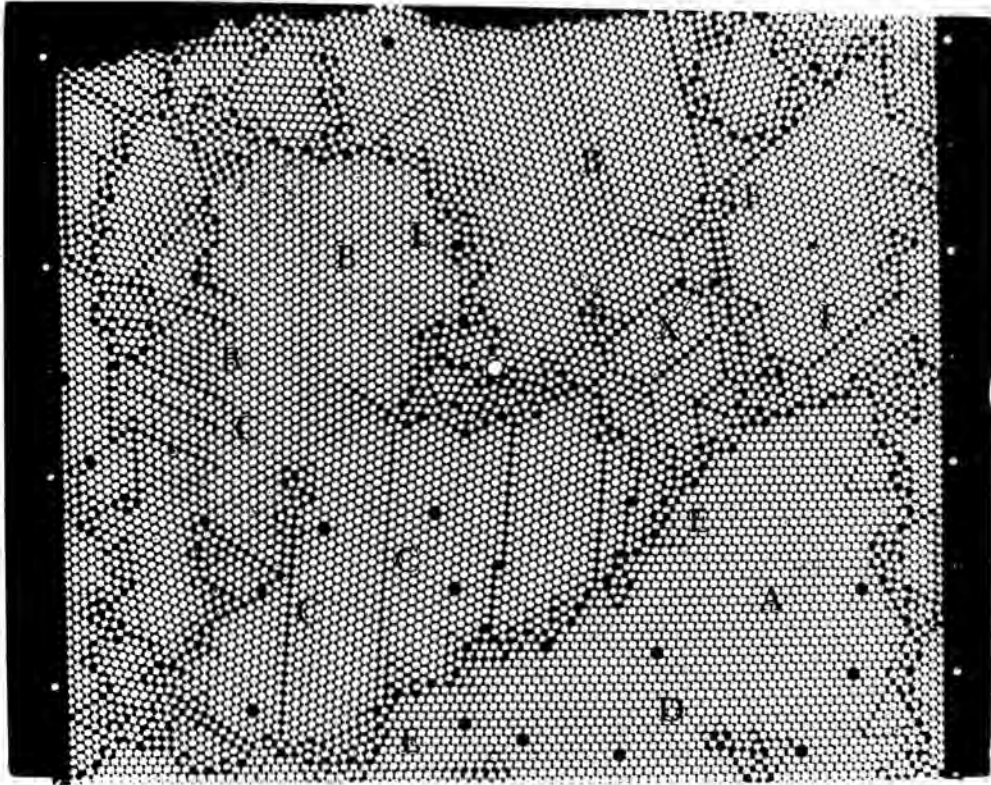
Ball bearing box model, modelling a plane through a crystal(s).
In this case the model represents a section through a highly
strained rock and shows the high energy situation while Pl.104
shows the low energy situation.

Page	Line	
ii	9	For 'held' read 'help'
28	3	Delete 'of' to read 'layer parallel'
30	25	For 'decusate' read 'decussate'
46	1	For 'strutures' read 'structures'
140	6	For 'microclase' read 'microcline'
167	2	For 'orthoganal' read 'orthogonal'
305	7	For 'myanite' read 'kyanite'
306	5	For 'metastabally' read 'metastably'
Throughout		For 'poikilolitic' read 'poikiloblastic'
"		For 'paracitic' read 'parasitic'
"		For 'schistocity' read 'schistosity'
"		For 'Nabbro' read 'Nabro'
"		For 'ameboid' read 'amoeboid'

Structural data added as Microfiche in vol. 2.

Fig 158.

Key as for Map 1

SECTIONS

BERGEN ARC THRUST D3+D4

S4

F3

F2

F3

F2

S3

F3

S3

1000 m

F3

0 m

S3

F2

D2 - D3

B

F6

BERGEN ARC THRUST
D3 + D4

hon

S3 (+ S4)

quartz vein D5

S6

Autochthon

TYSSE THRUST
D3

S3

1000 m

0 m

S1 + S2 + S3

D
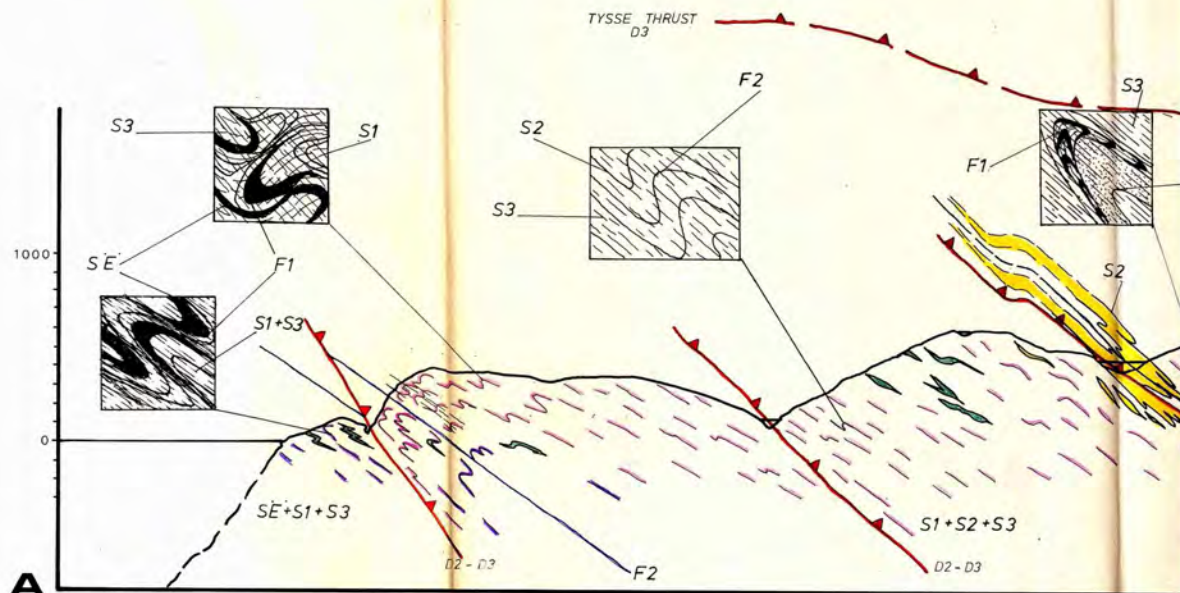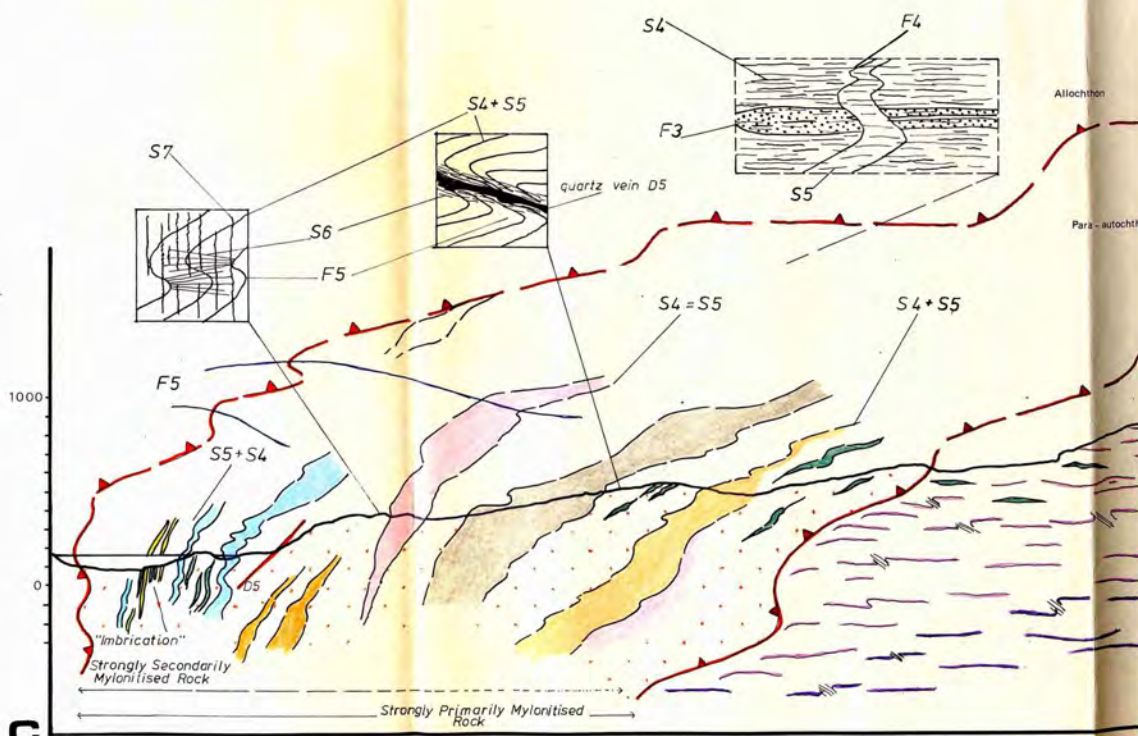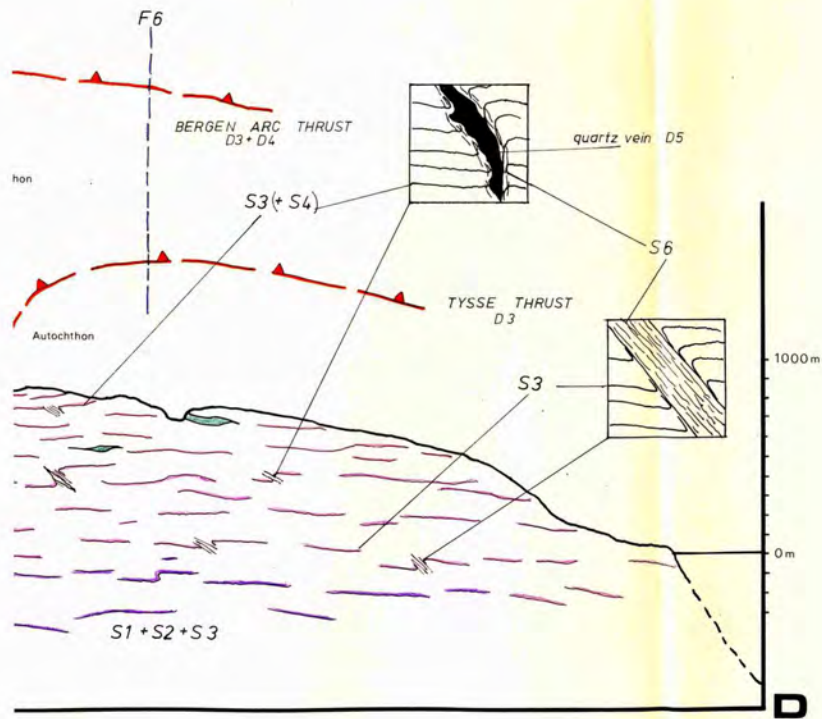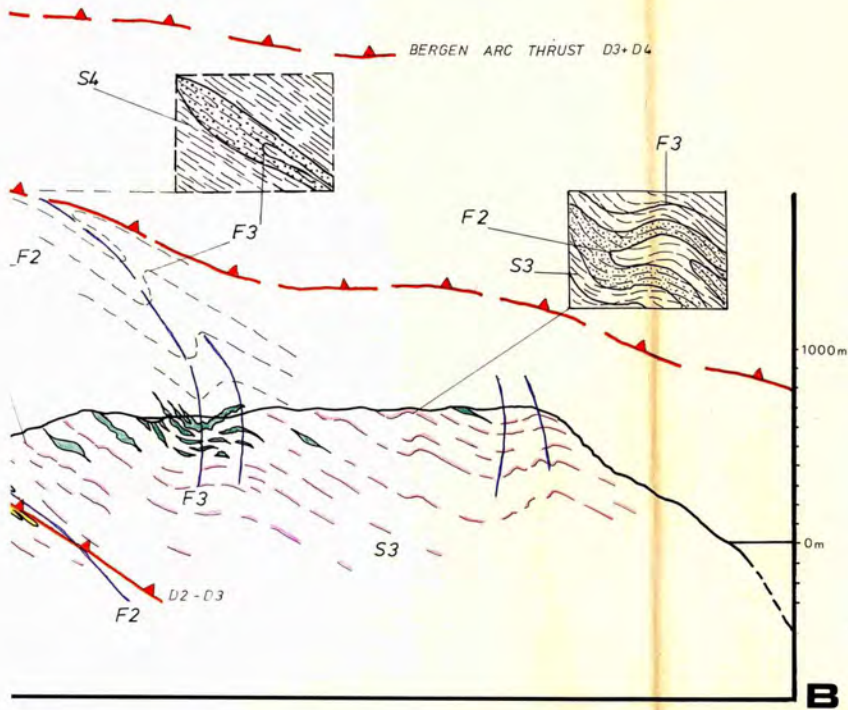
Scale   0   1   2 Km

Map:1

THE GEOLOGY

OF

NORTH OSTERØY,

NORWAY

VEAFJORDEN

Undifferentiated Gneiss

Rispingen Gneiss

Drangskollen Gneiss

Helldalsfjell Gneiss

Nonkletten Gneiss

Mica Schist

Quartzite

Quartzose Migmatite

Amphibolite

Pegmatite Rich Gneiss

Augen Gneiss

Granitic Gneiss

Flattened Gneiss & Migmatite

Gneiss & Migmatite

Unflattened Gneiss
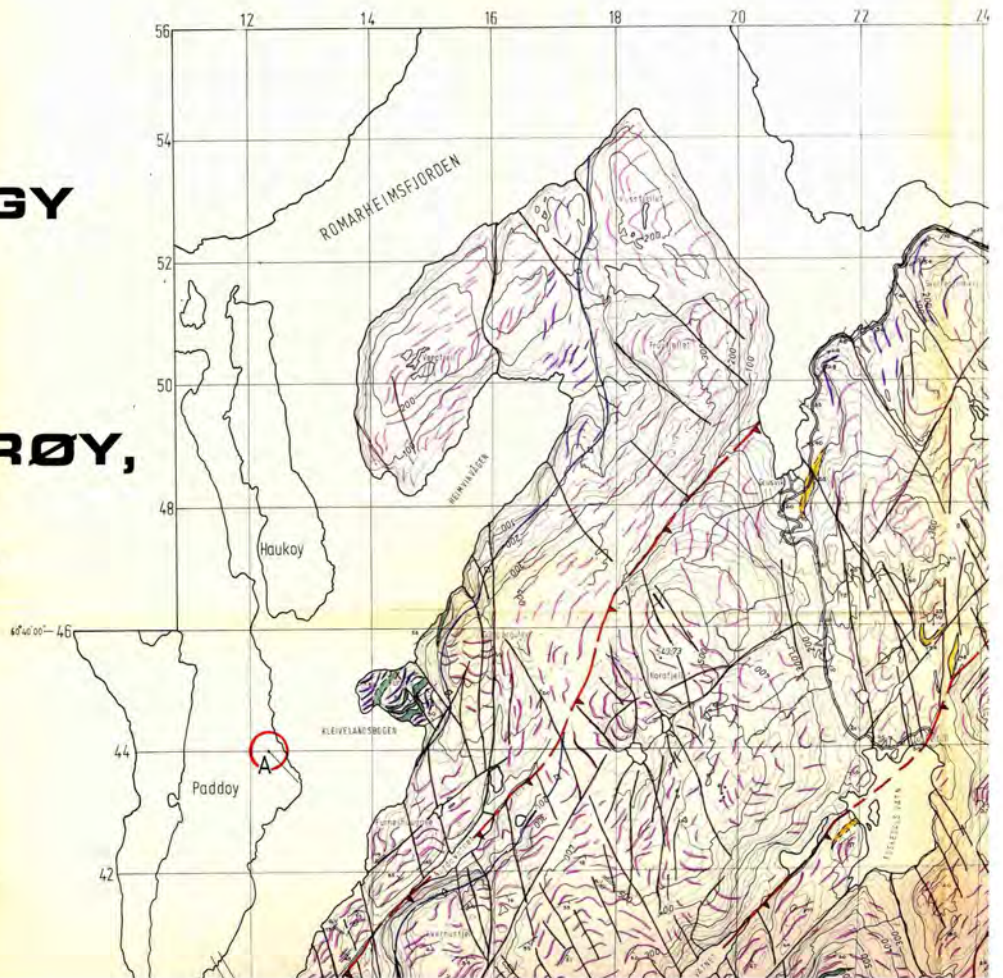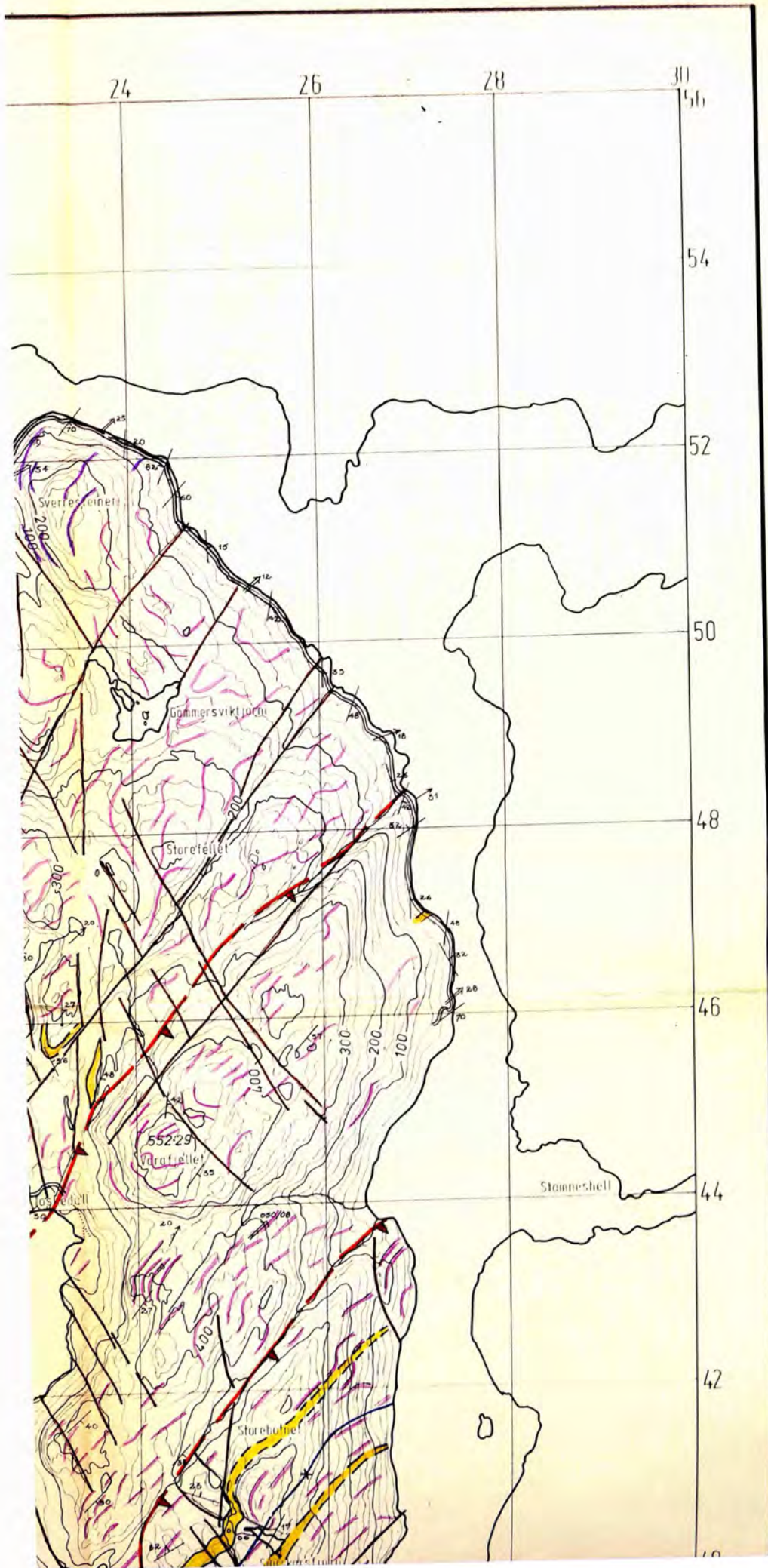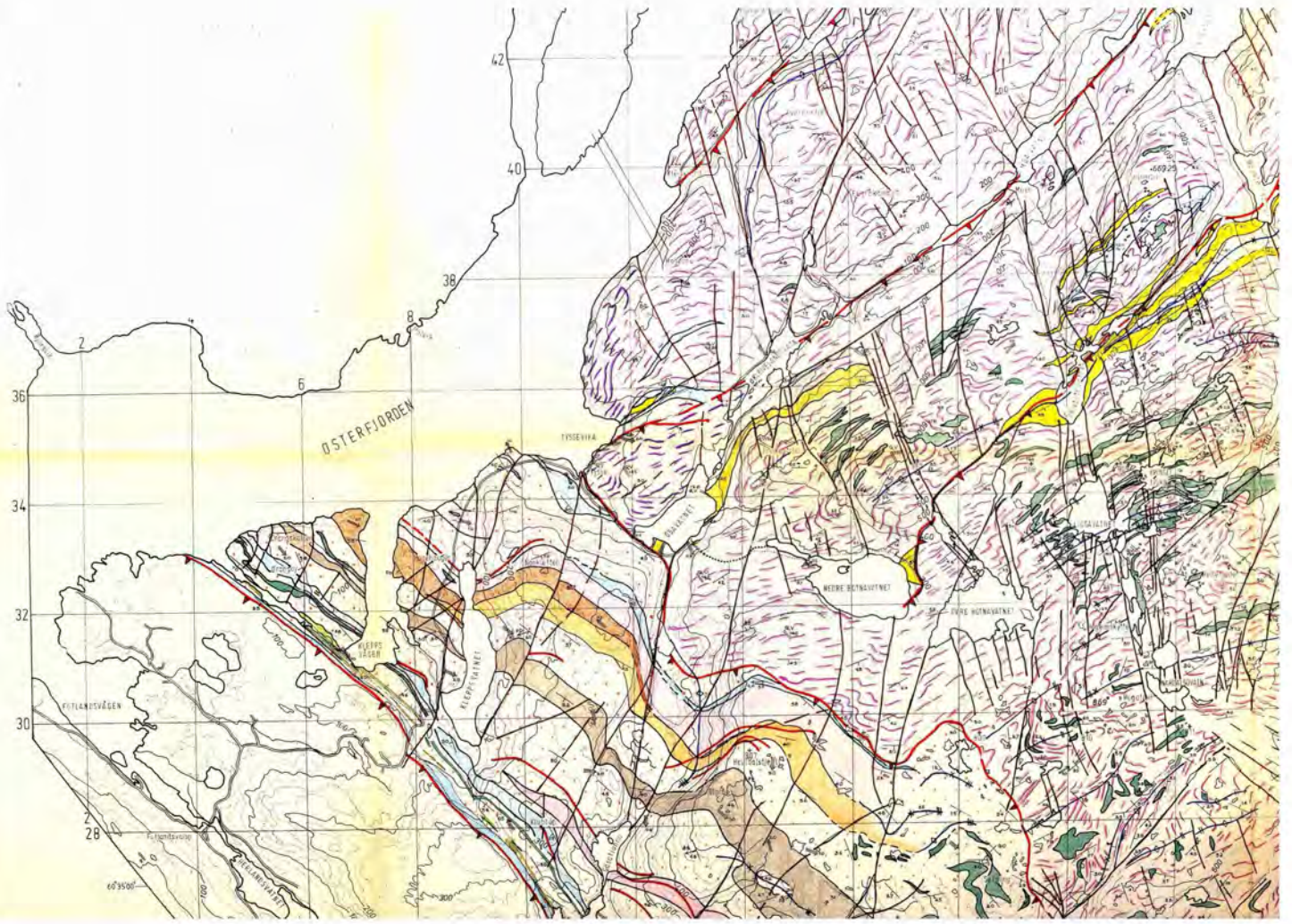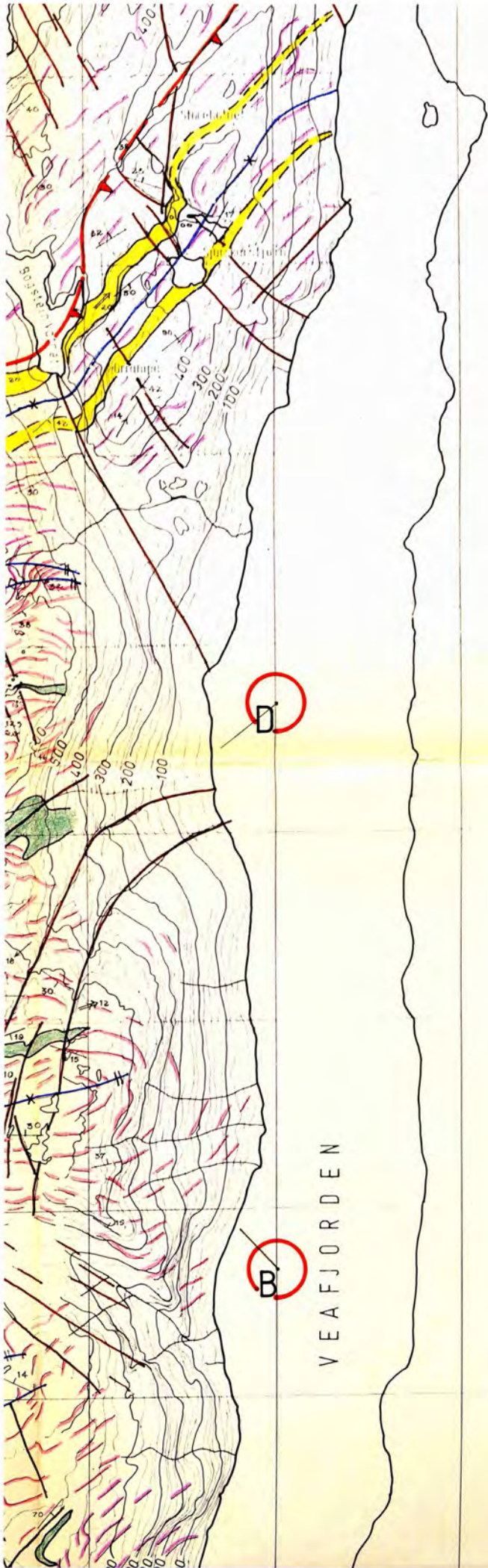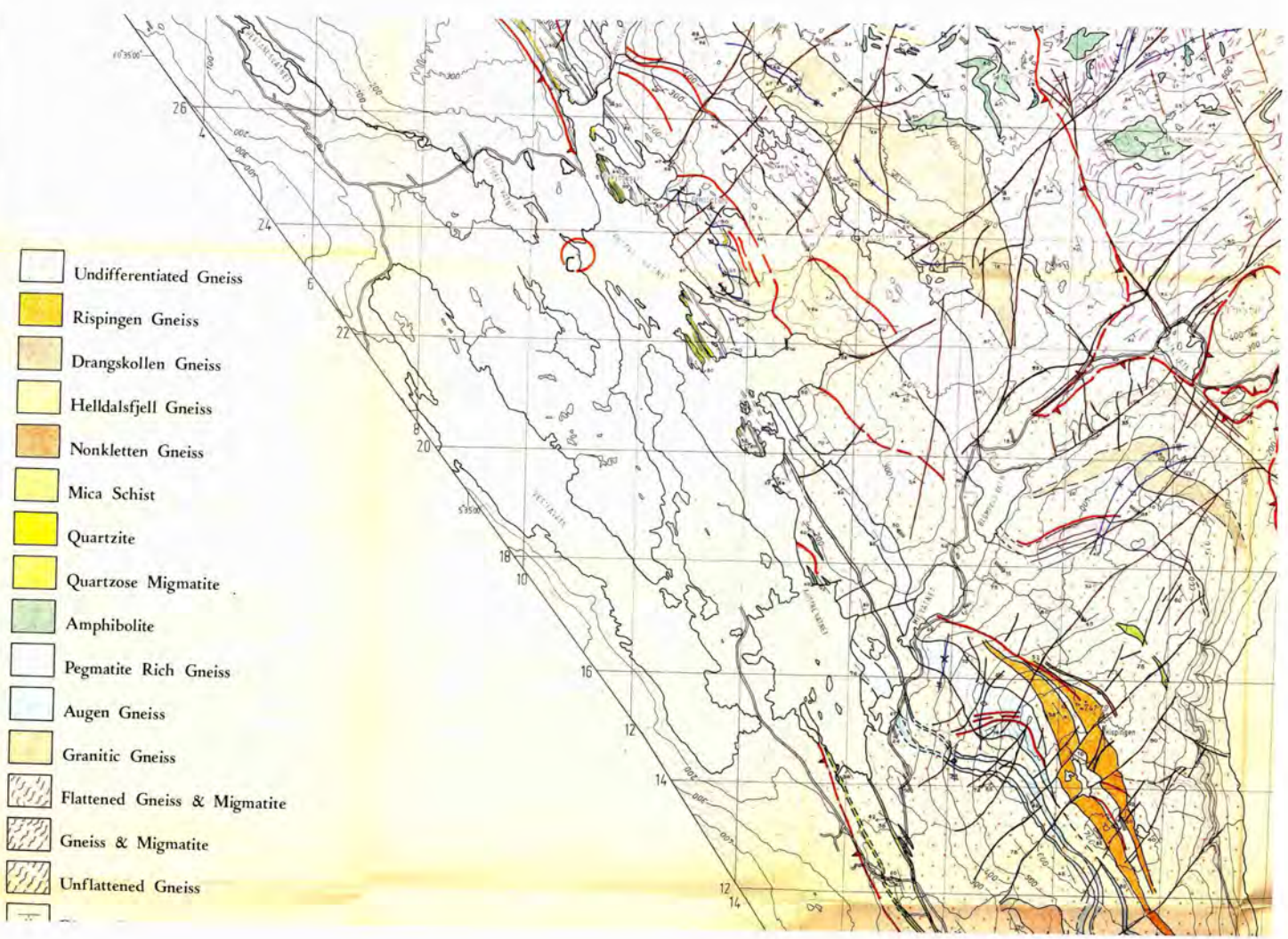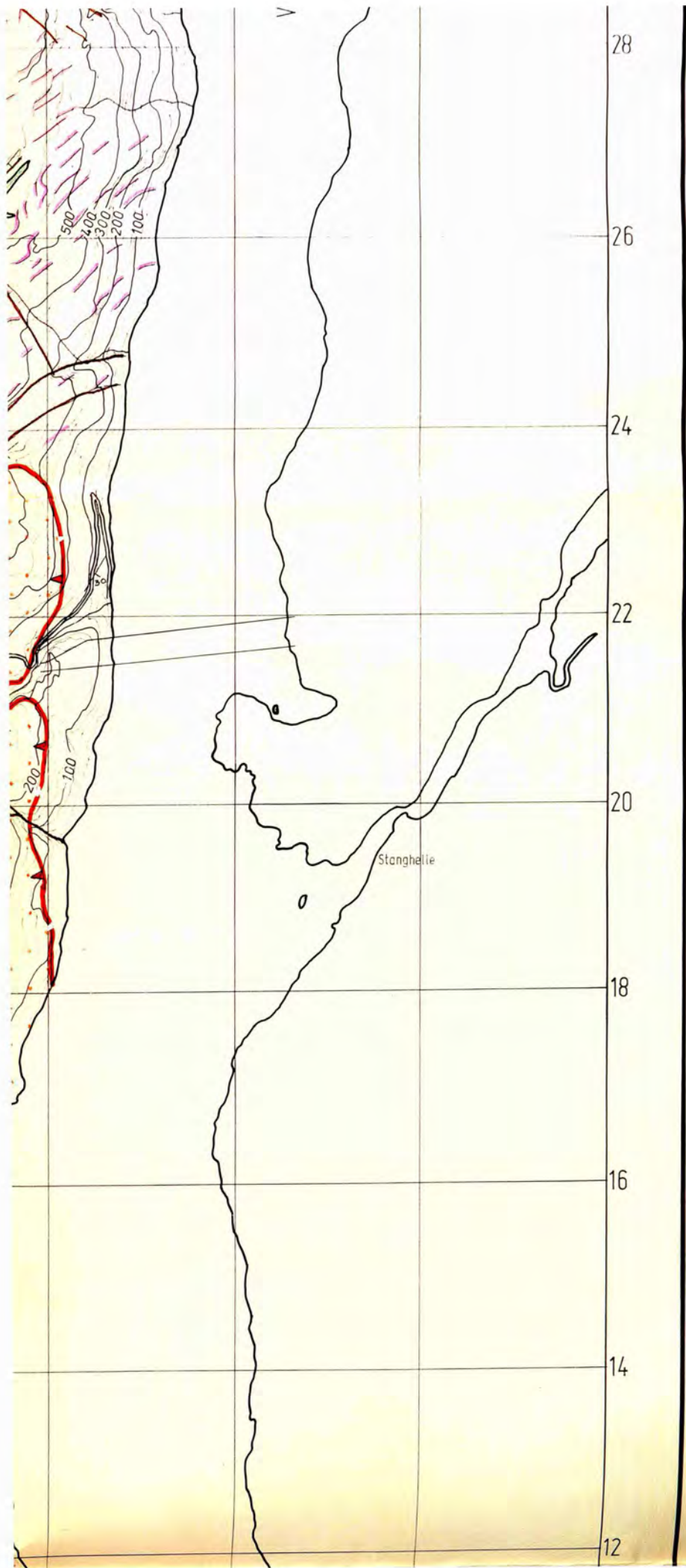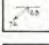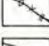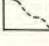
⬚	Dip & Strike of Foliation
⬚	Southern Gneiss Lineation, Pitch
⬚	Northern Gneiss Lineation, Plunge
⬚	F-5 Axial Plane Quartz Vein
⬚	F-2 Fold Plunge
⬚	F-3 Fold Plunge
⬚	F-5 Fold Plunge
⬚	F-2 Axial Plane Trace
⬚	F-3 Axial Plane Trace
⬚	F-5 Axial Plane Trace
⬚	Geological Boundaries
⬚	Joints
⬚	Major Thrust
⬚	Minor Thrust
⬚	Boundary or Structure Uncertain

⬚	Road
⬚	Footpath or Track
⬚	Steps
⬚	Water Pipe
⬚	Overhead Power Cable
⬚	Photo. Centre Number

N

SCALE 1:20,000

0   1   2   3   4   5 Kilometres

SORFJORDEN

Olfnesøy

VEA FJORDEN

nesay

24   26   28   5°45'00"   30

10

8

6

4

2

0